

KSC-DD-818-TR

SUMMARY OF MEASUREMENTS
OF KSC LAUNCH-INDUCED
ENVIRONMENTAL EFFECTS
(STS-1 THROUGH STS-11)

June 1984

ENGINEERING DEVELOPMENT DIRECTORATE

SUMMARY OF MEASUREMENTS
OF KSC LAUNCH-INDUCED
ENVIRONMENTAL EFFECTS
(STS-1 THROUGH STS-11)

PREPARED BY
PLANNING RESEARCH CORPORATION
Systems Services
for
ENGINEERING DEVELOPMENT
JOHN F. KENNEDY SPACE CENTER, NASA

PRC CONTROL NUMBER: 536-2610

June 1984

JOHN F. KENNEDY SPACE CENTER, NASA

TABLE OF CONTENTS

<u>Section</u>	<u>Title</u>	<u>Page</u>
I	INTRODUCTION	1-1
1.1	Purpose	1-1
1.2	Scope	1-1
1.3	Description	1-1
1.4	Authority	1-1
1.5	Data Processing	1-1
1.5.1	High-Frequency Data	1-1
1.5.2	Time Intervals and Parameters for Data Processing	1-12
1.5.2.1	Time Intervals	1-12
1.5.2.2	Parameters for Data Processing	1-13
1.5.2.3	Definitions of Parameters	1-14
1.6	Space Shuttle Launch Environment Reference Material . . .	1-15
II	PRESSURE AND ACOUSTICS	2-1
2.1	FSS Acoustics Summary	2-1
2.2	RSS Acoustics Summary	2-20
2.3	Centaur Rolling Beam Porch Assembly	2-39
2.4	Far Field Acoustics	2-71
2.4.1	Far Field Acoustic Pressures, Bearing 322° True	2-71
2.4.2	Near Field Acoustic Pressures on Three Light Posts . . .	2-72
2.4.3	Far Field Acoustic Pressures on the ECS Cooling Tower . .	2-73
2.4.4	Comparison of Actual Far Field Acoustic Data to Predictions	2-73
2.5	Deck 0 Pressures	2-105
2.6	TSM Pressures Summary	2-118
2.7	MLP Exterior Pressures (SRB Exhaust Wells, Sides 2 and 4, and Bottom)	2-131
2.8	West Side Deflector Pressures	2-159
2.9	MLP Interior Acoustics	2-167
III	STRAINS	3-1
3.1	SRB Holddown Post (HDP) Pedestal Strains on MLP	3-1
3.2	SRB HDP Strains and Loads During the Holddown Period (General Comments)	3-2
3.3	A Plausible Explanation of Strain Oscillations at SRB Ignition	3-4
IV	THERMAL DATA SUMMARY	4-1
4.1	MLP	4-1
4.2	FSS	4-1

TABLE OF CONTENTS (cont)

<u>Section</u>	<u>Title</u>	<u>Page</u>
V	VIBRATION	5-1
5.1	MLP	5-1
5.1.1	Vibration Inside MLP-1 and -2	5-2
5.1.2	MLP-1 and MLP-2 Vibration Data Comparison	5-3
5.2	FSS	5-52
5.3	RSS	5-92

LIST OF ILLUSTRATIONS

<u>Figure</u>	<u>Title</u>	<u>Page</u>
1-1	Shuttle Launch Environment Measurements Summary	1-2
1-2	Launch Configuration	1-3
1-3	MLP Deck A Floor Plan	1-5
1-4	MLP Deck B Floor Plan	1-6
1-5	Overpressure Measurement Locations (MLP-1)	1-7
1-6	Overpressure Measurement Locations (MLP-2)	1-8
1-7	STS-6 Sensors Installed at Pad	1-9
1-8	Time Periods and Intervals of the Launch Environment . .	1-13
2-1	STS-1 Through -9 FSS Acoustics at Lift-Off Peak - Sensor KSAPB001A at 125-ft Elevation	2-3
2-2	STS-1 Through -9 FSS Acoustics at Lift-Off Peak - Sensor KSAPB002A at 155-ft Elevation	2-4
2-3	STS-1 Through -9 FSS Acoustics at Lift-Off Peak - Sensor KSAPB003A at 185-ft Elevation	2-5
2-4	STS-1 Through -9 FSS Acoustics at Lift-Off Peak - Sensor KSAPB004A at 215-ft Elevation	2-6
2-5	STS-1 Through -9 FSS Acoustics at Lift-Off Peak - Sensor KSAPB005A at 245-ft Elevation	2-7
2-6	STS-1 Through -9 Summary of FSS Acoustics at Lift-Off Peak - 90 DOF PSD's (Mean and Limit Only)	2-8
2-7	STS-1 Through -9 Summary of FSS Acoustics at Lift-Off Peak - 90 DOF PSD's	2-9
2-8	STS-1 Through -9 Summary of FSS Acoustics at Lift-Off Peak - 3-Sigma Limit (Mean and Limit Only)	2-10
2-9	STS-1 Through -9 Summary of FSS Acoustics at Lift-Off Peak - 3-Sigma Limit	2-11
2-10	STS-1 Through -9 Summary of FSS Acoustics at Lift-Off Peak - 88 DOF PSD's (Mean and Limit Only)	2-12
2-11	STS-1 Through -9 Summary of FSS Acoustics at Lift-Off Peak - 88 DOF PSD's	2-13
2-12	STS-1 Through -9 Summary of FSS Acoustics at Lift-Off Peak - Data for 0 Hz to 50 Hz (Mean and Limit Only) . . .	2-14
2-13	STS-1 Through -9 Summary of FSS Acoustics at Lift-Off Peak - Data for 0 Hz to 50 Hz	2-15
2-14	STS-1 Through -8 Lift-Off Peak - FSS Acoustics at 245-ft Level, 16 DOF PSD's (Mean and Limit Only)	2-16
2-15	STS-1 Through -8 Lift-Off Peak - FSS Acoustics at 245-ft Level, 16 DOF PSD's	2-17
2-16	Plots of Predicted and Measured OBSPL's for STS-1 Through -6, FSS, All Tower Levels	2-18
2-17	STS-5, -6, -7, -8 Lift-Off Peak - Acoustics on ET Vent Arm, Top of Haunch Pivot	2-19

LIST OF ILLUSTRATIONS (cont)

<u>Figure</u>	<u>Title</u>	<u>Page</u>
2-18	Comparison of Predicted and Actual OBSPL's, Orbiter Holddown, RSS Side 1	2-21
2-19	Comparison of Predicted and Actual OBSPL's, Lift-Off Peak, RSS Side 1	2-22
2-20	Comparison of Predicted and Actual OBSPL's, Orbiter Holddown, RSS Side 2	2-23
2-21	Comparison of Predicted and Actual OBSPL's, Lift-Off Peak, RSS Side 2	2-24
2-22	Comparison of Predicted and Actual OBSPL's, Lift-Off Peak, PCR Side 3	2-25
2-23	Comparison of Predicted and Actual OBSPL's, Orbiter Holddown, All FSS Levels and Side 4 of RSS	2-26
2-24	Comparison of Predicted and Actual OBSPL's, Lift-Off Peak, RSS Side 4	2-27
2-25	Comparison of Predicted and Actual OBSPL's, Lift-Off Peak, RSS Interior Above 130.6-ft Level	2-28
2-26	STS-7 and -8 RSS Acoustics at Orbiter Holddown - Sensors on Side 1	2-29
2-27	STS-7 and -8 RSS Acoustics at Lift-Off Peak - Sensors on Side 1	2-30
2-28	STS-7 and -8 RSS Acoustics at Lift-Off Peak - Sensors on Side 1 (Zoom Plot)	2-31
2-29	STS-7 and -8 RSS Acoustics at Lift-Off Peak - Sensors at Grazing Incidence, Side 1	2-32
2-30	STS-7 and -8 RSS Acoustics at Lift-Off Peak - Sensors on Side 3	2-33
2-31	STS-7 and -8 RSS Acoustics at Lift-Off Peak - Sensors on Side 4 (Mean and Limit Only)	2-34
2-32	STS-7 and -8 RSS Acoustics at Lift-Off Peak - Sensors on Side 4	2-35
2-33	STS-7 and -8 RSS Acoustics at Lift-Off Peak - Sensors on Side 4 (Mean and Limit Only)	2-36
2-34	STS-7 and -8 RSS Acoustics at Lift-Off Peak - Sensors on Side 4	2-37
2-35	STS-7 and -8 RSS Free Field Acoustics at Lift-Off Peak - Sensors on Side 4	2-38
2-36	STS-9 and -11 Orbiter Holddown - Centaur Porch Assembly Pressures, All Sensor Data (Mean and Limit Only)	2-41
2-37	STS-9 and -11 Orbiter Holddown - Centaur Porch Assembly Pressures, All Sensor Data	2-42
2-38	STS-9 and -11 Orbiter Holddown - Centaur Porch Assem- bly Pressures, All Sensor Data (Zoom Plot)	2-43
2-39	STS-9 and -11 Lift-Off Peak - Centaur Porch Assembly Pressures (Mean and Limit; $F_{\max} = 5$ kHz)	2-44

LIST OF ILLUSTRATIONS (cont)

<u>Figure</u>	<u>Title</u>	<u>Page</u>
2-40	STS-9 and -11 Lift-Off Peak - Centaur Porth Assembly Pressures ($F_{\max} = 5$ kHz)	2-45
2-41	STS-9 and -11 Lift-Off Peak - Centaur Porth Assembly Pressures (No Hanning)	2-46
2-42	STS-9 and -11 Lift-Off Peak - Centaur Porth Assembly Pressures (Mean and Limit; $F_{\max} = 1$ kHz)	2-47
2-43	STS-9 and -11 Lift-Off Peak - Centaur Porth Assembly Pressures ($F_{\max} = 1$ kHz)	2-48
2-44	STS-9 and -11 Lift-Off Peak - Centaur Porth Assembly Pressures (Mean and Limit; $F_{\max} = 1,000$ Hz; High-Pass Filter at 1 Hz)	2-49
2-45	STS-9 and -11 Lift-Off Peak - Centaur Porth Assembly Pressures ($F_{\max} = 1,000$ Hz; High-Pass Filter at 1 Hz)	2-50
2-46	STS-9 and -11 Lift-Off Peak - Centaur Porth Assembly Pressures (Mean and Limit; $F_{\max} = 1,000$ Hz; High-Pass Filter at 1 Hz; No Hanning)	2-51
2-47	STS-9 and -11 Lift-Off Peak - Centaur Porth Assembly Pressures ($F_{\max} = 1$ kHz), Comparison of Hanned Data to Data Without Hanning	2-52
2-48	STS-9 and -11 Lift-Off Peak - Centaur Porth Assembly Pressures ($F_{\max} = 100$ Hz), Sensors Closest to Vehicle	2-53
2-49	STS-9 and -11 Lift-Off Peak - Centaur Porth Assembly Pressures ($F_{\max} = 100$ Hz), Sensors Farthest From Vehicle	2-54
2-50	STS-11 Lift-Off Peak - Centaur Porth Pressure Cross-Correlation (Adjacent Sensors; Sampling Rate = 10 kHz)	2-55
2-51	STS-11 Lift-Off Peak - Centaur Porth Pressure Cross-Correlation (Adjacent Sensors; Sampling Rate = 2 kHz)	2-56
2-52	STS-11 Lift-Off Peak - Centaur Porth Pressure Coherences (Adjacent Sensors; $F_{\max} = 5$ kHz)	2-57
2-53	STS-11 Lift-Off Peak - Centaur Porth Pressure Coherences (Adjacent Sensors; $F_{\max} = 1$ kHz)	2-58
2-54	STS-11 Lift-Off Peak - Centaur Porth Pressure Coherences (Adjacent Sensors; $F_{\max} = 100$ Hz)	2-59
2-55	STS-11 Lift-Off - Centaur Porth Assembly Pressures at East End, Sensor KSRPB002A (1 Hz to 10 Hz)	2-60
2-56	STS-11 Lift-Off - Centaur Porth Assembly Pressures at East End, Sensors KSRPB003A and -004A, 1 Hz to 10 Hz (From T to T + 10.24 s)	2-61
2-57	STS-11 Lift-Off - Centaur Porth Assembly Pressures at East End, Sensors KSRPB003A and -004A, 1 Hz to 10 Hz (From T + 5 to T + 15.24 s)	2-62
2-58	STS-11 Lift-Off - Centaur Porth Assembly Pressures at FSS Support, Sensors KSRPB005A and -006A, 1 Hz to 10 Hz (From T to T + 10.24 s)	2-63

LIST OF ILLUSTRATIONS (cont)

<u>Figure</u>	<u>Title</u>	<u>Page</u>
2-59	STS-11 Lift-Off - Centaur Porch Assembly Pressures at FSS Support, Sensors KSRPB005A and -006A, 1 Hz to 10 Hz (From T + 5 to T + 15.24 s)	2-64
2-60	STS-11 Lift-Off - Centaur Porch Assembly Pressures at FSS Support, Sensors KSRPB007A and -008A, 1 Hz to 10 Hz (From T to T + 10.24 s)	2-65
2-61	STS-11 Lift-Off - Centaur Porch Assembly Pressures at FSS Support, Sensors KSRPB007A and -008A, 1 Hz to 10 Hz (From T + 5 s to T + 16 s)	2-66
2-62	Typical RMS Plot of Centaur Porch Pressures Using a 2-Hz High-Pass Filter	2-67
2-63	Typical RMS Plot of Centaur Porch Pressures Using a 1-Hz High-Pass Filter	2-68
2-64	Typical RMS Plot of Centaur Porch Pressures Using a 1-Hz to 20-Hz Bandpass Filter	2-69
2-65	Typical Probability Density Plots	2-70
2-66	STS-11 Lift-Off - Sensor KAVYA003A at 610 ft From the Pad, Raw Data Time History.	2-74
2-67	STS-11 Lift-Off - Sensor KAVYA003A at 610 ft From the Pad, Hanned Time History	2-75
2-68	STS-11 Lift-Off - Sensor KAVYA004A at 1,200 ft From the Pad, Raw Data Time History	2-76
2-69	STS-11 Lift-Off - Sensor KAVYA004A at 1,200 ft From the Pad, Hanned Time History	2-77
2-70	STS-11 Lift-Off - Sensor KAVYA015A at 1,200 ft From the Pad, Raw Data Time History	2-78
2-71	STS-11 Lift-Off - Sensor KAVYA015A at 1,200 ft From the Pad, Hanned Time History	2-79
2-72	STS-11 Lift-Off - Sensor KAVYA005A at 2,500 ft From the Pad, Raw Data Time History	2-80
2-73	STS-11 Lift-Off - Sensor KAVYA005A at 2,500 ft From the Pad, Hanned Time History	2-81
2-74	STS-9 SRB Ignition - Cross-Correlation Between KAVYA003A, -004A, -015A, and -005A	2-82
2-75	STS-11 SRB Ignition - Cross-Correlation Between KAVYA003A, -004A, -013A, -015A, and -005A	2-83
2-76	STS-8, -9, and -11 SRB Ignition - Cross-Correlation Between KAVYA003A, -004A, -015A, and -013A	2-84
2-77	STS-9 and -11 SRB Ignition - Cross-Correlation Between KAVYA004A, -015A, and -005A	2-85
2-78	STS-9 and -11 SRB Ignition - Cross-Correlation Between KAVYA003A and -005A	2-86
2-79	STS-11 Lift-Off Peak - Coherence Between Adjacent KAVYA004A and -015A Sensor Data	2-87

LIST OF ILLUSTRATIONS (cont)

<u>Figure</u>	<u>Title</u>	<u>Page</u>
2-80	STS-11 Lift-Off Peak - Coherence Between Adjacent KAVYA004A and -015A Sensor Data (Mean)	2-88
2-81	STS-11 Lift-Off Peak - Coherence Between Adjacent KAVYA004A and -013A Sensor Data	2-89
2-82	STS-11 Lift-Off Peak - Coherence Between Adjacent KAVYA015A and -013A Sensor Data	2-90
2-83	STS-11 Lift-Off Peak and Peak End - PSD, Sensor KAVYA003A at 610 ft From the Pad	2-91
2-84	STS-11 Lift-Off Peak - PSD, Adjacent Sensors KAVYA004A, -015A, and -013A at 1,200 ft From the Pad	2-92
2-85	STS-11 Lift-Off Peak - PSD, Sensor KAVYA005A at 2,500 ft From the Pad	2-93
2-86	STS-11 SRB Ignition/Lift-Off - Probability Density, Sensors KAVYA003A and -004A	2-94
2-87	STS-8, -9, and -11 Summary at Lift-Off - PSD, Sensor KAVYA003A at 610 ft From the Pad	2-95
2-88	STS-8, -9, and -11 Summary at Lift-Off - PSD, Sensors at 1,200 ft From the Pad	2-96
2-89	STS-8, -9, and -11 Summary at Lift-Off - PSD, Sensors at 1,200 ft From the Pad (Mean and Limit Only)	2-97
2-90	STS-9 and -11 Summary at Lift-Off - PSD, Sensor KAVYA005A at 2,500 ft From the Pad	2-98
2-91	STS-6 Acoustic Pressure on Light Posts at the 98-ft Elevation With Sensors Facing the Vehicle (Averaging Block Time 1.024 s and 2.56 s)	2-99
2-92	STS-6 Acoustic Pressure on Light Posts at the 98-ft Elevation With Sensors Facing the Vehicle (0- to 50-Hz and 50- to 250-Hz Plot Range)	2-100
2-93	STS-6 Acoustic Pressure on Light Posts at the 98-ft Elevation With Sensors Facing the Vehicle (0- to 10-Hz and 10- to 50-Hz Plot Range)	2-101
2-94	STS-7 and -8 Lift-Off Peak - ECS Cooling Tower Acoustics (No Hanning)	2-102
2-95	STS-7 and -8 Lift-Off Peak - ECS Cooling Tower Acoustics (All PSD's Hanned)	2-103
2-96	Predicted and Actual Sound Pressure Levels Data Summary	2-104
2-97	MLP-1 Static Pressures and OASPL's	2-106
2-98	STS-1 MLP-1 Deck 0 Impinging Plume Pressure (TVM)	2-107
2-99	STS-2 MLP-1 Deck 0 Impinging Plume Pressure (TVM)	2-108
2-100	STS-3 MLP-1 Deck 0 Impinging Plume Pressure (TVM)	2-109
2-101	STS-9 MLP-1 Deck 0 Impinging Plume Pressure (TVM)	2-110
2-102	STS-1, -2, and -9 MLP-1 Deck 0 Impinging Plume Pressure (TVM)	2-111
2-103	STS-1, -2, -3, and -9 MLP-1 Deck 0 Impinging Plume Pressure (TVM) (Sensors: STS-1 and -2, KSRPF014A; STS-3 and -9, KSRPF005A)	2-112

LIST OF ILLUSTRATIONS (cont)

<u>Figure</u>	<u>Title</u>	<u>Page</u>
2-104	STS-1, -2, -3, and -9 MLP-1 Deck 0 Impinging Plume Pressure (TVM) (Sensors: STS-1, KSRPF017A; STS-2 and -9, -017A and -008A; STS-3, -008A)	2-113
2-105	STS-9 MLP-1 Deck 0 Impinging Plume Pressure PSD's - Lift-Off Peak	2-114
2-106	STS-1 Lift-Off Peak - KSRPF011A Raw Data and Dynamic Component of Data	2-115
2-107	STS-1 Lift-Off Peak - KSRPF011A Power Spectral Density, Probability Density, and Standard Deviation Time History	2-116
2-108	STS-1 Lift-Off Peak - KSRGF002A Raw Data (Filtered), Time Variable Mean, Dynamic Component of Data, and Power Spectral Density.	2-117
2-109	STS-6 and -8 Acoustics on TSM's at Lift-Off Peak - Sensors Oriented in -Z Direction (Mean and Limit Only). .	2-119
2-110	STS-6 and -8 Acoustics on TSM's at Lift-Off Peak - Sensors Oriented in -Z Direction.	2-120
2-111	STS-6 Acoustics on TSM's at Lift-Off Peak End - Sensors Oriented in -Z Direction (Mean and Limit)	2-121
2-112	STS-6 Acoustics on TSM's at Lift-Off Peak - Sensors Oriented in -Z Direction	2-122
2-113	STS-6 Lift-Off Peak - KSRPG001A Raw Data and Time Variable Mean	2-123
2-114	STS-6 Lift-Off Peak - KSRPG006A Raw Data and Time Variable Mean	2-124
2-115	STS-6 Lift-Off Peak - KSRPG007A Raw Data and Time Variable Mean	2-125
2-116	STS-4, -5, -7, and -8 Acoustics on Top of TSM's at Lift-Off Peak - Sensors in -Z Direction (Mean and Limit Only)	2-126
2-117	STS-4, -5, -6, -7, and -8 Acoustics on Top of TSM's at Lift-Off Peak - Sensors in -Z Direction	2-127
2-118	STS-4, -5, and -7 Acoustics on Top of TSM's at Lift-Off Peak - X and Y Directions (Mean and Limit Only)	2-128
2-119	STS-4, -5, and -7 Acoustics on Top of TSM's at Lift-Off Peak - X and Y Directions	2-129
2-120	STS-8 SRB Ignition - West SRB, Main Exhaust Well Pressures, T + 0.05 s to T + 0.35 s (MLP-2 Sensors on Side 1)	2-133
2-121	STS-8 SRB Ignition - West SRB, Main Exhaust Well Pressures T + 0.05 s to T + 0.35 s (MLP-2 Sensors on Side 2)	2-134
2-122	STS-8 SRB Ignition - Pressures at Bottom of West SRB Exhaust Well	2-135

LIST OF ILLUSTRATIONS (cont)

<u>Figure</u>	<u>Title</u>	<u>Page</u>
2-123	STS-8 SRB Ignition - West SRB, Secondary Exhaust Well Pressures, T + 0.05 s to T + 0.35 s	2-136
2-124	STS-8 SRB Ignition - West Exhaust Well Pressures Above Sound Suppression Water System	2-137
2-125	STS-9 SRB Ignition - West Exhaust Well Pressures Below Sound Suppression Water System (MLP-1 Sensors on South Side of West Exhaust Well)	2-138
2-126	STS-9 SRB Ignition - West Exhaust Well Pressures Below Sound Suppression Water System (MLP-1 Sensors on West Side of Primary West Exhaust Well)	2-139
2-127	STS-9 SRB Ignition - West Secondary Exhaust Well Pressures Below Sound Suppression Water System	2-140
2-128	STS-9 SRB Ignition - West Exhaust Well Pressures Above Sound Suppression Water System	2-141
2-129	STS-9 Lift-Off - West Primary Exhaust Well Pressures, South Side 1, Static Load	2-142
2-130	STS-9 Lift-Off - West Primary Exhaust Well Pressures, West Side 2, Static Load	2-143
2-131	STS-9 Lift-Off - West Secondary Exhaust Well Pressures, West Side 2, Static Load	2-144
2-132	STS-9 Lift-Off - West Secondary Exhaust Well Pressures, North Side 3, Static Load	2-145
2-133	STS-9 Lift-Off Peak - West Exhaust Well Pressures, Dynamic Part, Raw PSD's	2-146
2-134	STS-9 Lift-Off Peak - West Exhaust Well Pressures, Dynamic Part (Hanned)	2-147
2-135	STS-4, -5, -7, and -9 Lift-Off Peak - Acoustics on Sides 2 and 4 of MLP-1	2-148
2-136	STS-8 SRB Ignition - KSRPG014A Raw Data and TVM	2-149
2-137	STS-9 SRB Ignition - KSRPF062A Raw Data and TVM	2-150
2-138	STS-9 SRB Ignition - KSRPF060A Raw Data and TVM	2-151
2-139	STS-8 and -9 MLP-1 and MLP-2 Pressures on B Level, TVM	2-152
2-140	STS-4 Through -9 MLP-1 and MLP-2 Pressures on B Level Between T-1 and G-13, Dynamic Part	2-153
2-141	STS-4 Through -9 MLP-1 and MLP-2 Pressures on B Level Between T-1 and G-13, 0 to 100 Hz	2-154
2-142	STS-4 Through -9 MLP-1 and MLP-2 Pressures on B Level Between T-1 and G-13, 100 to 600 Hz	2-155
2-143	STS-4 and -6 Through -9 MLP-1 and MLP-2 Pressures on B Level Between SRB Exhausts, Dynamic Part	2-156
2-144	STS-4 Through -9 MLP-1 and MLP-2 Pressures on B Level Between SRB Exhausts, 0 Hz to 100 Hz	2-157
2-145	STS-4 and -6 Through -9 MLP-1 and MLP-2 Pressures on B Level Between SRB Exhausts, 100 Hz to 600 Hz	2-158

LIST OF ILLUSTRATIONS (cont)

<u>Figure</u>	<u>Title</u>	<u>Page</u>
2-146	STS-8 SRB Ignition - West Side Deflector Pressures, T + 0.15 s to T + 0.35 s	2-160
2-147	STS-9 SRB Ignition - West Side Deflector Pressures, T + 0.15 s to T + 0.35 s	2-161
2-148	STS-8 and -9 SRB Ignition - West Side Deflector Pressures T + 0.15 s to T + 0.35 s, Sensor KFDPA006A . . .	2-162
2-149	STS-8 and -9 SRB Ignition - West Side Deflector Pressures, T + 0.15 s to T + 0.35 s, Sensor KFDPA007A . . .	2-163
2-150	STS-8 and -9 SRB Ignition - West Side Deflector Pressures, T + 0.15 s to T + 0.35 s, Sensor KFDPA008A . . .	2-164
2-151	STS-8 and -9 Lift-Off - West Side Deflector Pressures, T + 0.5 s to T + 5.6 s	2-165
2-152	STS-7, -8, and -9 Lift-Off Peak - West Side Deflector Pressures, Dynamic Part	2-166
2-153	Lift-Off Peak - Summary of MLP Interior Acoustics, Room 15A	2-168
2-154	Lift-Off Peak - Summary of MLP Interior Acoustics, Rooms 7A, 8A, and 10A	2-169
2-155	Lift-Off Peak - Summary of MLP Interior Acoustics, Rooms 8B and 9B	2-170
2-156	Lift-Off Peak - Summary of MLP Interior Acoustics, Rooms 36AB and 37A.	2-171
2-157	Lift-Off Peak - Summary of MLP Interior Acoustics, Room 7A	2-172
2-158	STS-4 Through -11 Lift-Off Peak - Summary of MLP Interior Acoustics, PSD's (0 Hz to 51 Hz)	2-173
2-159	STS-4 Through -11 Lift-Off Peak - Summary of MLP Interior Acoustics, PSD's (Mean and Limit Only; 0 Hz to 51 Hz)	2-174
2-160	STS-4 Through -11 Lift-Off Peak - Summary of MLP Interior Acoustics, PSD's (50 Hz to 100 Hz)	2-175
2-161	STS-4 Through -11 Lift-Off Peak - Summary of MLP Interior Acoustics, PSD's, Mean and Limit Only (50 Hz to 100 Hz)	2-176
2-162	STS-4 Through -11 Lift-Off Peak - Summary of MLP Interior Acoustics, 2- and 3-Sigma Limits	2-177
2-163	Lift-Off Peak - Actual OBSPL's Compared With Predictions, MLP Compartments Around Exhaust Wells	2-178
2-164	Lift-Off Peak - Actual OBSPL's Compared With Predictions, MLP Compartments 36AB, 37A, and 37B	2-179
2-165	Lift-Off Peak - Actual OBSPL's Compared With Predictions, MLP Compartments Except Vicinity of Exhaust Wells	2-180
3-1	STS-9 East SRB HDP Pedestals (1, 2, 3, 4) Strains (T - 4.6 to T + 0.5 s)	3-9

LIST OF ILLUSTRATIONS (cont)

<u>Figure</u>	<u>Title</u>	<u>Page</u>
3-2	STS-9 West SRB HDP Pedestals (5, 6, 7, 8) Strains (T - 4.6 to T + 0.5 s)	3-11
3-3	STS-9 East SRB HDP Pedestals (1, 2, 3, 4) Strains (T - 0.015 to T + 0.01 s)	3-13
3-4	STS-9 East SRB HDP Pedestals (1, 2, 3, 4) Strains (T - 0.1 to T + 0.31 s)	3-14
3-5	STS-9 East SRB HDP Pedestal (1) Strains (T - 0.1 to T + 0.31 s)	3-15
3-6	STS-9 East SRB HDP Pedestal (2) Strains (T - 0.1 to T + 0.31 s)	3-16
3-7	STS-9 East SRB HDP Pedestal (3) Strains (T - 0.1 to T + 0.31 s)	3-17
3-8	STS-9 East SRB HDP Pedestal (4) Strains (T - 0.1 to T + 0.31 s)	3-18
3-9	STS-6, -7, -8, and -9 East SRB HDP Pedestal Strains at SRB Ignition	3-19
3-10	STS-6, -7, -8, and -9 West SRB HDP Pedestal Strains at SRB Ignition	3-21
3-11	STS-6, -7, -8, and -9 Summary of East and West SRB HDP Strains at SRB Ignition	3-23
3-12	Typical Strain Time History and Illustration of Terms in Text	3-26
3-13	Location of MLP HDP's	3-28
4-1	MLP-1 Thermal Data Recorded During STS-1, -3, -4, -5, -7, and -9 Launches	4-2
4-2	MLP-1 Heat Rate Data Recorded During STS-1 and -3 Launches	4-3
4-3	FSS Heat Rate Data Recorded During STS-3, -6, and -8 Launches	4-4
5-1	Room 43A - Girder Web Stiffener, Y Direction	5-5
5-2	Room 43A - Girder Web Stiffener, Z Direction	5-7
5-3	Room 36AB - Above Deck B Floor (6 ft), Z Direction	5-9
5-4	Room 40AB - Above Deck B Floor (11 ft), X Direction	5-11
5-5	Room 7A - C Bottom Flange Deck O Beam, Z Direction	5-13
5-6	Room 9A - C Bottom Flange Deck O Beam, Z Direction	5-15
5-7	Room 41B - Center Floor Beam, X Direction	5-17
5-8	Room 41B - Center Floor Beam, Y Direction	5-19
5-9	Room 8A - Truss T ₂ Vertical, Z Direction	5-21
5-10	Room 7A - Truss T ₁ Vertical, Z Direction	5-23
5-11	Room 10A - Truss T ₂ Top Chord, Z Direction	5-25
5-12	Room 10A - Truss T ₁ Top Chord, Z Direction	5-27
5-13	Room 9B - Floor Framing Stringer (E), Z Direction	5-29

LIST OF ILLUSTRATIONS (cont)

<u>Figure</u>	<u>Title</u>	<u>Page</u>
5-14	Room 9B - Floor Framing Stringer (W), Z Direction . . .	5-31
5-15	STS-6 MLP-2 Vibration Data Processing Parameters and Calculated RMS Displacements.	5-33
5-16	MLP-1 and MLP-2 Vibration, Deck 0 Beam, Room 9A at Centerline of East SRB, Z Direction	5-35
5-17	MLP-1 and MLP-2 Vibration, Deck 0 Beam, Room 7A, Z Direction	5-36
5-18	MLP-1 and MLP-2 Vibration, T-2 Truss Top Chord, Room 10A, Z Direction.	5-37
5-19	MLP-1 and MLP-2 Vibration, Deck B Floor Beam, Room 9B, Z Direction	5-38
5-20	MLP-1 and MLP-2 Vibration, Deck B Floor Beam, Room 9B, Z Direction, KSRDF129B, -DF129A, -DG006A	5-39
5-21	MLP-1 and MLP-2 Vibration, Deck B Floor Beam, Room 9B, Z Direction, KSRDF129A, -DG006C, -DF129B, -DG006B . . .	5-40
5-22	MLP-1 and MLP-2 Vibration, Deck B Floor Beam, Room 9B, at West SRB, Z Direction, KSRDF128B, -DG005A	5-41
5-23	MLP-1 and MLP-2 Vibration, Deck B Floor Beam, Room 9B, at West SRB, Z Direction, KSRDF128A, -DF129A, -DF129B, -DG005C, -DG006C	5-42
5-24	STS-6 MLP-2 Vibration of Deck 0 Beams, Z Direction, 0 to 100 Hz and 100 to 2,100 Hz	5-43
5-25	STS-6 MLP-2 Vibration of Deck 0 Beams, Z Direction, 0 to 100 Hz and 100 to 500 Hz	5-44
5-26	STS-6 MLP-2 Vibration of Deck 0 Beams, Z Direction, 0 to 100 Hz	5-45
5-27	STS-6 MLP-2 Vibration of T-2 Truss Top Chord, Z Direc- tion, 0 to 100 Hz and 100 to 2,100 Hz	5-46
5-28	STS-6 MLP-2 Vibration of T-2 Truss Top Chord, Z Direc- tion, 0 to 100 Hz and 100 to 500 Hz	5-47
5-29	STS-6 MLP-2 Vibration of T-2 Truss Top Chord, Z Direc- tion, 0 to 100 Hz	5-48
5-30	STS-6 MLP-2 Vibration of Deck B Floor Beams, Z Direc- tion, 0 to 100 Hz and 100 to 250 Hz	5-49
5-31	STS-6 MLP-2 Vibration of Deck B Floor Beams, Z Direc- tion, 0 to 50 Hz	5-50
5-32	STS-6 Data Pertinent to MLP-2 Fundamental Resonances After SRB Ignition	5-51
5-33	Floor Beam Side 2, 75-ft Level, Z Direction	5-53
5-34	Floor Beam Center Side 4, 115-ft Level, Z Direction . .	5-55
5-35	Floor Beam Center Side 1, 115-ft Level, Z Direction . .	5-57
5-36	Floor Beam Side 1, 195-ft Level, Z Direction	5-59
5-37	Floor Beam Center Side 1, 195-ft Level, Z Direction . .	5-61
5-38	Floor Beam Side 1, 255-ft Level, Z Direction	5-63

LIST OF ILLUSTRATIONS (cont)

<u>Figure</u>	<u>Title</u>	<u>Page</u>
5-39	Floor Beam Center Side 1, 255-ft Level, Z Direction . .	5-65
5-40	ET Arm Vertical Member, 215-ft Level, Z Direction . . .	5-67
5-41	LH ₂ Dewar Gage Panel Center, 155-ft Level, X Direction	5-69
5-42	LO ₂ Dewar Gage Panel Center, 155-ft Level, X Direction	5-71
5-43	STS-3 FSS Vibration at 115- and 155-ft Levels, X and Y Directions	5-73
5-44	STS-3 Lift-Off Peak - FSS Vibration at 115-ft Level, Z Direction	5-74
5-45	STS-3 Lift-Off Peak - FSS Vibration at 115-ft Level, Z Direction, (Only KSADB014B Is Visible)	5-75
5-46	STS-3 Lift-Off Peak - FSS Vibration at 115-ft Level, Z Direction (Deleted KSADB014B)	5-76
5-47	STS-3 Lift-Off Peak - FSS Vibration at 115-ft Level, Z Direction (All PSD'S Hanned)	5-77
5-48	STS-3 Lift-Off Peak - FSS Vibration at 155-ft Level, Z Direction (KSADB015A, -16A, -17A, -21B, and -22B) . . .	5-78
5-49	STS-3 Lift-Off Peak - FSS Vibration at 155-ft Level, Z Direction (KSADB016A, -21B, and -22B)	5-79
5-50	STS-3 Lift-Off Peak - FSS Vibration at 155-ft Level, Z Direction (All PSD's Hanned)	5-80
5-51	STS-3 FSS Vibration at 195-ft Level, X and Y Direc- tions	5-81
5-52	STS-3 Lift-Off Peak - FSS Vibration at 195-ft Level, Z Direction (KSADB023A, -29A, -24B, and 35B; Delta F = 0.3906 Hz)	5-82
5-53	STS-3 Lift-Off Peak - FSS Vibration at 195-ft Level, Z Direction	5-83
5-54	STS-3 Lift-Off Peak - FSS Vibration at 195-ft Level, Z Direction (All PSD's Hanned)	5-84
5-55	STS-3 FSS Vibration at 215-ft Level, Z Direction . . .	5-85
5-56	STS-3 FSS Vibration at 255-ft Level, X Direction . . .	5-86
5-57	STS-3 FSS Vibration at 255-ft Level, Y Direction . . .	5-87
5-58	STS-3 FSS Vibration at 255-ft Level, Z Direction . . .	5-88
5-59	STS-3 Lift-Off Peak - FSS Vibration at 255-ft Level, Z Direction (All PSD's Hanned)	5-89
5-60	STS-3 Lift-Off Peak - FSS Vibration on Side 1 at 115-, 195-, and 255-ft Levels, Z Direction	5-90
5-61	STS-3 Lift-Off Peak - FSS Vibration on Side 1 at 255- ft Level, Z Direction	5-91
5-62	Main Floor Beam, 107-ft Level, Z-Direction	5-93
5-63	Floor Beam, Side 4, 158-ft 5-in- Level, Z-Direction . .	5-95
5-64	Platform 2-in-Floor Beam, Side 3, 131-ft Level	5-97
5-65	Outside Flange, Side 4, 135-ft Level	5-99
5-66	Platform Floor Beam (Point 1), 107-ft Level	5-101

LIST OF ILLUSTRATIONS (cont)

<u>Figure</u>	<u>Title</u>	<u>Page</u>
5-67	Platform Floor Beam (Point 2), 107-ft Level	5-103
5-68	Platform Floor Beam (Middle), 120-ft Level	5-105
5-69	STS-3 RSS Vibration Data Comparison, Bottom Flange, 130-ft 7-in Level	5-107
5-70	STS-3 RSS Vibration on Hypergol Platform, X and Y Directions	5-108
5-71	STS-3 RSS Vibration on Hypergol Platform, Z Direction	5-109
5-72	STS-3 RSS Vibration on APU Platform, Z Direction	5-111
5-73	STS-3 RSS Vibration on PCR Floor, Z Direction	5-113
5-74	STS-3 RSS Vibration, High-Frequency Sensors on Floors, X Direction	5-114
5-75	STS-3 RSS Vibration, High-Frequency Sensors on Floors, Y Direction	5-115
5-76	STS-3 RSS Vibration, Side 4 Girts, X Direction	5-117
5-77	STS-3 RSS Vibration, Side 3 Girts, Y Direction	5-118
5-78	STS-3 Lift-Off - Vibration Inside HIM Rack 6396A1, Sensors in X, Y, and Z Directions	5-119
5-79	STS-3 Malfunction of High-Frequency Sensors KSRDC042A (X), -43A (Y), and -44A (Z)	5-120
5-80	STS-3 KSRDC042A (X), -43A (Y), and -44A (Z) Before and After Malfunction	5-121
5-81	STS-2 and -3 PCR Floor Beam, X and Y Directions	5-122
5-82	STS-2 and -3 PCR Floor Beam, Z Direction, and Side Girt, X Direction	5-123
5-83	STS-2 and -3 Side 3 Girt, Y Direction	5-124
5-84	STS-2 and -3 APS Floor Beam, X and Y Directions	5-126
5-85	STS-2 and -3 Hypergol Electronic Equipment Platform Floor Beam at 117-ft Elevation, X Direction	5-127
5-86	STS-2 and -3 Hypergol Electronic Equipment Platform Floor Beam at 117-ft Elevation, Y Direction	5-128
5-87	STS-2 and -3 Hypergol Electronic Equipment Platform Floor Beam, X and Y Directions	5-129
5-88	STS-2 and -3 Hypergol Electronic Equipment Platform Floor Beam, Z Direction	5-130
5-89	STS-2 and -3 PCR Floor Beam, X and Y Directions	5-131
5-90	STS-2 Lift-Off Peak - Comparison Between KSRDC006A (X) and -007A (Y)	5-132
5-91	STS-3 Lift-Off Peak - Comparison Between KSRDC049A (X) and -050A (Y)	5-134
5-92	STS-3 Lift-Off Peak - Low-Frequency Sensors KSRDC006A (X), -007A (Y), -049A (X), and -050A (Y)	5-137
5-93	STS-2 Lift-Off Peak End - High-Frequency Sensors Inside HIM Rack 6396A1	5-139

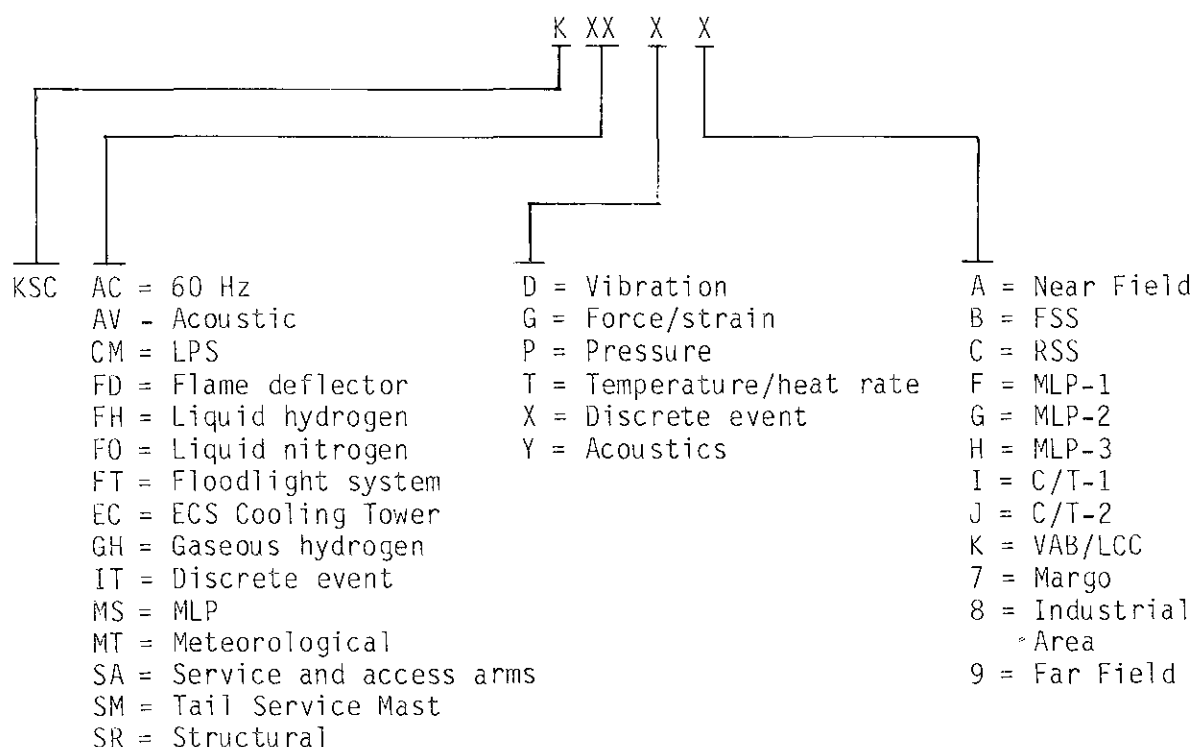
ABBREVIATIONS AND ACRONYMS

APS	Aft Propulsion System
APU	Auxiliary Propulsion Unit
Btu	British thermal unit
CCFC	cross-correlation function coefficient
CF	calibration factor
C _L	centerline
cm ²	square centimeter
DAS	Data Acquisition System
dB	decibel
DOF	degree(s) of freedom
ECS	Environmental Control System
EL	elevation
ET	External Tank
F _{max}	maximum analysis frequency
FSS	Fixed Service Structure
ft	foot
g	acceleration due to gravity
G ₁	girder (no. 1)
GLOW	Orbiter gross lift-off weight
GO ₂	gaseous oxygen
GP	general publication
HDP	holddown post
HIM	hardware interface module
Hz	hertz
in	inch
kHz	kilohertz
kips	thousands of pounds
KSC	John F. Kennedy Space Center
LH ₂	liquid hydrogen
LO ₂	liquid oxygen
MLP	Mobile Launcher Platform
μin	microinch
μs	microsecond
ms	millisecond
NASA	National Aeronautics and Space Administration
OASPL	overall sound pressure level
OB SPL	octave band sound pressure level
oct	octave
PD	probability density
PIC	Pyro Initiator Controller
PMS	Permanent Measurement System
PRC	Planning Research Corporation
PSD	power spectral density
psia	pounds per square inch, absolute
psig	pounds per square inch, gage
rms	root mean square

ABBREVIATIONS AND ACRONYMS (cont)

RSS	Rotating Service Structure
s	second (of time)
SRB	Solid Rocket Booster
STS	Space Transportation System
T(T-0)	instant of time when the PIC is energized
T ₁	truss (no. 1)
TSM	Tail Service Mast
TVM	time variable mean

DECIPHERING THE DESIGNATION



Ergo: KSRPG = Plot of the launch-induced reaction of a pressure (P) transducer installed (see figure 1-1 for location) on the structure (SR) of MLP-2 (G) at KSC (K).

The time period (holddown or lift-off) or interval within a time period (SRB ignition or lift-off peak) during which the reaction was recorded is indicated on each plot.

The numerical suffixes (001A, 002A, . . . 014A, etc.) are sequential.

SECTION I

INTRODUCTION

1.1 PURPOSE

The purpose of this document is to present a summary of Shuttle launch-induced environment data acquired at KSC during Space Transportation System (STS) launches.

1.2 SCOPE

The data presented include launch data from STS-1 through STS-11. All Space Shuttles were launched at Pad A from Mobile Launcher Platform (MLP)-1, except STS-6, -8, and -9, which were launched from MLP-2.

1.3 DESCRIPTION

Selection of measurement type, location, range, and sampling frequencies was based primarily on the Shuttle Environment Prediction, GP-1059. Figure 1-1 shows a summary of the measurement type, location, and ranges presented in this document.

Figure 1-2 shows an elevation of LC-39A. Figures 1-3 and 1-4 show the compartment arrangement and main structural members of the MLP. Figures 1-5 and 1-6 show the overpressure sensor locations for both MLP-1 and MLP-2. Figure 1-7 shows the pressure sensors installed on the lightposts for STS-6 launch.

1.4 AUTHORITY

This document was prepared by Planning Research Corporation (PRC) Systems Services Aerospace Division for the NASA/KSC Engineering Development Directorate. Mr. Valentin Sepcenko and Mr. Rocco Sannicandro comprised the PRC technical team for this project. Mr. Frank McInerny and Mr. Bill Tolson of NASA provided direction.

1.5 DATA PROCESSING

The data are initially recorded on magnetic tapes during the launch. These tapes are reduced to raw oscillograms for quick-look analysis and selection of significant time intervals for further processing. Processing was performed in NASA's Wave Analysis Laboratory.

1.5.1 HIGH-FREQUENCY DATA. Launch environment data such as plume pressures, acoustics, strains in structural members, and vibration may be classified as wideband, random, and nonstationary. Data time histories represent long-duration transients where, in a general case, the mean value and the standard deviation calculated within a short time interval are also variable with

Measurement Type	Location	Qty	Range
Pressure	MLP		
	Deck	6	0 to 150 psia
	TSM	12	0 to 25 psia
	Exhaust wells	40	0 to 50 psia
	Flame deflector	8	0 to 300 psia
	FSS	6	0 to 20 psia
	Centaur Porch	8	±5 psig
Acoustics	MLP (inside)	15	110 dB to 170 dB
	FSS	7	138 dB to 180 dB
	RSS	12	130 dB to 175 dB
	Pad (far field)	18	120 dB to 180 dB
Strain	MLP (inside)	18	±1,500 μ in/in
	Holddown posts	48	±500 μ in/in
	TSM	8	±350 to 1,250 μ in/in
	RSS	15	±900 μ in/in
Load	MLP holddown posts	12	0 to 2,124 kips
Temperature	MLP		
	Deck	9	32°F to 1,900°F
	Flame deflector	2	32°F to 4,200°F
Heat Rate	MLP deck	6	0 to 820 Btu/ft ² /s
	FSS ET vent arm	1	0 to 300 Btu/ft ² /s
Vibration	MLP (inside)	150	±5 g to ±100 g
	FSS	47	±15 g to ±100 g
	RSS	41	±7 g to ±65 g

Figure 1-1. Shuttle Launch Environment Measurements Summary

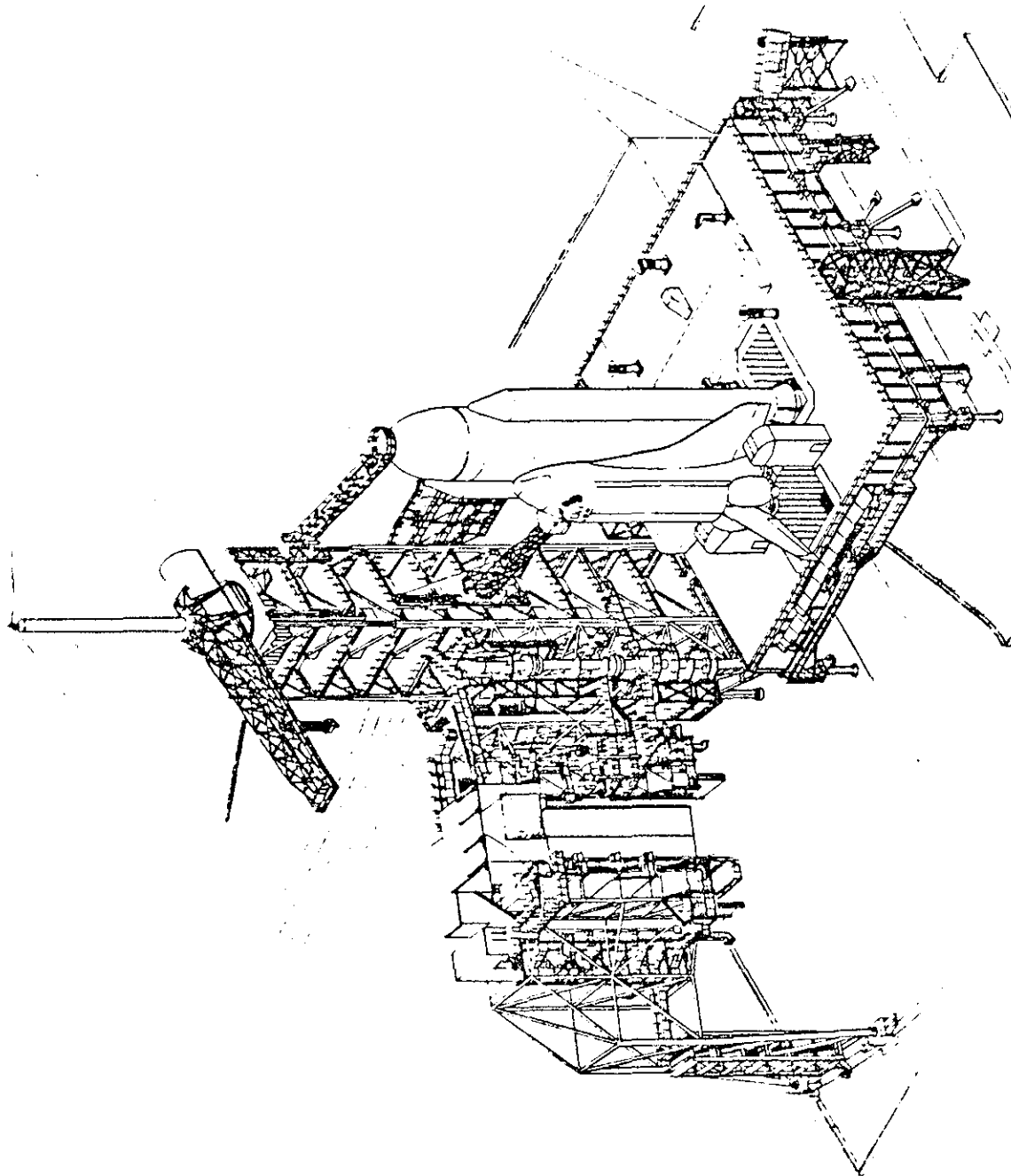


Figure 1-2. Launch Configuration (Sheet 1 of 2)

KSC-DD-818-TR

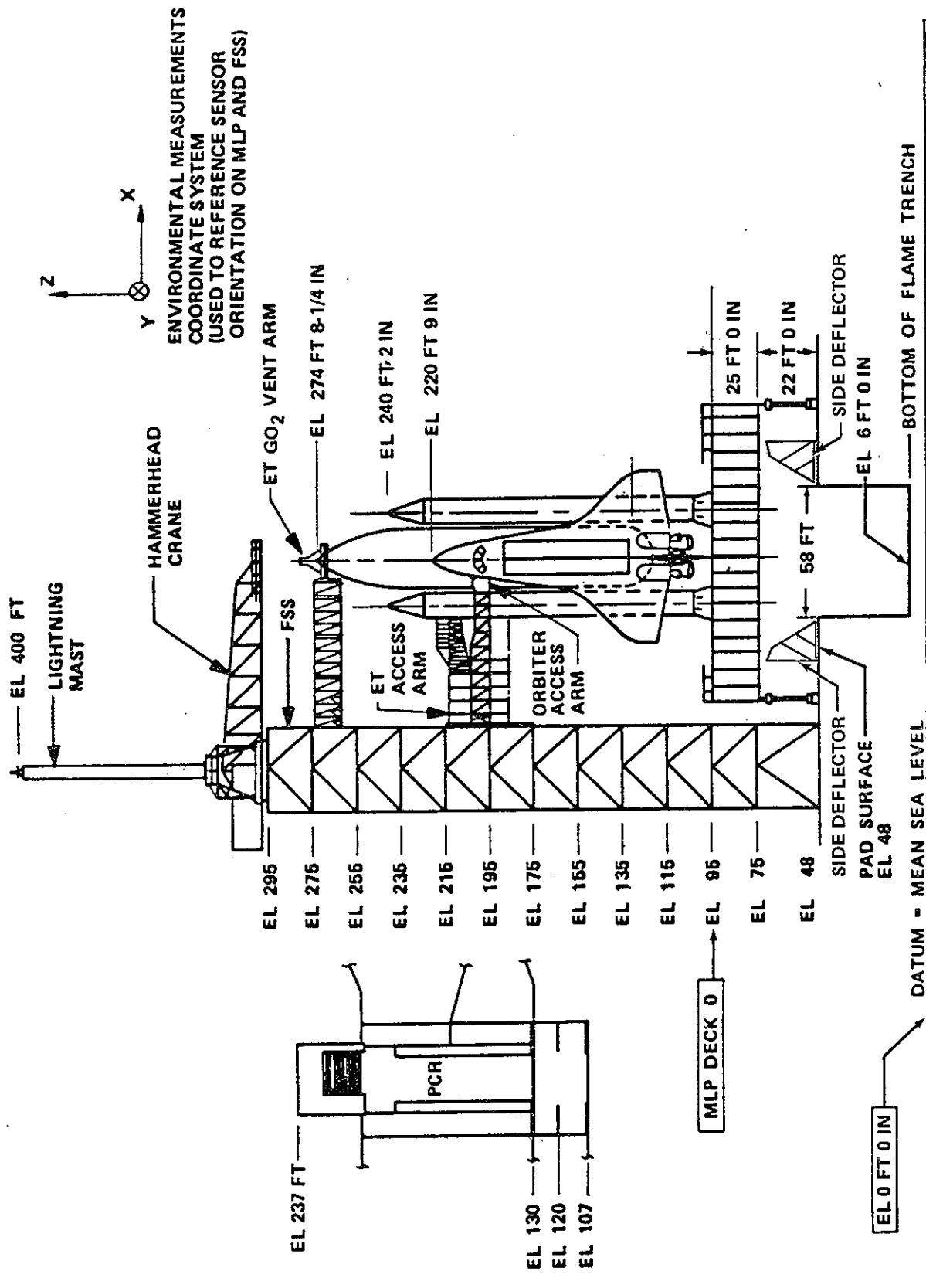


Figure 1-2. Launch Configuration (Sheet 2 of 2)

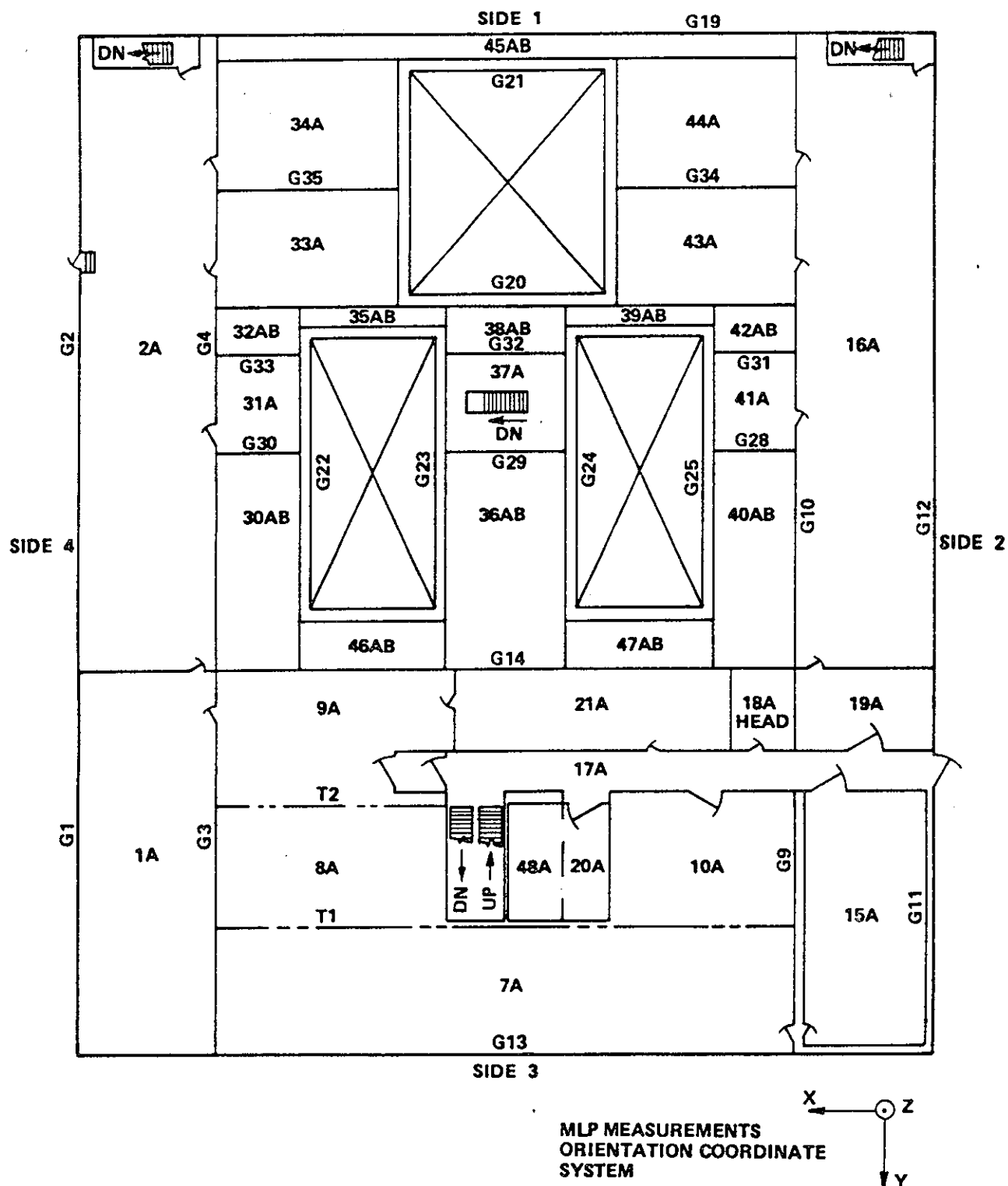


Figure 1-3. MLP Deck A Floor Plan.

KSC-DD-818-TR

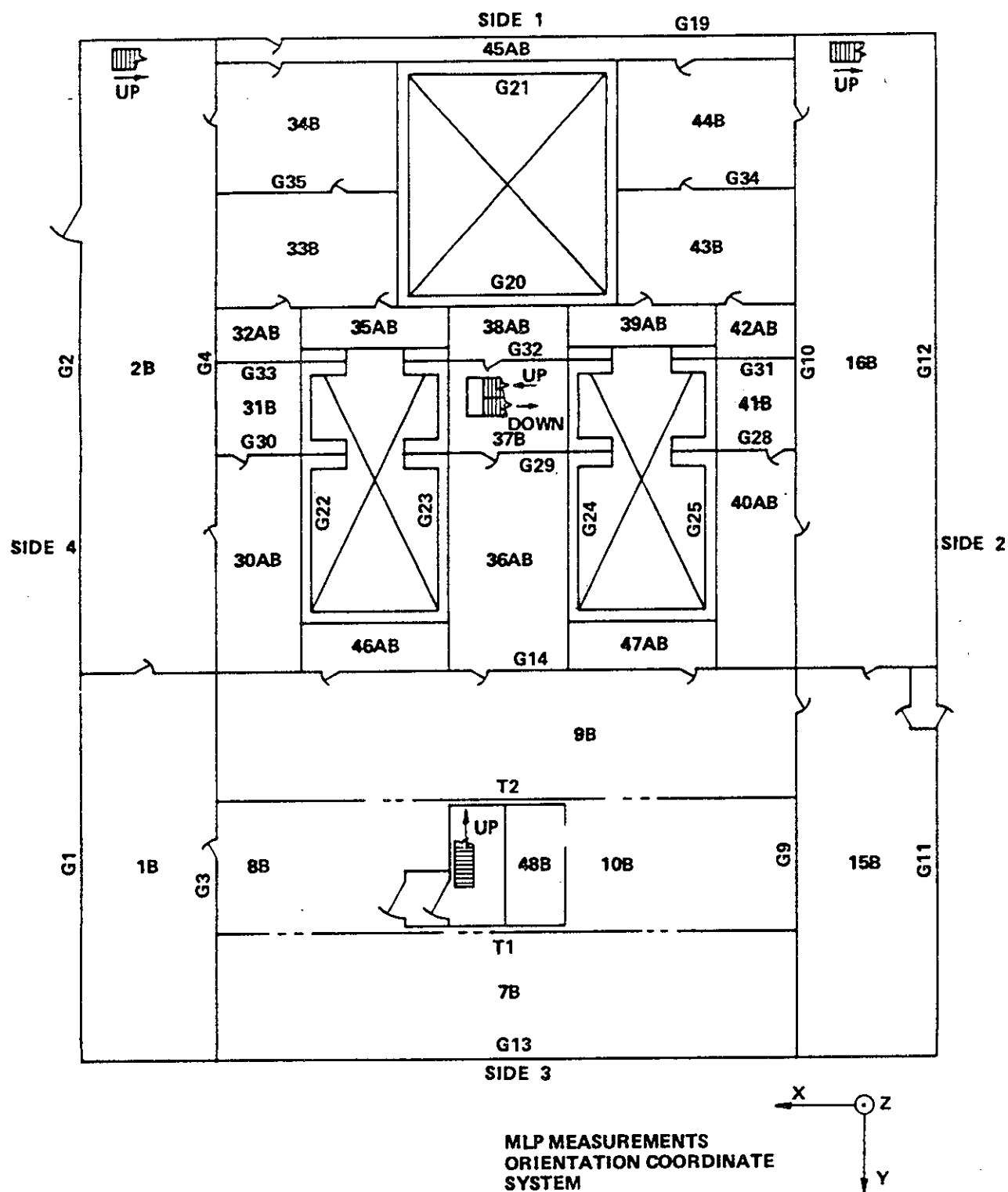


Figure 1-4. MLP Deck B Floor Plan

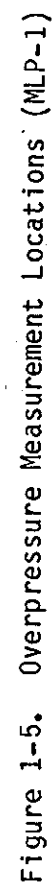


Figure 1-6. Overpressure Measurement Locations (MLP-2)

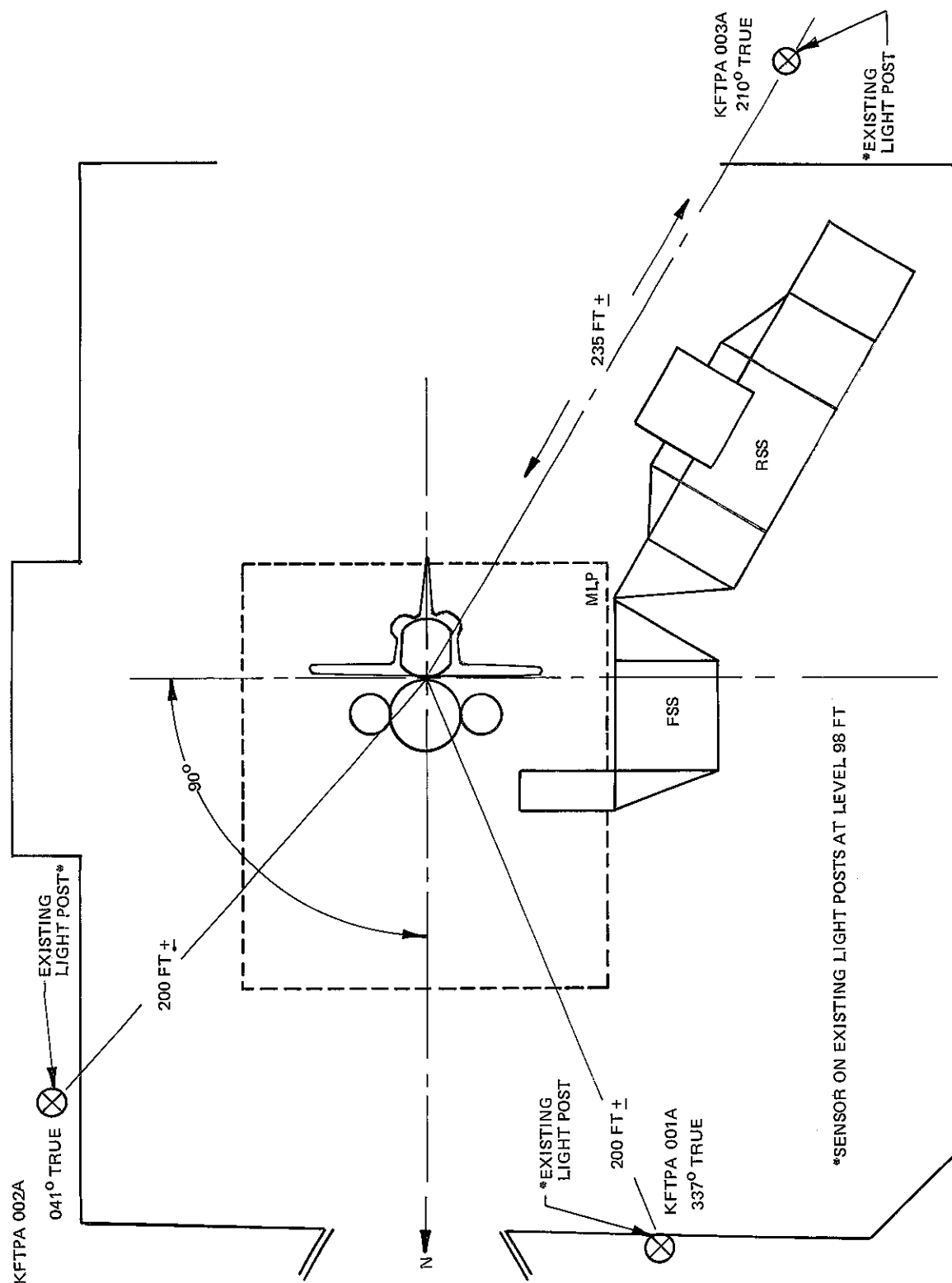


Figure 1-7. STS-6 Sensors Installed at Pad

time. The procedure used to process random nonstationary data in terms of well-developed statistical functions used in stationary data processing is outlined further.

All processing was performed on Hewlett-Packard 5451C Fourier analyzer equipment. The inherent features of the analyzer, such as the choice of a data block size and maximum analysis frequency, have an effect on the processed results because of the nonstationary character of the data. In most cases, statistical accuracy (random error) of processed data was limited by the available duration of the data.

The first step in data processing is the separation of raw data into two components: time variable mean (TVM) and the dynamic component. TVM is calculated from raw data by means of a multiple application of a Hanning smoothing algorithm. The calculated difference between the raw data and the TVM is the dynamic component. The chosen method of digital separation via Hanning algorithm has an advantage over filtering because it does not introduce any phase shift in the data. All further statistical processing involves only the dynamic component.

Certain types of data (vibration, acoustic, and some strains) have an inherent zero mean and did not require the preceding step.

Whenever available memory space permitted, a type of overlap processing was used by generating intermediate data blocks from two adjacent blocks containing a dynamic component. This operation was necessary to reduce random error, a consequence of the short duration of available data and the small number of data blocks. The number of degrees of freedom (DOF) for statistical estimates is almost doubled by overlap processing.

Standard deviation, or the root mean square (rms) of the dynamic component, is calculated on a data block basis. Averaging is performed for the time interval contained within a data block. A plot of standard deviation time history on a data block basis is always presented in this report to depict the nonstationary character of the data during the total time interval of analysis.

Calculation of the dynamic component frequency composition and related cross-functions (power spectra, cross-power spectra, and auto- and cross-correlation function coefficients) via Fourier transformation, followed by conjugate multiplication and averaging of resulting data blocks, required weighting of data blocks prior to averaging. Such a requirement is peculiar only to nonstationary data. A weighting factor, equal to the reciprocal of the data block standard deviation, reduces the time variable standard deviation of the dynamic component to a constant unit value. Normalization was performed on each data block in the time domain to reduce the dynamic component to a stationary data form. From this point on, calculations of power spectra, cross-power spectra, auto- and cross-correlation function coefficients, and coherences follow the standard procedure for stationary data.

Two different windowing functions were applied to the normalized time domain data in order to reduce leakage before taking the Fourier transforms. Both windows use a cosine tapering function applied at each end of a data block to a variable number of points (window taper width). In cases where the overlap processing was used, the window taper width is equal to one-quarter of the data block. In all other cases, the window taper width is equal to one-tenth of the data block. While the data processing program allows specification of any window taper width, the choice of assumed windows was found to be an optimum compromise between the leakage reduction and the alteration of data amplitudes. Preservation of data amplitudes was a governing factor because of the short duration of available data. The correction required to preserve the normalized unit value of standard deviation after windowing is calculated for each window type and applied to the processed data.

Normalized power spectra having a unit area, together with the time history of standard deviation, are a sufficient representation of a class of nonstationary data having a constant frequency composition within the total analysis interval. It should be noted that actual launch data do not perfectly fit such a model. Some frequency variation does occur although relatively slowly and in a continuous manner. In this case, processed power and cross-power spectra represent average rms amplitudes occurring within the total processed time interval.

The final step in calculating power spectra and cross-power spectra was affected by practical considerations of data usage. For the sake of convenience, normalized power spectra were multiplied by the value of variance corresponding to a data block with a maximum value of standard deviation. Similarly, normalized cross-power spectra magnitude was multiplied by the product of maximum values of a pair of standard deviations of data channels entering the cross-power spectrum calculations. Final presentations are in engineering units (squared) per unit bandwidth.

Estimated power spectra and cross-power spectra have a very jagged appearance, caused mainly by the small number of DOF available for these estimates rather than by the actual presence of narrow-band peaks in the data. Plume pressure and acoustic data are inherently wideband. Vibration and strain data contain legitimate peaks at resonance frequencies. It was considered that some frequency domain averaging would improve the legibility and, in the case of plume pressures and acoustics, the quality of the estimates. Therefore, frequency domain averaging using a Hanning algorithm was performed on all data in the frequency domain. However, the presentations always include data before and after performed averaging with an understanding that the user's judgement and experience are necessary to interpret the validity of narrow-band peaks.

The amplitude distribution probability density (PD) function is obtained from the nonstationary dynamic component prior to normalization and by means of histograms on a data block basis. Thus, PD represents a time-averaged estimate for the total duration of an analyzed interval. These estimates deviate from normal (Gaussian) distribution, reflecting the nonstationary character of

the data and, to a lesser degree, the procedure. For presentation, the PD was reduced to a standardized form whereby the abscissas are expressed in units of standard deviations (sigmas) and the ordinates are a product of PD and the standard deviation. The assumed value of the standard deviation is the calculated maximum on a data block basis. Such a presentation facilitates direct comparison with standardized Gaussian distribution.

In practical applications, integrals of PD (i.e., the cumulative probability) are of importance. These integrals were calculated between limits (-1, +1) to (-3, +3) standard deviations in 0.5 intervals.

In addition to the previously described processing, the acoustic and pressure dynamic components were processed in terms of octave band sound pressure levels (OBSPL's). The OBSPL's were calculated from power spectra for standard octave center frequencies and bandwidths. It should be noted that the last point of an OBSPL curve is always affected by the cutoff frequency of an anti-aliasing filter. Also, the accuracy at the lower end of the OBSPL curve is affected by the resolution bandwidth of the calculated power spectral density (PSD) curve. Thus, the accurate range of the OBSPL curve is from about 16 Hz and up to the frequency preceding the last center frequency shown on the OBSPL plots. Below this range (approximately 16 Hz), the dispersion among OBSPL curves from sensors, which should have measured about the same values, is increasing toward the first OBSPL center frequency of 2 Hz. The cause of such a decrease in accuracy is not in the data processing but rather in the fact that within the total available analysis interval there is an insufficient number of cycles at these low frequencies for a reliable statistical estimate. Conversely, at the low frequency end, 4 Hz and below, there is an insufficient number of cycles to produce full resonances in the affected structures.

1.5.2 TIME INTERVALS AND PARAMETERS FOR DATA PROCESSING.

1.5.2.1 Time Intervals. Time intervals (as shown in figure 1-8) selected for high-frequency data processing are referenced to an instant of time, T (often called T-zero), which is the time of a signal sent to the Pyrotechnic Initiator Controller (PIC).

Figure 1-8 depicts a typical data-time history where T divides a total data duration into two periods: Orbiter holddown and lift-off.

1.5.2.1.1 Orbiter Holddown Period. The Orbiter holddown period begins with Space Shuttle Main Engine (SSME) ignition and the occurrence of measurable data; it ends at T. It is characterized by a rapid rise of the standard deviation to a peak followed by a small decay and transition into a steady state. The total duration of this period is about 5.5 s.

1.5.2.1.2 Lift-off Period. By definition, the lift-off period begins at time T. The extent and the end of this period are vaguely defined by a decay of data amplitudes beyond significant values. Usually this decay is accompanied by a visible shift in the data frequency composition toward the lower end of the spectrum.

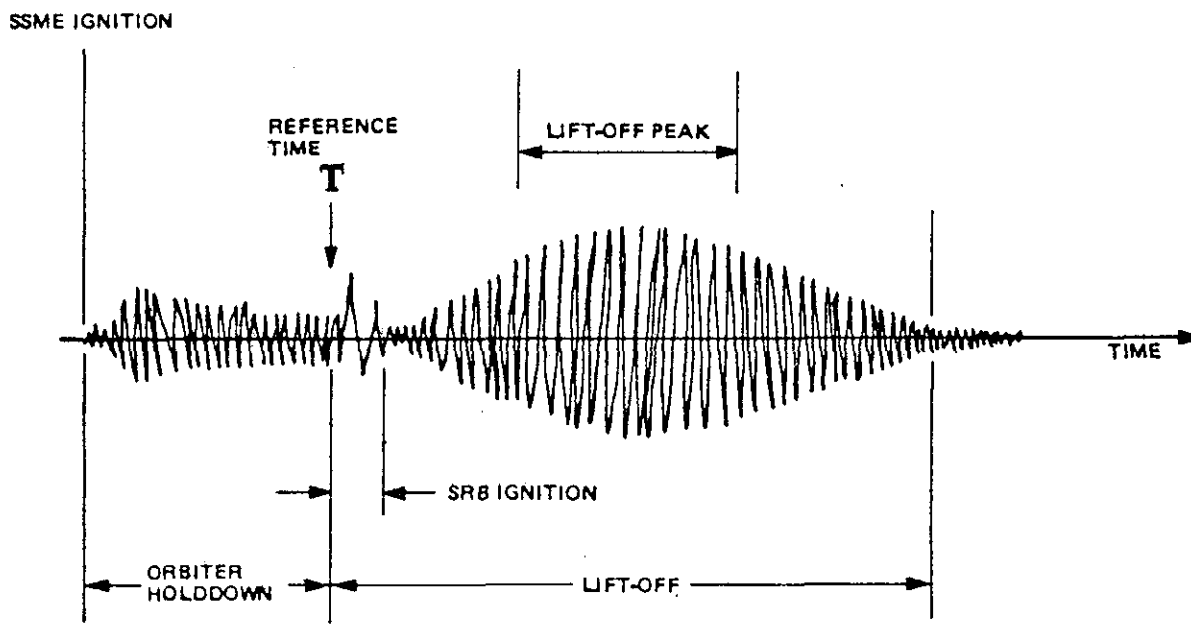


Figure 1-8. Time Periods and Intervals of the Launch Environment

1.5.2.1.3 Lift-off Period Intervals. Within the lift-off period, there are two intervals containing different types of data. The first interval is designated SRB ignition. This interval contains a distinct pulse caused by the SRB ignition overpressure that is superimposed over a steady-state environment generated by the SSME exhaust plumes. The second interval, designated lift-off peak, is centered on the lift-off period to contain the peak data amplitudes recorded during lift-off.

In a general case, processing was performed on data from the period of Orbiter holddown and from the two lift-off intervals: SRB ignition and lift-off peak.

Since sensor calibration was performed to accommodate the anticipated peak amplitudes at lift-off, there are cases where holddown data are either near or below the usable sensor range; i.e., the data are in the noise domain. In such cases, holddown data were not processed. Similarly, there are cases where the SRB ignition did not induce significant response and, consequently, processing was omitted. In each case, a judgement was involved in the selection within the general classification of outlined launch-time intervals.

1.5.2.2 Parameters for Data Processing. The choice of parameters governing data processing [block size, maximum analysis frequency (F_{\max}), total analysis time (TAT), etc.] was made after examination of launch data oscillograms. The appearance of raw data within the time interval selected for processing and the frequency-response range of the sensor imposed the upper limit on the selection of F_{\max} .

The choice of a data block size is usually a compromise among a desired resolution bandwidth, the available length of data for a desired large number of DOF affecting the random error, and a requirement to have essentially stationary data within the selected block size. The last requirement could not always be met because of the nonstationary character of the data. In order to improve the resolution in the lower frequency range, a few processing runs were necessary using the lower values of F_{\max} rather than the upper limit governed by the total frequency content in the data. Thus, most of the processed data are presented for two and sometimes three values of F_{\max} and other parameters. All pertinent parameters appear on the plots of processed data.

1.5.2.3 Definitions of Parameters. Following are definitions of some parameters appearing in the data plots of this publication.

- a. Sample rate is always set to be twice F_{\max} . Anti-aliasing filter setting is always one-half F_{\max} .
- b. Start time defines the beginning of the total interval used in processing. It is always referenced with respect to time, T.
- c. Time domain filter taper width defines the number of data points at each end of a data block in the time domain window smoothed by the cosine function.
- d. Standard deviation and rms are used interchangeably and pertain to the dynamic component only.
- e. Filter bandwidth represents the resolution bandwidth of a frequency domain plot; i.e., the spacing of plotted data points.
- f. Raw data, TVM, or dynamic component. Whenever these terms are presented, the plots correspond to a data block having a maximum value of standard deviation. The location of this data block within the total processing interval may be found from the plot of standard deviation time history on a data block basis.
- g. Number of Hanning smoothings represents the number of passes of the smoothing algorithm applied to separate the TVM from the raw data (in the time domain) or to provide averaging in the frequency domain (PSD plots).

The remaining parameters and plot titles appearing in this document are self-explanatory.

1.6 SPACE SHUTTLE LAUNCH ENVIRONMENT REFERENCE MATERIAL

<u>Document No.</u>	<u>Title</u>
KSC-DD-457-TR	Space Shuttle STS-1 Launch Processed Ground Measurements; Volumes 1 and 2, September 1981
KSC-DD-593-TR	Space Shuttle STS-2 Launch Processed Ground Measurements; Volumes 1 and 2, May 1982
KSC-DD-651-TR	Space Shuttle STS-3 Launch Processed Ground Measurements; Volumes 1 and 2, October 1982 Appendix A STS-3 MLP Vibration Data Appendix B STS-3 RSS Vibration Data Appendix C STS-3 FSS Vibration Data
KSC-DD-655-TR	Space Shuttle STS-4 Launch Processed Ground Measurements; February 1982 Appendix A FSS Acoustic Summary
KSC-DD-677-TR	Space Shuttle STS-3 Launch Vibration Displacements and Acceleration Spectral Densities of the MLP, RSS, and FSS; February 1983
KSC-DD-684-TR	Vibration Environment Effect on Payload Ground Handling Mechanism During STS-6 Flight Readiness Firing; March 1983
KSC-DD-688-TR	Space Shuttle STS-5 Launch Processed Ground Measurements; April 1982 Appendix A FSS Acoustics Summary Appendix B SRB Holddown Post Strains and Loads During the Holddown Period
KSC-DD-712-TR	Space Shuttle STS-6 Launch Processed Ground Measurements; July 1983 Appendix A FSS Acoustics Summary Appendix B TSM Acoustics Summary Appendix C STS-6 Near-Field Pressure on Light Posts Appendix D Acoustics Inside MLP-1 and MLP-2 Appendix E Vibration Inside MLP-1 and MLP-2

SECTION II

PRESSURE AND ACOUSTICS

2.1 FSS ACOUSTICS SUMMARY

The FSS acoustics summary includes data from five pressure sensors, KSAPB001A through KSAPB005A, recorded during STS-1 through STS-9 launches. All sensors were oriented horizontally and located on the corner column of sides 1 and 4 of the FSS. Figures 2-1 through 2-5 show mean and limit (limit = mean + 2 sigma) PSD's for each sensor, processed using two different sets of processing parameters and different time intervals during peak environment at lift-off. The left frame of each figure (2-1 through 2-5) presents peak PSD's of pressure components above approximately 50 Hz, up to the plot limit of 750 Hz. The right frame of each figure (2-1 through 2-5) presents peak PSD's of pressure components below approximately 50 Hz. This dual presentation accounts for observed variation in the pressure waveform frequency composition, which occurs in a continuous manner during a launch.

PSD statistics (mean and limit) obtained by lumping all FSS sensor data are shown on figures 2-6 through 2-13. Heading text that accompanies each figure (plot) provides information pertinent to data processing and rms (standard deviation) values of pressures within presented frequency range. Statistics on figures 2-6, -8, -10, and -12 present separate mean and limit PSD's obtained from measurements shown on figures 2-7, -9, -11, and -13, which serve mainly as illustrations of data dispersion on the FSS. For applications such as a test specification or a design criterion, or both, limit curves on figures 2-6 and 2-10 (or 2-12) are recommended. Limit curve on figure 2-6 will govern for frequencies above approximately 50 Hz, while limit curve on figure 2-10 will govern for frequencies below approximately 50 Hz. It is necessary to mention that below about 10 or 12 Hz, the number of pressure cycles occurring during the peak is insufficient to induce full resonance. The peak environment is usually contained within a single data block of about 0.5 s duration. Within a longer interval of about 1.5 s, the peak environment decays to about 85 percent of its peak value. The user is advised to examine individual measurement rms time histories published for launches STS-1 through STS-6, and, whenever responses were calculated assuming steady-state theory, to introduce a correction for a limited number of excitation cycles. Without such correction, responses below 12 Hz will be overestimated.

Figures 2-14 and 2-15 present enlarged PSD plots obtained from the output of sensor KSAPB005A located on the 245-ft level for STS-1 through STS-8. Both mean and limit curves are nearly identical to those on figure 2-5 (right frame) showing that the addition of one series of launch data (STS-9) does not introduce any significant change to presented statistics. The limit curve on figure 2-14 was used to check ET G0₂ vent arm for dynamic loads.

KSC-DD-818-TR

Figure 2-16 presents comparative plots between predicted and measured (STS-1 through STS-6) OBSPL's. For applications, we recommend the use of presented PSD's rather than OBSPL's because these PSD's have a substantially better resolution than that obtainable from conversion of OBSPL's into an average octave band PSD.

No distinct "static" type pressures were measured on the FSS during STS-1 through STS-9 launches. Measured pressures are clearly dynamic transients. Same low baseline drifts were noticed in the outputs of all pressure sensors on the FSS. These drifts were becoming progressively worse as the number of launches increased, and during STS-11 two FSS sensors failed. Baseline drifts, both positive and negative, which may be mistaken for pseudostatic pressures, are caused mainly by radiating heat and a very high rate of heat input resulting in nonuniform temperature distribution and consequent thermal deformations within sensor bodies.

Figure 2-17 presents a summary of PSD's obtained from the output of sensor KSAPB006A. This sensor is located on the ET vent arm at the top of haunch pivot and is oriented upward. Because of its proximity to the exhaust plume, the output of this sensor was significantly affected by heat; therefore, the data were processed using a high-pass filter to eliminate high baseline drift, and so it is not known whether there were any "static" pressure components (below 2 Hz) present in the sensor output.

Vehicle trajectory and engine gimbaling have a significant effect on this measurement. Two lowest PSD curves on figures 2-17 (STS-5 and STS-6) have a magnitude similar to data recorded on the FSS proper (sensors KSAPB001A through KSAPB005A). STS-7 and especially STS-8 data are significantly higher.

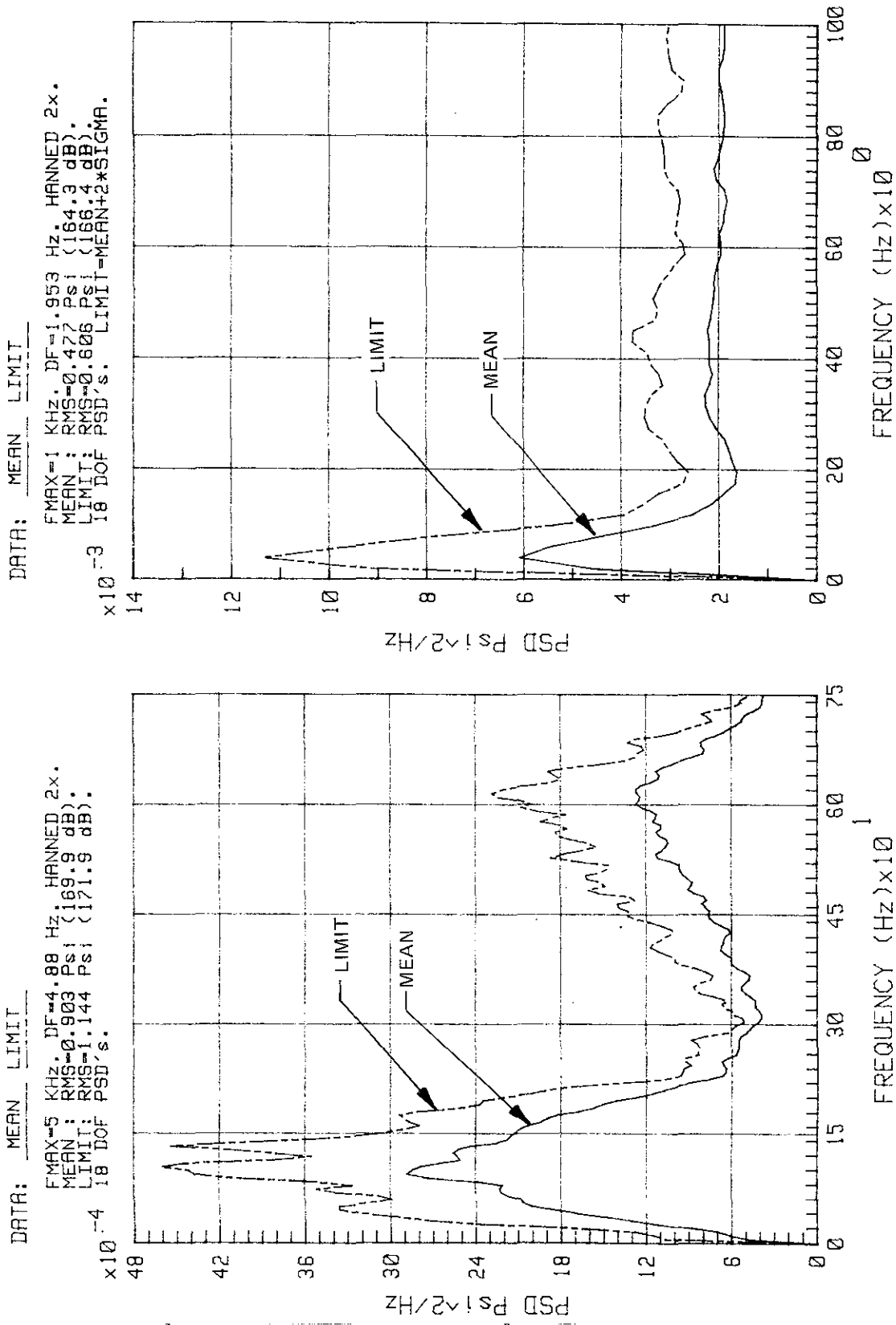


Figure 2-1. STS-1 Through -9 FSS Acoustics at Lift-Off Peak - Sensor KSAPB001A at 125-ft Elevation

KSC-DD-818-TR

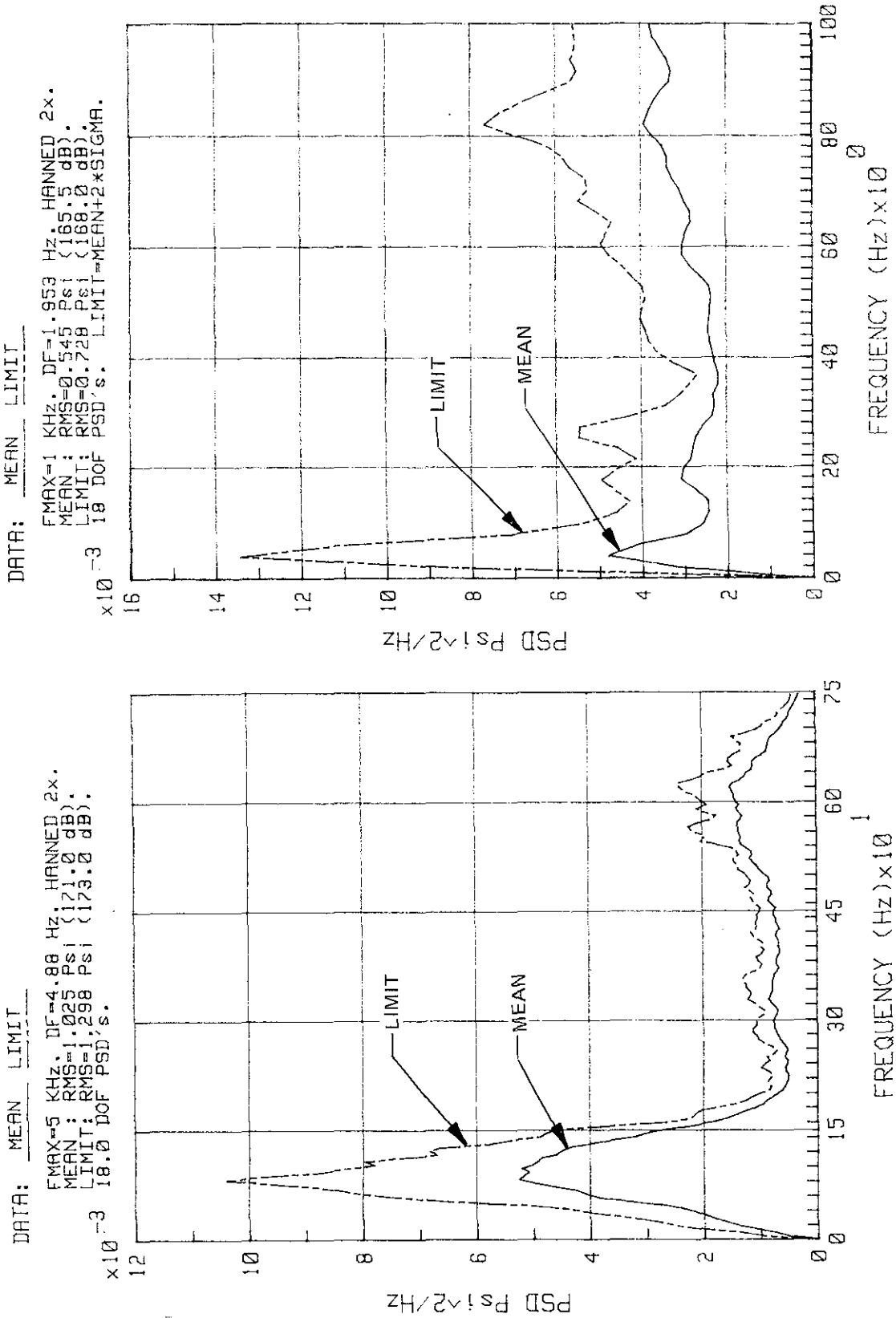


Figure 2-2. STS-1 Through -9 FSS Acoustics at Lift-Off Peak - Sensor KSAPB002A at 155-ft Elevation

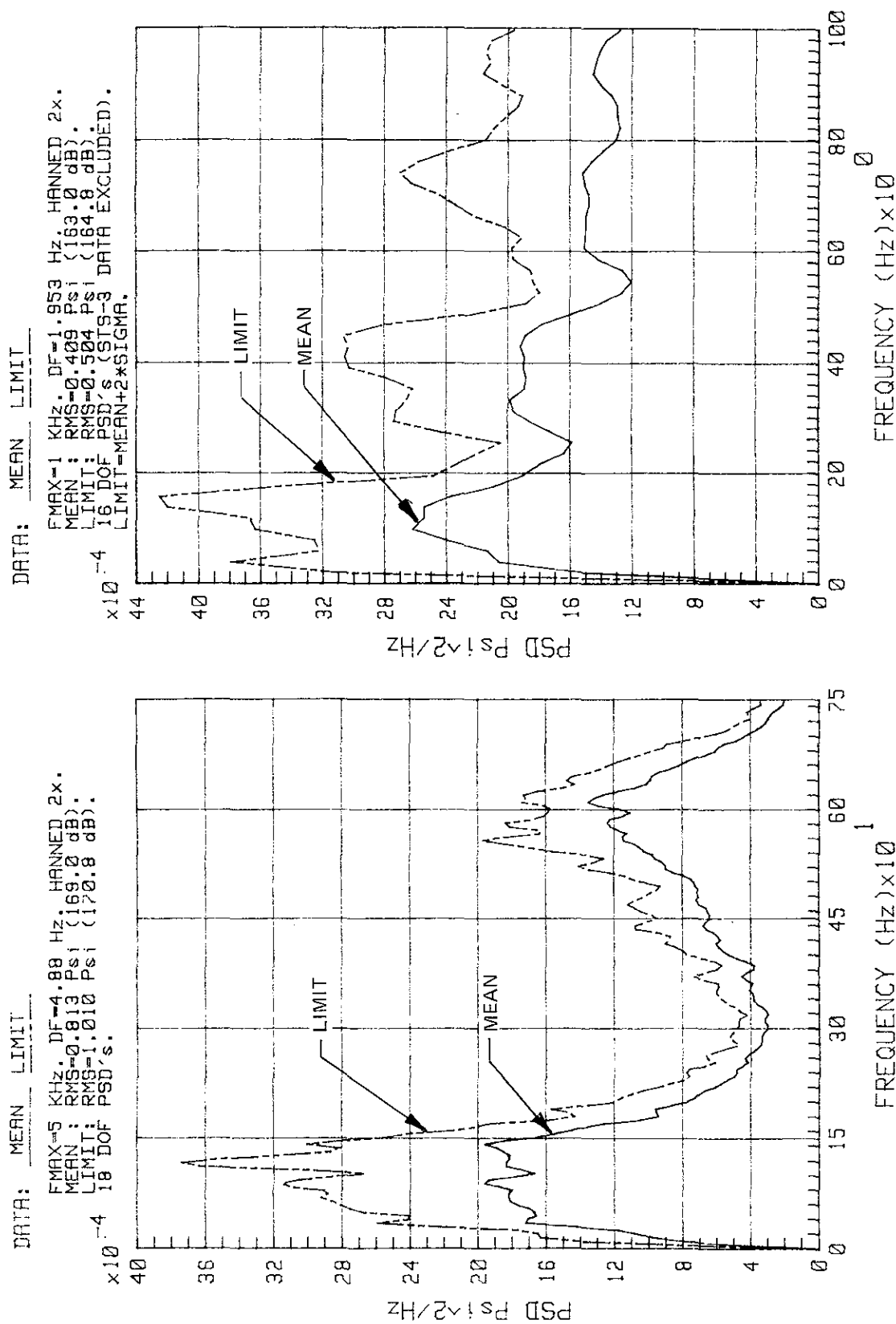


Figure 2-3. STS-1 Through -9 FSS Acoustics at Lift-Off Peak - Sensor KSAPB003A at 185-ft Elevation

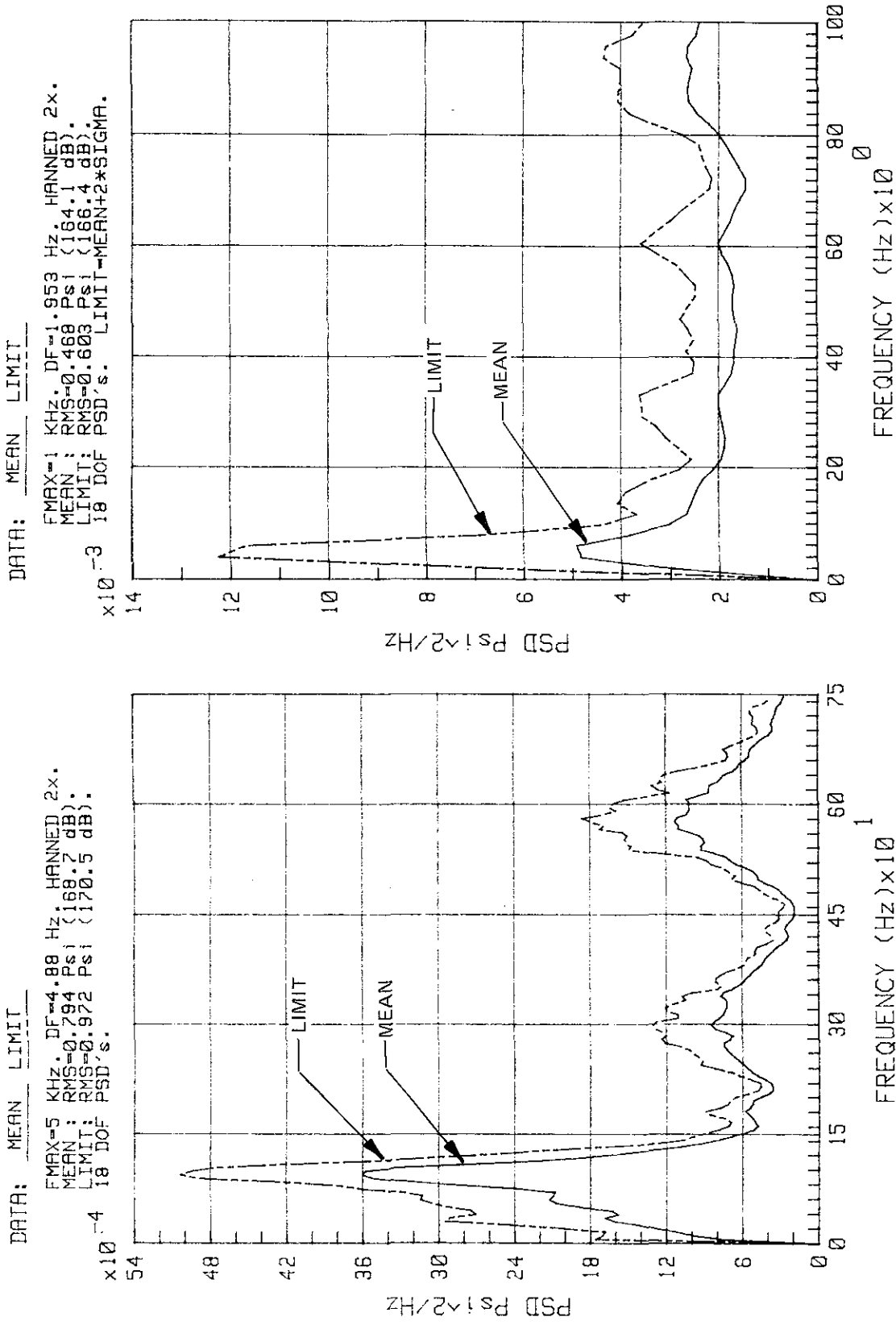


Figure 2-4. STS-1 Through -9 FSS Acoustics at Lift-Off Peak - Sensor KSAPB004A at 215-ft Elevation

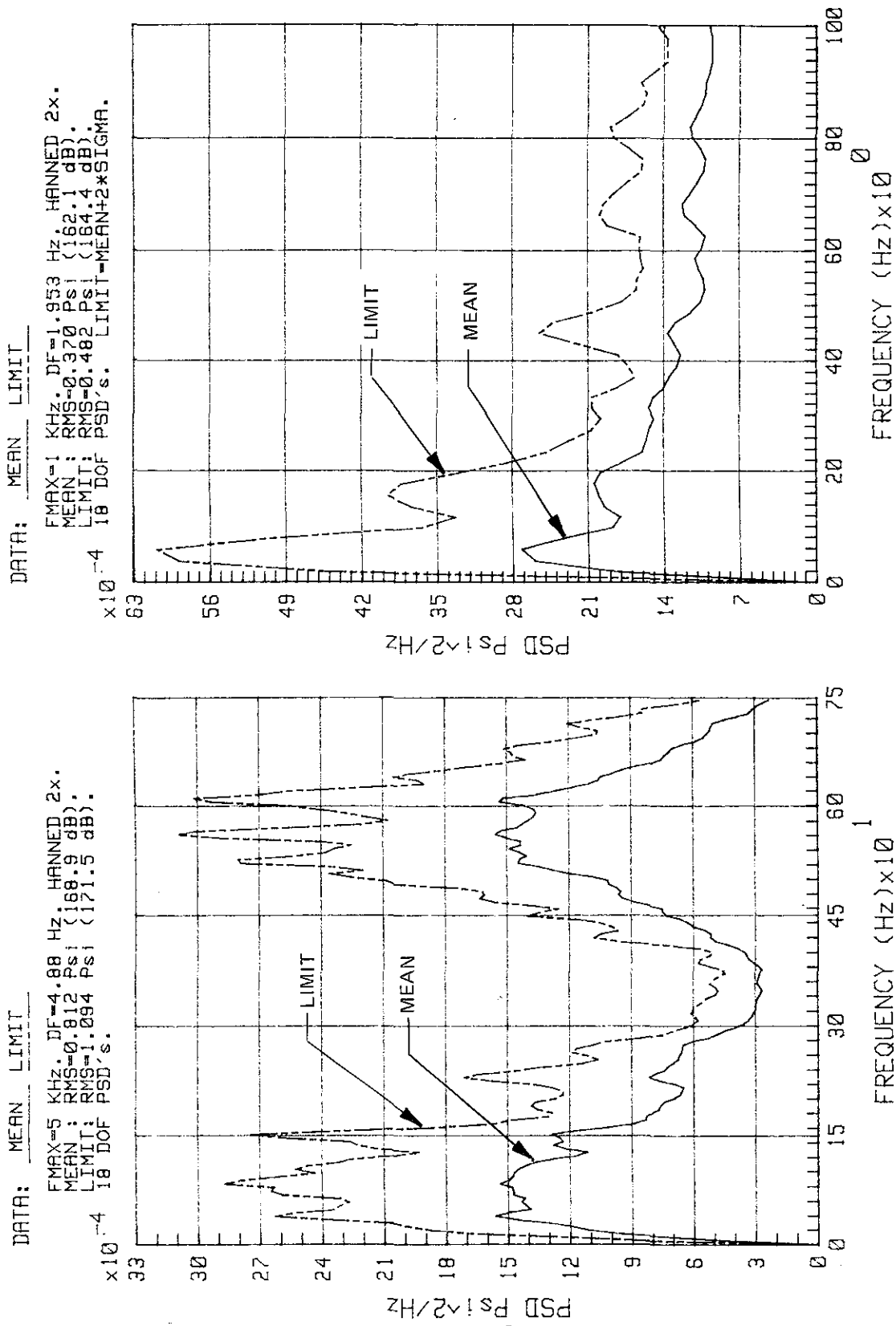


Figure 2-5. STS-1 Through -9 FSS Acoustics at Lift-Off Peak - Sensor KSAPB005A at 245-ft Elevation

KSC-DD-818-TR

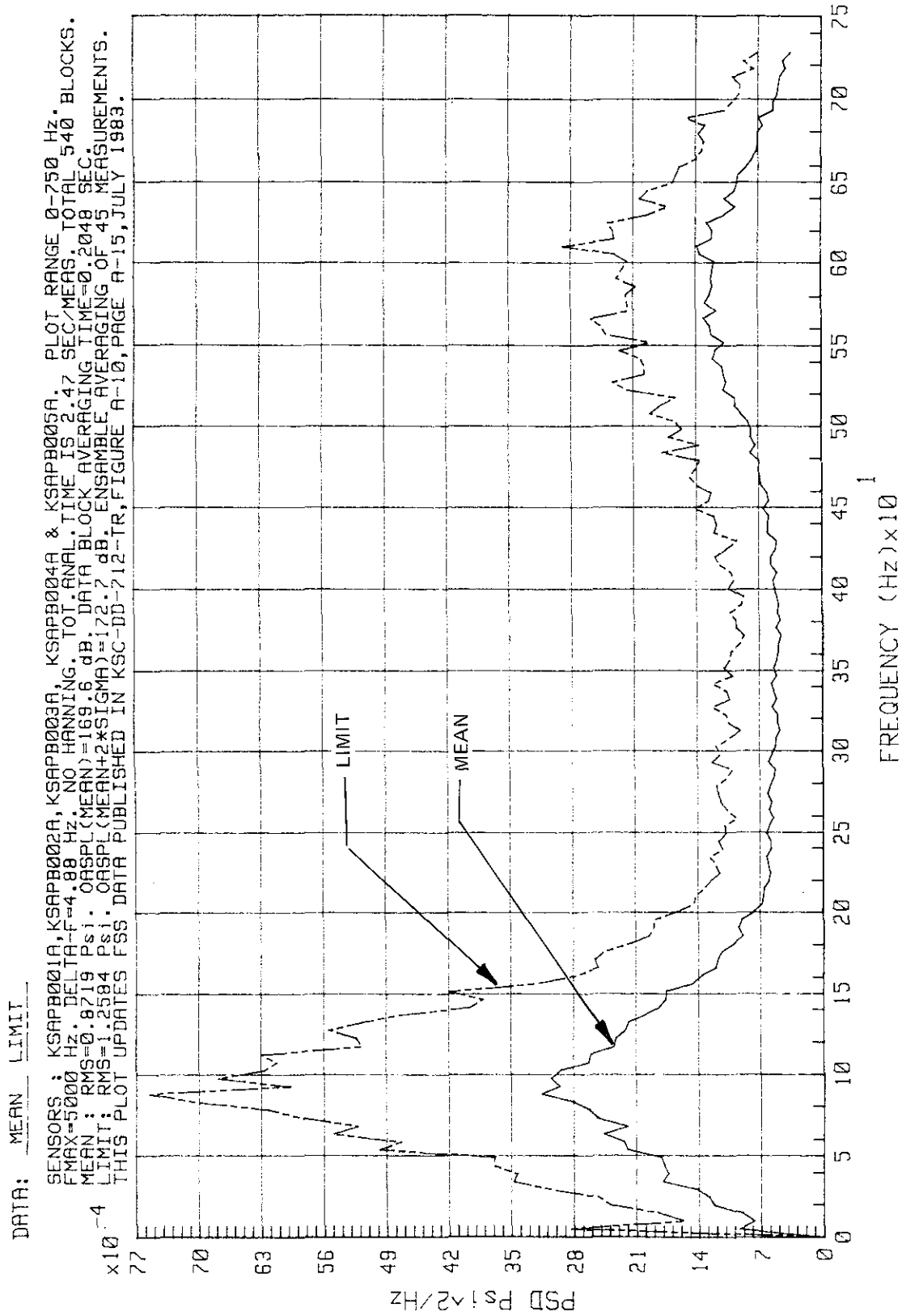


Figure 2-6. STS-1 Through -9 Summary of FSS Acoustics at Lift-Off Peak - 90 DCF PSI's (Mean and Limit Only)

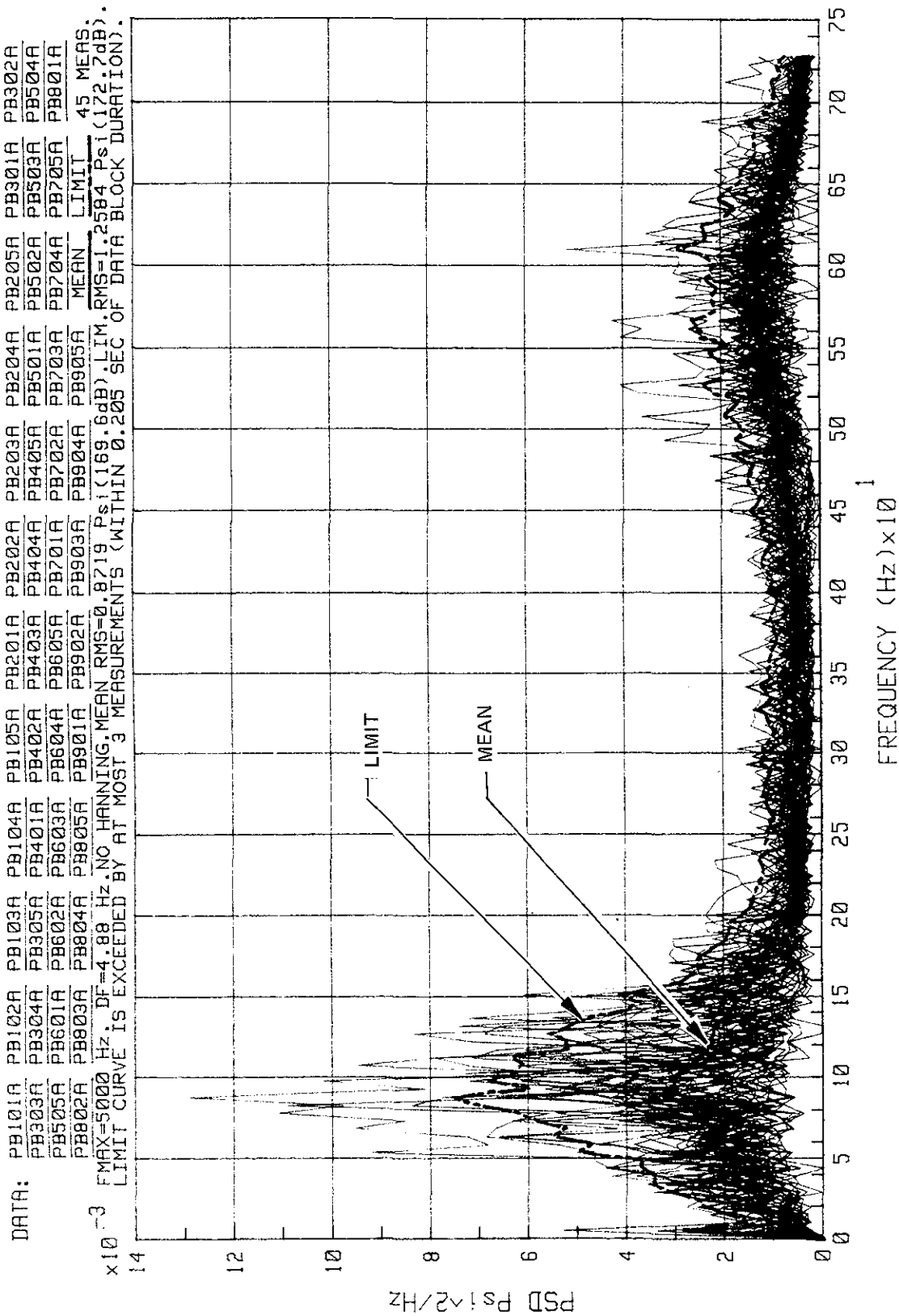


Figure 2-7. STS-1 Through -9 Summary of FSS Acoustics at Lift-Off Peak - 90 DOF PSD's

KSC-DD-818-TR

DATA: MEAN LIMIT

SENSORS : KSAPB001A, KSAPB002A, KSAPB003A, KSAPB004A & KSAPB005A. 90 DOF. PLOT RANGE 0-750 Hz.
 FMAX=5000 Hz. DELTA-F=4.88 Hz. NO HANNING. TOT. ANAL. TIME IS 2.47 SEC/MEAS. TOTAL 540 BLOCKS.
 MEAN : RMS=0.872 Psi. ORASPL(MEAN)=169.6 dB. DATA BLOCK AVERAGING TIME=0.2048 SEC.
 LIMIT: RMS=1.413 Psi. ORASPL(MEAN+3*SIGMA)=173.8 dB. ENSEMBLE AVERAGING OF 45 MEASUREMENTS.

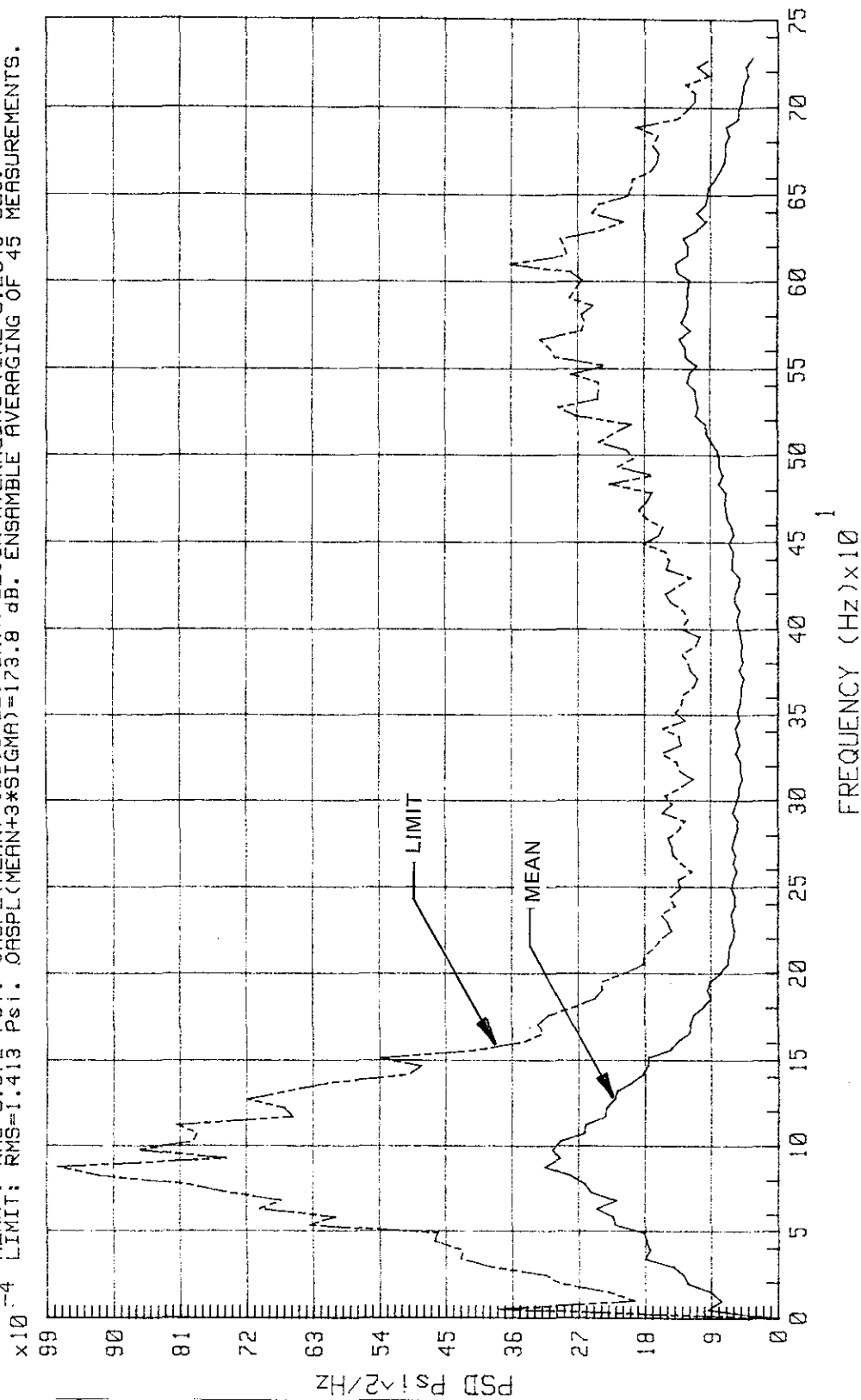


Figure 2-8. STS-1 Through -9 Summary of FSS Acoustics at Lift-Off
 Peak - 3-Sigma Limit (Mean and Limit Only)

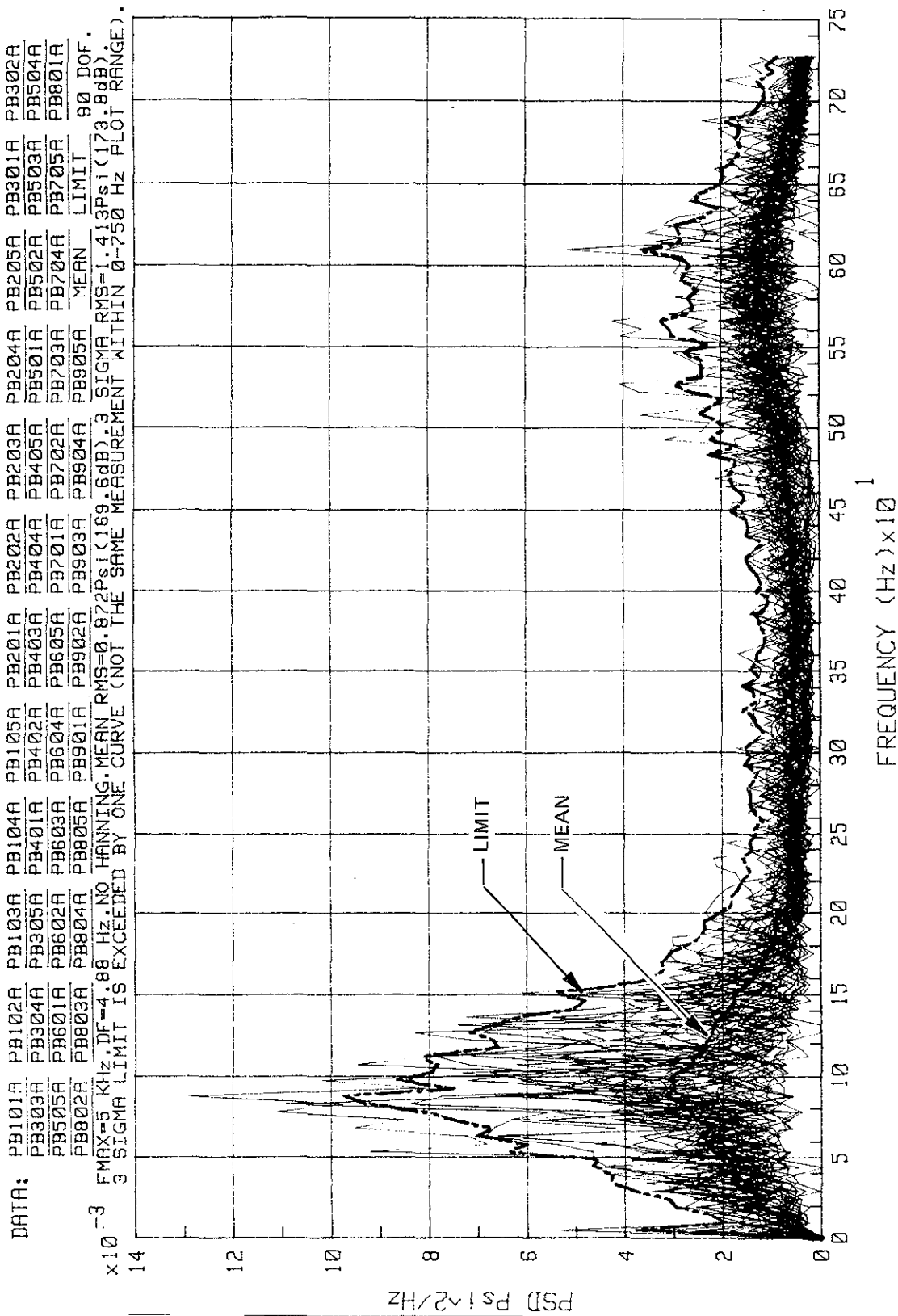


Figure 2-9. STS-1 Through -9 Summary of FSS Acoustics at Lift-Off Peak -
 3-Sigma Limit

KSC-DD-818-TR

DATA: MEAN LIMIT

x10⁻³
 18
16
14
12
10
8
6
4
2
0

0 1 2 3 4 5 6 7 8 9 10 11 12 13 14 15 16 17 18 19 20
 FREQUENCY (Hz) x 10¹

PSD Ps1/2/Hz
 LIMIT
 MEAN

SENSORS : KSAPB001A, KSAPB002A, KSAPB003A, KSAPB004A & KSAPB005A. PLOT RANGE 0-200 Hz.
 FMAX=1000 Hz. DELTA-F=1.953 Hz. NO HANNING. TOT.ANAL.TIME VARIES (4.6 TO 6.7 SEC/MEAS.)
 MEAN : RMS=0.5810 Psi. OASPL(MEAN)=166.0 dB. DATA BLOCK AVERAGING TIME=0.512 SEC. TOT.1084 BK.
 LIMIT : RMS=0.8515 Psi. OASPL(MEAN+2*SIGMA)=169.4 dB. ENSAMBLE AVERAGING OF 44 MEASUREMENTS.
 THIS PLOT UPDATES FSS DATA PUBLISHED IN KSC-DD-712-TR, FIGURE A-14, PAGE A-19, JULY 1983.

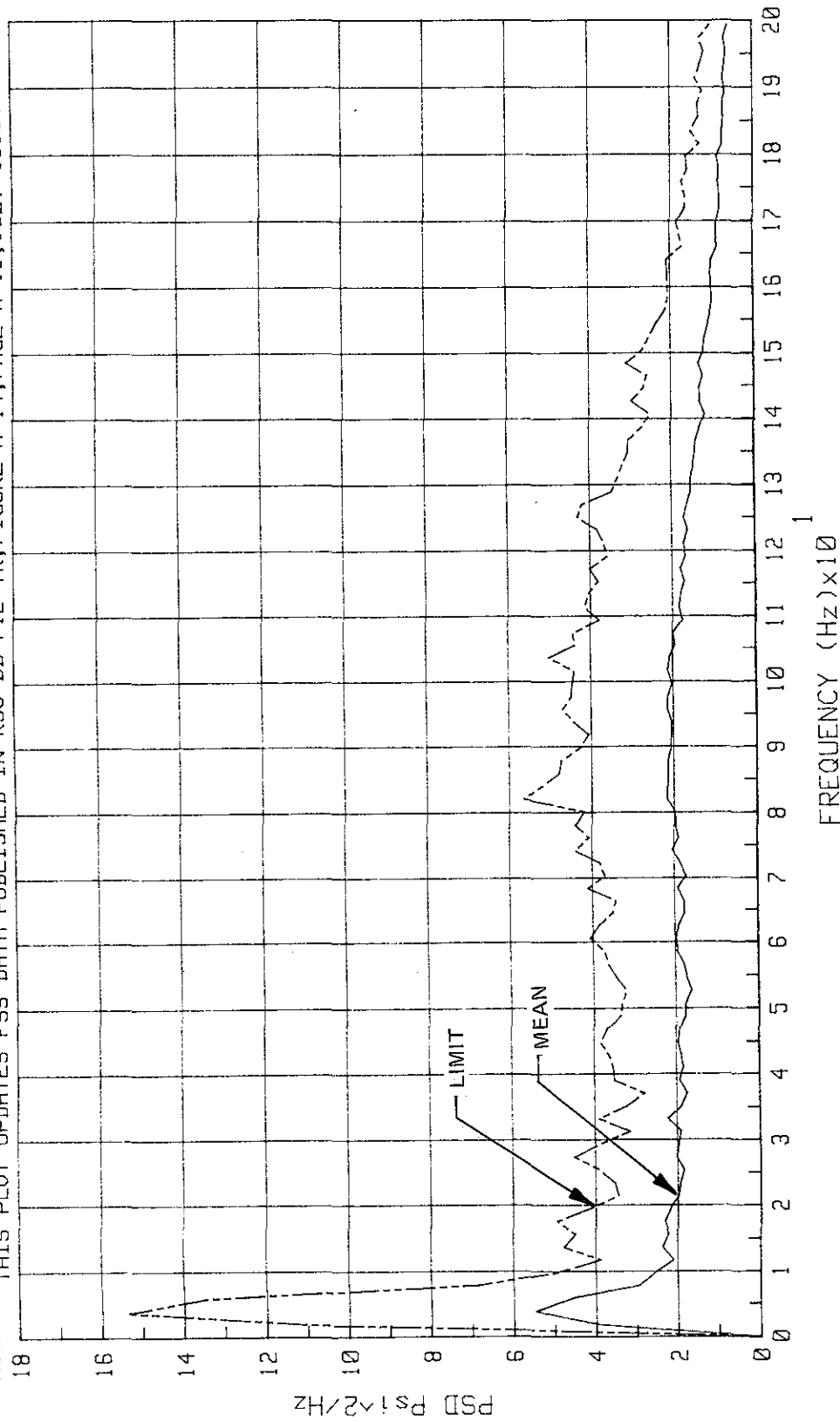
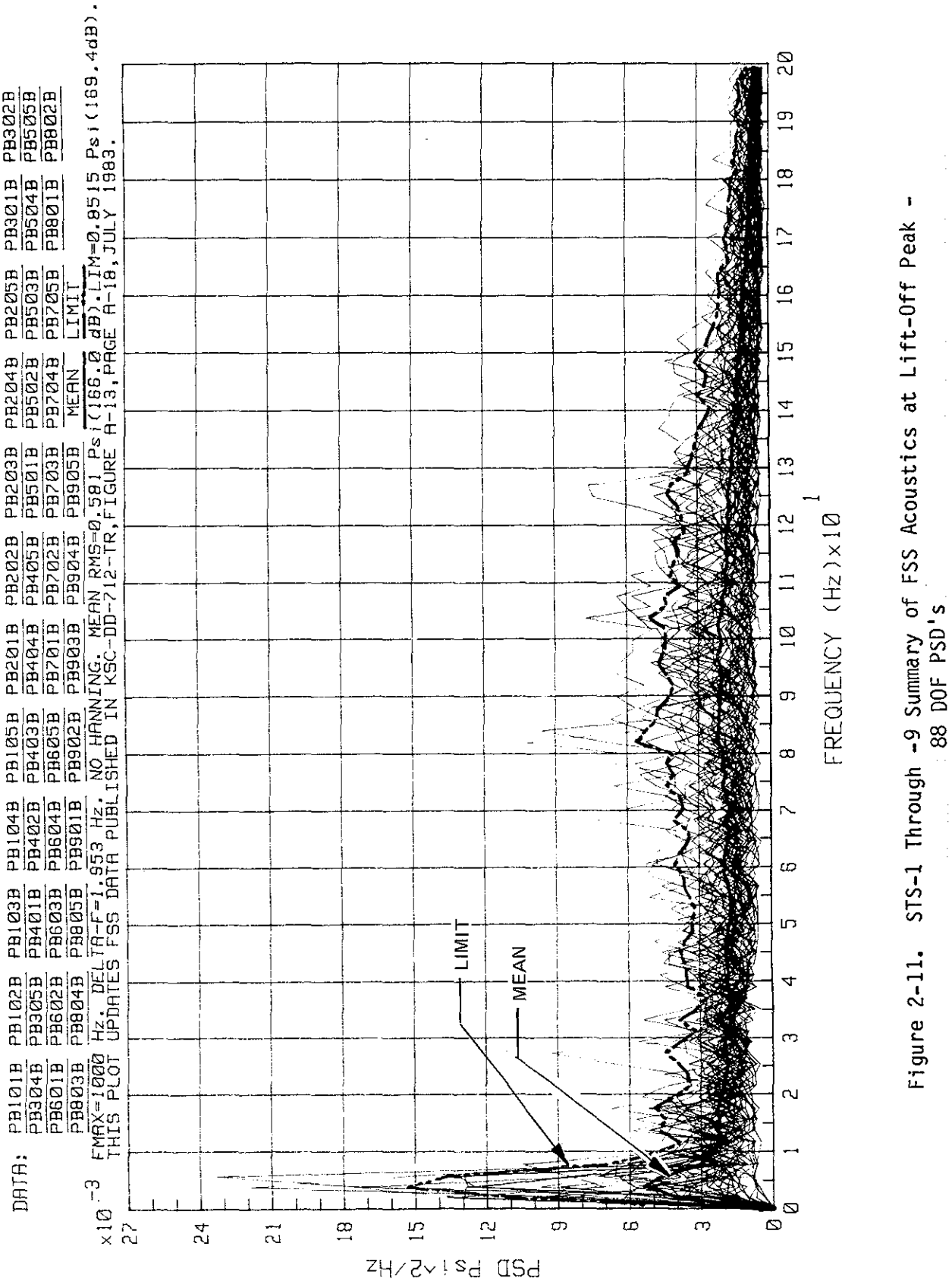


Figure 2-10. STS-1 Through -9 Summary of FSS Acoustics at Lift-Off Peak - 88 DOF PSD's (Mean and Limit Only)



KSC-DD-818-TR

DATA: MEAN LIMIT

SENSORS : KSAPB001A, KSAPB002A, KSAPB003A, KSAPB004A & KSAPB005A. 88 DOF PSD's.
 FMAX=1000 Hz. DELTA-F=1.953 Hz. NO HANNING. TOT. ANAL. TIME VARIES (4.6 TO 6.7 SEC/MEAS.).
 MEAN : RMS=0.3410 Psi. ORSPL(MEAN)=161.4 dB. DATA BLOCK AVER. TIME=0.512 SEC. TOT. 1084 BLOCKS.
 LIMIT: RMS=0.5000 Psi. ORSPL(MEAN+2*SIGMA)=164.7 dB. ENSEMBLE AVERAGING OF 44 MEASUREMENTS.

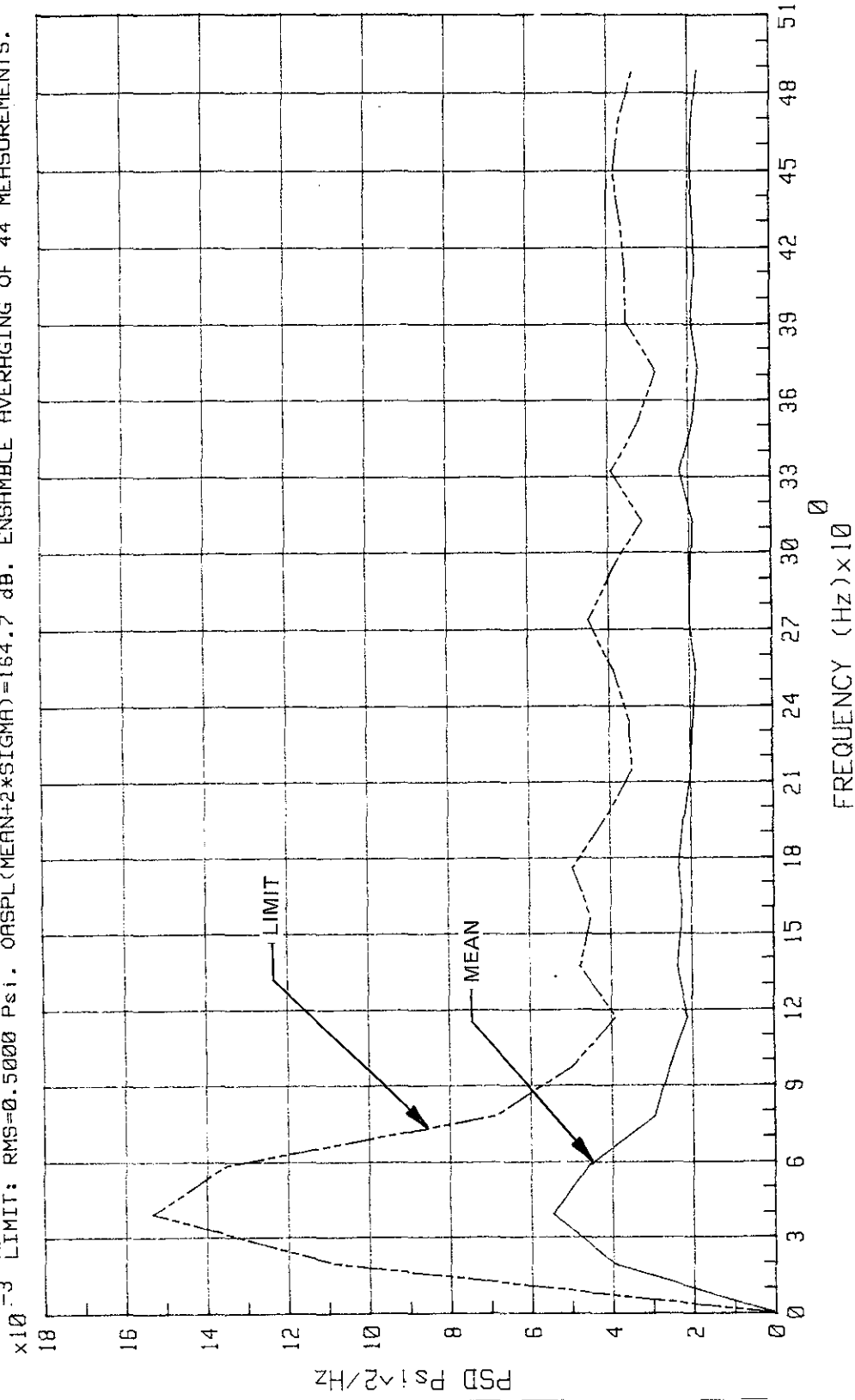


Figure 2-12. STS-1 Through -9 Summary of FSS Acoustics at Lift-Off Peak - Data for 0 Hz to 50 Hz
 (Mean and Limit Only)

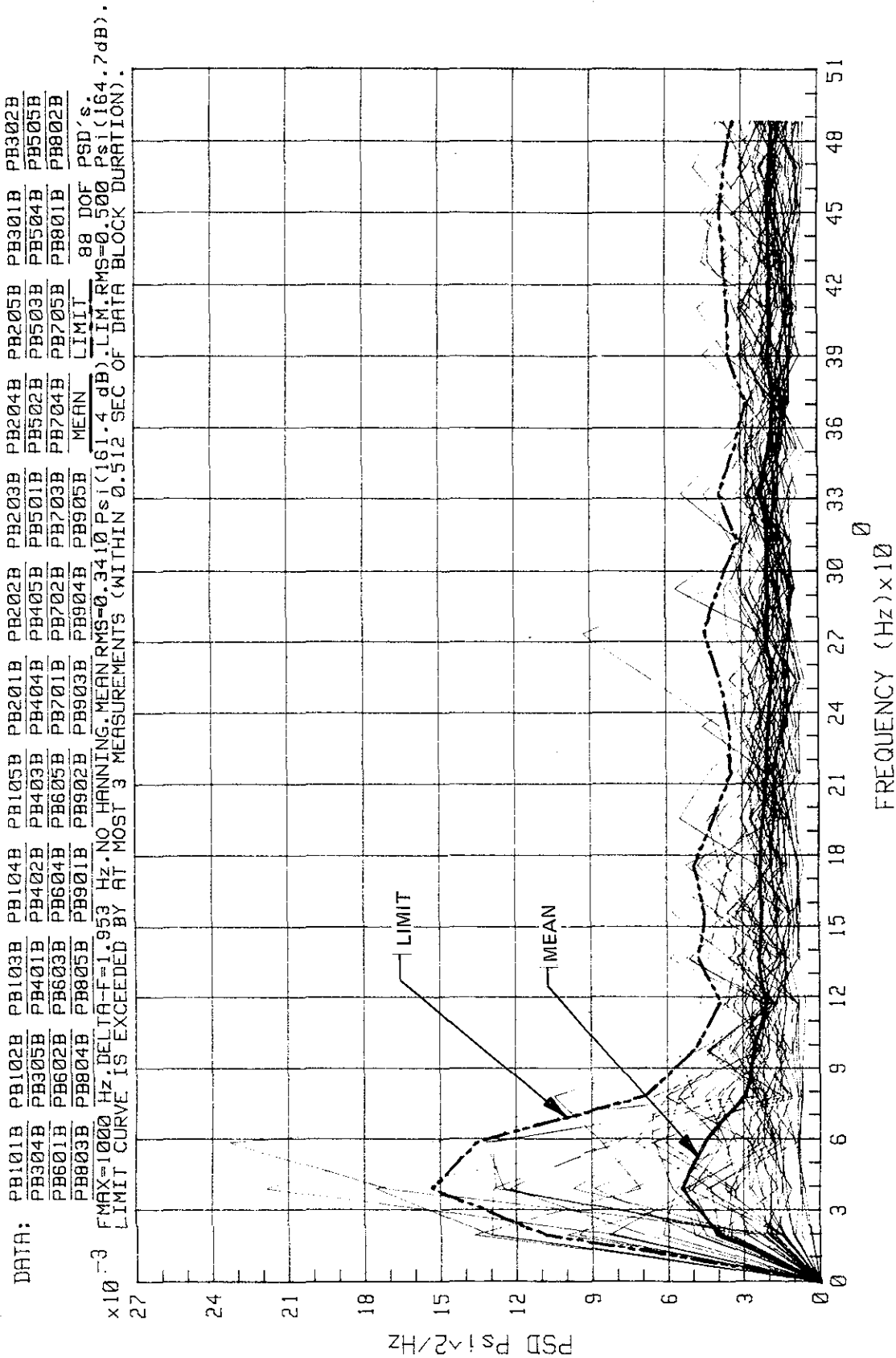


Figure 2-13. SIS-1 Through -9 Summary of FSS Acoustics at Lift-Off Peak - Data for 0 Hz to 50 Hz

KSC-DD-818-TR

DATA: MEAN LIMIT

FMAX=1000 Hz. DELTA-F=1.953 Hz. ALL PSD'S HANNED 2x. BLOCK AVERAGING TIME 0.512 SEC.
 MEAN : RMS=0.3730 Psi. ORSPL(MEAN)=162.2 dB. MEAN & LIMIT DATA FOR PLOT RANGE 0-100 Hz.
 LIMIT : RMS=0.4862 Psi. ORSPL(X+2S)=164.5 dB. LIMIT=MEAN+2*SIGMA.

$\times 10^{-4}$

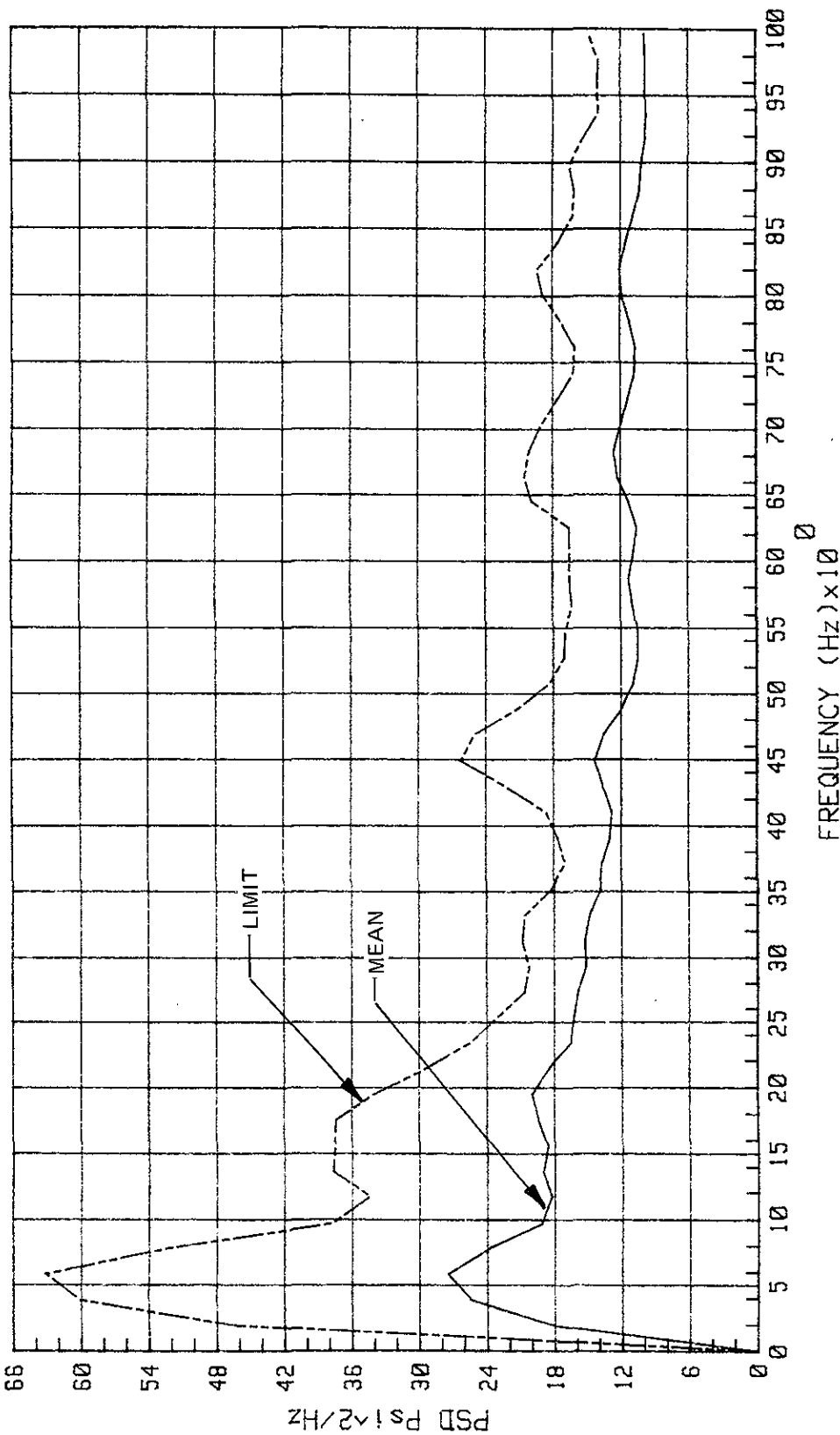


Figure 2-14. STS-1 Through -8 Lift-Off Peak - FSS Acoustics at 245-ft Level, 16 DOF PSD's (Mean and Limit Only)

KSA#: PB105B PB205B PB305B PB405B PB505B PB605B PB705B PB805B MEAN LIMIT

FMAX=1000 Hz. DELTA-F=1.953 Hz. ALL PSD'S HANNED 2x. BLOCK AVERAGING TIME 0.512 SEC.
 MEAN : RMS=0.3730 Psi. OASPL(MEAN)=162.2 dB. MEAN & LIMIT DATA FOR PLOT RANGE 0-100 Hz.
 LIMIT : RMS=0.4862 Psi. OASPL(X+2S)=164.5 dB. LIMIT=MEAN+2*SIGMA. LIMIT CURVE IS AN
 ENVELOPE OF ALL DATA

NOTE: THIS PLOT IS FOR ILLUSTRATION ONLY. SEE PLOT CONTAINING SEPARATE MEAN & LIMIT CURVES.

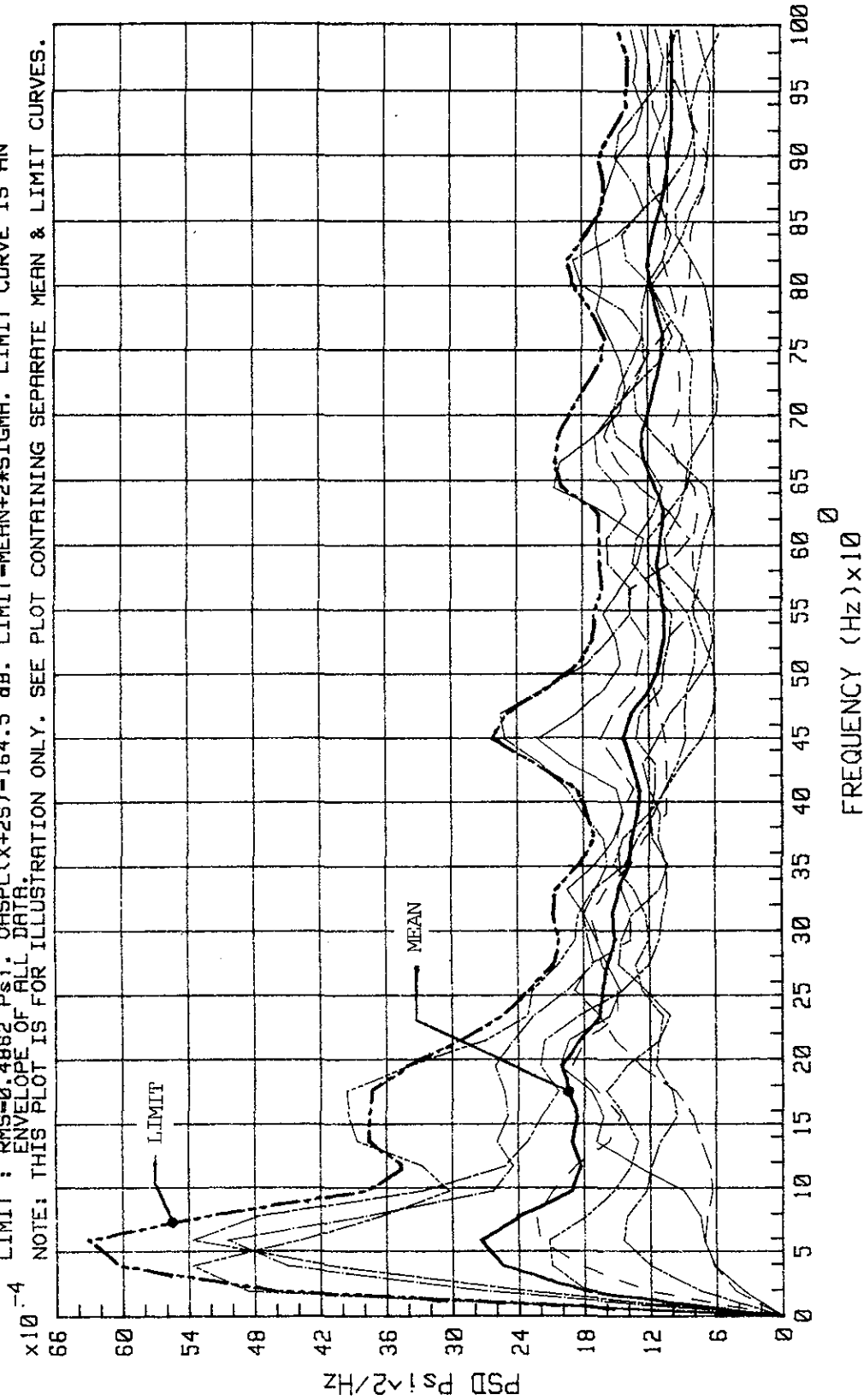


Figure 2-15. STS-1 Through -8 Lift-Off Peak - FSS Acoustics at 245-ft Level, 16 DOF PSD's

KSC-DD-818-TR

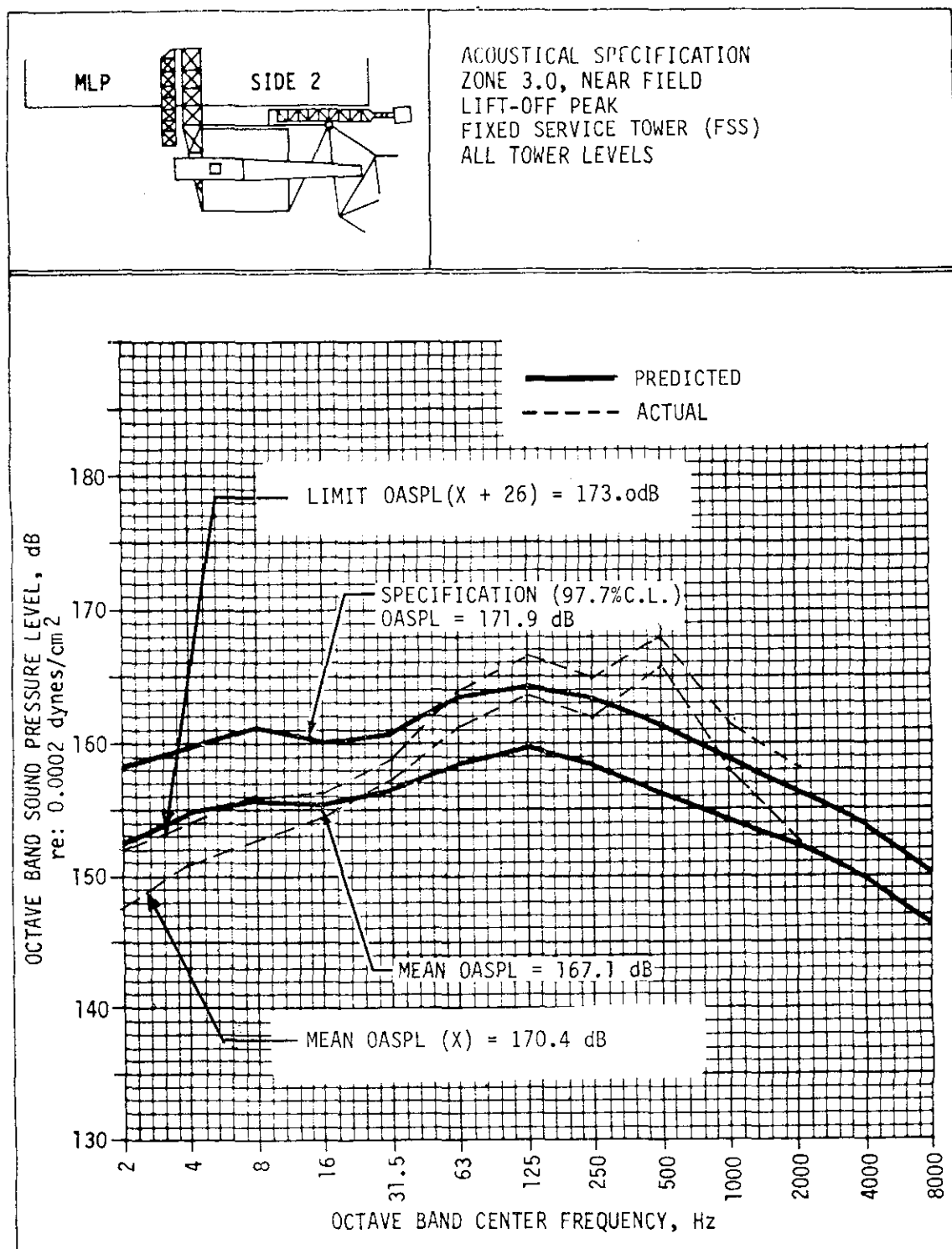


Figure 2-16. Plots of Predicted and Measured OBSPL's for STS-1 Through -6, FSS, All Tower Levels

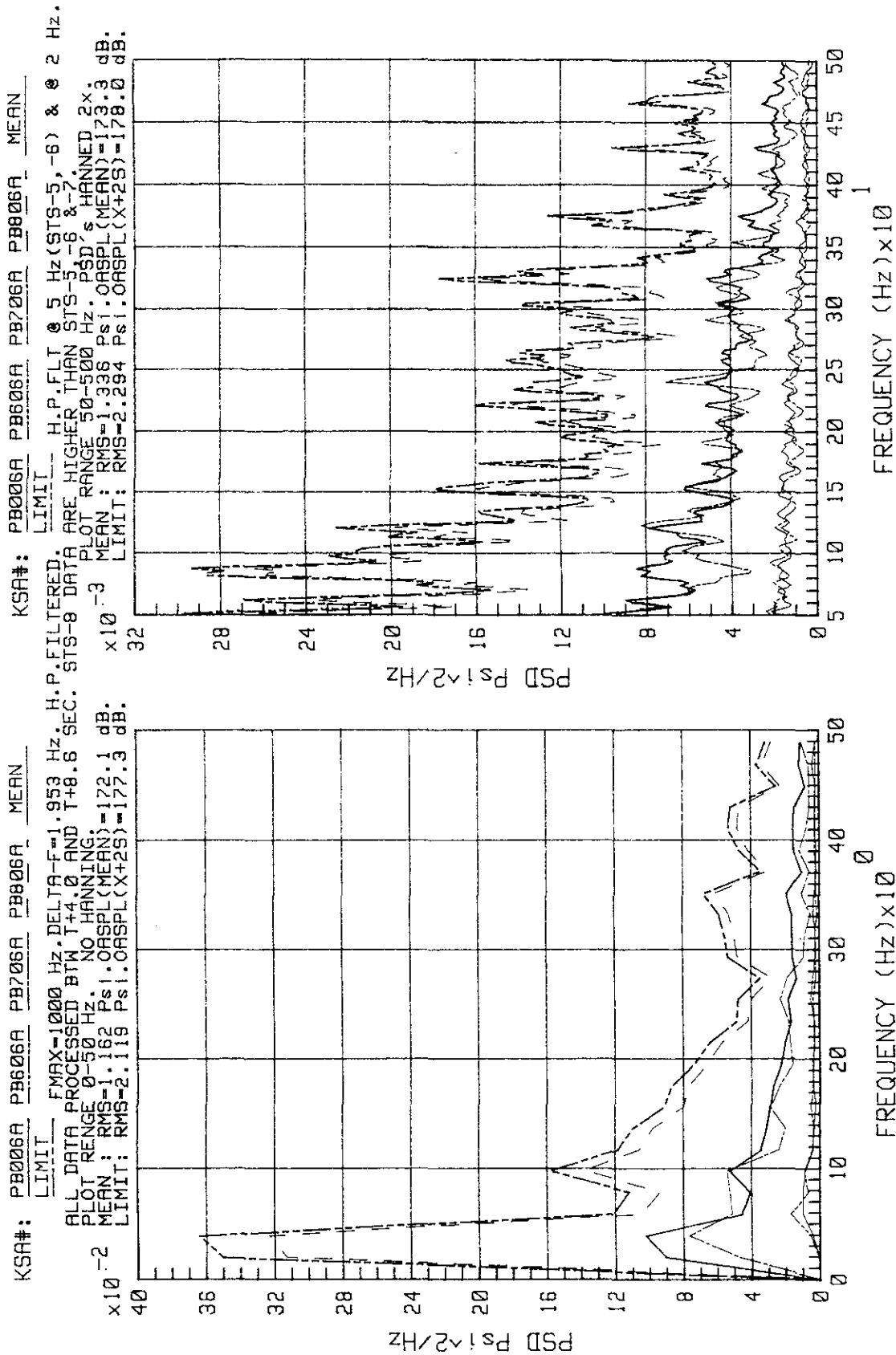


Figure 2-17. STS-5, -6, -7, -8 Lift-off Peak - Acoustics on ET Vent Arm, Top of Haunch Pivot

KSC-DD-818--TR

2.2 RSS ACOUSTICS SUMMARY

The summary of RSS acoustics was obtained from data collected in two separate measurement efforts. The first effort was conducted for STS-1 through STS-3 launches, using sensors used during the Saturn V program. Data are presented in the form of OBSPL's on figures 2-18 through 2-25 and compared to predictions. Because the STS-1 through STS-3 measured data did not compare well with predictions, a second effort was initiated for STS-7 and STS-8, using new acoustic sensors. Resulting data are presented in the form of PSD's on figures 2-26 through 2-35. In either case, measured data were similar, as can be seen from the comparison of overall sound pressure level (OASPL) values calculated from PSD's and shown on the plot headings. Acoustic pressures at a given sensor location are comparable between launches; however, because of diffraction, shielding, and ground reflections, the output of different sensors, although located on the same side, are not always comparable. Sensor locations and orientations are shown on plot headings on figures 2-26 through 2-35 to alert the user to these differences.

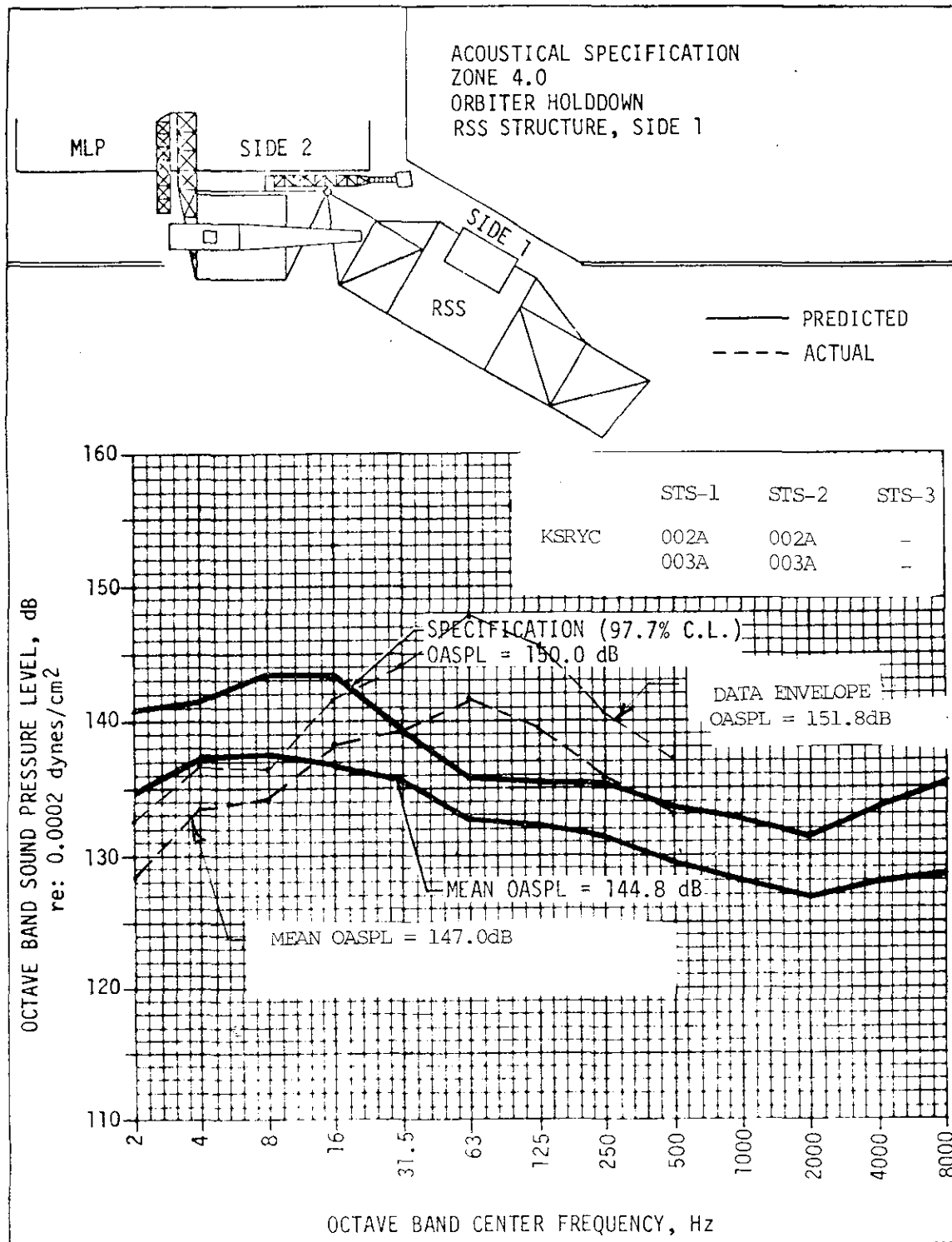


Figure 2-18. Comparison of Predicted and Actual OBSPL's,
Orbiter Holddown, RSS Side 1

KSC-DD-818-TR

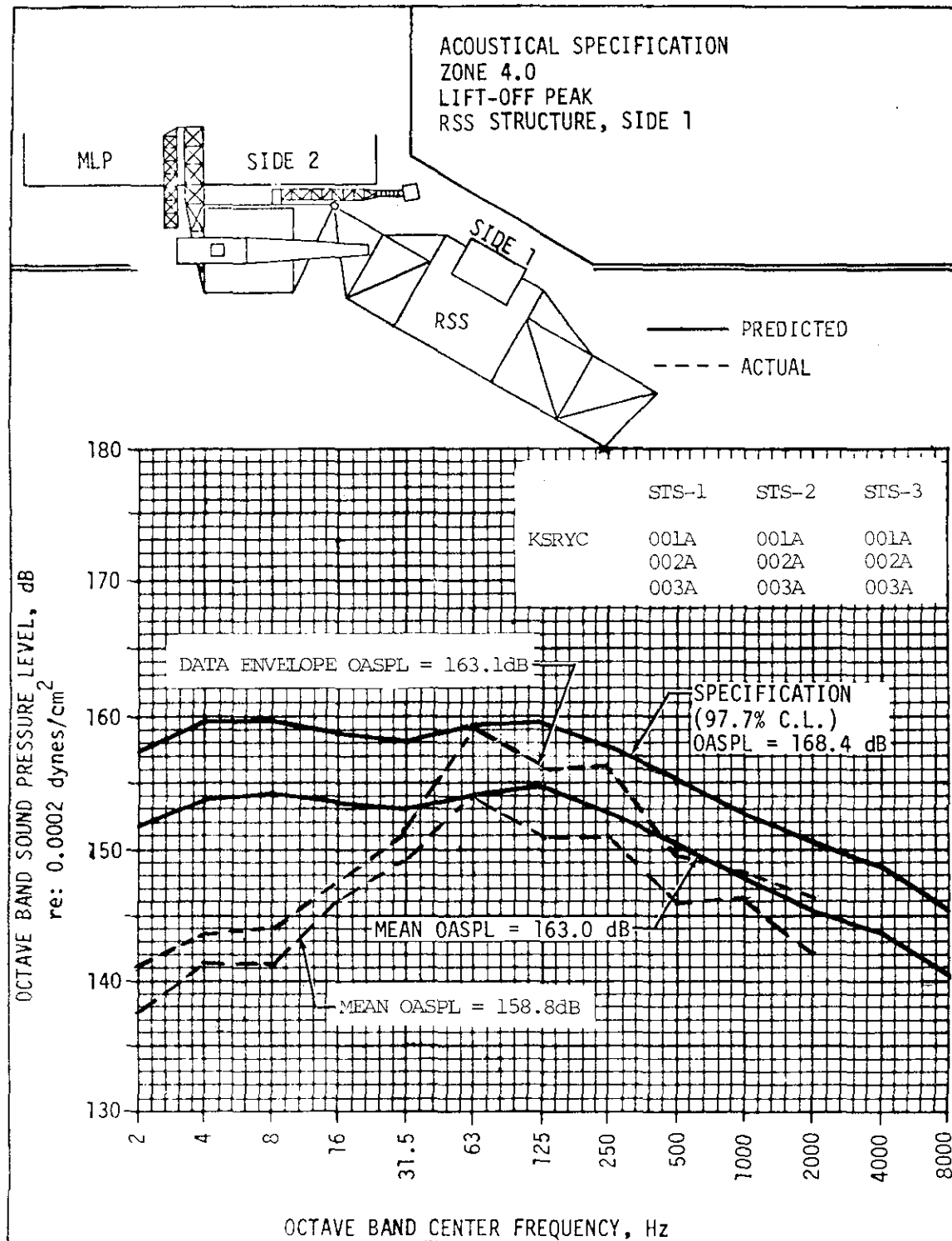


Figure 2-19. Comparison of Predicted and Actual OBSPL's,
Lift-Off Peak, RSS Side 1

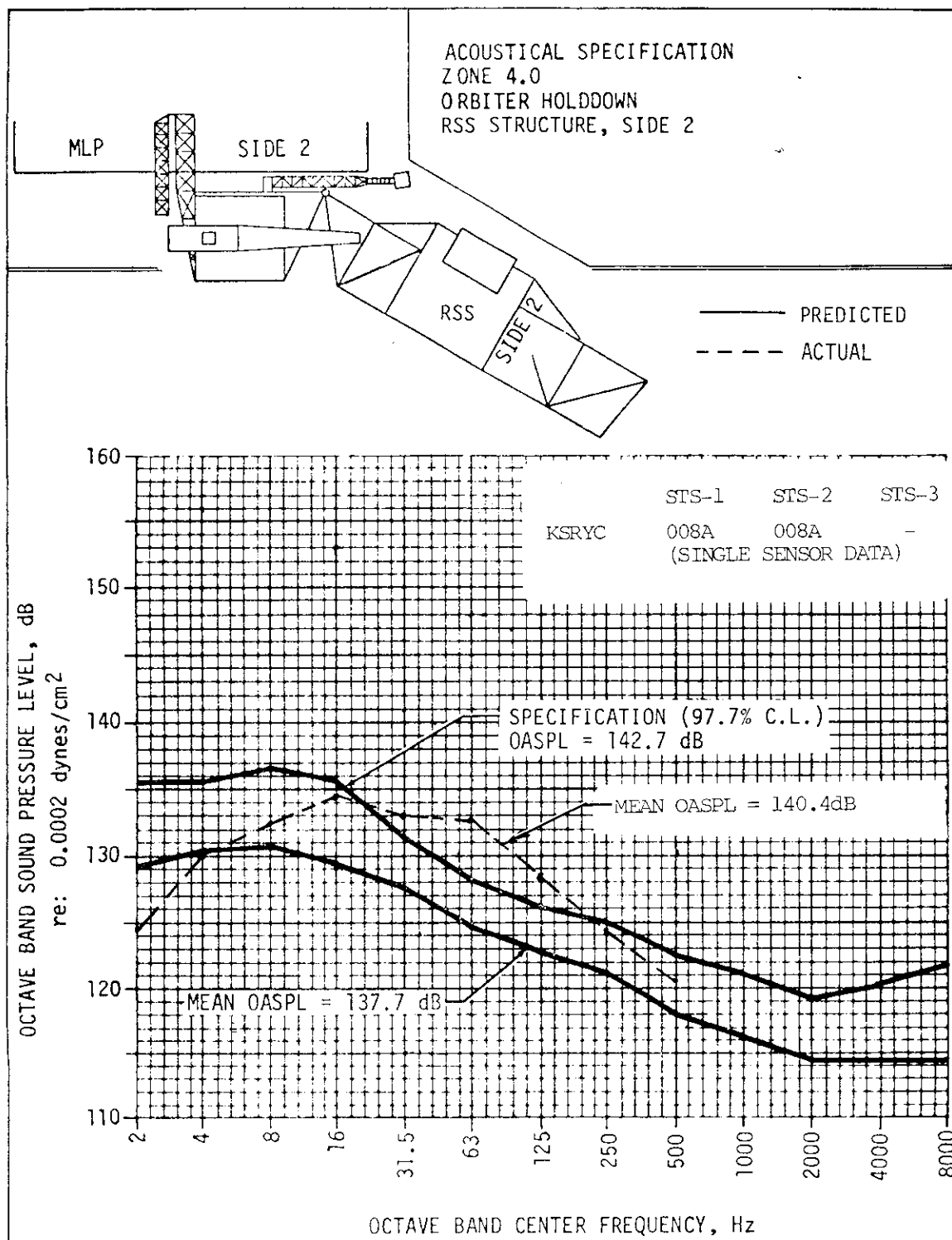


Figure 2-20. Comparison of Predicted and Actual OBSPL's,
Orbiter Holddown, RSS Side 2

KSC-DD-818-TR

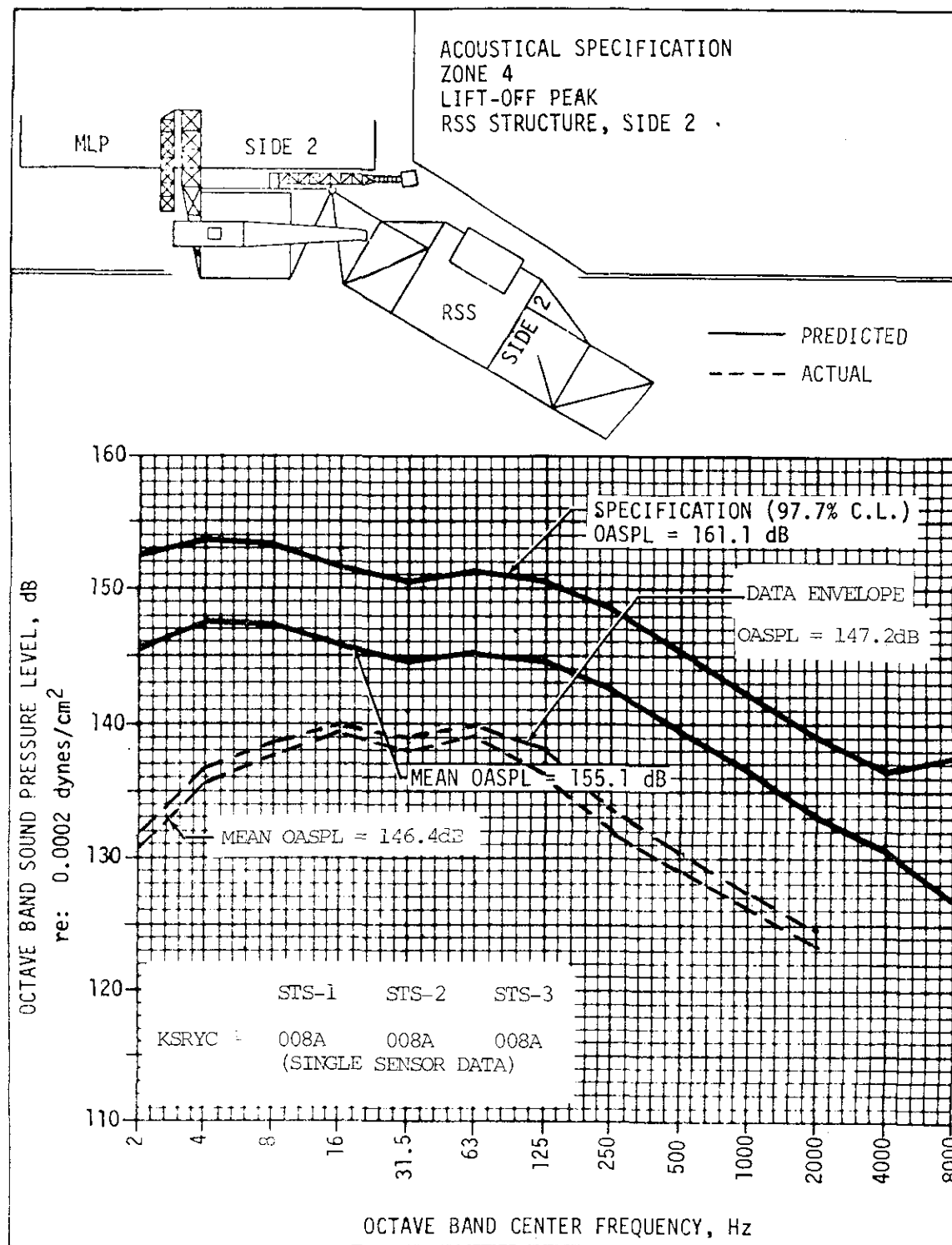


Figure 2-21. Comparison of Predicted and Actual OBSPL's,
Lift-Off Peak, RSS Side 2

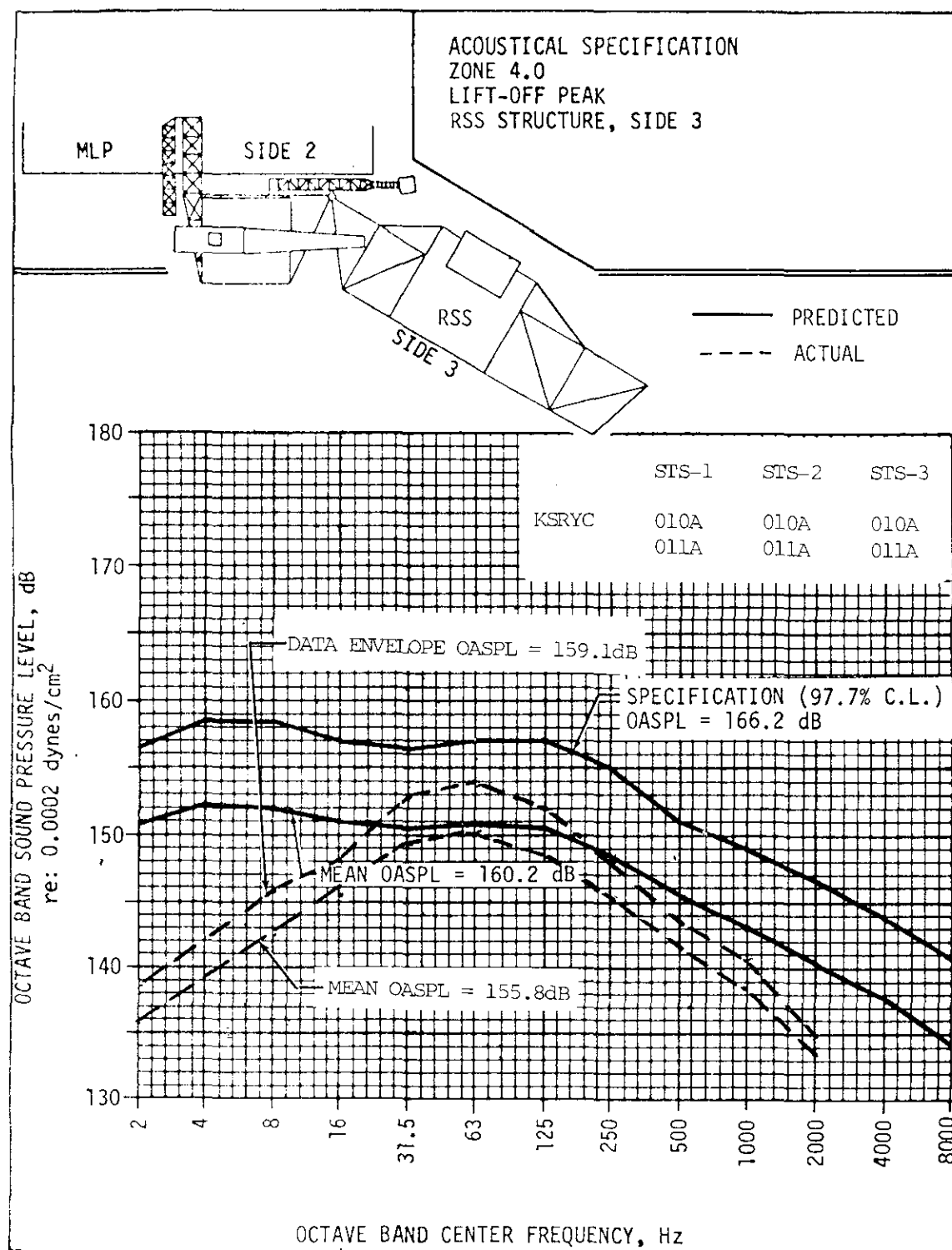


Figure 2-22. Comparison of Predicted and Actual OBSPL's,
Lift-Off Peak, PCR Side 3

KSC-DD-818-TR

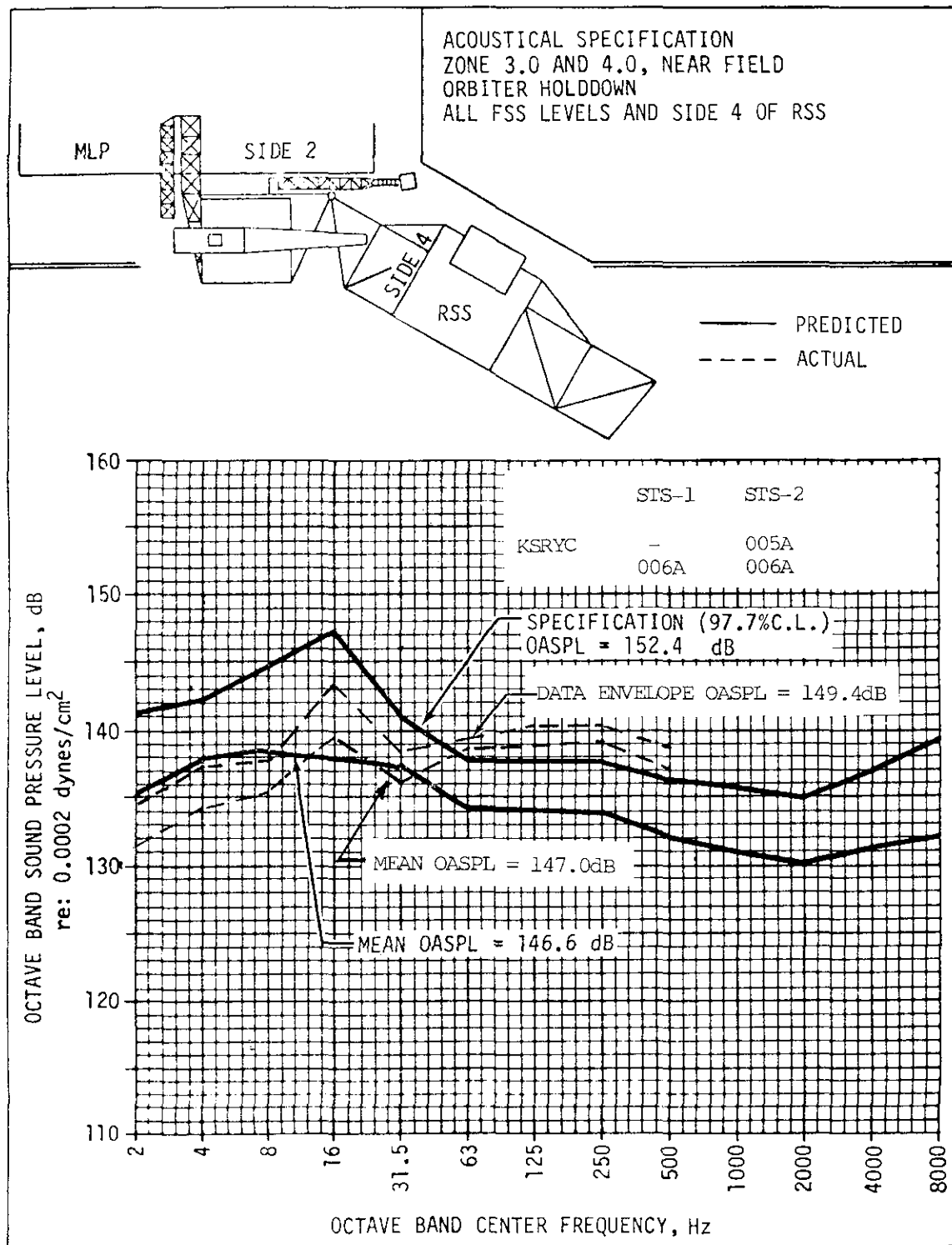


Figure 2-23. Comparison of Predicted and Actual OBSPL's, Orbiter Holddown, All FSS Levels and Side 4 of RSS

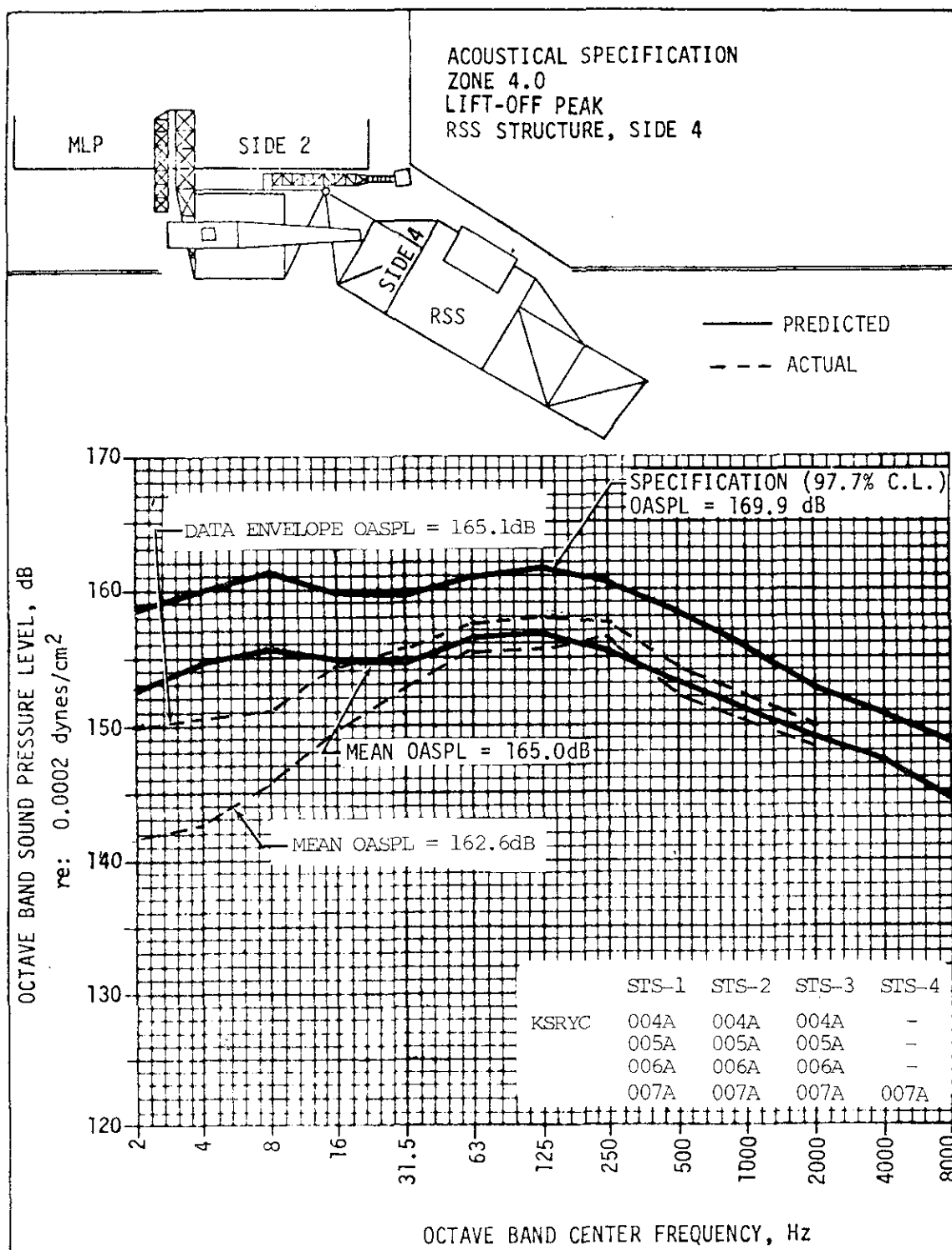


Figure 2-24. Comparison of Predicted and Actual OBSPL's,
Lift-Off Peak, RSS Side 4

KSC-DD-818-TR

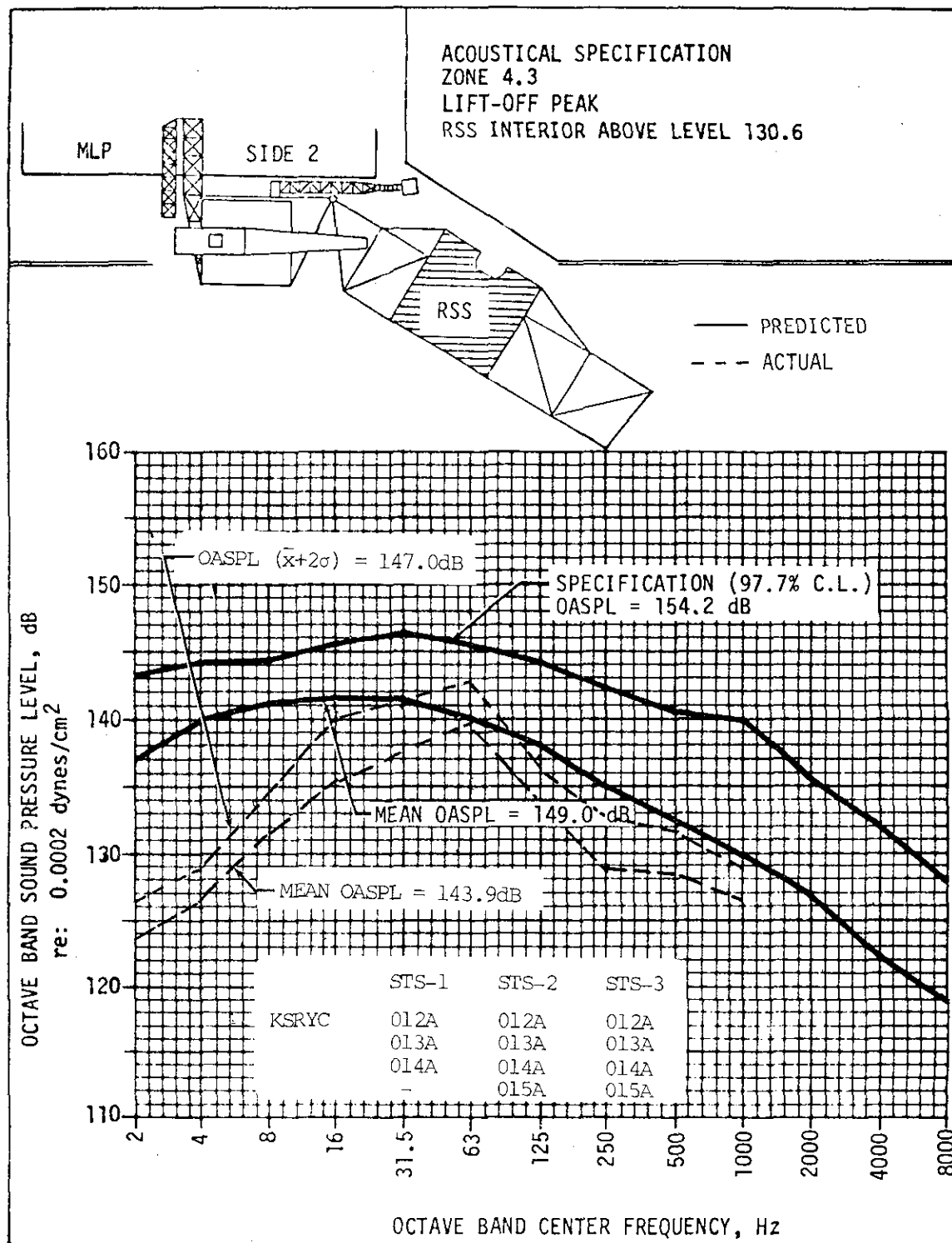


Figure 2-25. Comparison of Predicted and Actual OBSPL's,
Lift-Off Peak, RSS Interior Above 130.6-ft Level

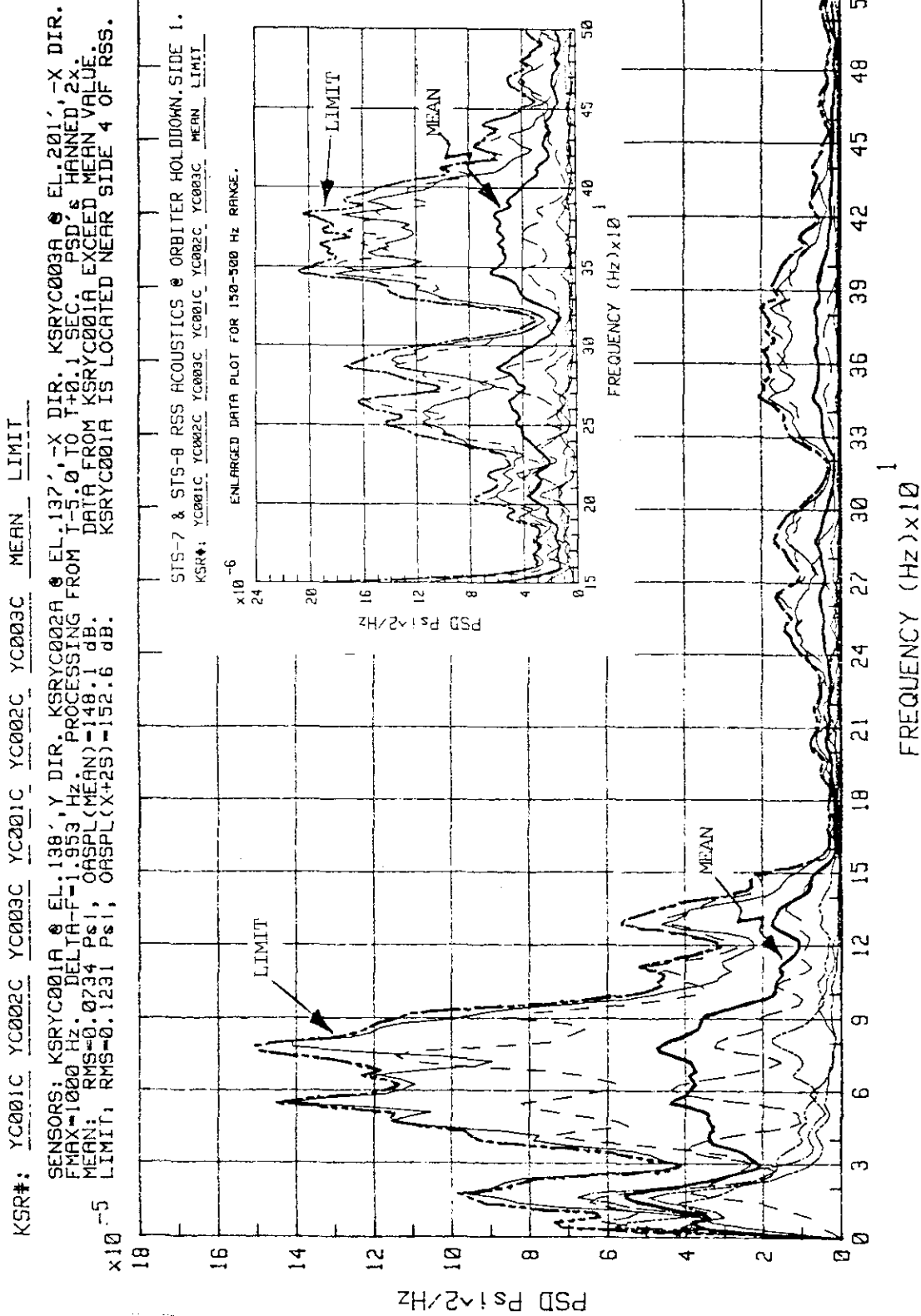


Figure 2-26. STS-7 and -8 RSS Acoustics at Orbiter Holddown - Sensors on Side 1

KSC-DD-818-TR

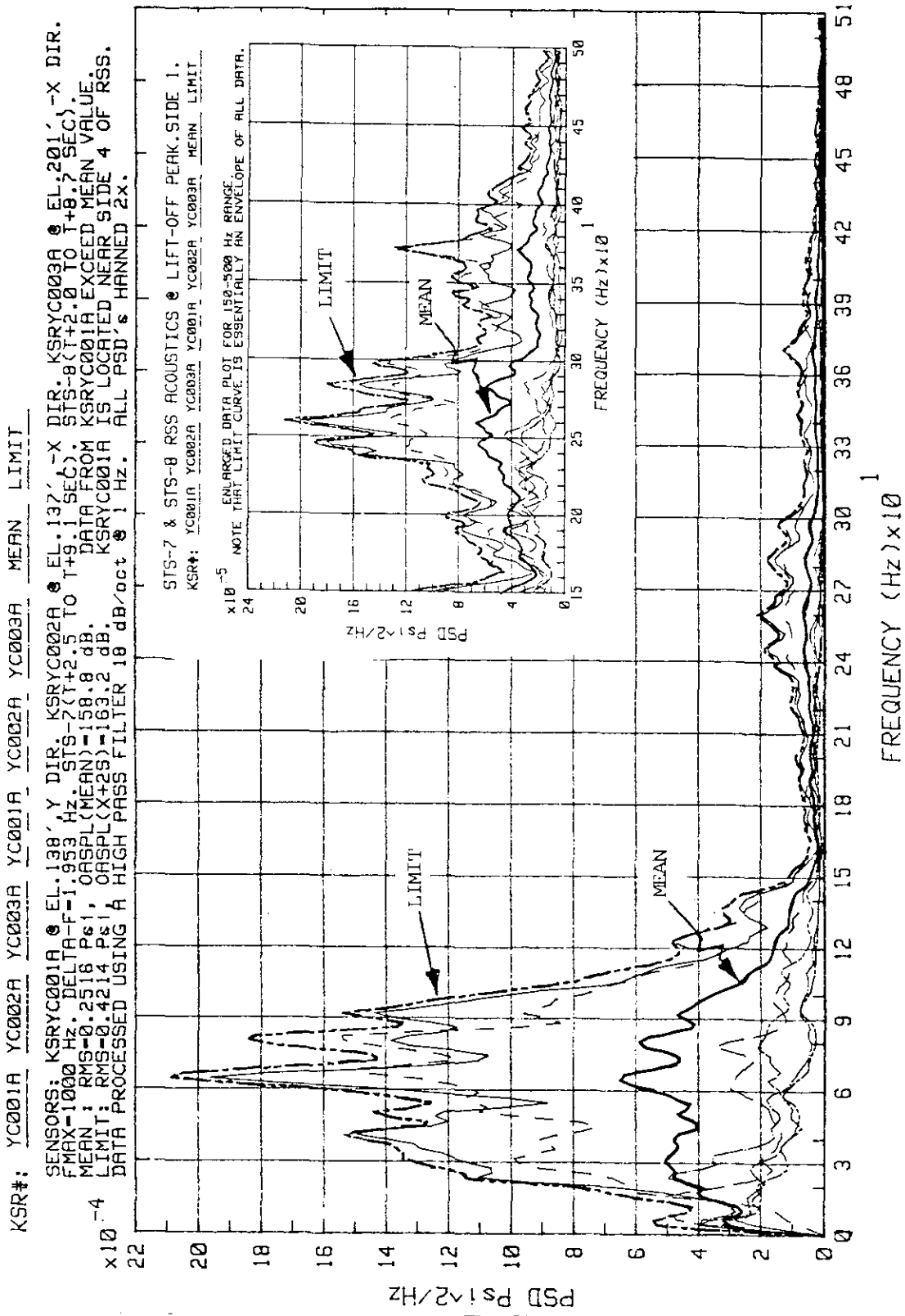


Figure 2-27. STS-7 and -8 RSS Acoustics at Lift-Off Peak - Sensors on Side 1

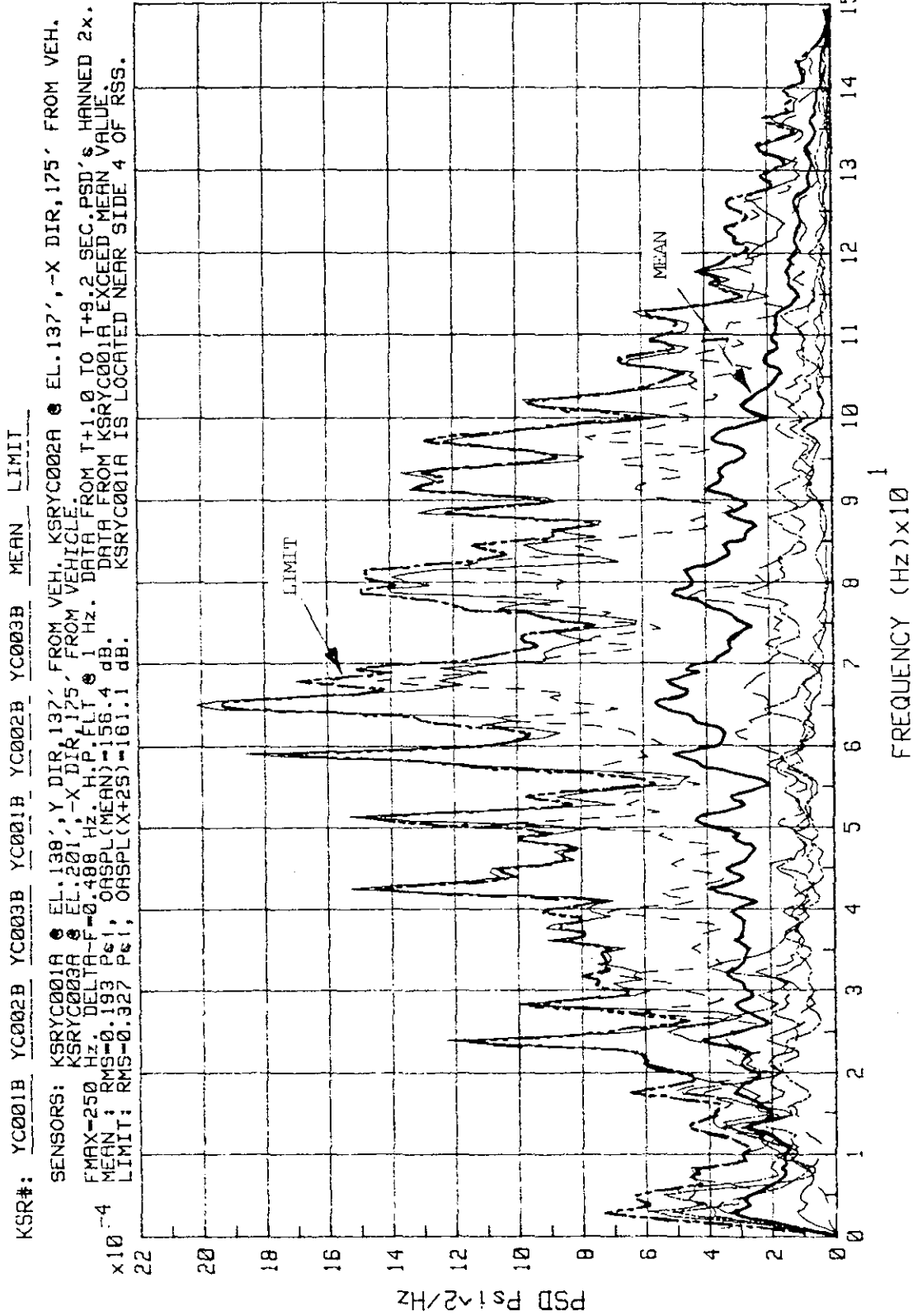


Figure 2-28. STS-7 and -8 RSS Acoustics at Lift-Off Peak - Sensors on Side 1 (Zoom Plot)

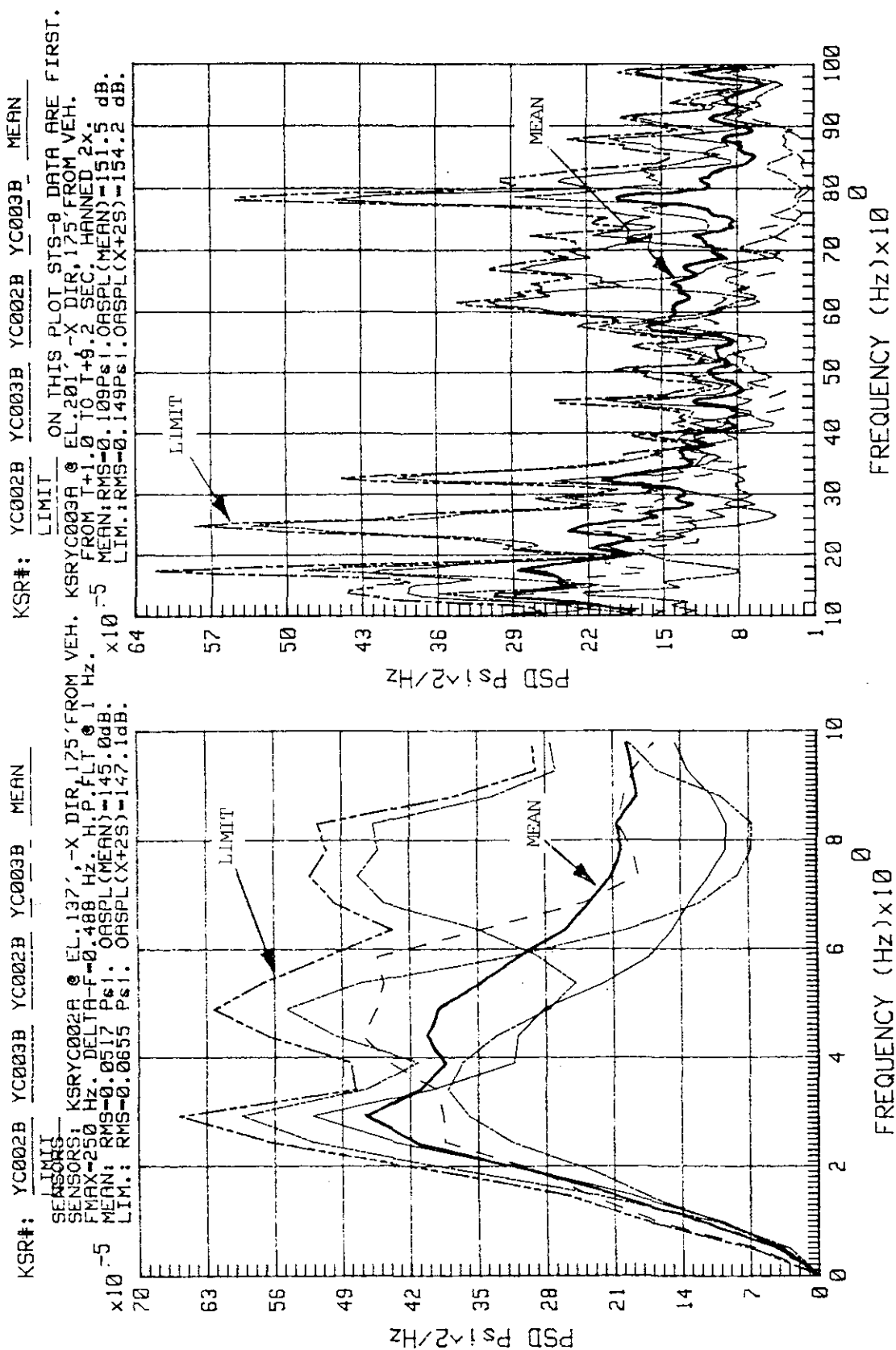


Figure 2-29. STS-7 and -8 RSS Acoustics at Lift-Off Peak - Sensors at Grazing Incidence, Side 1

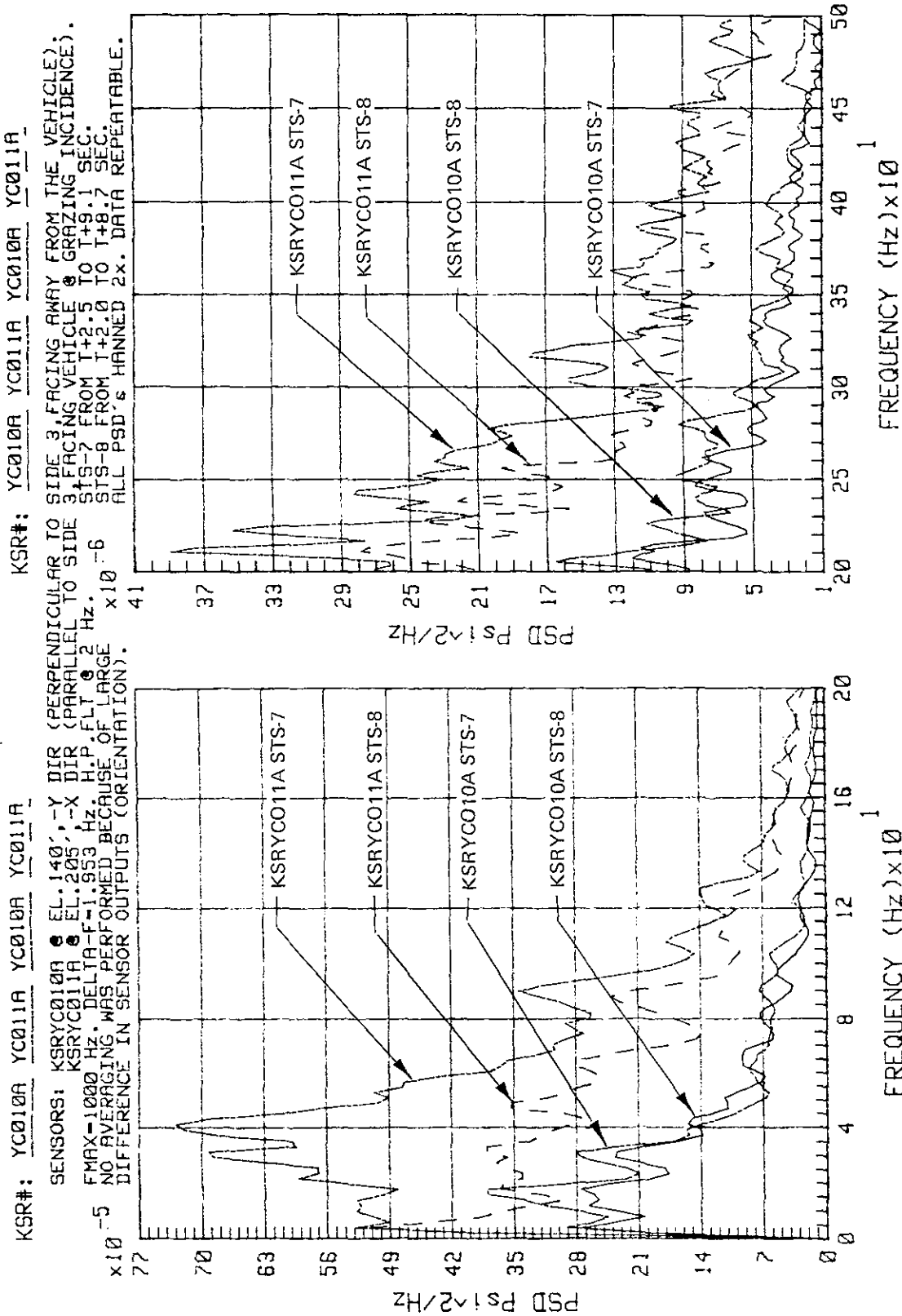


Figure 2-30. STS-7 and -8 RSS Acoustics at Lift-Off Peak - Sensors on Side 3

KSC-DD-818-TR

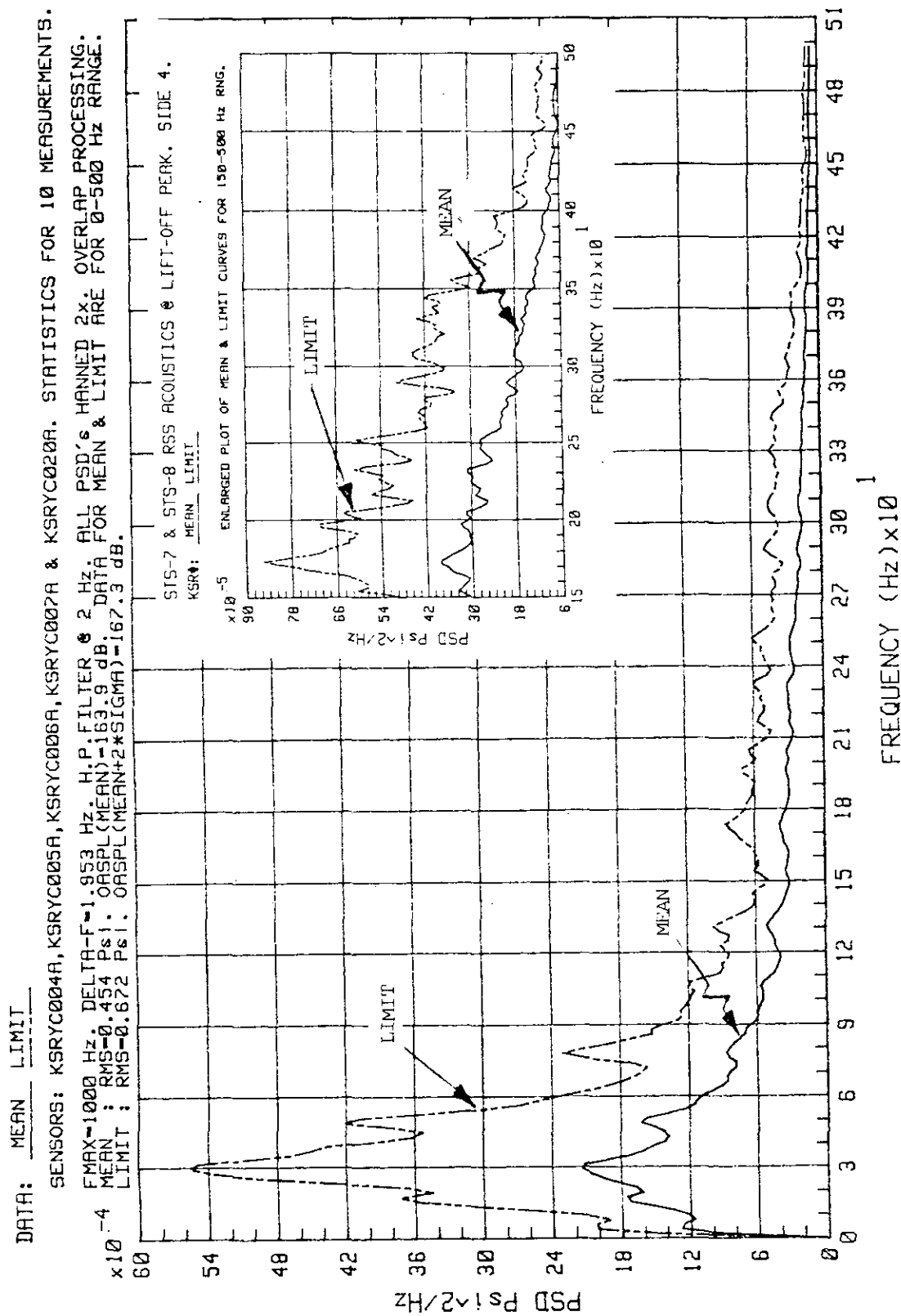
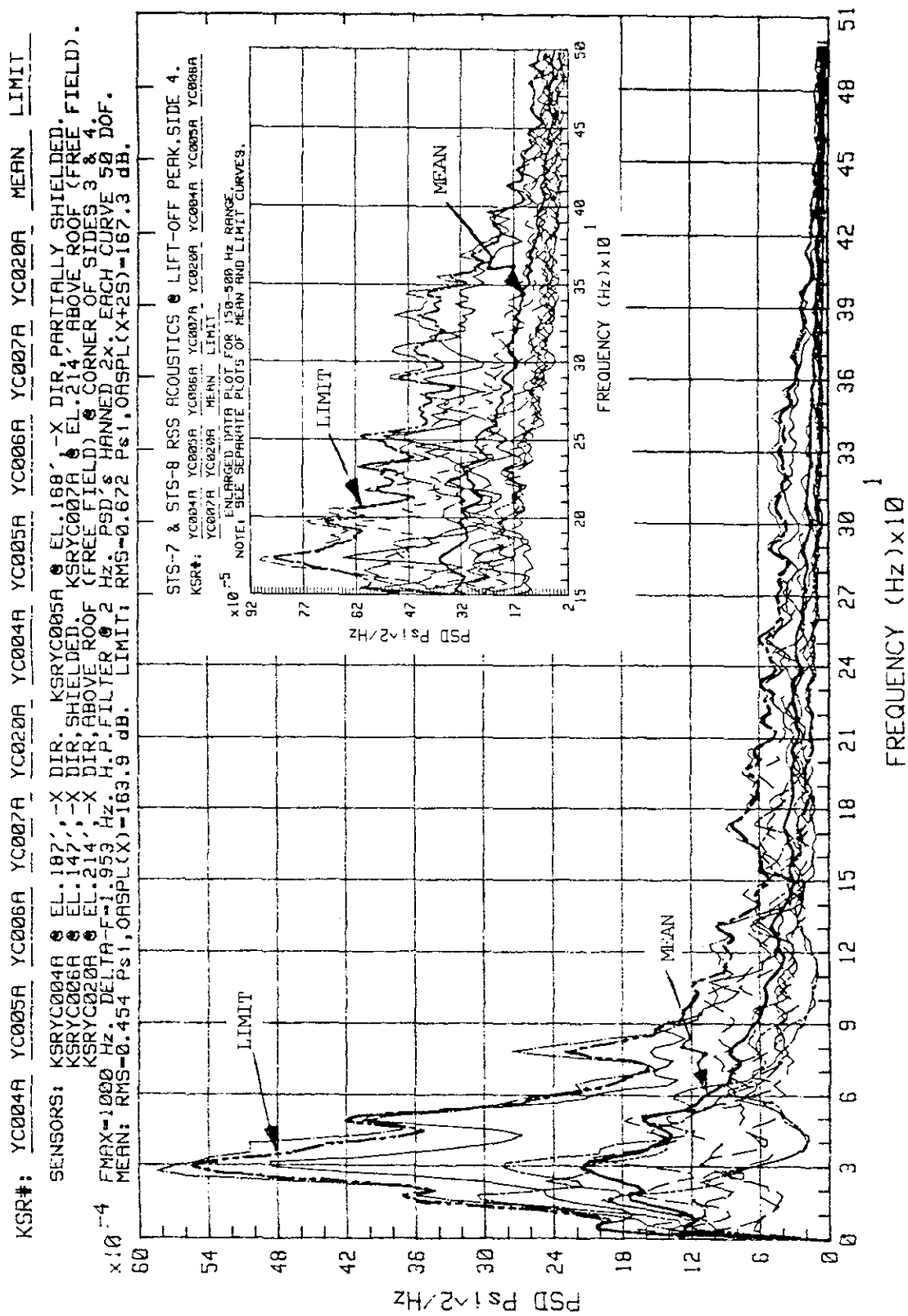


Figure 2-31. STS-7 and -8 RSS Acoustics at Lift-Off Peak - Sensors on Side 4 (Mean and Limit Only)



KSC-DD-818-TR

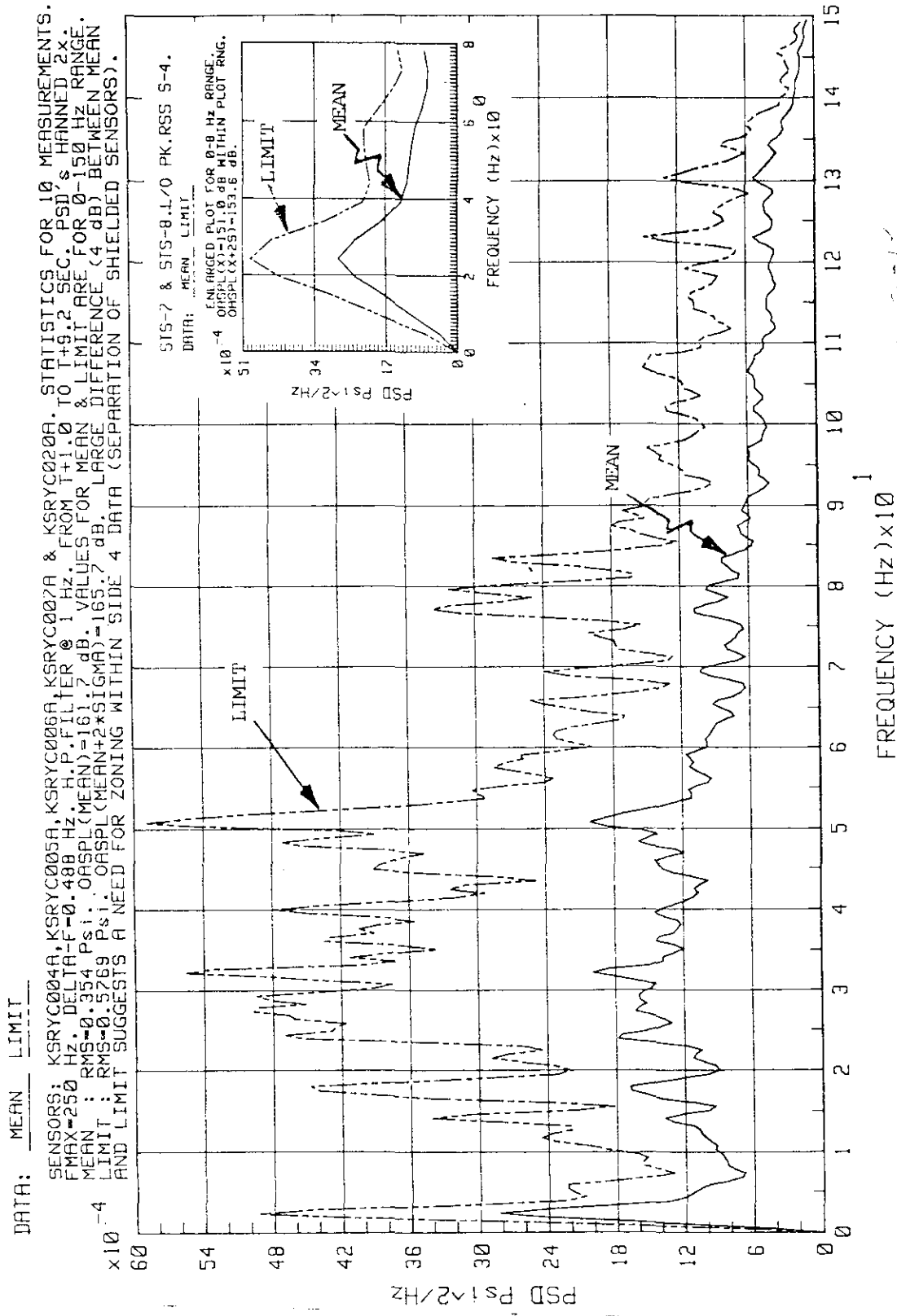


Figure 2-33. STS-7 and -8 RSS Acoustics at Lift-Off Peak - Sensors on Side 4 (Mean and Limit Only)

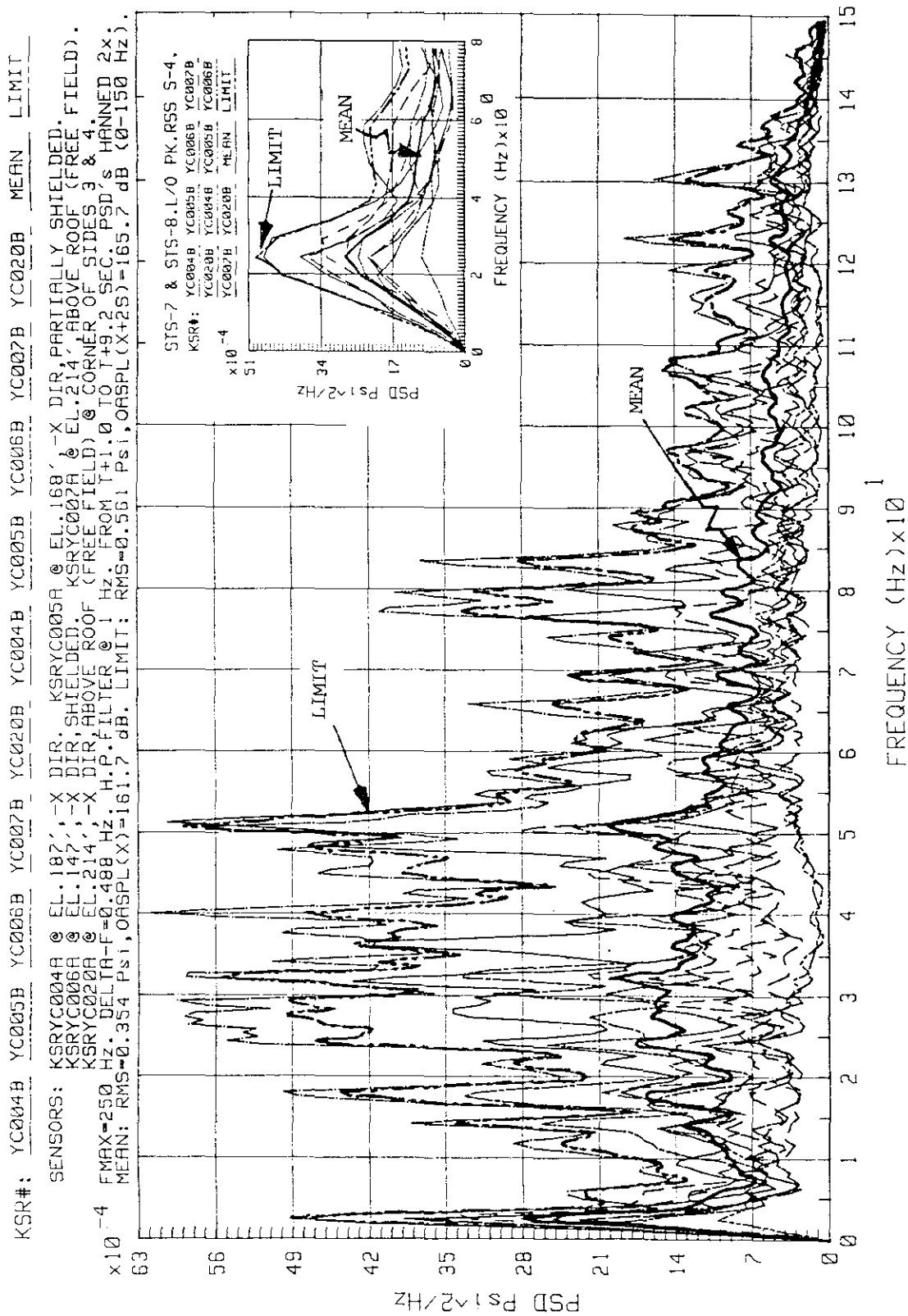


Figure 2-34. STS-7 and -8 RSS Acoustics at Lift-Off Peak - Sensors on Side 4

KSR#: YC007B YC020B YC007B YC020B MEAN LIMIT

SENSORS: KSRYC007A @ EL.214', ABOVE RSS ROOF, FACING VEHICLE, @ APPROX. 150' FROM VEHICLE.
KSRYC020A @ EL.214', ABOVE RSS ROOF, FACING VEHICLE, @ APPROX. 170' FROM VEHICLE.
FMAX=250 Hz. DELTA-F=0.488 Hz. H.P. FILTER @ 1 Hz. FROM T+1.0 TO T+9.2 SEC. PSD's HANNED 2x.
MEAN: RMS=0.273 PSI, ORSPL(X)=159.5 dB. LIMIT: RMS=0.365 PSI, ORSPL(X)=162.0 dB (0-100 Hz).
FREE FIELD DATA ARE NOT AFFECTED BY LOCAL REFLECTIONS. STS-8 DATA ARE HIGHER THEN STS-7.

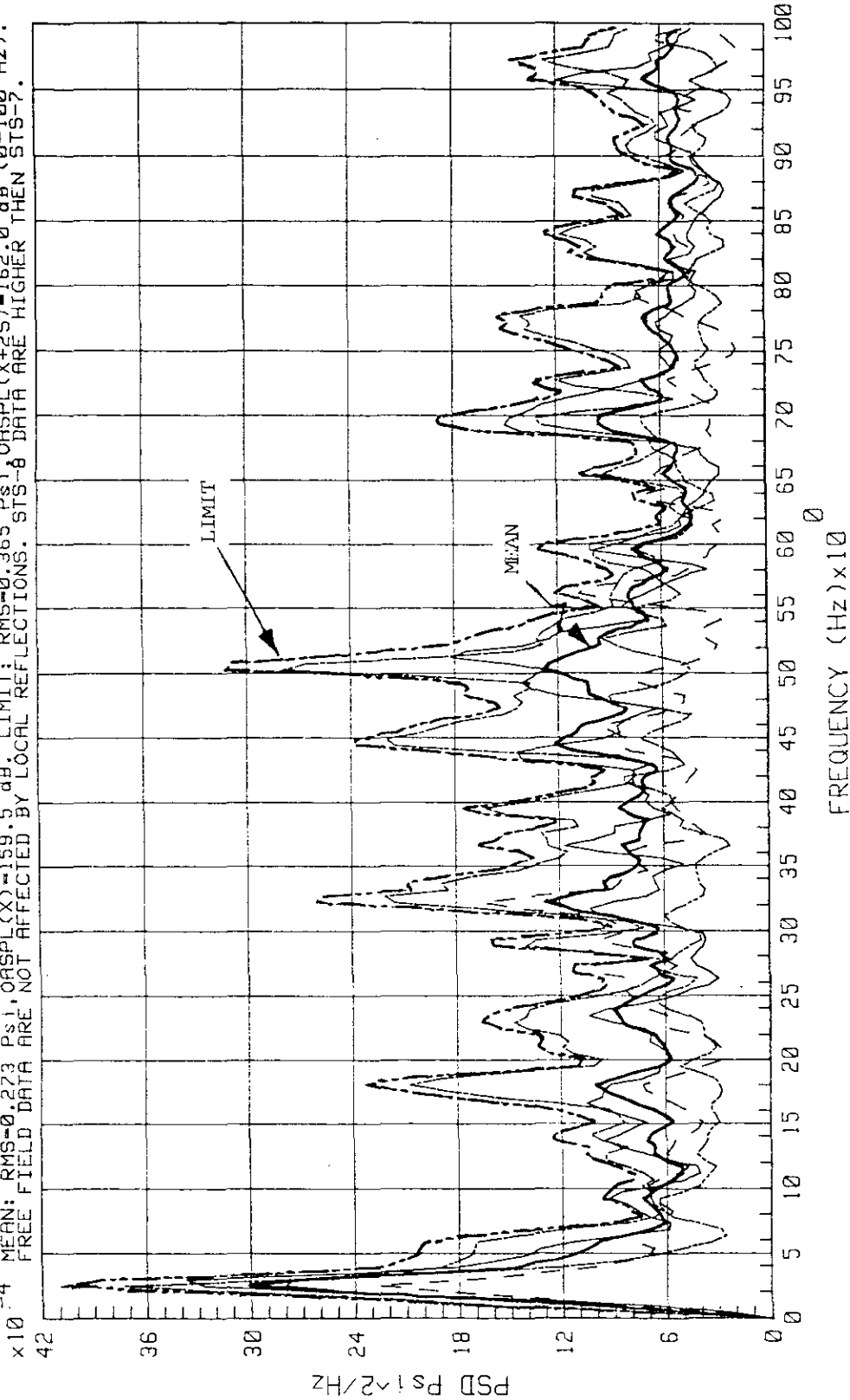


Figure 2-35. STS-7 and -8 RSS Free Field Acoustics at Lift-Off Peak - Sensors on Side 4

2.3 CENTAUR ROLLING BEAM PORCH ASSEMBLY

This summary of acoustic pressures on the Centaur porch assembly is based on data from pressure sensors KSRPB001A through KSRPB008A, recorded during STS-9 and STS-11 launches. Eight pressure sensors were installed in pairs at four locations on the porch, two pairs at the east cantilevered end and two pairs at FSS support. Within each sensor pair, one was oriented vertically (Z-direction) and another horizontally (X-direction). Sensors were installed at the end of bent (45°) tubes in order to protect diaphragms from direct exposure to radiating heat. Additional protection from heat in the form of ablative coating was applied to all sensor housings for STS-11. In spite of these precautions, all sensor outputs contained some baseline drift. Because of the baseline drift, data were processed using a high-pass filter.

No distinct "static" type pressures were measured on the porch during STS-9 and STS-11. This conclusion is based on the following observations, disregarding the possibility that baseline drift could have masked "static" pressures:

- a. The amount of baseline drift was the same in each sensor pair during STS-9. STS-11 data show a substantial reduction in the baseline drift as a consequence of additional thermal protection, while the sign of drift in the majority of sensors reversed to negative.
- b. If there were any static pressures, they would be recorded by sensors oriented vertically, in the opposite direction to the exhaust flow. Examination of low-frequency end of spectra shows that horizontally oriented sensors always have higher PSD ordinates at these frequencies than their vertically oriented pairs. This indicates dominant direction of pressure waves to be closer to horizontal than to vertical direction, and an absence of continuous exhaust flow at sensor locations.

The summary of acoustic environment on the porch assembly is presented on figures 2-36 through 2-49 in terms of PSD's. Figures 2-36 through 2-38 depict environment during Orbiter holddown period caused by the burn of SSME's. All pertinent data processing parameters are shown in the plot headings. There are no substantial differences between acoustic environments recorded by sensors at the cantilever end and at FSS support during this period.

Figures 2-39 through 2-49 present summary of acoustic environment recorded during the lift-off peak period. Data processing was performed using three different values of F_{\max} (Nyquist frequency) with corresponding different analysis time intervals. Such processing was necessary in order to account for the continuous variation in the data frequency composition. In processing cases corresponding to $F_{\max} = 5$ kHz and 1 kHz, all PSD's were lumped together regardless of sensor locations. The case corresponding to $F_{\max} = 5$ kHz, where PSD's are dominated by a wideband peak between 500 and 800 kHz, shows no significant difference between environments at porch end and FSS support. The

case corresponding to $F_{\max} = 1$ kHz shows that below approximately 25 Hz, higher values of PSD's (near factor of 2) were derived from sensors located closer to the vehicle (on the porch end). Figure 2-45, which shows all PSD mean and limit curve calculations, illustrates this difference.

The case corresponding to $F_{\max} = 100$ Hz required separate mean and limit curve plots for sensors at cantilever end and FSS support because of 6.2-dB difference in the mean values within the 0- to 20-Hz range. Figures 2-48 and 2-49 present summaries for the case $F_{\max} = 100$ Hz. The user should keep in mind that data are nonstationary and the number of cycles of waveform components below approximately 10 Hz at peak amplitudes is limited and cannot induce full response resonances.

Figures 2-50 and 2-51 present STS-11 cross-correlation function coefficients (CCFC's) between adjacent sensor pairs calculated at sampling rate 10 kHz ($F_{\max} = 5$ kHz) and at sampling rate 2 kHz ($F_{\max} = 1$ kHz). The timelag of the peak is about 0.5 ms. The sign of the lag at peak is positive whenever the first sensor entering cross-correlation calculations is oriented in the X direction. The sign becomes negative when the first sensor is oriented in the Z direction. This indicates that the prevailing direction of pressures wave propagation is close to horizontal, since a sensor oriented in the horizontal (X) direction records a wave before (by 0.5 ms) it reaches a sensor oriented in the vertical (Z) direction. The base of the first CCFC peak (theoretically this is the time between zero crossings, but in practical computations it may be taken as a crossing of ± 0.1 CCFC noise line), which defines correlation length as a function of analysis bandwidth and thus, of F_{\max} . For the case of $F_{\max} = 1$ kHz, the base of CCFC peak (figure 2-51) is about 3 ms. Thus, the average correlation length (essentially an average of all waveform components within the range 0 to 500 kHz) is less than 3.5 ft. The value of CCFC peak (less than 1) is a consequence of multiple sources within the exhaust plumes where pressure waves are generated.

Figures 2-52 through 2-54 present coherences between adjacent sensors calculated for processing cases of $F_{\max} = 5$ kHz, 1 kHz, and 100 Hz. There is a trend toward higher coherences between sensor pairs located farther away from the exhaust plumes.

Figures 2-55 through 2-61 show narrow band, 1 to 10 Hz, pressure time histories for STS-11. For adjacent sensors, both time histories are shown on the same plot.

Figures 2-62 through 2-64 show typical rms time histories for two sensors (KSRPB002A and KSRPB003A) corresponding to each of the processing cases of F_{\max} .

Figure 2-65 shows probability density plots of KSRPB002A for two cases of F_{\max} .

FILE: MEAN LIMIT

SENSORS: STS-9 (KSRPB001A THRU KSRPB009A) & STS-11 (KSRPB002A THRU KSRPB008A).
 FMAX=1000 Hz. DELTA-F=1.953 Hz. A-A FILTER @ 500 Hz. FROM 1-5.0 TO 1+0.12 SEC. HANNED 2x.
 MEAN: RMS=0.205 Psi (157 dB). LIMIT(MEAN+2*SIGMA): RMS=0.297 Psi (160.2 dB).
 MEAN & LIMIT DATA ARE FOR PLOT RANGE 0-800 Hz.

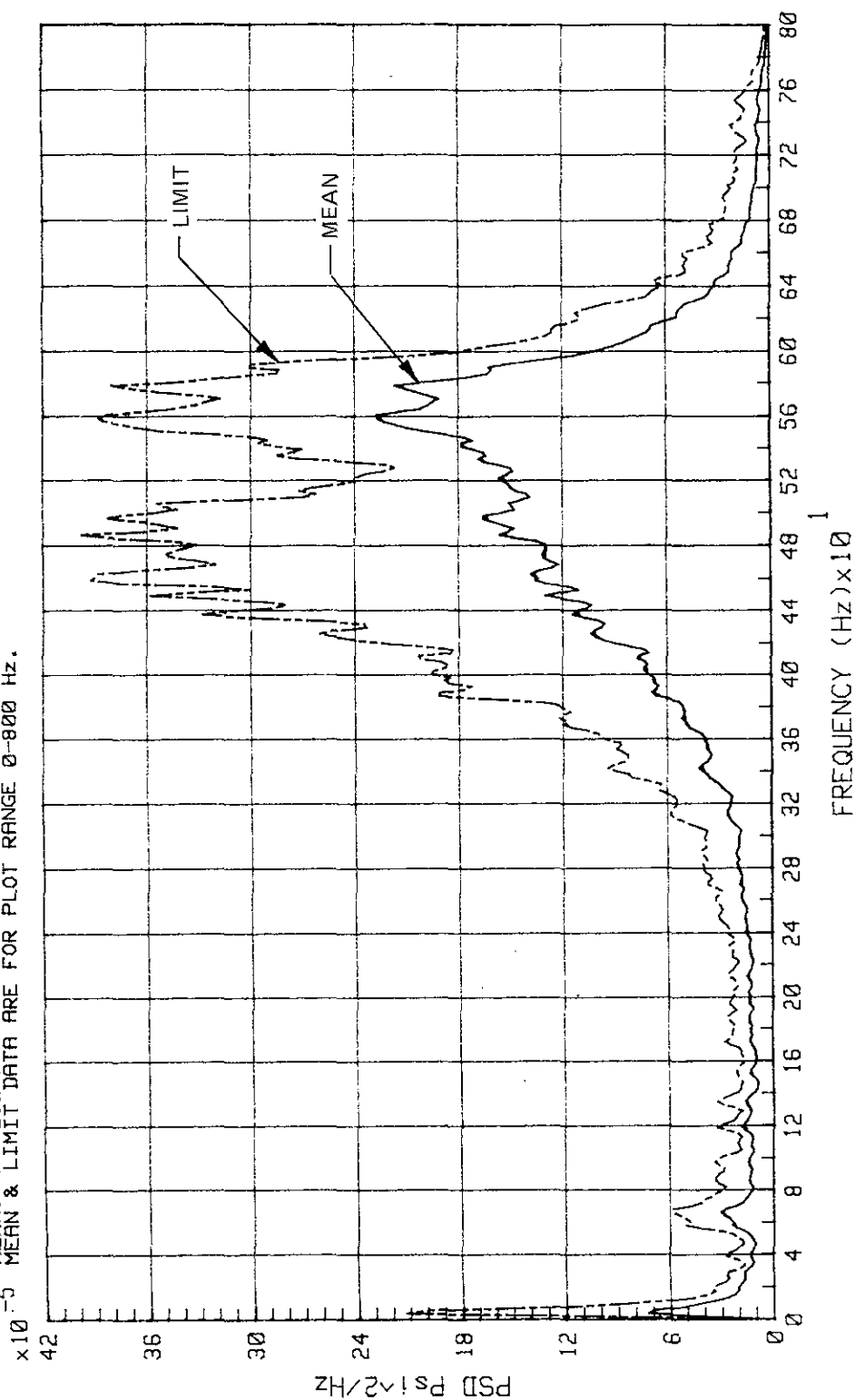


Figure 2-36. STS-9 and -11 Orbiter Holddown - Centaur Porch Assembly Pressures, All Sensor Data (Mean and Limit Only)

KSC-DD-818-TR

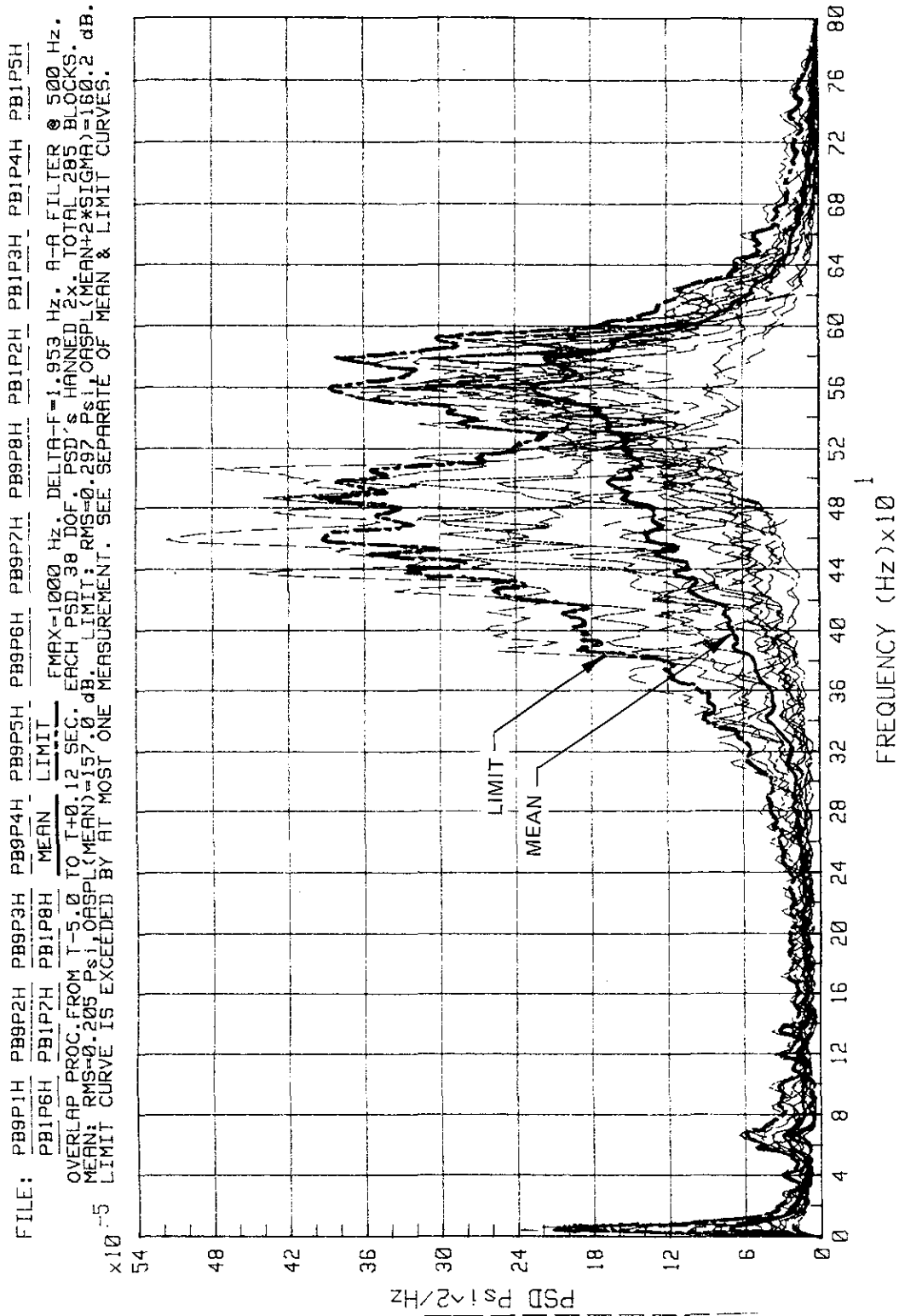


Figure 2-37. STS-9 and -11 Orbiter Holddown - Centaur Porch Assembly Pressures, All Sensor Data

FILE: MEAN LIMIT

SENSORS: STS-9 (KSRPB001A THRU KSRPB008A) & STS-11 (KSRPB002A THRU KSRPB008A).
 FMAX=1000 Hz. DELTA-F=1.953 Hz. A-A FILTER @ 500 Hz. FROM T-5.0 TO T+0.12 SEC. HANNED 2x.
 MEAN: RMS=0.0458 Psi (144.0 dB). LIMIT(MEAN+2*SIGMA): RMS=0.0667 Psi (147.2 dB).
 MEAN & LIMIT DATA ARE FOR PLOT RANGE 0-100 Hz.

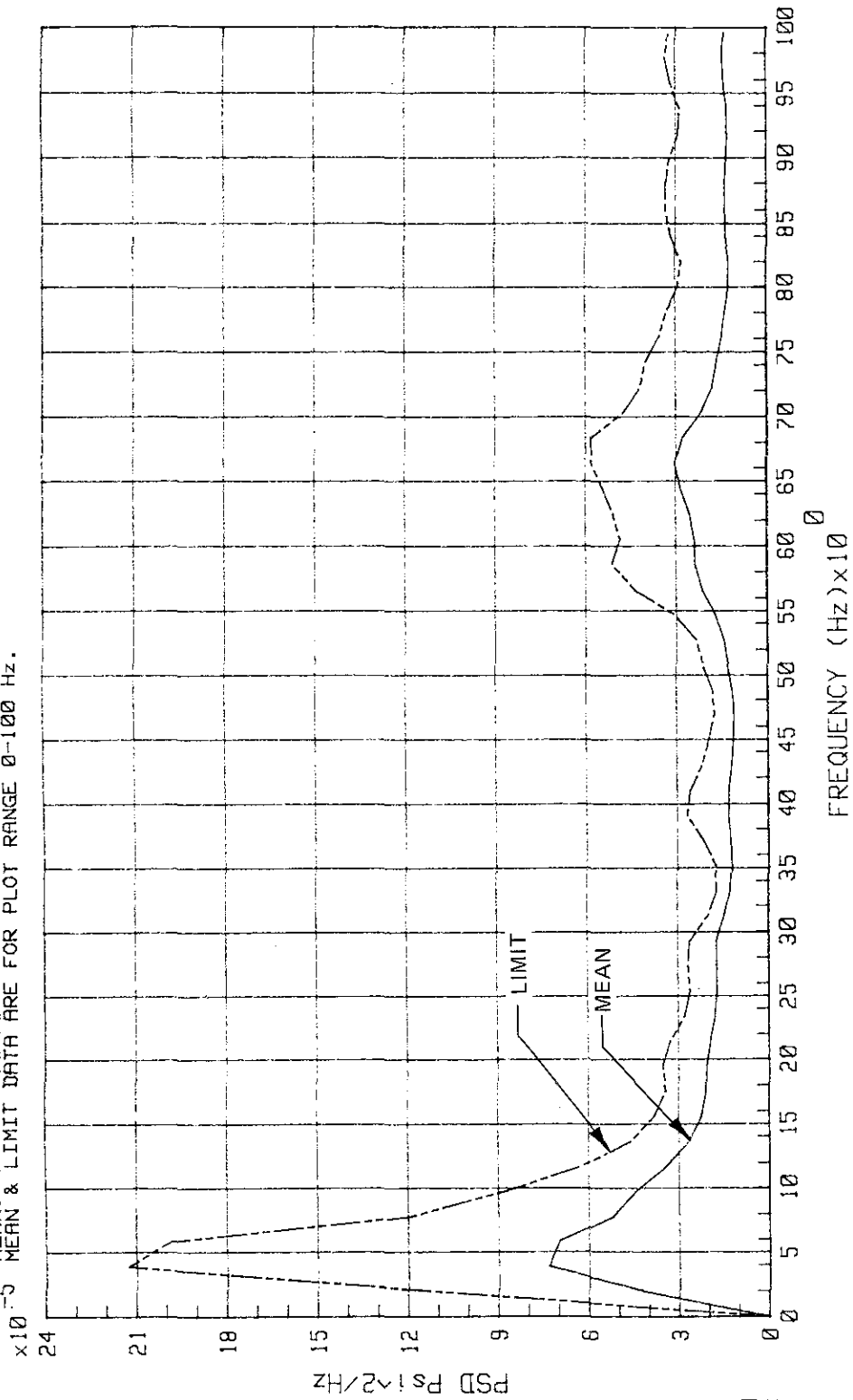


Figure 2-38. STS-9 and -11 Orbiter Holddown - Centaur Porch Assembly Pressures, All Sensor Data (Zoom Plot)

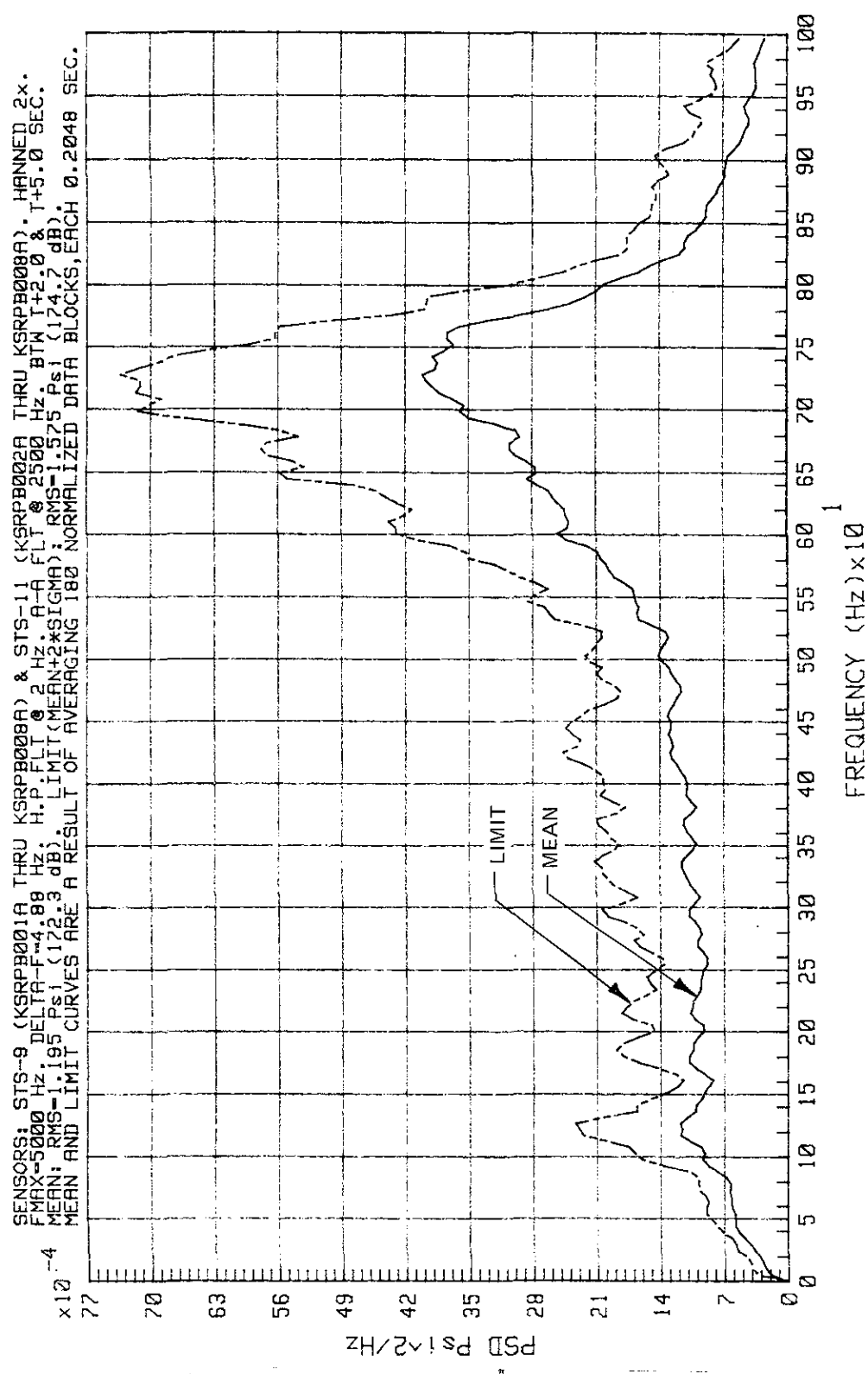


Figure 2-39. STS-9 and -11 Lift-Off Peak - Centaur Porth Assembly Pressures
 (Mean and Limit; $F_{\text{max}} = 5 \text{ kHz}$)

FILE: PB9P1A PB9P2A PB9P3A PB9P4A PB9P5A PB9P6A PB9P7A PB9P8A PB9P2A PB9P3A PB9P4A PB9P5A

PB9P6A PB9P7A PB9P8A MEAN LIMIT

SEE SEPARATE PLOT OF MEAN AND LIMIT CURVES.
 SENSORS: STS-9 (KSRP0001A) THRU KSRP0008A) & STS-11 (KSRP0002A THRU KSRP0008A). HANNED 2x.
 FMAX=5000 Hz. DELTA F=4.88 Hz. H.P. FLT @ 2500 Hz BTW 1+2.0 & 1+5.0 SEC.
 MEAN: RMS=1.195 Psi (172.3 dB). LIMIT(MEAN+2*SIGMA): RMS=1.575 Psi (174.7 dB).
 MEAN AND LIMIT CURVES ARE A RESULT OF AVERAGING 180 NORMALIZED DATA BLOCKS, EACH 0.2048 SEC.

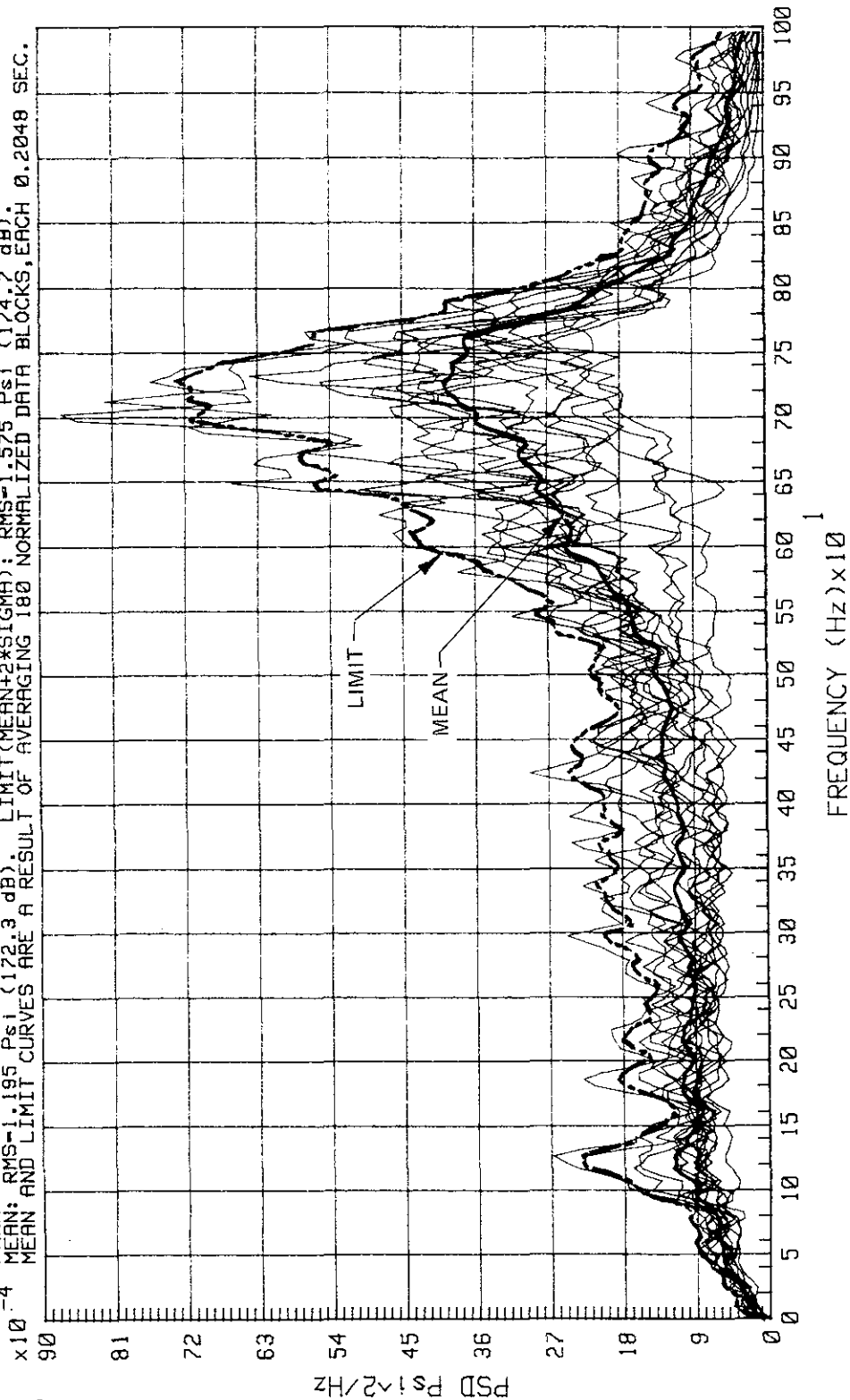


Figure 2-40. STS-9 and -11 Lift-Off Peak - Centaur Porch Assembly Pressures ($F_{max} \approx 5$ kHz)

FILE: MEAN LIMIT

THIS PLOT IS PRESENTED FOR COMPARISON OF MEAN & LIMIT CURVES CALCULATED WITHOUT HANNING.
 SENSORS: STS-9 (KSRP0001A THRU KSRP0008A) & STS-11 (KSRP0002A THRU KSRP0008A). NO HANNING.
 FMAX=5000 Hz. DELTA-F=4.88 Hz. H.P.FLT @ 2 Hz. A-A FLT @ 2500 Hz. BTW T+2.0 & T+5.0 SEC.
 MEAN: RMS-1.196 Psi (122.3 dB). LIMIT: MEAN+2*SIGMA: RMS-1.645 Psi (125.1 dB).
 MEAN AND LIMIT CURVES ARE A RESULT OF AVERAGING 180 NORMALIZED DATA BLOCKS, EACH 0.2048 SEC.

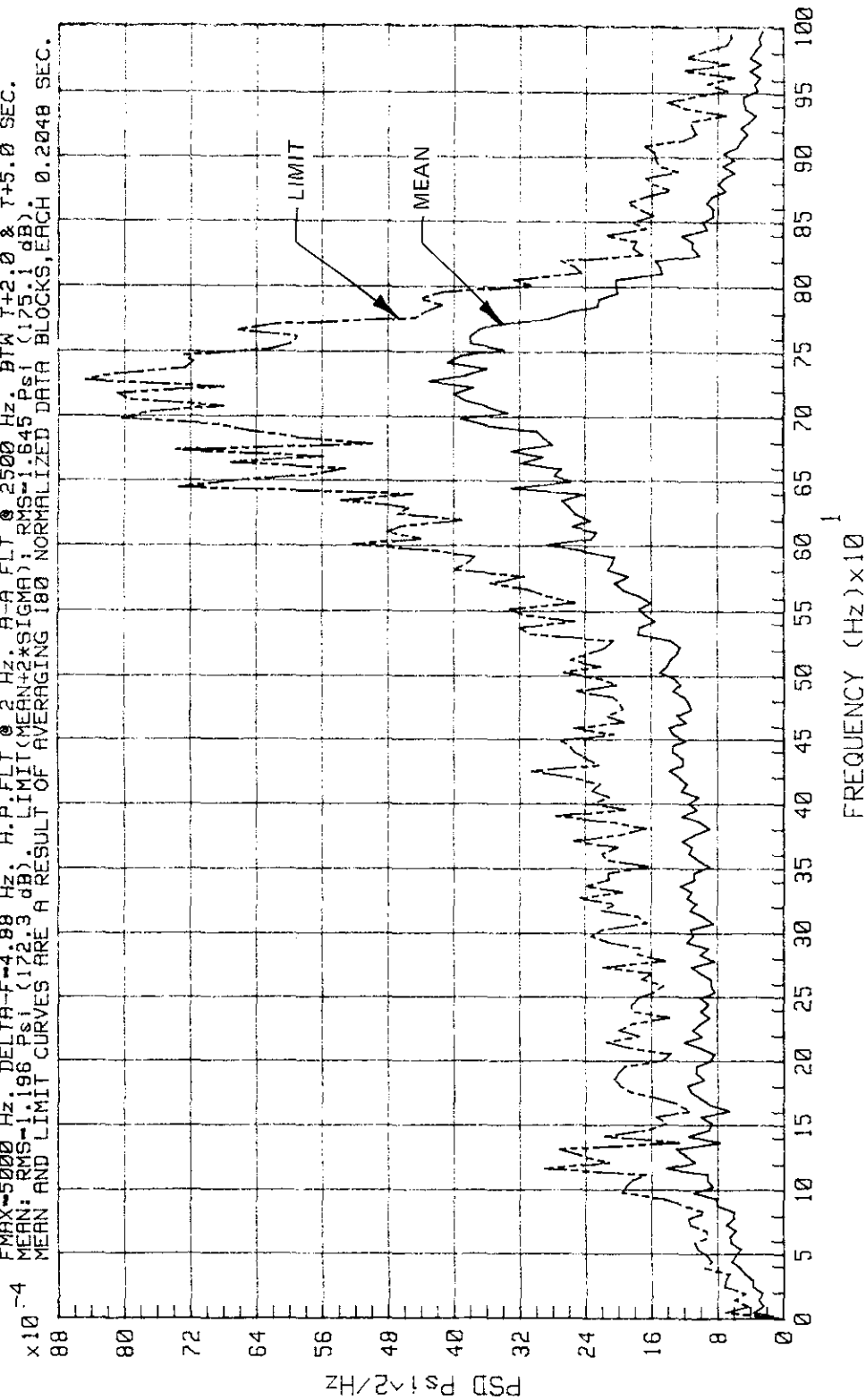


Figure 2-41. STS-9 and -11 Lift-Off Peak - Centaur Porch Assembly Pressures (No Hanning)

FILE: MEAN LIMIT

LIMIT CURVE GOVERNS PORCH DESIGN LOADS AT FREQUENCIES BELOW APPROXIMATELY 100 Hz.
 SENSORS: STS-9 (KSRP0018 THRU KSRP008A) & STS-11 (KSRP0028 THRU KSRP008A), HANNED 2x.
 FMAX=1000 Hz, DELTA-F=1.953 Hz, H.P.FLT=1 Hz, A-A FLT=500 Hz, FROM T+1.5 TO T+8.17 SEC.
 MEAN: RMS=0.711 Psi (167.8 dB), LIMIT (MEAN+2*SIGMA): RMS=0.926 Psi (170.1 dB).
 MEAN AND LIMIT CURVES ARE A RESULT OF AVERAGING 375 NORMALIZED DATA BLOCKS, EACH 0.512 SEC.

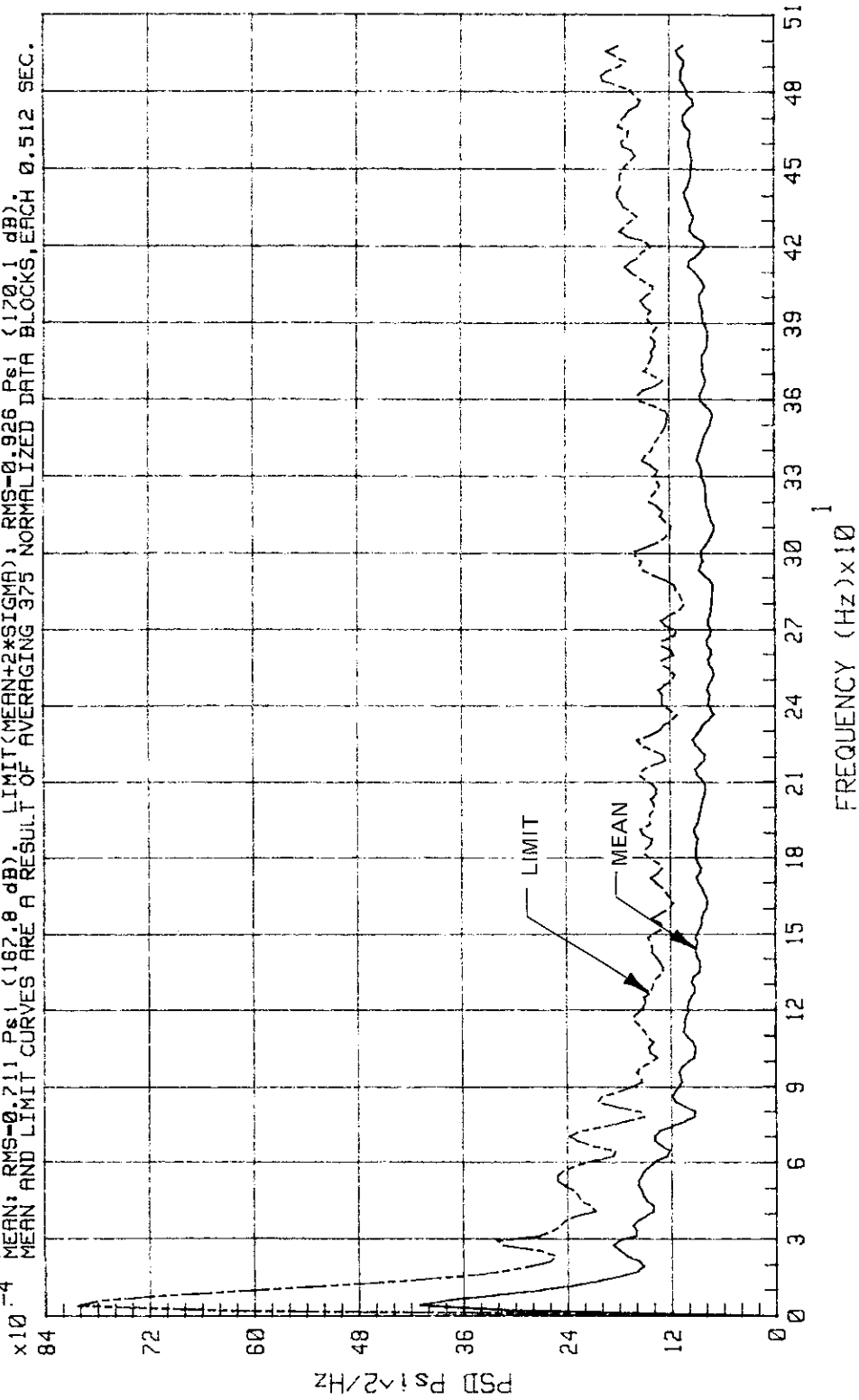
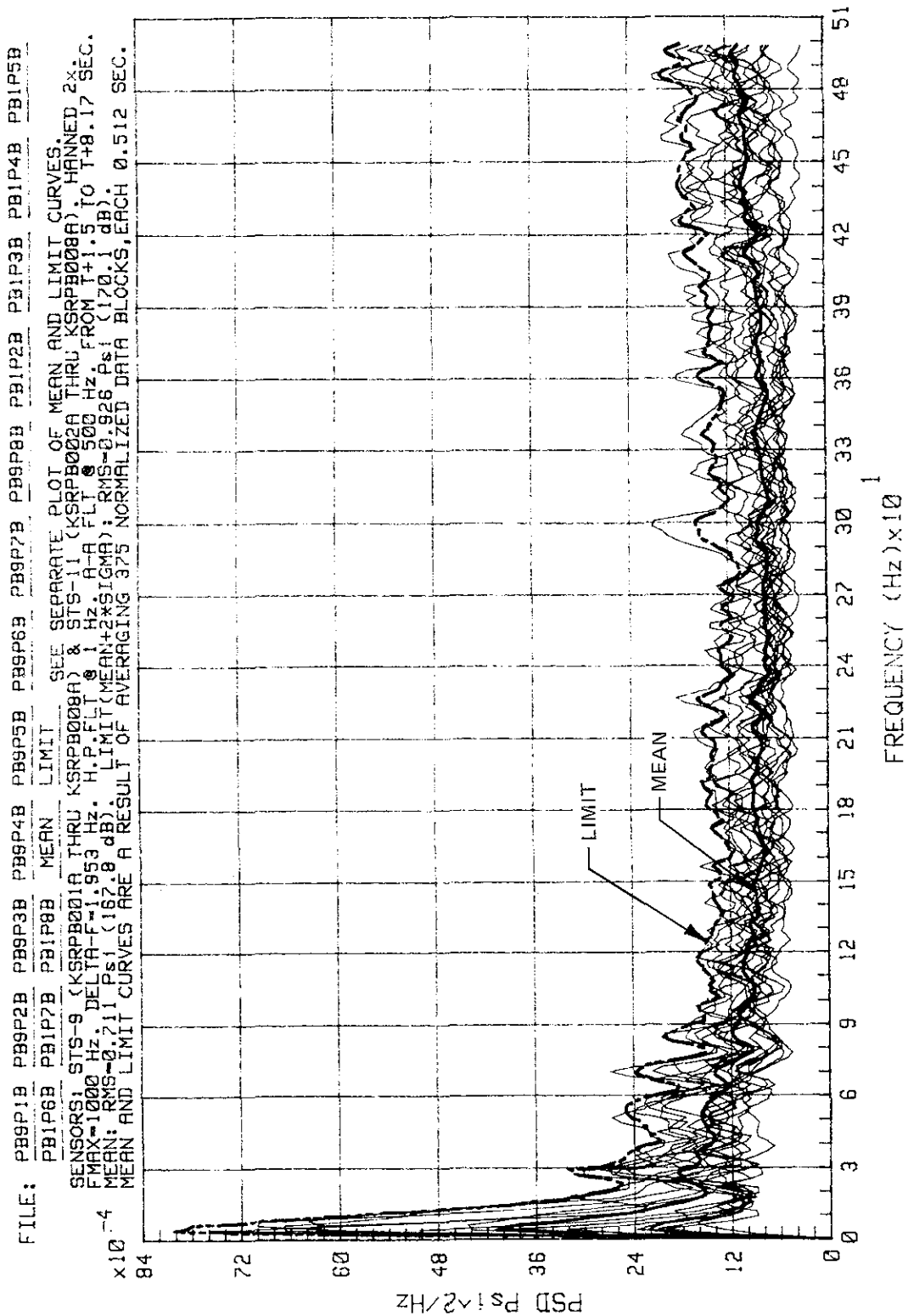


Figure 2-42. STS-9 and -11 Lift-Off Peak - Centaur Porch Assembly Pressures
 (Mean and Limit; $F_{max} = 1 \text{ kHz}$)

KSC-DD-818-TR

Figure 2-43. STS-9 and -11 Lift-off Peak - Centaur Porch Assembly Pressures ($F_{\text{max}} = 1 \text{ kHz}$)

FILE: MEAN LIMIT

SENSORS: STS-9 (KSRP0001A THRU KSRP0008A) & STS-11 (KSRP0002A THRU KSRP0008A), HANNED 2X.
 FMAX=1000 Hz, DELTA-F=1.953 Hz, H.P.FLT @ 1 Hz, A-A FLT @ 500 Hz, FROM 1+1.5 TO 1+8.17 SEC.
 MEAN: RMS=0.401 Psi (162.8 dB), LIMIT(MEAN+2*SIGMA): RMS=0.529 Psi (165.2 dB).
 MEAN AND LIMIT CURVES ARE A RESULT OF AVERAGING 375 NORMALIZED DATA BLOCKS, EACH 0.512 SEC.

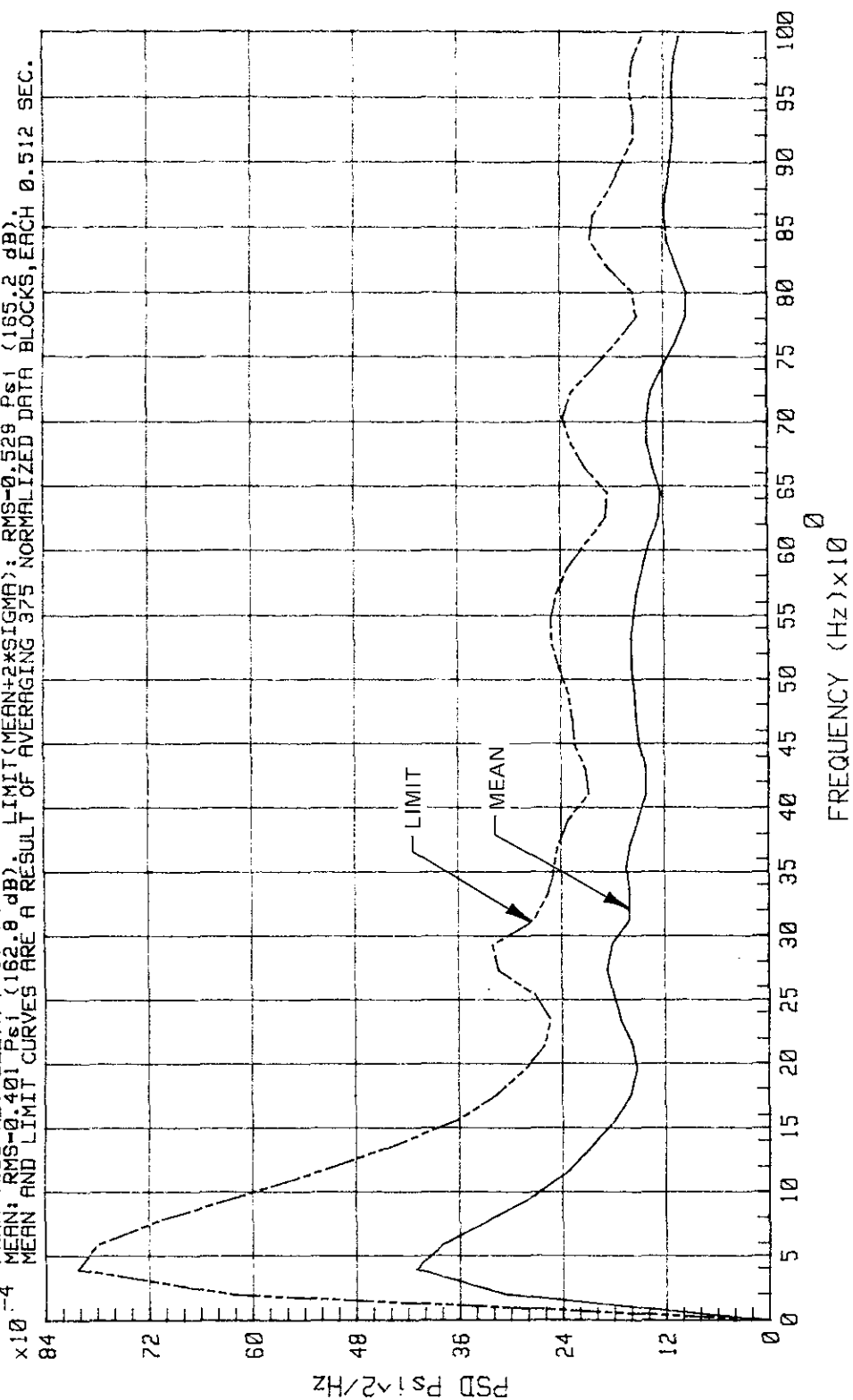


Figure 2-44. STS-9 and -11 Lift-Off Peak - Centaur Porch Assembly Pressures
 (Mean and Limit; F_{max} = 1,000 Hz; High-Pass Filter at 1 Hz)

KSC-DD-818-TR

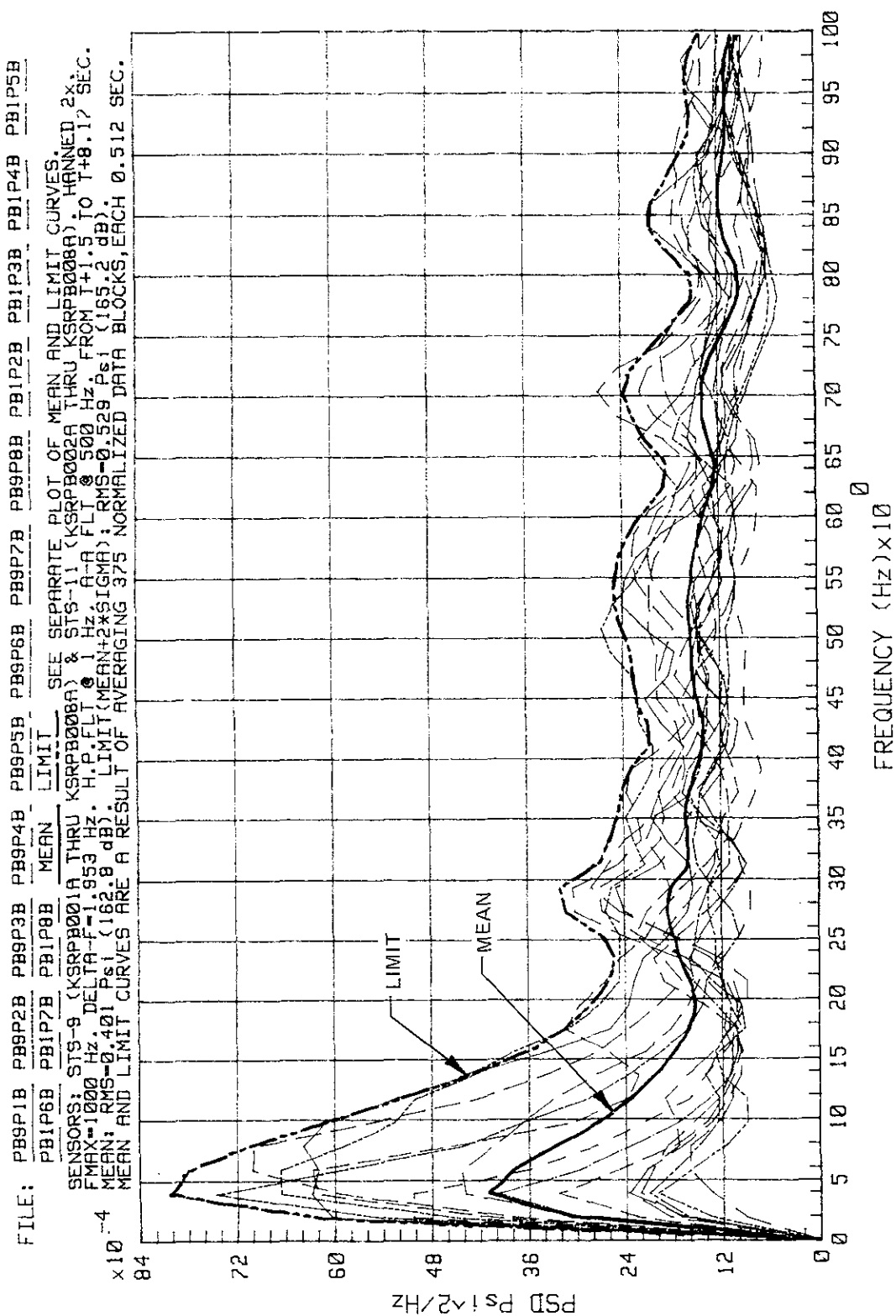


Figure 2-45. STS-9 and -11 Lift-Off Peak - Centaur Porch Assembly Pressures
($F_{\max} = 1,000$ Hz; High-Pass Filter at 1 Hz)

FILE: MEAN LIMIT

THIS PLOT IS PRESENTED FOR COMPARISON OF MEAN AND LIMIT CURVES CALCULATED WITHOUT HANNING.
 SENSORS: STS-9 (KSRP0001A THRU KSRP0008A) & STS-11 (KSRP0002A THRU KSRP0008A), NO HANNING.
 FMAX=1000 Hz. DELTA-F=1.953 Hz. H.P.FLT @ 1 Hz. A-A FLT @ 500 Hz. FROM T+1.5 TO T+8.17 SEC.
 MEAN: RMS=0.409 Psi (163.0 dB). LIMIT (MEAN+2*SIGMA): RMS=0.562 Psi (165.7 dB).
 MEAN AND LIMIT CURVES ARE A RESULT OF AVERAGING 375 NORMALIZED DATA BLOCKS, EACH 0.512 SEC.

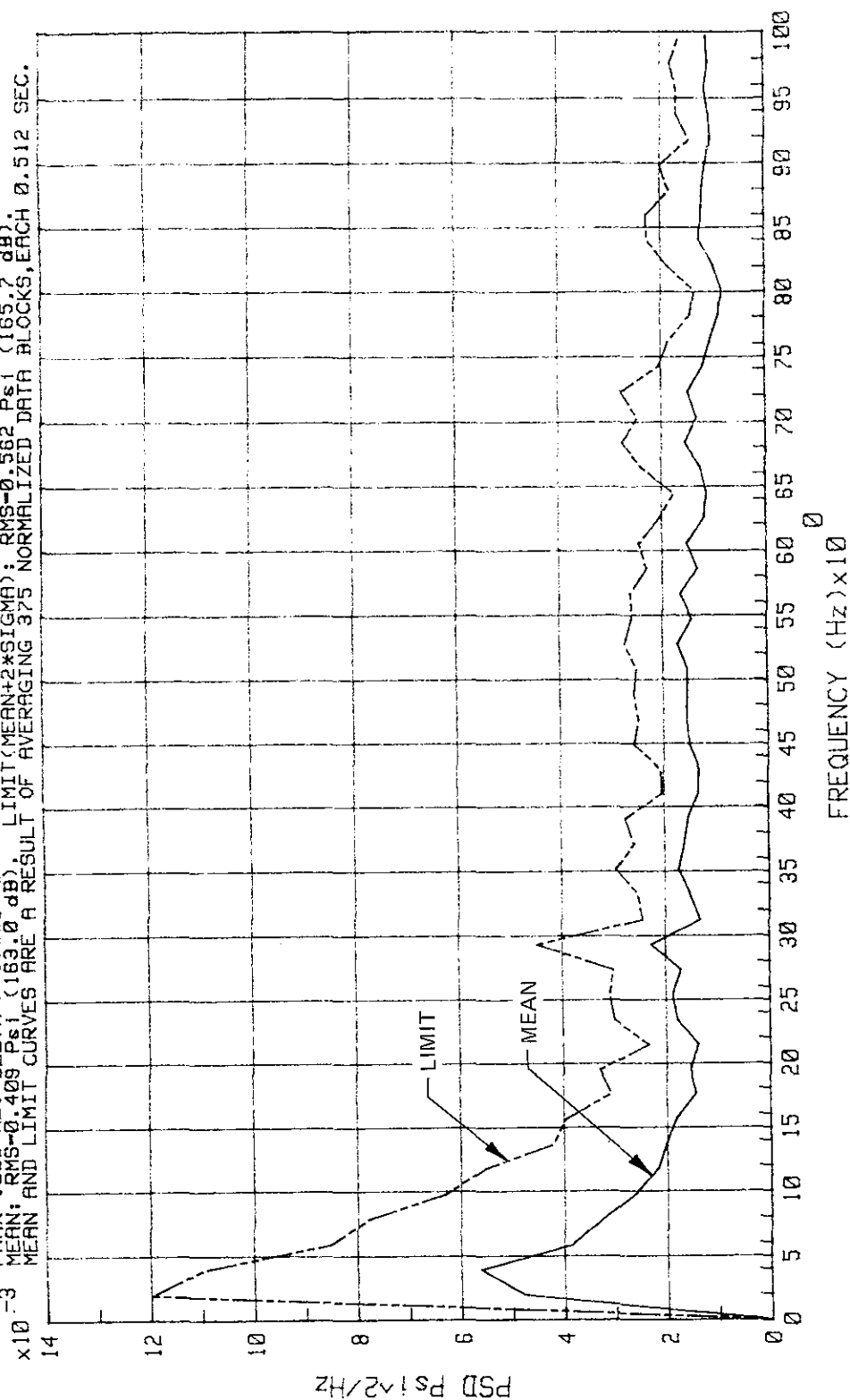
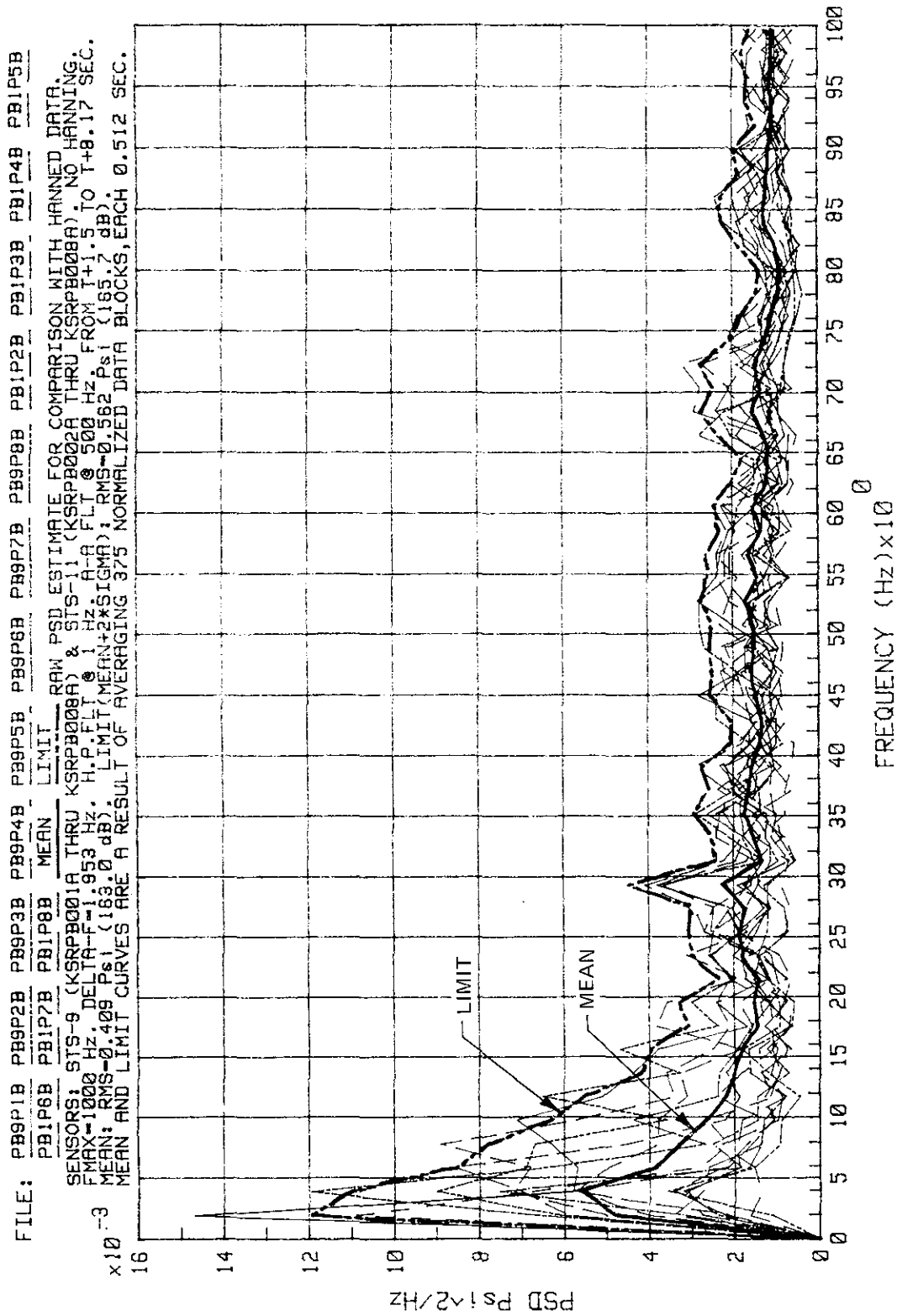


Figure 2-46. STS-9 and -11 Lift-Off Peak - Centaur Porch Assembly Pressures
 (Mean and Limit; $F_{max} = 1,000$ Hz; High-Pass Filter at 1 Hz; No Hanning)



FILE: PB9P1E PB9P2E PB9P3E PB9P4E PB1P2E PB1P3E PB1P4E MEAN LIMIT

LIMIT CURVE MAY GOVERN PORCH DESIGN LOADS AT FREQUENCIES BELOW APPROX. 5 Hz (LIMITED # OF CIC'S).
 SENSORS: STS-9 (KSRPB001A THRU KSRPB004A) & STS-11 (KSRPB002A THRU KSRPB004A). NO HANNING.
 FMAX=100 Hz. DELTA F=0.3906 Hz. H.P. FLT @ 1 Hz. A-A FLT @ 20 Hz. FROM T+1.5 TO T+11.74 SEC.
 MEAN: RMS=0.241 Psi. (158.4 dB). LIMIT (MEAN+2*SIGMA): RMS=0.332 Psi (161.2 dB).
 MEAN AND LIMIT CURVES ARE A RESULT OF AVERAGING 49 NORMALIZED DATA BLOCKS, EACH 2.56 SEC.

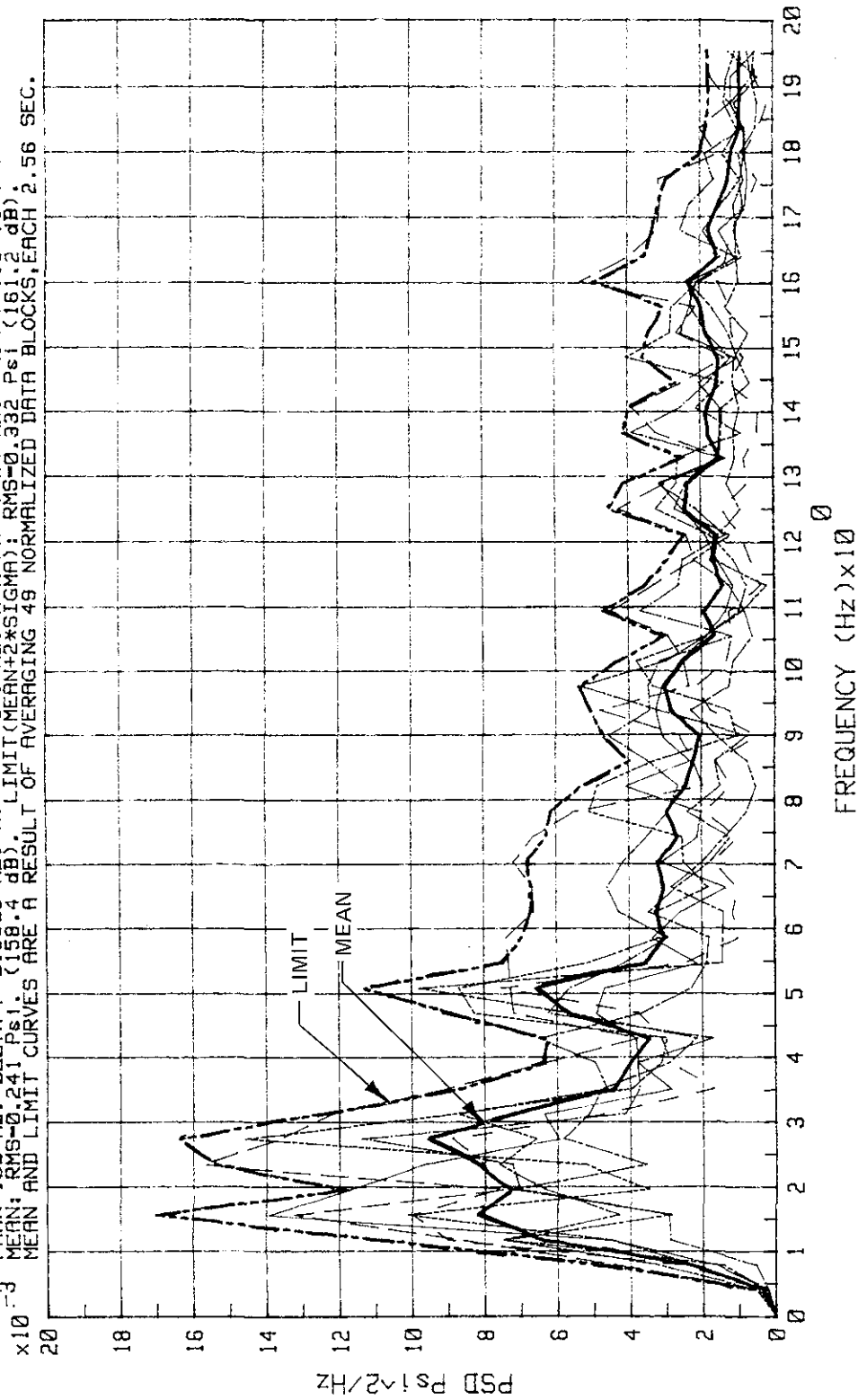


Figure 2-48. STS-9 and -11 Lift-Off Peak - Centaur Porch Assembly Pressures
 ($F_{\max} = 100 \text{ Hz}$), Sensors Closest to Vehicle

KSC-DD-818-TR

FILE: PB9P5E PB9P6E PB9P7E PB9P8E PB9P9E PB1P5E PB1P6E PB1P7E PB1P8E MEAN LIMIT

SENSORS: STS-9 (KSRPB005A THRU KSRPB008A) & STS-11 (KSRPB005A THRU KSRPB008A). NO HANNING.
 FMAX=100 Hz. DELTA-F=0.3906 Hz. H.P.FLT @ 1 Hz. A-A FLT @ 20 Hz. FROM T+1.5 TO T+11.74 SEC.
 MEAN: RMS=0.119 Psi. (152.2 dB). LIMIT(MEAN+2*SIGMA): RMS=0.161 Psi (154.9 dB).
 MEAN AND LIMIT CURVES ARE A RESULT OF AVERAGING 56 NORMALIZED DATA BLOCKS, EACH 2.55 SEC.

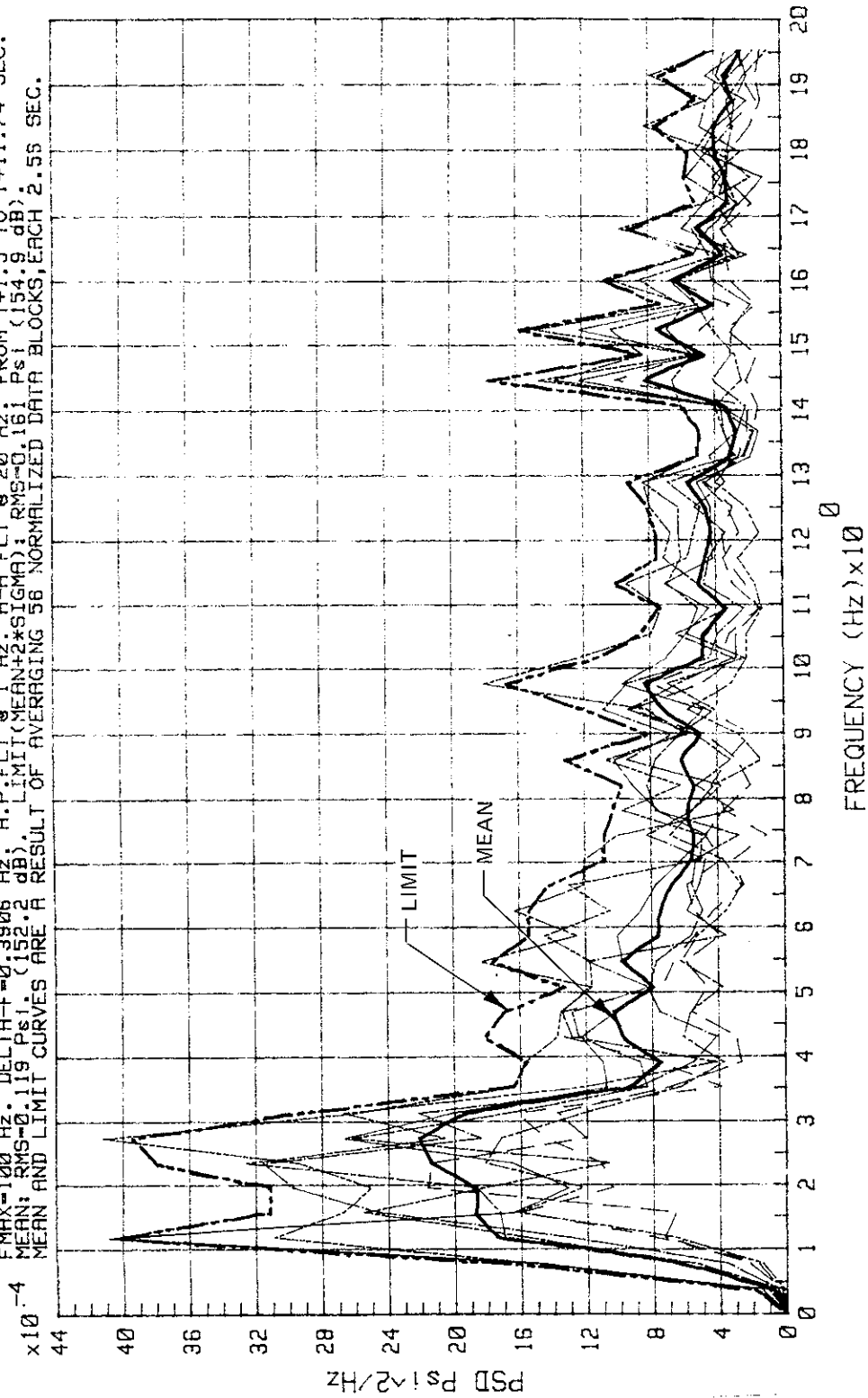


Figure 2-49. STS-9 and -11 Lift-Off Peak - Centaur Porch Assembly Pressures
 ($F_{\text{max}} = 100 \text{ Hz}$), Sensors Farthest From Vehicle

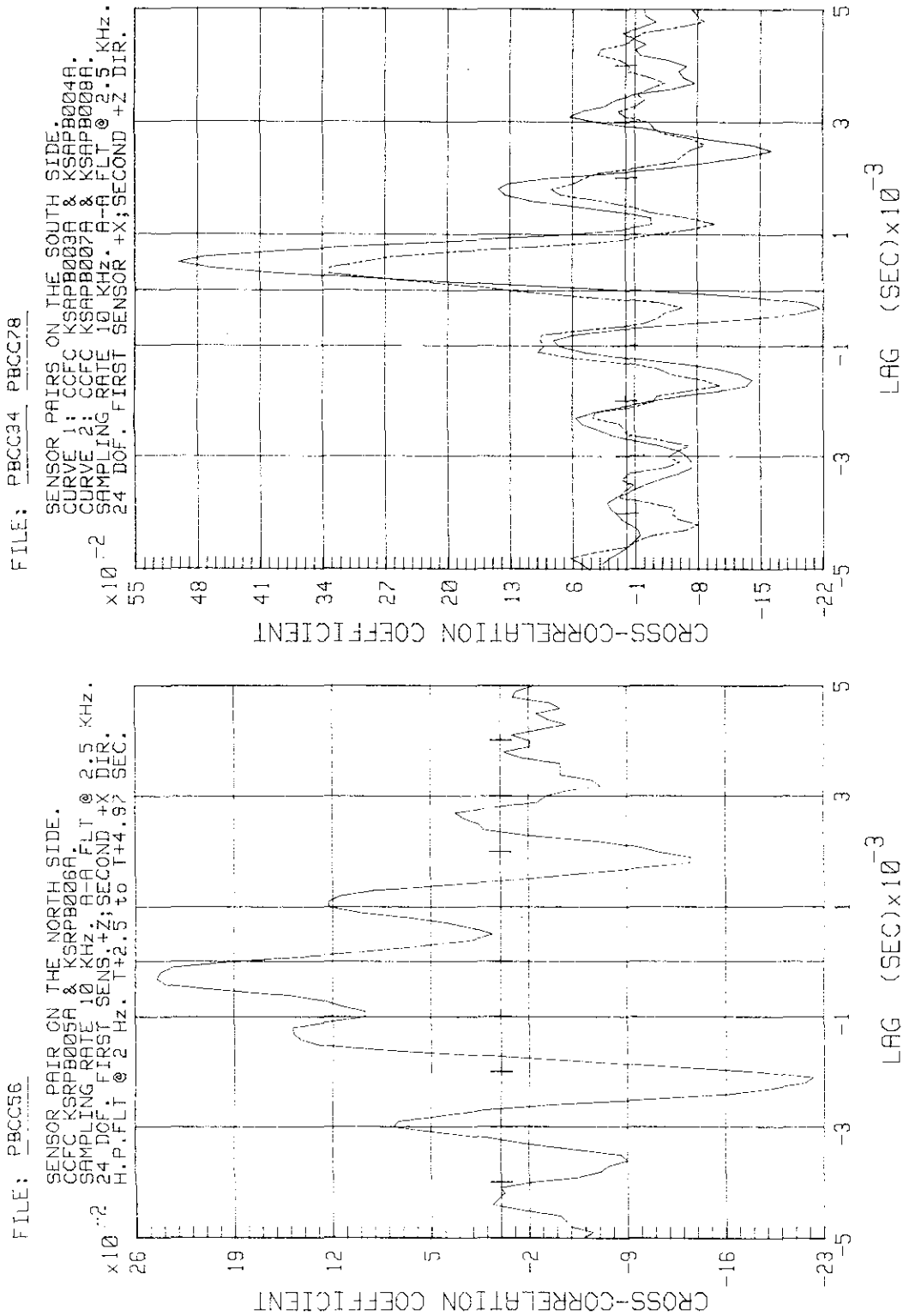


Figure 2-50. STS-11 Lift-Off Peak - Centaur Porch Pressure Cross-Correlation
 (Adjacent Sensors; Sampling Rate = 10 KHz)

KSC-DD-818-TR

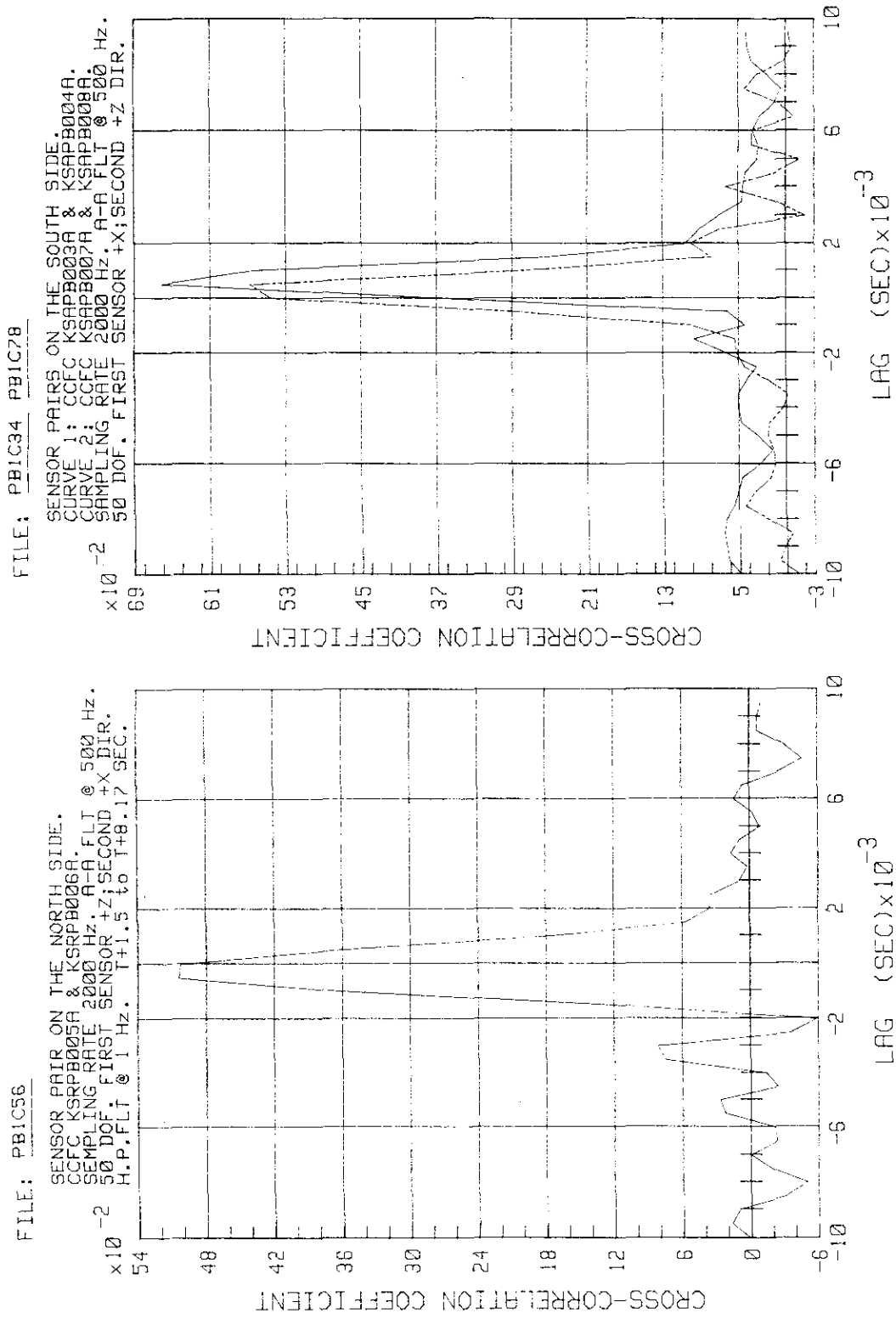


Figure 2-51. STS-11 Lift-Off Peak - Centaur Porch Pressure Cross-Correlation
 (Adjacent Sensors; Sampling Rate = 2 kHz)

FILE: PBCL34 PBCL56 PBCL78

F_{MAX}=5000 HZ. DELTA-F=4.88 HZ. A-A FILTER @ 2500 HZ. PROCESSING BTW T+2.0 & T+4.97 SEC.
EACH COHERENCE 24 DOF. HANNED 5x IN ORDER TO EMPHASIZE TRENDS.

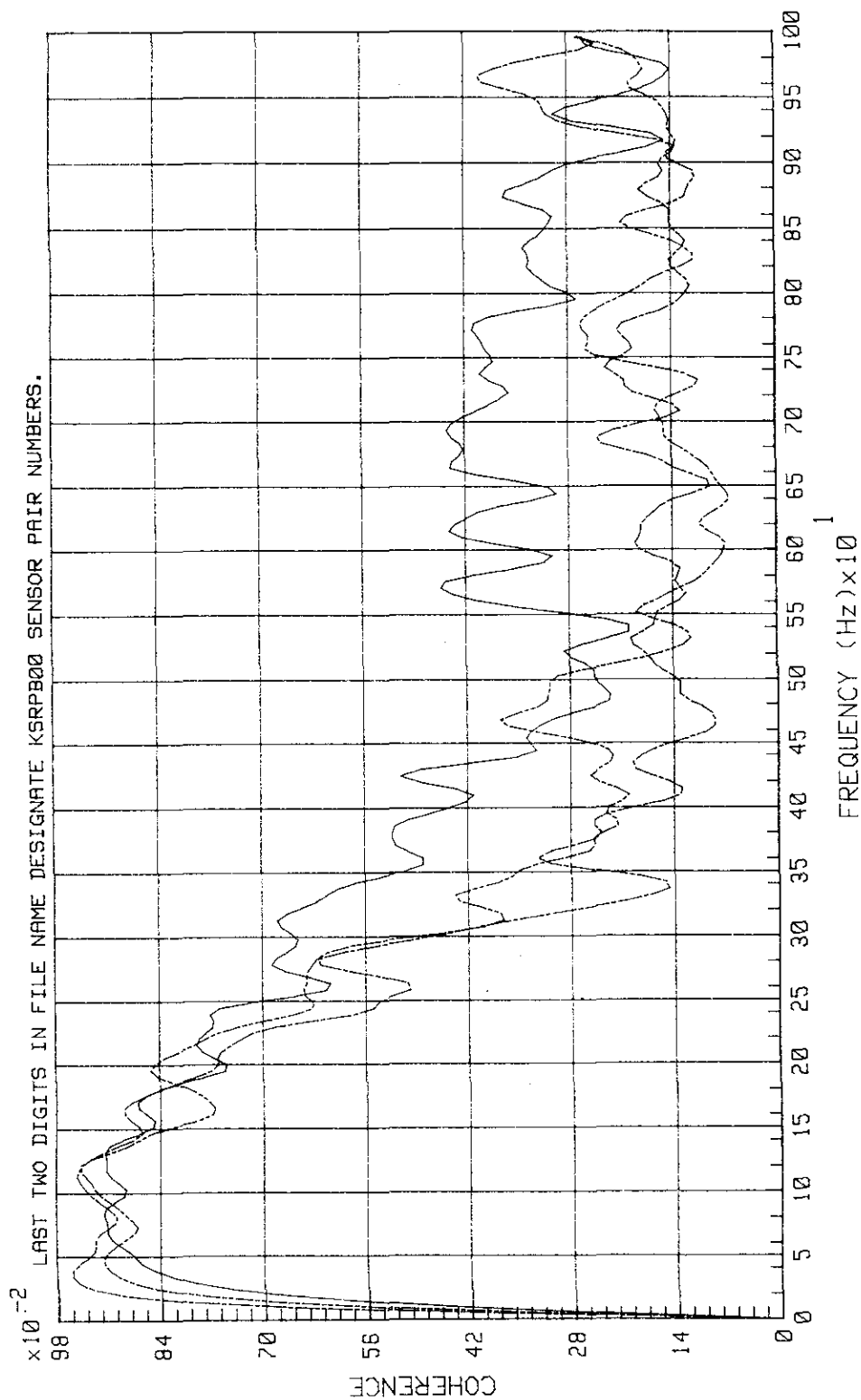


Figure 2-52. STS-11 Lift-Off Peak - Centaur Porth Pressure Coherences
(Adjacent Sensors; F_{max} = 5 kHz)

KSC-DD-818-TR

FILE: PBIL34 PBIL56 PBIL78

F_{MAX}=1000 Hz. DELTA-F=1.953 Hz. A-A FILTER @ 500 Hz. PROCESSING FROM T+1.5 TO T+8.17 SEC.
 EACH COHERENCE 50 DOF. HANNED 5x IN ORDER TO EMPHASIZE TRENDS.

LAST TWO DIGITS IN FILE NAME DESIGNATE KSRPB00 SENSOR PAIR NUMBERS.

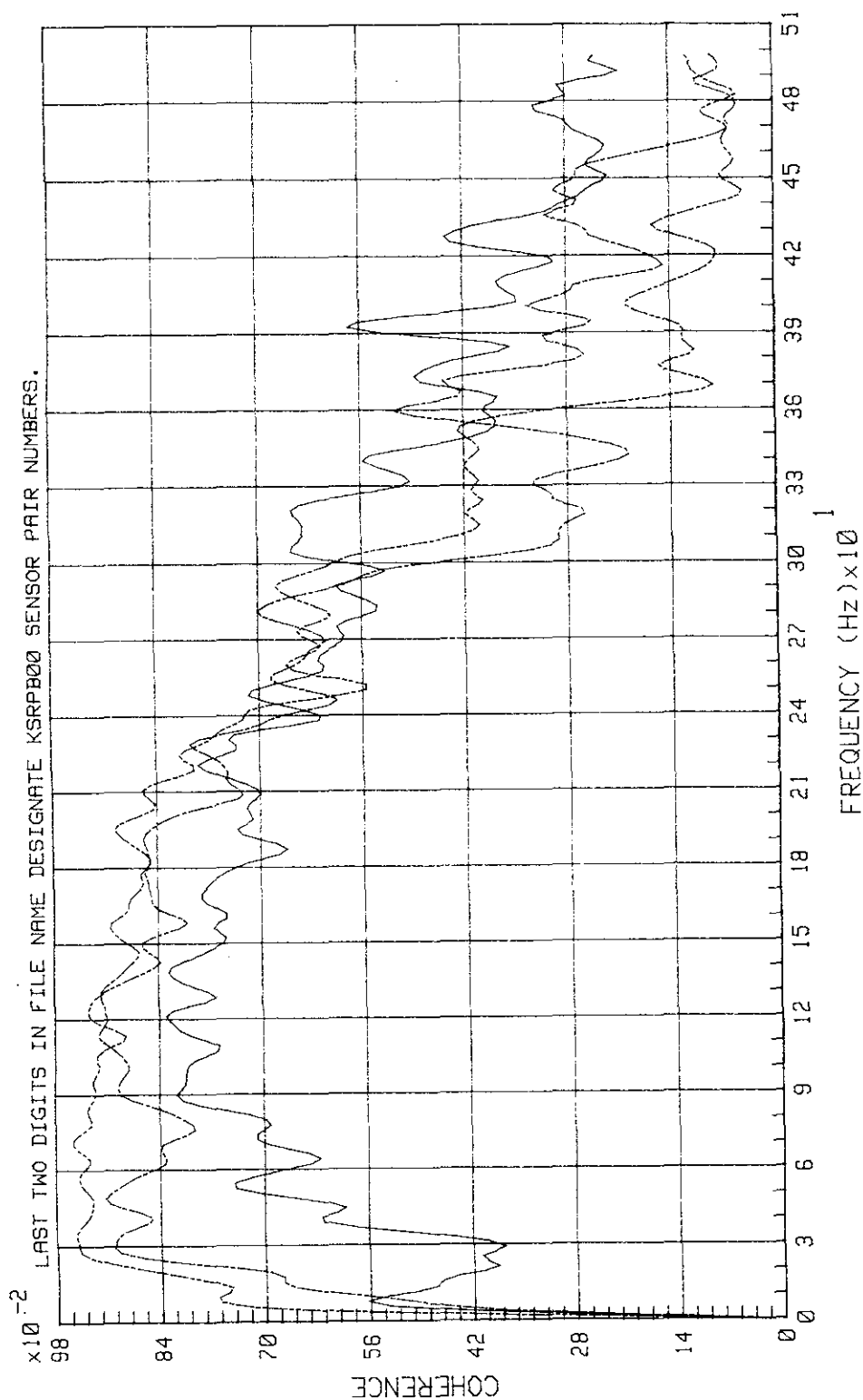


Figure 2-53. STS-11 Lift-Off Peak - Centaur Porch Pressure Coherences
 (Adjacent Sensors; $F_{MAX} = 1 \text{ kHz}$)

FILE: PB1M34 PB1M56 PB1M78

F_{MAX} = 100 Hz, DELTA-F = 0.3908 Hz, A-A FILTER @ 50 Hz, PROCESSING FROM T+1.5 TO T+11.74 SEC.
EACH COHERENCE 14 DOF, NO HANNING.

LAST TWO DIGITS IN FILE NAME DESIGNATE KSRPB00 SENSOR PAIR NUMBERS.

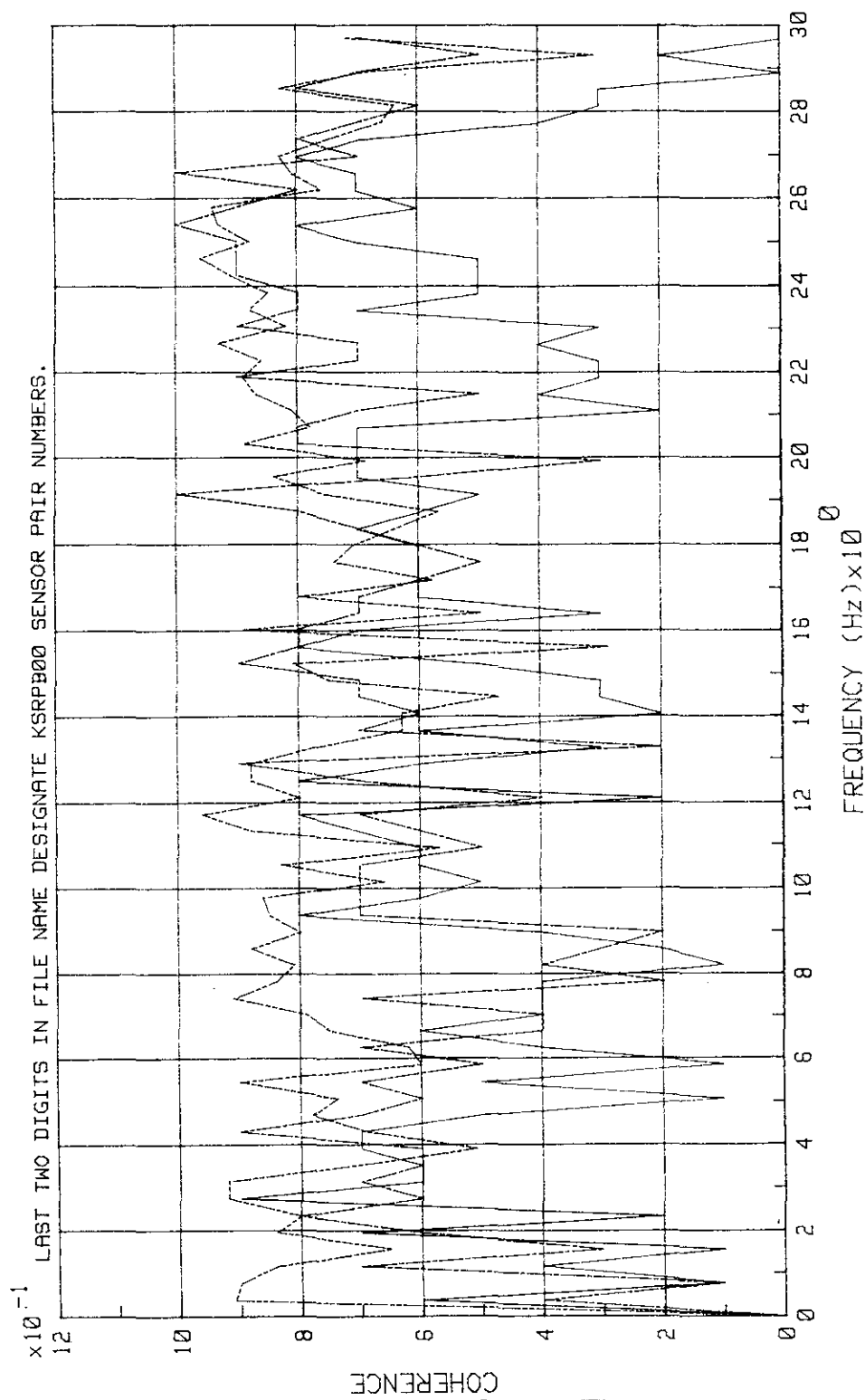


Figure 2-54. STS-11 Lift-Off Peak - Centaur Porth Pressure Coherences
(Adjacent Sensors; $F_{max} = 100$ Hz)

KSC-DD-818-TR

FILE: PB1R2A PB1R2B

LOW FREQUENCY PRESSURE TIME HISTORY FROM T=5.0 TO T+15.24 SEC. BANDPASS FILTER 1-10 Hz.
 SENSOR KSRPB002A (X-DIR HORIZONTAL). SAMPLING RATE 200 Hz.
 NOTE: ADJACENT SENSOR KSRPB001A (Z-DIR VERTICAL) FAILED. THIS PLOT IS A SINGLE SENSOR OUTPUT.
 PLOT TIME SCALE IS REFERENCED TO T-ZERO=34:13:00.0016 GMT (1984).

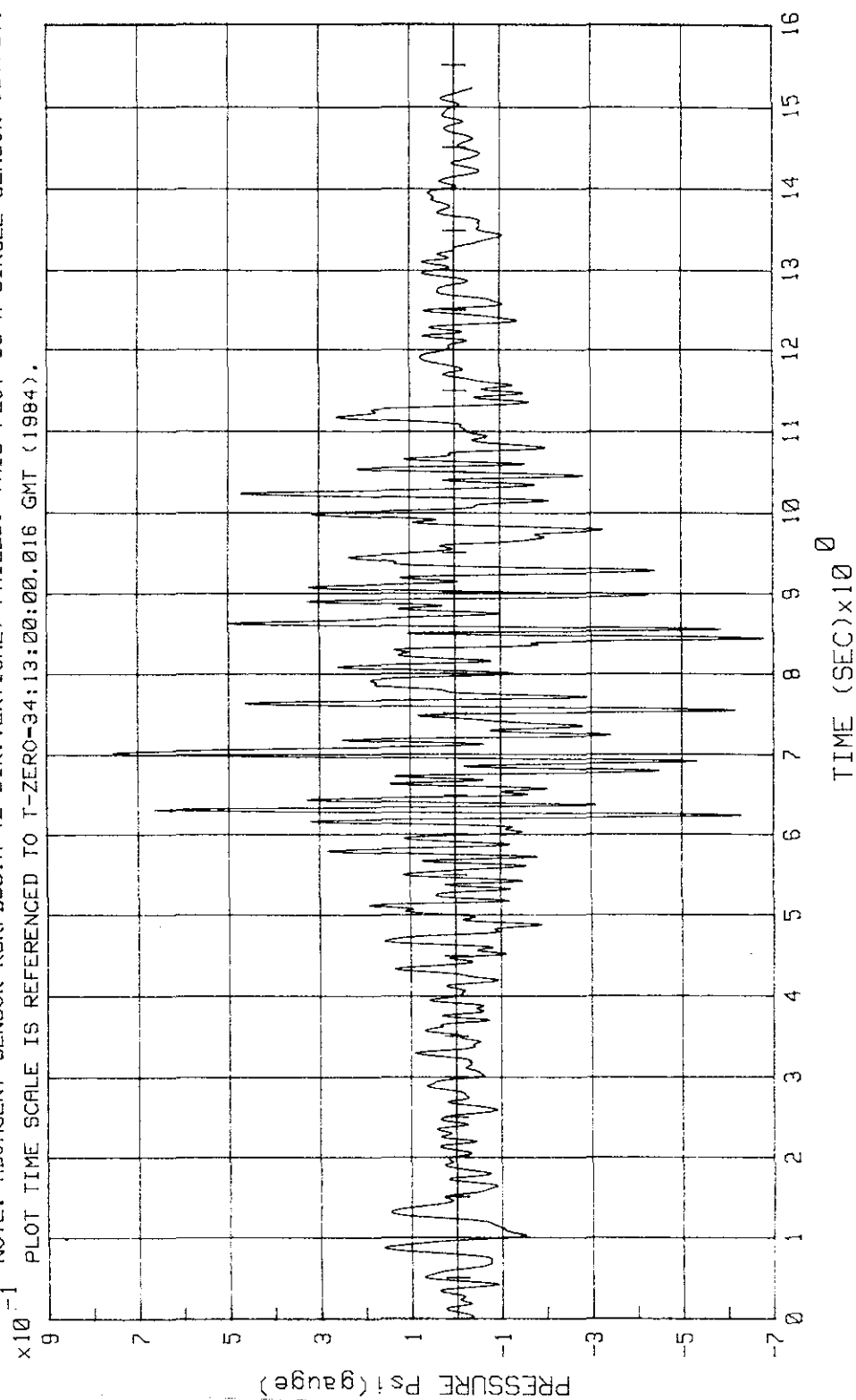


Figure 2-55. STS-11 Lift-Off - Centaur Porch Assembly Pressures at East End, Sensor KSRPB002A
 (1 Hz to 10 Hz)

FILE: PBIR4A PBIR3A

LOW FREQUENCY PRESSURE TIME HISTORY FROM T=0.0 TO T+10.24 SEC. BANDPASS FILTER 1-10 Hz.
SENSORS: KSRPB004A (Z-DIR.VERTICAL) & KSRPB003A (X-DIR.HORIZONTAL). SAMPLING RATE 200 Hz.

$\times 10^{-1}$ PLOT TIME SCALE IS REFERENCED TO T-ZERO=34:13:00.016 GMT (1984).

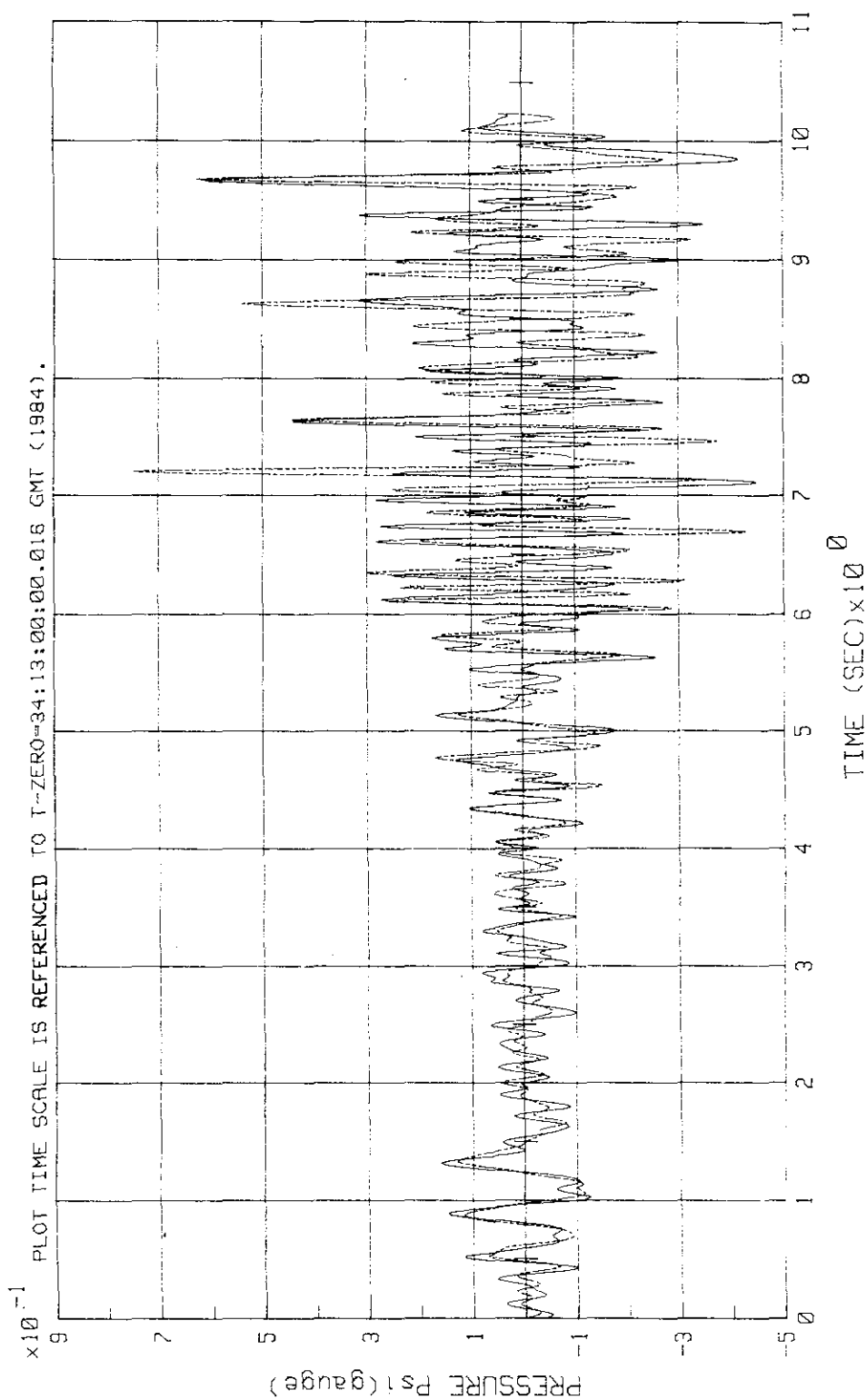


Figure 2-56. STS-11 Lift-Off - Centaur Porch Assembly Pressures at East End, Sensors KSRPB003A and -004A, 1 Hz to 10 Hz (From T to T + 10.24 s)

KSC-DD-818-TR

FILE: PB1R4B PB1R3B

LOW FREQUENCY PRESSURE TIME HISTORY FROM T=5.0 TO T+15.24 SEC. BANDPASS FILTER 1-10 Hz.
 SENSORS: KSRPB004A (Z-DIR.VERTICAL) & KSRPB003A (X-DIR.HORIZONTAL). SAMPLING RATE 200 Hz.

PLOT TIME SCALE IS REFERENCED TO T-ZERO=34:13:00.0016 GMT (1984).

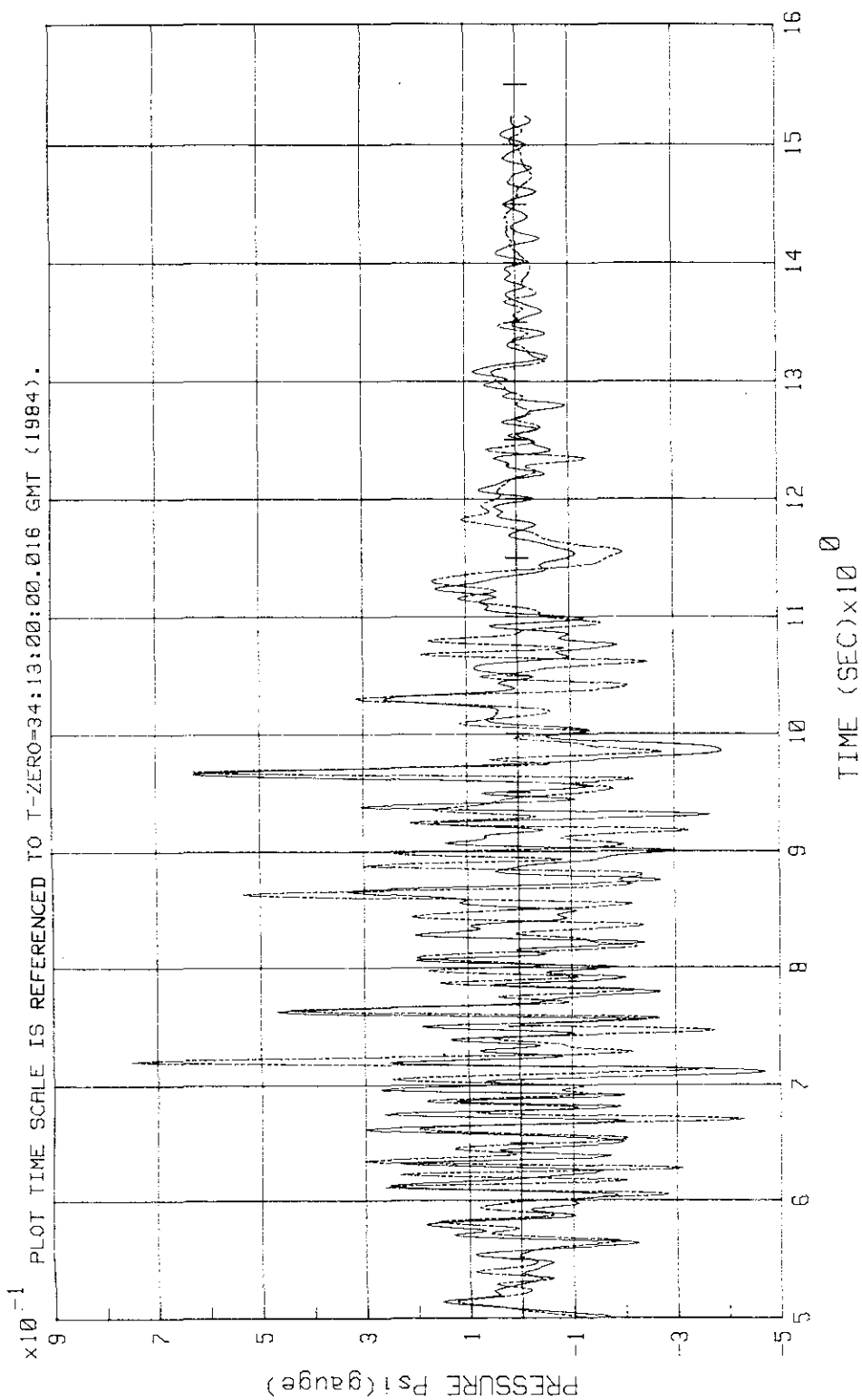


Figure 2-57. STS-11 Lift-Off - Centaur Porch Assembly Pressures at East End,
 Sensors KSRPB003A and -004A, 1 Hz to 10 Hz (From T + 5 to T + 15.24 s)

FILE: PB1R5A PB1R6A

LOW FREQUENCY PRESSURE TIME HISTORY FROM T=0.0 TO T+10.24 SEC. BANDPASS FILTER 1-10 Hz.
 SENSORS: KSRPB005A (Z-DIR, VERTICAL) & KSRPB006A (X-DIR, HORIZONTAL). SAMPLING RATE 200 Hz.
 NOTE: BOTH SENSORS RECORDED NEARLY IDENTICAL PRESSURE TIME HISTORIES. SEE CALCULATED
 COHERENCES FOR INTERVALS T+1.5 TO T+8.17 SEC & T+1.5 TO T+11.74 SEC.
 PLOT TIME SCALE IS REFERENCED TO T-ZERO=34:13:00:00.016 GMT (1984).

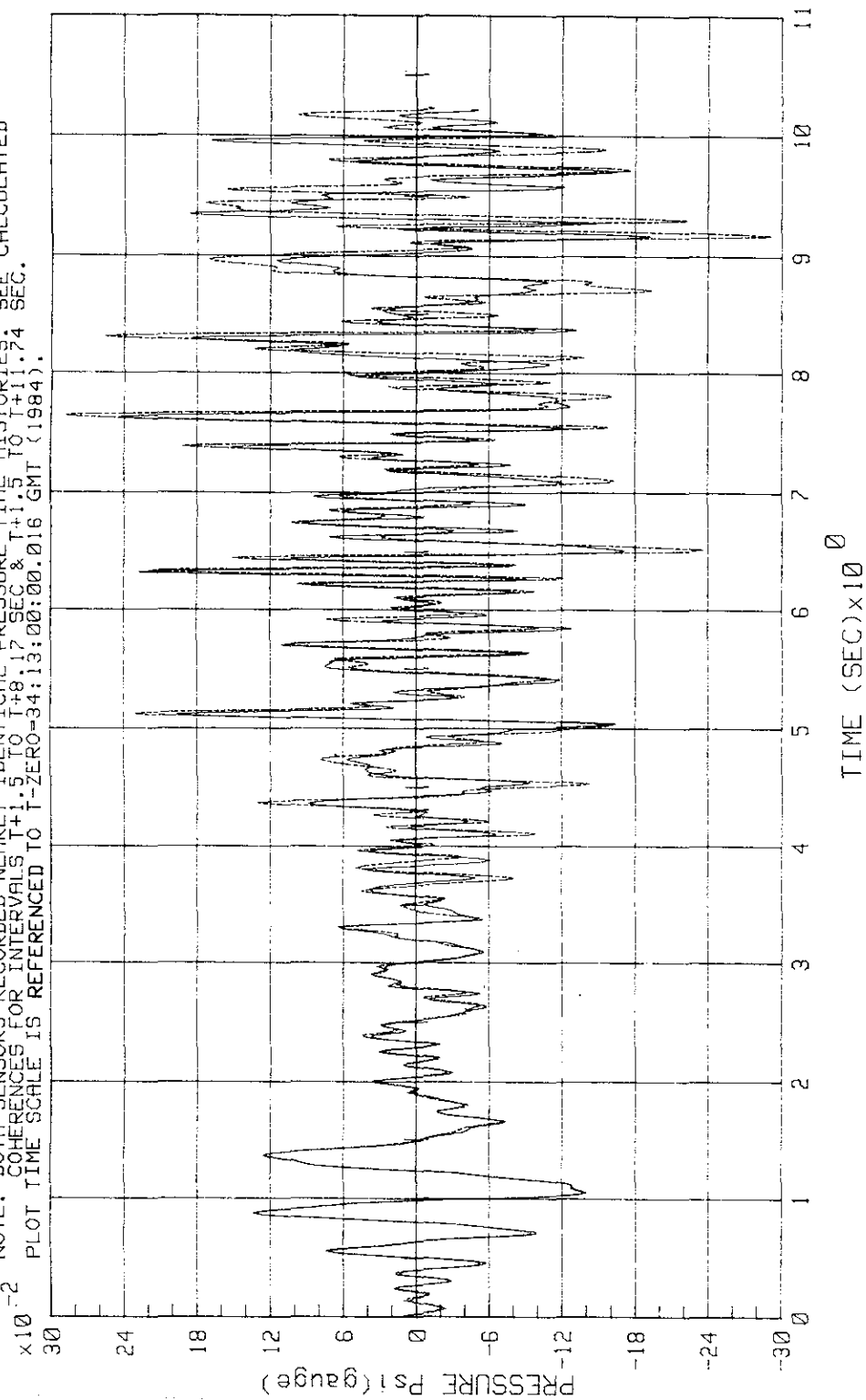


Figure 2-58. STS-11 Lift-Off - Centaur Porch Assembly Pressures at FSS Support,
 Sensors KSRPB005A and -006A, 1 Hz to 10 Hz (From T to T + 10.24 s)

KSC-DD-818-TR

FILE: PB1R5B PB1R6B

LOW FREQUENCY PRESSURE TIME HISTORY FROM T=5.0 TO T+15.24 SEC. BANDPASS FILTER 1-10 Hz.
 SENSORS: KSRPB005A (Z-DIR.VERTICAL) & KSRPB006A (X-DIR.HORIZONTAL). SAMPLING RATE 200 Hz.

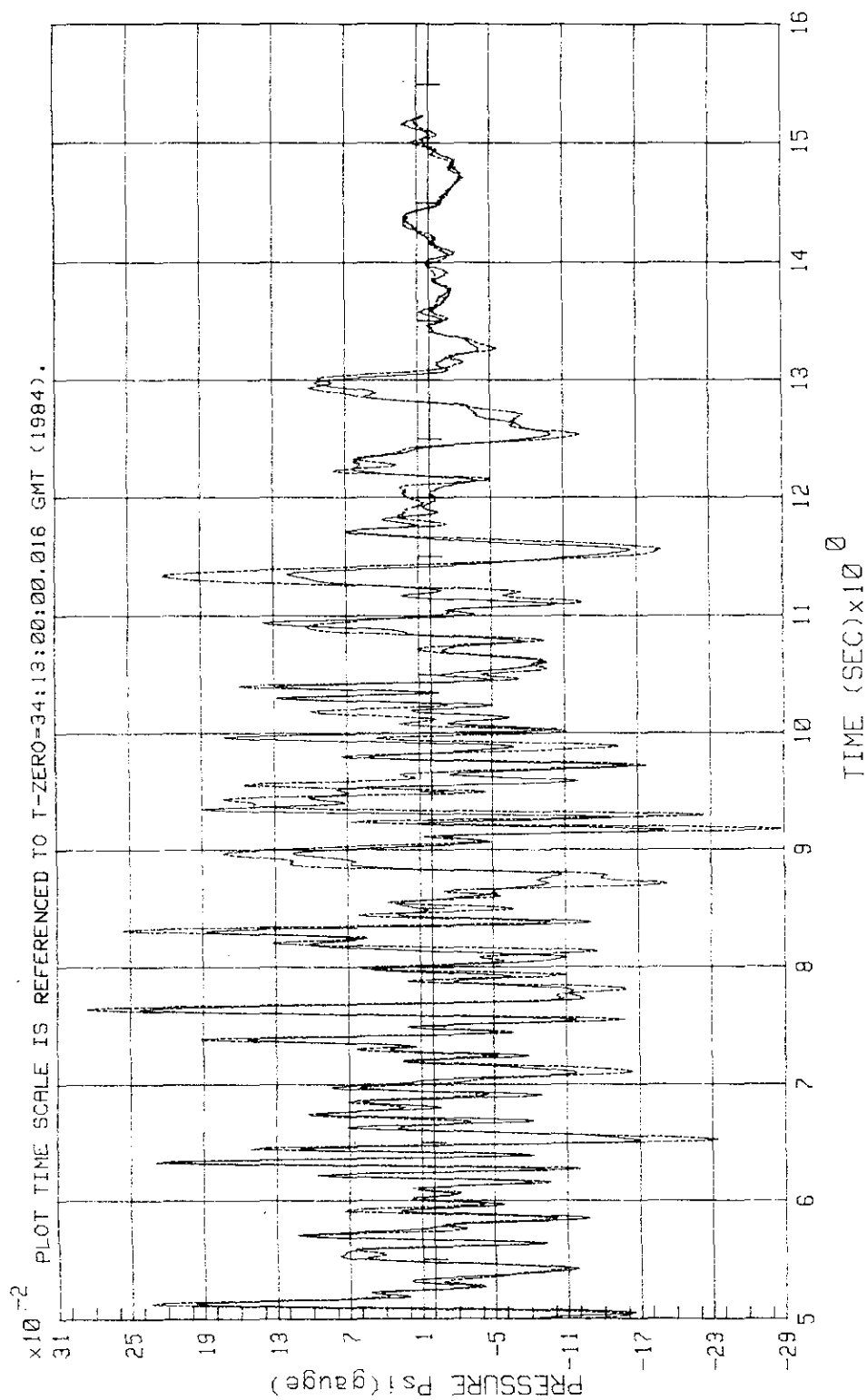


Figure 2-59. STS-11 Lift-Off - Centaur Porch Assembly Pressures at FSS Support,
 Sensors KSRPB005A and -006A, 1 Hz to 10 Hz (From T + 5 to T + 15.24 s)

FILE: PB1R8A PB1R7A

LOW FREQUENCY PRESSURE TIME HISTORY FROM T=0.0 TO T+10.24 SEC. BANDPASS FILTER 1-10 Hz.
SENSORS: KSRPB008A (Z-DIR.VERTICAL) & KSRPB007A (X-DIR.HORIZONTAL). SAMPLING RATE 200 Hz.

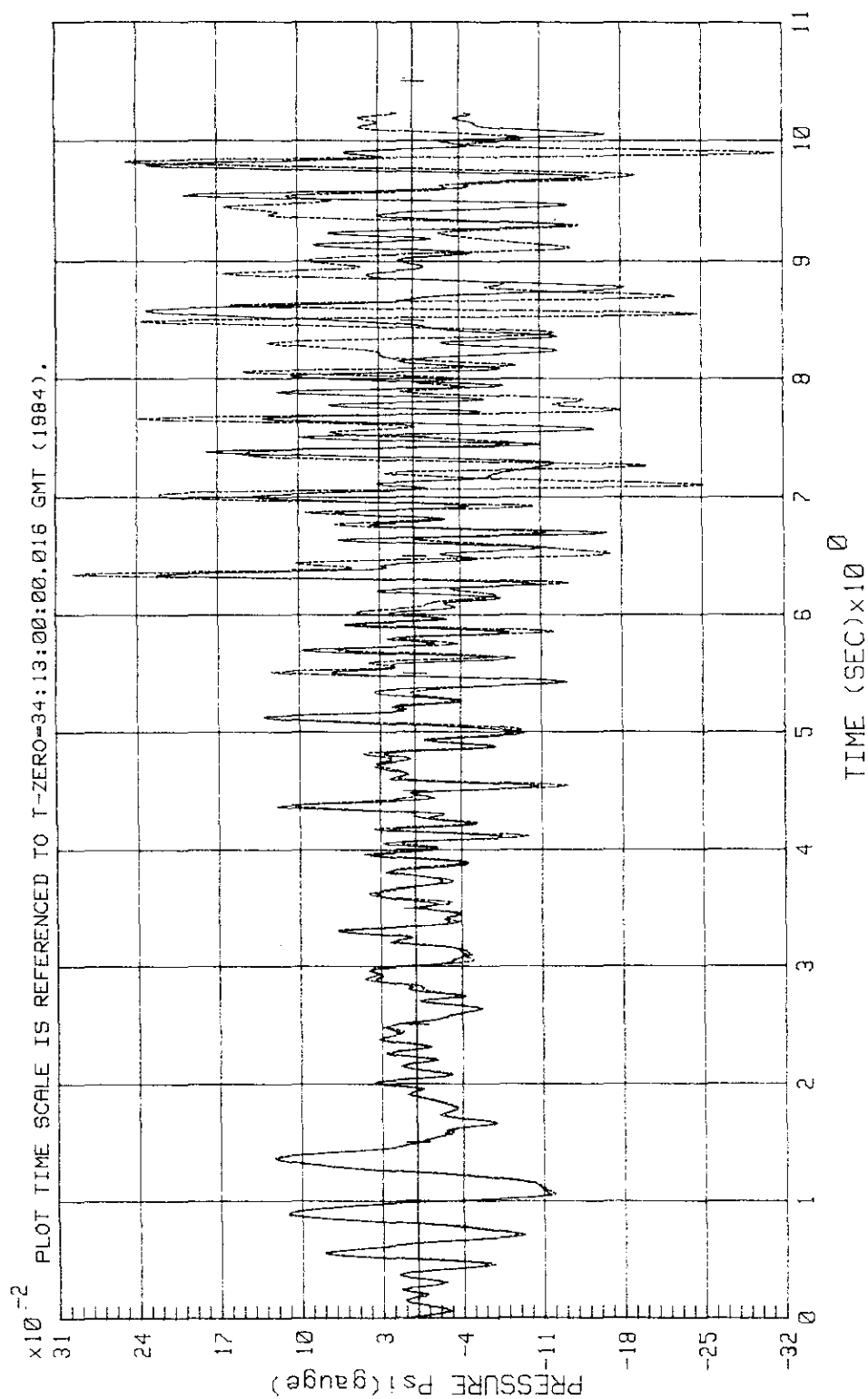


Figure 2-60. STS-11 Lift-Off - Centaur Porch Assembly Pressures at FSS Support, Sensors KSRPB007A and -C08A, 1 Hz to 10 Hz (From T to T + 10.24 s)

KSC-DD-818-TR

FILE: PB1R8B PB1R7B

LOW FREQUENCY PRESSURE TIME HISTORY FROM T=5.0 TO T+15.24 SEC. BANDPASS FILTER 1-10 Hz.
 SENSORS: KSRPB008A (Z-DIR.VERTICAL) & KSRPB007A (X-DIR.HORIZONTAL). SAMPLING RATE 200 Hz.

x10⁻² PLOT TIME SCALE IS REFERENCED TO T-ZERO=34:13:00.0016 GMT (1984).

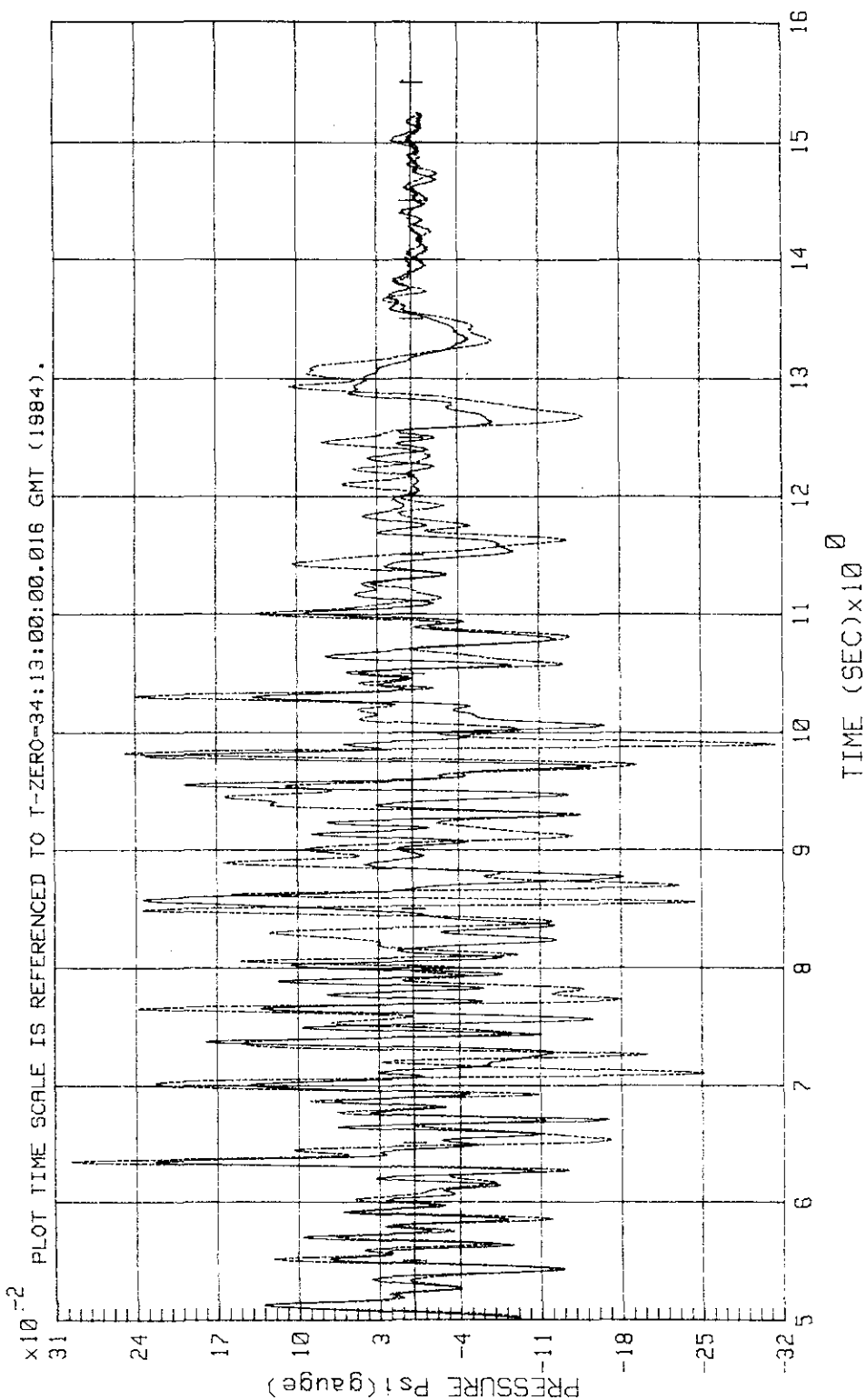
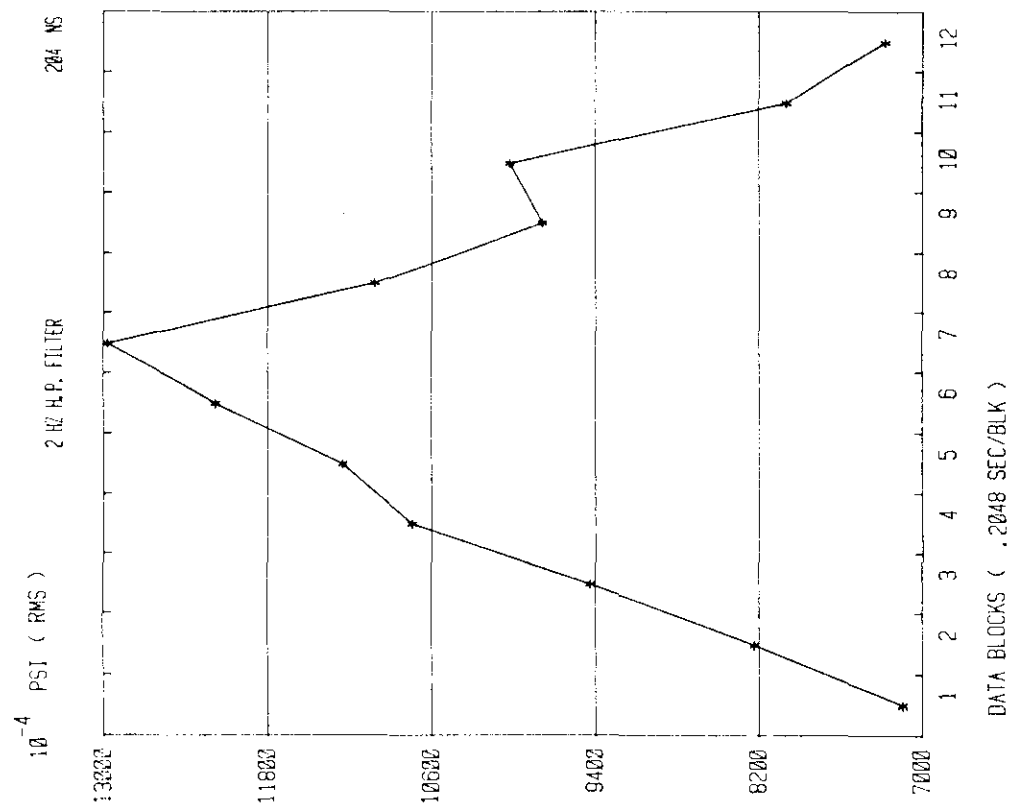


Figure 2-61. STS-11 Lift-Off - Centaur Porch Assembly Pressures at FSS Support, Sensors KSRPB007A and -008A, 1 Hz to 10 Hz (From T + 5 s to T + 16 s)

STS-11 LIFT-OFF PEAK
TIME HISTORY
KSC2002A CHANNEL A
START TIME = 1 + 2.00 SEC

BLOCK SIZE = 2048
SAMPLE RATE = 10000 HZ
TOTAL TIME = 2.458 SEC



BLOCK SIZE = 2048
SAMPLE RATE = 10000 HZ
TOTAL TIME = 2.458 SEC

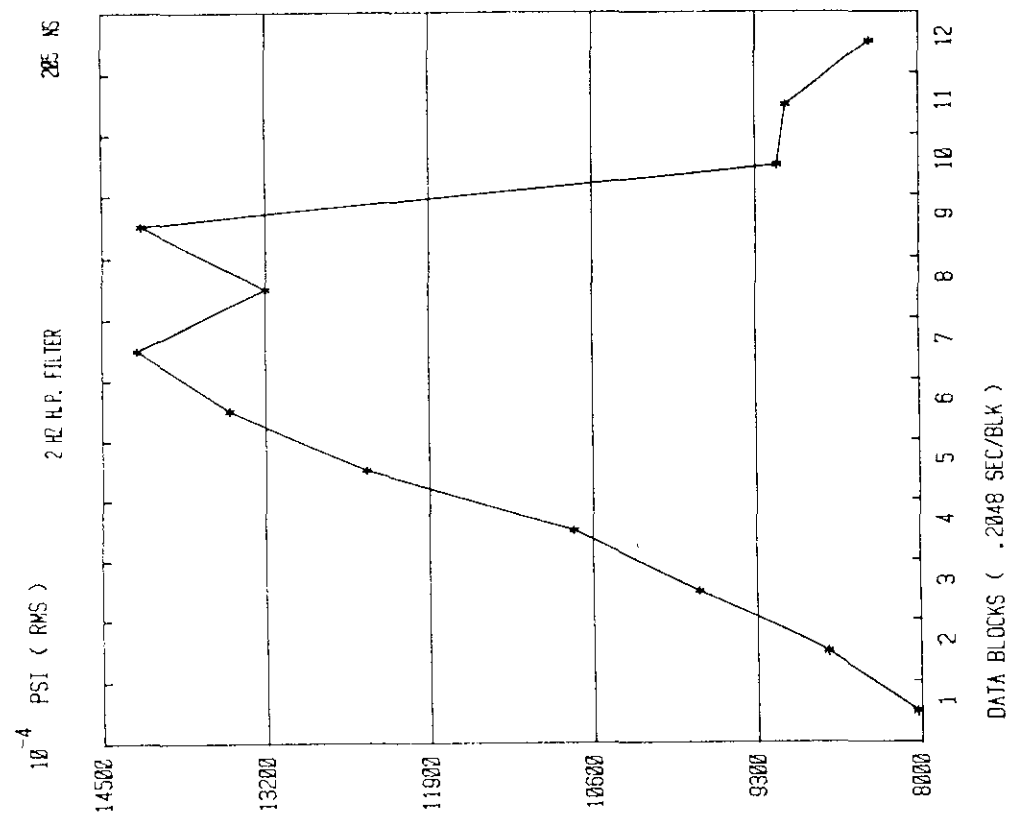


Figure 2-62. Typical RMS Plot of Centaur Porch Pressures Using a 2-Hz High-Pass Filter

KSC-DD-818-TR

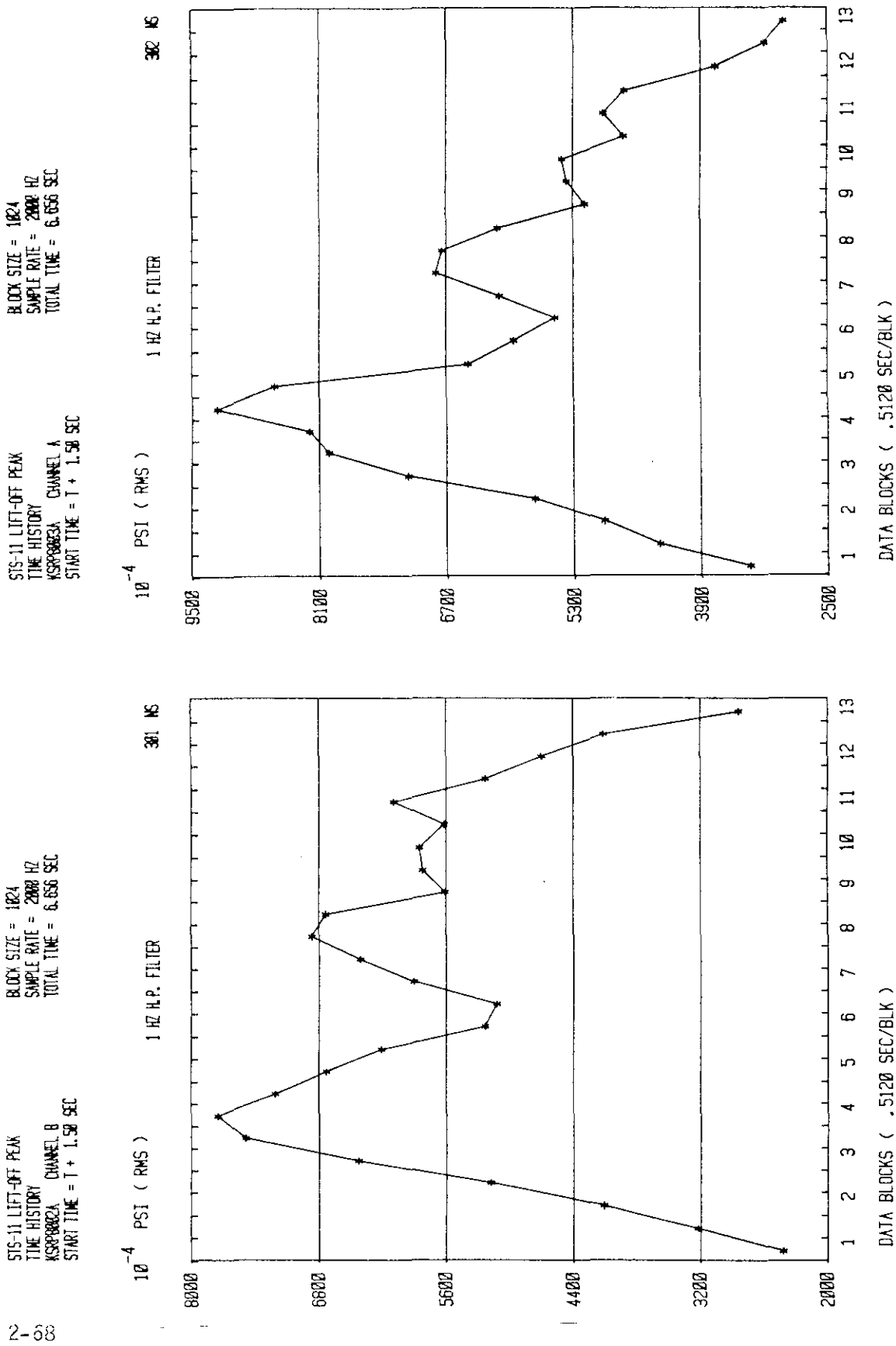
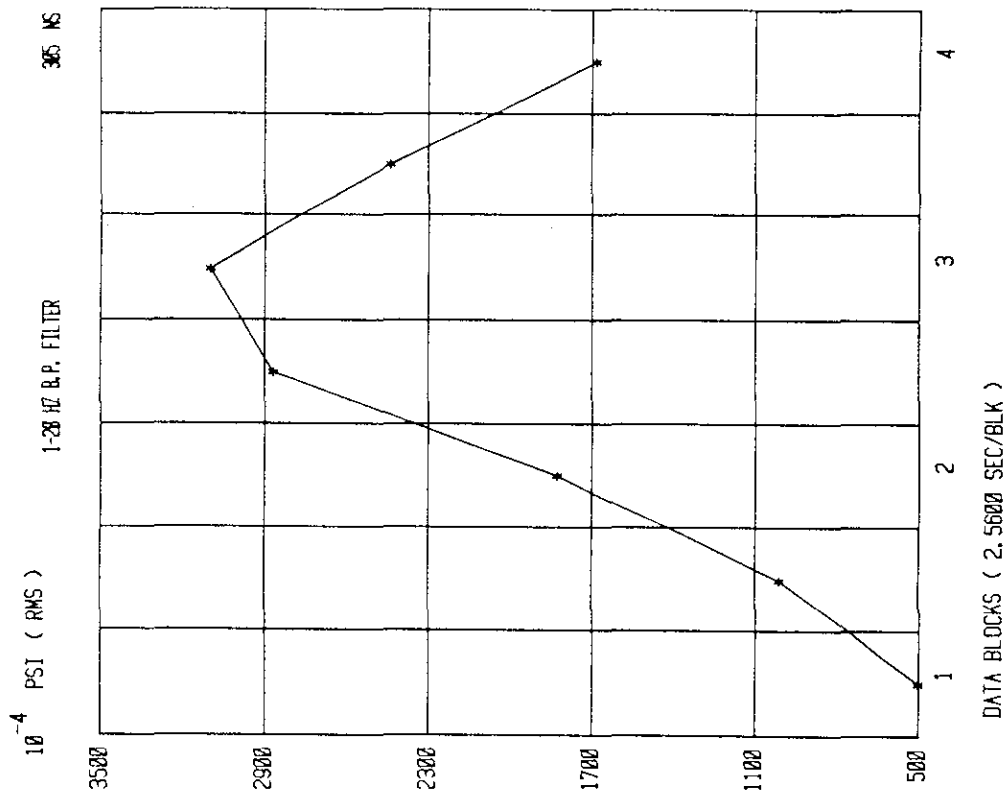


Figure 2-63. Typical RMS Plot of Centaur Porch Pressures Using a 1-Hz High-Pass Filter

STS-11 LIFT-OFF PEAK
TIME HISTORY
KSC00002A CHANNEL B
START TIME = T + 1.50 SEC

BLOCK SIZE = 512
SAMPLE RATE = 200 HZ
TOTAL TIME = 10.240 SEC



STS-11 LIFT-OFF PEAK
TIME HISTORY
KSC00003A CHANNEL A
START TIME = T + 1.50 SEC

BLOCK SIZE = 512
SAMPLE RATE = 200 HZ
TOTAL TIME = 10.240 SEC

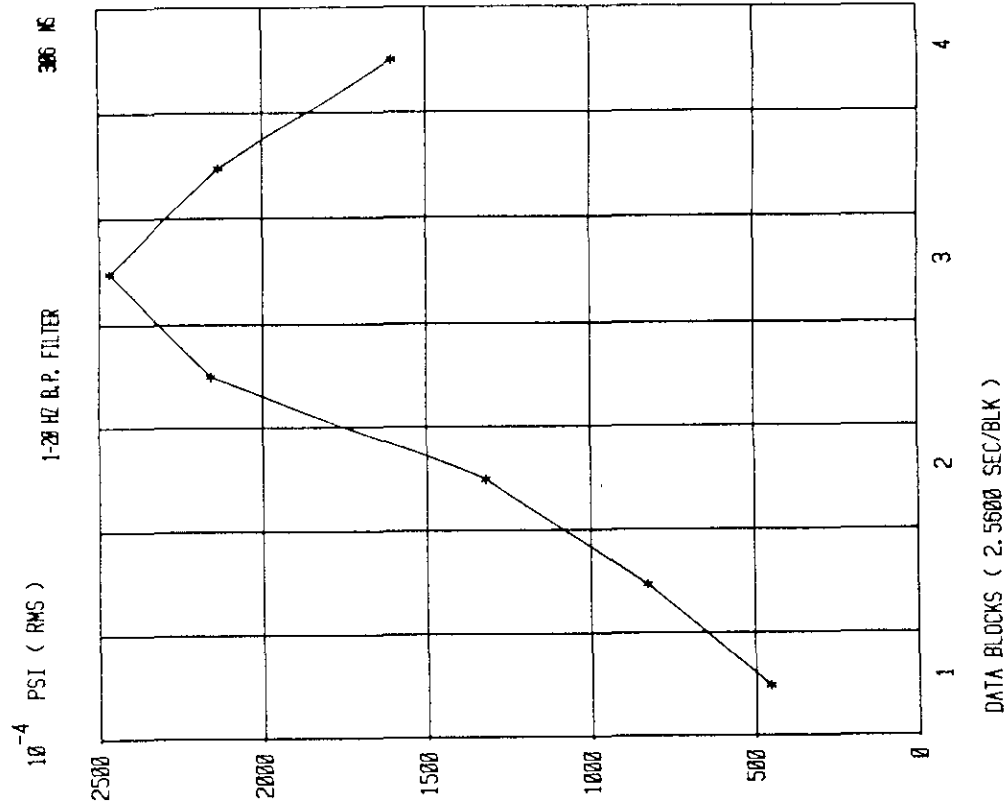
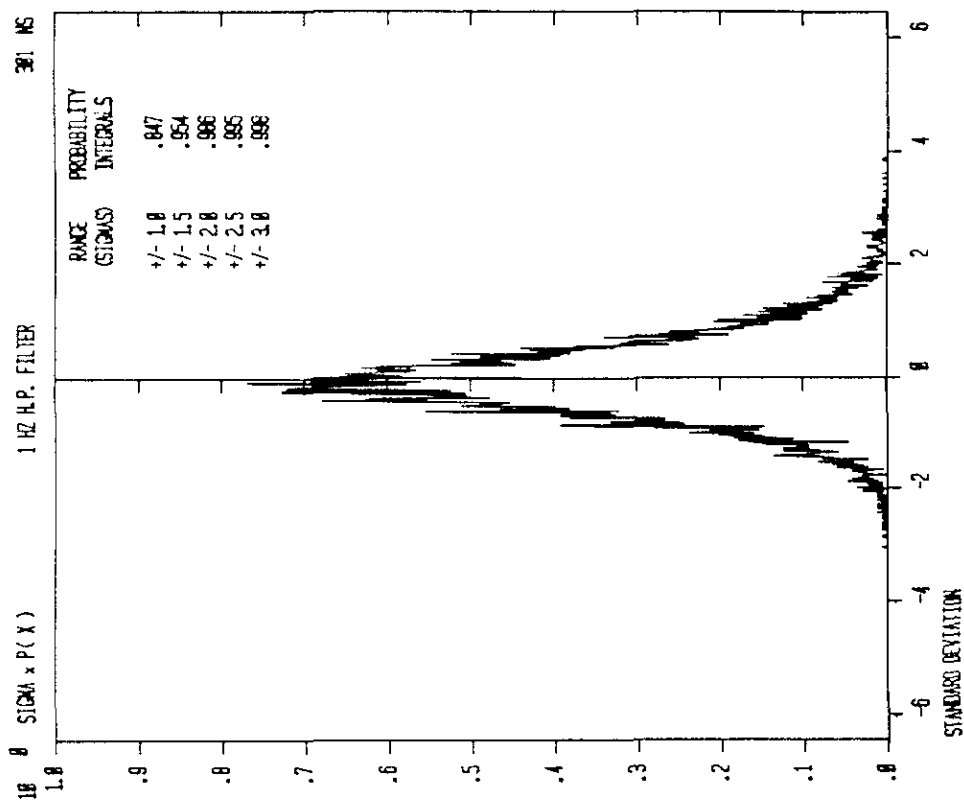


Figure 2-64. Typical RMS Plot of Centaur Porch Pressures Using a 1-Hz to 20-Hz Bandpass Filter

KSC-DD-818-TR

STS-11 LIFT-OFF PEAK
PROBABILITY DENSITY
KSPB002A CHANNEL B
START TIME = 1 + 1.50 SEC

BLOCK SIZE = 1024
SAMPLE RATE = 2000 HZ
TOTAL TIME = 6.056 SEC
RMS = .775 PSIS
AVERAGES = 13



STS-11 LIFT-OFF PEAK
PROBABILITY DENSITY
KSPB002A CHANNEL B
START TIME = 1 + 2.00 SEC

BLOCK SIZE = 2048
SAMPLE RATE = 10000 HZ
TOTAL TIME = 2.458 SEC
RMS = 1.297 PSIS
AVERAGES = 12

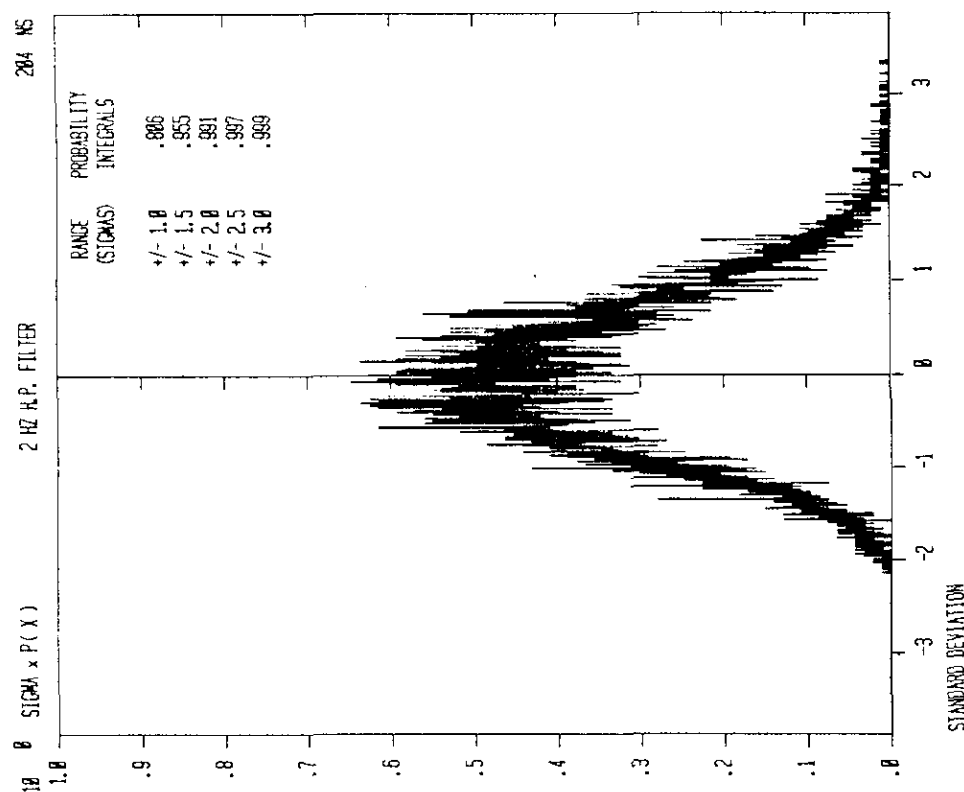


Figure 2-65. Typical Standard Deviation Plot of Centaur Porch Pressures Using 1- and 2-Hz High-Pass Filters

2.4 FAR FIELD ACOUSTICS

This section includes a summary of measured far field acoustic pressures at various distances and azimuths from the center of Pad A.

2.4.1 FAR FIELD ACOUSTIC PRESSURES, BEARING 322° TRUE. The following sensors recorded the acoustics along the line from Pad A to Pad B.

<u>Measurement No.</u>	<u>Distance From Pad A Center (ft)</u>
KAVYA001A	257
KAVYA003A	610
KAVYA004A, 13A, and 15A	1,200
KAVYA005A	2,754

During STS-1, -2, and -3 launches, KAVYA005A was reported to be 2,500 ft from Pad A center. Cross-correlation data obtained during STS-9 and STS-11 showed that the actual distance of this sensor from Pad A was 2,754 ft. A cross-country survey confirmed this distance.

Figures 2-66 through 2-73 show far field raw data and smoothed (Hanned) time histories for the STS-11 launch. Since all measurements contained baseline drift caused by radiating heat, data processing required the use of high-pass filter at 1 Hz in order to eliminate the drift.

Figures 2-74 and 2-75 present CCFC's obtained from STS-9 and STS-11 measurements for a time period involving transients generated at SRB ignition. Close examination of these data and enlarged summaries presented on figures 2-76 through 2-78 show the effect of atmospheric conditions on the trace velocity of sound propagation. Time delay (lag) of the CCFC's first peaks varies between launches. The average velocity of pressure wave propagation calculated from the peak lags for STS-9, -10, and -11 launches (figure 2-76) is 1,153 ft/s.

Figures 2-79 through 2-82 present coherences calculated between adjacent (about 4 in apart) sensors at 1,200 ft. Such high coherences exist only between closely spaced sensors. These coherences confirm validity of sensor outputs at 1,200 ft.

Figures 2-83 through 2-85 present STS-11 PSD's. Headings on each figure show selected processing time intervals and other pertinent processing parameters. Output of KAVYA003A (see figure 2-83) was processed using four different total analysis time intervals because of variations observed in its time history (see figures 2-66 and 2-67). This sensor appeared to have been hit by the reflected SRB plume splashing over the sloping pad apron at approximately T + 12.0 s. The output was lost at T + 13.8 s. Plume splash was observed during

KSC-DD-818-TR

STS-11 only and did not occur during STS-8 or STS-9 launches. Outputs of all other sensors, figures 2-84 and 2-85, were processed twice, using intervals that included and excluded SRB ignition transient.

Figure 2-86 presents typical probability densities calculated from the outputs of KAVYA003A and KAVYA004A sensors. It should be noted that because of inadvertent reversal of sensor polarity and consequent use of negative values for calibration constants, signs of probability integrals are reversed. It should be noted also, that the values of probability integrals below the range ± 2.5 sigma are substantially different from a normal (Gaussian) distribution as a consequence of nonstationary data. Presented probability densities in standardized form are referenced to maximum rms (maximum sigma) values. The 99% confidence limit, often used in design considerations, occurs within ± 2.2 -sigma range, while in a Gaussian distribution, the same confidence limit is within ± 2.58 -sigma range, about 17% higher.

Summaries of derived PSD's at each sensor location are presented on figures 2-87 through 2-90. In each case, a mean and limit (limit = mean + 2 sigma) curve are calculated. Because of the small number of collected measurements, the limit curve is essentially an envelope of all measurements. The use of limit curve is recommended for design applications.

Launch-to-launch dispersion is obtained from the difference between OASPL's, calculated by integrating limit and mean PSD curves within presented range 0 to 50 Hz, and converting these into dB. Calculated dispersions are 2 dB, 1.7 dB, and 1.3 dB at respective distances 610, 1,200, and 2,754 ft. It is of interest to note that within the same 0- to 50-Hz range, dispersion on the FSS calculated from 45 measurements (STS-1 through STS-9) is 3.3 dB.

2.4.2 NEAR FIELD ACOUSTIC PRESSURES ON THREE LIGHT POSTS. The following measurements recorded acoustic pressures on three existing light posts during the STS-6 launch at elevation 98 ft (3 ft above MLP deck 0) shown on figure 1-7:

<u>Measurement No.</u>	<u>Distance from Pad A Center</u>	<u>Azimuth From Pad A Center</u>
KFTPA001A	200	337° true
KFTPA002A	200	41° true
KFTPA003A	235	210° true

The purpose of these measurements was to establish pressure on structures surrounding the MLP when SRB plumes splash over the deck 0 and, after being deflected, impinge on surrounding structures that are elevated above the MLP.

Pressure time histories from all three measurements were affected by heat input and contain baseline drift corresponding to unreal negative pressures. This malfunction begins at T + 6.0 s in the output of KFTPA001A and KFTPA002A, and at T + 7.7 s in the output of KFTPA003, which is located on the south side

of Pad A and was least exposed to plume impingement. A high-pass filter (at 1 Hz, 18 dB/oct) was required to eliminate baseline drift in the output of all sensors. The remaining data above 1 Hz are considered to be valid.

Figure 2-91 shows overplots of data processed using two different sets of parameters. The left frame presents data essentially before the SRB plumes splash over the MLP. The splash begins at about $T + 6.0$ s.

The right frame is a relatively long-duration (up to $T + 13.9$ s) processing of a fairly narrow (0 to 50 Hz) band of data that include effects of the splash. Notice a substantial increase in all amplitudes (0 to 50 Hz) on the right frame compared to those on the left frame.

Figure 2-92 presents an enlarged zoom plot of the same data as the left frame on figure 2-91. Data on both figures were Hanned two times in order to reduce jogged appearance of PSD's resulting from a low number of DOF's available for these estimates.

Figure 2-93 presents an enlarged zoom plot of the same data as the right frame on figure 2-91, except that no Hanning was applied in order to obtain the highest value of PSD peak at 1.24 Hz, which indicates that sensor KFTPA002A was exposed to impingement by the east SRB plume deflected from the MLP deck. The peak at 1.24 Hz exceeds data obtained on the FSS by narrow band analysis. Examination of raw data time history confirms that this peak is real and not a consequence of the baseline drift. The peak amplitude of 1.24 Hz raw data component is about 0.25 psi and only about 5 cycles were recorded. Thus, presented PSD on figure 2-93 below approximately 5 Hz, should not be considered as a steady-state input.

2.4.3 FAR FIELD ACOUSTIC PRESSURES ON THE ECS COOLING TOWER. Measurements KECYA001 and KECYA002 were installed on the ECS cooling tower located approximately 450 ft and 270° true from Pad A center during STS-7 and -8 launches. Damage to the tower walls was occurring. Hardening of the structure solved the problem. PSD plots are presented for both launches, including the mean and limit (mean plus 2-sigma) curves in figures 2-94 and 2-95.

2.4.4 COMPARISON OF ACTUAL FAR FIELD ACOUSTIC DATA TO PREDICTIONS. Figure 2-96 shows a comparison between predicted far field acoustic levels at various distances from Pad A center to the average of actual data recorded at the distances shown.

KSC-DD-818-TR

FILE: YAR03B YAR03C

SAMPLING RATE 200 Hz. HIGH-PASS FILTER @ 1 Hz. ANTI-ALIASING FILTER @ 50 Hz.

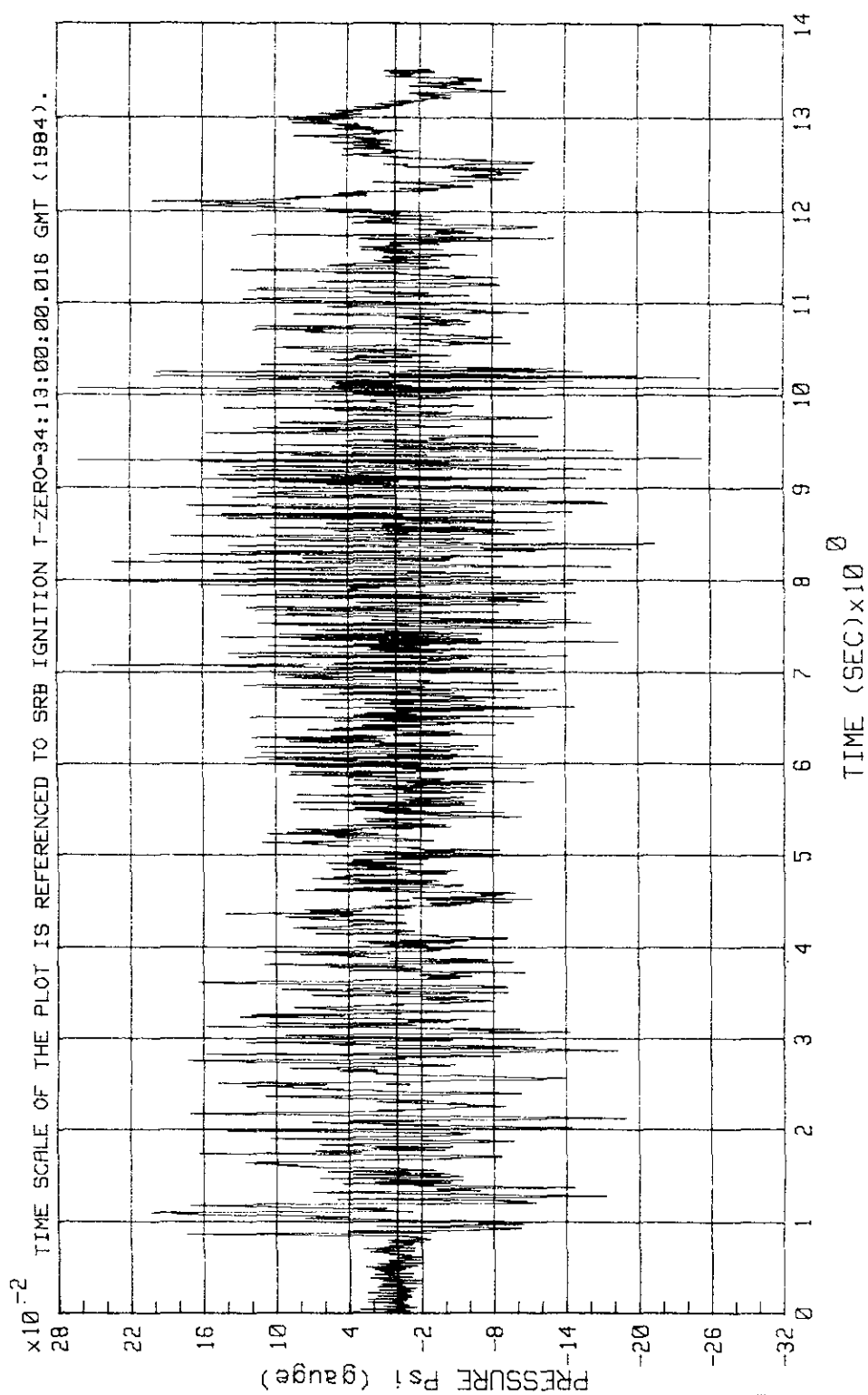


Figure 2-66. STS-11 Lift-Off - Sensor KAVYA003A at 610 ft From the Pad, Raw Data Time History

FILE: YAR03B YAR03C

SAMPLING RATE 200 HZ, HIGH-PASS FILTER @ 1 HZ, ANTI-ALIASING FILTER @ 50 HZ.

RAW DATA WERE HANNED 50X IN ORDER TO EMPHASIZE LOW FREQUENCY COMPONENTS.

NOTE: PEAK @ T+12 SEC IS CAUSED BY THE SPLASH OF THE END OF SRB PLUMES OVER SLOPING PAD APRON.

NOTE: REFLECTED PRESSURE WAVE HITS THE SENSOR. THIS IS A RANDOM OCCURRENCE.

TIME SCALE OF THE PLOT IS REFERENCED TO SRB IGNITION T-ZERO-34:13:00:00.016 GMT (1984).

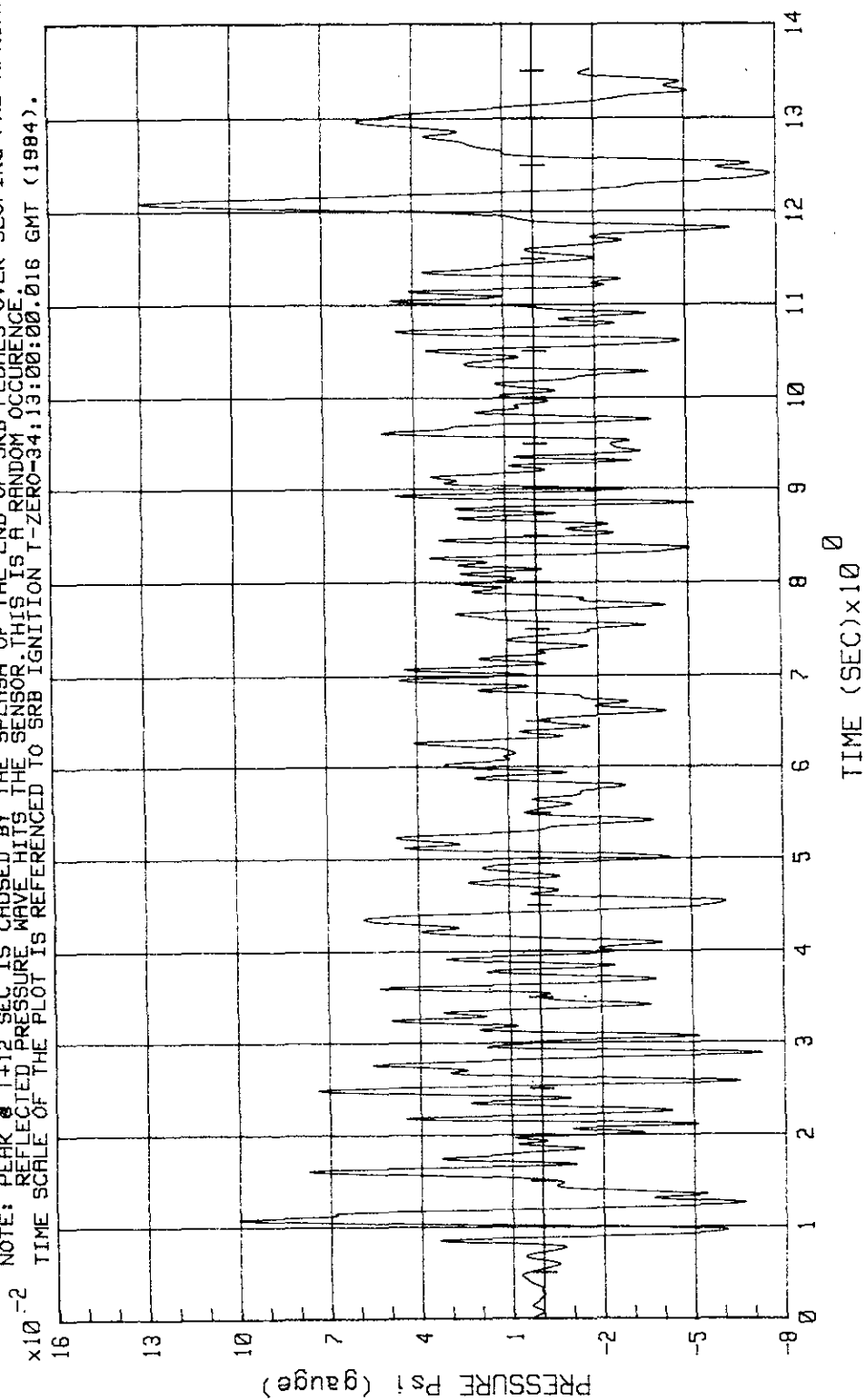


Figure 2-67. STS-11 Lift-Off - Sensor KAVYA003A at 610 ft From the Pad, Hanned Time History

KSC-DD-818-TR

FILE: YAR04B YAR04C

SAMPLING RATE 200 Hz. HIGH-PASS FILTER @ 1 Hz. ANTI-ALIASING FILTER @ 50 Hz.

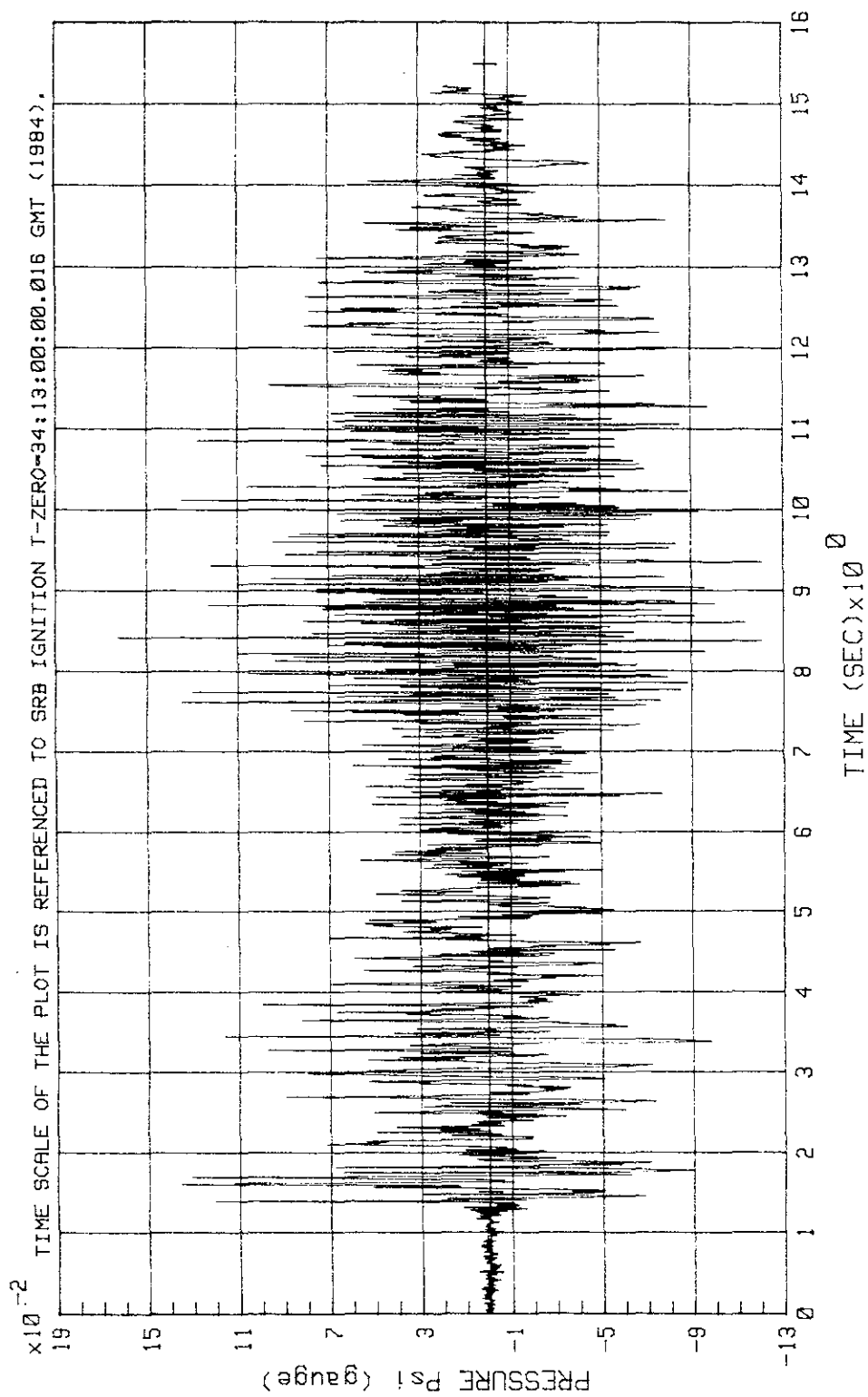


Figure 2-68. STS-11 Lift-Off - Sensor KAVYA004A at 1,200 ft From the Pad, Raw Data Time History

FILE: YAR04B YAR04C

SAMPLING RATE 200 Hz. HIGH-PASS FILTER @ 1 Hz. ANTI-ALIASING FILTER @ 50 Hz.
RAW DATA WERE HANNED 50x IN ORDER TO EMPHASIZE LOW FREQUENCY COMPONENTS.

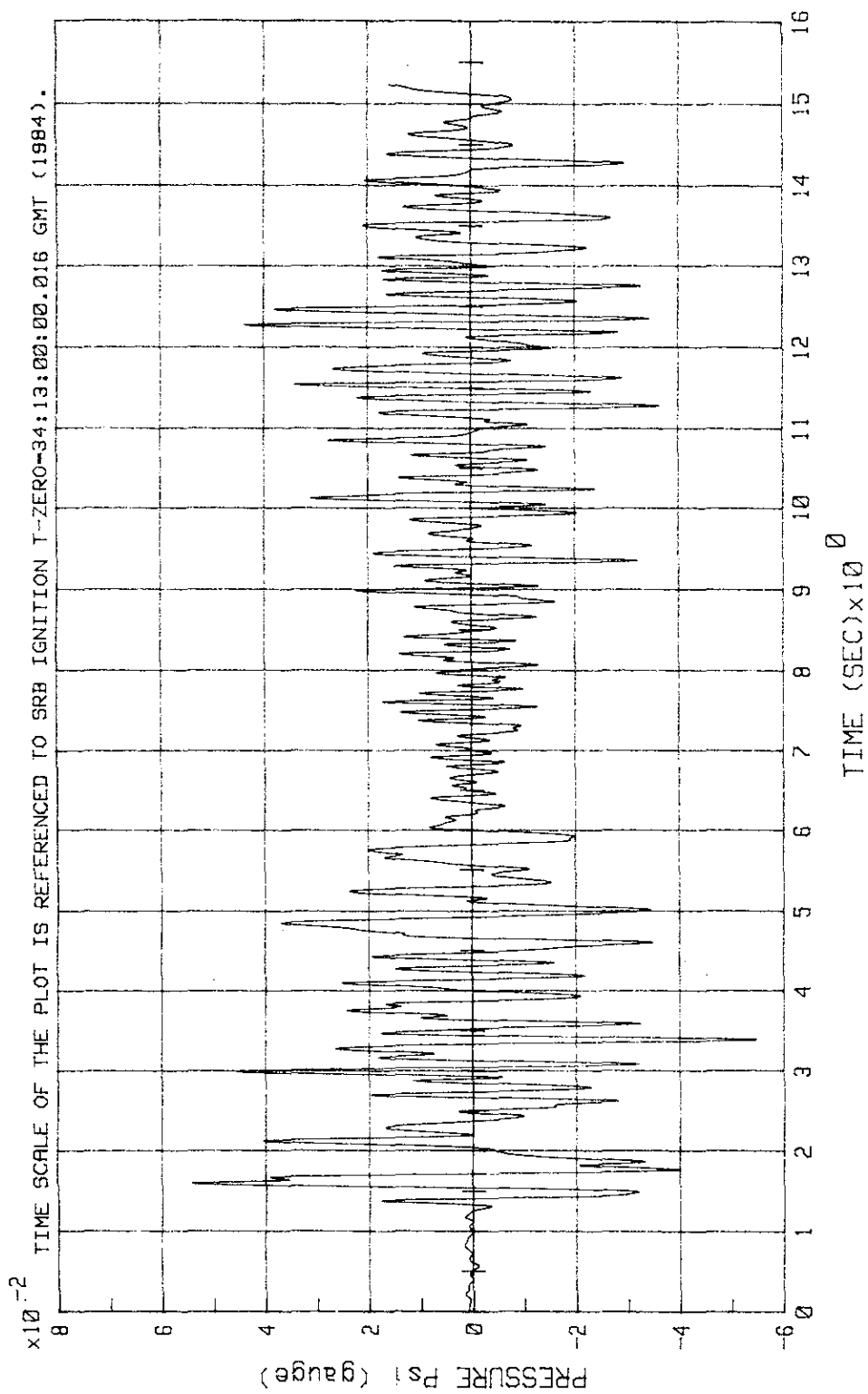


Figure 2-69. STS-11 Lift-Off - Sensor KAVYA0004A at 1,200 ft From the Pad, Hanned Time History

KSC-DD-818-TR

FILE: YAR15B YAR15C

SAMPLING RATE 200 Hz. HIGH-PASS FILTER @ 1 Hz. ANTI-ALIASING FILTER @ 50 Hz.

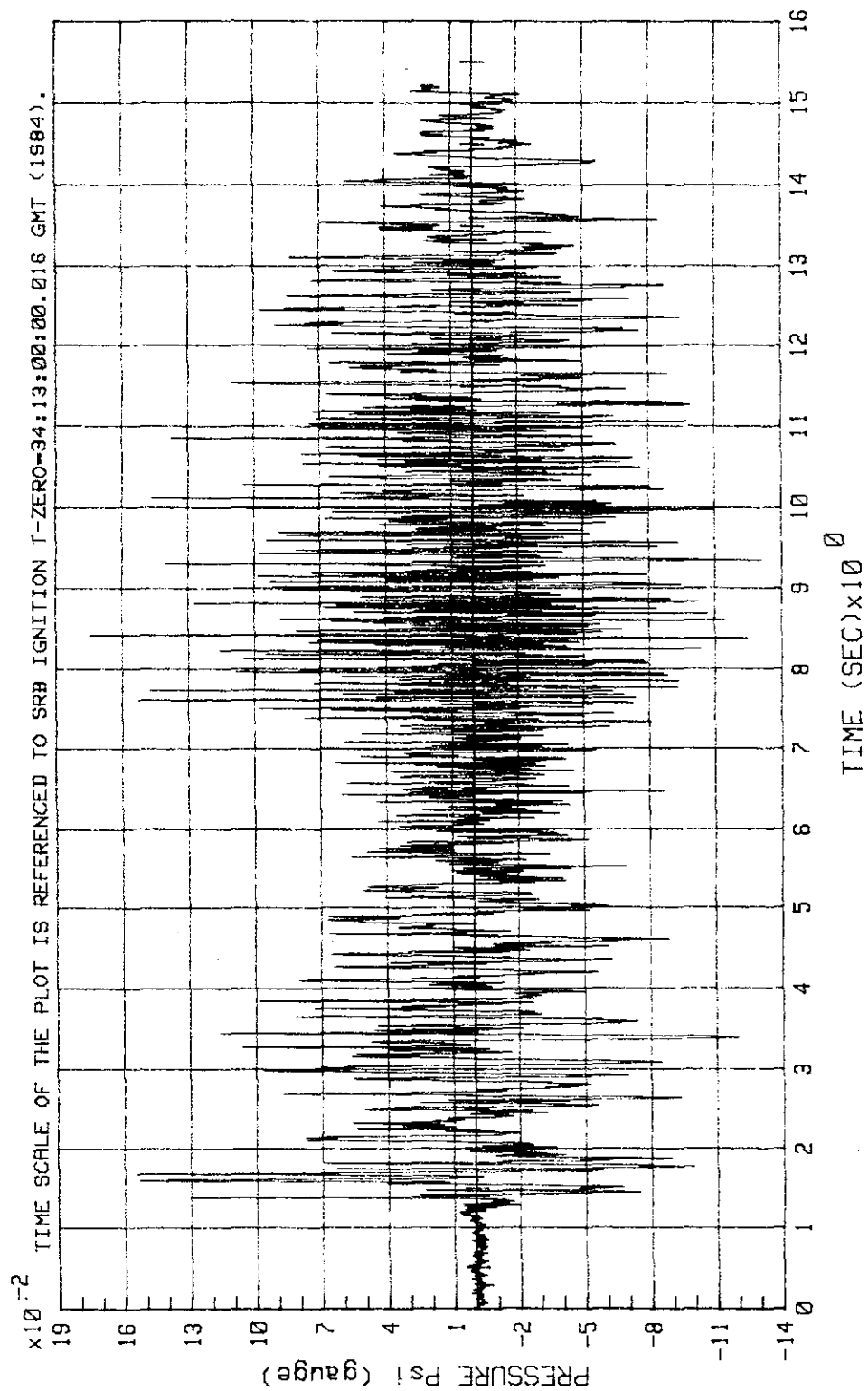


Figure 2-70. STS-11 Lift-Off - Sensor KAVYA015A at 1,200 ft From the Pad, Raw Data Time History

FILE: YAR15B YAR15C

SAMPLING RATE 200 Hz. HIGH-PASS FILTER @ 1 Hz. ANTI-ALIASING FILTER @ 50 Hz.
RAW DATA WERE HANNED 50x IN ORDER TO EMPHASIZE LOW FREQUENCY COMPONENTS.

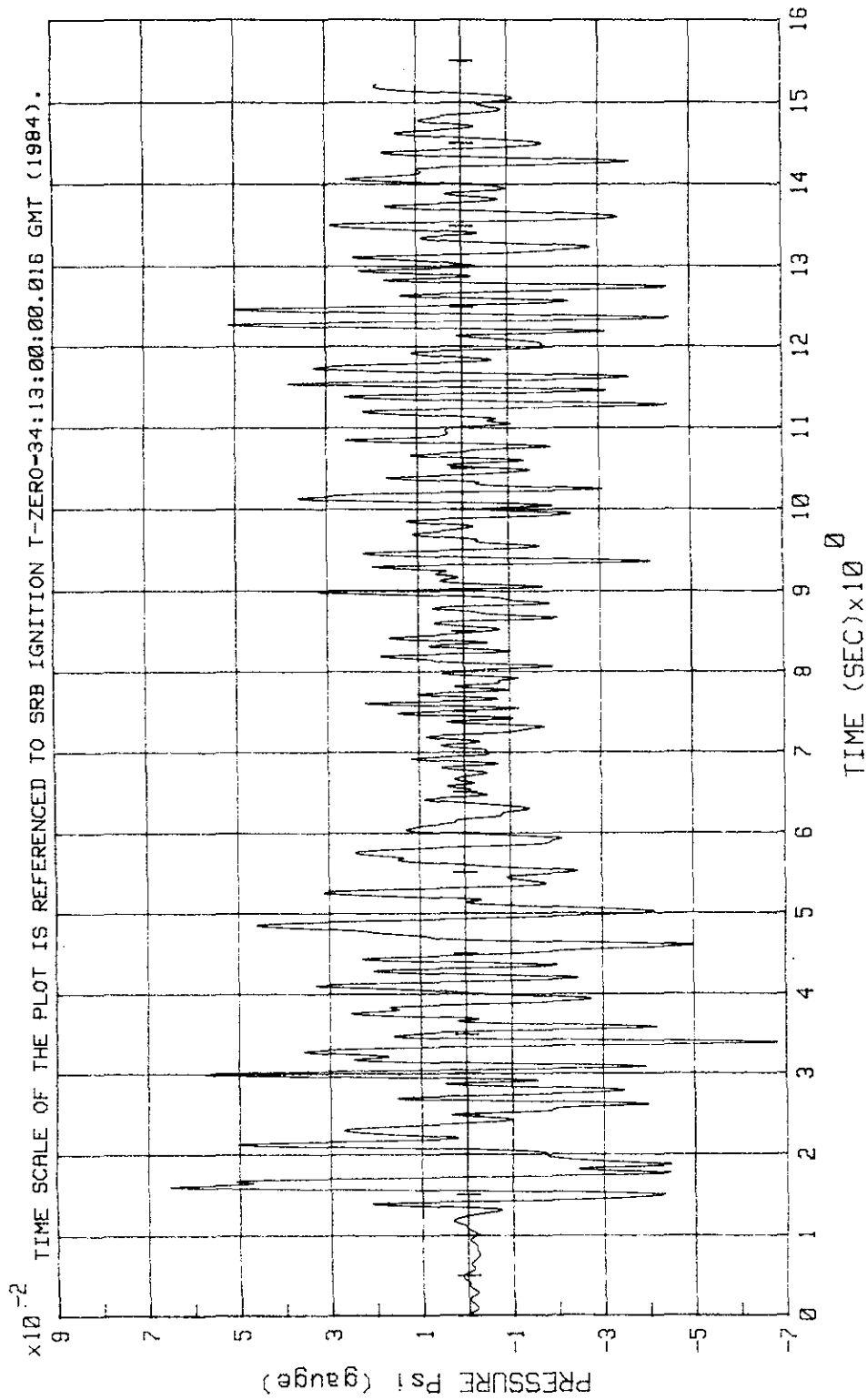


Figure 2-71. STS-11 Lift-Off - Sensor KAVYA015A at 1,200 ft From the Pad, Hanned Time History

KSC-DD-818-TR

FILE: YAR05B YAR05C

SAMPLING RATE 200 Hz. HIGH-PASS FILTER @ 1 Hz. ANTI-ALIASING FILTER @ 50 Hz.

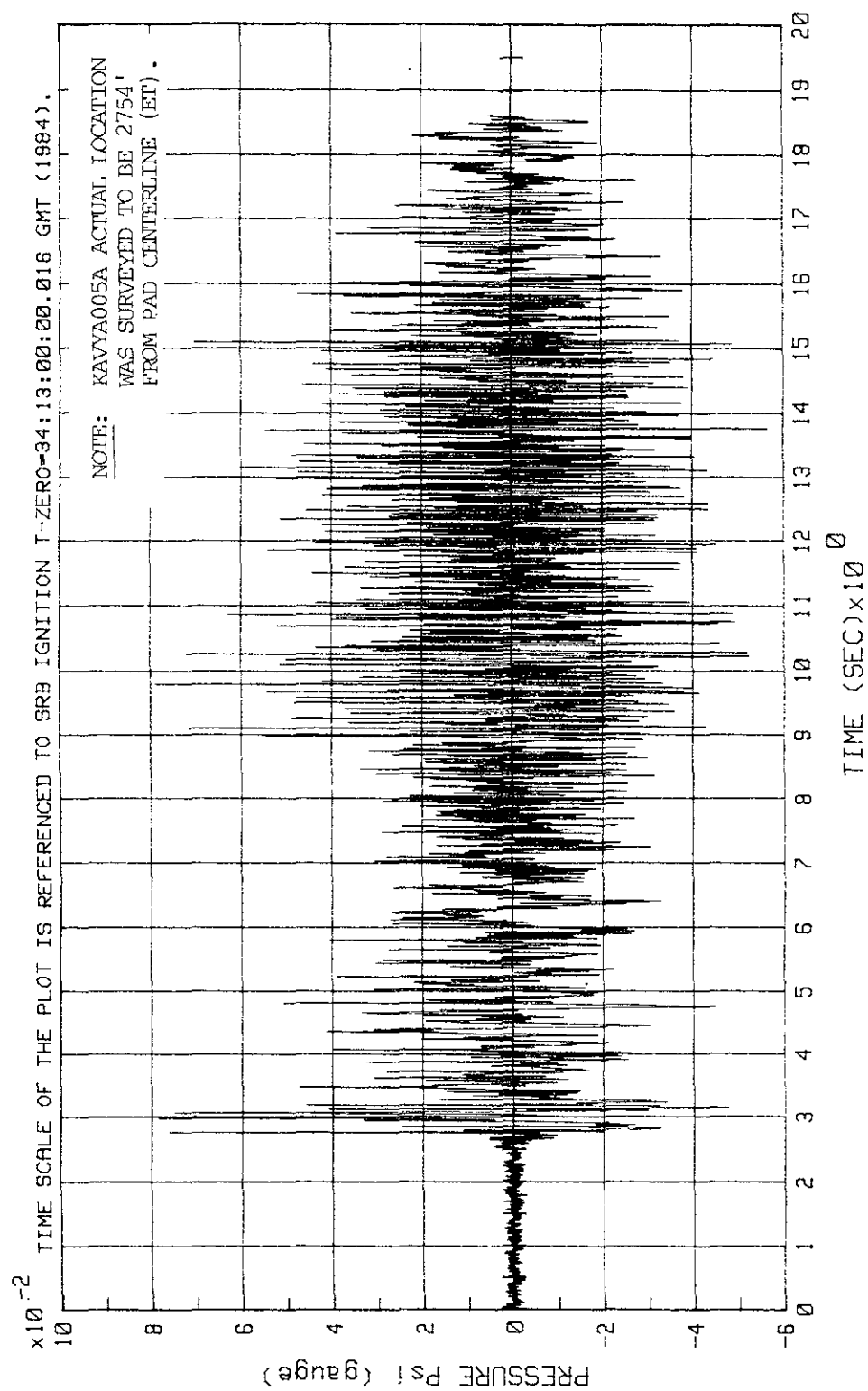


Figure 2-72. STS-11 Lift-Off - Sensor KAVYA005A at 2,500 ft From the Pad, Raw Data Time History

FILE: YAR05B YAR05C

SAMPLING RATE 200 Hz. HIGH-PASS FILTER @ 1 Hz. ANTI-ALIASING FILTER @ 50 Hz.

RAW DATA WERE HANNED 50x IN ORDER TO EMPHASIZE LOW FREQUENCY COMPONENTS.

NOTE: BECAUSE OF TWO DIFFERENT FILES WHICH JOIN @ T=8.4 SEC) THERE IS A DISCONTINUITY IN

THE PLOT @ T=8.4 SEC. NO SUCH DISCONTINUITY EXISTS IN THE RAW DATA PLOT.

TIME SCALE OF THE PLOT IS REFERENCED TO SRB IGNITION T=ZERO-34:13:00:00.016 GMT (1984).

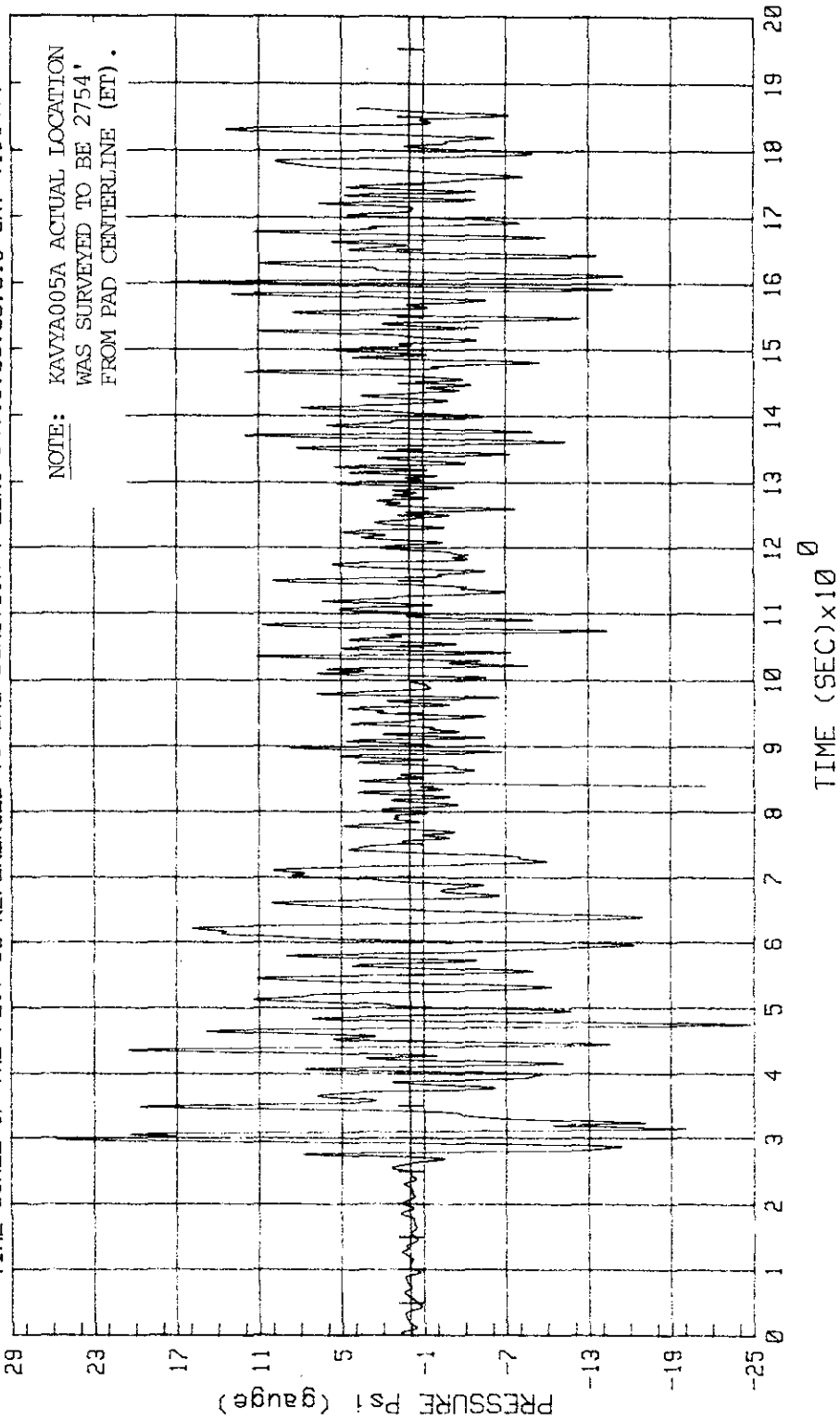


Figure 2-73. STS-11 Lift-Off - Sensor KAVYA005A at 2,500 ft From the Pad, Hanned Time History

KSC-DD-818-TR

FILE: C0304A C0315A C0305B C0415A C0405B C1505B

MAXIMUM CROSS-CORRELATION FUNCTION COEFFICIENTS (COFC's) WERE OBTAINED WITHIN TIME INTERVALS
 T+0.28 TO T+3.34 SEC (FOR "A"-FILES) AND T+0.76 TO T+5.88 SEC (FOR "B"-FILES). (KAVYA003A),
 NOMINAL SENSOR DISTANCES FROM THE CENTER OF THE LAUNCH PAD (SRB's) ARE: 610' (KAVYA003A),
 1200' (KAVYA004A & KAVYA015A) AND 2500' (KAVYA005A). SAMPLING RATE 200 Hz. A-A FLT @ 50 Hz.
 DATA PLOTTED IN THE VICINITY OF THE FIRST PEAK ONLY. PLOT RESOLUTION DELTA-T=0.005 SEC.

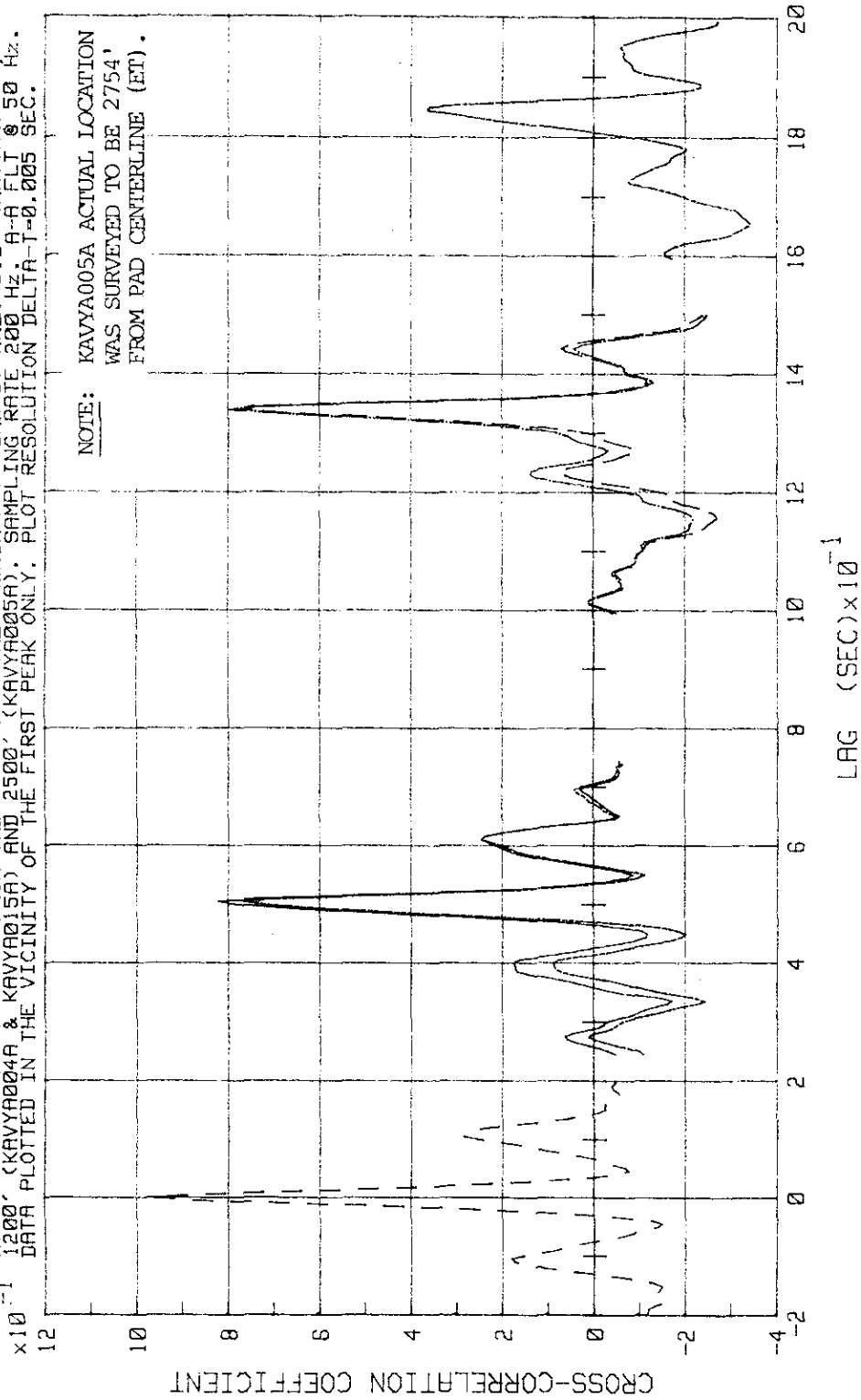


Figure 2-74. STS-9 SRB Ignition - Cross-Correlation Between KAVYA003A,
 -004A, -015A, and -005A

FILE: C0304A C0315A C0313A C0415A C0413A C1513A C0305B C0405B C1505B

MAXIMUM CROSS-CORRELATION FUNCTION COEFFICIENTS (CCFC's) WERE OBTAINED WITHIN TIME INTERVALS
 $T=0.78$ TO $T+3.34$ SEC (FOR 'A'-FILES) AND $T+0.76$ TO $T+5.88$ SEC (FOR 'B'-FILES).
 NOMINAL SENSOR DISTANCES FROM THE CENTER OF THE LAUNCH PAD (SRB's) ARE: 610' (KAVYA003A),
 1200' (KAVYA004A, -13A & -15A) AND 2500' (KAVYA005A). SAMPLING RATE 200 Hz. A-A FLT @ 50 Hz.
 H.P. FLT @ 1 Hz. DELTA-T=0.005 SEC. CCFC's PLOTTED IN THE VICINITY OF THE FIRST PEAK ONLY.

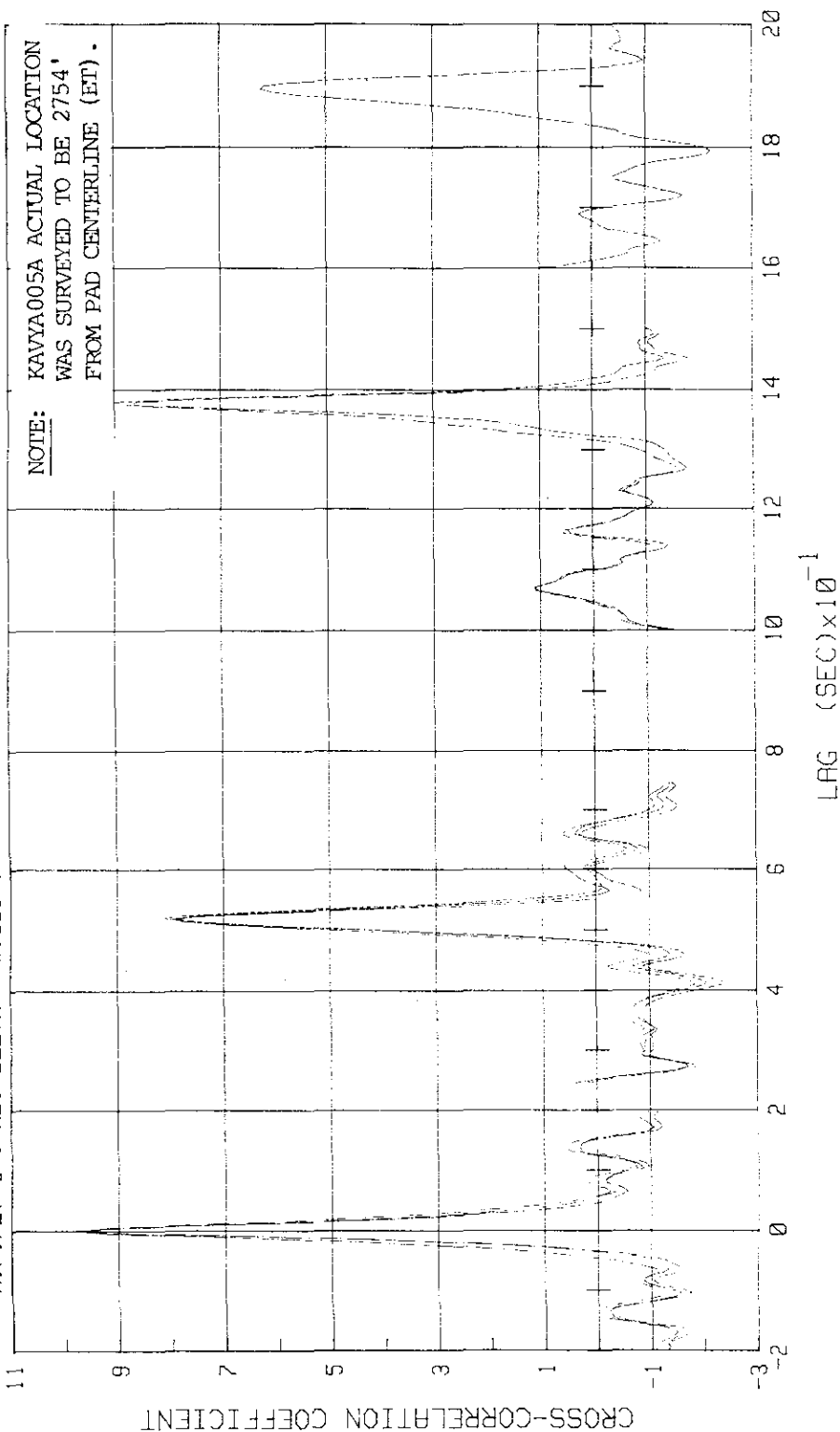


Figure 2-75. STS-11 SRB Ignition -- Cross-Correlation Between KAVYA003A, -004A, -013A, and -015A, and -005A

FILE: YAC34B C0304A C0304A C0315A C0313A

MAXIMUM CROSS-CORRELATION FUNCTION COEFFICIENTS (CCFC's) WERE OBTAINED WITHIN TIME INTERVALS T+0.28 TO T+2.84 SEC FOR STS-8 AND T+0.28 TO T+3.34 SEC FOR STS-9 & STS-11. NOMINAL SENSOR DISTANCES FROM THE CENTER OF THE LAUNCH PAD (SRB's) ARE: 610' (KAVYA003A) AND 1200' (KAVYA004A, -15A & -13A). SAMPLING RATE 200 HZ. A-R FLT @ 50 HZ. H.P. FLT @ 1 Hz (STS-11 ONLY). FILES: STS-8 (YAC34B), STS-9 (C0304A), STS-11 (C0304A, C0315A & C0313A).

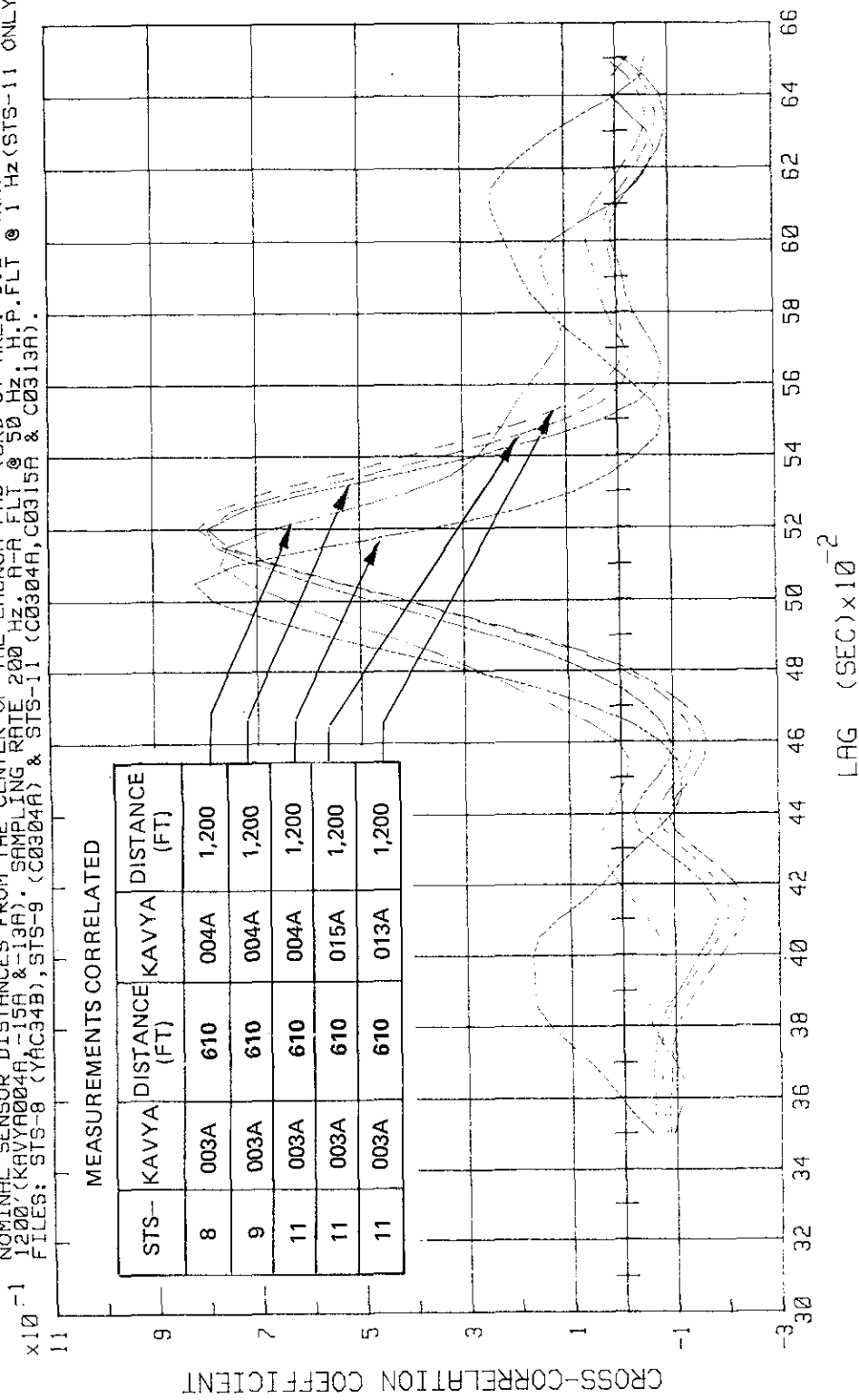


Figure 2-76. STS-8, -9, and -11 SRB Ignition - Cross-Correlation Between KAVYA003A, -004A, -015A, and -005A

FILE: C0405B C1505B C0405B C1505B

MAXIMUM CROSS-CORRELATION FUNCTION COEFFICIENTS (CCFC's) WERE OBTAINED WITHIN TIME INTERVALS
T+0.76 TO T+5.88 SEC FOR BOTH LAUNCHES USING IDENTICAL PROCESSING (EXCEPT H.P. FILTER FOR STS-11).
NOMINAL SENSOR DISTANCES FROM THE CENTER OF THE LAUNCH PAD (SRB's) ARE: 1200' (KAVYA004A, -15A) &
2500' (KAVYA005A). SAMPLING RATE 200 Hz; A-A FLT @ 50 Hz; H.P. FLT @ 1 Hz (STS-11 ONLY).
FILES: STS-9 (C0405B & C1504B) & STS-11 (C0405B & C1505B).

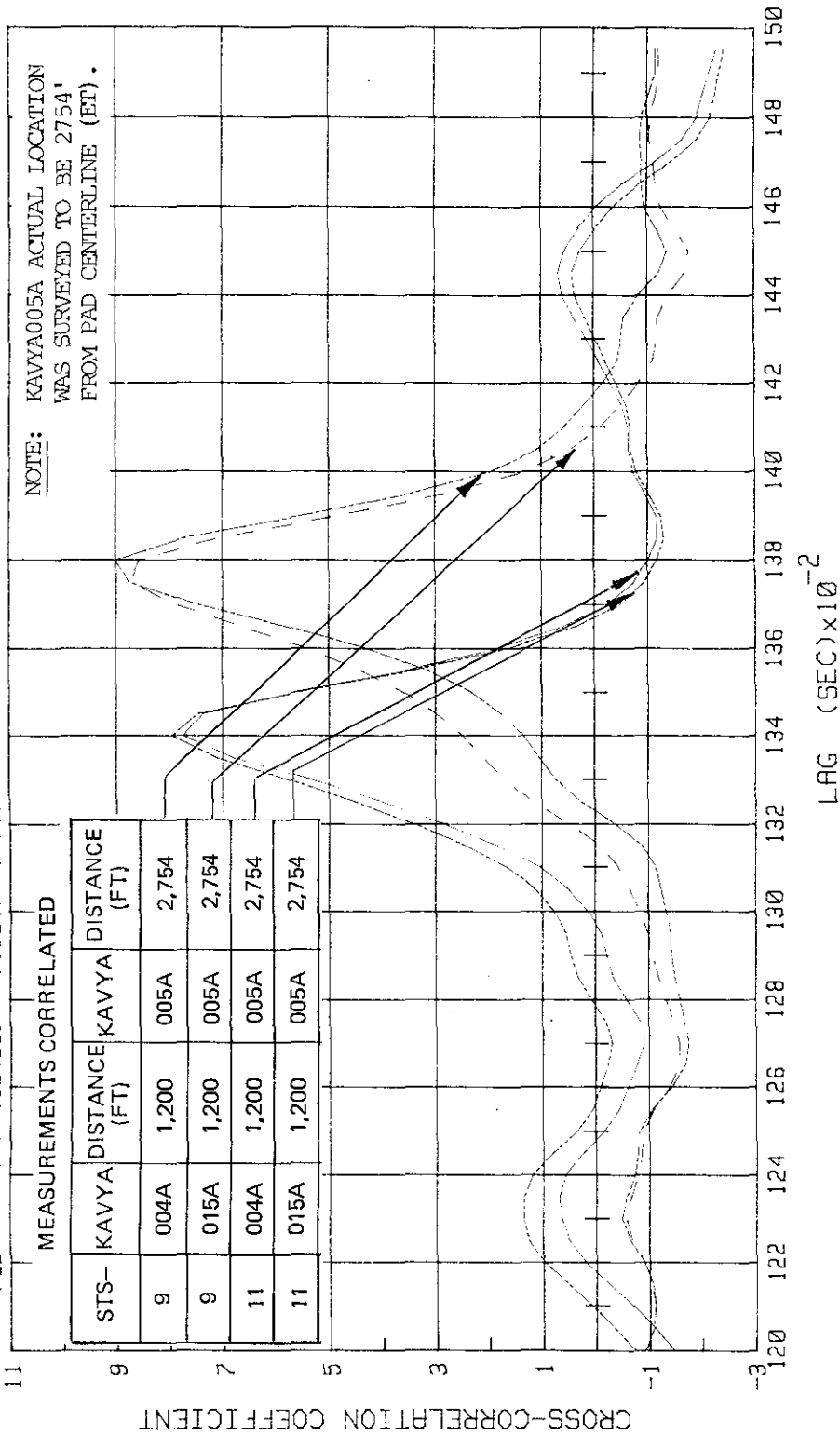


Figure 2-77. STS-9 and -11 SRB Ignition - Cross-Correlation Between
KAVYA004A, -015A, and -005A

FILE: C0305B C0305B

MAXIMUM CROSS-CORRELATION FUNCTION COEFFICIENTS (CCFC's) WERE OBTAINED WITHIN TIME INTERVALS T+0.76 TO T+5.88 SEC FOR BOTH LAUNCHES USING IDENTICAL PROCESSING (EXCEPT H.P. FILTER FOR STS-11). NOMINAL SENSOR DISTANCES FROM THE CENTER OF THE LAUNCH PAD (SRB's) ARE: 610 (KAVYA003A) AND 2500 (KAVYA005A). SAMPLING RATE 200 Hz. A-A FLT @ 50 Hz. H.P. FLT @ 1 Hz (STS-11 ONLY). CCFC FOR STS-9 IS SHIFTED DOWN ABOUT ZERO AXIS BECAUSE MEAN WAS NOT ZERO (DATA DRIFT & NO H.P. FLT).

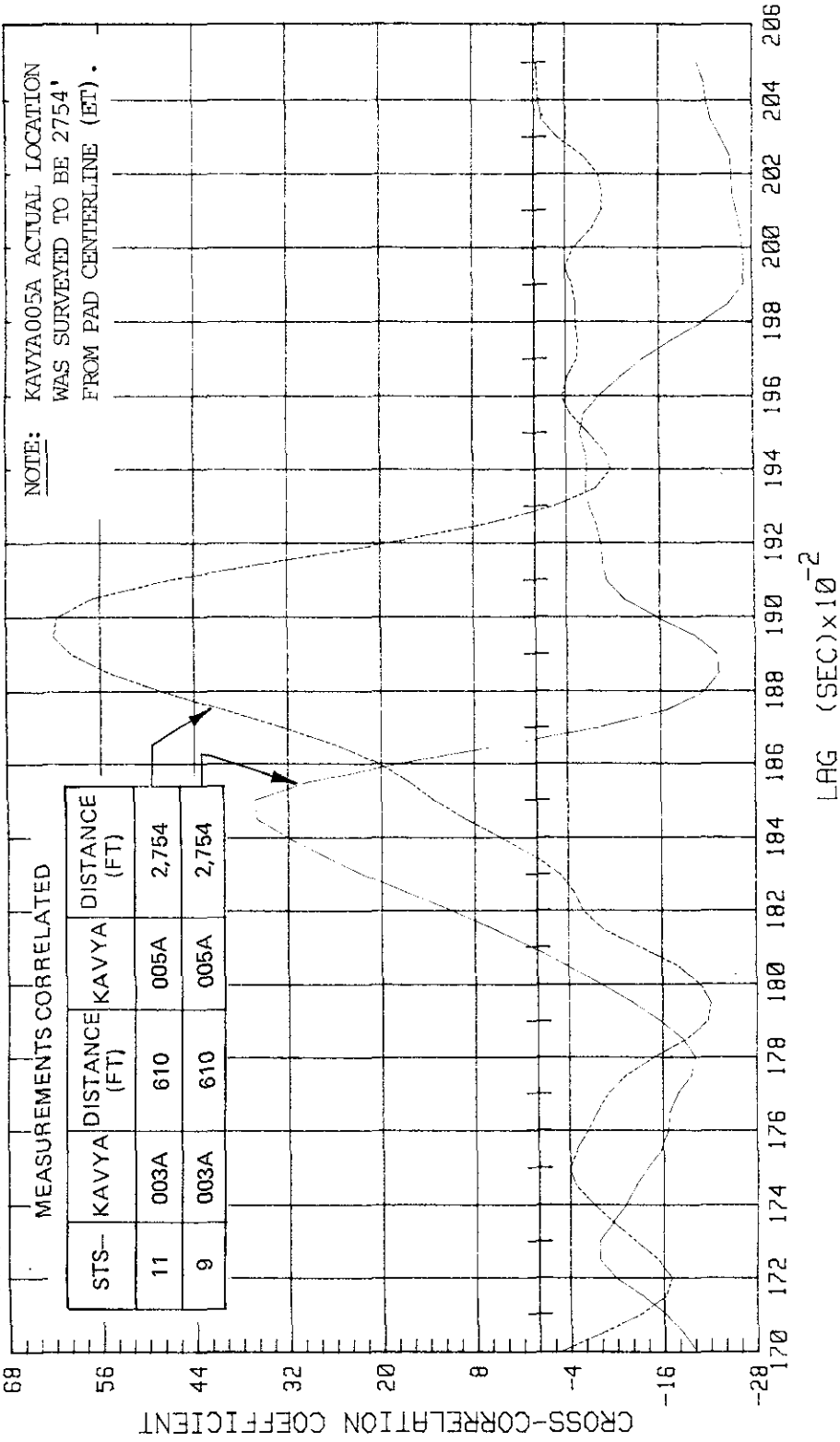


Figure 2-78. STS-9 and -11 SRB Ignition - Cross-Correlation Between KAVYA003A, and -005A.

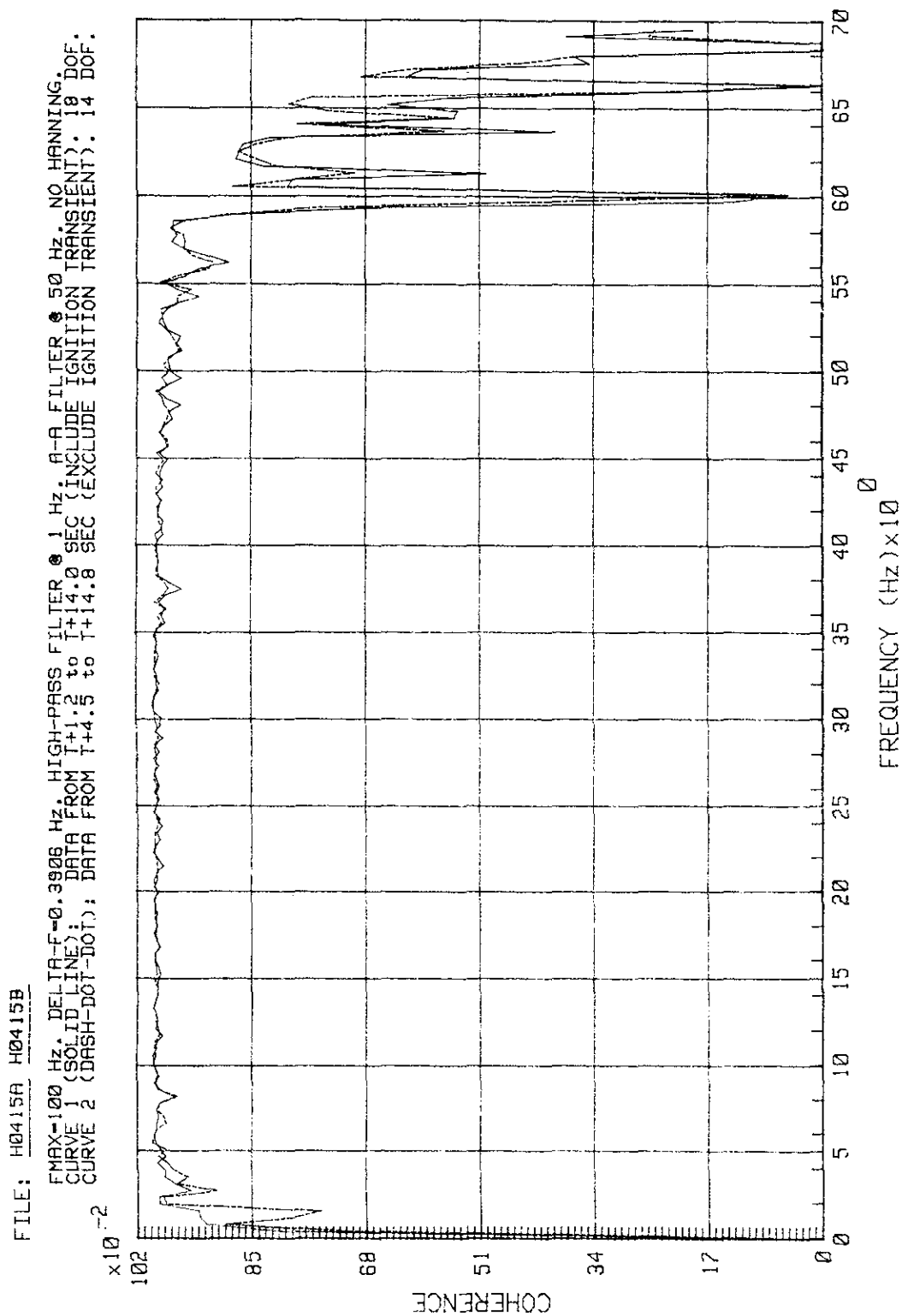


Figure 2-79. STS-11 Lift-Off Peak - Coherence Between Adjacent KAVYA004A and -015A Sensor Data

KSC-DD-818-TR

FILE: H0415A H0415B MEAN

FMAX=100 Hz, DELTA-F=0.3908 Hz, HIGH-PASS FILTER @ 1 Hz, A-A FILTER @ 50 Hz, NO HANNING.
 CURVE 1 (SOLID LINE); DATA FROM T+1.2 to T+14.0 SEC (INCLUDE IGNITION TRANSIENT); 18 DOF.
 CURVE 2 (DASH-DOT-DOT); DATA FROM T+4.5 to T+14.8 SEC (EXCLUDE IGNITION TRANSIENT); 14 DOF.

ENLARGED COHERENCE PLOT FOR 5-55 Hz RANGE.

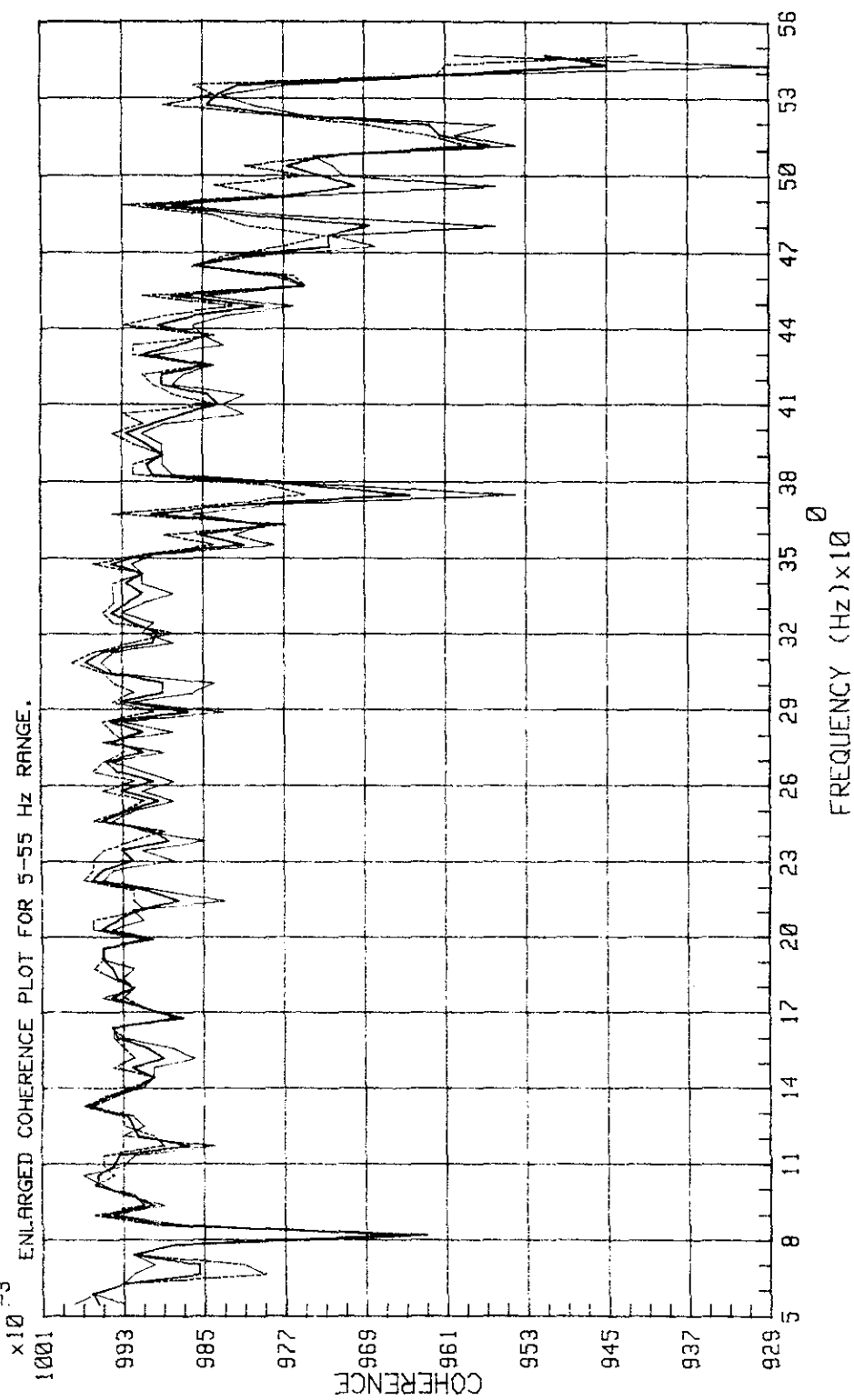


Figure 2-80. STS-11 Lift-Off Peak -
 Coherence Between Adjacent KAVYA004A and -015A Sensor Data (Near)

FILE: H0413A H0413B

FMAX=100 Hz. DELTA-F=0.3908 Hz. HIGH-PASS FILTER @ 1 Hz. A-A FILTER @ 50 Hz. NO HANNING.
 CURVE 1 (SOLID LINE): DATA FROM T+1.2 to T+14.0 SEC (INCLUDE IGNITION TRANSIENT). 18 DOF.
 CURVE 2 (DASH-DOT-DOT): DATA FROM T+4.5 to T+14.8 SEC (EXCLUDE IGNITION TRANSIENT). 14 DOF.

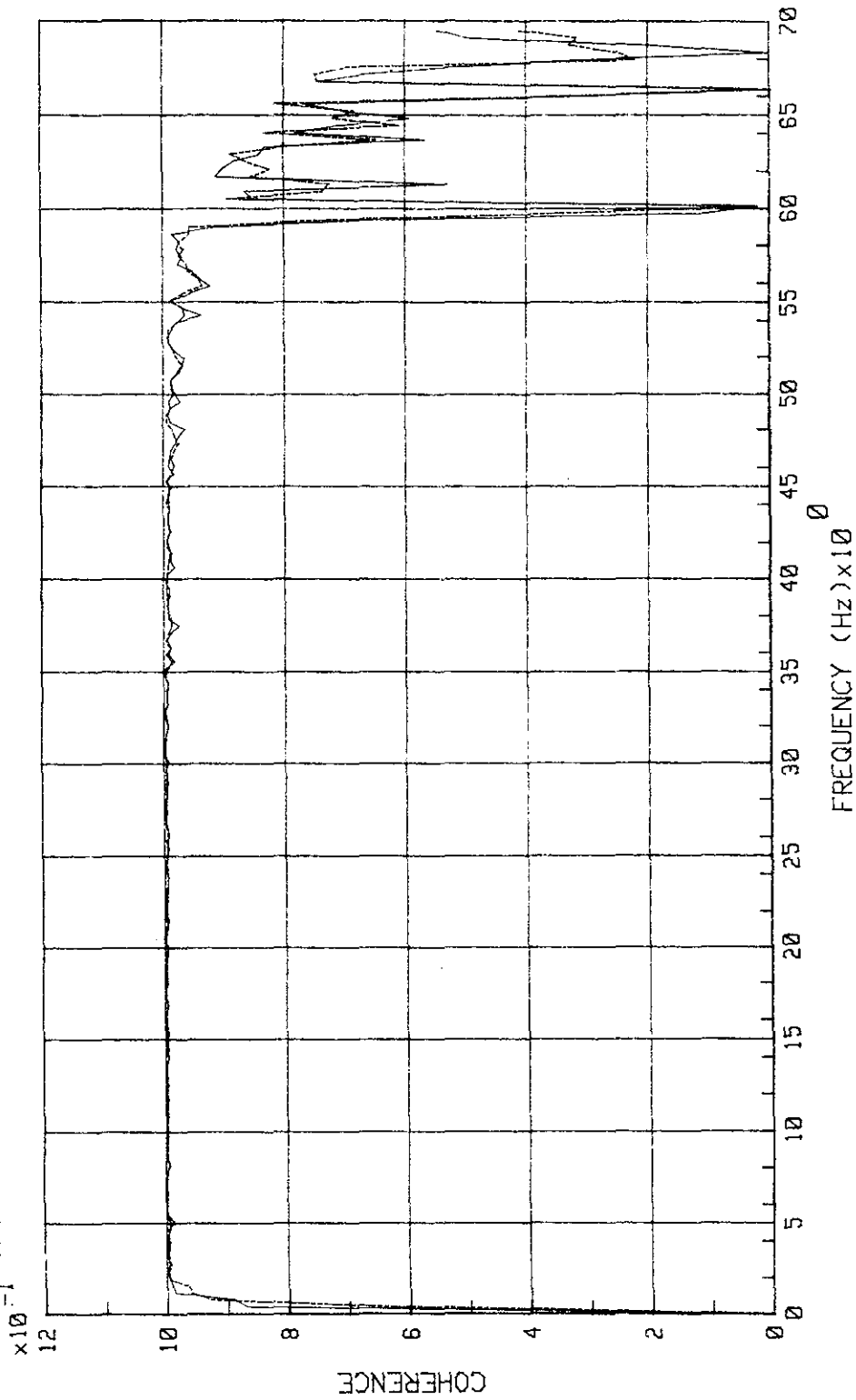


Figure 2-81. STS-11 Lift-Off Peak - Coherence Between Adjacent KAVYA004A and -013A Sensor Data

KSC-DD-818-TR

FILE: H1513A H1513B

FMAX=100 Hz. DELTA-F=0.3906 Hz. HIGH-PASS FILTER @ 1 Hz. A-A FILTER @ 50 Hz. NO HANNING.
 CURVE 1 (SOLID LINE); DATA FROM T+1.2 to T+14.0 SEC (INCLUDE IGNITION TRANSIENT); 18 DOF.
 CURVE 2 (DASH-DOT-DOT); DATA FROM T+4.5 to T+14.8 SEC (EXCLUDE IGNITION TRANSIENT); 14 DOF.

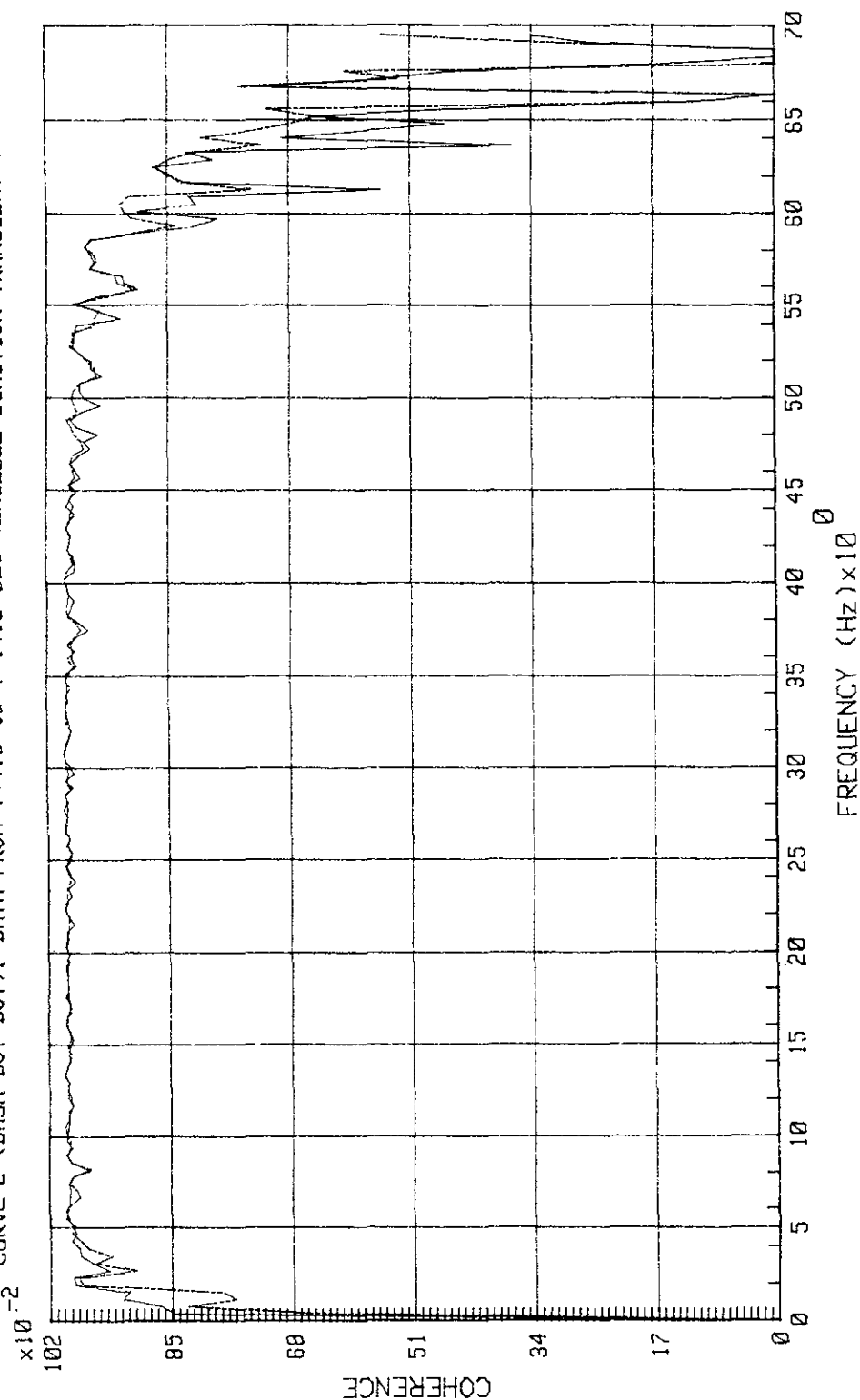


Figure 2-82. STS-11 Lift-Off Peak - Coherence Between Adjacent KAVYA015A and -013A Sensor Data

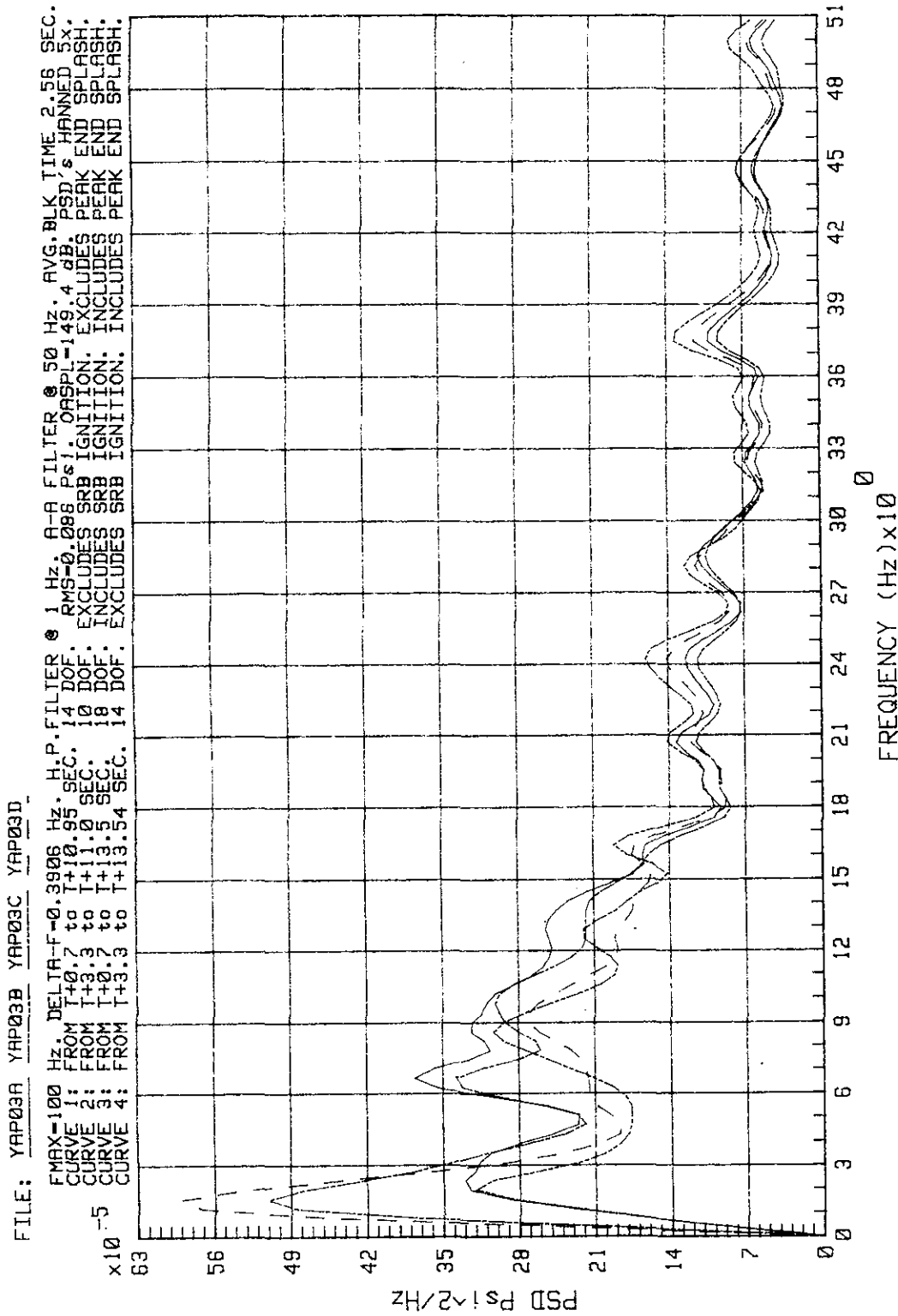


Figure 2-83. STS-11 Lift-Off Peak and Peak End - PSD, Sensor KAVYA003A at 610 ft From the Pad

KSC-DD-818-TR

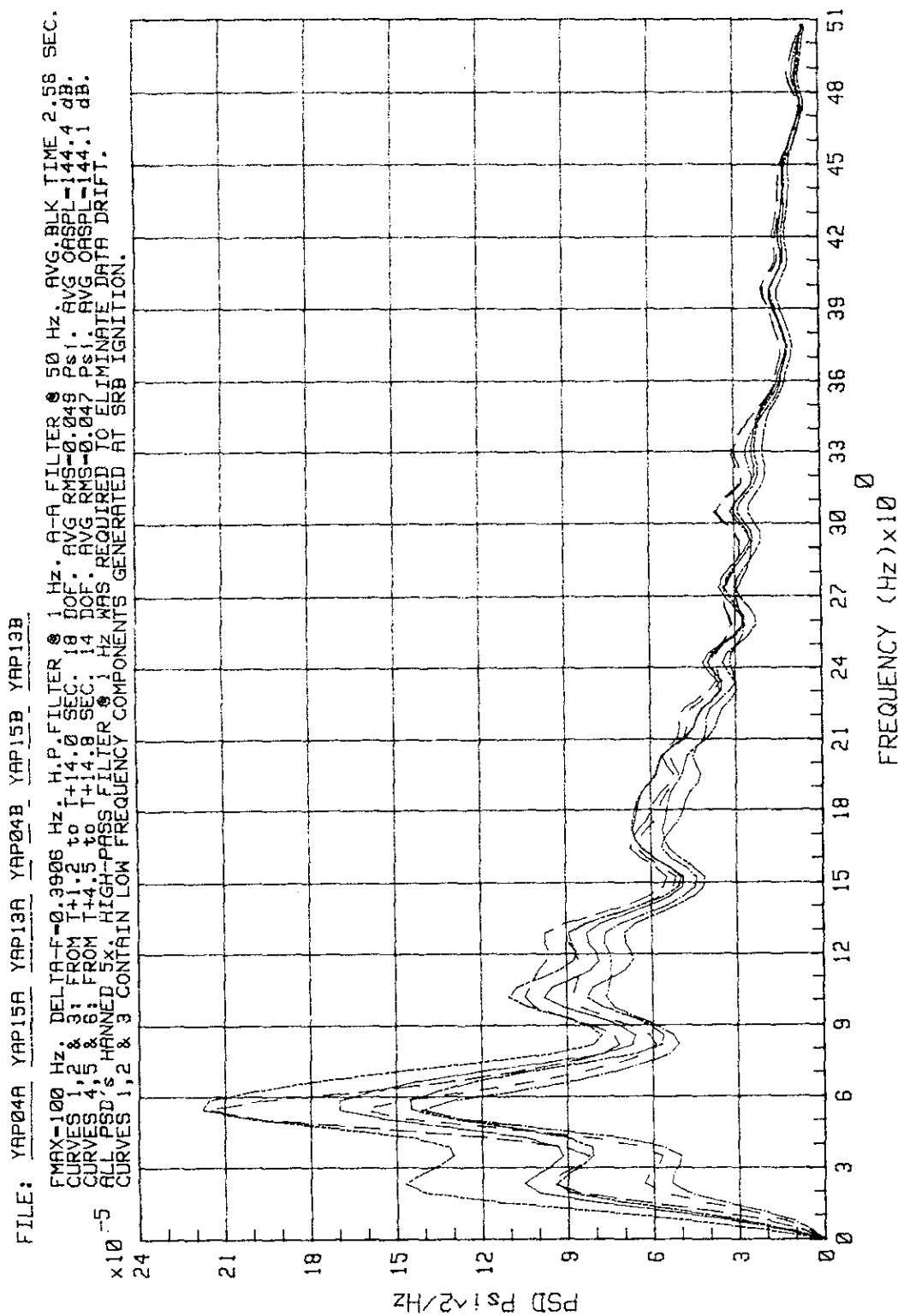


Figure 2-84. STS-11 Lift-Off Peak - PSD, Adjacent Sensors
 KAVYA004A, -015A, and -013A at 1,200 ft from the Pad

FILE: YAP05A YAP05B

EMAX=100 HZ. DELTA-F=0.3906 HZ. H.P. FILTER @ 50 HZ. AVG. BLK TIME 2.56 SEC.
 CURVE 1: FROM T+2.5 TO T+23.0 SEC. 30 DOF. RMS=0.023 PSI. OR SPL=138.0 dB. PSD'S HANNED 5x.
 CURVE 2: FROM T+6.5 TO T+21.9 SEC. 22 DOF. RMS=0.023 PSI (SAME AS CURVE 1).
 CURVE 1 INCLUDES SRB IGNITION TRANSIENT.

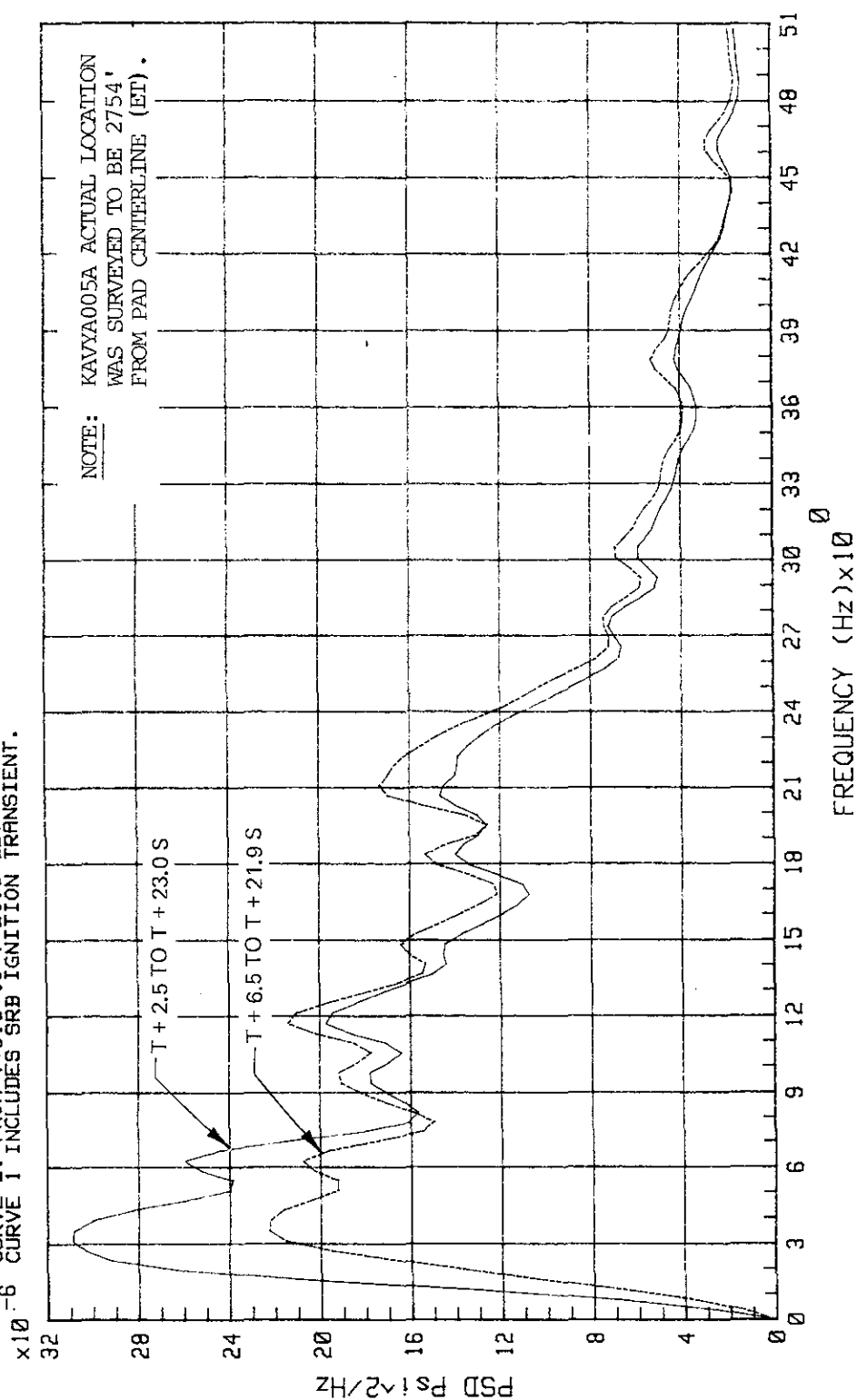


Figure 2-85. STS-11 Lift-Off Peak - PSD, Sensor KAVYA005A at 2,500 ft From the Pad

KSC-DD-818-TR

STS-11 SRB IGNITION/LIFT-OFF
 PROBABILITY DENSITY
 KAVYA003A CHANNEL A
 START TIME = 1 + .78 SEC

BLOCK SIZE = 512
 SAMPLE RATE = 200 HZ
 TOTAL TIME = 10.24 SEC
 RMS = .006 PSIG
 AVERAGES = 4

STS-11 SRB IGNITION/LIFT-OFF
 PROBABILITY DENSITY
 KAVYA003A CHANNEL A
 START TIME = 1 + 1.20 SEC

BLOCK SIZE = 512
 SAMPLE RATE = 200 HZ
 TOTAL TIME = 12.00 SEC
 RMS = .049 PSIG
 AVERAGES = 5

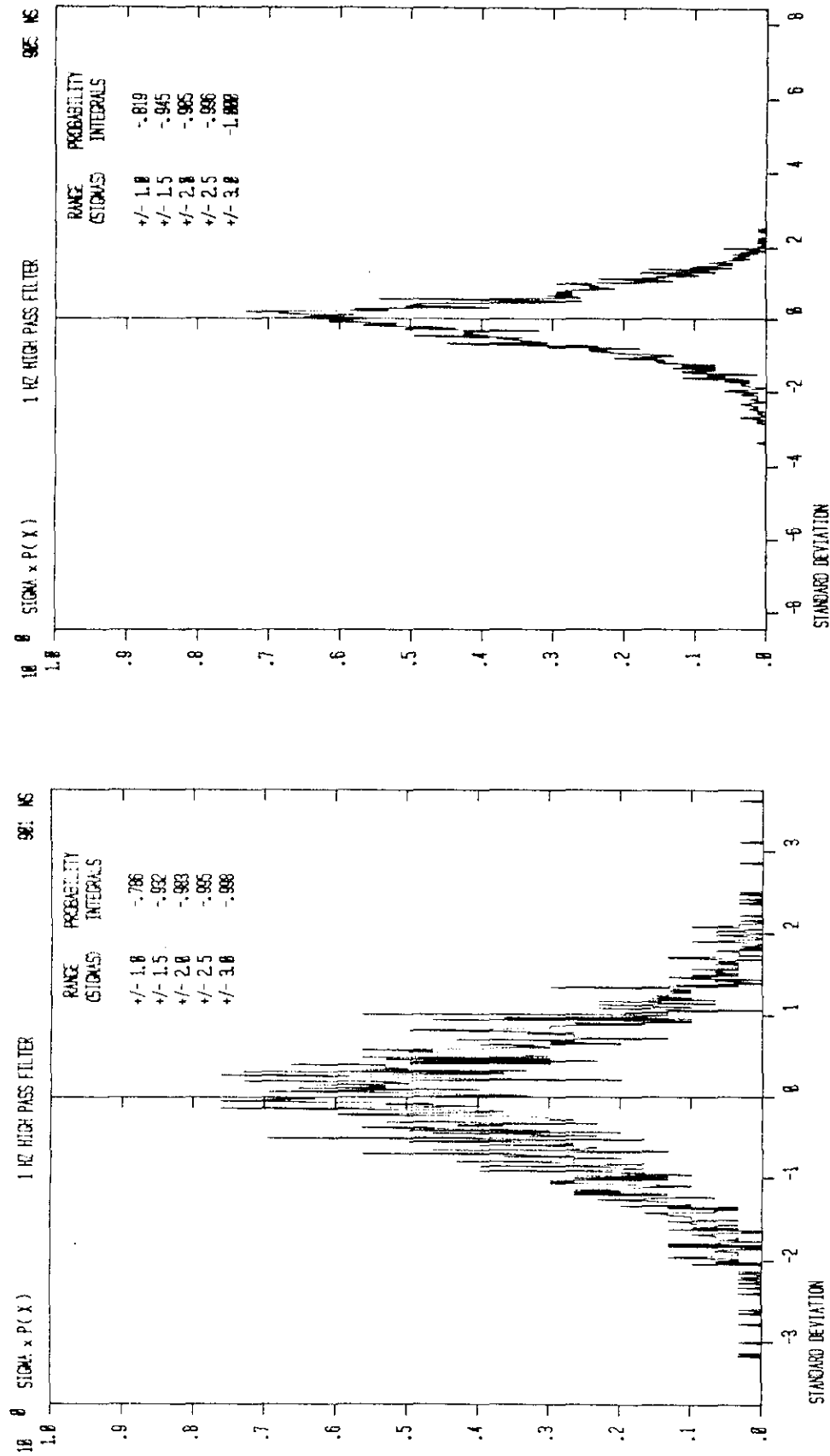


Figure 2-86. STS-11 SRB Ignition/Lift-Off - Probability Density, Sensors KAVYA003A and -004A.

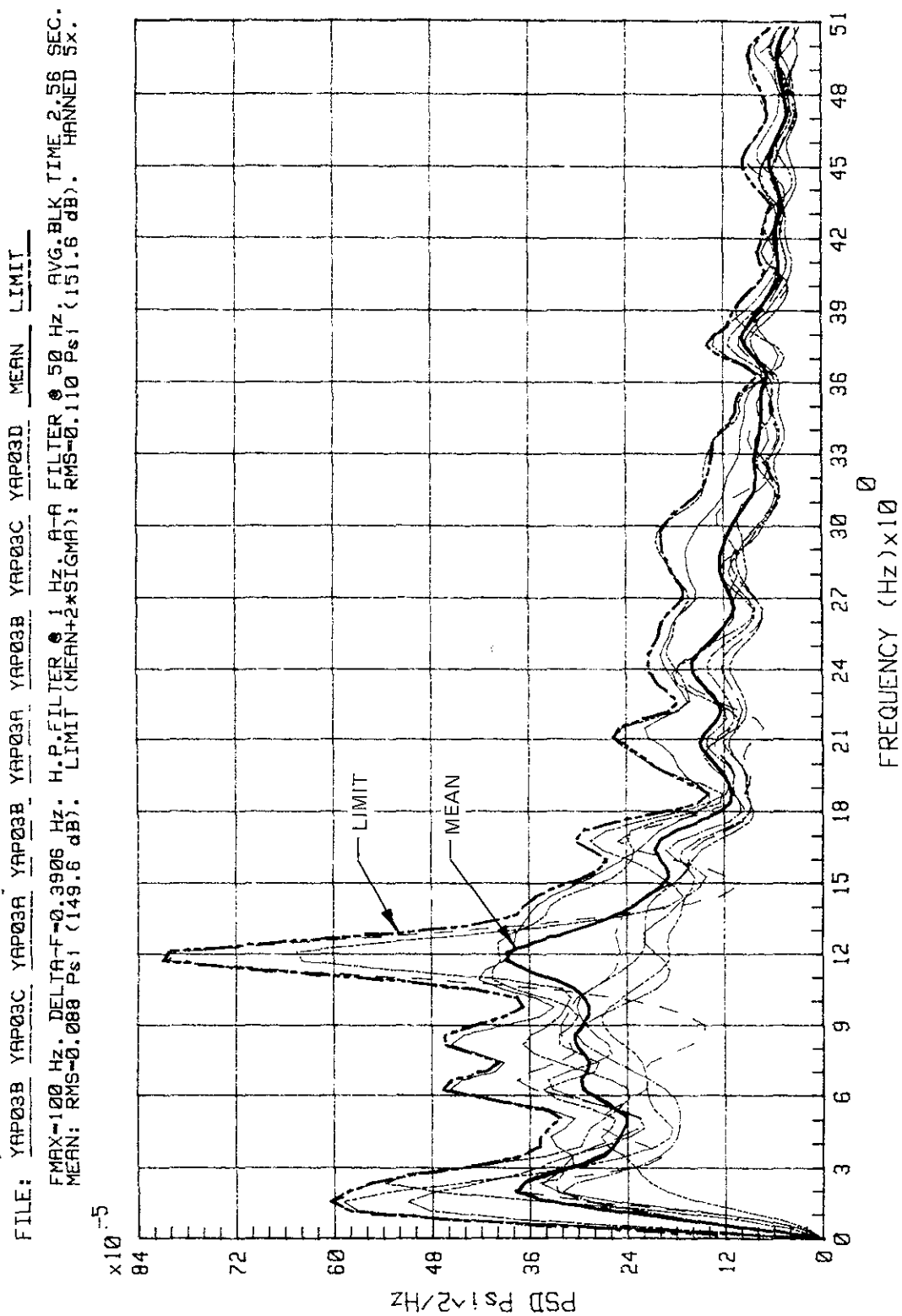


Figure 2-87. STS-8, -9, and -11 Summary at Lift-Off - PSD,
 Sensor KAVYA003A at 610 ft From the Pad

KSC-DD-818-TR

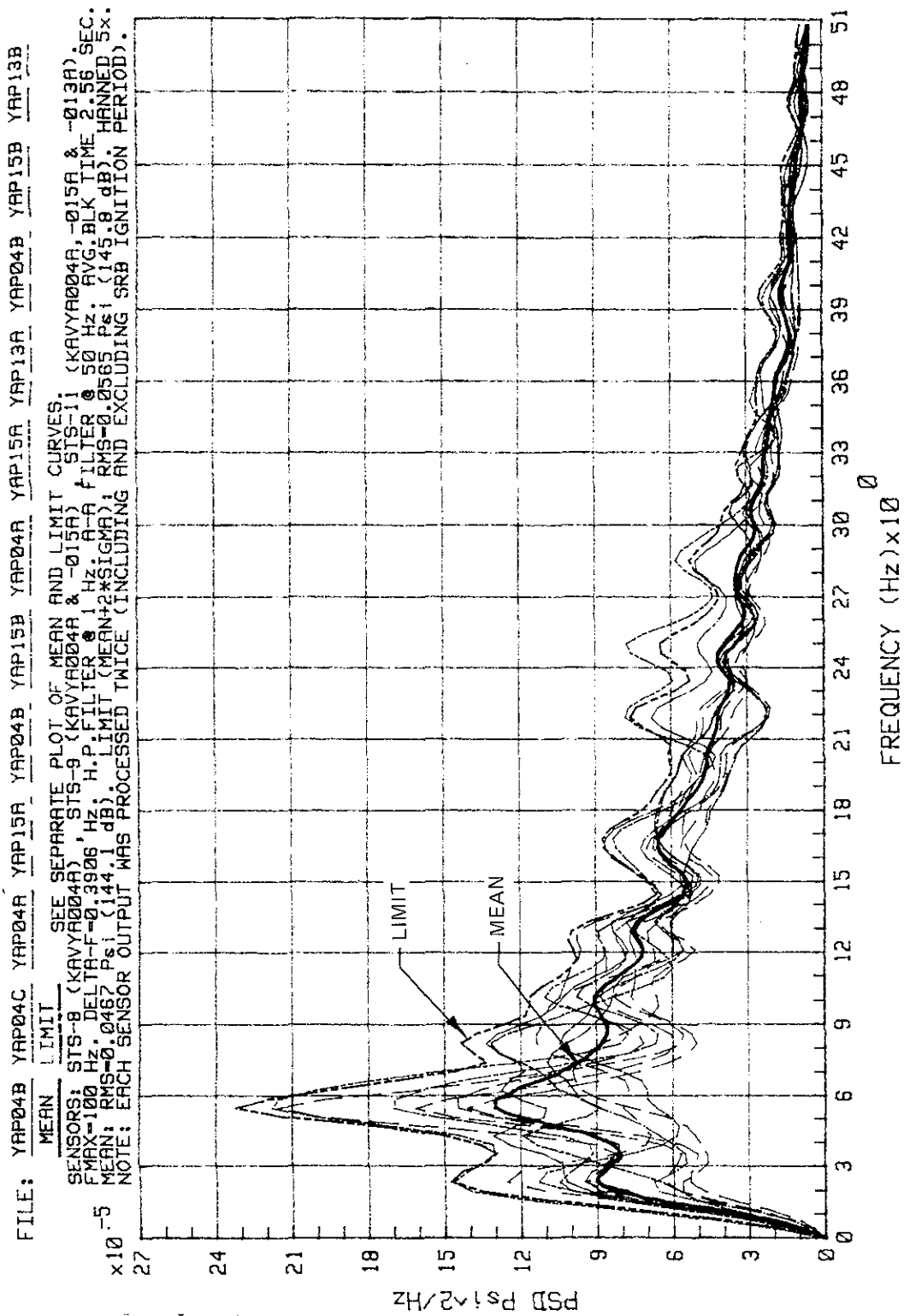


Figure 2-88. STS-8, -9, and -11 Summary at Lift-Off - PSD, Sensors at 1,200 ft From the Pad

FILE: MEAN LIMIT

SENSORS: STS-8 (KAVYA004R), STS-9 (KAVYA004R & -015R), STS-11 (KAVYA004R, -015R & -013R)
 FMAX=100 Hz. DELTA-F=0.3906 Hz. H.P. FILTER @ 1 Hz. A-A FILTER @ 50 Hz. AVG. BLK TIME 2.56 SEC.
 MEAN: RMS=0.0467 Psi (144.1 dB). LIMIT (MEAN+2*SIGMA): RMS=0.0565 Psi (145.8 dB). HANNED 5x.
 NOTE: EACH SENSOR OUTPUT WAS PROCESSED TWICE (INCLUDING AND EXCLUDING SRB IGNITION PERIOD).

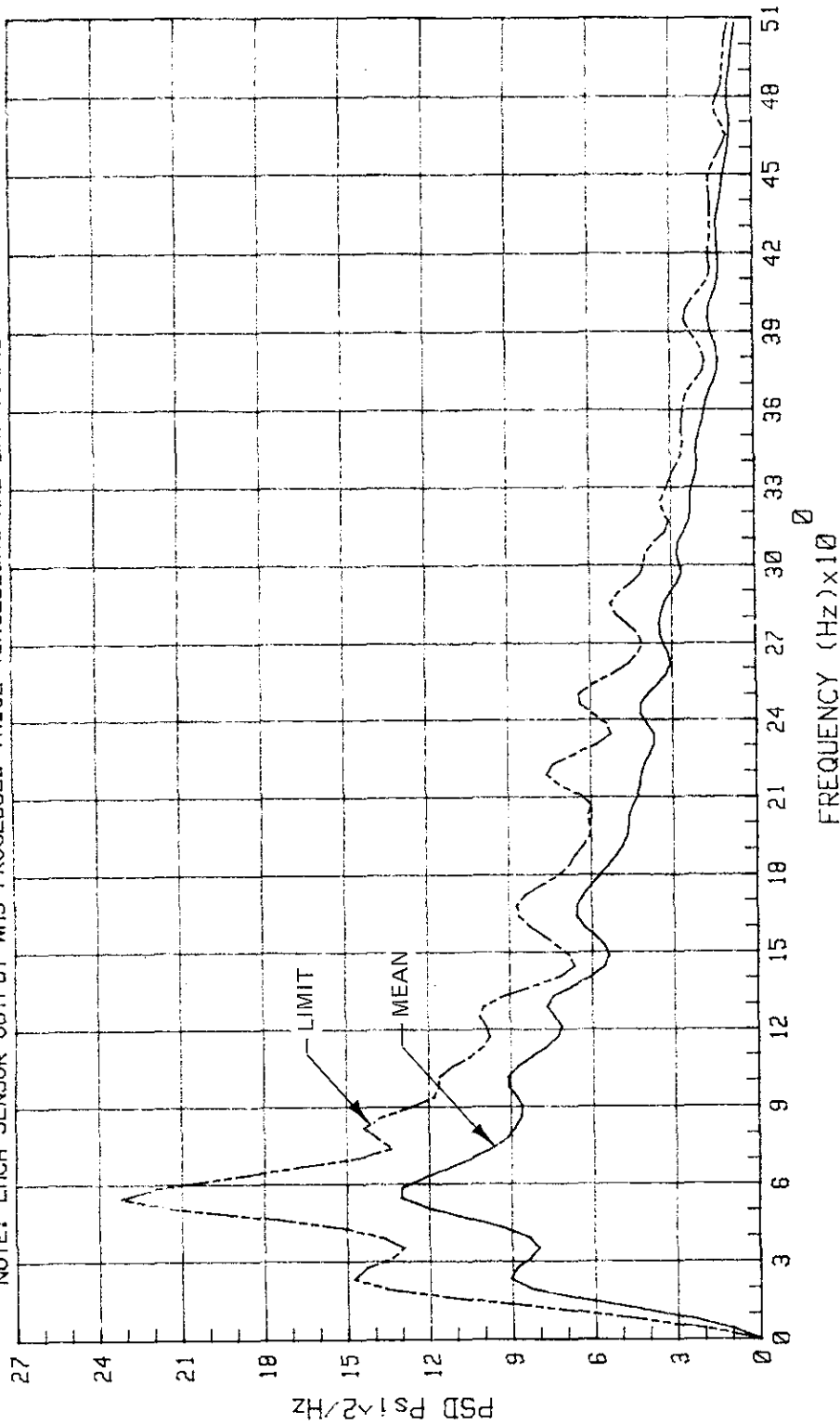


Figure 2-89. STS-8, -9, and -11 Summary at Lift-Off - PSD, Sensors at 1,200 ft From the Pad
 (Mean and Limit Only)

KSC-DD-818-TR

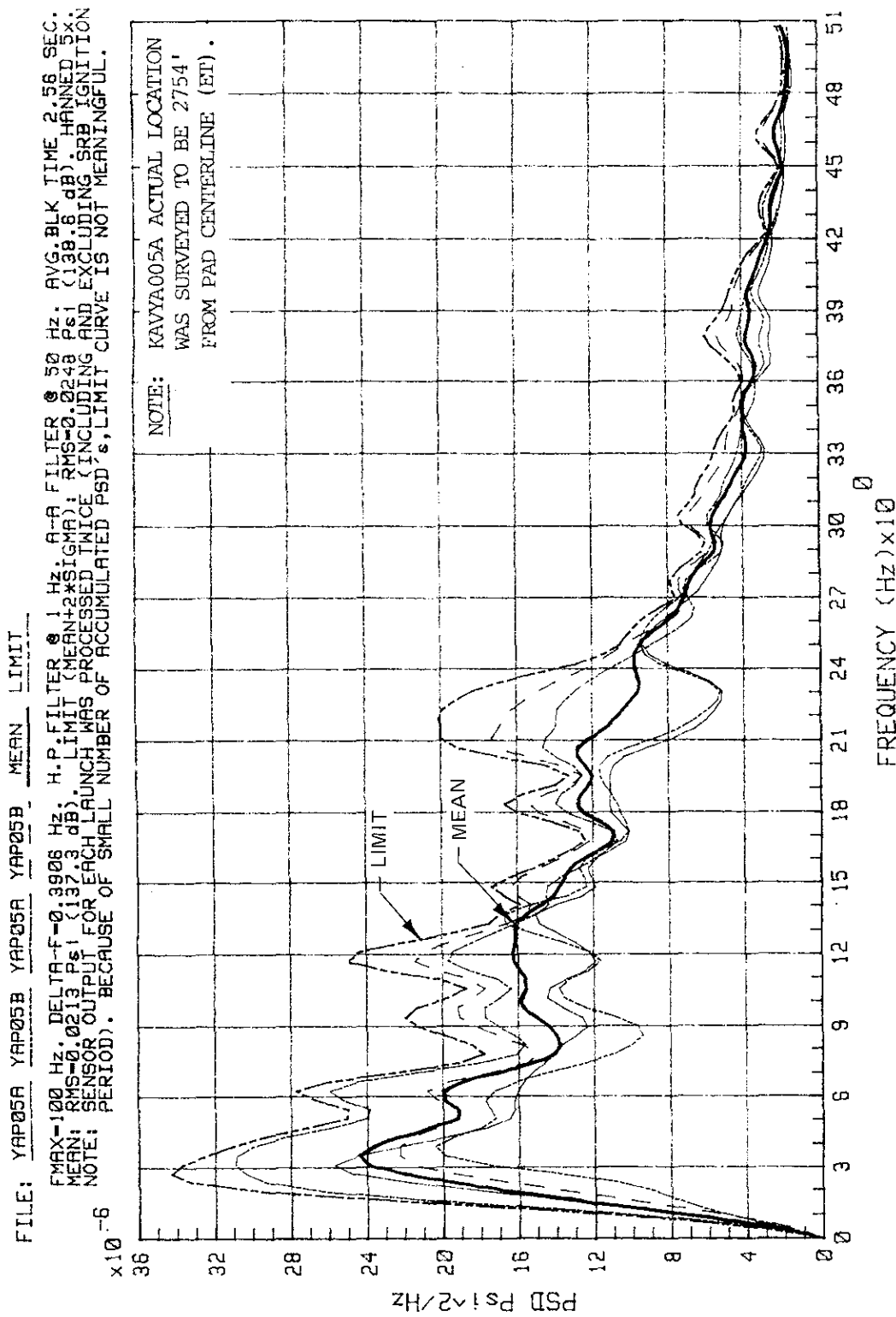


Figure 2-90. STS-9 and -11 Summary at Lift-Off - PSD, Sensor KAVYA005A at 2,500 ft From the Pad

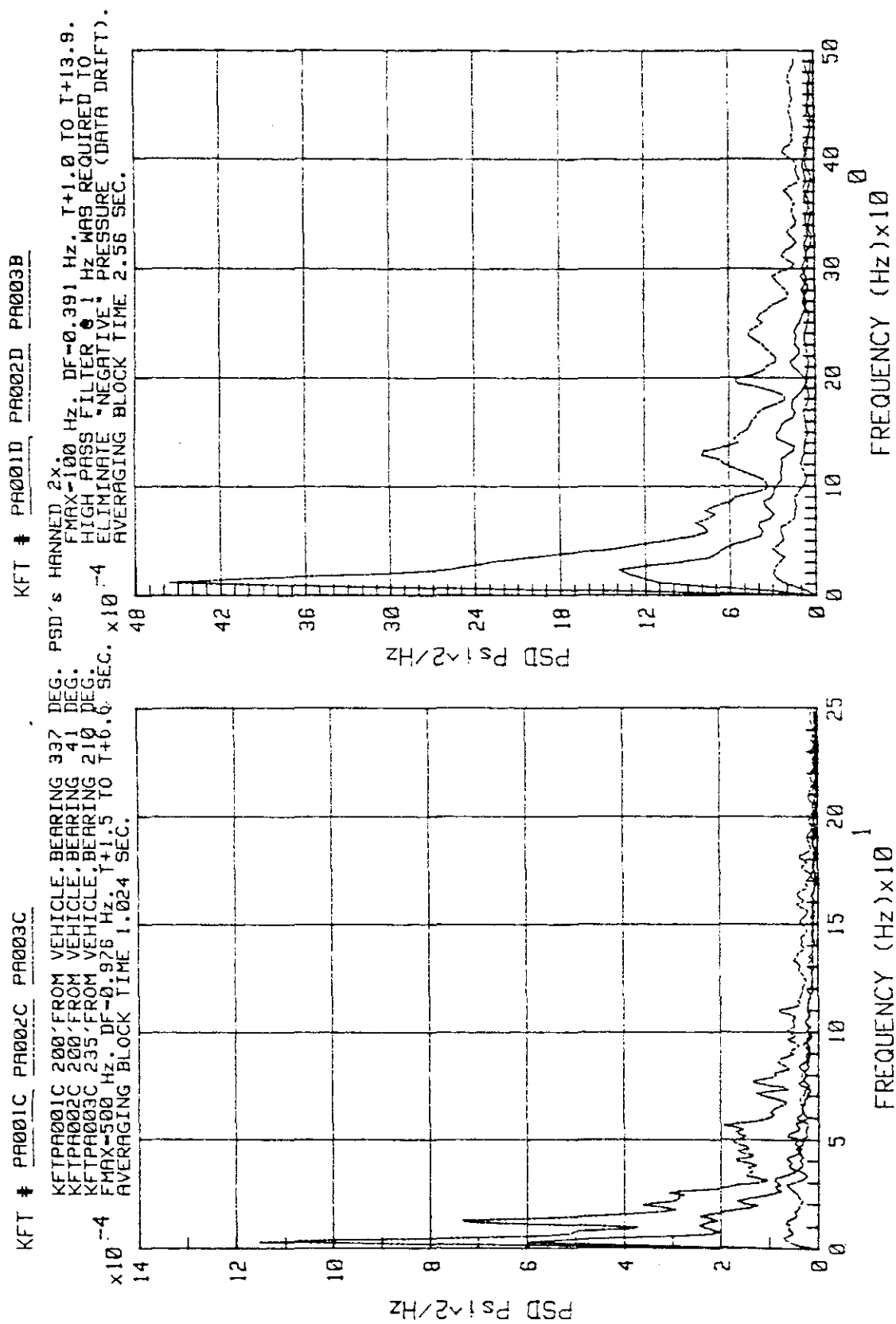


Figure 2-91. STS-6 Acoustic Pressure on Light Posts at the 98-ft Elevation with Sensors Facing the Vehicle (Averaging Block Time 1.024 s and 2.56 s)

KSC-DD-818-TR

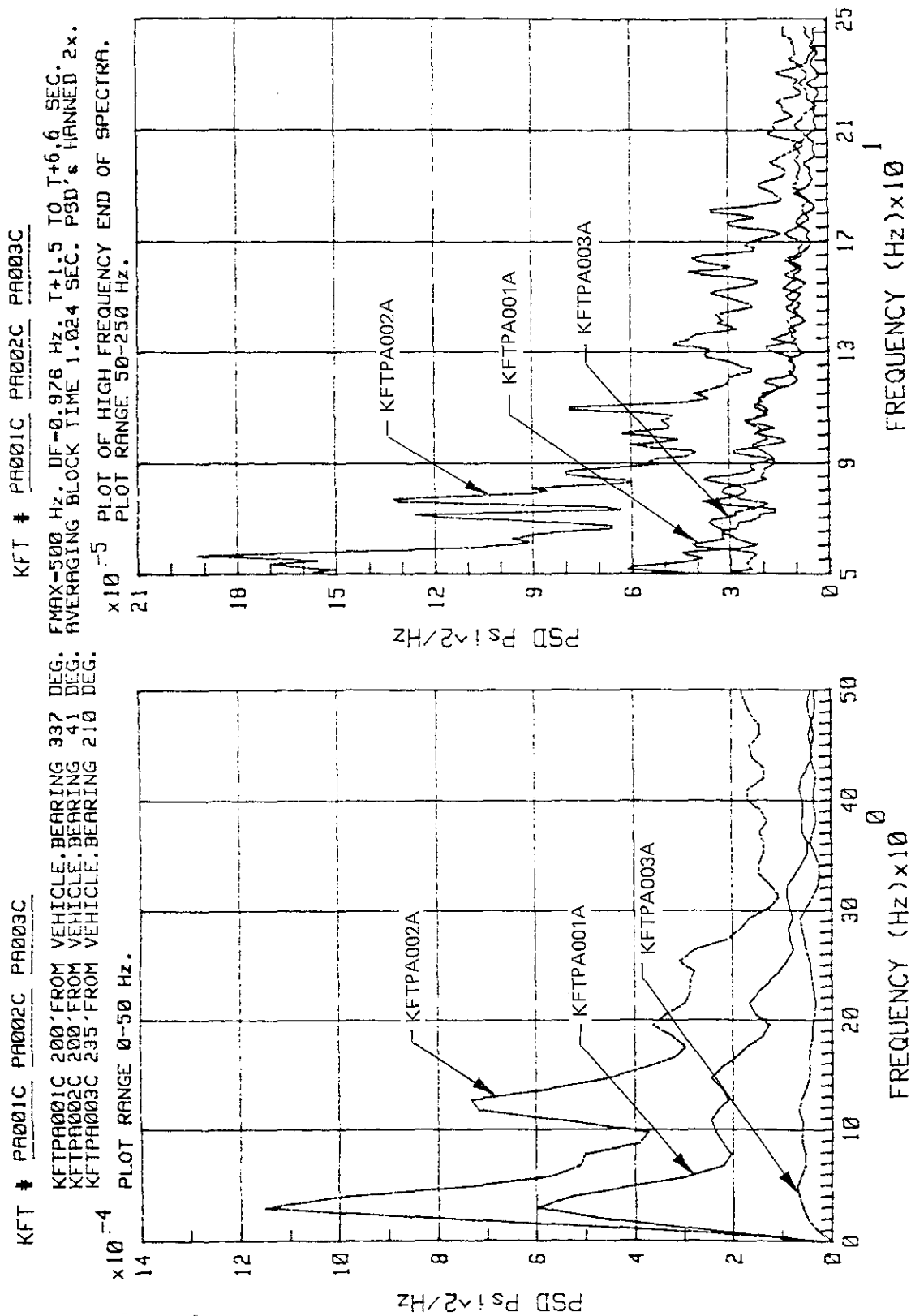


Figure 2-92. STS-6 Acoustic Pressure on Light Posts at the 98-ft Elevation with Sensors Facing the Vehicle (0- to 50-Hz and 50- to 250-Hz Plot Range)

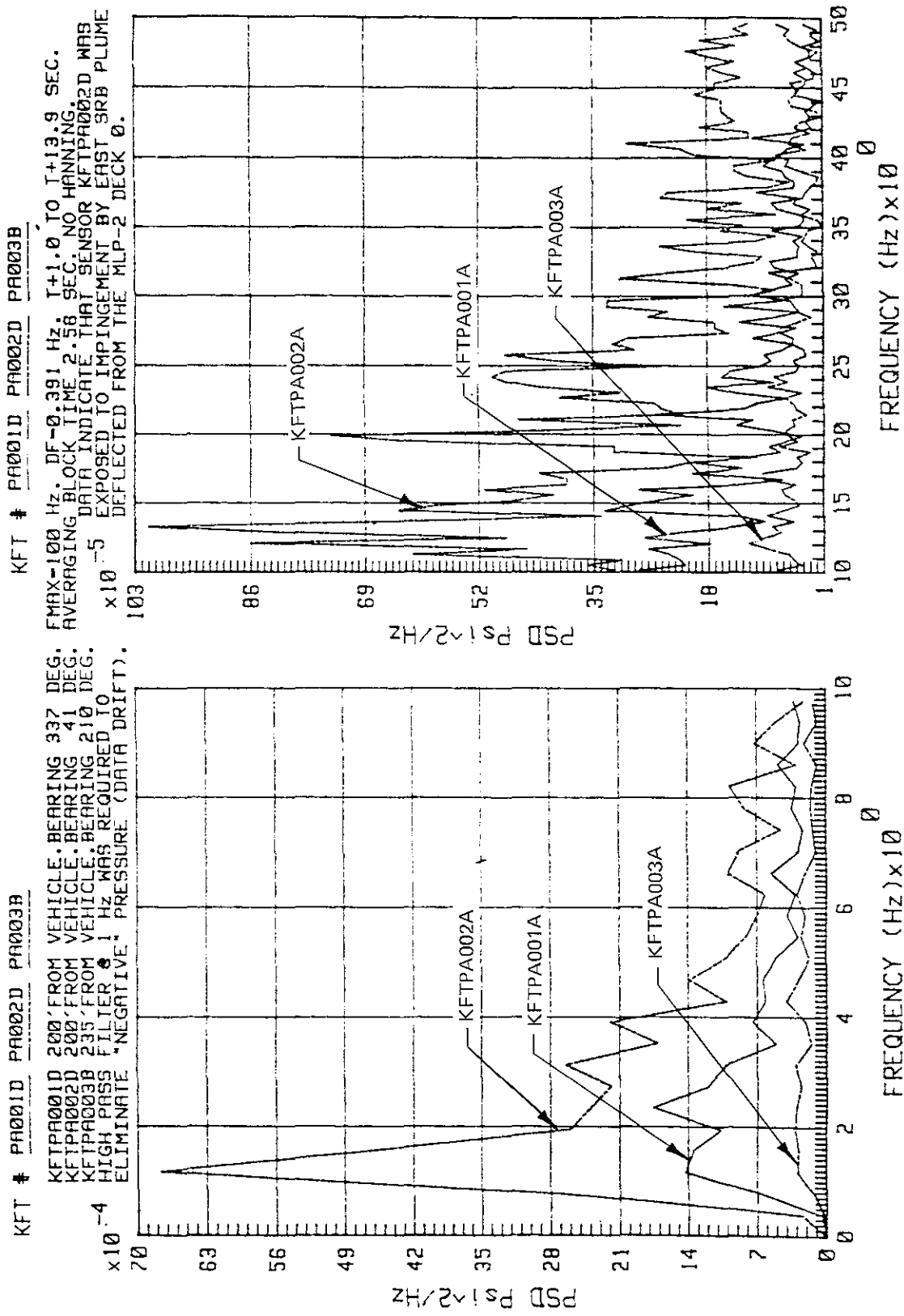


Figure 2-93. STS-6 Acoustic Pressure on Light Posts at the 98-ft Elevation with Sensors Facing the Vehicle (0- to 10-Hz and 10- to 50-Hz Plot Range)

KSC-DD-818-TR

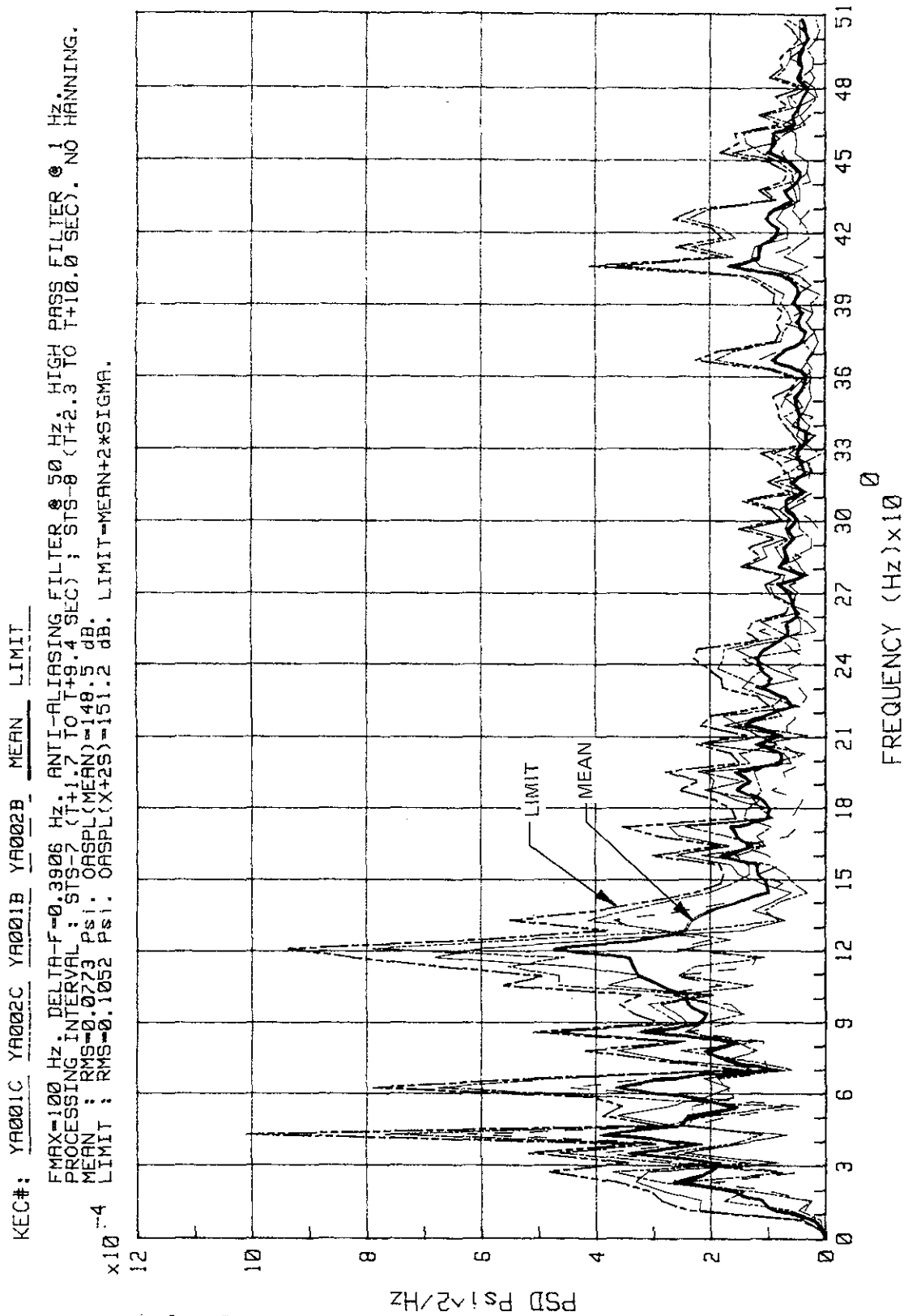


Figure 2-94. STS-7 and -8 Lift-Off Peak - ECS Cooling Tower Acoustics (No Hanning)

KEC#: YA001C YA002C YA001B YA002B MEAN LIMIT

FMAX=100 Hz. DELTA-F=0.3906 Hz. ANTI-ALIASING FILTER @ 50 Hz. HIGH PASS FILTER @ 1 Hz.
 PROC. INTERVAL: STS-7 (T+1.7 TO T+9.4 SEC); STS-8 (T+2.3 TO T+10.0 SEC). ALL PSD's HANNED 2x.
 MEAN: RMS=0.0773 Psi. OASPL(MEAN)=148.5 dB. OVERLAP PROCESSING RESULTS IN 5 DATA BLOCKS/MEAS.
 LIMIT: RMS=0.1000 Psi. OASPL(X+2S)=150.8 dB. LIMIT=MEAN+2*SIGMA. MEAN & LIMIT VALUES ARE FOR
 x10⁻⁵ LIMIT: DATA PLOT RANGE 0-51 Hz. TOTAL NUMBER OF NORMALIZED DATA BLOCKS FOR AVERAGING IS 20.

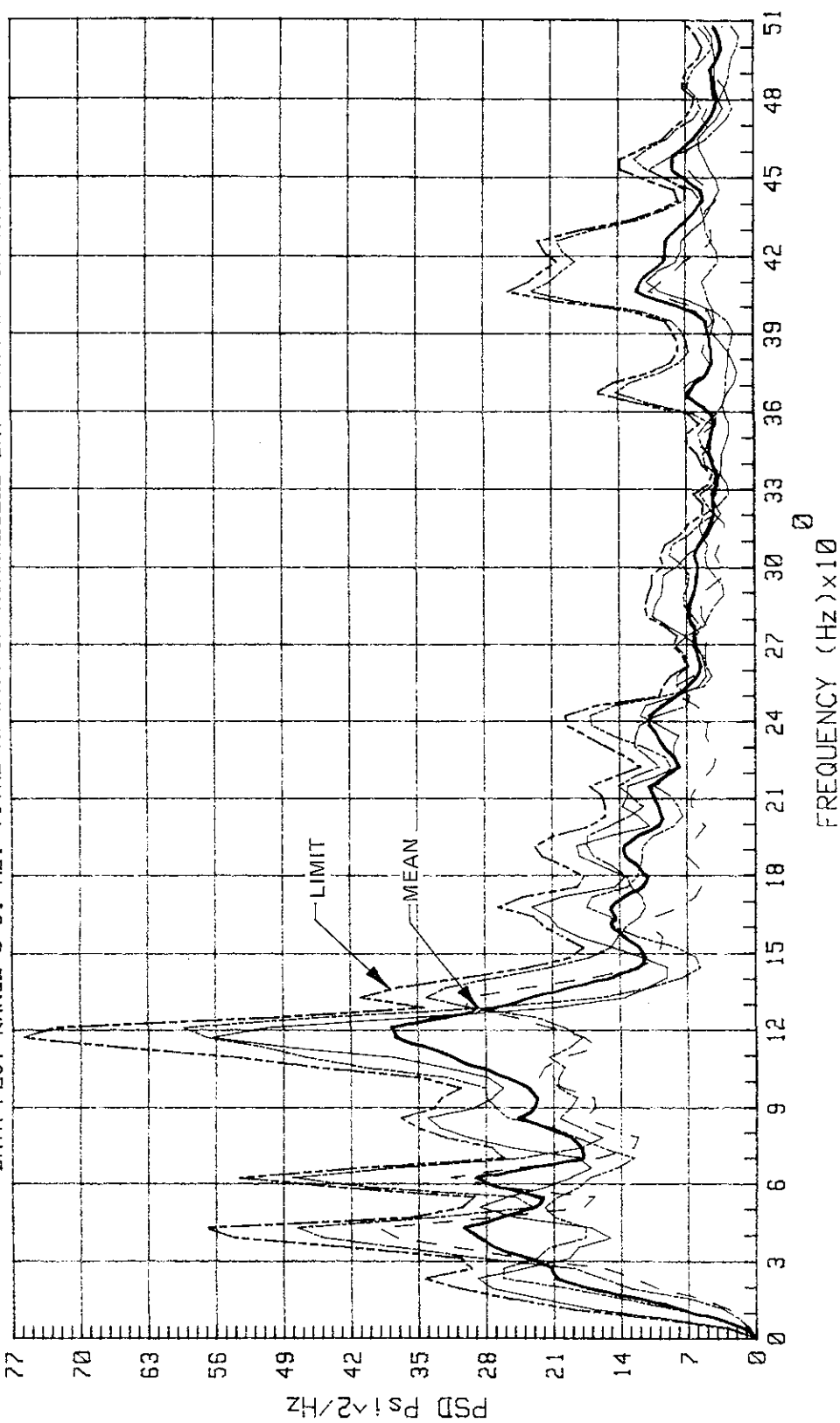


Figure 2-95. STS-7 and -8 Lift-Off Peak - ECS Cooling Tower Acoustics (All PSD's Hanned)

KSC-DD-818-TR

FAR FIELD
PREDICTED AVERAGE SOUND PRESSURE LEVELS
(50 PERCENT CONFIDENCE LEVELS)

Direction:
322° T from Pad Centerline

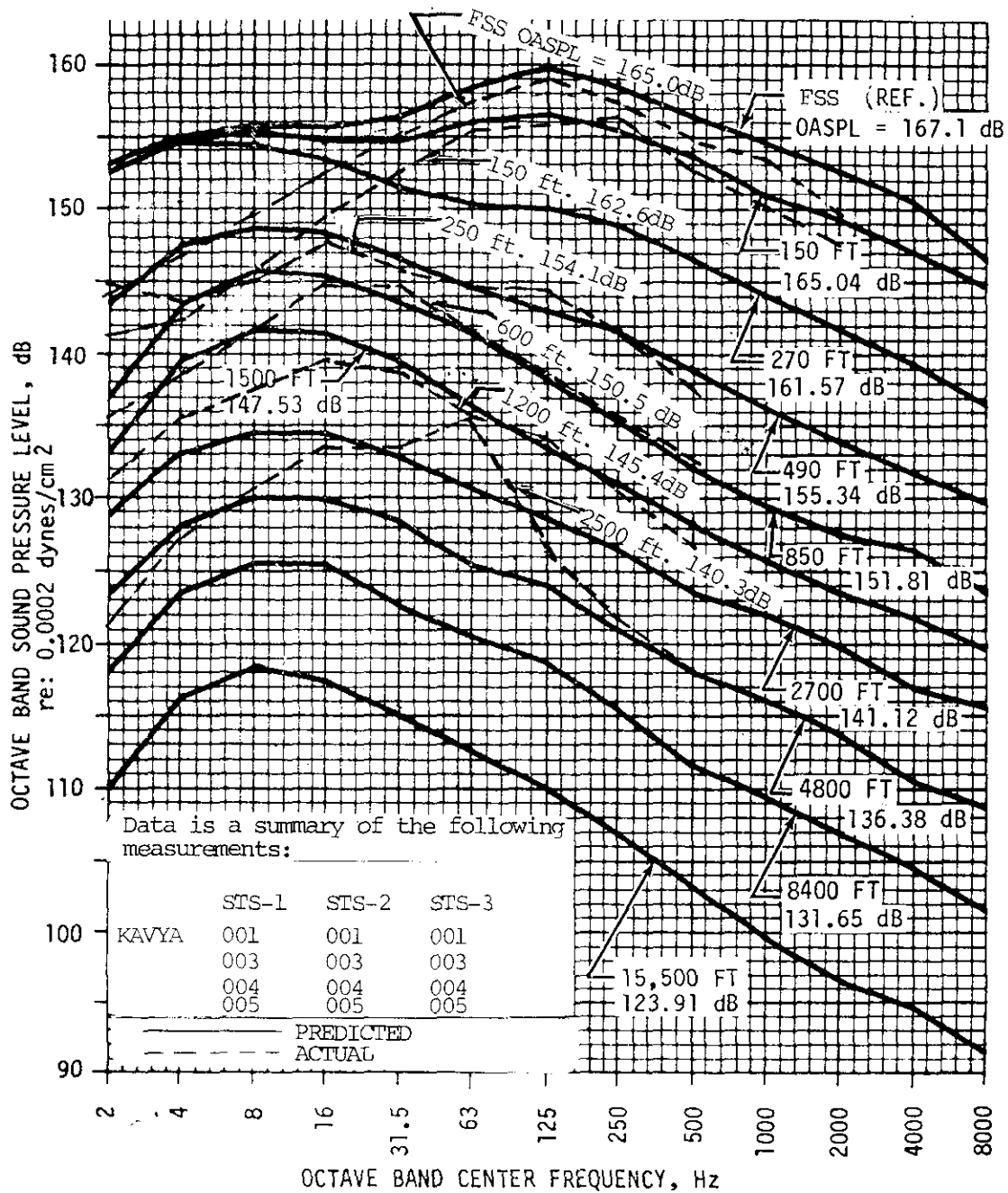


Figure 2-96. Predicted and Actual Sound Pressure Levels Data Summary

2.5 MLP DECK 0 PRESSURES

This section presents a summary of plume impingement pressures recorded by six pressure sensors during STS-1, -2, -3, and -9 launches. The thermally protected sensors were located only on MLP-1 as shown in figure 2-97. Not all sensors provided valid data for each launch. Data losses, mainly dropouts, were caused by the severe vibration environment affecting the data acquisition system (DAS). Remaining valid data were processed to provide slow varying pressure components designated as TVM and rapidly varying dynamic components, further processed to yield PSD's. Extraction of TVM used multiple application of time domain averaging by means of Hanning algorithm, a symmetric coefficient digital filter that acts as a low-pass filter but without introducing time delay (phase shift) in filtered data.

Extracted TVM's, often identified as "static" pressures, for each launch are shown on figures 2-98 through 2-101. Sensors that provided data and other pertinent information are shown in plot headings.

A summary of static pressures recorded by each pair of sensors equidistant from the SRB's in prelaunch position is shown on figures 2-102 through 2-104.

Typical PSD's obtained from dynamic pressure components (dynamic component is the difference between raw data and TVM) for STS-9 are shown on figure 2-105. The user is referred to previously published STS-1 through STS-3 data documents for additional information (PSD's, rms time histories, probability densities, etc.) on processed dynamic components. The highest values of dynamic components were recorded during STS-1 by sensor KSRPF011A (14.7 psi rms average within 0.512 s data block). Pertinent plots are shown on figures 2-106 and 2-107. The right plot on figure 2-106 shows probability density with asymmetric distribution of dynamic pressure components.

As an illustration of response to both static and dynamic pressure components, figure 2-108 presents STS-1 strain time histories (raw data, TVM, and dynamic components) recorded by a strain gage on the bottom flange of T-2 truss top chord. These time histories are similar to those of pressures. Note that after the peak, a slow decay of TVM to ambient is delayed (by a few minutes) by induced thermal strains in the deck 0. Peak amplitudes of dynamic strain components slightly exceed peak values of TVM strains.

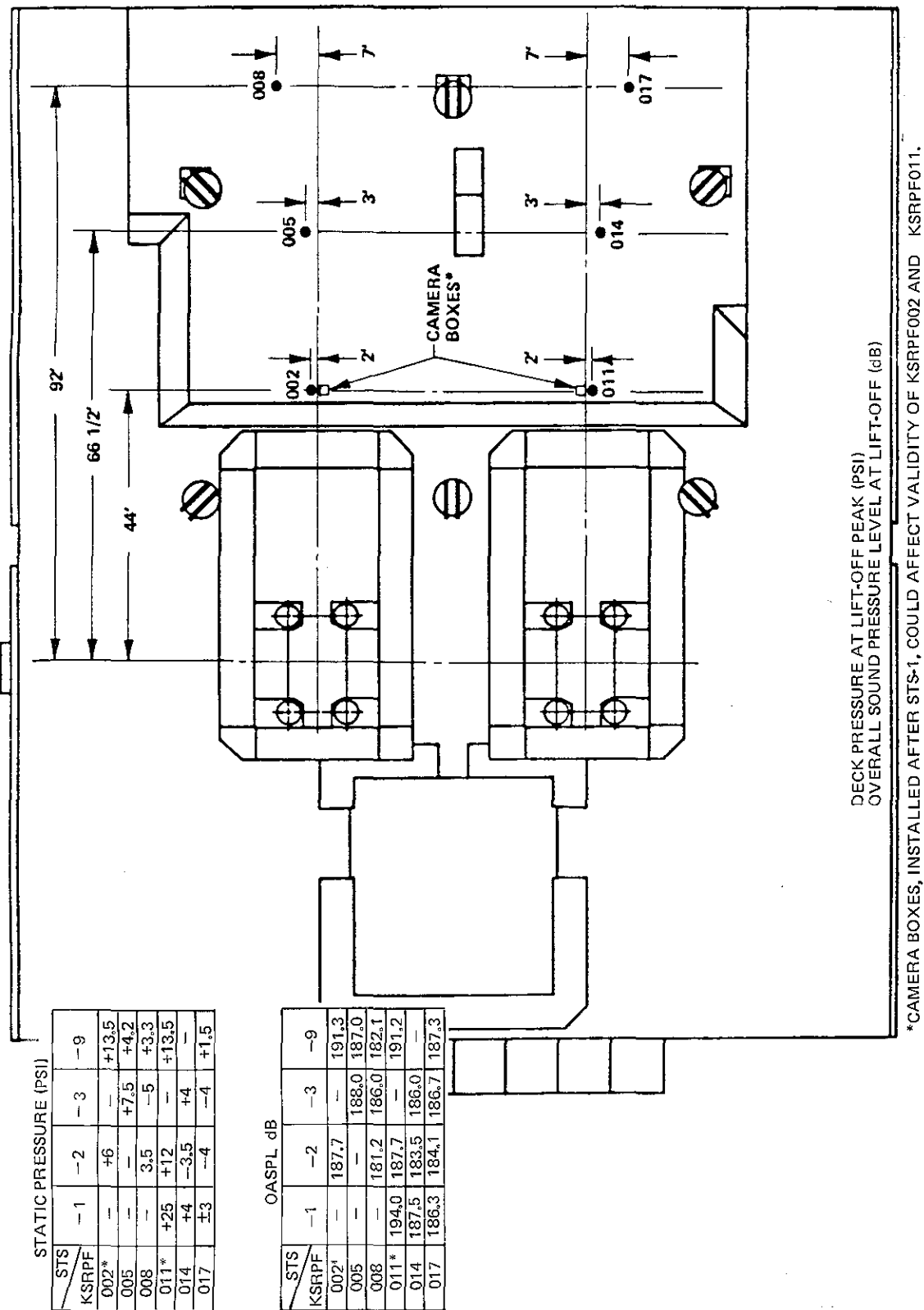


Figure 2-97. MLP-1 Static Pressures and OASPL's

FILE: PFT11A PFT14A PFT17A

SENSORS: KSRPF011A, KSRPF014A & KSRPF017A.
 SAMPLING RATE 200 Hz. A-A FILTER @ 50 Hz.
 BY HANNING 200X. TIME SCALE REFERENCED TO T-ZERO-102:12:00:03.983 GMT (1981).
 x10.0 PLOT START TIME-T+5.00 SEC.

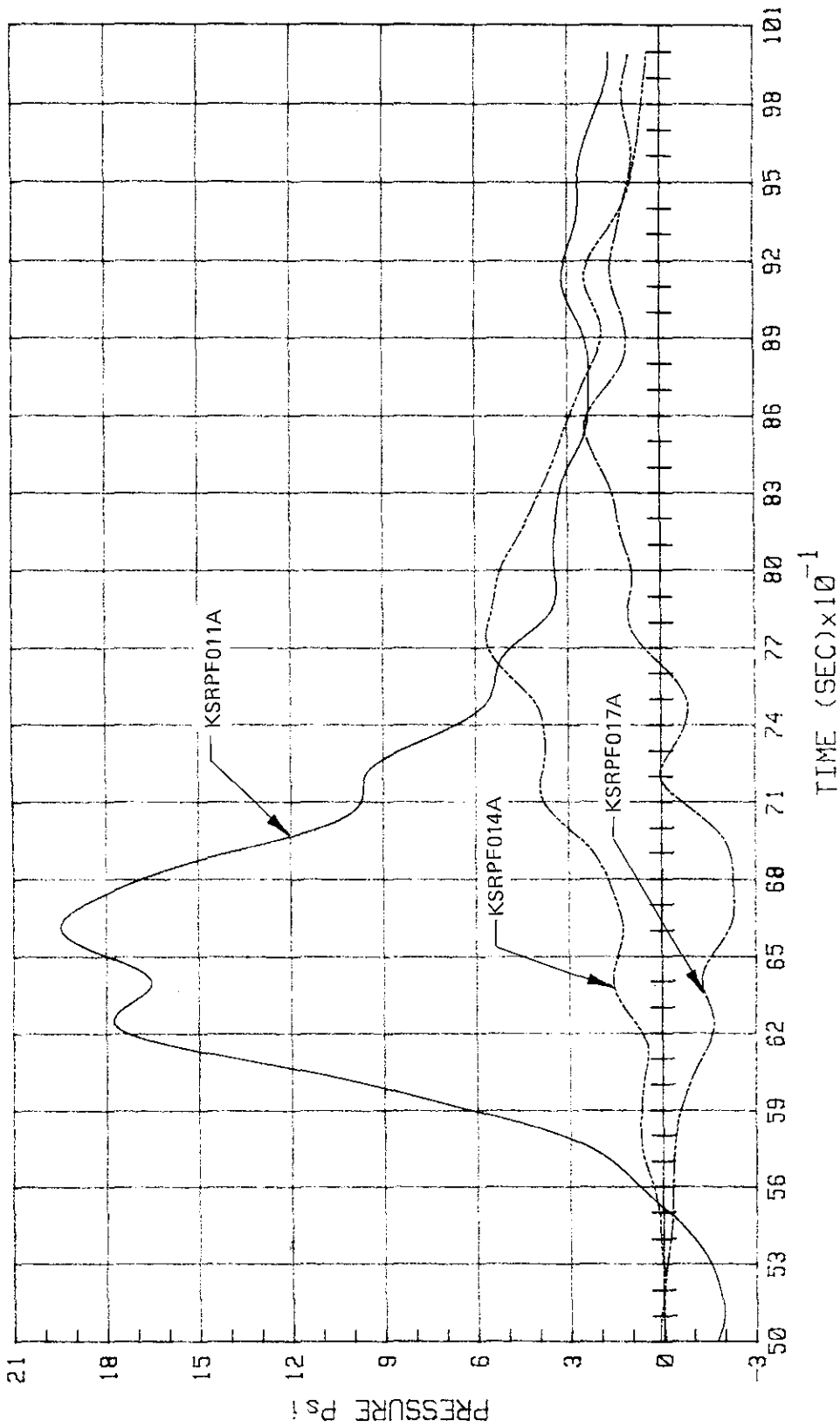


Figure 2-98. STS-1 MLP-1 Deck 0 Impinging Plume Pressure (TVM)

KSC-DD-818-TR

FILE: PFT02B PFT08B PFT11B PFT14B PFT17B

SENSORS: KSRPF002A, KSRPF008A, KSRPF011A, KSRPF014A & KSRPF017A.
 SAMPLING RATE 200 Hz. A-A FILTER @ 50 Hz. TVM (Time Variable Mean) EXTRACTED FROM RAW DATA
 BY HANNING 200X. TIME SCALE REFERENCED TO T-ZERO=316:15:09:59.833 GMT (1981).
 0 PLOT START TIME=T+5.00 SEC.

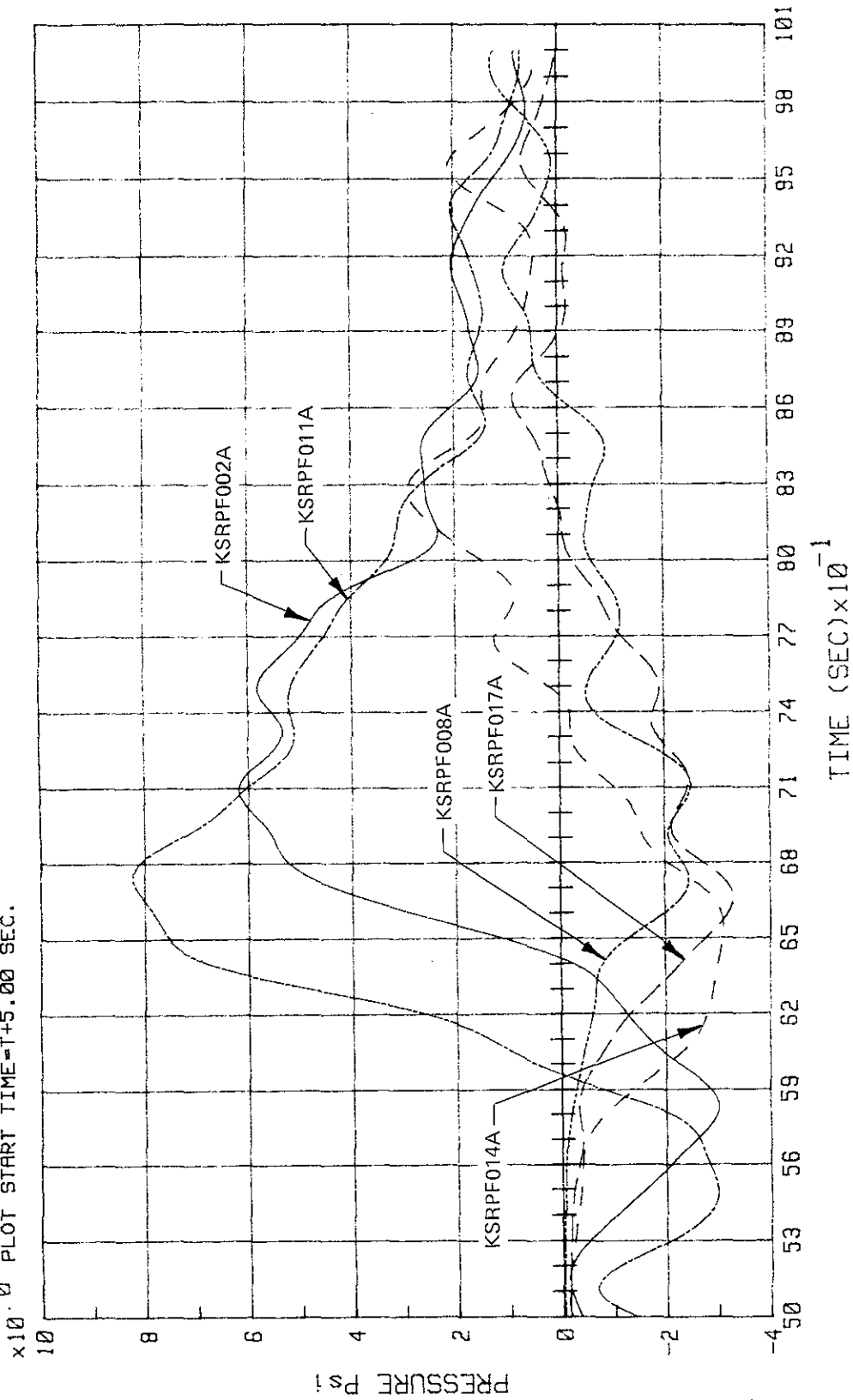


Figure 2-99. STS-2 MLP-1 Deck 0 Impinging Plume Pressure (TVM)

FILE: PFT05C PFT08C

SENSORS: KSRPF005A & KSRPF008A.
 SAMPLING RATE 200 Hz. A-A FILTER @ 50 Hz. TVM (Time Variable Mean) EXTRACTED FROM RAW DATA
 BY HANNING 200x. TIME SCALE REFERENCED TO T-ZERO=081:15:59.801 GMT (1982).
 PLOT START TIME -15.00 SEC.

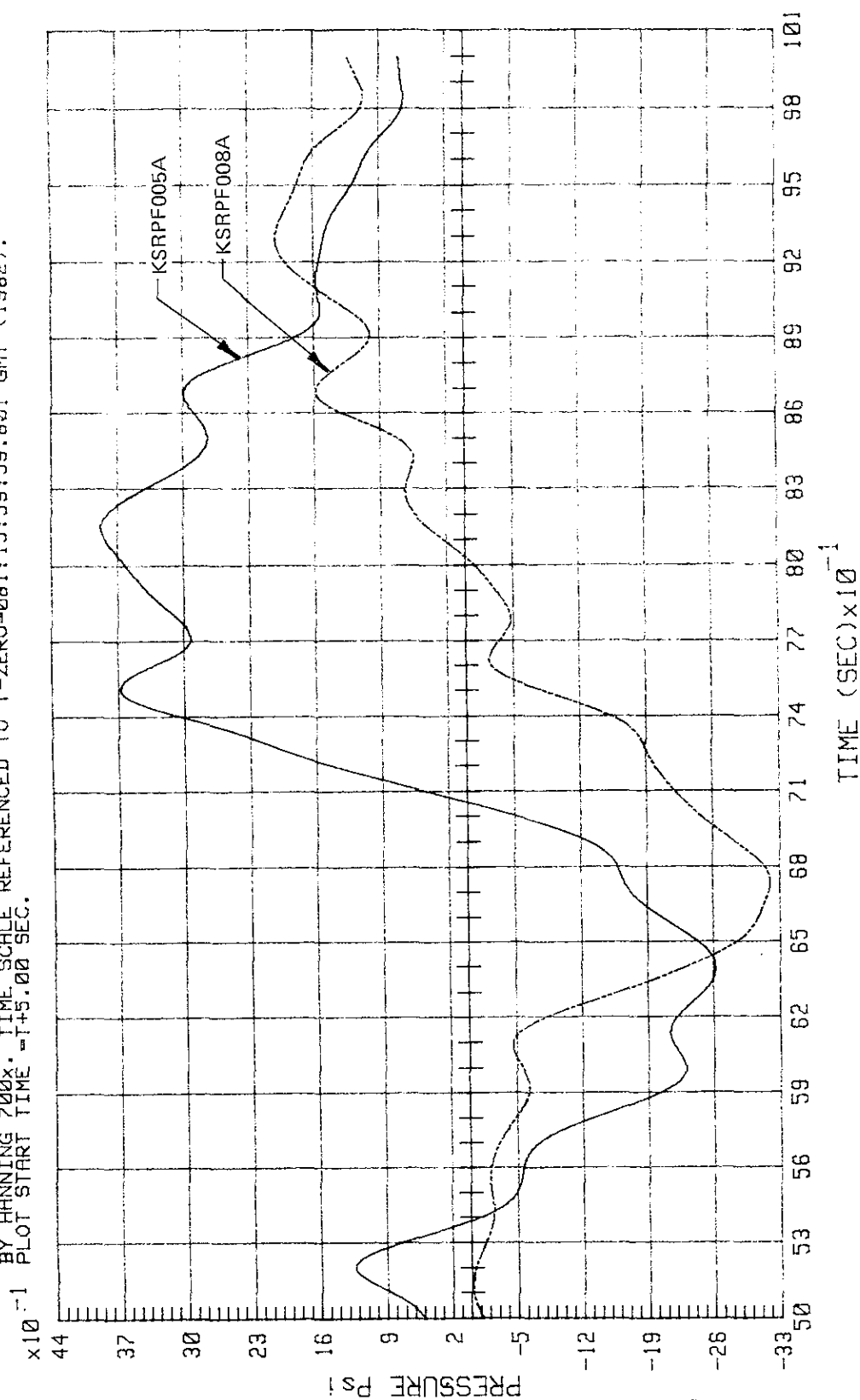


Figure 2-100. STS-3 MLP-1 Deck 0 Impinging Plume Pressure (TVM)

KSC-DD-818-TR

FILE: PFT02D PFT05D PFT08D PFT11D PFT17D

SENSORS: KSRPF002A, KSRPF005A, KSRPF008A, KSRPF011A & KSRPF017A.
 SAMPLING RATE 200 Hz. A-A FILTER @ 50 Hz. TVM (Time Variable Mean) EXTRACTED FROM RAW DATA
 BY HANNING 200x. TIME SCALE REFERENCED TO T-ZERO-332:16:00:00 GMT (1983).
 0 PLOT SCALE START TIME-14.00 SEC. DATA DROPOUTS IN THE OUTPUTS OF KSRPF002A & KSRPF005A
 PREVENTED TVM PLOTS BEYOND T+7.8 SEC FOR THESE SENSORS.

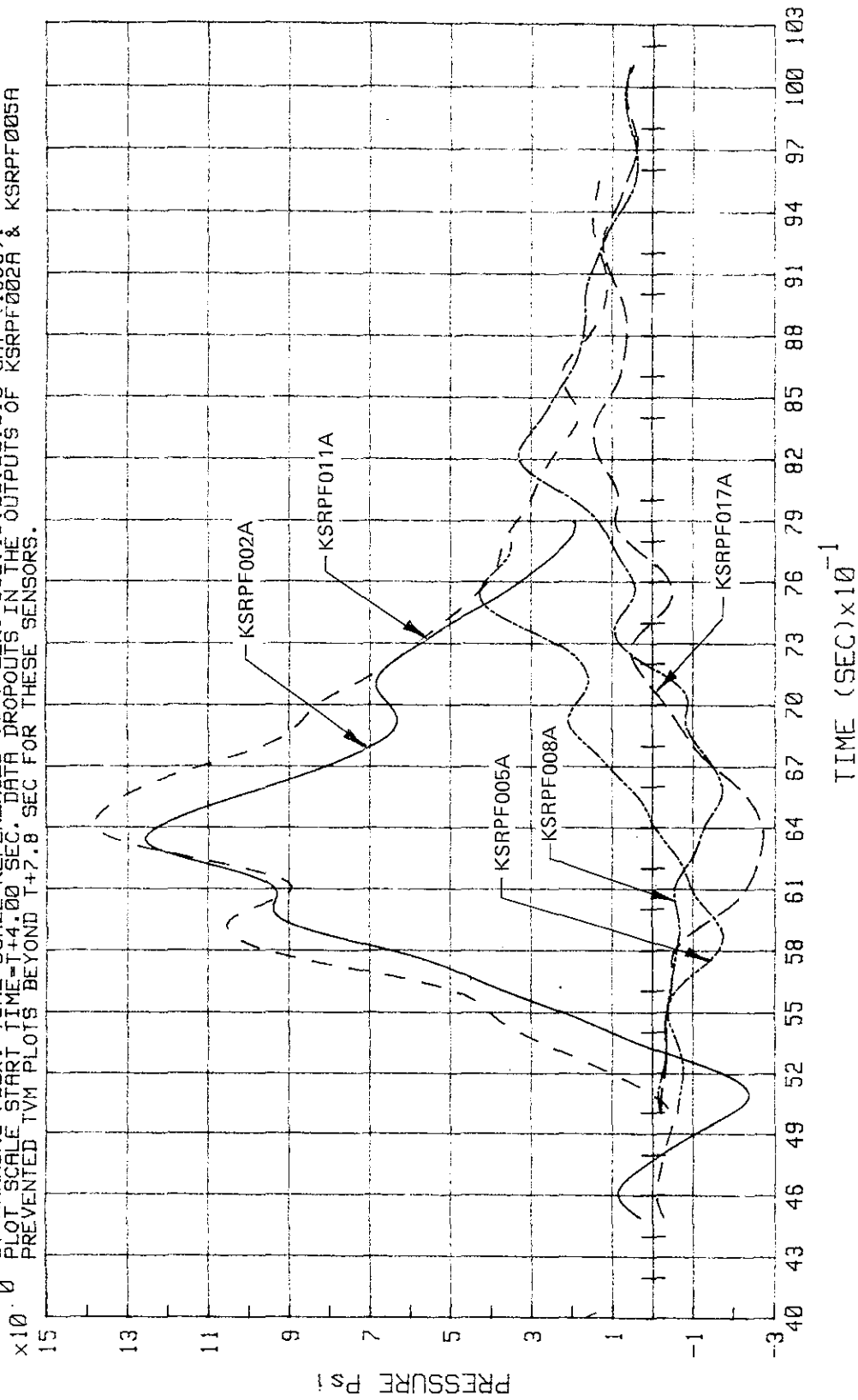


Figure 2-101. STS-9 MLP-1 Deck 0 Impinging Plume Pressure (TVM)

FILE: PFT11A PFT11B PFT02B PFT11D PFT02D

STS-1 SENSOR KSRPF011A, STS-2 & STS-9 SENSORS KSRPF011A & KSRPF002A. EXTRACTED FROM RAW DATA
 SAMPLING RATE 200 Hz. A-A FILTER @ 50 Hz. TVM (Time Variable Mean) FOR EACH LAUNCH.
 BY HANNING 200x. TIME SCALE IS REFERENCED TO T-ZERO (SRB IGNITION) FOR EACH LAUNCH.
 DROP IN PEAK POSITIVE PRESSURE AFTER STS-1 IS CAUSED BY A CAMERA BOX, INSTALLED ABOUT 1.5 FT
 FROM THE SENSORS, DEFLECTING LOCAL FLOW. PLOT SCALE START TIME = T+4.00 SEC.

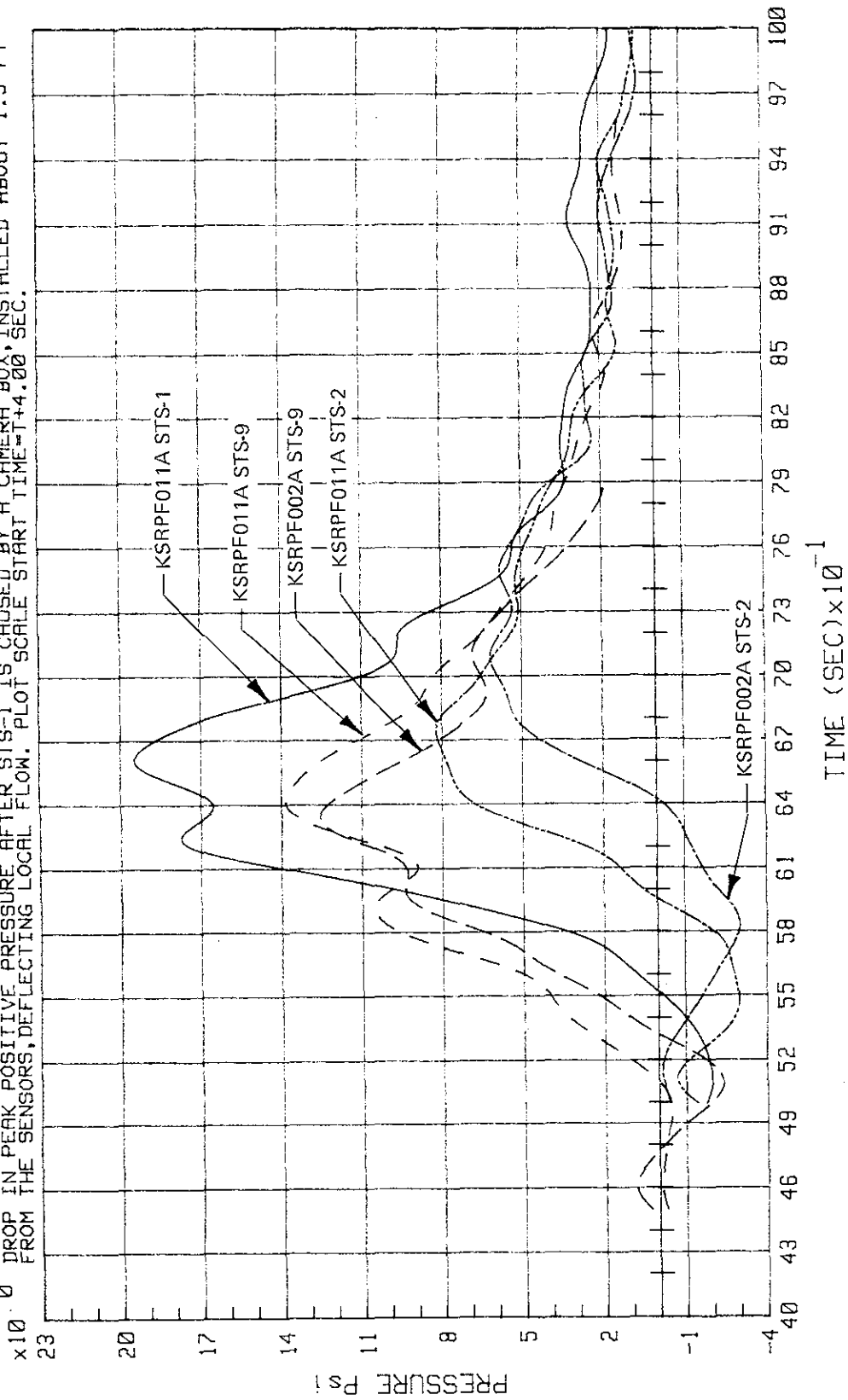


Figure 2-102. STS-1, -2, and -9 MLP-1 Deck 0 Impinging Plume Pressure (TVM)

KSC-DD-818-TR

FILE: PFT14A PFT14B PFT05C PFT05D

STS-1 & STS-2 SENSOR KSRPF014A, STS-3 & STS-9 SENSOR KSRPF005A.
 SAMPLING RATE 200 Hz. H-A FILTER @ 50 Hz. TVM (Time Variable Mean) EXTRACTED FROM RAW DATA
 BY HANNING 200x. TIME SCALE IS REFERENCED TO T-ZERO (SRB IGNITION) FOR EACH LAUNCH.
 x10⁻¹ PLOT SCALE START TIME = T+5.00 SEC.

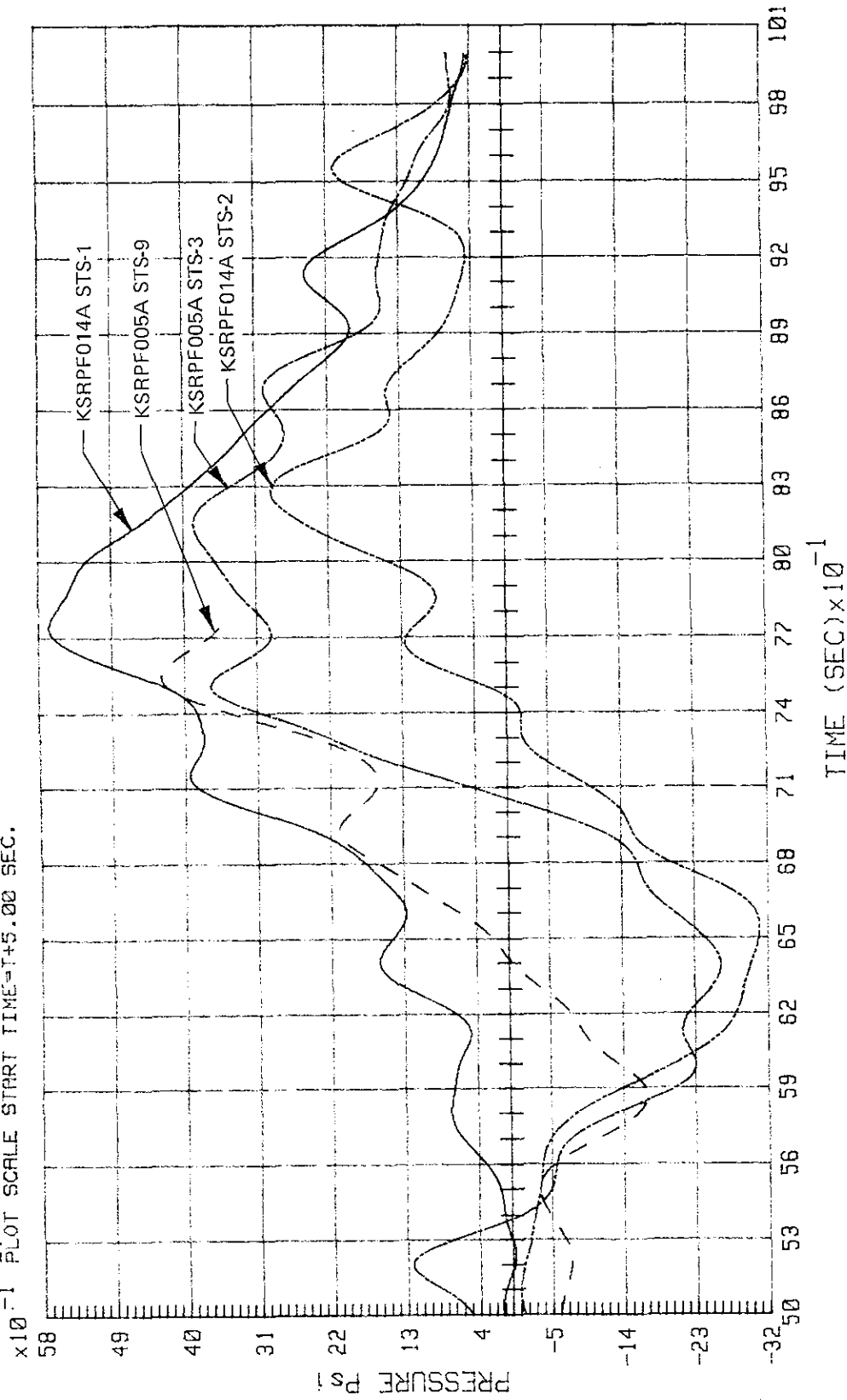


Figure 2-103. STS-1, -2, -3, and -9 MLP-1 Deck 0 Impinging Plume Pressure (TVM)
 (Sensors: STS-1 and -2, KSRPF014A; and STS-3 and -9, -005A)

FILE: PFT17A PFT17B PFT08B PFT08C PFT12D PFT08D

STS-1 SENSOR KSRPF017A, STS-2 SENSORS KSRPF017A & KSRPF008A, STS-3 SENSOR KSRPF008A.
 STS-9 SENSORS KSRPF017A & KSRPF008A. SAMPLING RATE 200 Hz. A-A FILTER @ 50 Hz.
 TVM (Time Variable Mean) EXTRACTED FROM RAW DATA BY HANNING 200x. TIME SCALE IS REFERENCED
 -1 TO T-ZERO (SRB IGNITION) FOR EACH LAUNCH. PLOT SCALE START TIME=T+5.00 SEC.

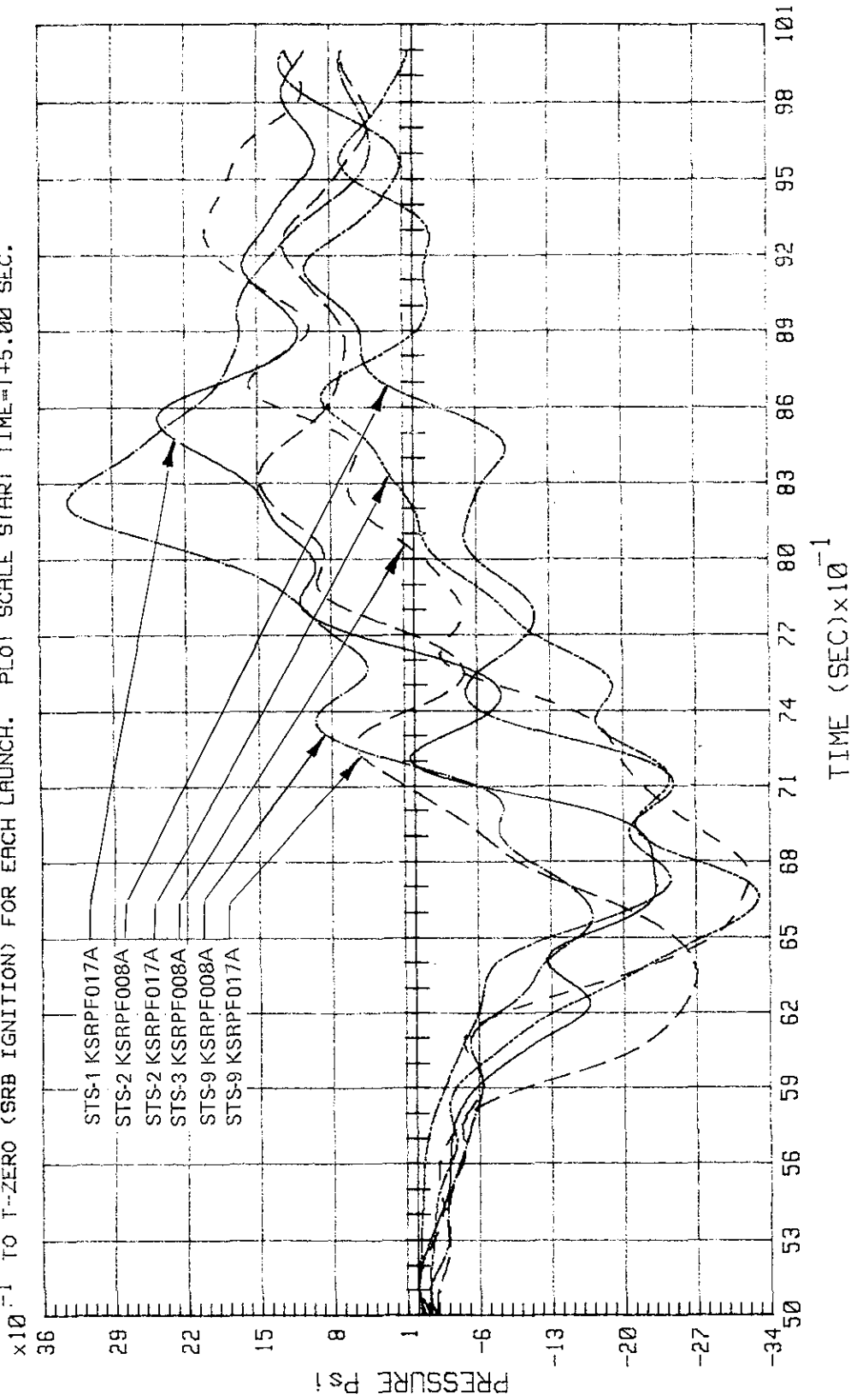


Figure 2-104. STS-1, -2, -3, and -9 MLP-1 Deck 0 Impinging Plume Pressure (TVM)
 (Sensors: STS-1, KSRPF017A; STS-2 and -9, -017A and -008A; and STS-3, -008A)

KSC-DD-818-TR

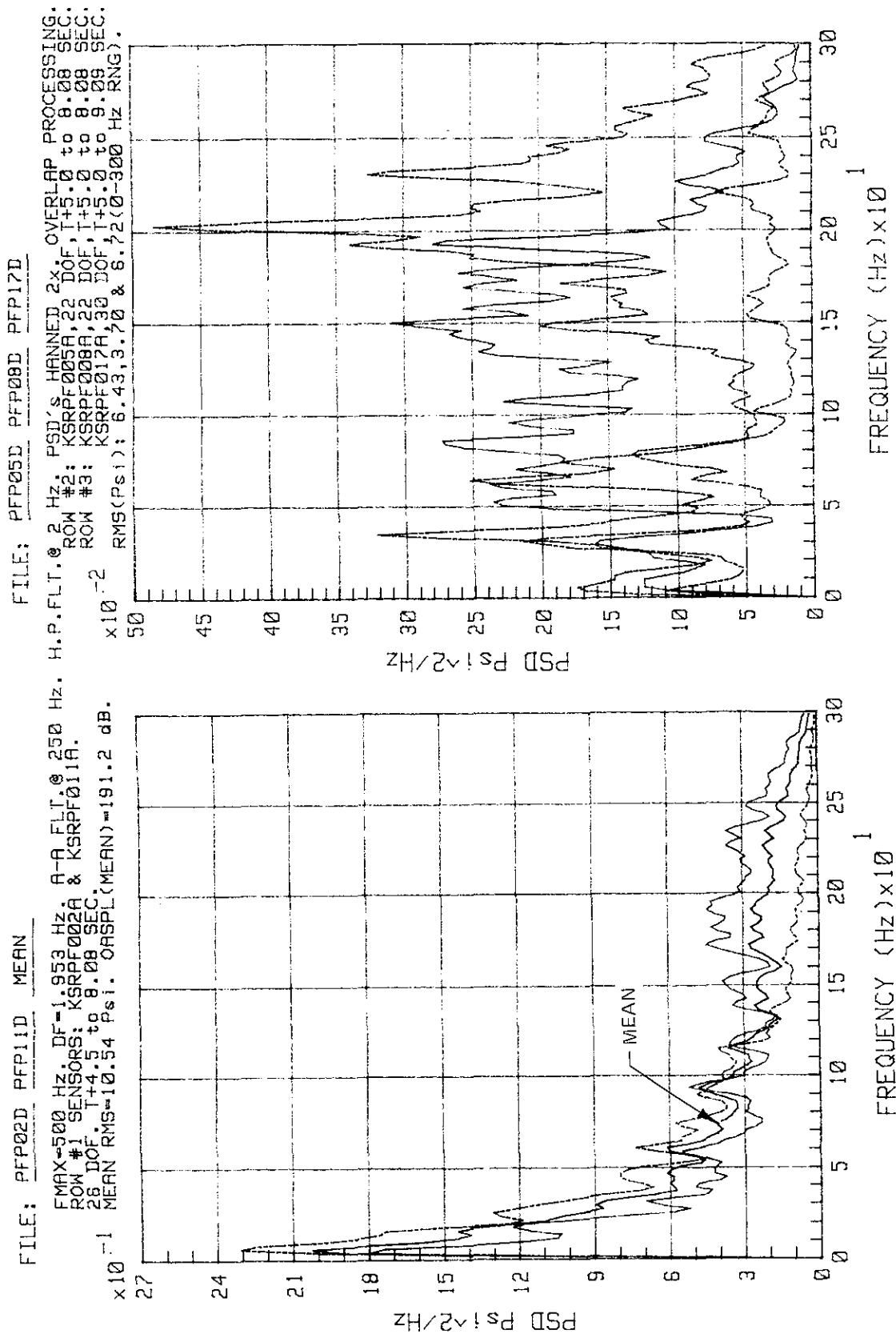


Figure 2-105. STS-9 MLP-1 Deck 0 Impinging Plume Pressure PSD's - Lift-Off Peak

STS-1 LIFT-OFF PEAK
 RAW DATA
 KSRPF011A
 START TIME = 1 + 5.36000 SEC
 TOTAL ANALYSIS TIME = 2.04000 SEC
 1603

BLOCK SIZE = 2048
 SAMPLE RATE = 1000.00000 SAMPLES/SEC
 CHANNEL A
 RMS = 0.60238 PSI
 TOTAL ANALYSIS TIME = 2.04000 SEC

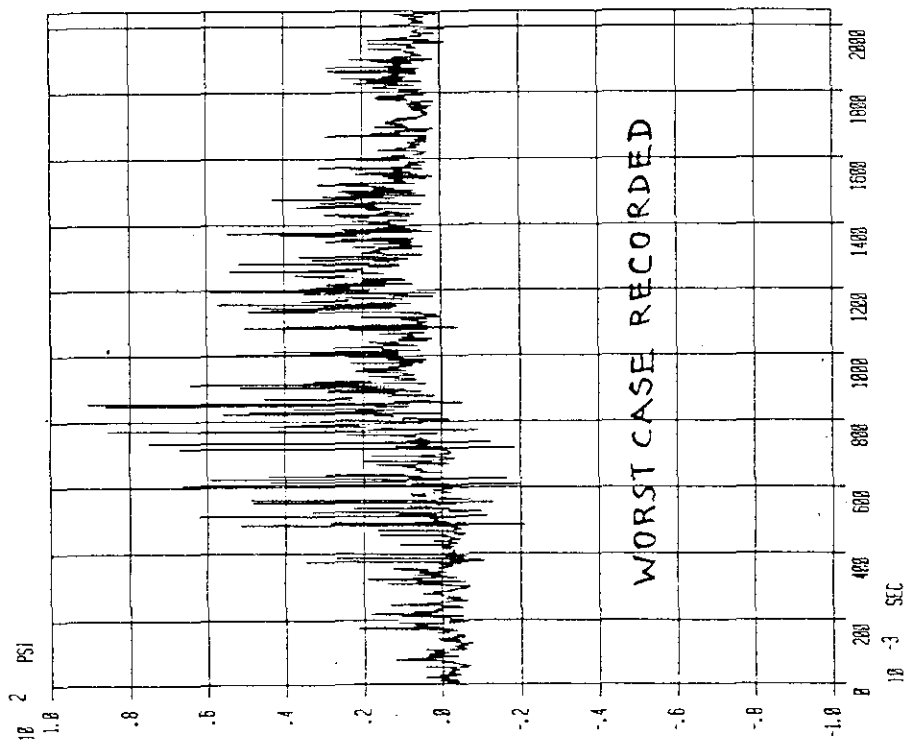
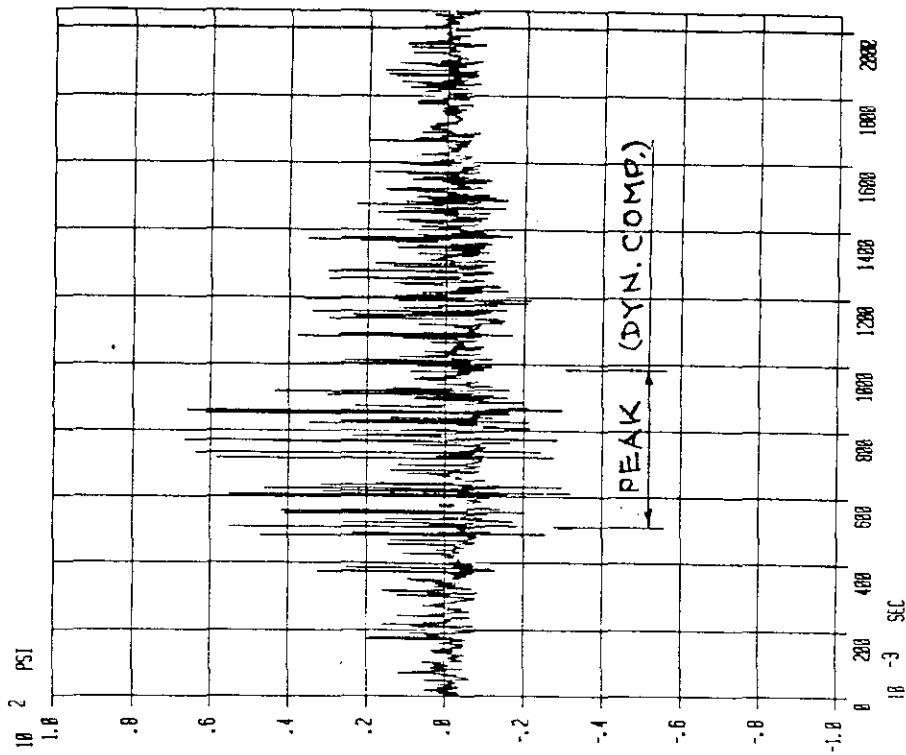


Figure 2-106. STS-1 Lift-Off Peak - KSRPF011A Raw Data and Dynamic Component of Data

KSC-DD-818-TR

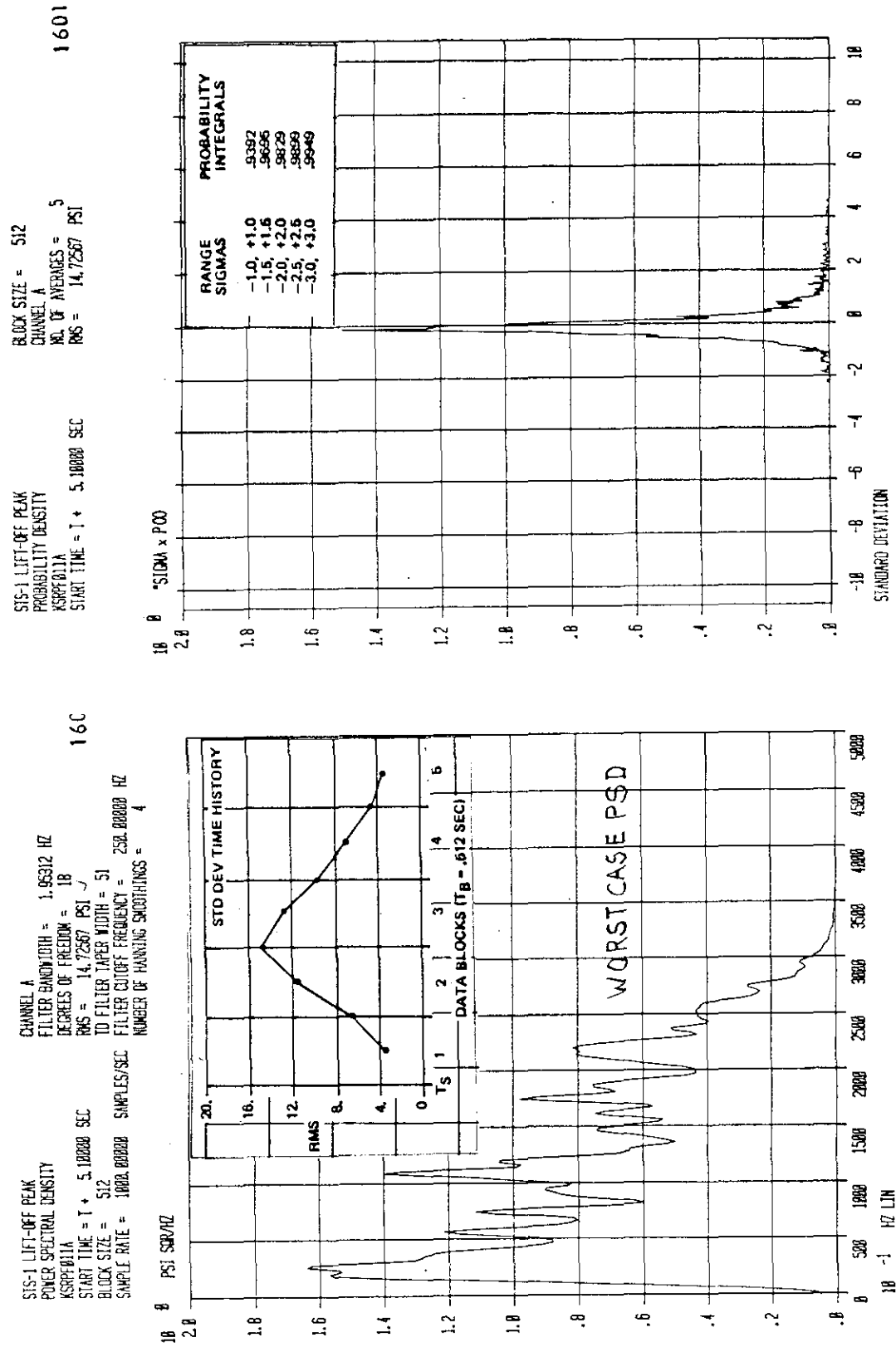
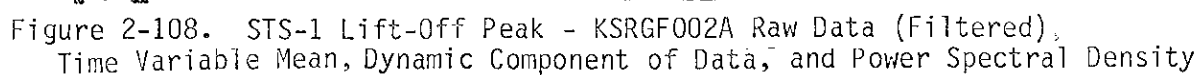


Figure 2-107. STS-1 Lift-Off Peak - KSRPF011A Power Spectral Density, Probability Density, and Standard Deviation Time History



2.6 TSM PRESSURES SUMMARY

This section presents a summary of pressures recorded by sensors on both TSM's (LH₂ and LO₂) during STS-4 through STS-8 launches. Statistical data in terms of OBSPL's were derived from STS-1 through STS-5 measurements (X- and Y-direction sensors) and are included in this summary. Since the acoustic environment on TSM's is very nonstationary, orientation of sensor orifice (X, Y, or Z) and time intervals selected for processing were major factors affecting the results.

Figures 2-109 and 2-110 present PSD's derived from MLP-2 TSM's sensor data during lift-off peak ($T + 1.5$ s to $T + 5.6$ s). Orifices of these sensors were oriented in the -Z direction (looking down). PSD's from the same sensor outputs for processing time interval $T + 5.5$ s to $T + 12.2$ s (lift-off peak end) for STS-6 are shown on figures 2-111 and 2-112. Comparing the PSD plots of figures 2-109 and 2-111 reveals significant differences in their frequency composition.

TSM sensors with orifices in the -Z direction recorded apparent "static" pressures as a result of indirect impingement from the SRB plumes after these plumes impinge on the north part of MLP deck 0 (peak at about $T + 8$ s), and are deflected horizontally toward TSM's. Deflected splash impinges on the base of TSM's where they are again deflected by the TSM's. Thus, apparent "static" pressures are associated with an upward flow of twice deflected and splashing plumes. Figures 2-113 through 2-115 show STS-6 time histories of raw data and TVM extracted from the raw data for the period $T + 3.0$ s to $T + 13.24$ s.

When all PSD's from -Z-direction sensors on MLP-1 and MLP-2 recorded during STS-4 through STS-8 are averaged, the resulting PSD's are shown on figure 2-116 and 2-117. These PSD's are similar to those on figures 2-109 and 2-110, thus confirming similarity and validity of TSM pressure data recorded on two different MLP's by two different data acquisition systems.

A number of sensors on the MLP-1 TSM's had their orifices oriented in X and Y directions. Figures 2-118 and 2-119 show PSD's derived from the outputs of X- and Y-direction sensors for STS-4, -5, and -7 launches. These sensors did not record significant "static" pressures mainly because the direction of their orifices is perpendicular to the direction of splash flow. Generally X- and Y-direction sensors recorded higher dynamic pressures within the 0- to 200-Hz range shown on figures 2-118 and 2-119 than did their Z-direction counterparts.

Table 2-1 presents a statistical summary of acoustic pressures on TSM's recorded by X- and Y-direction sensors during STS-1 through STS-5 launches. Data are presented in terms of OBSPL's. A total of 18 measurements comprises these statistics, which essentially reflect data on figures 2-118 and 2-119, except that OBSPL's range is extended to 2.0 kHz.

DATA: MEAN LIMIT

SENSORS: KSRPG001A, KSRPG006A & KSRPG007A ON MLP-2. PROCESSING FROM T+1.5 TO T+5.6 SEC.
 FMAX=1000 Hz. DELTA-F=1.953 Hz. A-A FILTER @ 500 Hz. TOTAL 90 DATA BLOCKS. PSD'S HANNED 2x.
 MEAN: RMS=2.000 Psi. ORSPL(X)=176.8 dB. LIMIT: RMS=2.864 Psi. ORSPL(X+25)=179.9 dB (0-600 Hz).
 THIS PLOT UPDATES MLP-2 TSM'S DATA PUBLISHED IN KSC-DD-712-TR, FIGURE B-1, PAGE B-4, JULY 1983.

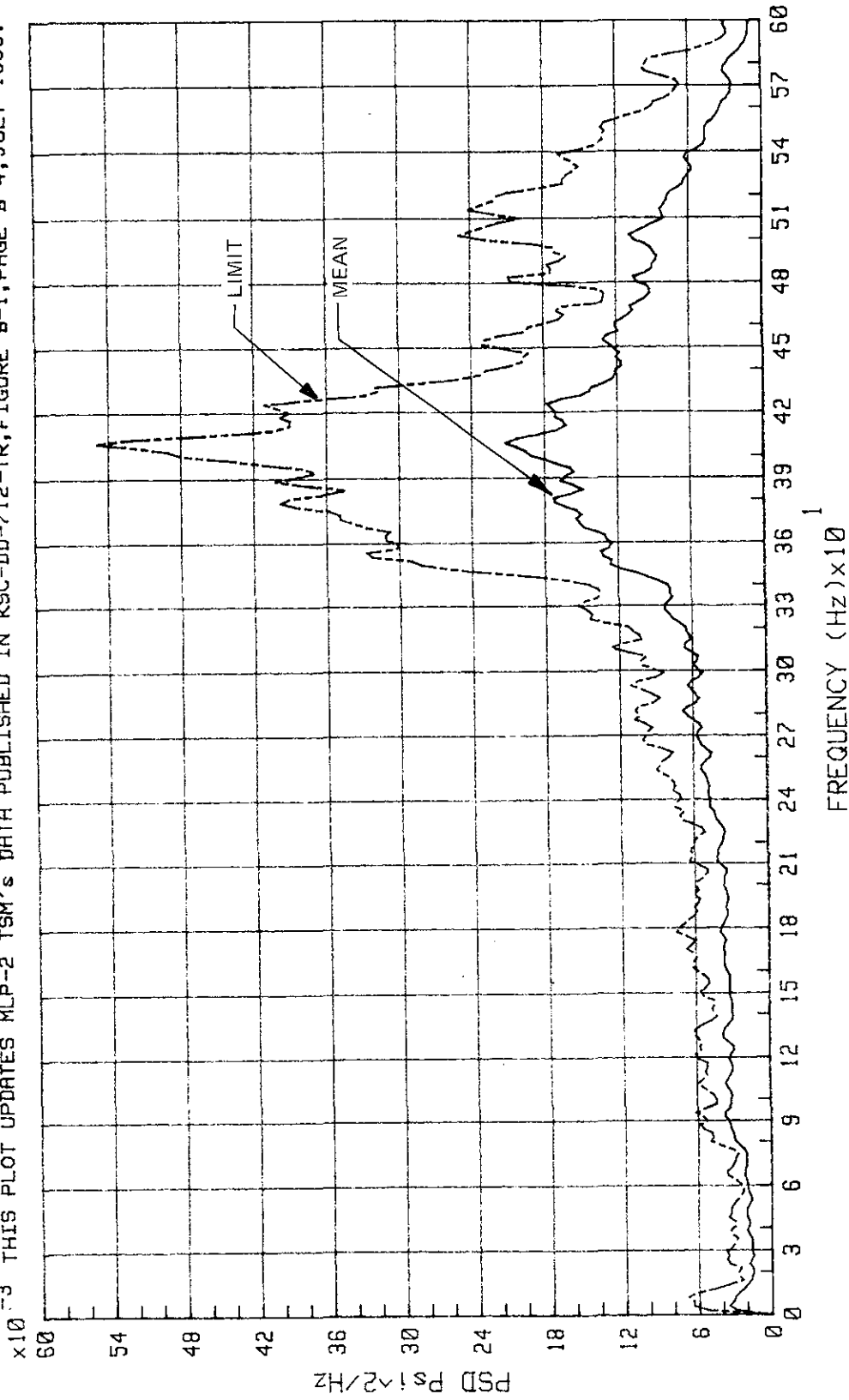


Figure 2-109. STS-6 and -8 Acoustics on TSM's at Lift-Off Peak - Sensors Oriented in -Z Direction (Mean and Limit Only)

KSC-DD-818-TR

KSR#: PG001C PG006C PG007C PG001C PG006C PG007C MEAN LIMIT

KSRPG001A NEAR TOP OF LOX TSM. KSRPG006A NEAR CENTER OF LOX TSM. KSRPG007A NEAR CENTER OF LH2 TSM. FMAX=1000 Hz. DELTA-F=1.953 Hz. PROCESSING FROM T+1.5 TO T+5.6 SEC. PSD's HANNED 2X. MEAN: RMS=2.000 Psi, OASPL(X)=176.8 dB. LIMIT: RMS=2.864 Psi, OASPL(X)=179.9 dB (0-600 Hz). THIS PLOT UPDATES MLP-2 TSM's DATA PUBLISHED IN KSC-DD-712-TR, FIGURE B-2, PAGE B-5, JULY 1983. LAUNCH-TO-LAUNCH DISPERSION IS HIGH. DATA FOR EACH LAUNCH ARE CONSISTENT & DISPERSION IS LOW.

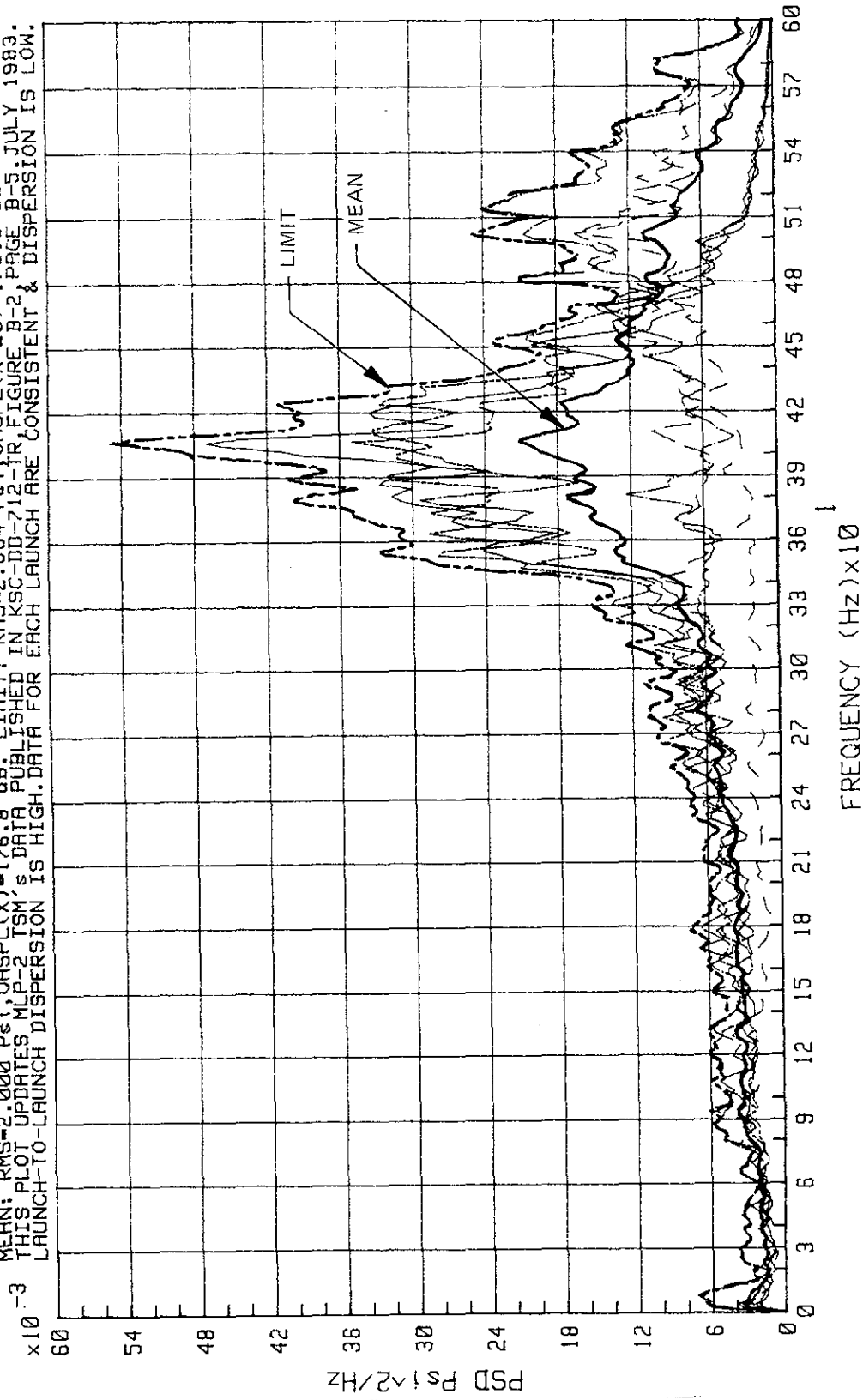


Figure 2-110. STS-6 and -8 Acoustics on TSM's at Lift-Off Peak - Sensors Oriented in -Z Direction

SENSORS: KSRPG001A, KSRPG006A & KSRPG007A, PROCESSING FROM T+5.5 TO T+12.2 SEC.
 FMAX=1000 Hz, DELTA F=1.953 Hz, PSD's HANNED 2x.
 MEAN RMS=1.600 Psi, OASPL(X)=174.8 dB, VALUES FOR MEAN AND LIMIT ARE FOR 0-600 Hz RANGE.
 LIMIT CURVE (MEAN+2*SIGMA) RMS=1.863 Psi, OASPL(X+2S)=176.2 dB.
 SINGLE LAUNCH DATA ARE CONSISTENT AND SHOW VERY LOW DISPERSION.

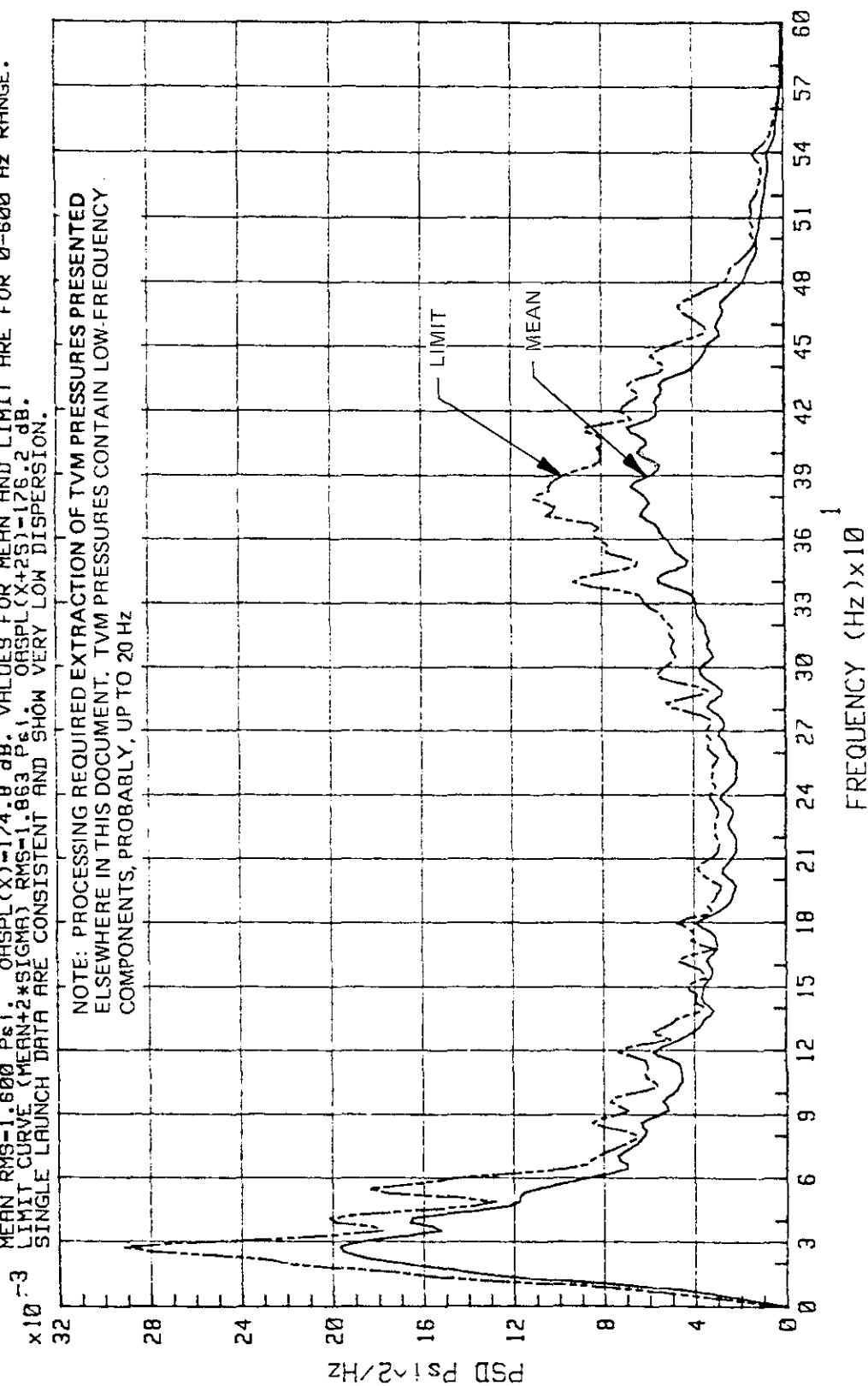


Figure 2-111. STS-6 Acoustics on TSM's at Lift-Off Peak End - Sensors Oriented in -Z Direction
 (Mean and Limit)

KSC-DD-818-TR

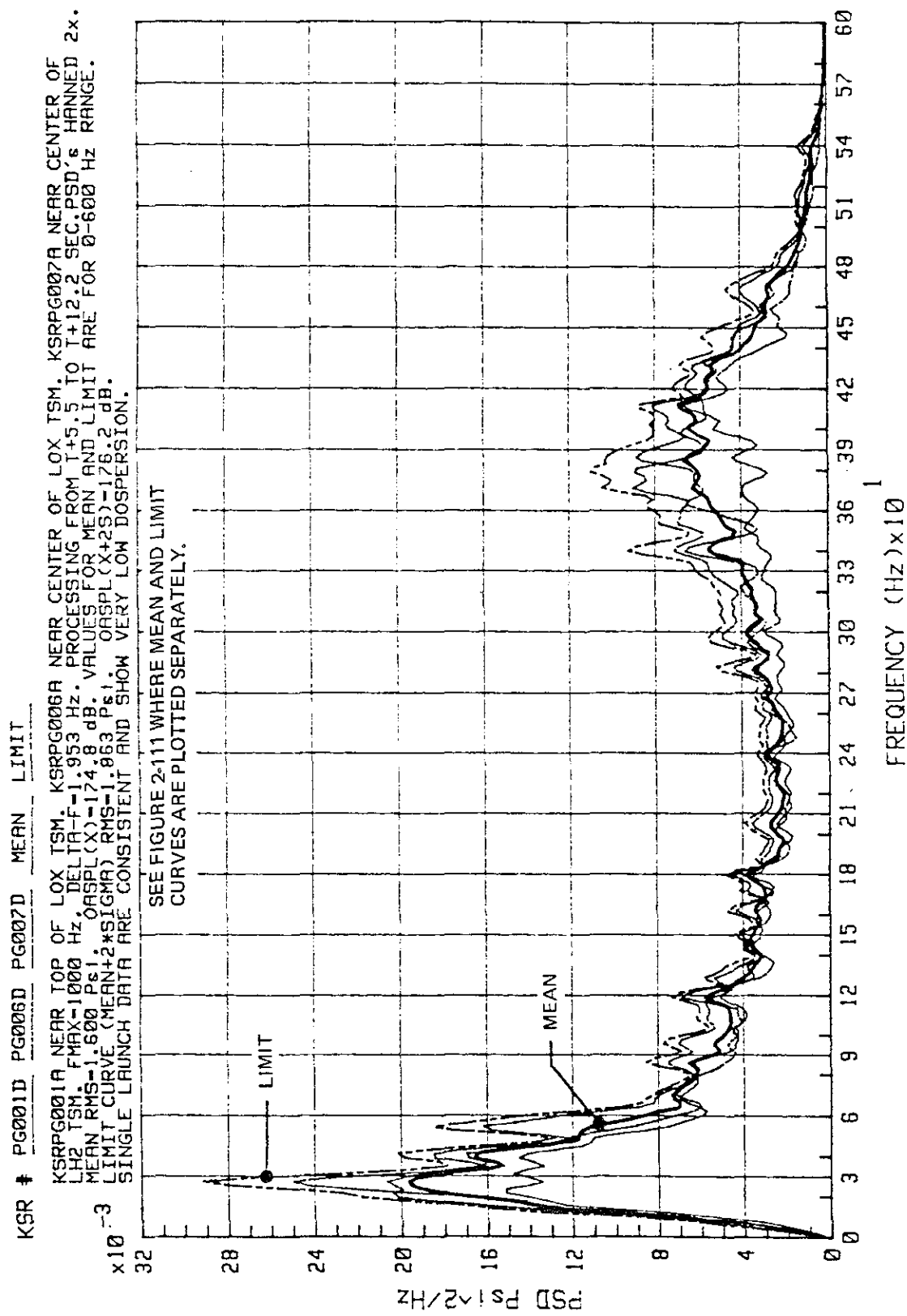
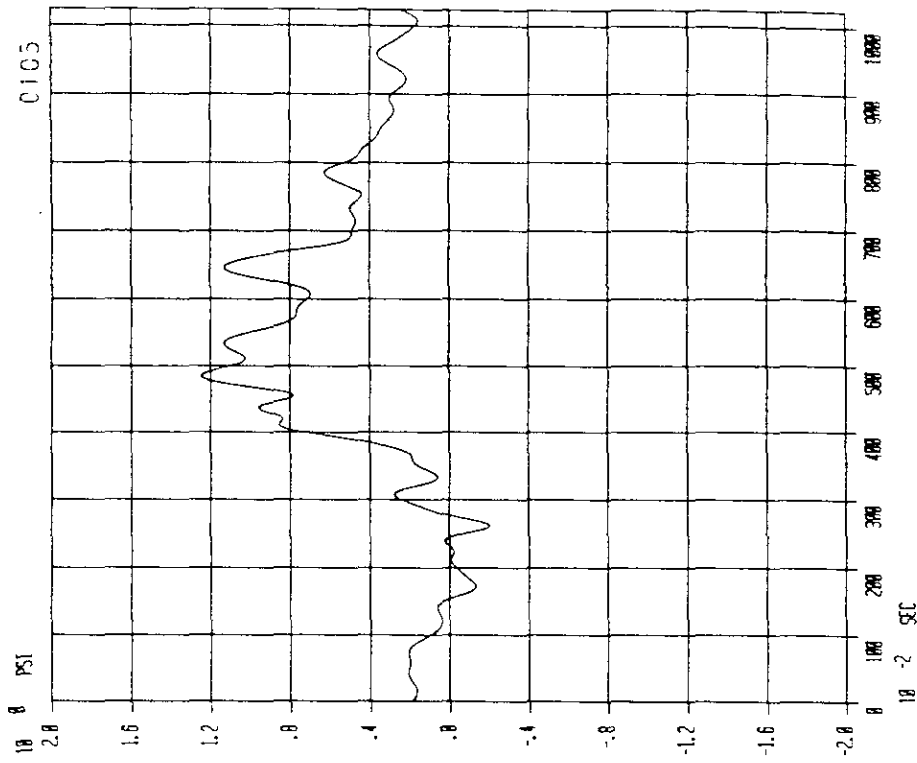


Figure 2-112. STS-6 Acoustics on TSM's at Lift-Off Peak - Sensors Oriented in -Z Direction

STS-6 LIFT-OFF PEAK
TIME VARIABLE MEAN
KSRPG001A CHANNEL A
START TIME = 7 + 3.00 SEC

BLOCK SIZE = 2048
HANNING SMOOTHING = 750
TOTAL TIME = 10.240 SEC



BLOCK SIZE = 2048
SAMPLE RATE = 200 HZ
TOTAL TIME = 10.240 SEC

STS-6 LIFT-OFF PEAK
RAW DATA
KSRPG001A CHANNEL A
START TIME = 7 + 3.00 SEC

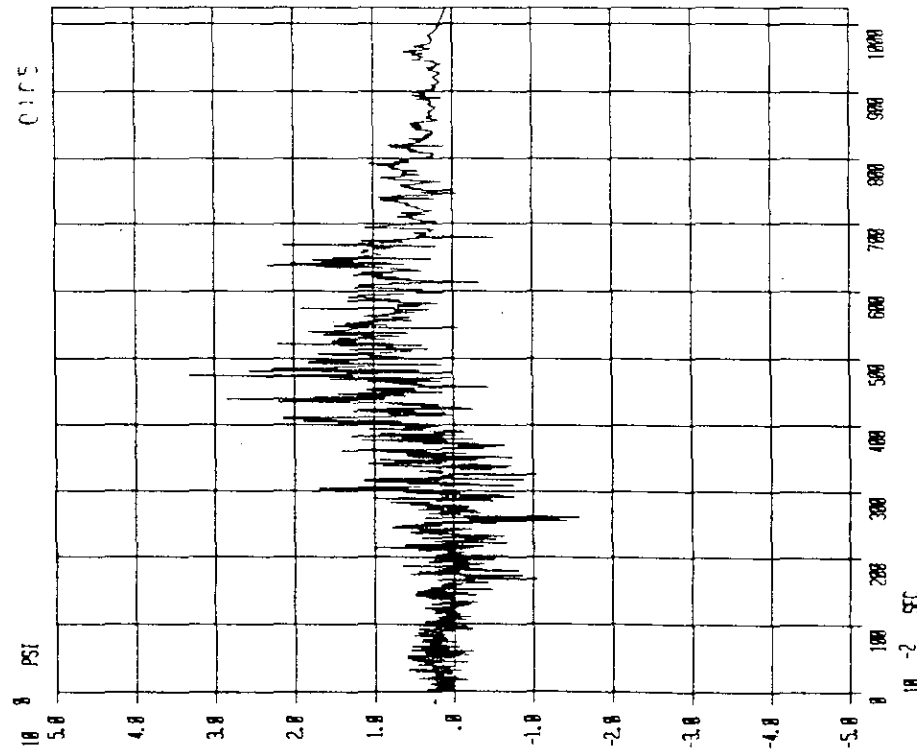


Figure 2-113. STS-6 Lift-Off Peak - KSRPG001A Raw Data and Time Variable Mean

KSC-DD-818-TR

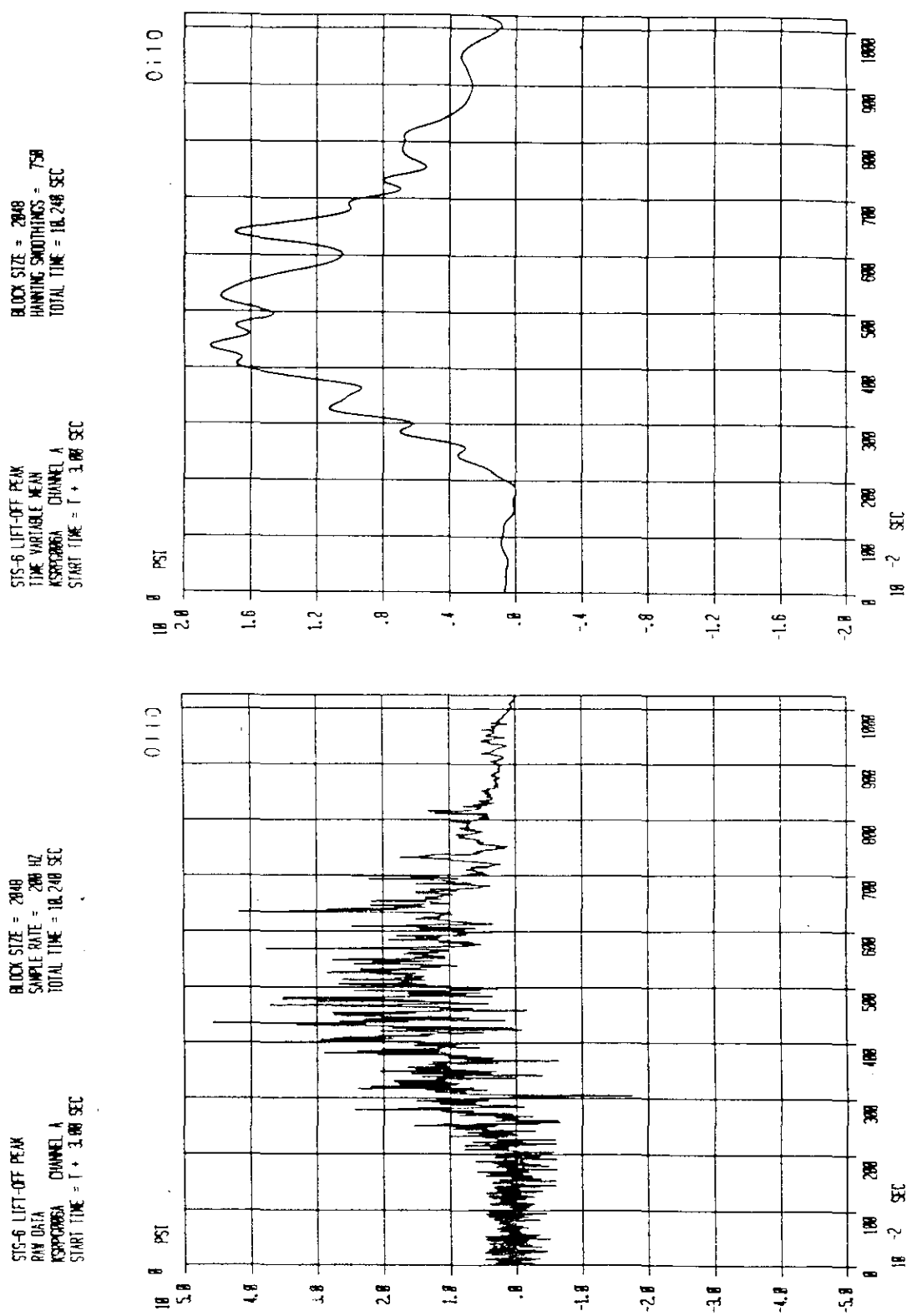
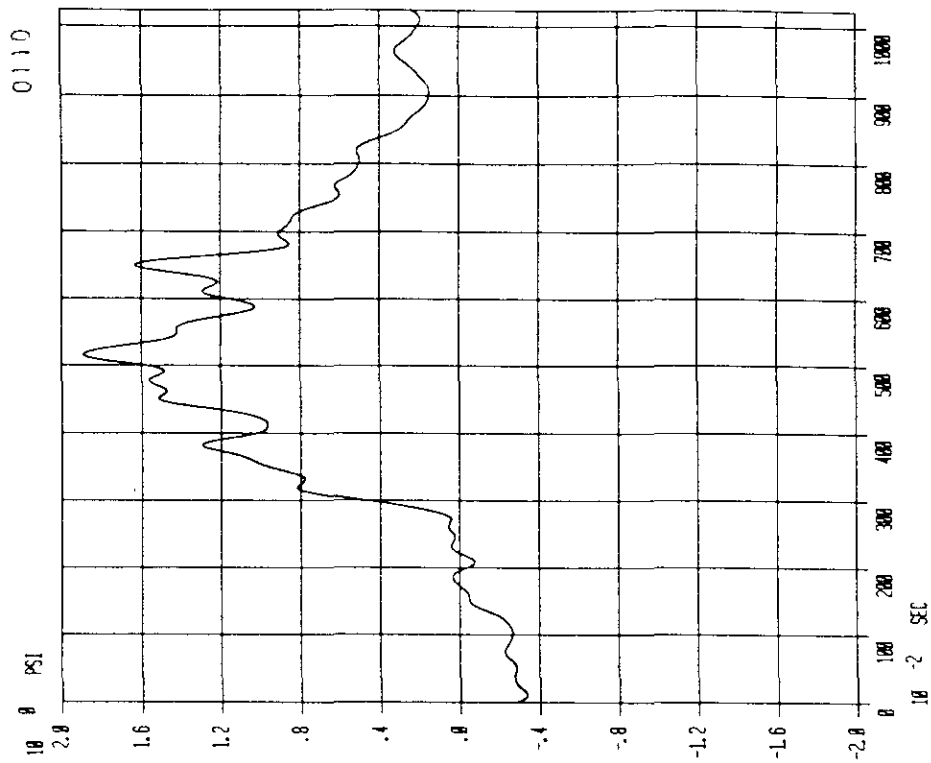


Figure 2-114. STS-6 Lift-Off Peak - KSRPG006A Raw Data and Time Variable Mean

STS-6 LIFT-OFF PEAK
 TIME VARIABLE MEAN
 KSRPG007A CHANNEL 8
 START TIME = 1 + 3.00 SEC
 BLOCK SIZE = 2048
 HANNING SMOOTHING = 0.50
 TOTAL TIME = 10.240 SEC



STS-6 LIFT-OFF PEAK
 RAW DATA
 KSRPG007A CHANNEL 8
 START TIME = 1 + 3.00 SEC
 BLOCK SIZE = 2048
 SAMPLE RATE = 200 HZ
 TOTAL TIME = 10.240 SEC

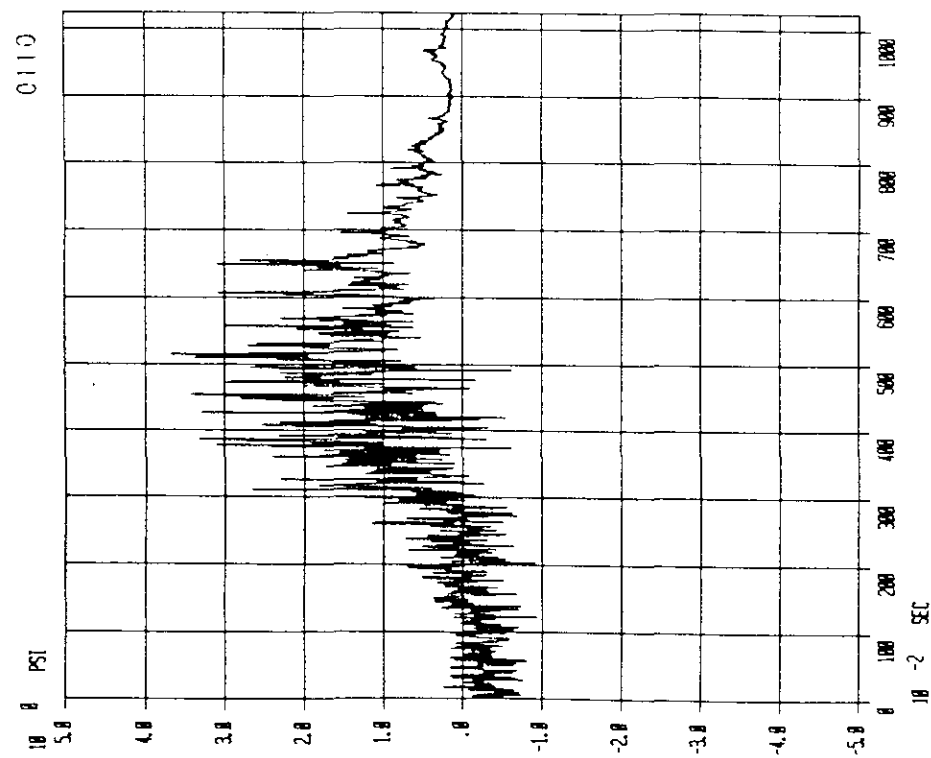


Figure 2-115. STS-6 Lift-Off Peak - KSRPG007A Raw Data and Time Variable Mean

KSC-DD-818-TR

DATA: MEAN LIMIT

MLP-1 SENSORS: KSRPF020A, -23A, -43A & -45A. MLP-2 SENSORS: KSRPG001A, -6A & -7A.
 FMAX=1000 Hz. DELTA-F=1.953 Hz. A-A FILTER @ 500 Hz. FROM T+1.5 TO T+5.6 SEC. HANNED 2x.
 MEAN: RMS=1.790 Psi, ORASPL(X)=175.8 dB. LIMIT: RMS=2.722 Psi, ORASPL(X+2S)=179.5 dB. (0-600 Hz).
 THIS PLOT UPDATES TSM's DATA PUBLISHED IN KSC-DD-712-TR, FIGURE B-9, PAGE B-12, JULY 1983.

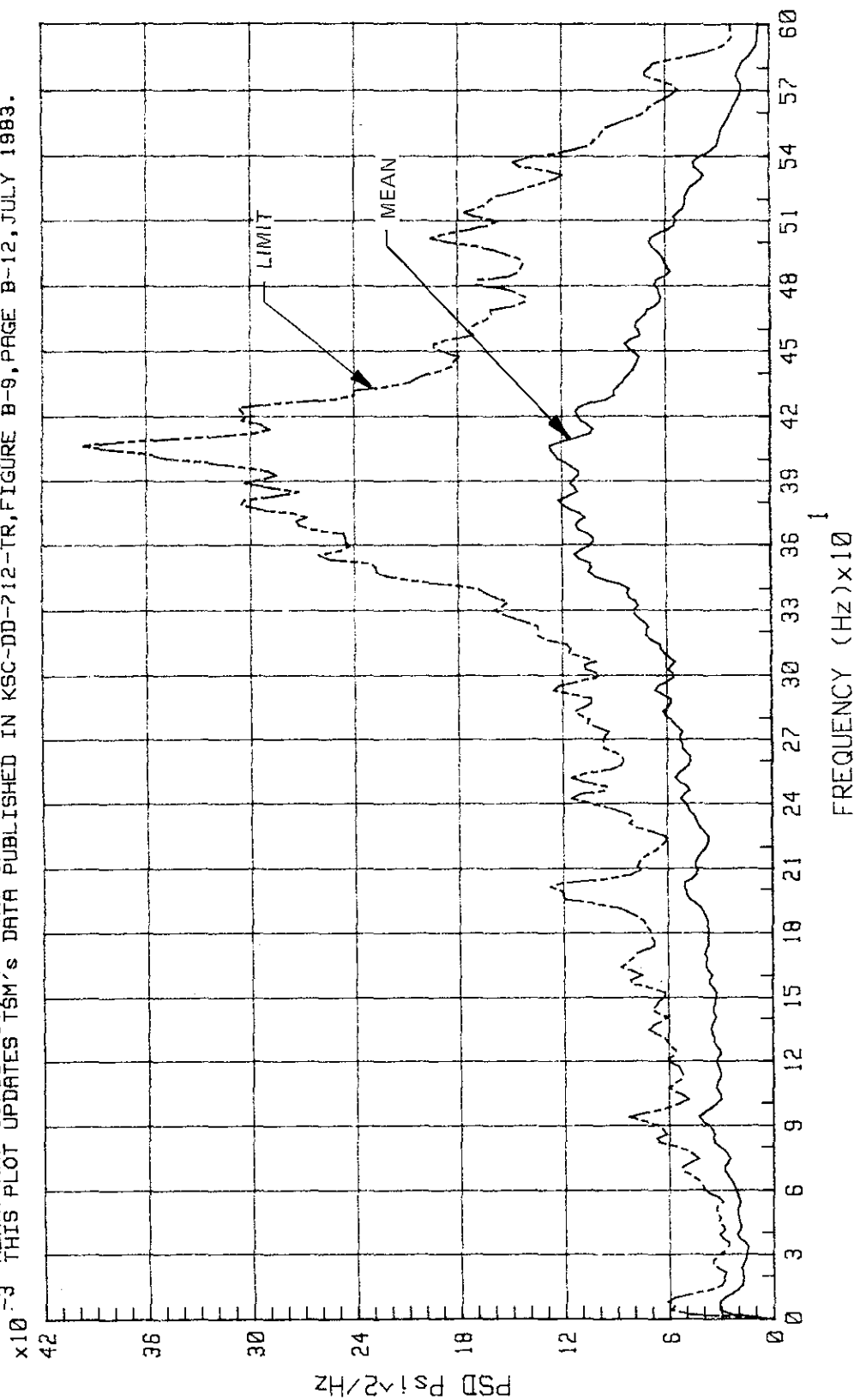


Figure 2-116. STS-4, -5, -7, and -8 Acoustics on Top of TSM's at Lift-Off Peak -
 Sensors in -Z Direction (Mean and Limit Only)

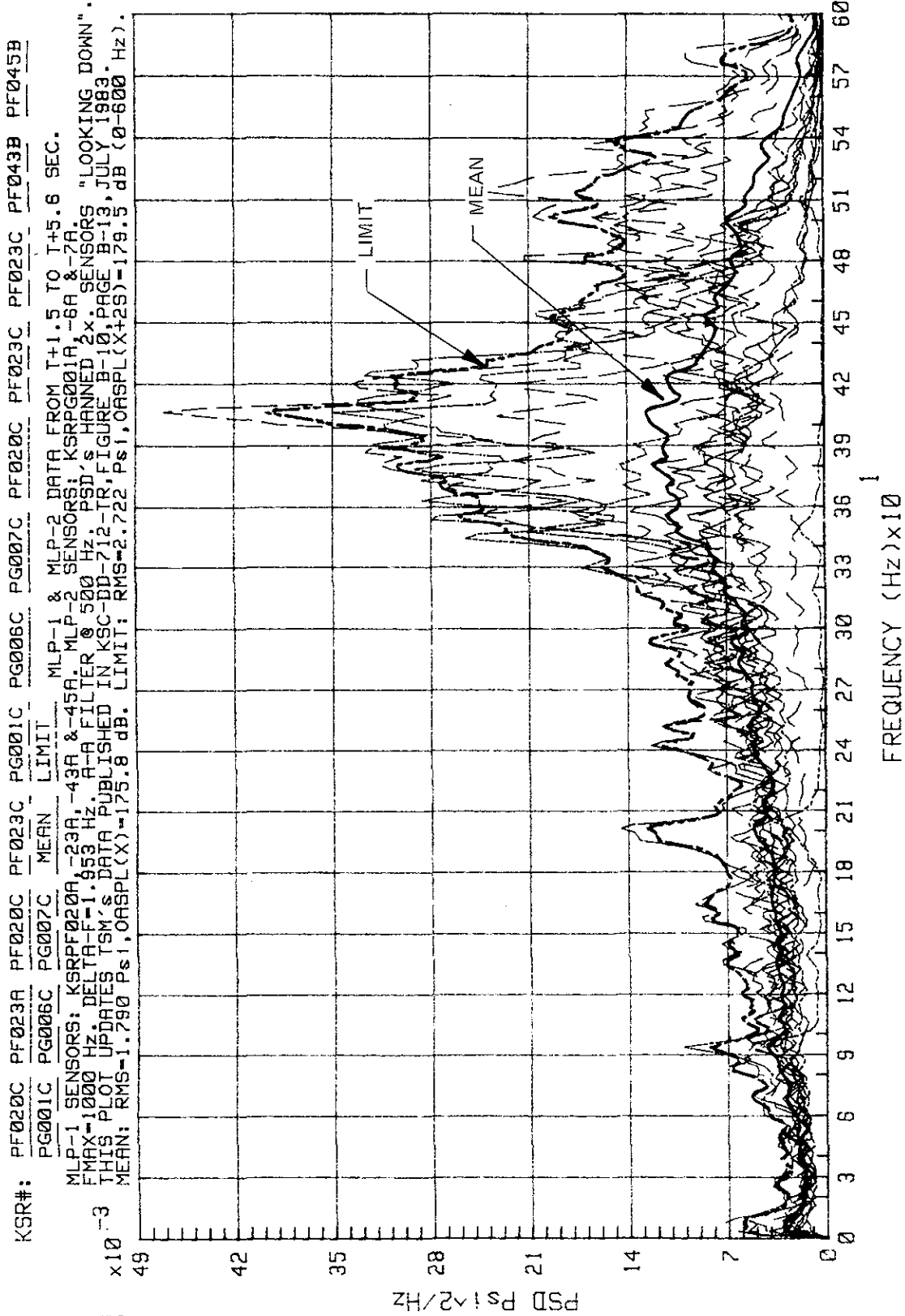


Figure 2-117. STS-4, -5, -6, -7, and -8 Acoustics on Top of TSM's at Lift-Off Peak - Sensors in -Z Direction

KSC-DD-818-TR

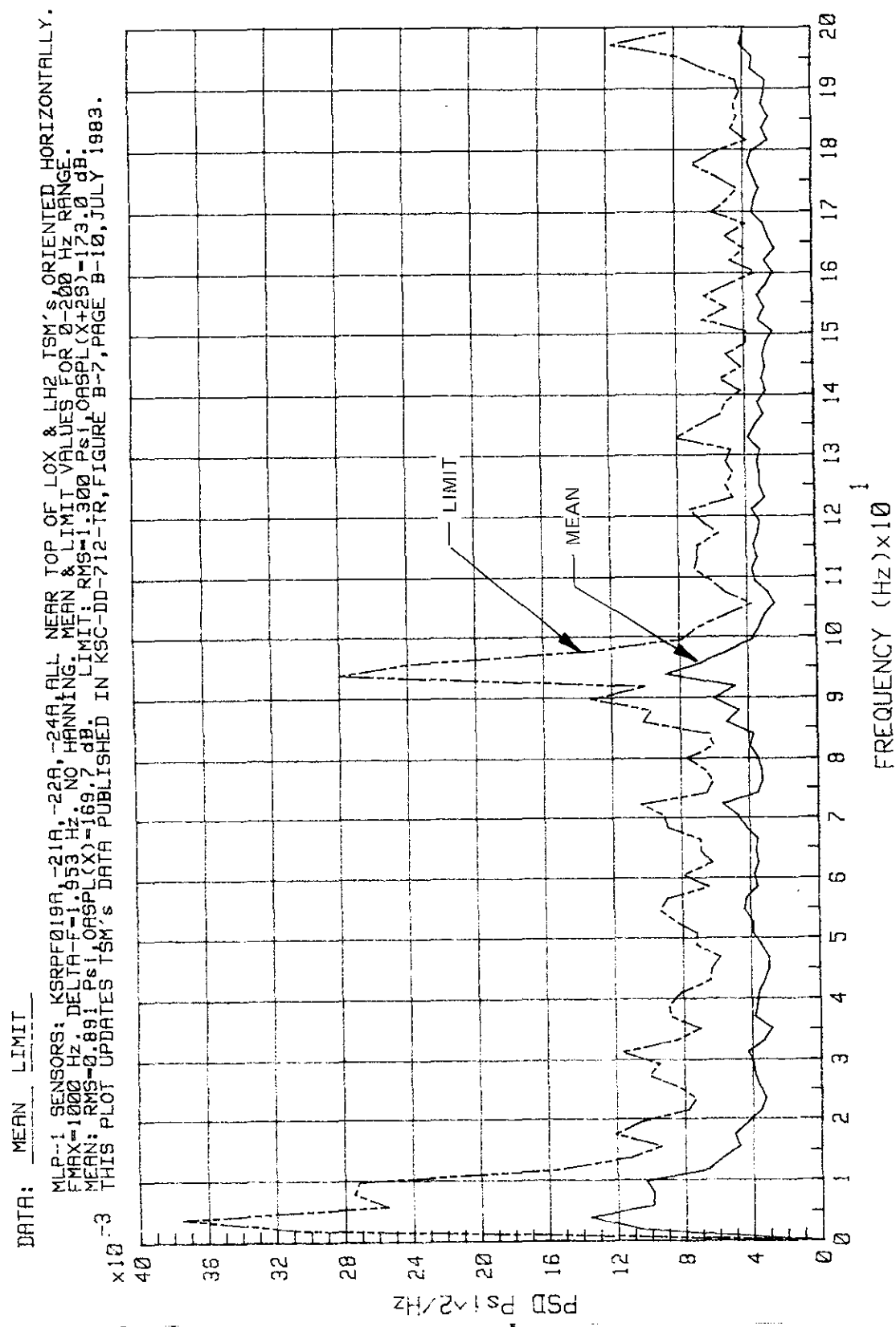


Figure 2-118. STS-4, -5, and -7 Acoustics on Top of TSM's at Lift-Off Peak - X and Y Directions (Mean and Limit Only)

DATA: PF019C PF021A PF022A PF024C PF019C PF021C PF022C PF024C PF021C MEAN LIMIT
 MLP-1 SENSORS NEAR TOP OF LOX & LH2 TSM's ORIENTED HORIZONTALLY (X&Y), FACING VEHICLE (X).
 FMAX=1000 Hz. DELTA-F=1.953 Hz. NO HANNING. MEAN & LIMIT VALUES FOR 0-200 Hz RANGE.
 MEAN: RMS=0.891 Psi, ORSPL(X)=169.7 dB. LIMIT: RMS=1.300 Psi, ORSPL(X+2S)=173.0 dB.
 THIS PLOT UPDATES TSM's DATA PUBLISHED IN KSC-DD-712-TR, FIGURE B-8, PAGE B-11, JULY 1983.
 THIS UPDATE ADDS STS-7 KSRPF021A DATA.

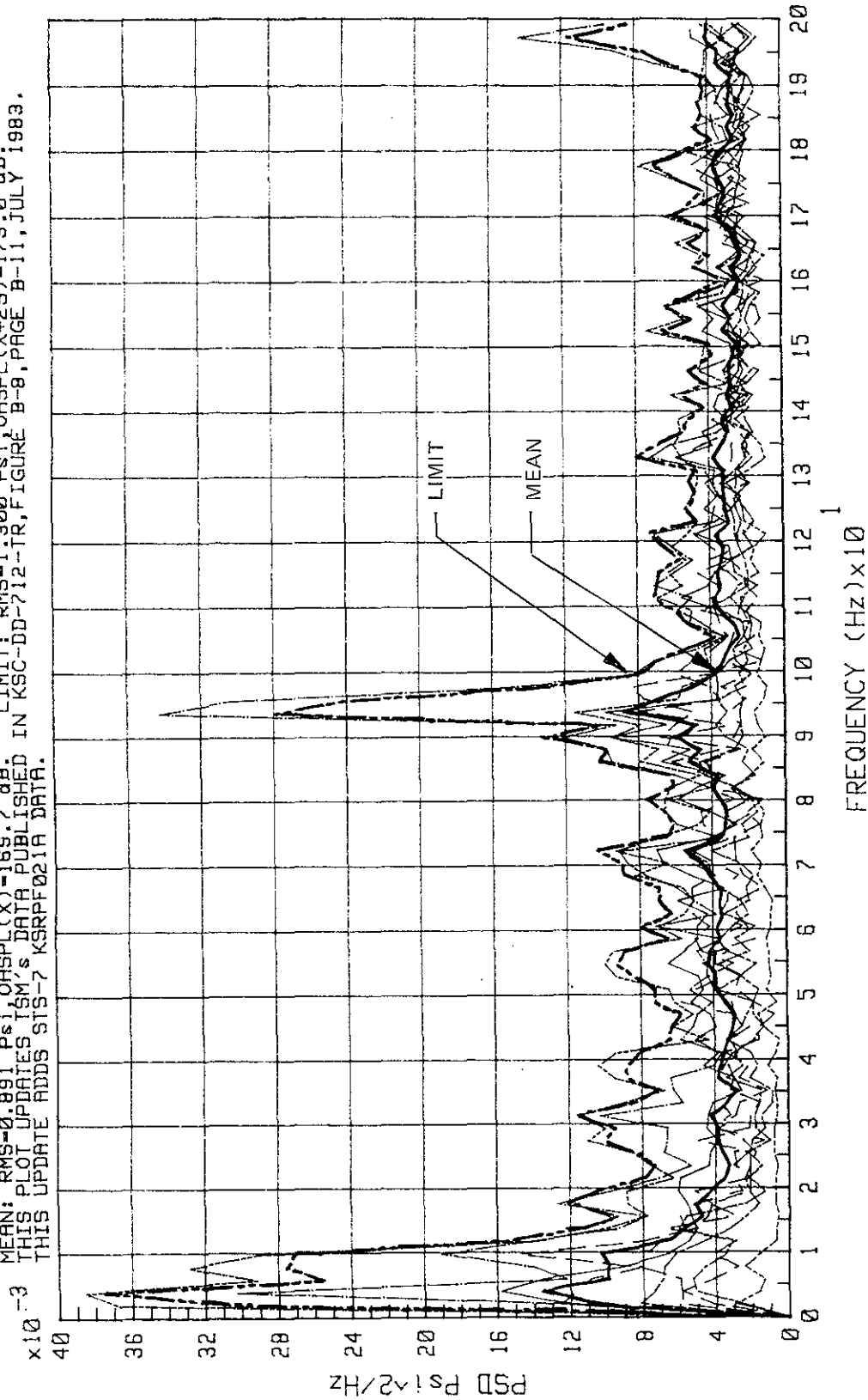


Figure 2-119. STS-4, -5, and -7 Acoustics on Top of TSM's at Lift-Off Peak - X and Y Directions

Table 2-1. Statistical Data From TSM Pressure Sensors
(X and Y Directions) for STS-1 Through STS-5 Launches

Octave Band Center Frequency (Hz)	Statistical Summary		
	Mean (50% CL) Sound Pressure Level (\bar{X}) (dB)	97.7% CL Sound Pressure Level ($\bar{X} + 2\sigma$) (dB)	97.7% CL Octave Band Average PSD (psi /Hz)
2	153.1	156.9	2.913 E-2
4	156.8	160.3	3.186 E-2
8	157.9	161.5	2.100 E-2
16	158.8	161.6	1.074 E-2
31.5	160.1	163.4	8.261 E-3
63	163.4	166.1	7.691 E-3
125	165.6	168.5	6.736 E-3
250	172.3	176.3	2.029 E-2
500	173.8	176.9	1.165 E-2
1,000	163.8	166.9	5.825 E-4
2,000	158.7	162.7	1.107 E-4
Overall sound pres- sure level (OASPL)	177.3	180.7	

NOTE

Statistical summary is applicable to north side of TSM's, where measurements were made. STS-6 data are not included because on MLP-2 all TSM sensors are oriented downward (-Z direction) and data recorded at lift-off peak are lower than similar data recorded on MLP-1 by sensors oriented horizontally (X and Y directions). Presented data do not include pressures from impingement of SRB plumes deflected by the MLP deck 0.

2.7 MLP EXTERIOR PRESSURES (SRB EXHAUST WELLS, SIDES 2 AND 4, AND BOTTOM)

This section presents exterior pressures recorded on MLP-1 and MLP-2 by sensors located in the SRB exhaust wells, on MLP sides 2 and 4, and on the MLP bottom (B-level). Since the pressures are distinctly transient at some locations, the data are presented in the time domain; however, when longer duration data are available, PSD's are plotted. Plot headings provide information on parameters used in data processing and on sensor locations. Figures 1-5 and 1-6 show the overpressure sensor locations for MLP-1 and MLP-2.

Figures 2-120 through 2-124 present STS-8 SRB ignition overpressure transients recorded by MLP-2 sensors at various locations on the sides of SRB exhaust wells. Data processing time interval $T + 0.05$ to $T + 0.35$ s includes highest recorded SRB ignition overpressure transients. All raw data were smoothed (Hanned) between 3 and 10 times in order to eliminate high-frequency noise, which obscures underlying pressure pulses. Figures 2-120 through 2-123 present overpressures at sensor locations below water spray nozzles. Figure 2-124 presents overpressures at locations above water spray nozzles and water troughs where pressures are substantially reduced by these devices.

Figures 2-125 through 2-128 present STS-9 SRB ignition overpressure transients recorded by MLP-1 sensors for the same time interval as above, $T + 0.05$ to $T + 0.35$ s. Although MLP-1 and MLP-2 sensors do not have an identical correspondence (their corresponding locations are slightly different), pressures recorded by corresponding groups of sensors are similar. Thus, corresponding STS-8 and STS-9 data are on figures 2-120 and 2-125 (south side), 2-121 and 2-126 (west side, primary well), 2-123 and 2-127 (west side, secondary well), and figures 2-124 and 2-128 (locations above water spray nozzles).

Figures 2-129 through 2-132 present STS-9 lift-off ($T + 1.0$ s to $T + 11.0$ s) pressures on different sides of the west SRB exhaust well measured by 14 sensors on MLP-1. These pressures, obtained from raw data by digital filtering (extraction of TVM) are slow varying pressure components that, in most applications, may be identified as "static" loads. In this group, a few sensors were affected by heat, and their outputs did not return to ambient. Corresponding invalid data are noted in plot headings.

Dynamic pressures during STS-9 lift-off, obtained from the outputs of 14 sensors located in the west SRB exhaust well and using high-pass filter at 2 Hz, were processed in terms of PSD's. Figures 2-133 and 2-134 show raw and smoothed (Hanned) PSD's and derived mean and limit (limit = mean + 2 sigma) PSD's. The limit PSD is exceeded by only one measurement, KSRPF074A, located near the bottom of SRB secondary exhaust well. For application, both static (figures 2-129 through 2-132) and dynamic (figures 2-133 and 2-134) pressures should be considered to occur simultaneously, although peak rms pressures usually precede peak TVM by about 1 to 2 s.

KSC-DD-818-TR

The summary of pressures on MLP sides 2 and 4 obtained from a total of 11 measurements is shown on figure 2-135. Sensors KSRPF037A through -40A were installed on MLP-1 only. They do not have counterparts on MLP-2. Sides 2 and 4 are shielded from direct exhaust impingement and no "static" type pressures were recorded. Recorded maximum rms pressures are below those on the FSS, probably because of diffraction effects and shielding (sensor orifices cannot "see" exhaust plumes).

Pressures on the bottom of MLP were measured by three sensors, KSRPF062A and -60A on MLP-1, and KSRPG014A on MLP-2. Figures 2-136 through 2-138 present typical pulses occurring during SRB ignition. These pulses are higher than TVM pressures occurring at lift-off shown on figure 2-139. Corresponding dynamic pressures at lift-off at locations of KSRPF062A and KSRPG014A (between T-1 and G-13) are shown on figure 2-140 with enlarged plots on figure 2-141 and 2-142. Similarly, pressures between SRB exhausts are shown on figures 2-143 through 2-145. It should be noted that pressure pulses at SRB ignition and TVM at lift-off show highest "static" type, slow varying pressures to be negative; thus, as load, their prevailing effect is downward. PSD's on figures 2-141 and 2-144 have a peak around 4 Hz near fundamental MLP resonance and apparently these pressures, in addition to MLP level 0 pressures, are responsible for relatively large MLP motions in the vertical direction.

FILE: PGR22T PGR23T PGR04T

MLP-2 SENSORS ON SOUTH SIDE (SIDE 1) OF EXHAUST WELL, BELOW WATER SPRAY NOZZLES.
 CURVE 1: KSRPG0228A, 4'-9" BELOW DECK 0. SAMPLE RATE 2 KHZ. A-A FILTER @ 500 Hz. HANNED 3x.
 CURVE 2: KSRPG0238A, 18'-0" BELOW DECK 0. SAMPLE RATE 2 KHZ. A-A FILTER @ 500 Hz. HANNED 3x.
 CURVE 3: KSRPG004A, 21'-9" BELOW DECK 0. SAMPLE RATE 5 KHZ. A-A FILTER @ 1250 Hz. HANNED 3x.
 NOTE: TIME SCALE IS REFERENCED TO NOMINAL T-ZERO=242:06:32:00.027 GMT.

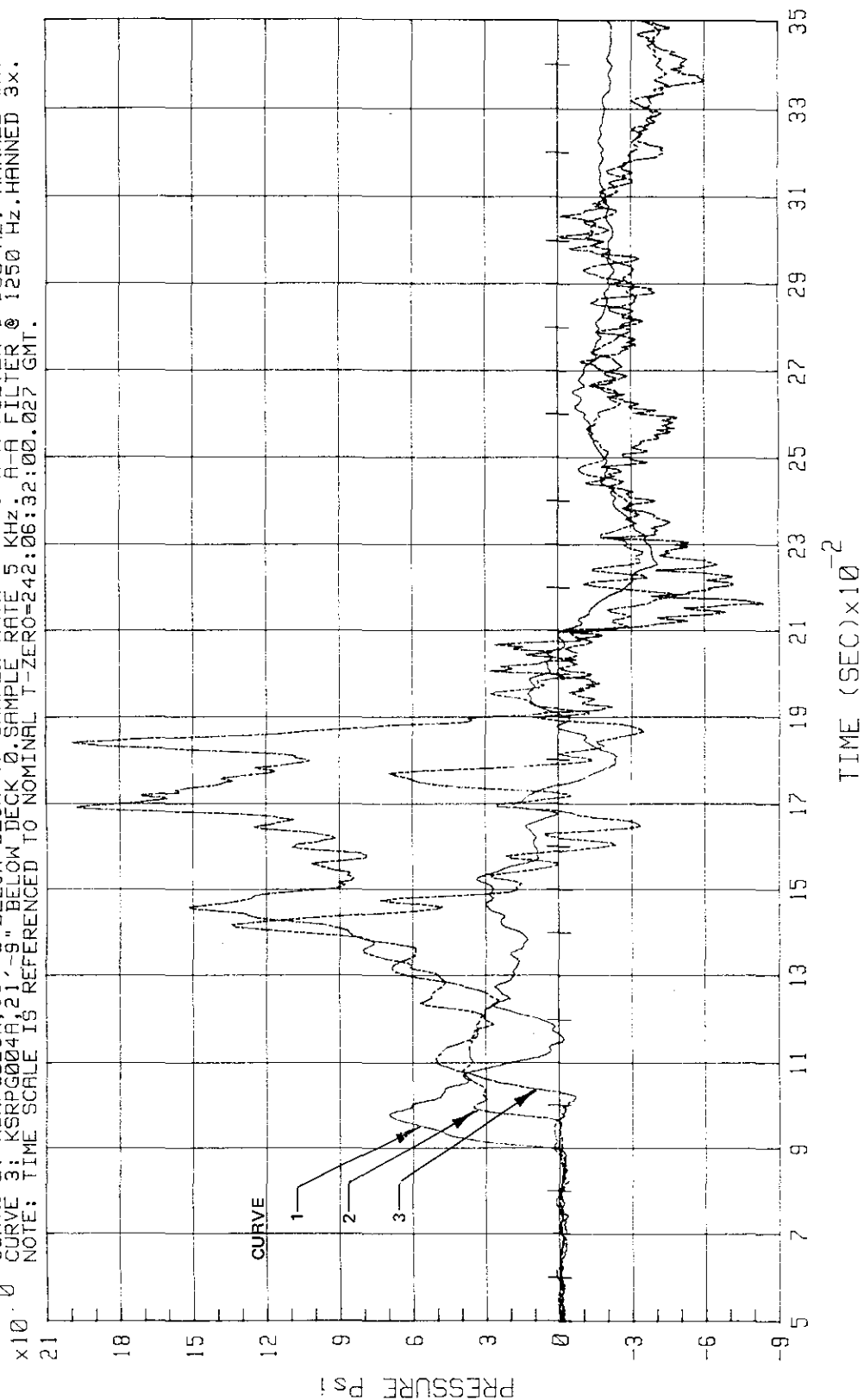


Figure 2-120. STS-8 SRB Ignition - West SRB, Main Exhaust Well Pressures, T + 0.05 s to T + 0.35 s (MLP-2 Sensors on Side 1)

KSC-DD-818-TR

FILE: PGR16T PGR17T PGR18T

MLP-2 SENSORS ON WEST SIDE (SIDE 2) OF EXHAUST WELL, BELOW WATER SPRAY NOZZLES.
 CURVE 1: KSRPG016A, 6'-3" BELOW DECK 0. SAMPLE RATE 2 KHz. A-A FILTER @ 500 Hz. HANNED 3x.
 CURVE 2: KSRPG017A, 11'-0" BELOW DECK 0. SAMPLE RATE 2 KHz. A-A FILTER @ 500 Hz. HANNED 3x.
 CURVE 3: KSRPG018A, 21'-0" BELOW DECK 0. SAMPLE RATE 2 KHz. A-A FILTER @ 500 Hz. HANNED 3x.
 NOTE: TIME SCALE IS REFERENCED TO NOMINAL T-ZERO=242:05:32:00.027 GMT.

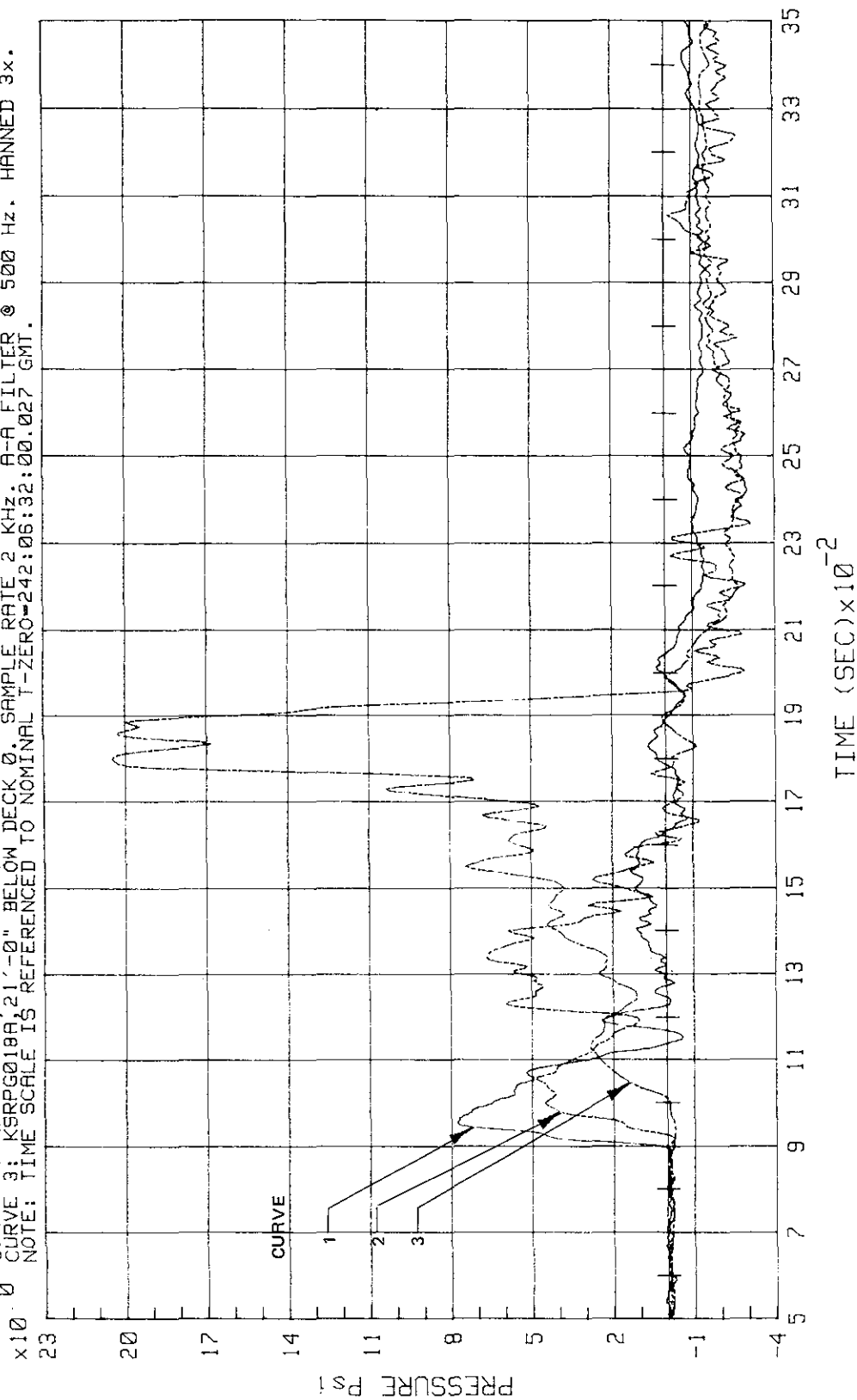


Figure 2-121. STS-8 SRB Ignition - West SRB, Main Exhaust Well Pressures
 T + 0.05 s to T + 0.35 s (MLP-2 Sensors on Side 2)

FILE: PGR04T PGR18T PGR21T PGR12T

MLP-2 SENSORS ON SOUTH, WEST & NORTH SIDES OF WEST EXHAUST WELL, AT THE BOTTOM OF THE WELL.
 CURVE 1: KSRPG004A, SIDE 1, 3'-6" ABOVE BOTTOM OF MLP. CURVE 2: KSRPG018A, SIDE 2, PRIMARY WELL.
 4'-0" ABOVE BOTTOM OF MLP. CURVE 3: KSRPG021A, SIDE 2, SECONDARY WELL, 4'-0" ABOVE BOTTOM OF MLP.
 CURVE 4: KSRPG012A, SIDE 3, SECONDARY WELL, 4'-3" ABOVE BOTTOM OF MLP. ALL DATA HANNED 3x.
 TIME SCALE REF. T-ZERO=242:06:32:00 GMT. REF. AMBIENT PRESSURE=0.0 Psi. T+0.05 to T+0.35 sec.

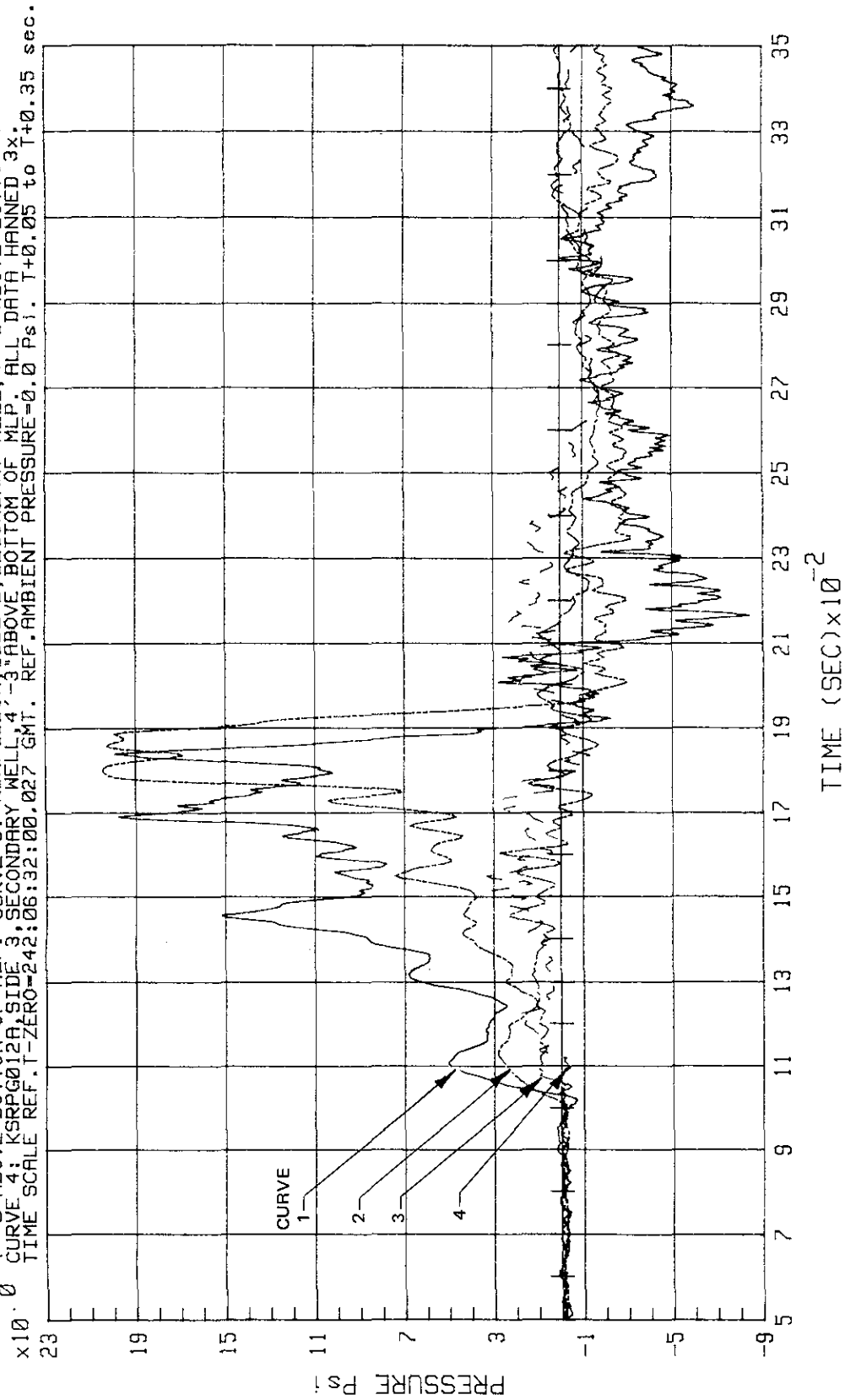


Figure 2-122. STS-8 SRB Ignition - Pressures at Bottom of West SRB Exhaust Well

KSC-DD-818-TR

FILE: PGR20T PGR21T PGR11T PGR12T

MLP-2 SENSORS ON WEST (SIDE 2) & NORTH (SIDE 3) SIDES OF EXHAUST WELL, BELOW WATER SPRAY NOZZLES.
 CURVE 1: KSRPG020A, 16'-3" BELOW DECK 0.
 CURVE 2: KSRPG021A, 21'-0" BELOW DECK 0.
 CURVE 3: KSRPG011A, 16'-0" BELOW DECK 0.
 CURVE 4: KSRPG012A, 20'-9" BELOW DECK 0.
 SAMPLE RATE 2 KHz, A-A FILTER @ 500 Hz, ALL RAW DATA HANNED 5x. REF. AMBIENT PRESSURE = 0.0 Psi.
 NOTE: TIME SCALE IS REFERENCED TO NOMINAL T-ZERO=242:06:32:00.027 GMT.

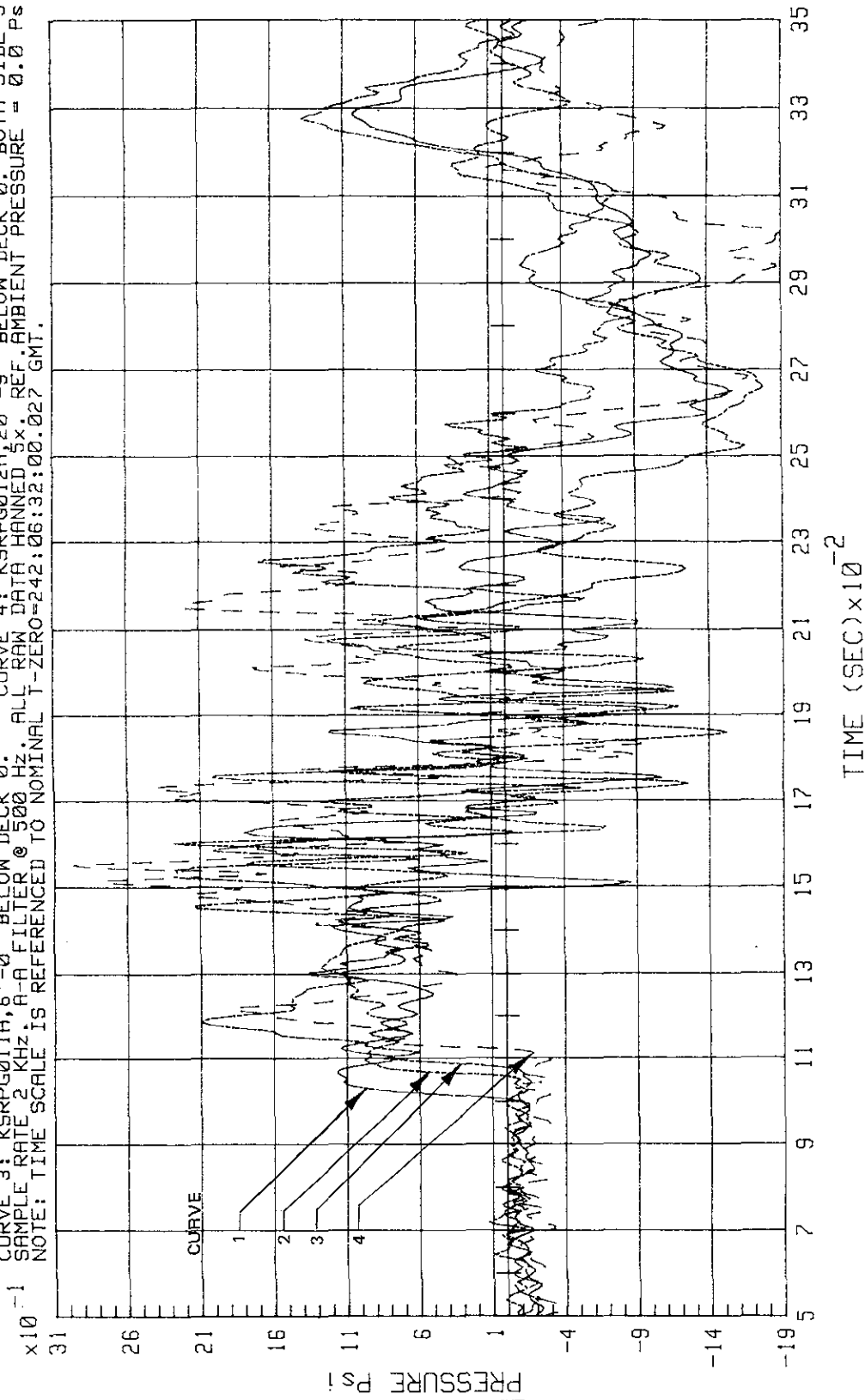


Figure 2-123. STS-8 SRB Ignition - West SRB, Secondary Exhaust Well Pressures, T + 0.05 s to T + 0.35 s

FILE: PGR10T PGR15T PGR19T PGR24T

MLP-2 SENSORS ON SOUTH, WEST & NORTH SIDES OF WEST EXHAUST WELL, ABOVE SPRAY NOZZLES & TROUGHS.
 CURVE 1: KSRPG010A, SIDE 1, 4'-3" BELOW DECK 0. CURVE 2: KSRPG015A, SIDE 2, PRIMARY WELL, 2'-6" BELOW
 DECK 0. CURVE 3: KSRPG019A, SIDE 2, SECONDARY WELL, 2'-6" BELOW DECK 0. CURVE 4: KSRPG024A, SIDE 3,
 SECONDARY WELL, 3'-3" BELOW DECK 0. SAMPLE RATE 2 KHz. A-A FLT @ 500 Hz. ALL DATA HANNED 10x.
 TIME SCALE REF. T-ZERO=242:06:32:00.027 GMT. REF. AMBIENT PRESSURE=0.0 Psi. T+0.05 to T+0.35 sec.

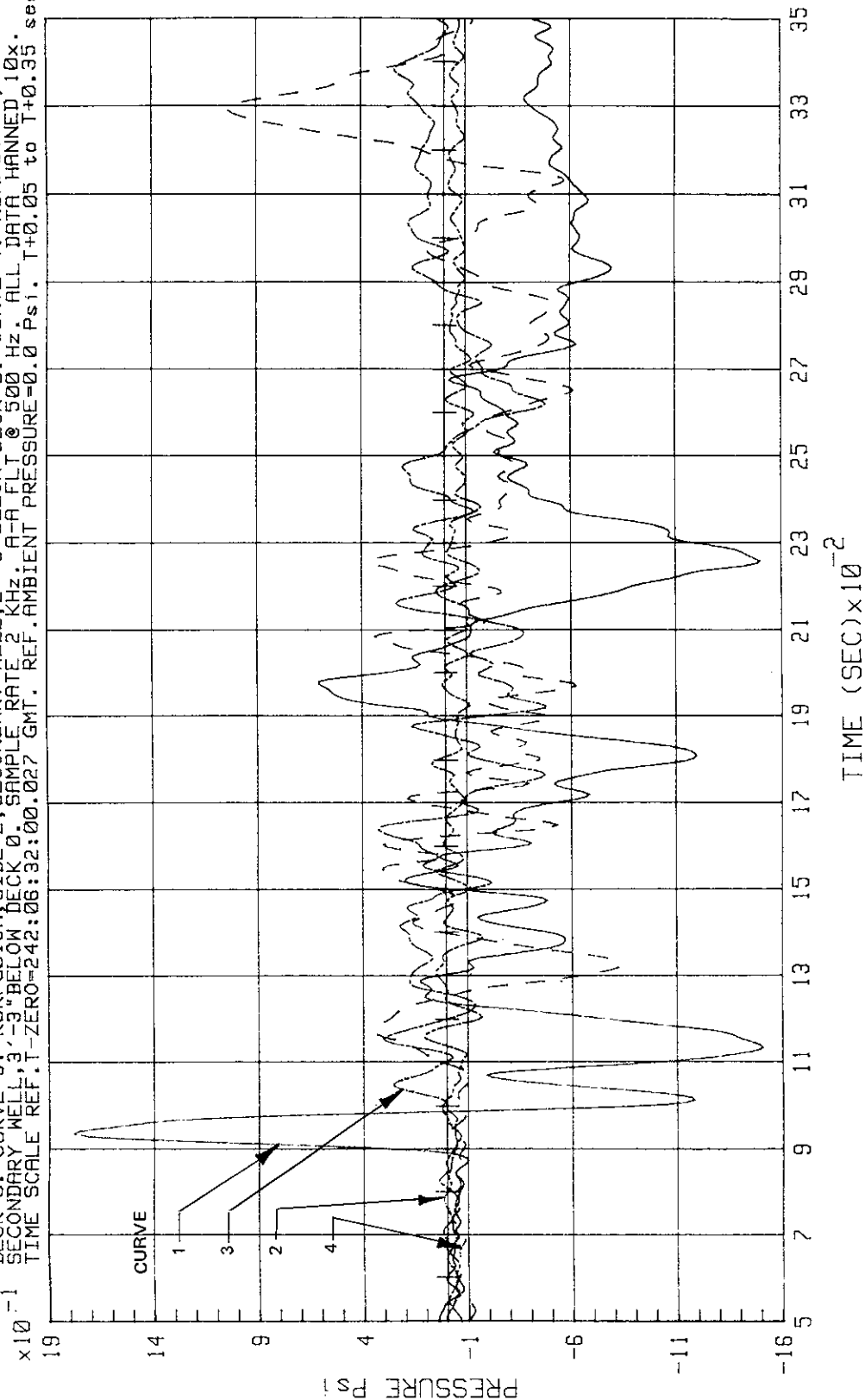


Figure 2-124. STS-8 SRB Ignition - West Exhaust Well Pressures Above Sound Suppression Water System

KSC-DD-818-TR

FILE: PFR25A PFR27A PFR35D PFR36D

MLP-1 SENSORS ON SOUTH SIDE OF WEST EXHAUST WELL, BELOW WATER SPRAY NOZZLES.
 CURVE 1: KSRPF075A, 6.0', BELOW DECK 0. CURVE 2: KSRPF072A, 16.0', BELOW DECK 0.
 CURVE 3: KSRPF035A, 21.3', BELOW DECK 0. CURVE 4: KSRPF036A, 21.8', BELOW DECK 0.
 0 SAMPLING RATE 2 KHz. A-A FILTER @ 500 Hz. ALL DATA HANNED 10x. T+0.05 TO T+0.35 sec.
 TIME SCALE REFERENCED TO T-ZERO-332:16:00:00.010 GMT (1983).

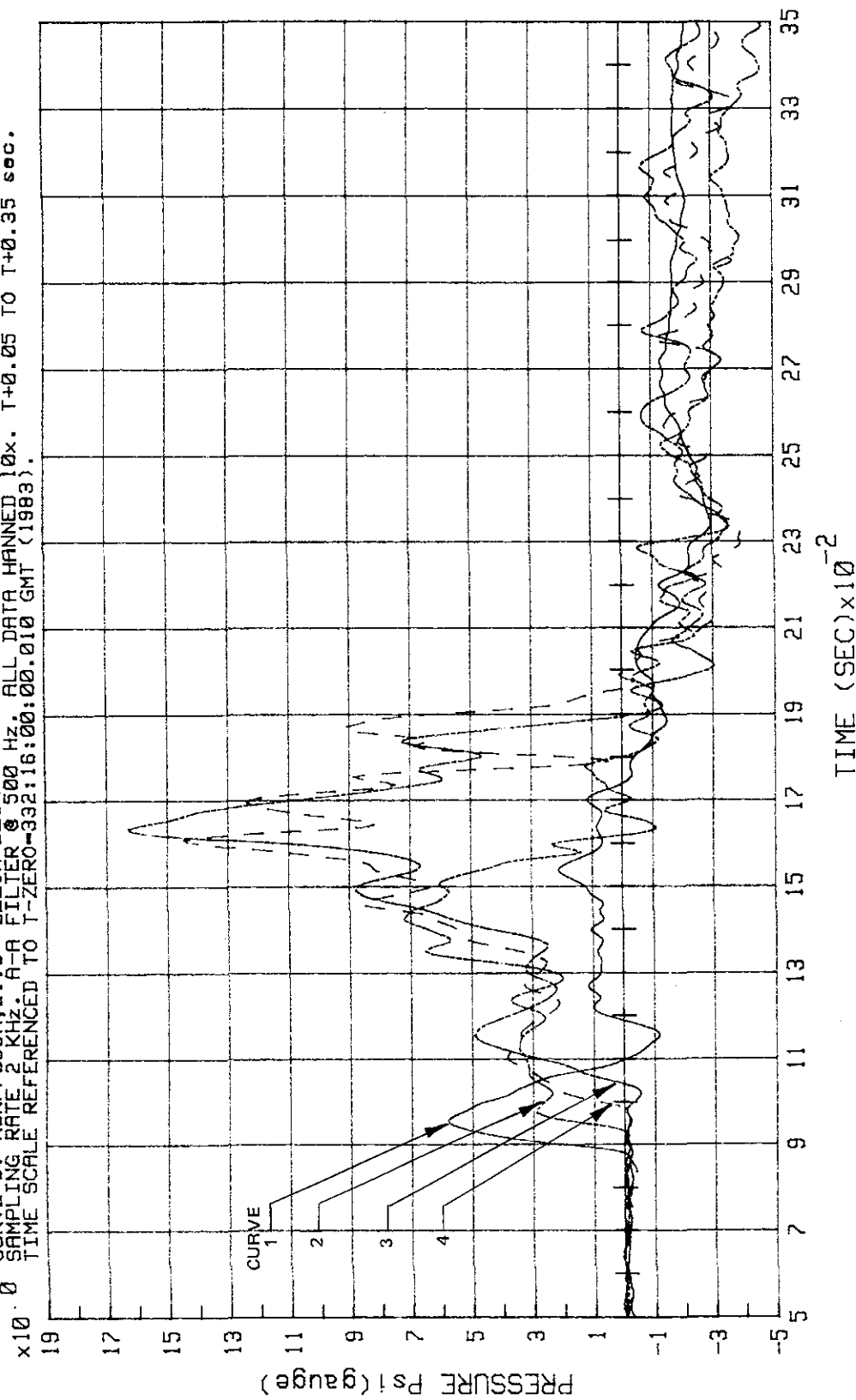


Figure 2-125. STS-9 SRB Ignition - West Exhaust Well Pressures Below Sound Suppression Water System (MLP-1 Sensors on South Side of West Exhaust Well)

FILE: PFR84A PFR65A PFR66A

MLP-1 SENSORS ON WEST SIDE OF PRIMARY WEST EXHAUST WELL BELOW WATER SPRAY NOZZLES.
 CURVE 1: KSRPF064A, 6.3' BELOW DECK 0. CURVE 2: KSRPF065A, 11.0' BELOW DECK 0.
 CURVE 3: KSRPF066A, 16.0' BELOW DECK 0. ALL SENSORS LOCATED @ CENTERLINE OF WEST SRB.
 0 SAMPLING RATE 2 KHz. A-A FILTER @ 500 Hz. ALL DATA HANNED 10x. T+0.05 TO T+0.35 sec.
 TIME SCALE REFERENCED TO T-ZERO-332:16:00:00.010 GMT (1983).

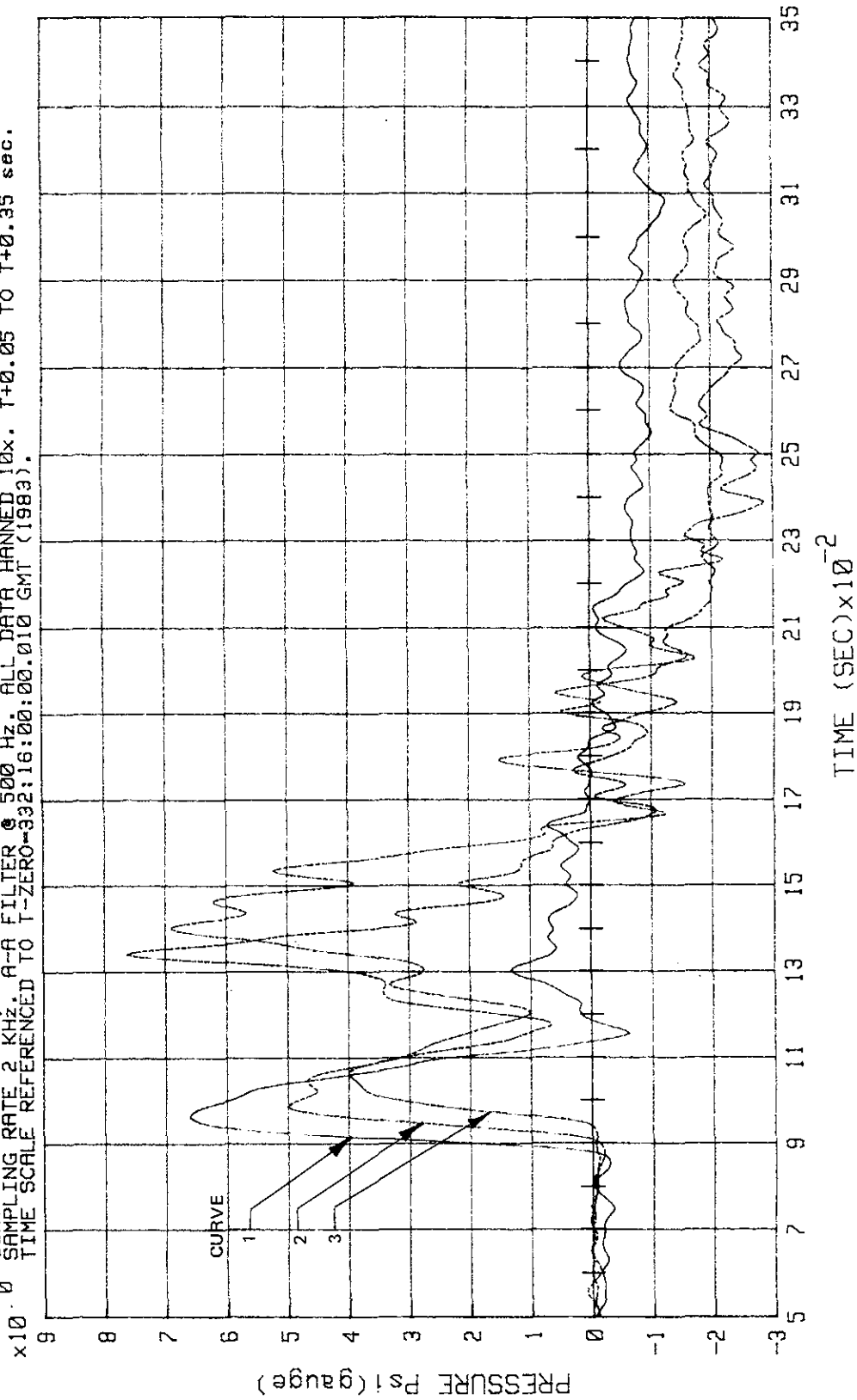


Figure 2-126. STS-9 SRB Ignition - West Exhaust Well Pressures Below Sound Suppression Water System (MLP-1 Sensors on West Side of Primary West Exhaust Well)

KSC-DD-818-TR

FILE: PFR71A PFR74A PFR80A PFR58A

MLP-1 SENSORS ON WEST & NORTH SIDES OF SECONDARY WEST EXH. WELL BELOW WATER SPRAY NOZZLES.
 CURVE 1: KSRPF071A, 16.3' BELOW DECK 0.
 CURVE 2: KSRPF074A, 21.0' BELOW DECK 0. WEST SIDE.
 CURVE 3: KSRPF080A, 16.0' BELOW DECK 0.
 CURVE 4: KSRPF058A, 21.8' BELOW DECK 0. NORTH SIDE.
 -1 SAMPLING RATE 2 KHz. A-A FILTER @ 500 Hz. ALL DATA HANNED 10x. T+0.05 TO T+0.35 sec.
 TIME SCALE REFERENCED TO T-ZERO-332:16:00:00.010 GMT (1983).

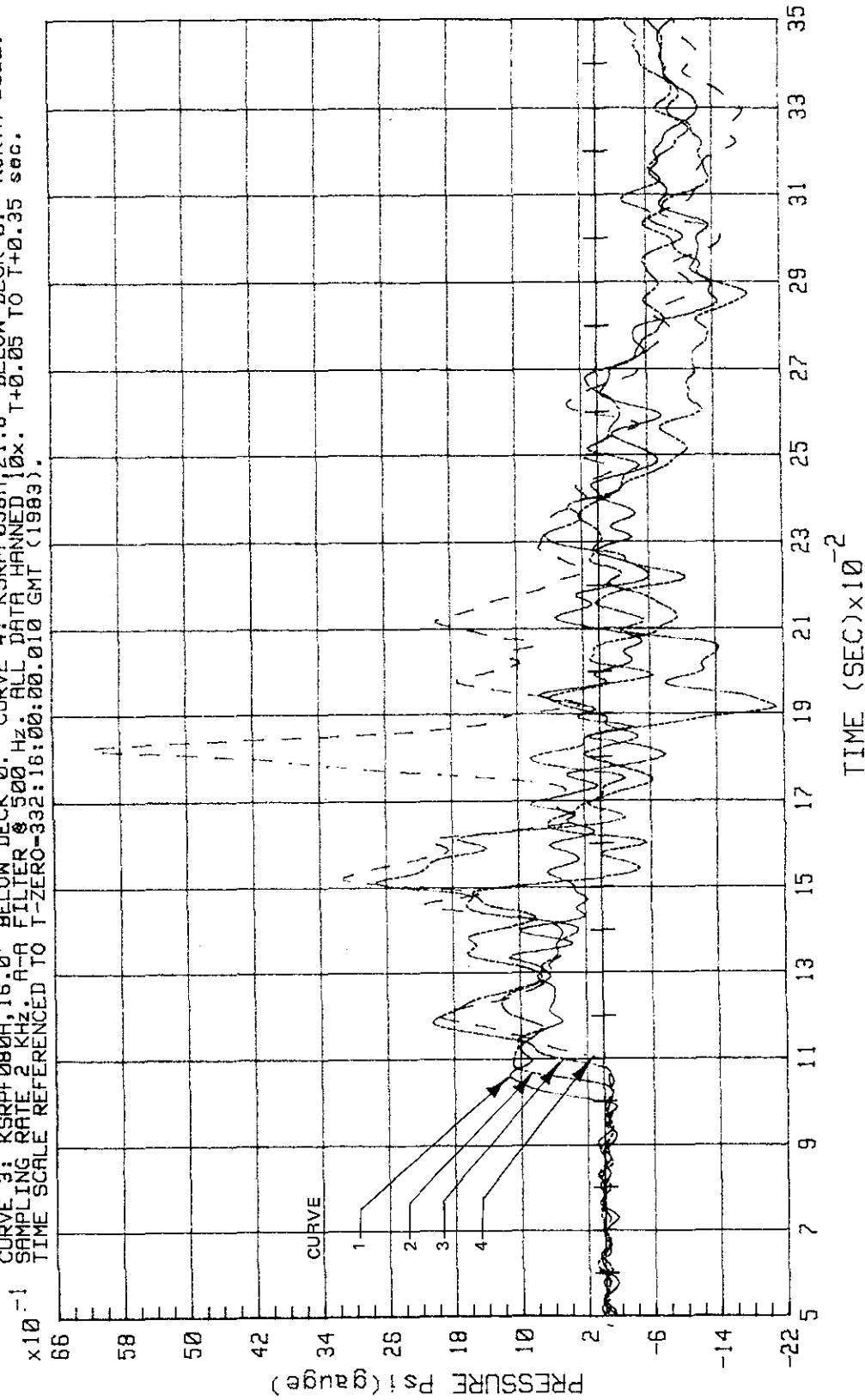


Figure 2-127. STS-9 SRB Ignition - West Secondary Exhaust Well Pressures
 Below Sound Suppression Water System

FILE: PFR54A PFR63A PFR70A PFR78A

MLP-1 SENSORS ON SOUTH, WEST & NORTH SIDES OF WEST EXHAUST WELL ABOVE SPRAY NOZZLES & TROUGHS.
 CURVE 1: KSRPF054A, SIDE 1, 4.75' BELOW DECK 0. CURVE 2: KSRPF063A, SIDE 2, PRIMARY WELL, 2.5' BELOW
 DECK 0. CURVE 3: KSRPF070A, SIDE 2, SECONDARY WELL, 2.5' BELOW DECK 0. CURVE 4: KSRPF078A, SIDE 3,
 SECONDARY WELL, 3.25' BELOW DECK 0. SAMPLE RATE 2 KHz. A-A FLT @ 500 Hz. ALL DATA HANNED 10x.
 TIME SCALE REFERENCED TO T-ZERO-332:16:00:00.010 GMT (1983). T+0.05 TO T+0.35 sec.

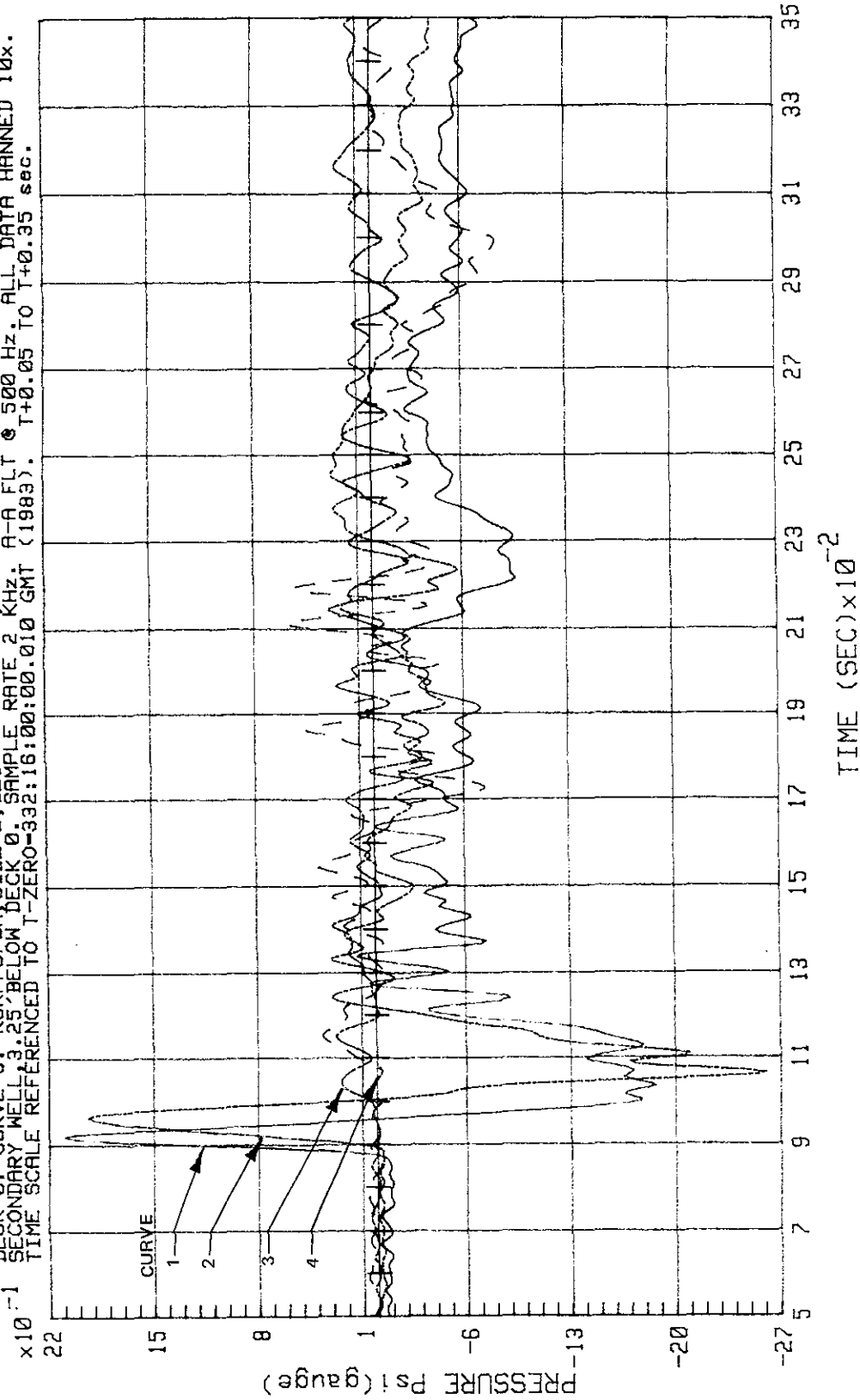


Figure 2-128. STS-9 SRB Ignition - West Exhaust Well Pressures Above Sound Suppression Water System

KSC-DD-818-TR

FILE: PFT54C PFT75C PFT77I PFT35C

MLP-1 SENSORS ON SOUTH SIDE 1 OF PRIMARY WEST EXHAUST WELL. EXTRACTED TIME VARIABLE MEAN.

CURVE 1: KSRPF054A, 4.75' BELOW DECK 0. CURVE 2: KSRPF075A, 8.0' BELOW DECK 0.

CURVE 3: KSRPF077A, 16.0' BELOW DECK 0. CURVE 4: KSRPF035A, 31.3' BELOW DECK 0.

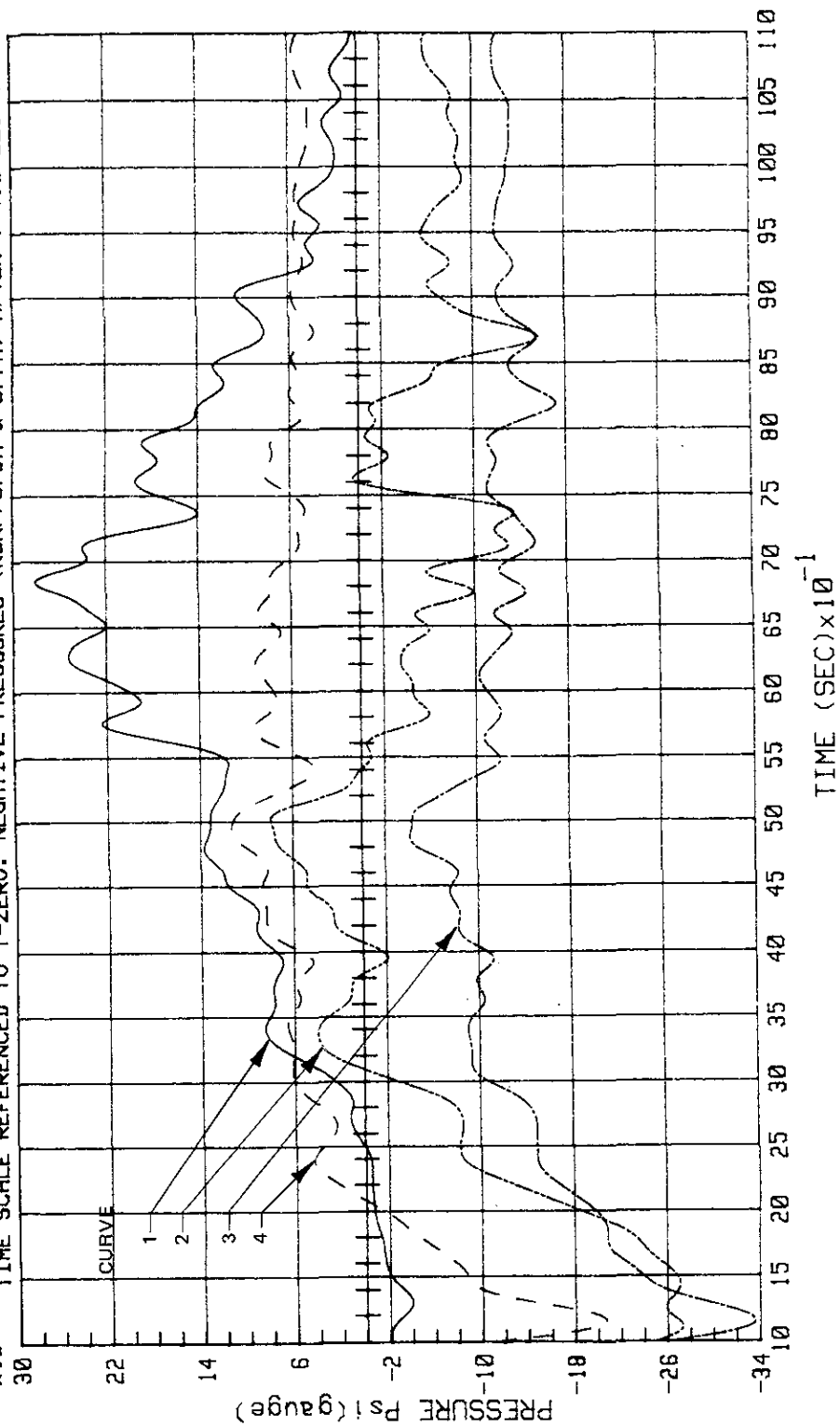
x10⁻¹ SAMPLING RATE 200 Hz. A-R FILTER 0.50 Hz. ALL DATA HANNED 500X. FROM T+1.0 TO T+11.0 SEC. TIME SCALE REFERENCED TO T-ZERO. NEGATIVE PRESSURES (KSRPF075A & 077A) AFTER T+4.0 SEC ARE INVALID.

Figure 2-129. STS-9 Lift-Off - West Primary Exhaust Well Pressures, South Side 1, Static Load

FILE: PFT63C PFT64C PFT65C PFT66C

MLP-1 SENSORS ON WEST SIDE 2 OF PRIMARY WEST EXHAUST WELL. EXTRACTED TIME VARIABLE MEAN.
 CURVE 1: KSRPF063A, 2.5' BELOW DECK 0. CURVE 2: KSRPF064A, 6.3' BELOW DECK 0.
 CURVE 3: KSRPF065A, 11.0' BELOW DECK 0. CURVE 4: KSRPF066A, 16.0' BELOW DECK 0.
 -1 SAMPLING RATE 200 Hz. A-A FILTER @ 50 Hz. ALL DATA HANNED 500x. FROM T+1.0 TO T+11.0 sec.
 x10⁻¹ TIME SCALE REFERENCED TO T-ZERO.

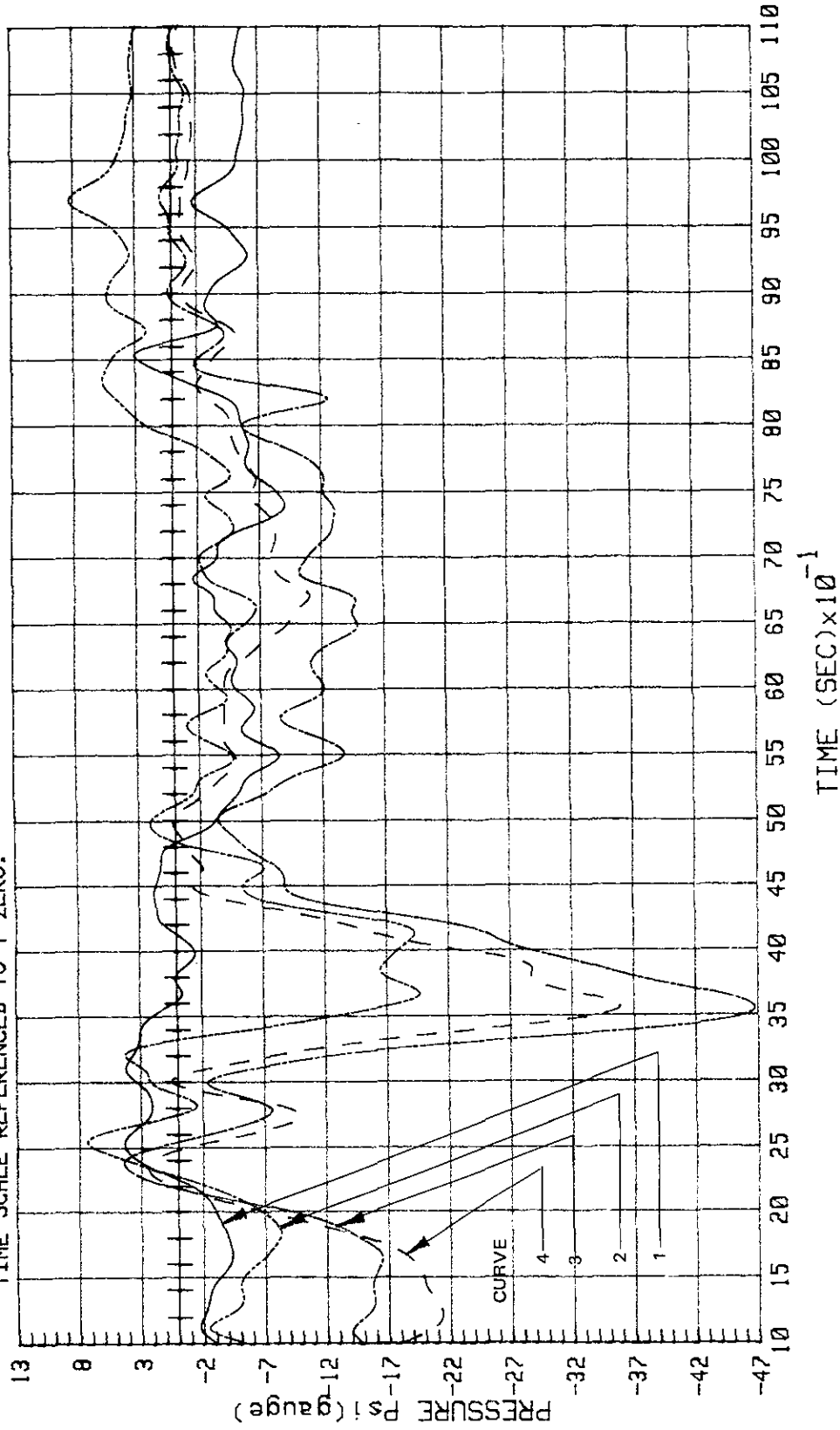


Figure 2-130. STS-9 Lift-Off - West Primary Exhaust Well Pressures, West Side 2, Static Load

KSC-DD-818-TR

FILE: PFT70C PFT71C PFT74C

MLP-1 SENSORS ON WEST SIDE OF SECONDARY WEST EXHAUST WELL, EXTRACED TIME VARIABLE MEAN.
 CURVE 1: KSRPF071A, 2.5' BELOW DECK 0. CURVE 2: KSRPF071A, 8.3' BELOW DECK 0.
 CURVE 3: KSRPF071A, 21.0' BELOW DECK 0. OUTPUT OF KSRPF071A DID NOT RETURN TO AMBIENT.
 x10⁻¹ SAMPLING RATE 200 HZ. A-A FILTER @ 50 HZ. ALL DATA HANNED 500x. FROM T+1.0 TO T+11.0 SEC.
 TIME SCALE REFERENCED TO T-ZERO. ALL SENSORS SHOW DRIFT AFTER T+10.0 SEC.

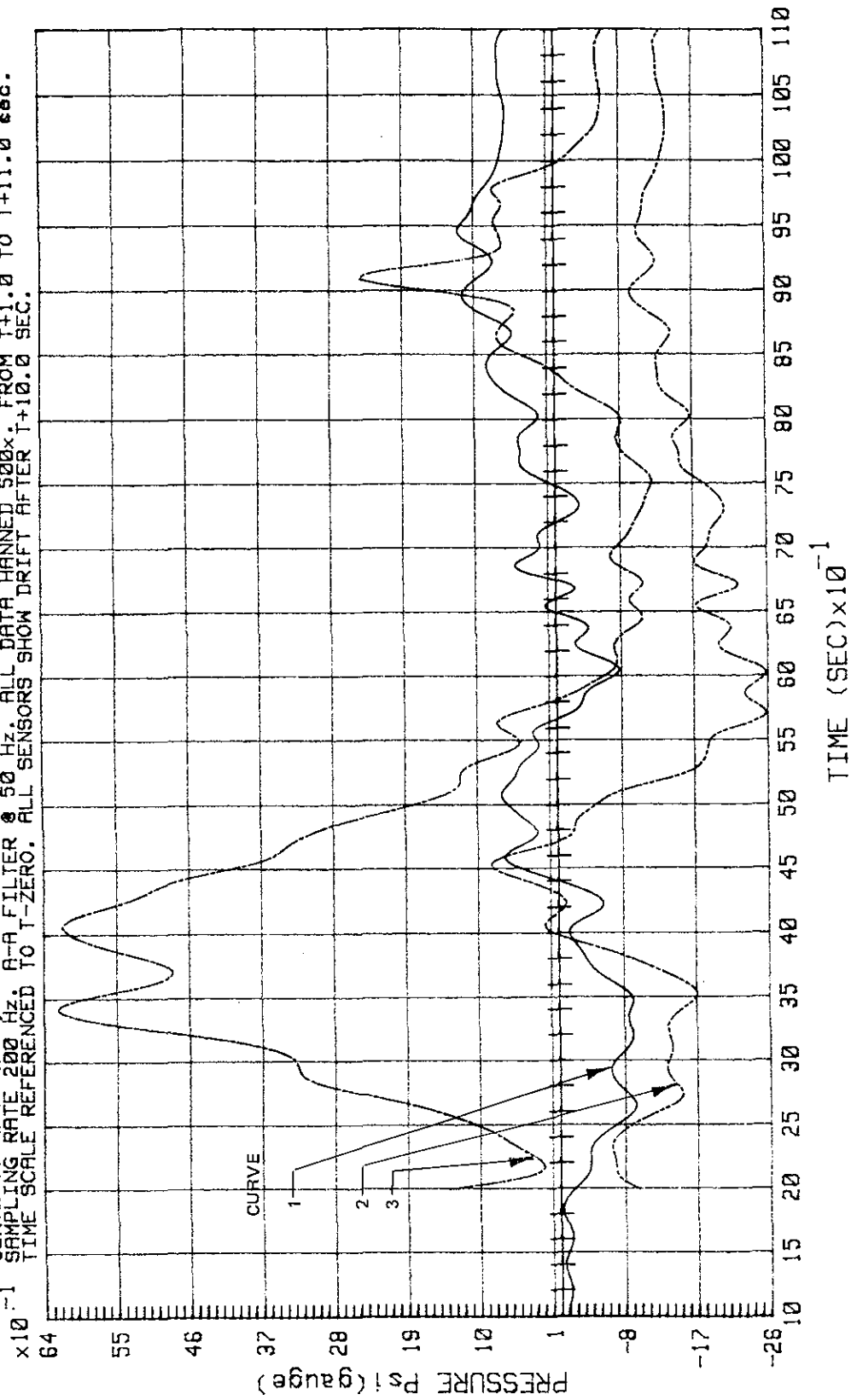


Figure 2-131. STS-9 Lift-Off - West Secondary Exhaust Well Pressures, West Side 2, Static Load

FILE: PFT80C PFT58C

MLP-1 SENSORS ON NORTH SIDE OF SECONDARY WEST EXHAUST WELL. EXTRACTED TIME VARIABLE MEAN.
 CURVE 1: KSRPF080A, 18.0' BELOW DECK 0. CURVE 2: KSRPF058A, 21.8' BELOW DECK 0.
 AFTER T+7.5 SEC KSRPF080A DATA CONTAIN DRIFT & KSRPF058A OUTPUT HAS DROPOUT.
 x10⁻¹ SAMPLING RATE 200 HZ, A-A FILTER 50 HZ. ALL DATA HANNED 500x. FROM T+1.0 TO T+11.0 SEC.
 TIME SCALE REFERENCED TO T-ZERO. AFTER T+7.5 SEC DATA INVALID.

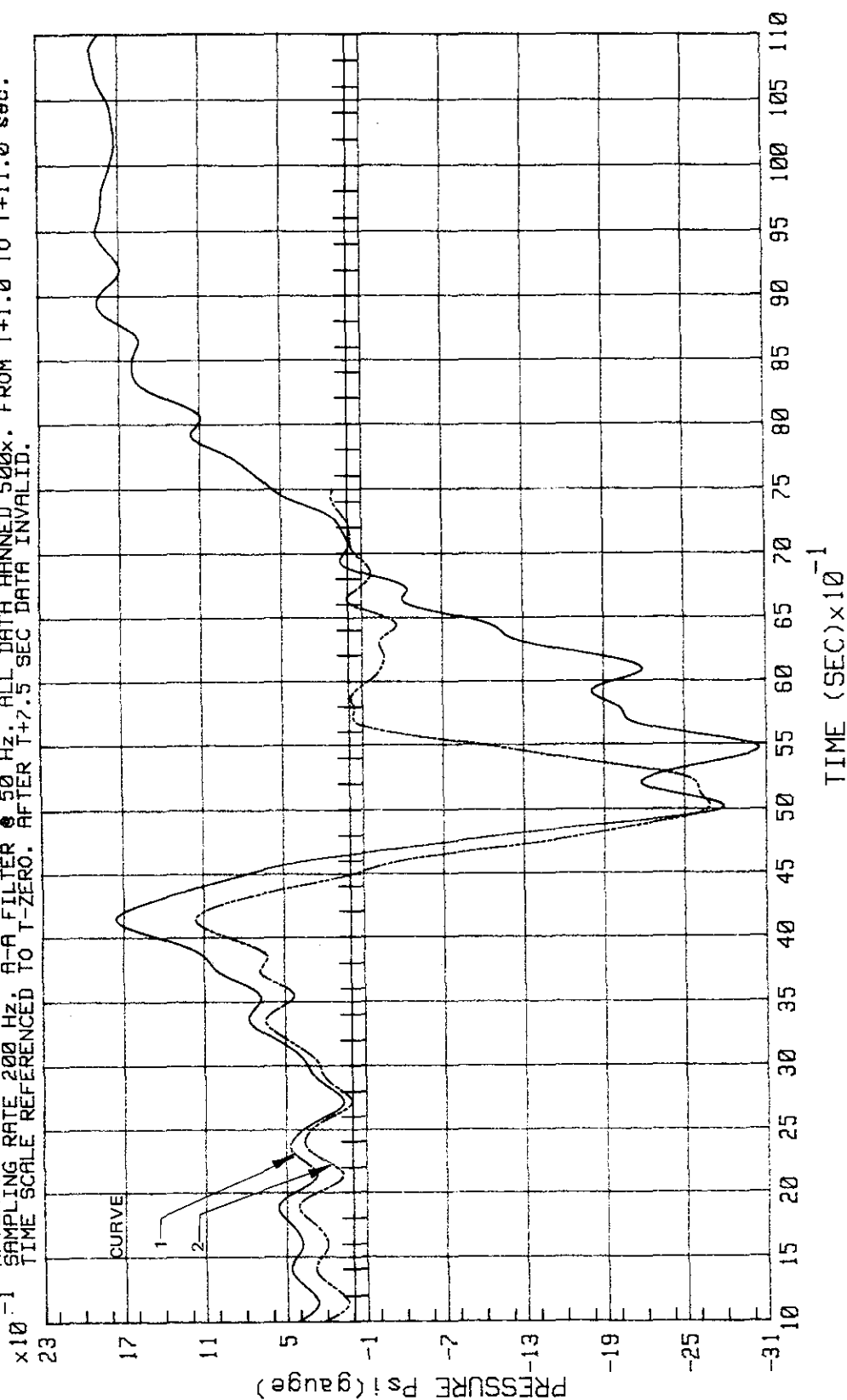


Figure 2-132. STS-9 Lift-Off - West Secondary Exhaust Well Pressures, North Side 3, Static Load

KSC-DD-818-TR

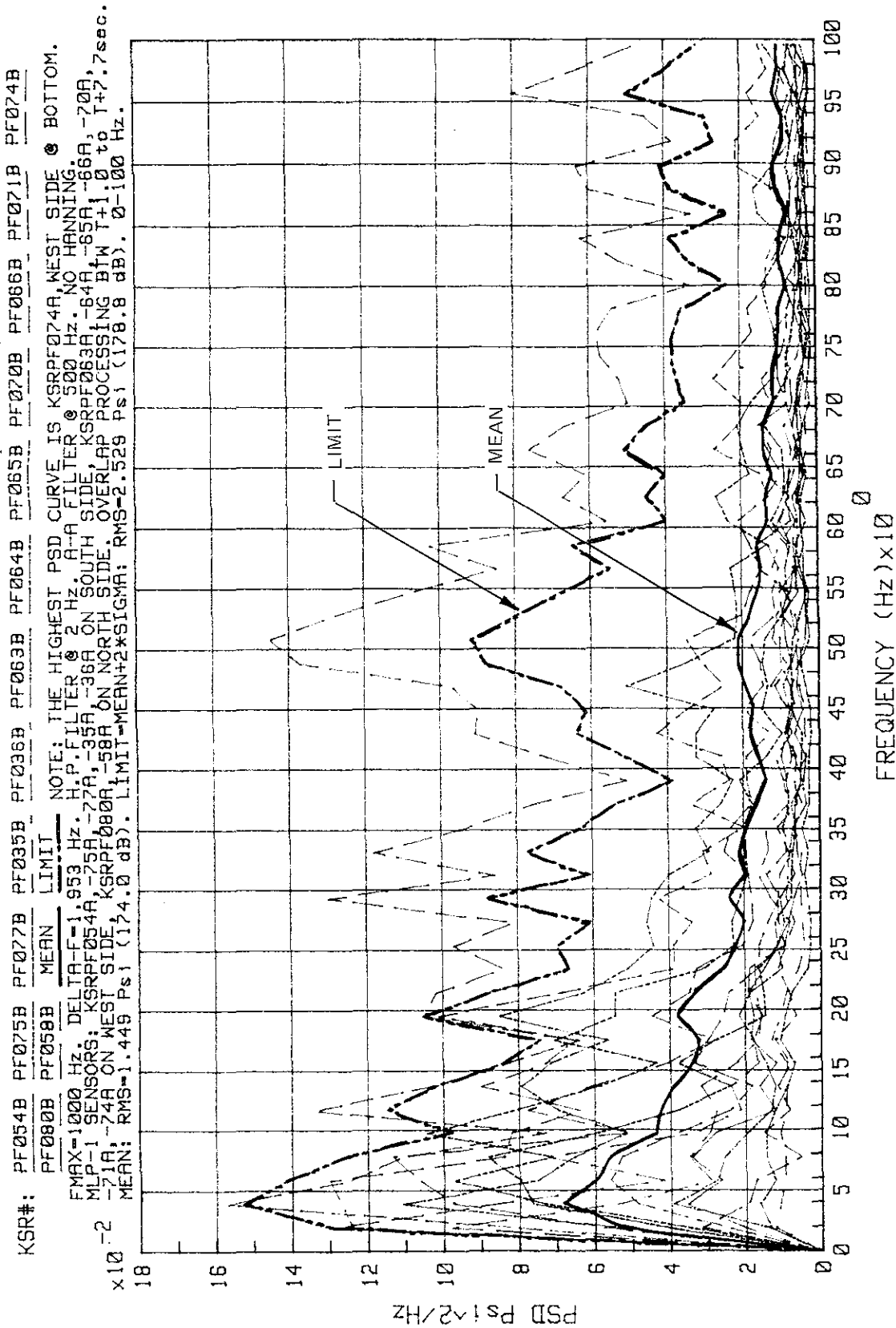


Figure 2-133. STS-9 Lift-Off Peak - West Exhaust Well Pressures, Dynamic Part, Raw PSD's

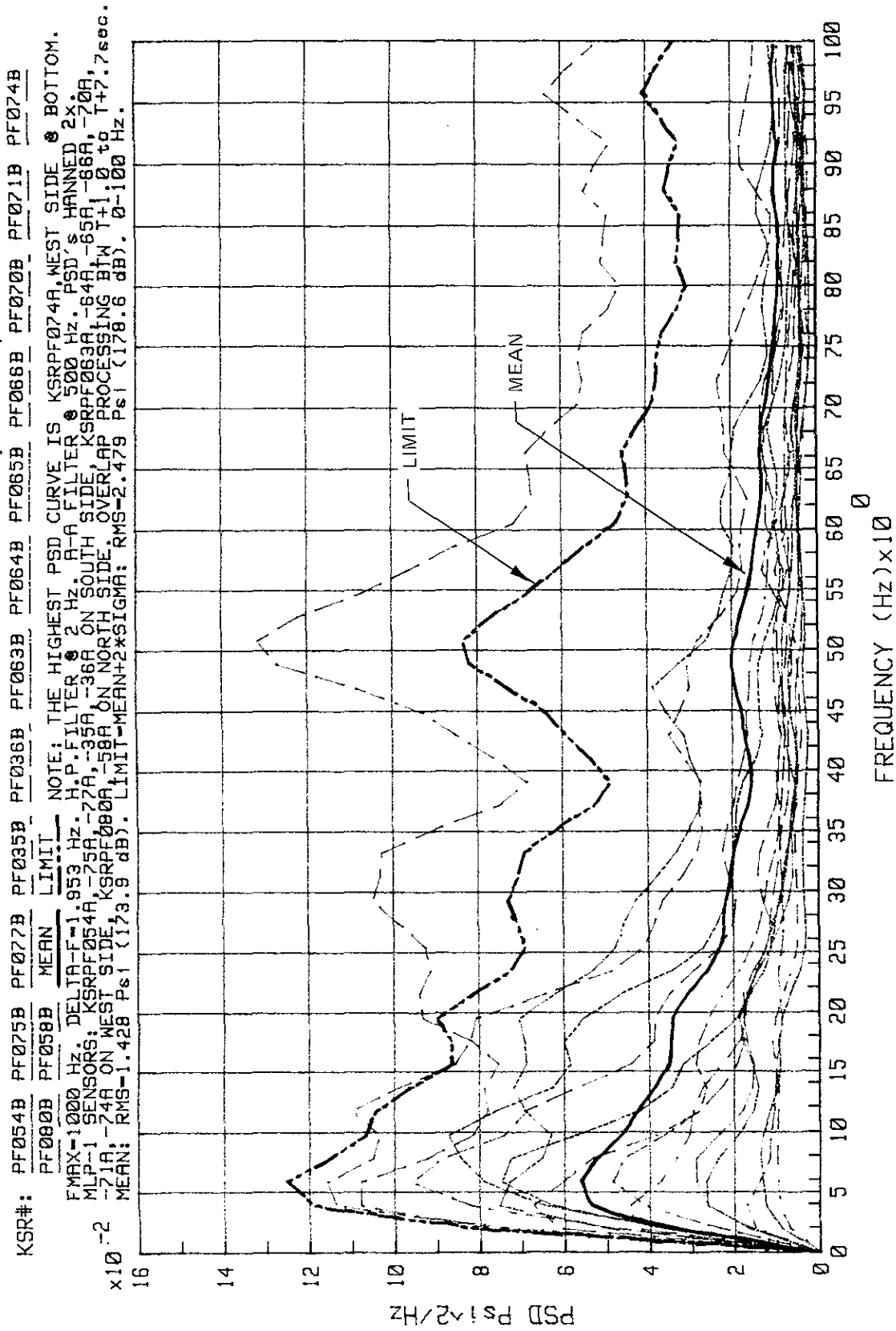


Figure 2-134. STS-9 Lift-Off Peak - West Exhaust Well Pressures, Dynamic Part (Hanned)

KSC-DD-818-TR

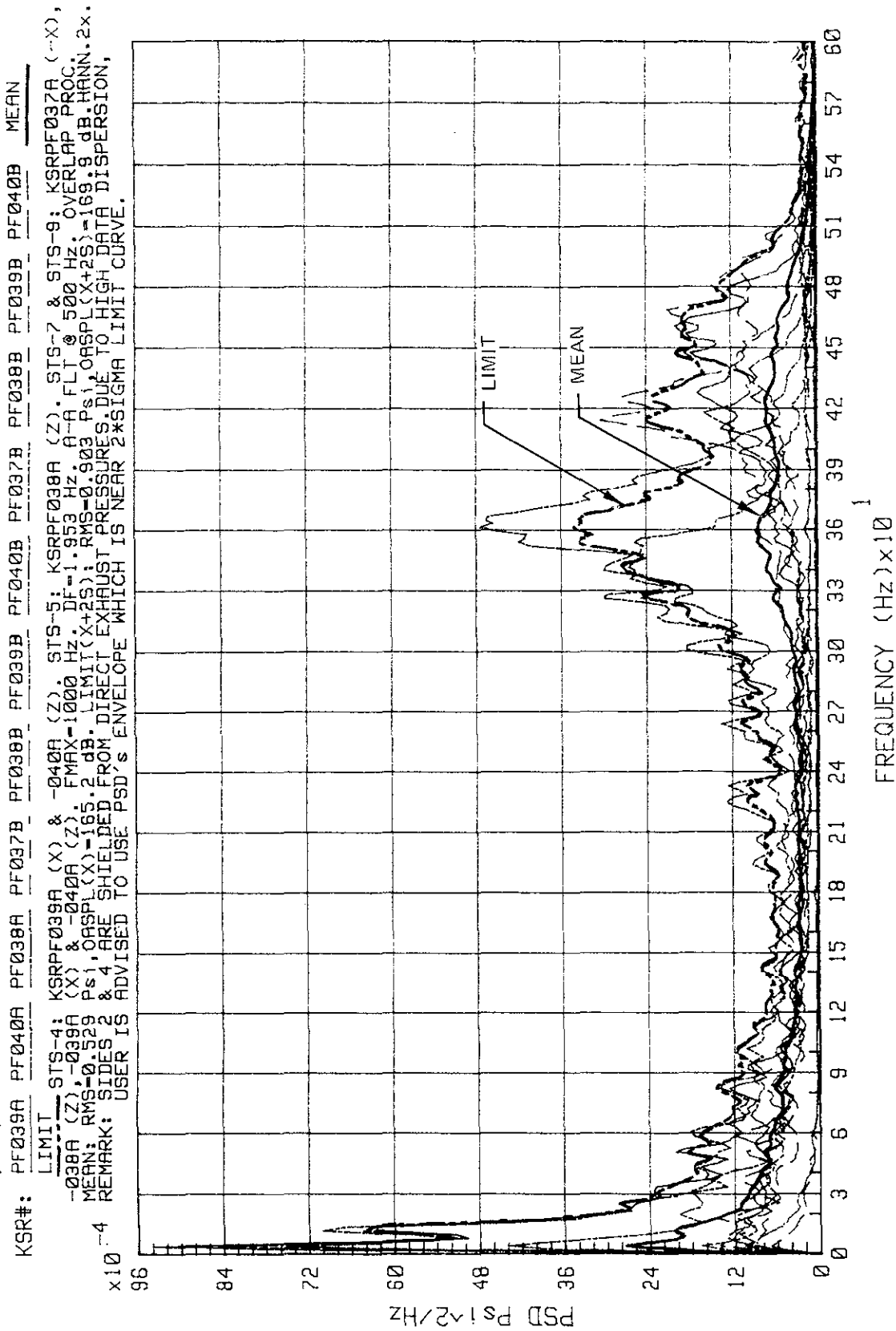


Figure 2-135. STS-4, -5, -7, and -9 Lift-Off Peak - Acoustics on Sides 2 and 4 of MLP-1

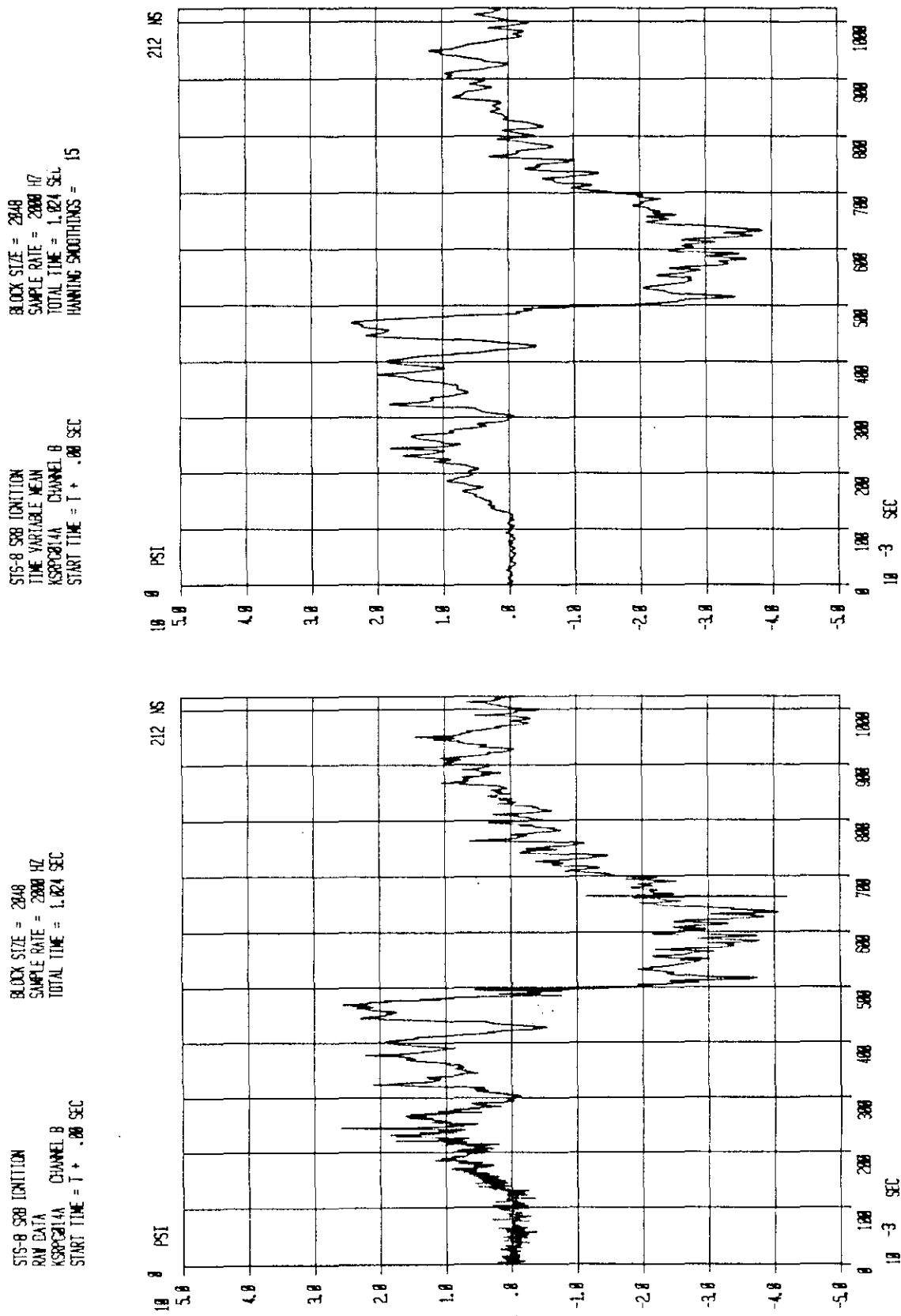
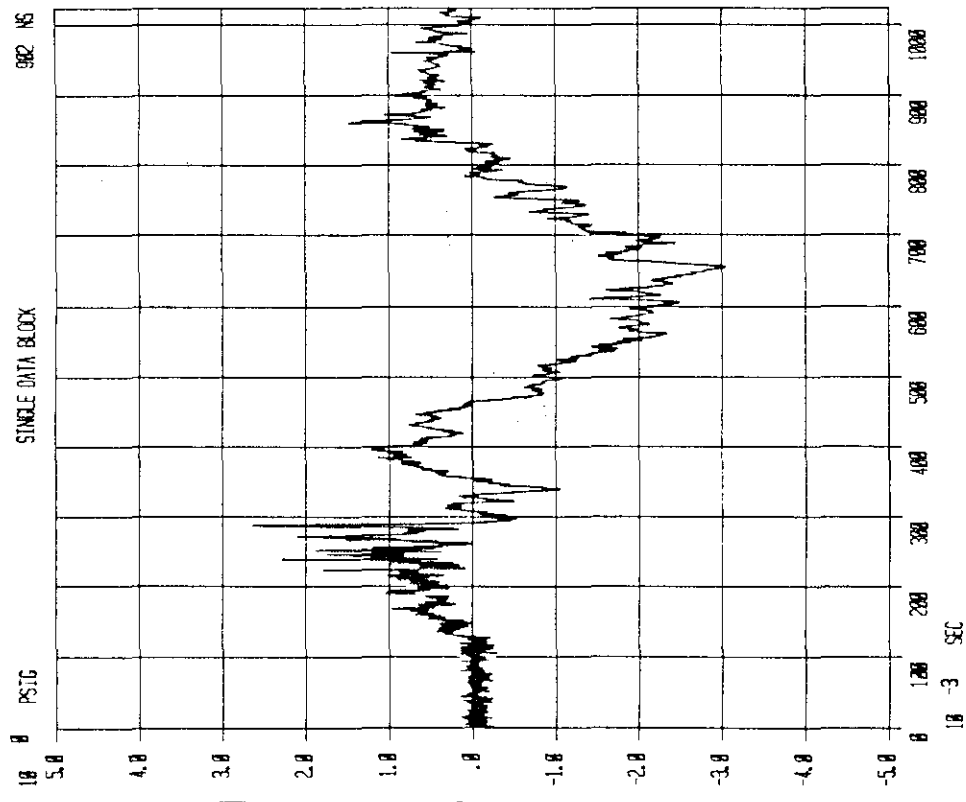


Figure 2-136. STS-8 SRB Ignition - KSRPG014A Raw Data and TVN

KSC-DD-818-TR

STS-9 SRB IGNITION
RAW DATA
KSRPF062A CHANNEL A
START TIME = 1 + .00 SEC

BLOCK SIZE = 2048
SAMPLE RATE = 2000 HZ
TOTAL TIME = 1.024 SEC



STS-9 SRB IGNITION
TIME VARIABLE MEAN
KSRPF062A CHANNEL A
START TIME = 1 + .00 SEC

BLOCK SIZE = 2048
SAMPLE RATE = 2000 HZ
TOTAL TIME = 1.024 SEC
HANNING SMOOTHINGS = 15

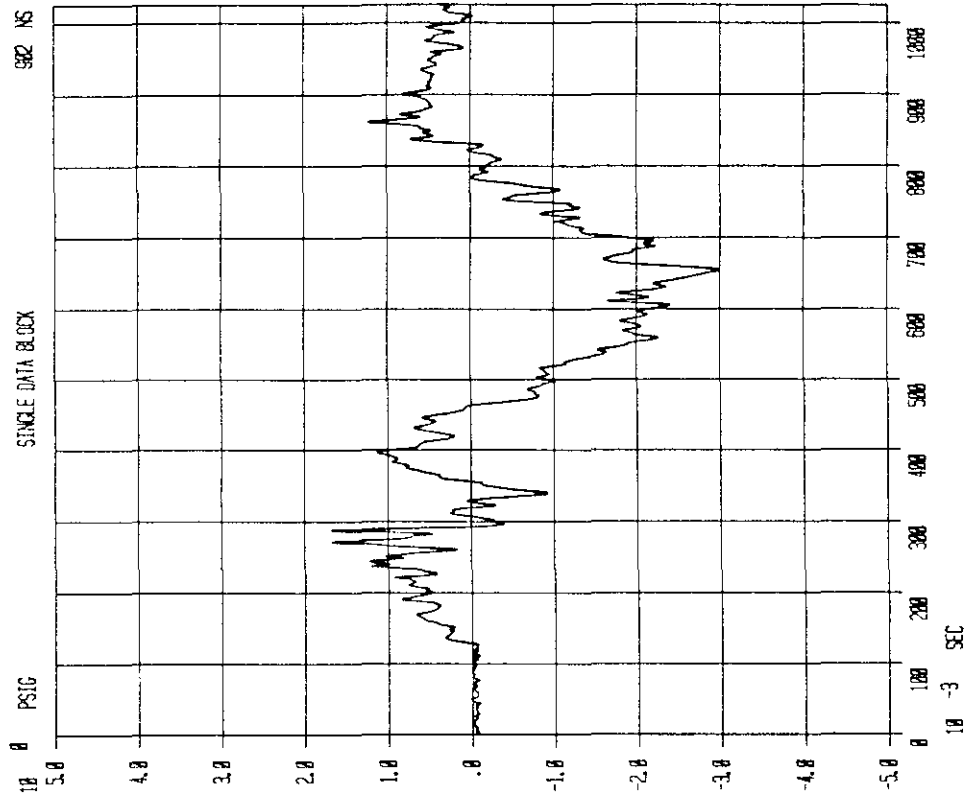
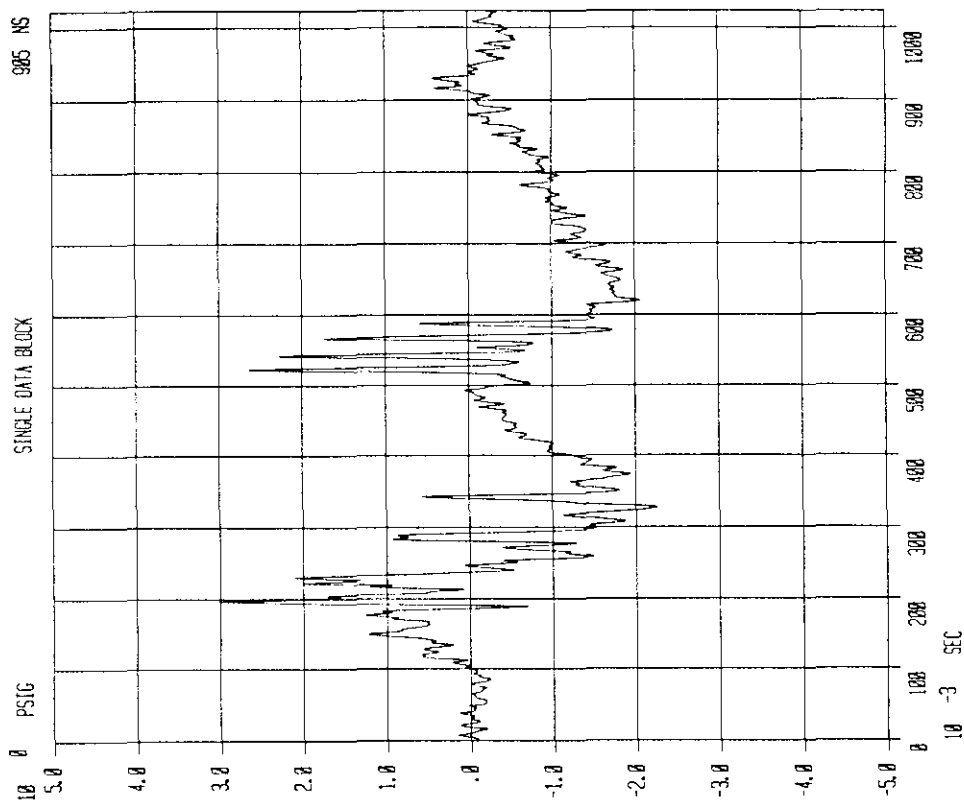


Figure 2-137. STS-9 SRB Ignition - KSRPF062A Raw Data and TVM

STS-9 SRB IGNITION
BLOCK SIZE = 2048
SAMPLE RATE = 2000 HZ
TOTAL TIME = 1.024 SEC
HANNING SMOOTHINGS = 15

TIME VARIABLE MEAN
KSRPF060A CHANNEL A
START TIME = T + .20 SEC



STS-9 SRB IGNITION
BLOCK SIZE = 2048
SAMPLE RATE = 2000 HZ
TOTAL TIME = 1.024 SEC

TIME VARIABLE MEAN
KSRPF060A CHANNEL A
START TIME = T + .20 SEC

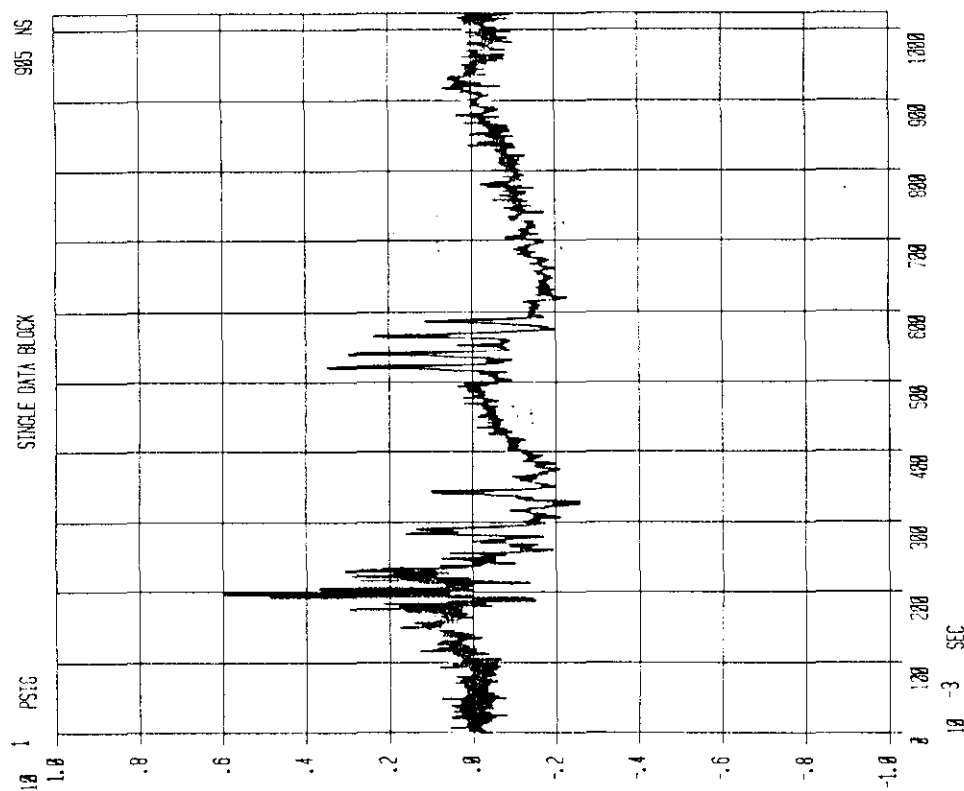


Figure 2-138. STS-9 SRB Ignition - KSRPF060A Raw Data and TVM

KSC-DD-818-TR

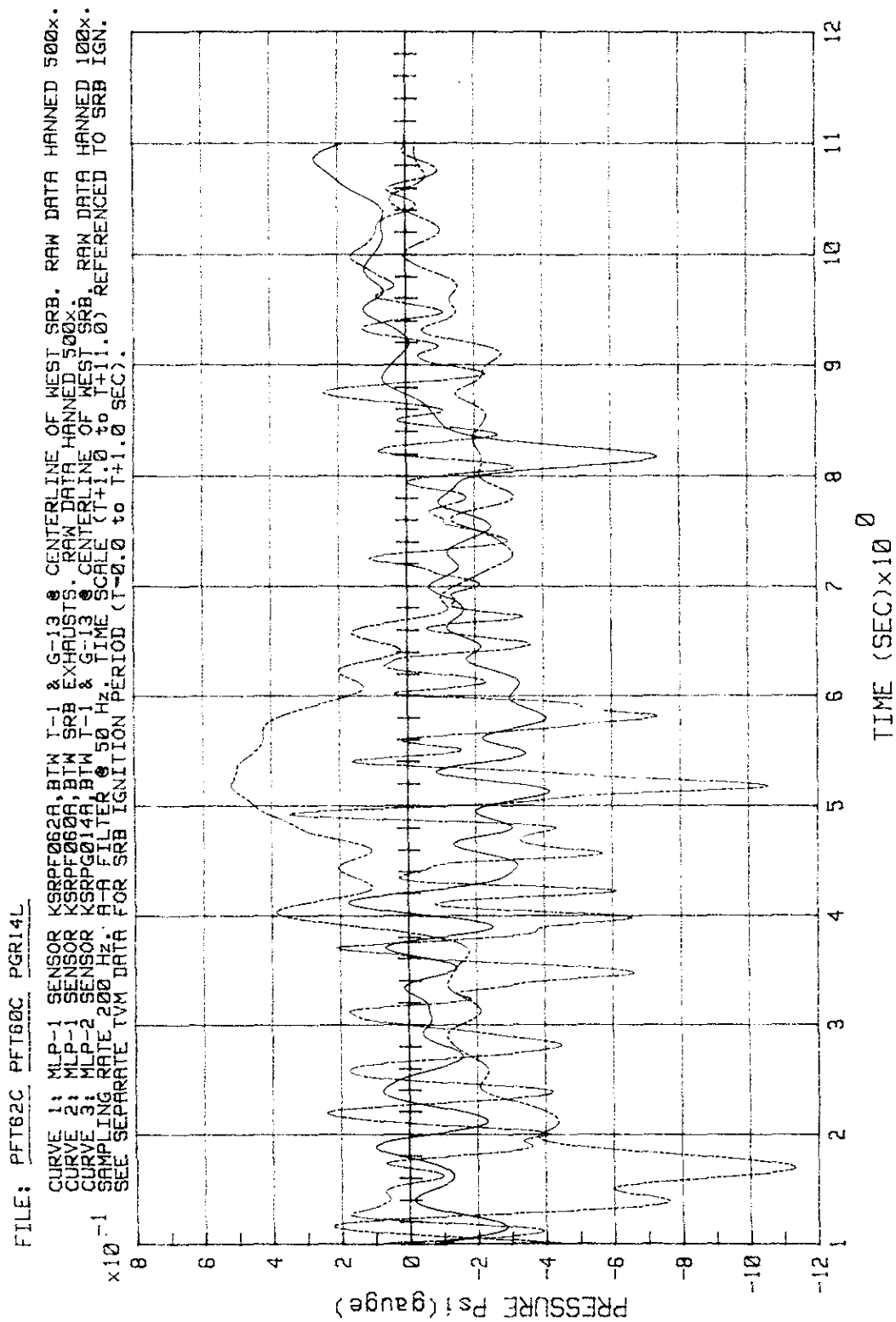


Figure 2-139. STS-8 and -9 MLP-1 and MLP-2 Pressures on B Level, TVM

FILE: PF062C PF062C PG014C PF062B PG014C PF062B MEAN LIMIT

SENSORS: KSRPF062A ON MLP-1 & KSRPF062A ON MLP-2, FMAX=1000 Hz, DELTA-F=1.953 & 0.976 Hz.
OVERLAP PROC, STS-4 & STS-5 (NO H.P.FLT OR TDM), STS-6 (TVM EXTRACTED), STS-7 (2 Hz H.P.FLT),
STS-8 (TVM EXTRACTED), STS-9 (2 Hz H.P.FLT), ALL PSD & HANNED 2x, DATA FOR 0-600 Hz RANGE.
x10⁻³ MEAN: RMS=1.1739 Psi (172.1 dB), LIMIT (MEAN+2*SIGMA): RMS=1.5887 Psi (174.8 dB).
SEE SEPARATE PLOTS FOR 0-100 Hz & 100-600 Hz RANGES, FOR "STATIC" PRESSURES SEE TVM DATA.

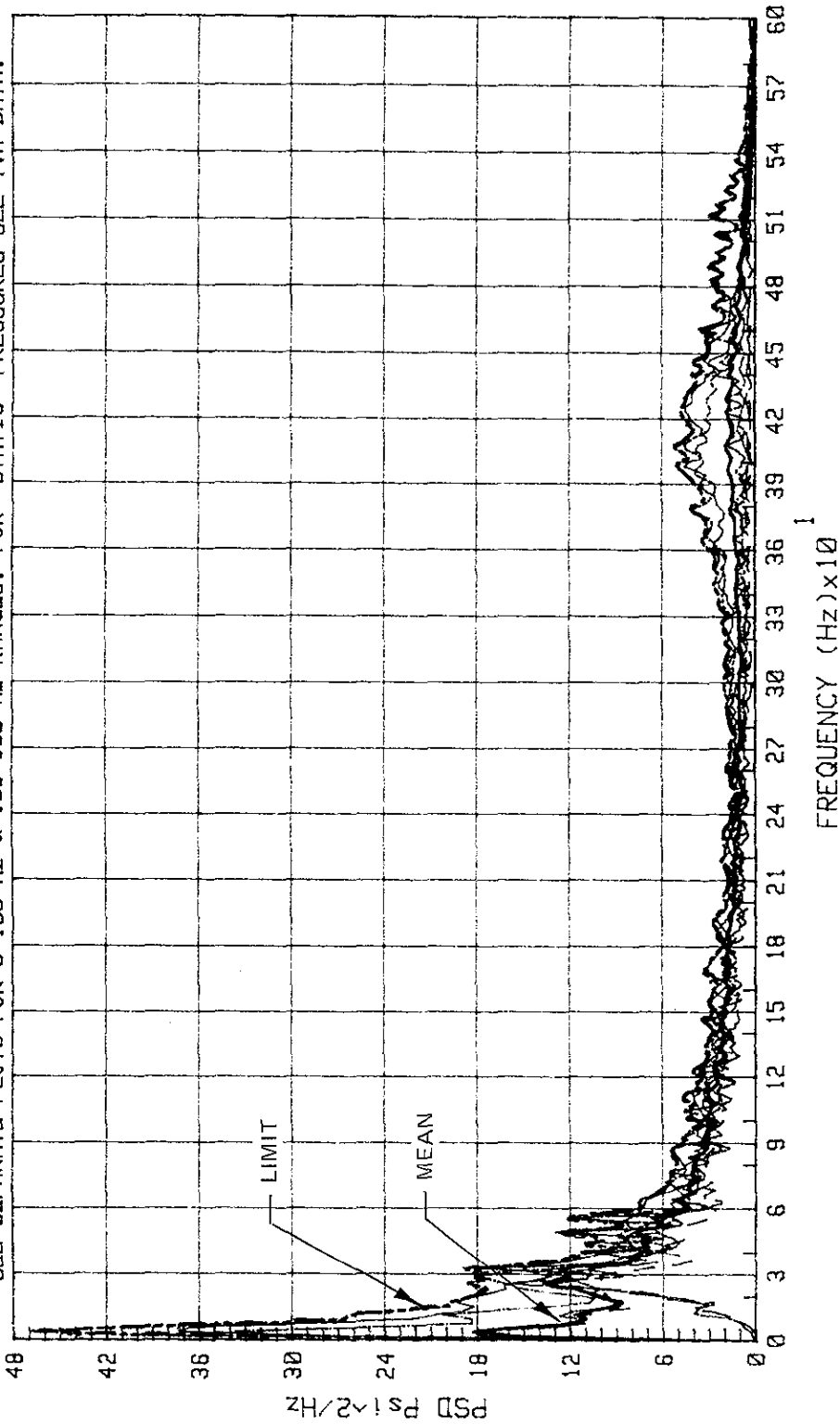


Figure 2-140. STS-4 Through -9 MLP-1 and MLP-2 Pressures on B Level Between T-1 and G-13, Dynamic Part

KSC-DD-818-TR

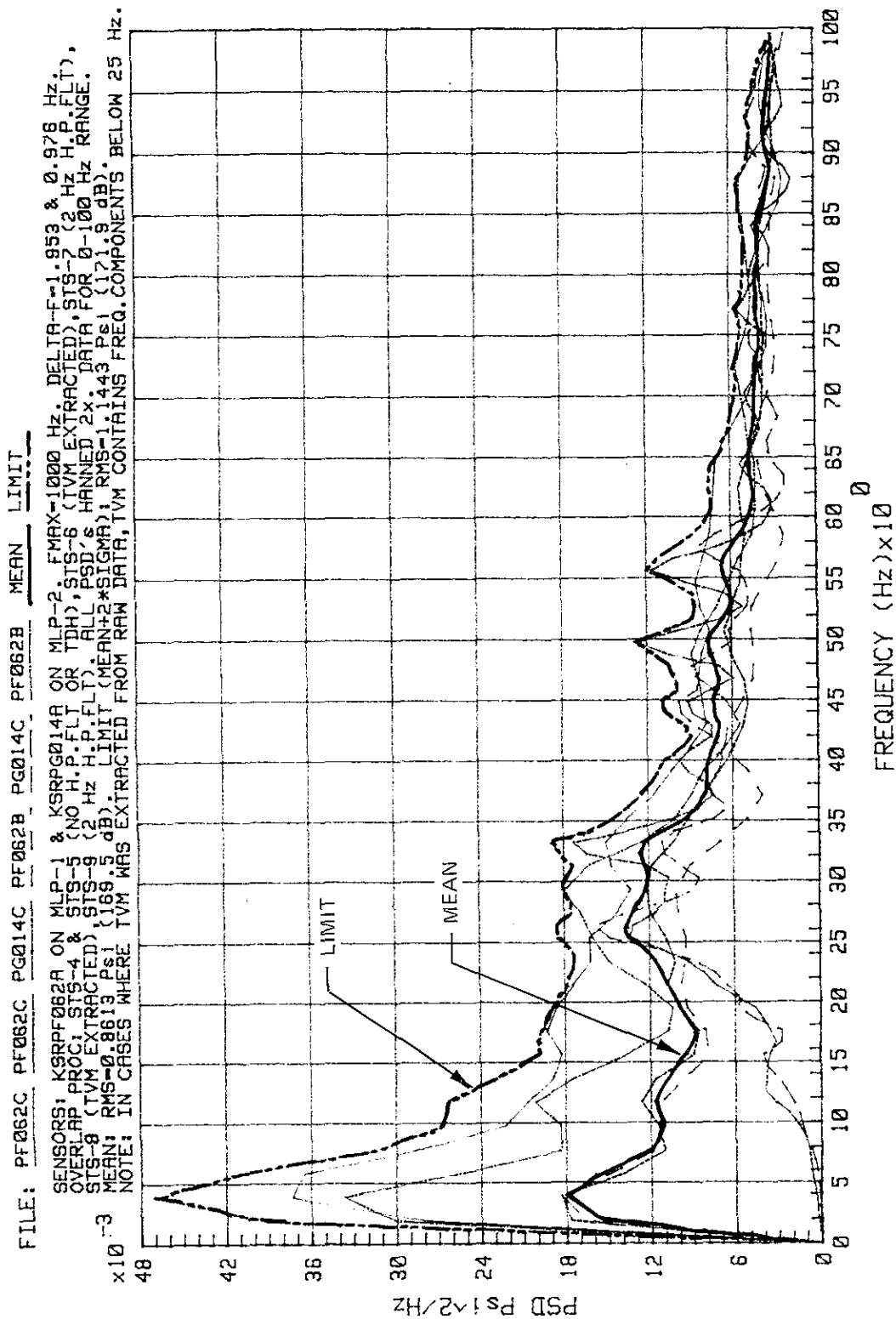


Figure 2-141. STS-4 Through -9 MLP-1 and MLP-2 Pressures on B Level
Between T-1 and G-13, 0 to 100 Hz

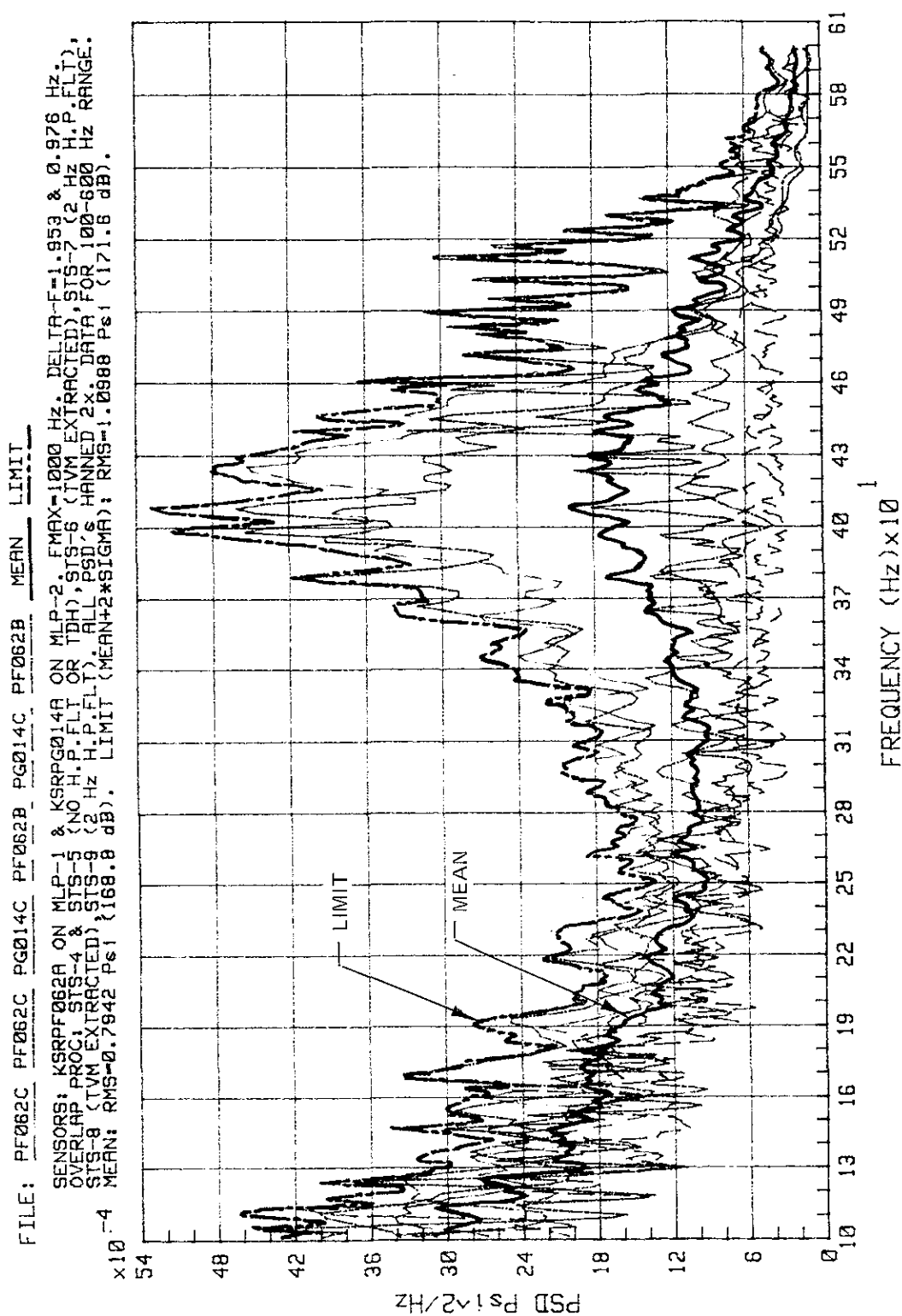


Figure 2-142. STS-4 Through -9 MLP-1 and MLP-2 Pressures on B Level
 Between T-1 and G-13, 100 to 600 Hz

KSC-DD-818-TR

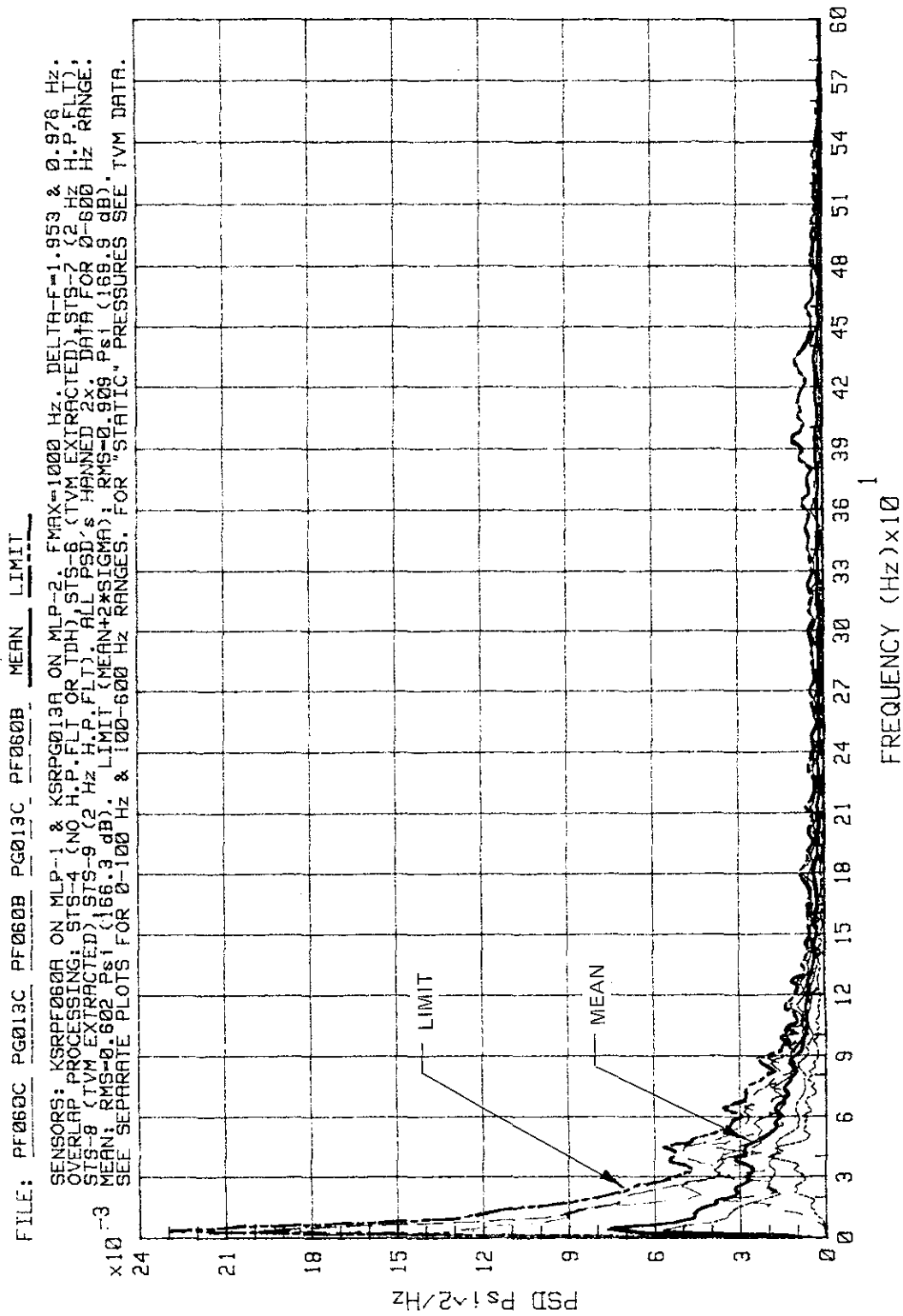


Figure 2-143. STS-4 and -6 Through -9 MLP-1 and MLP-2 Pressures on B Level
Between SRB Exhausts, Dynamic Part

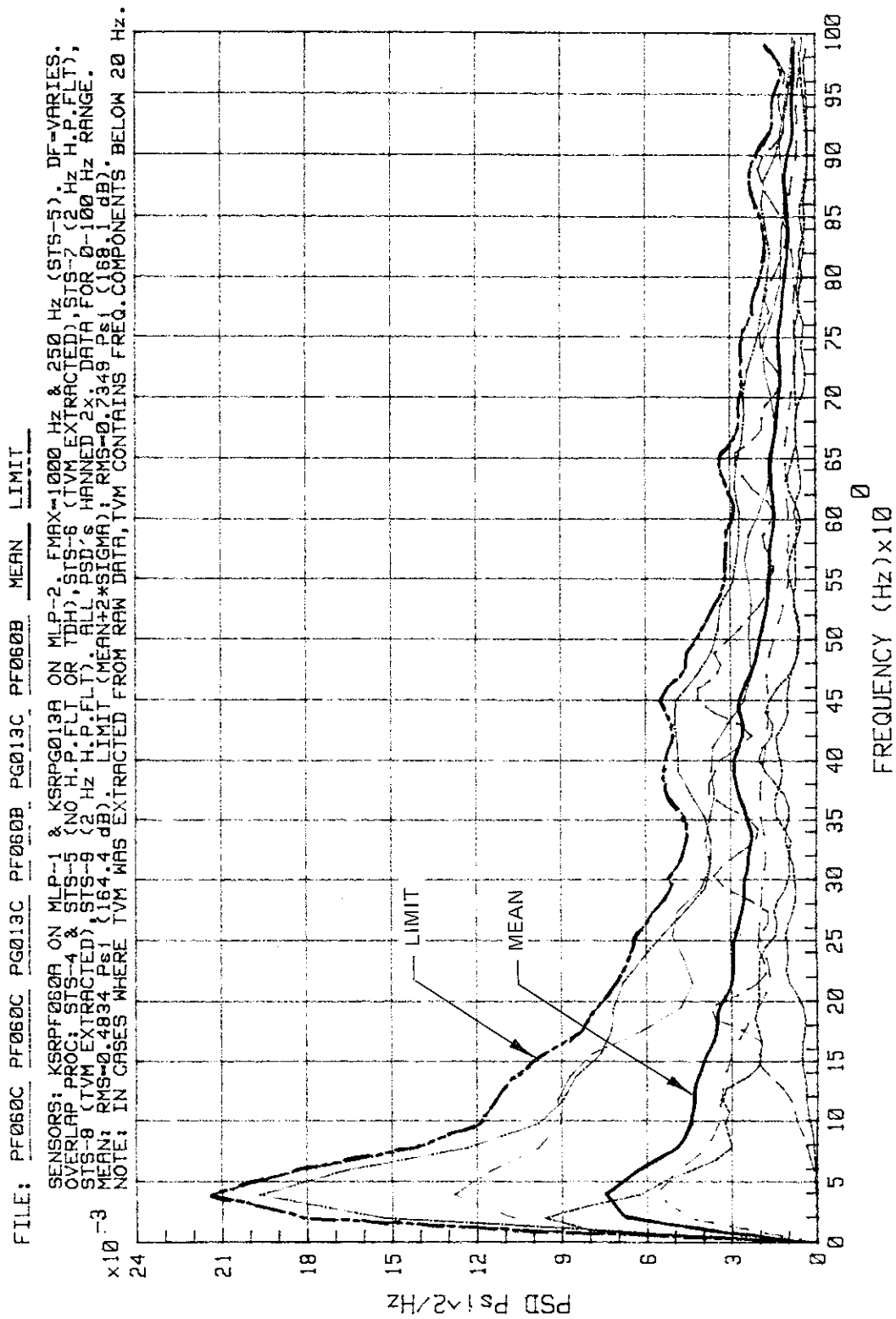


Figure 2-144. STS-4 Through -9 MLP-1 and MLP-2 Pressures on B Level Between SRB Exhausts, 0 Hz to 100 Hz

KSC-DD-818-TR

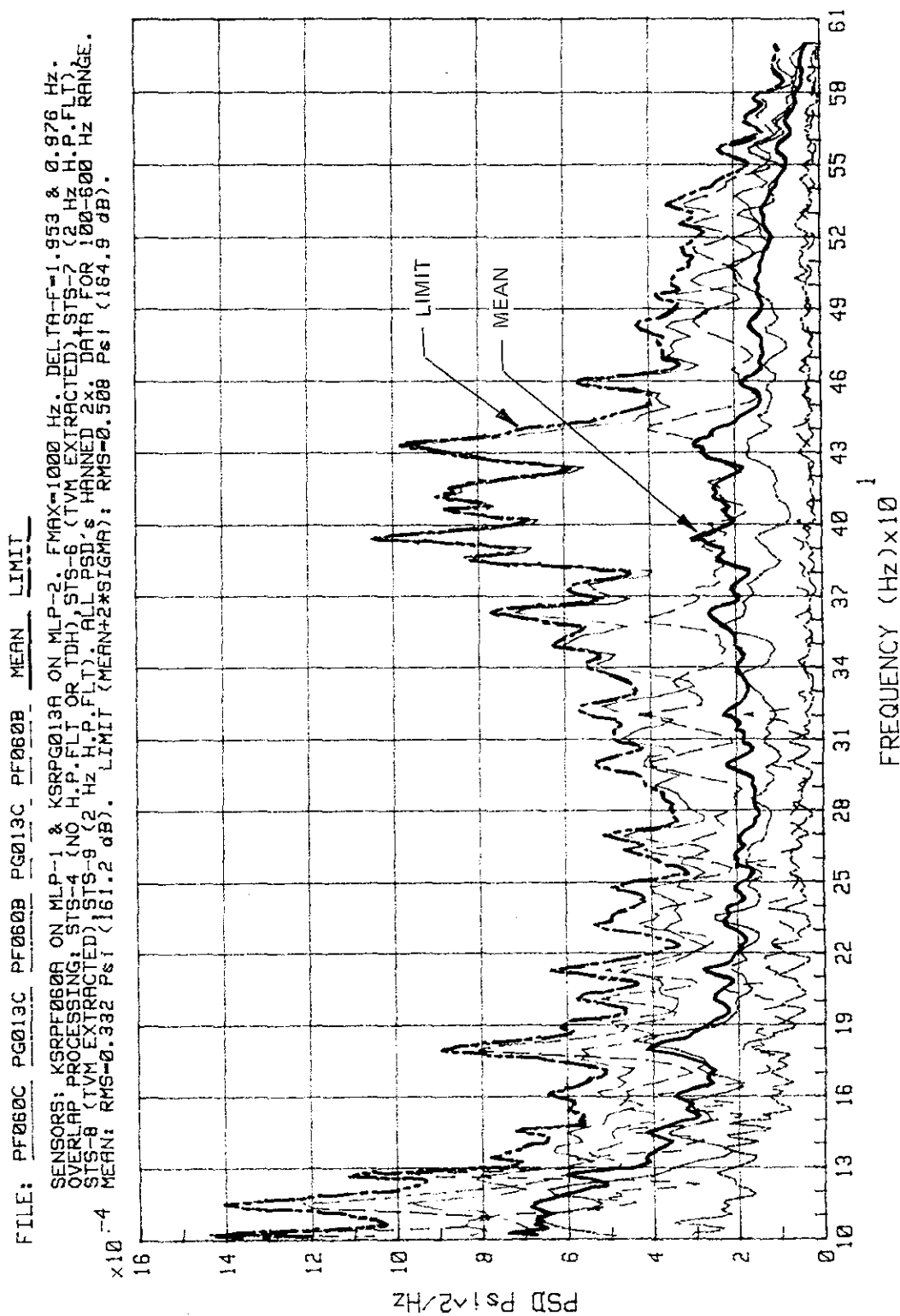


Figure 2-145. STS-4 and -6 Through -9 MLP-1 and MLP-2 Pressures on B Level
Between SRB Exhausts, 100 Hz to 600 Hz

2.8 WEST SIDE DEFLECTOR PRESSURES

This summary of pressures on the west side deflector is based on data from sensors KRFPA006A, -07A, and -08A, recorded during the launch of STS-8 and STS-9.

Figures 2-146 and 2-147 present raw data time histories for a short interval ($T + 0.15$ s to $T + 0.35$ s) when the highest pressure pulses occur. Figures 2-148 through 2-150 compare outputs of the same sensors for two launches. Of interest are the highest pressure peaks on these figures. All three sensors recorded these peaks for STS-9, while only KFDPA008A recorded such a peak for STS-8. The timing of these peaks (KFDPA006A with 27 psi at $T + 0.269$ s, KFDPA007A with 100 psi at $T + 0.272$ s, and KFDPA008A with 106 psi at $T + 0.293$ s) indicates their propagation to occur from the middle of the side deflector downward with a velocity that is substantially less than the speed of sound. Thus, the source of these peaks is the main SRB plume at ignition and not the deflected plume, as supposed.

Figure 2-151 presents a summary of slow varying "static" pressures for time interval $T + 0.5$ s to $T + 5.6$ s. At each sensor location, these pressures are repeatable between launches. A high pressure gradient exists along the height of the deflector from $T + 0.5$ s until $T + 3.5$ s, with increasing pressures toward the base of the deflector.

The summary of dynamic pressures is shown on figure 2-152 in terms of PSD's. A 2-Hz high-pass filter was used to separate dynamic components from the static components shown on figure 2-151. PSD's show a similar dispersion along the height of the deflector as do the slow varying pressure components. Highest dynamic pressures occur at the base of the deflector.

KSC-DD-818-TR

FILE: PAR06I PAR07I PAR08I

SAMPLING RATE 2 KHZ. A-A FILTER @ 500 HZ. NO HANNING. T-ZERO=242:06:32:00.027 GMT (1983)
 CURVE 1: KFDPA006A, ABOVE MIDDLE OF DEFLECTOR. PRESSURES ARE LOWEST.
 CURVE 2: KFDPA007A, BELOW MIDDLE OF DEFLECTOR. PRESSURES ARE HIGHEST.
 CURVE 3: KFDPA008A, AT THE BOTTOM OF DEFLECTOR. PRESSURES ARE HIGHEST.
 TIME SCALE OF THE PLOT IS REFERENCED TO T-ZERO.

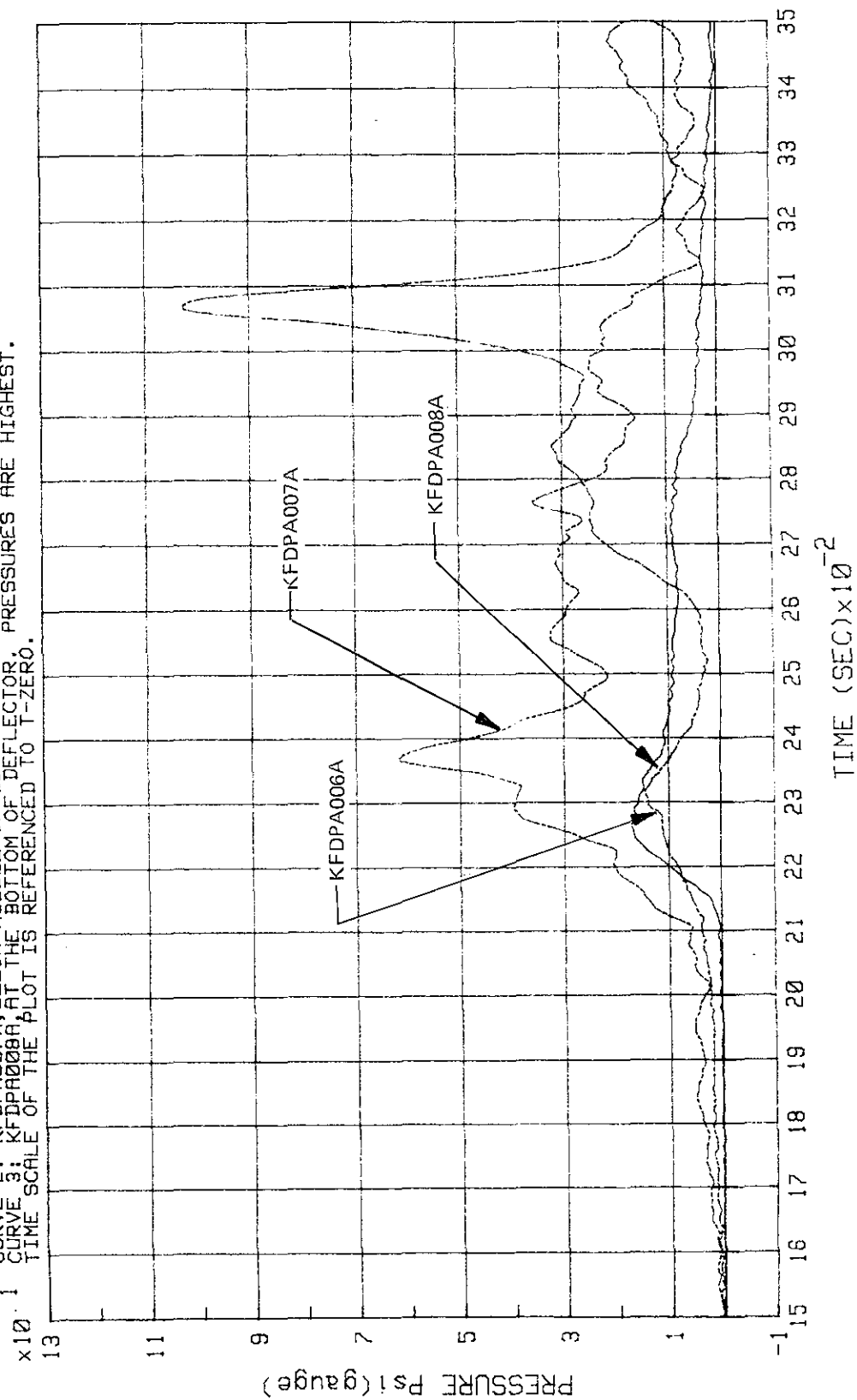


Figure 2-146. STS-8 SRB Ignition -
 West Side Deflector Pressures, T + 0.15 s to T + 0.35 s

FILE: PAR061 PAR071 PAR081

SAMPLING RATE 2 KHz. A-A FILTER @ 500 Hz. NO HUNNING. T-ZERO-332:16:00:00.010 GMT (1983).
 CURVE 1: KFDPA006A, ABOVE MIDDLE OF DEFLECTOR. PRESSURES ARE LOWEST.
 CURVE 2: KFDPA007A, BELOW MIDDLE OF DEFLECTOR.
 CURVE 3: KFDPA008A, AT THE BOTTOM OF DEFLECTOR. PRESSURES ARE HIGHEST.
 TIME SCALE OF THE PLOT IS REFERENCED TO T-ZERO.

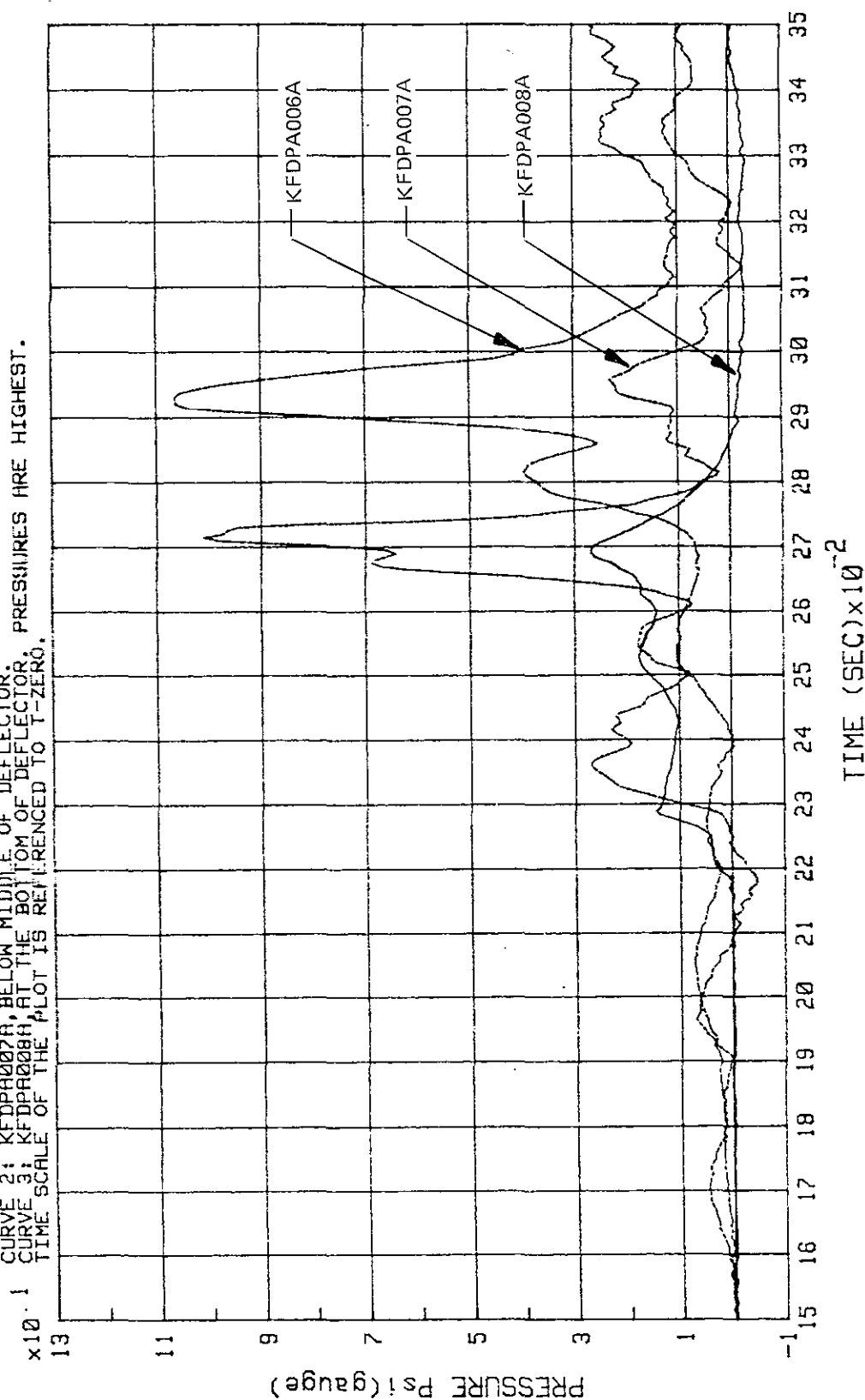


Figure 2-147. STS-9 SKB Ignition -
 West Side Deflector Pressures, T + 0.15 s to T + 0.35 s

KSC-DD-818-TR

FILE: PAR061 PAR061

SAMPLING RATE 2 KHz, A-A FILTER @ 500 Hz, NO HANNING. TIME SCALE REFERENCED TO T-ZERO.
 SENSOR KFDPA006A, ABOVE MIDDLE OF DEFLECTOR. SOLID LINE IS STS-8 MEASUREMENT.

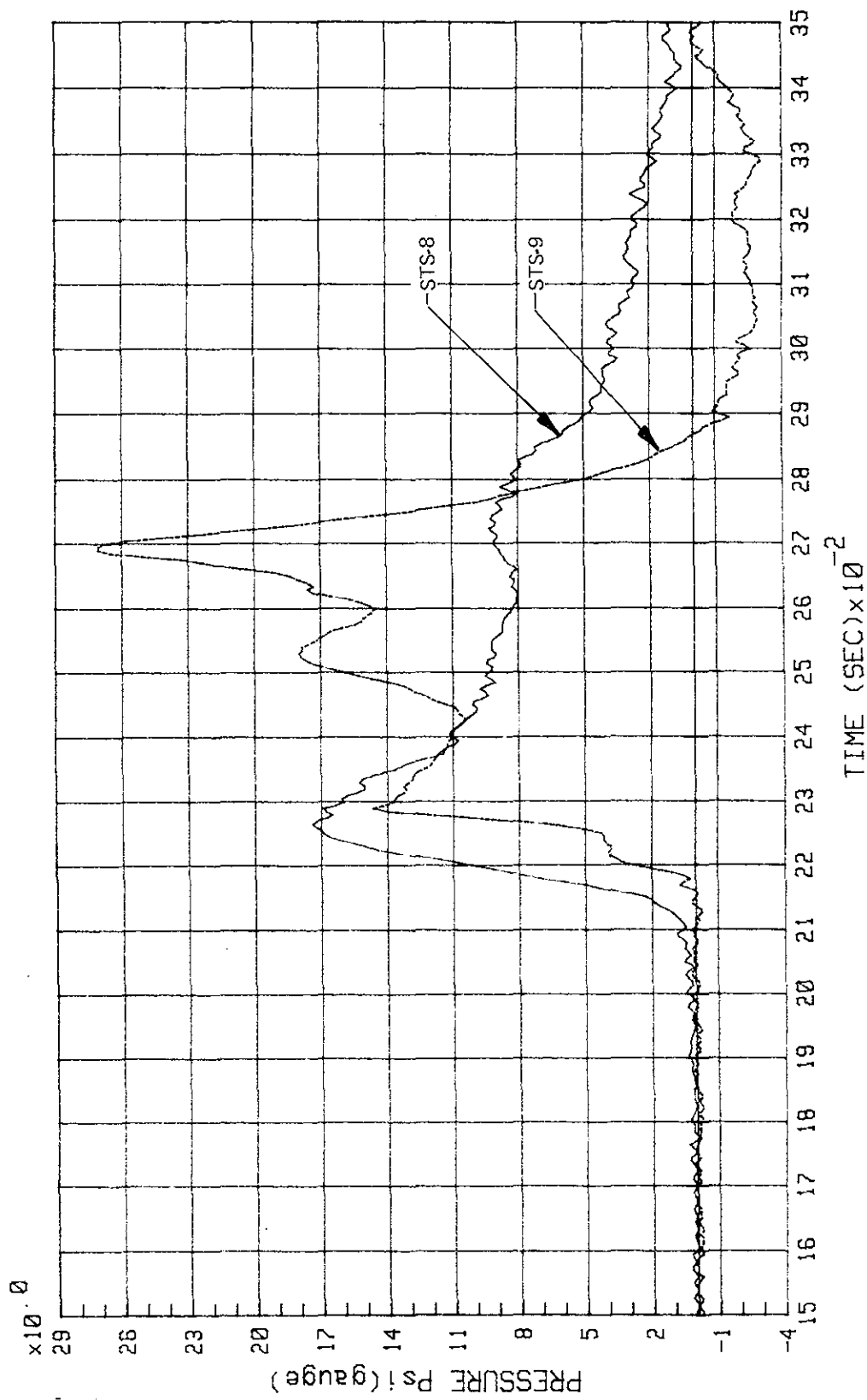


Figure 2-148. STS-8 and -9 SRB Ignition - West Side Deflector Pressures,
 T + 0.15 s to T + 0.35 s, Sensor KFDPA006A

FILE: PAR07I PAR07I

SAMPLING RATE 2 KHZ. A-A FILTER @ 500 HZ. NO HANNING. TIME SCALE REFERENCED TO T-ZERO.
SENSOR KFDPA007A, BELOW MIDDLE OF DEFLECTOR. SOLID LINE IS STS-8 MEASUREMENT.

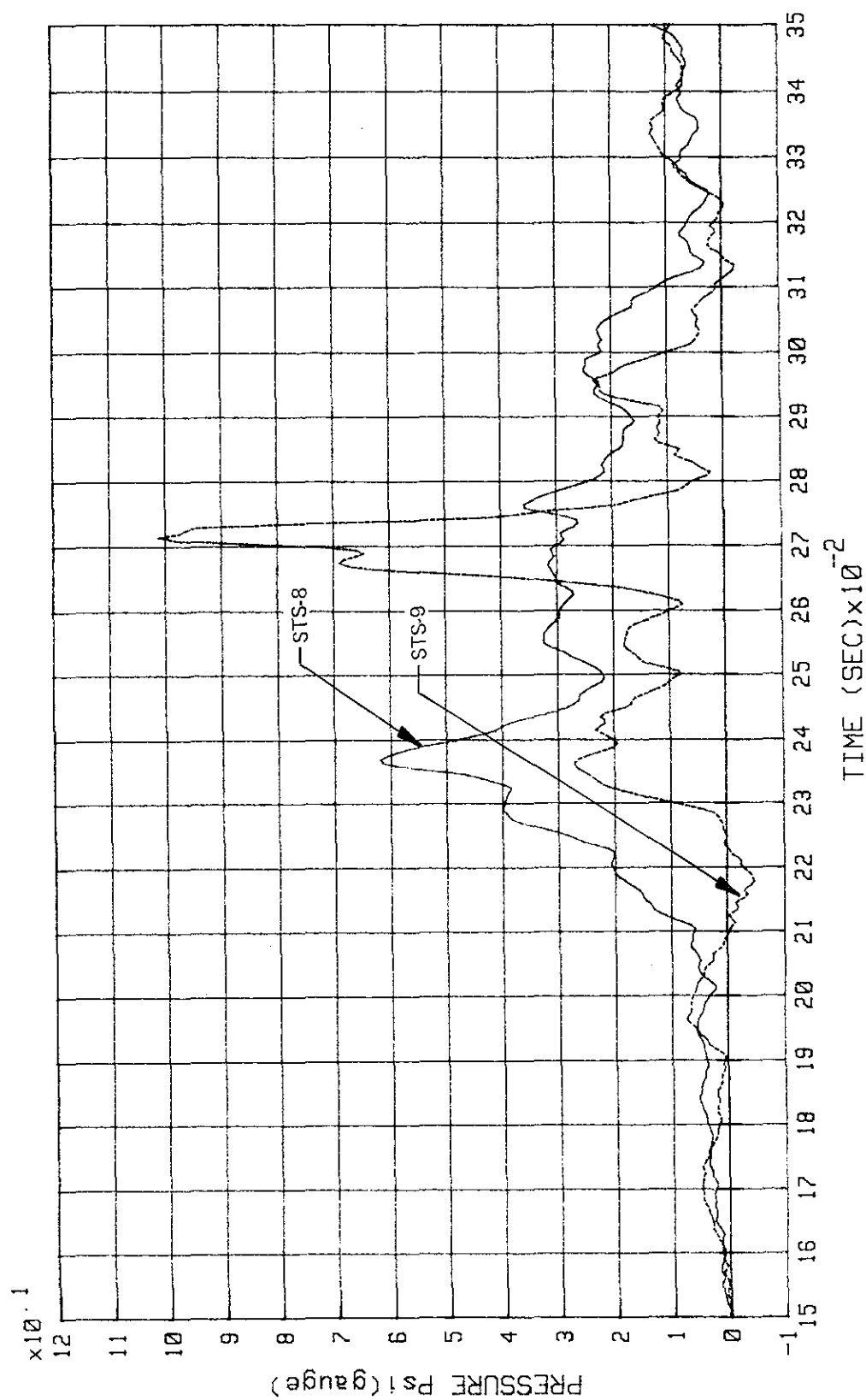


Figure 2-149. STS-8 and -9 SRB Ignition - West Side Deflector Pressures,
T + 0.15 s to T + 0.35 s, Sensor KFDPA007A

FILE: PAR001 PAR001

SAMPLING RATE 2 KHz. A-A FILTER @ 500 Hz. NO HANNING. TIME SCALE REFERENCED TO T-ZERO.
SENSOR KFDPA008A, AT THE BOTTOM OF DEFLECTOR. SOLID LINE IS STS-8 MEASUREMENT.

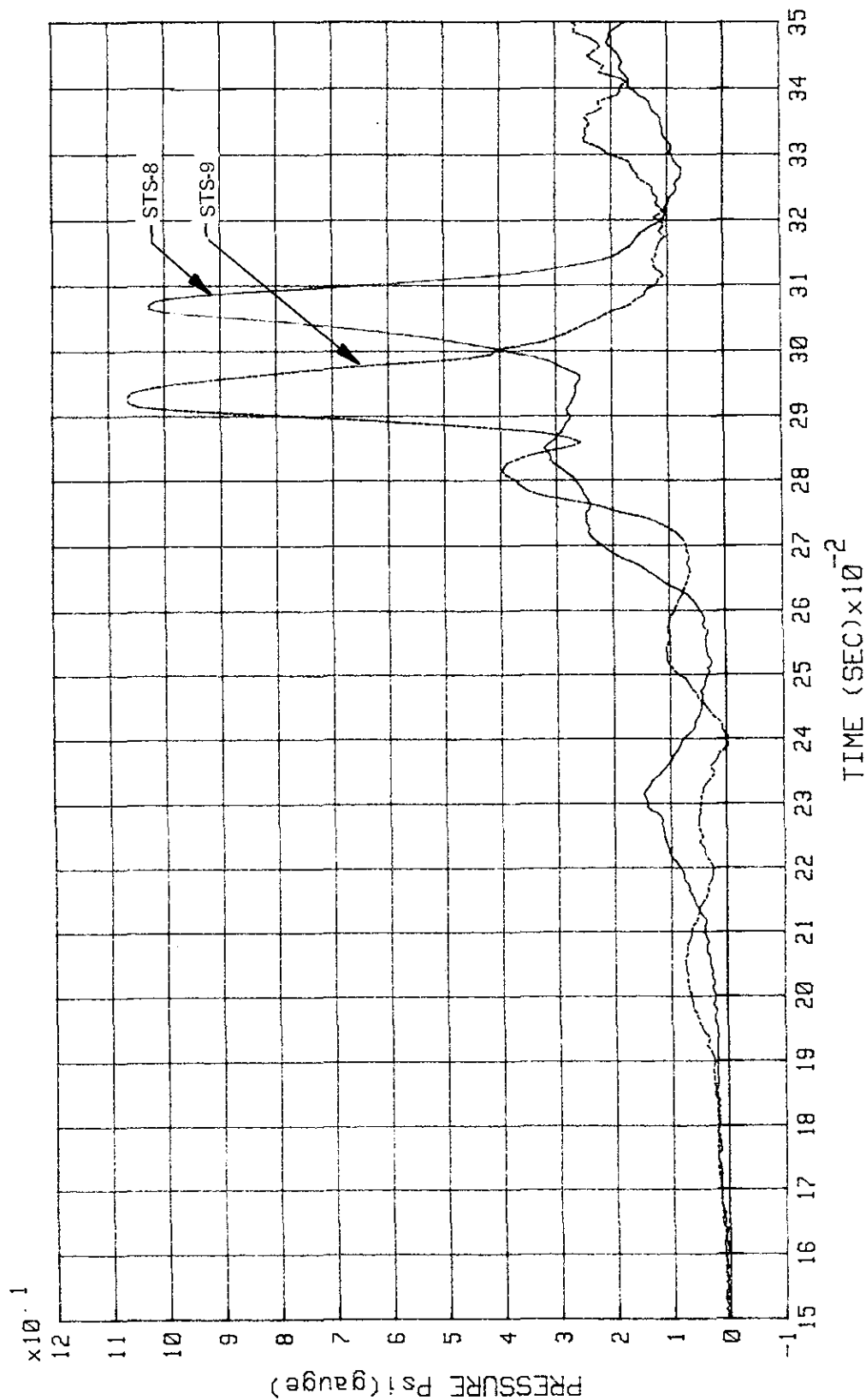


Figure 2-150. STS-8 and -9 SRB Ignition - West Side Deflector Pressures,
T + 0.15 s to T + 0.35 s, Sensor KFDPA008A

FILE: PAR06L PAR07L PAR08L PAR06L PAR07L PAR08L

SAMPLING RATE 200 Hz. A-A FILTER @ 50 Hz. HANNED 30x. TIME SCALE REFERENCED TO T-ZERO.

CURVES 1 & 4: KFDPA006A, ABOVE MIDDLE OF DEFLECTOR. PRESSURES ARE LOWEST.

CURVES 2 & 5: KFDPA007A, BELOW MIDDLE OF DEFLECTOR.

CURVES 3 & 6: KFDPA008A, AT THE BOTTOM OF DEFLECTOR. PRESSURES ARE HIGHEST.

CURVES 1, 2 & 3 ARE STS-8 MEASUREMENTS. EACH SENSOR RECORDED REPEATABLE DATA FOR TWO LAUNCHES.

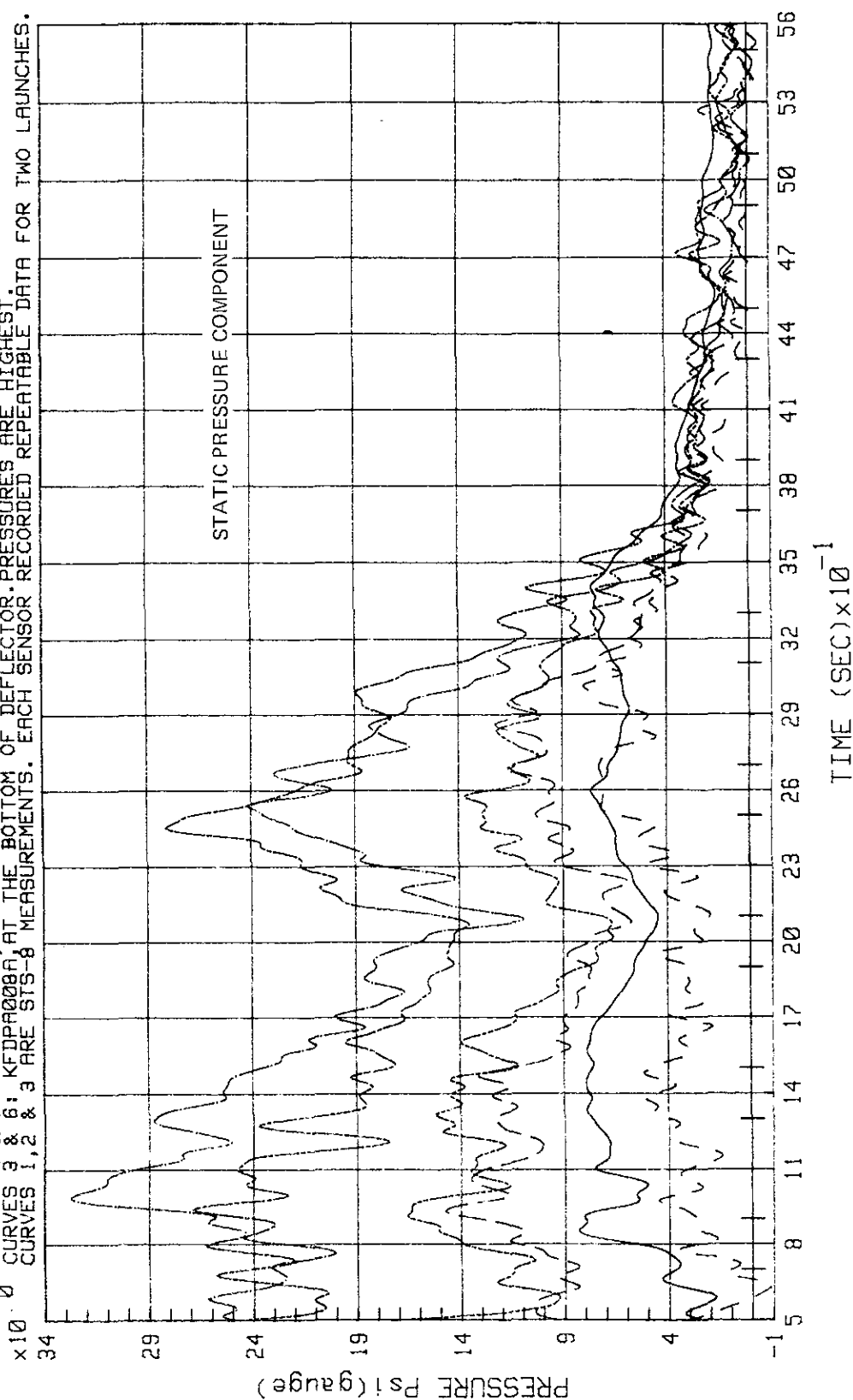


Figure 2-151. STS-8 and - 9 Lift-Off - West Side Deflector Pressures,
T + 0.5 s to T + 5.6 s

KFD#: PA006C PA007C PA008C PA006B PA007B PA008B PA003B PA007B PA008B MEAN LIMIT

FMAX=1000 Hz. DELTA-F=1.953 Hz. H.P. FILTER @ 2 Hz. A-A FILTER @ 500 Hz. PSD'S HANNED 2x.
 SENSORS: KFDPA006A, -007A & -008A. OVERLAP PROCESSING FROM T+0.5 TO T+8.1 SEC(STS-7), TO T+4.1
 SEC(STS-8) & TO T+4.6 SEC(STS-9). 18 DOF MEAN & LIMIT-MEAN+2*SIGMA PSD'S.
 MEAN: RMS=4.036 PSI, ORSPL(X)=182.9 dB. LIMIT: RMS=6.686 PSI, ORSPL(X+2S)=187.3 dB, 0-100 Hz.
 NOTE: FOR "STATIC" PRESSURE COMPONENTS SEE TIME DOMAIN PLOT FROM T+0.5 TO T+5.6 SEC.

$\times 10^{-2}$

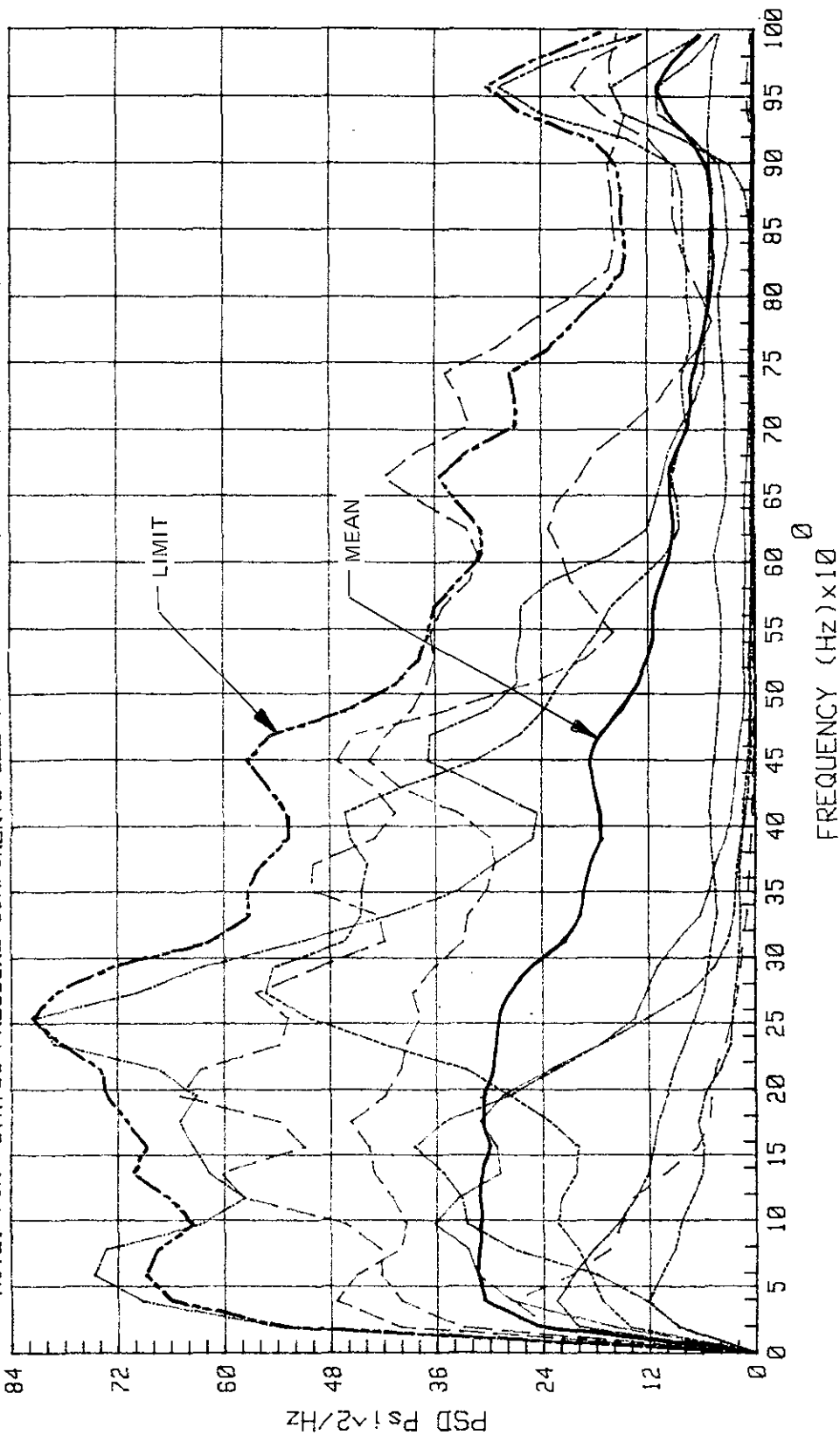


Figure 2-152. STS-7, -8, and -9 Lift-Off Peak -
 West Side Deflector Pressures, Dynamic Part

2.9 MLP INTERIOR ACOUSTICS

The summary of MLP (1 and 2) interior acoustics includes STS-4 through STS-11 measurements. All measured acoustic pressures are substantially below predicted OBSPL's. This summary includes only pressure PSD's; because presentation in terms of OBSPL's does not provide necessary resolution, while pressure PSD's contain distinct, repeatable narrow band peaks.

Figures 2-153 through 2-157 contain acoustic pressure summaries for rooms on A and B levels. The right frame on these figures presents separate plots of mean and limit (limit = mean + 2 sigma) curves. Processing parameters and other pertinent information are contained on the plot headings.

Because of substantial dispersion of acoustic pressures between different MLP rooms and rather low, noncritical acoustic levels in these room, all available measurements were lumped together. Figures 2-158 through 2-161 provide corresponding plots in high-resolution scales. Since the 2-sigma limit curve is below two to three actual measurements, the summary curves on figure 2-162 present both 2- and 3-sigma limits. The dispersion between mean and 3-sigma limit of all MLP measurements is 6.9 dB, and 3-sigma limit OASPL = 147.2 dB, substantially below all predictions which were in the range from 150dB to 164 dB. Figures 2-163 through 2-165 present OBSPL's from STS-1 through STS-4 compared with predictions. For application, curves on figure 2-162 are recommended.

KSC-DD-818-TR

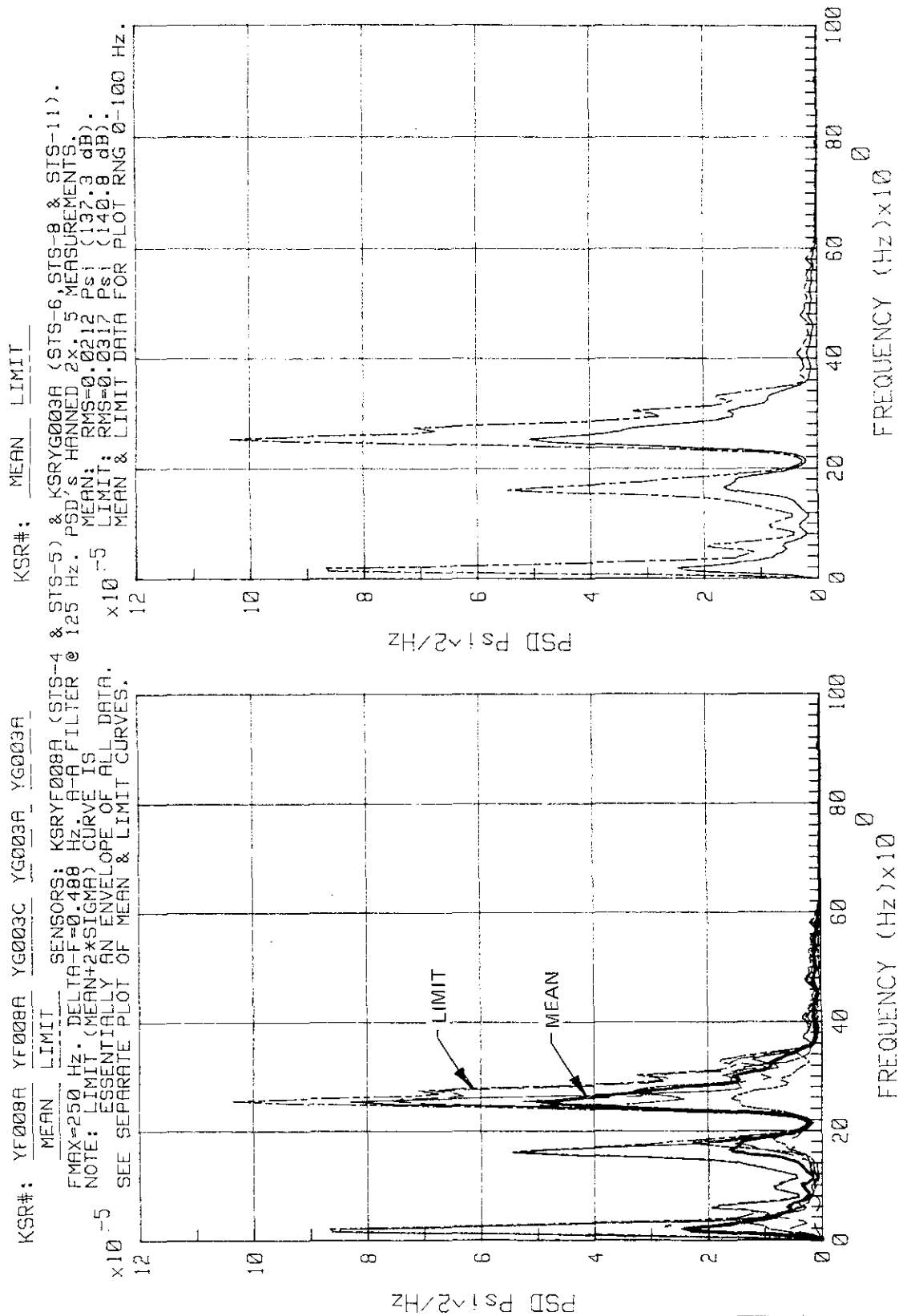


Figure 2-153. Lift-Off Peak - Summary of MLP Interior Acoustics, Room 15A

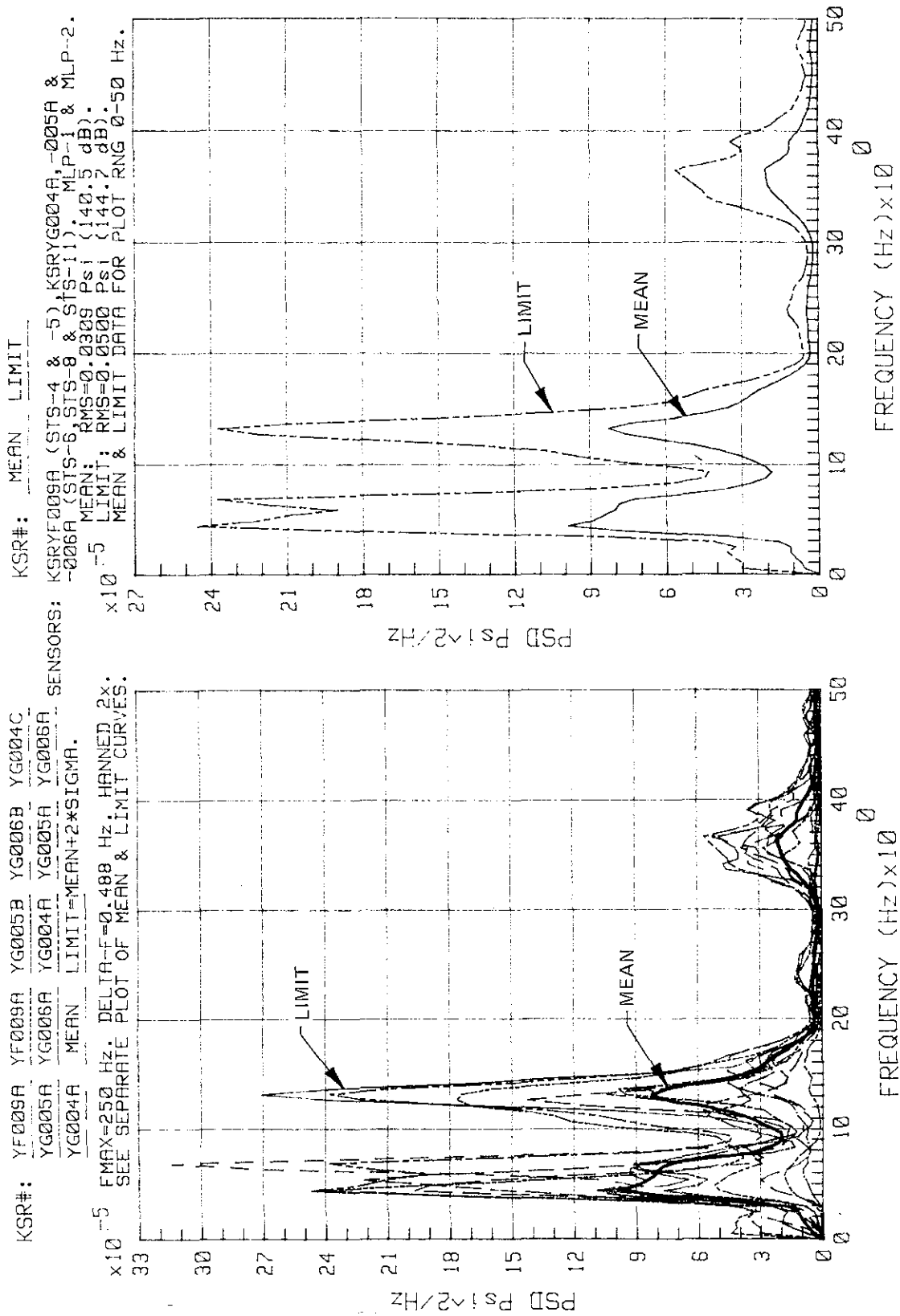


Figure 2-154. Lift-Off Peak - Summary of MLP Interior Acoustics, Rooms 7A, 8A, and 10A

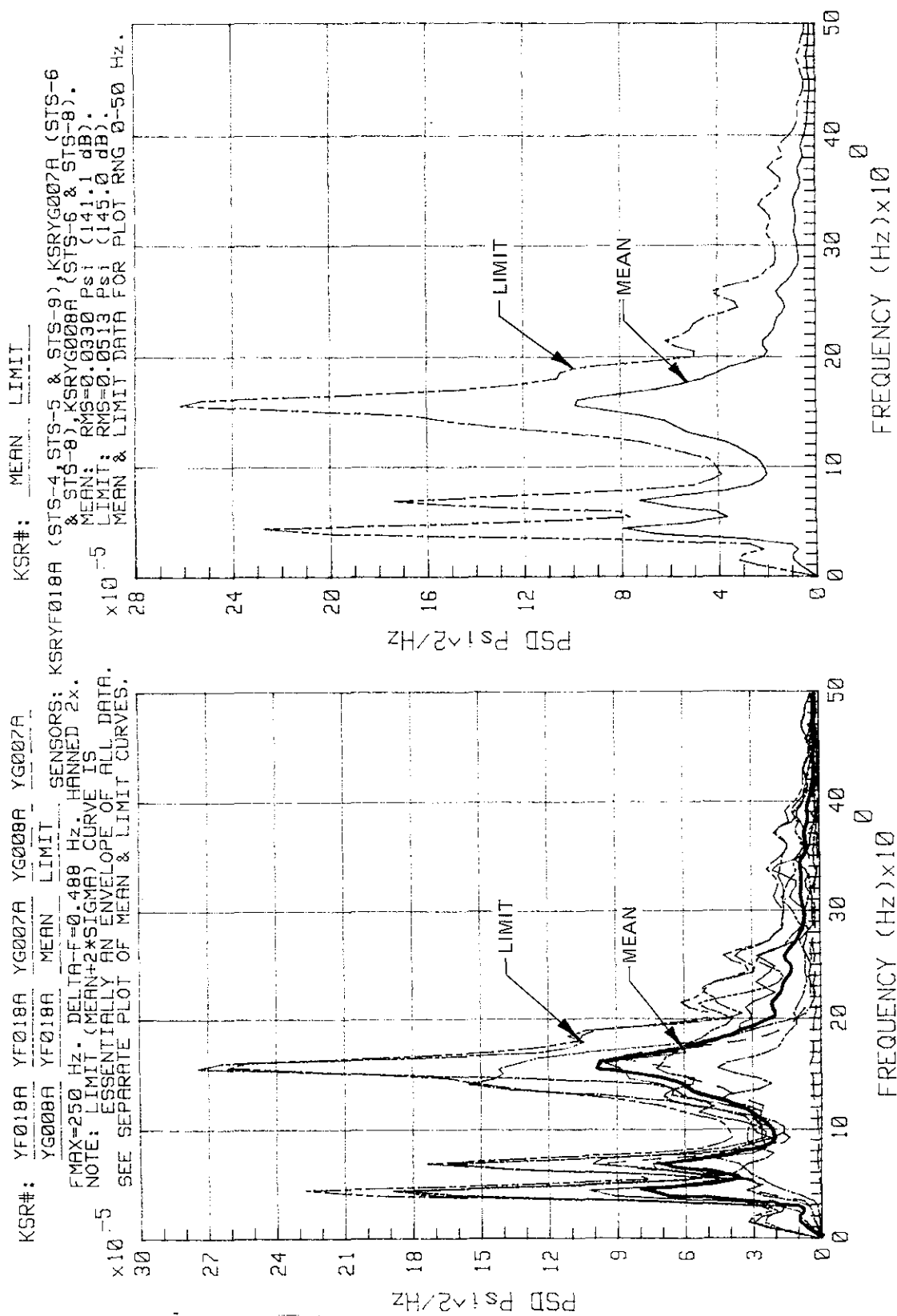


Figure 2-155. Lift-Off Peak - Summary of MLP Interior Acoustics, Rooms 8B and 9B

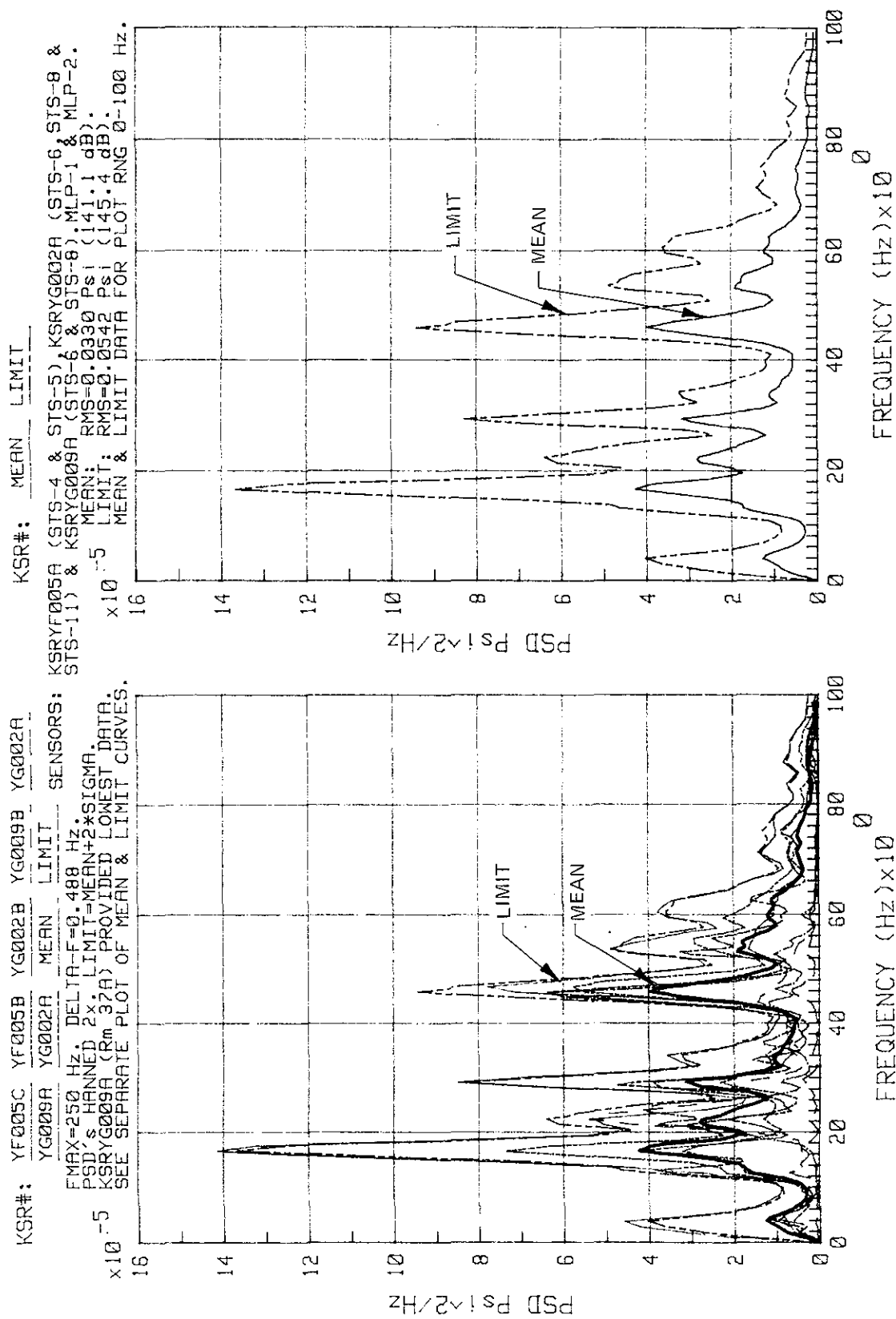


Figure 2-156. Lift-Off Peak - Summary of MLP Interior Acoustics, Rooms 36AB and 37A

KSC-DD-818-TR

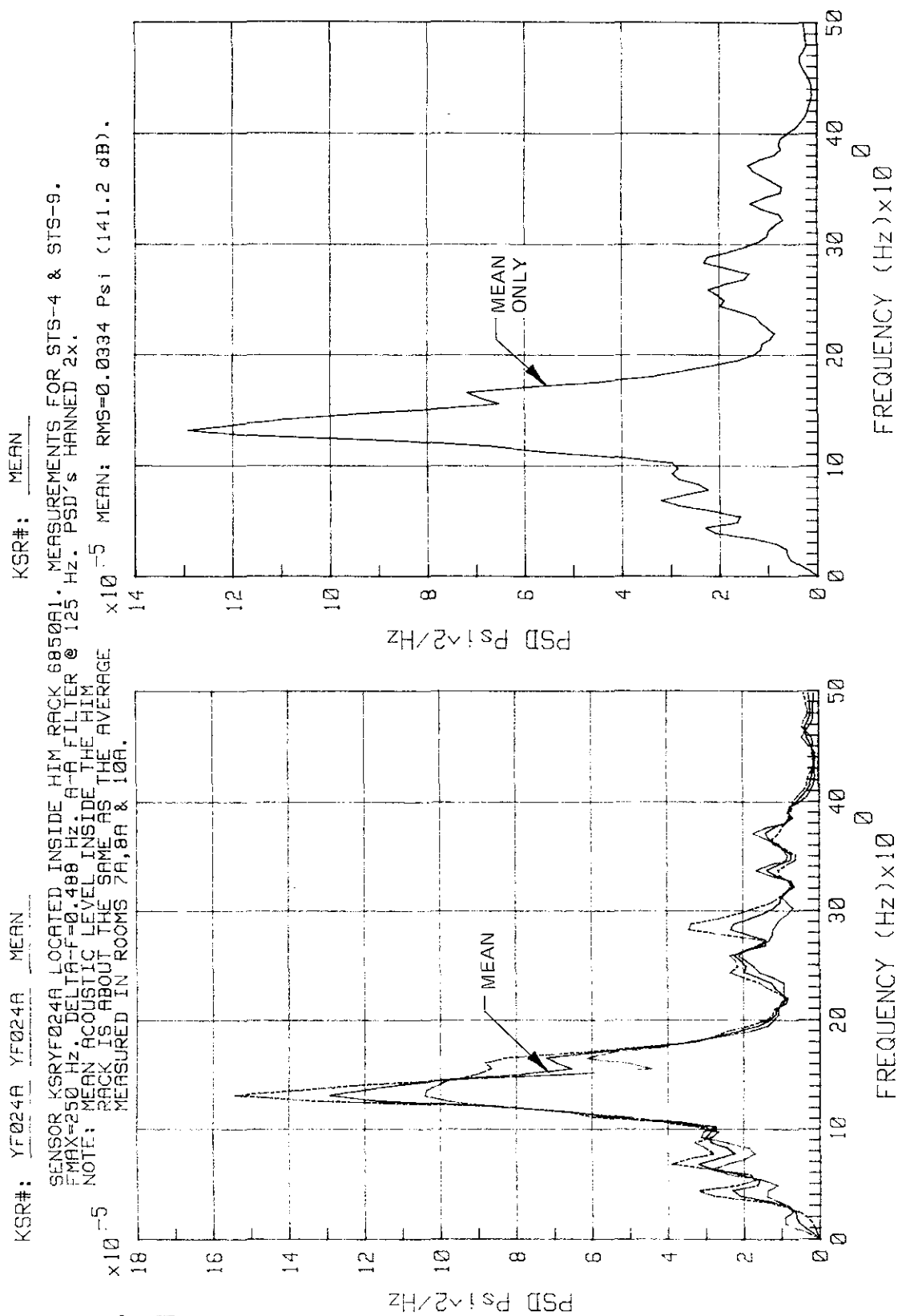


Figure 2-157. Lift-off Peak - Summary of MLP Interior Acoustics, Room 7A

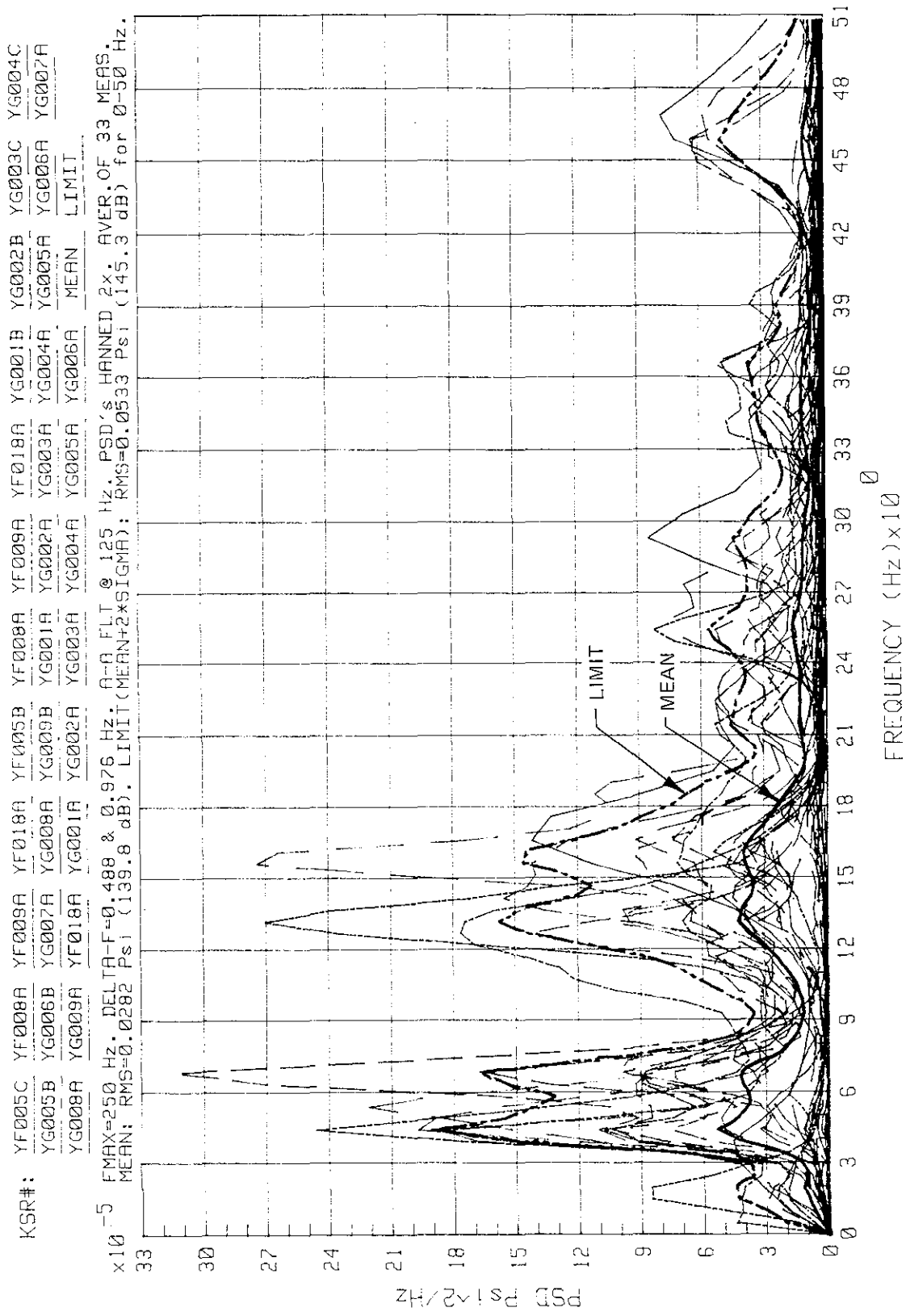


Figure 2-158. STS-4 Through -11 Lift-Off Peak - Summary of MLP Interior Acoustics, PSD's (0 Hz to 51 Hz)

KSC-DD-818-TR

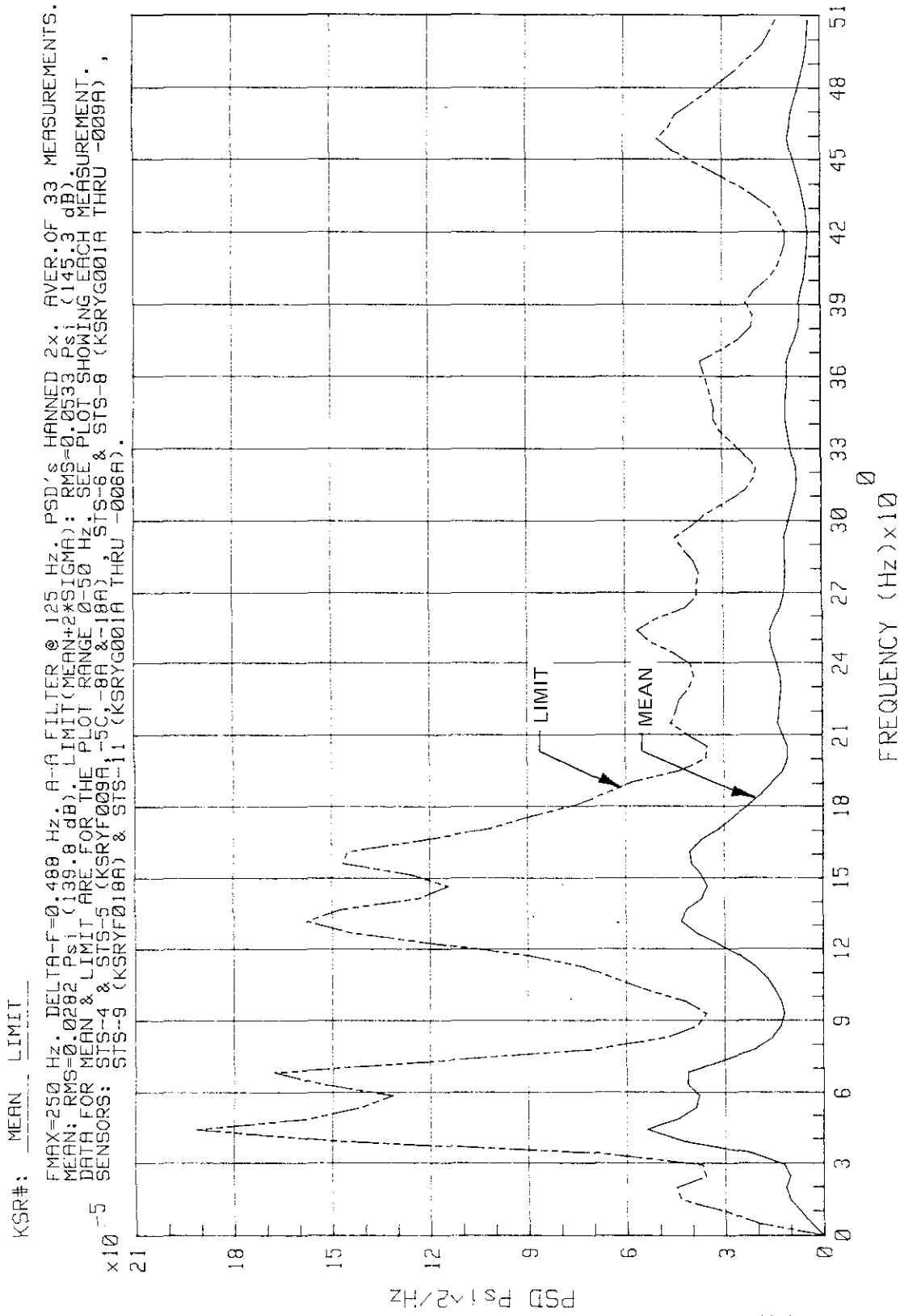


Figure 2-159. STS-4 Through -11 Lift-Off Peak - Summary of MLP Interior Acoustics,
 PSD's (Mean and Limit Only; 0 Hz to 51 Hz)

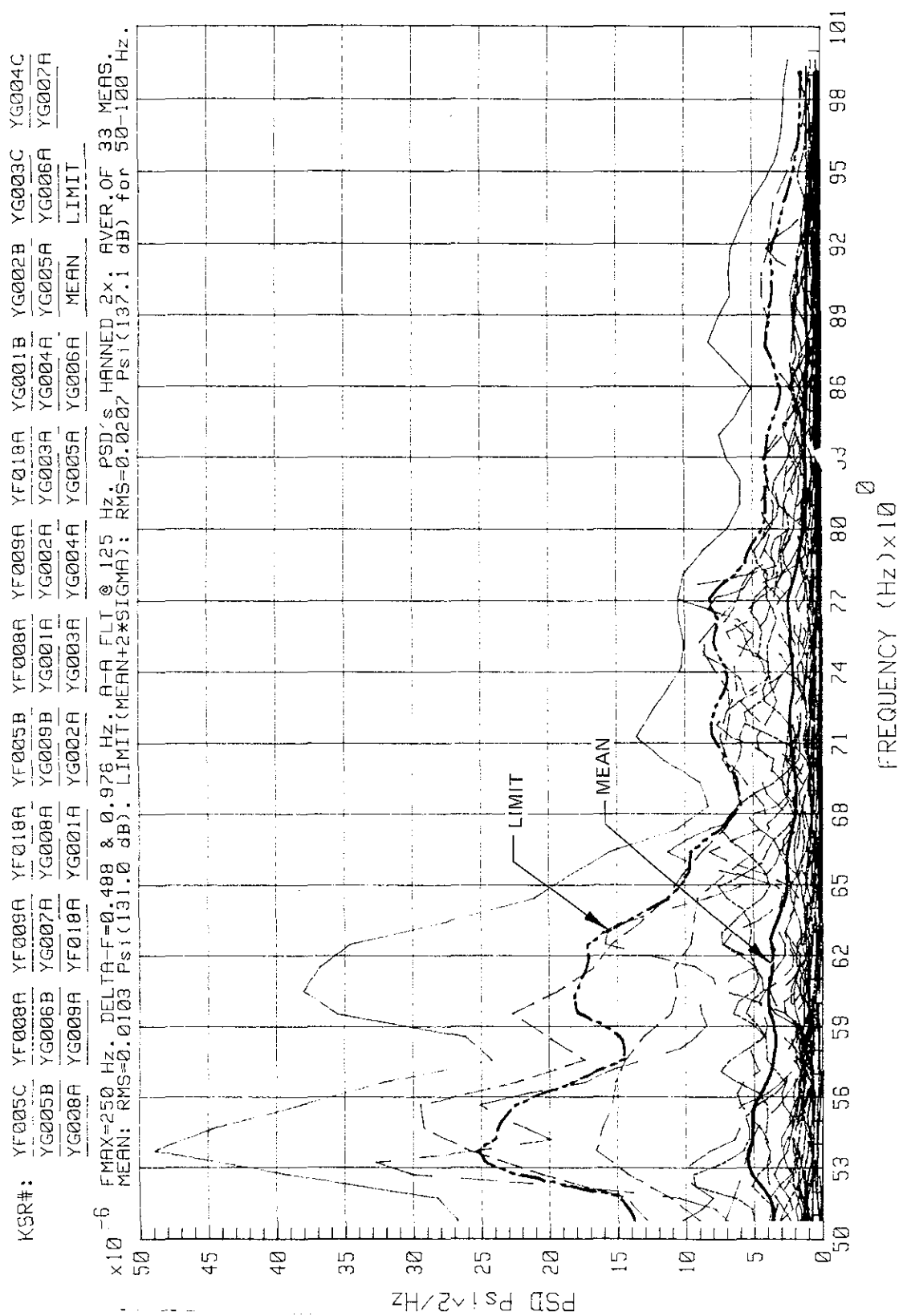


Figure 2-160. STS-4 Through -11 Lift-Off Peak - Summary of MLP Interior Acoustics, PSD's (50 Hz to 100 Hz)

KSC-DD-818-TR

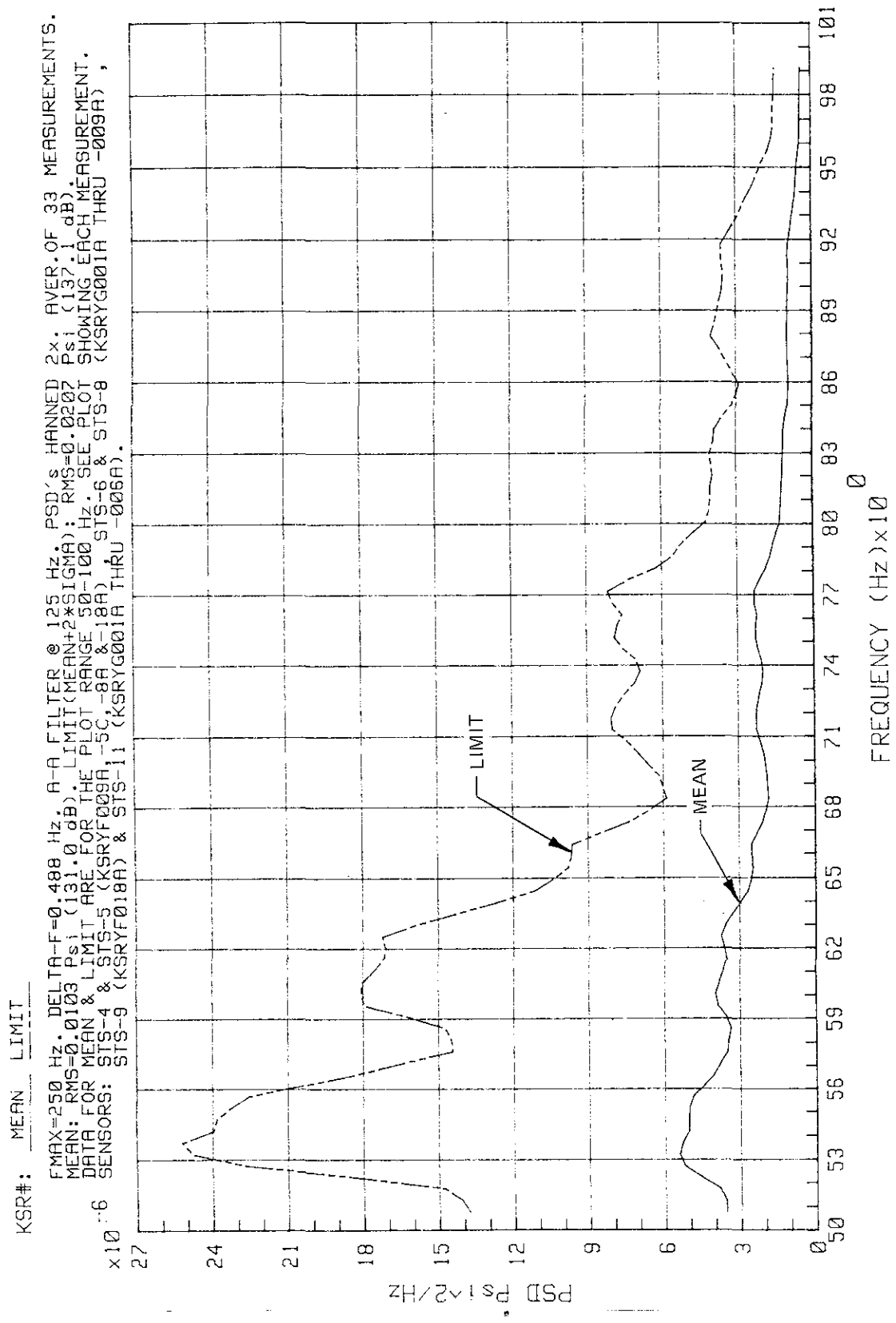


Figure 2-161. STS-4 Through -11 Lift-Off Peak - Summary of MLP Interior Acoustics, PSD's, Mean and Limit Only (50 Hz to 100 Hz)

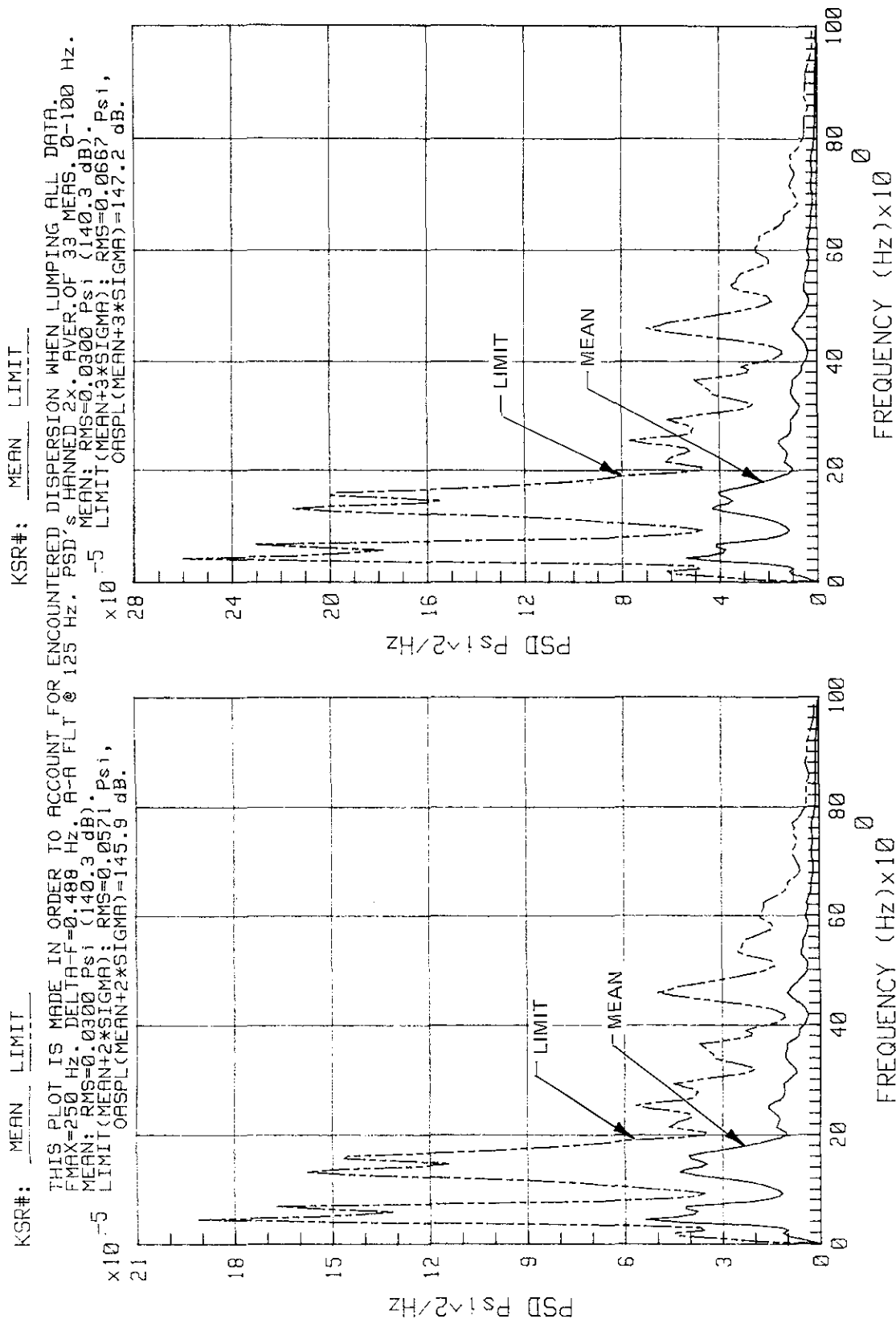
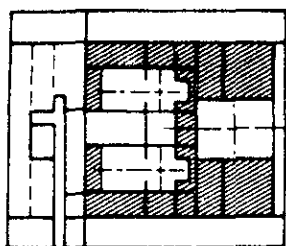


Figure 2-162. STS-4 Through -11 Lift-Off Peak - Summary of MLP Interior Acoustics,
 2- and 3-Sigma Limits

KSC-DD-818-TR



DECKS A & B

ACOUSTICAL SPECIFICATION
 ZONE 1.2 AND 1.3
 LIFT-OFF PEAK
 MOBILE LAUNCHER PLATFORM COMPARTMENTS
 AROUND EXHAUST WELLS

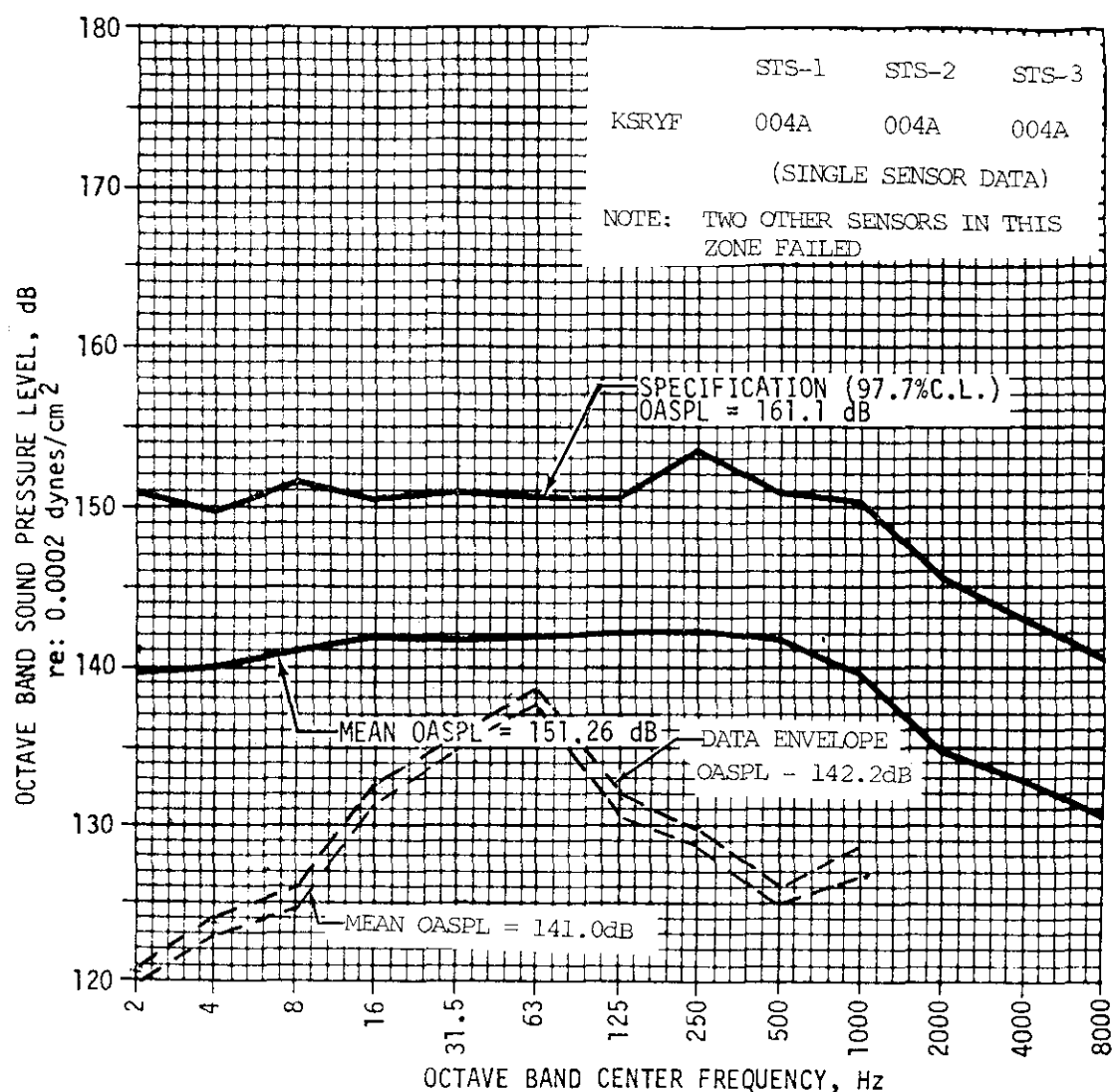
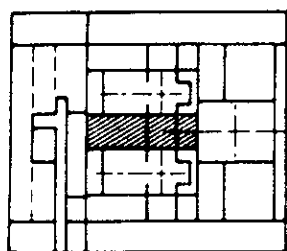


Figure 2-163. Lift-Off Peak - Actual OBSPL's Compared With Predictions,
 MLP Compartments Around Exhaust Wells



DECKS A & B

ACOUSTICAL SPECIFICATION
 ZONE 1.2 AND 1.3
 LIFT-OFF PEAK
 MOBILE LAUNCHER PLATFORM COMPARTMENTS 36AB,
 37A AND 37B

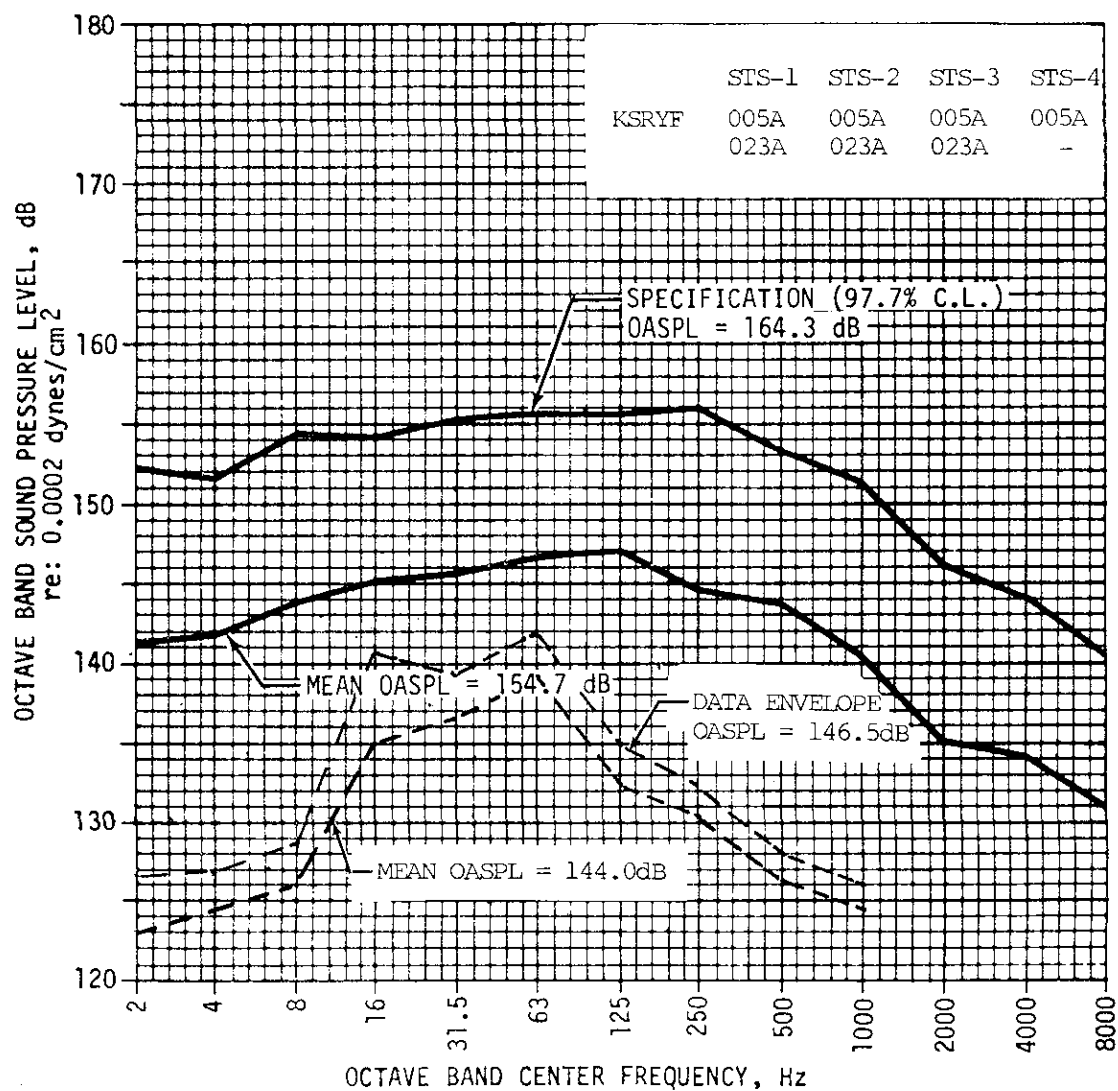
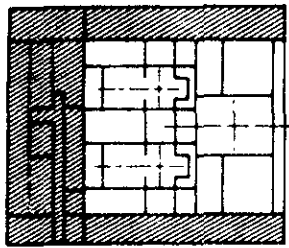


Figure 2-164. Lift-Off Peak - Actual OBSPL's Compared With Predictions,
 MLP Compartments 36AB, 37A, and 37B

KSC-DD-818-TR



DECKS A & B

ACOUSTICAL SPECIFICATION
 ZONE 1.2, 1.3, 2.2 AND 2.3
 LIFT-OFF PEAK
 MOBILE LAUNCHER PLATFORM COMPARTMENTS
 EXCEPT VICINITY OF EXHAUST WELLS

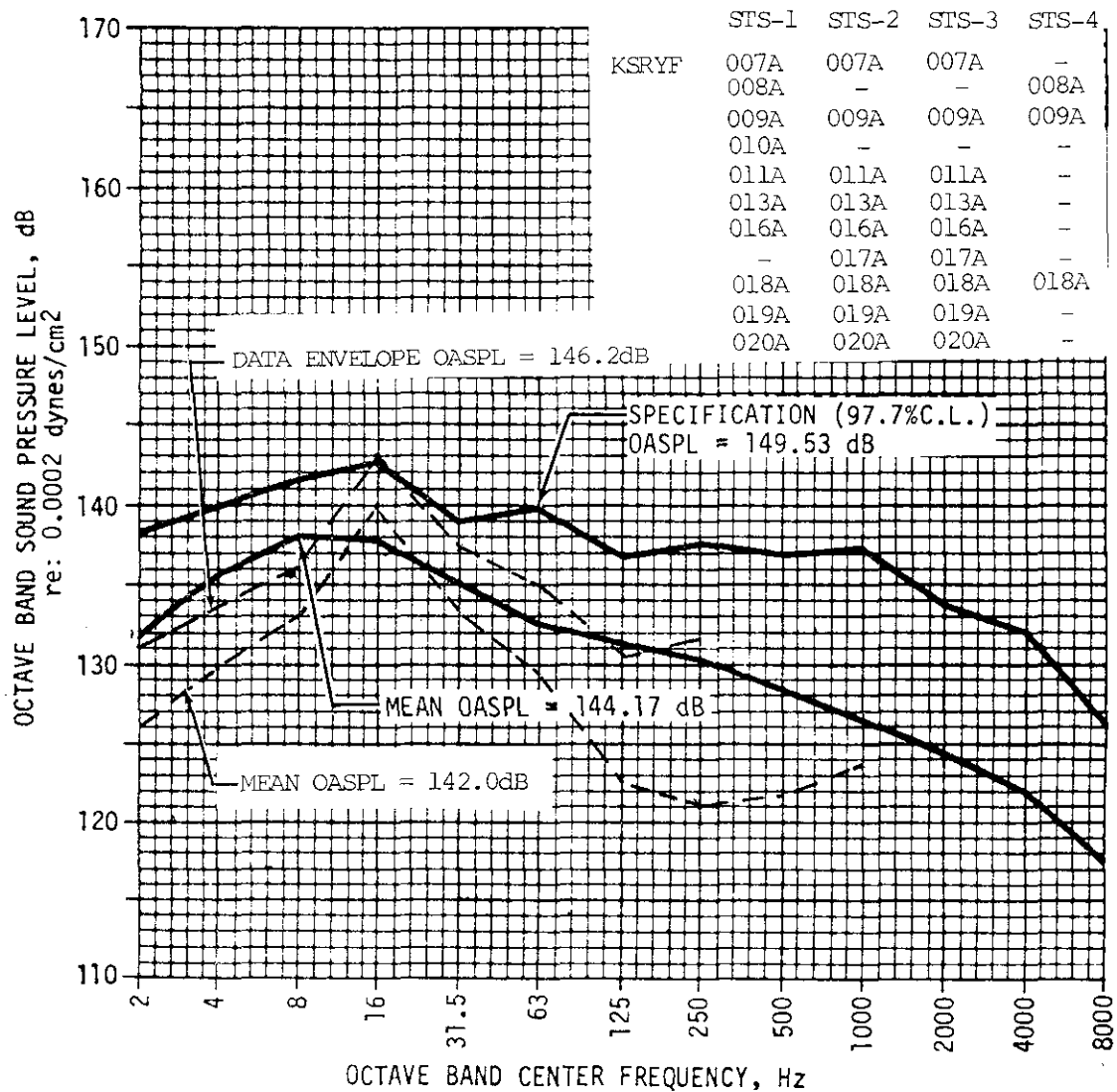


Figure 2-165. Lift-Off Peak - Actual OBSPL's Compared With Predictions, MLP Compartments Except Vicinity of Exhaust Wells

SECTION III

STRAINS

3.1 SRB HOLDDOWN POST (HDP) PEDESTAL STRAINS ON MLP (STS-6 THROUGH -9)

This summary presents results of strain measurements on the HDP pedestals. Previous publications include similar strain time histories for STS-1 through STS-8. Oscillatory strain components that occur between $T - 0.01$ s to $T + 0.3$ s are presented in terms of their PSD's, using STS-6 through STS-9 data after some of these components were related to dilatational waves generated within SRB's at ignition. The last part of this summary presents text previously published with STS-5 data (KSC-DD-688-TR) pertinent to pedestal loads before SRB ignition and to strain oscillations at SRB ignition.

Each SRB HDP pedestal was instrumented with two sets of strain gages, further designated as either type 1 or type 2. Each set consisted of eight strain gages, wired in a manner ensuring temperature compensation and recording of only axial load-induced strains while eliminating voltage output caused by the bending of the pedestal. Each set, further referred to as a strain gage, represents an uncalibrated load cell.

Figures 3-1 and 3-2 present raw strain time histories sampled at a 200-Hz rate for time interval $T - 4.6$ s to $T + 0.5$ s for STS-9. Each figure contains four time histories corresponding to either type 1 or type 2 gages on east pedestals (nos. 1, 2, 3, and 4) or on west pedestals (nos. 5, 6, 7, and 8). Similar and repeatable time histories were recorded during STS-1 through STS-8. Figure 3-3 presents time histories of type 1 gages sampled at a 5-kHz rate for a short time interval of 25 ms ($T - 0.15$ s to $T + 0.01$ s). This interval includes shocks generated by the activation of explosive bolts. Figure 3-4 presents the four (type 1 gage) time histories for time interval $T - 0.1$ s to $T + 0.31$ s, which show decay of pedestal loads at lift-off to no-load condition beginning at approximately $T + 0.28$ s.

Figures 3-5 through 3-8 present strain time histories from each gage shown on figure 3-4 and extracted TVM (see explanation in figure headings). The dynamic strain components, which are defined as the difference between raw strain data and TVM, were used in subsequent computations of PSD's from STS-6 through STS-9 measurements presented on figures 3-9 through 3-11. It should be noted that the effect of dynamic strain components on the HDP pedestals is insignificant. They may have a significance as dynamic loads on the vehicle, because these strains are a result of longitudinal oscillations of SRB's recorded at the interface between the SRB's and the MLP. High PSD peak, around 70 Hz, may be explained considering propagation of dilatational waves through SRB casings. Measured PSD's on pedestals under either the east SRB (figure 3-9) or the west SRB (figure 3-10) show relatively low dispersion; the limit curves

are essentially envelopes of all data. When both east and west pedestal measurements are combined (figure 3-11, sheets 1 and 2), the limit (mean + 2 sigma) curve is exceeded by two to three measurements. Therefore, a new limit (mean + 3 sigma) curve is calculated and presented on figure 3-11 (sheet 3). Included in this section is the text portion of appendix B of KSC-DD-688-TR, which discusses a method of calibrating strain gage outputs to represent dynamic loads. The appendix B text contains assumptions about the distribution of dead load on HDP pedestals critical for the calculation of calibration factors to convert recorded strains into loads. Peak load estimates from measured strains cannot be improved without knowledge of actual dead load on each pedestal. If Orbiter weight eccentricity with respect to HDP pedestals were used, it would result in a nonuniform distribution of HDP pedestal dead loads and calibration factors different from those calculated. This information was not available at the time of publication. Information from appendix B, SRB HDP Strains and Loads During the Holddown Period (KSC-DD-688-TR) follows (3.2 through 3.3).

3.2 SRB HDP STRAINS AND LOADS DURING THE HOLDDOWN PERIOD (STS-1 THROUGH -5)

This paragraph presents Shuttle HDP loads obtained from strain measurements KSRGF013A through -028A during STS-2, STS-3, and STS-5 launches. Each SRB HDP pedestal was instrumented with two sets of strain gages and represents an uncalibrated load cell. Each set consisted of eight strain gages, wired in a manner ensuring temperature compensation and recording of axial load-induced strains while eliminating voltage output caused by the bending. Each set, further referred to as a strain gage, provided an independent measurement of an average axial strain in HDP's. The knowledge of static load carried by each HDP before SSME ignition and recorded strain time histories provide necessary information for the calibration of improvised load cells. Then, recalibrated strain time histories represent dynamic load time histories for each HDP for the period from SSME ignition until the separation of tie-down explosive bolts and lift-off. Required calibration procedure is as follows:

$$CF = \frac{GLOW + \Delta}{8(\epsilon_{DL} - \epsilon_{L/O})} \quad \text{kips}/(\mu\text{in/in})$$

$$P(t) = CF[\epsilon(t) - \epsilon_{L/O}] \quad \text{kips}$$

Where:

CF = load cell calibration factor that converts recorded strain ($\mu\text{in/in}$) into load (kips). The expression for CF contains an assumption that the total vehicle weight (before SSME ignition) is equally distributed among all eight HDP's. This assumption neglects the eccentricity of Orbiter weight with respect to SRB support.

GLOW = Gross lift-off weight of Shuttle vehicle at nominal lift-off (approximately 0.21 s after SRB ignition). For STS-2, GLOW = 4,030.4 kips. For STS-3, GLOW = 4,016.6 kips. Estimated numbers account for a decrease in the total Shuttle weight by the amount of fuel burned by the SSME's during holddown period and by SRB's until development of lift-off thrust.

Δ = weight of fuel ($\text{LH}_2 + \text{LO}_2$ + about 0.21 s of SRB propellant) burned during the holddown period and until SRB's thrust develops, estimated to be 441.6 kips for STS-2 and 456.1 kips for STS-3.

$\text{GLOW} + \Delta$ = 4,472.0 kips for STS-2 and 4,472.7 kips for STS-3 (gross Shuttle vehicle weights before SSME ignition)

ϵ_{DL} = strain gage output before SSME ignition. For STS-2 and STS-5, this output was zeroed ($\epsilon_{\text{DL}} = 0$).

$\epsilon_{\text{L/O}}$ = strain gage output after lift-off. This is a no-load condition on HDP's and represents a zero reference line for dynamic load time histories.

$P(t)$ = dynamic load on HDP at time t . Using the sign of recorded strains in expression for $P(t)$, a positive value of $P(t)$ represents a downward load on the HDP. A negative $P(t)$ represents an upward (tensile) load on the HDP.

$\epsilon(t)$ = strain gage output at time t . For extreme values of dynamic loads, $\epsilon(t)$ corresponds to either a maximum (ϵ_{max}) or a minimum (min) of a recorded strain time history.

Figure 3-12 (right side) illustrates strain values required to obtain calibration factors from a typical strain time history. Table 3-1 and figure 3-13 present calibration factors (CF), dead load strain differences ($\epsilon_{\text{DL}} - \epsilon_{\text{L/O}}$), of peak strain differences ($\epsilon_{\text{max/min}} - \epsilon_{\text{L/O}}$), and peak dynamic loads (and locations of HDP's) for all strain measurements on SRB HDP pedestals. In computations, the total dead load on each HDP $(\text{GLOW} + \Delta)/8 = 559.0$ kips. For STS-3 measurements, some roundings and extrapolations were necessary in order to obtain $\epsilon_{\text{DL}} - \epsilon_{\text{L/O}}$, since ϵ_{DL} was not zeroed and processed data began at $T - 4.60$ s, while first SSME ignition occurred at approximately $T - 6.0$ s. For convenience and reference, STS-2 and STS-3 SRB HDP strain time histories, previously published in KSC-DD-593-TR and KSC-DD-651-TR, are presented. Strain time histories for STS-5 can be found elsewhere in this document.

The peak load values presented in table 3-1 show significant differences between loads obtained by two independent measurements on each HDP pedestal, as well as differences between loads on different pedestals. The only emerging

pattern is that the second measurement (gage 2) in most cases shows higher loads than gage 1. The output of gage 2 is also more susceptible to bending strains in the pedestals. It appears that the effect of HDP pedestal bending has not been entirely eliminated from sensor outputs. Consequently, peak downward loads appear to be overestimated, and peak upward loads are underestimated. Some differences between the two measurements on the same HDP pedestal may be caused by details in strain gage installations or in their locations with respect to possible asymmetries in the HDP's. Because the pedestal is very short, the assumption about the plane section containing strain gages and remaining plane after the deformation takes place may not be sufficiently accurate, and some warping of the plane cross section may be responsible for differences in the gage 1 and gage 2 outputs.

The assumption of equal dead load distribution (before SSME ignition) on each HDP may be responsible for generally higher loads on HDP's 3 and 7. Because of MLP flexibility, HDP's 3 and 7 are points of lower MLP stiffness than the opposite HDP's 4 and 8. It is possible that, in the statically indeterminate Shuttle support structure, HDP's 3 and 7 carry a lower-than-assumed dead load (559 kips). If so, then the calibration factors (CF) and the peak dynamic loads on these HDP's will be proportionally lower than the values presented in table 3-1, while HDP's 4 and 8 would attain higher-than-presented dynamic loads. Unfortunately, these questions cannot be answered based on available test data. An analysis of HDP dead load, which would consider Shuttle erection procedure, eccentricity of Orbiter weight, and fueling of ET tank, would eliminate the assumption made in this report about equal distribution of Shuttle weight among all HDP's.

3.3 A PLAUSIBLE EXPLANATION OF STRAIN OSCILLATIONS AT SRB IGNITION

Figure 3-12 (left side) shows an enlarged plot of raw data beginning at $T - 0.1$ s (nominal) for a duration of 0.41 s. Although the sampling rate of analog signal was 5 kHz, the DAS limits the frequency content of data to maximum 2 kHz. Of principal interest is the strain time history from the instant of explosive bolt actuation ($T - 0.01$ s) until the separation of the SRB from the HDP (approximately $T + 0.21$ s). Two distinct peaks, a maximum and a minimum, separated by approximately 10 ms, occur in the time history of each HDP pedestal strain. These peaks are followed by a shift of the average strain line (see figure 3-12, left side) about which a few oscillations occur at a frequency of about 82 Hz. Because this is a relatively high frequency, substantially higher than the first longitudinal SRB mode (below 15 to 16 Hz), a few initial and highest oscillations may be caused by propagating waves rather than by a "standard" standing wave-type vibration. If this hypothesis is true, then a strong argument can be made that the stiffness and mass of SRB HDP supporting structure, in this case the MLP, has no significant effect on Shuttle dynamics for the period of about 70 ms, beginning at about $T + 0.07$ s when large oscillations in the recorded HDP strains occur. For this period, a plausible explanation of the strain time history, presented further, is based on known concepts of wave propagation developed in mechanics of continuum. The explanation is prompted by an unexpected coincidence of three minima peak

(figure 3-1, left side) with the calculated results obtained considering propagation and reflection of dilatational waves within the SRB's solid propellant casing structure. First, we list necessary data:

- a. Distance from the top of the SRB casing dome (base of igniter) in the forward segment to the strain gage on HDP's is estimated to be $\simeq 117.8$ ft
- b. For SRB steel casing, using standard steel properties, data are:

Modulus of elasticity	$E = 29 \times 10^6$ lb/in ²
Poisson's ratio	$\nu = 0.3$
Elastic (Lame') constants	
$\lambda = E\nu / [(1 + \nu)(1 - 2\nu)]$	$= 16.73 \times 10^6$ lb/in ²
$\mu = E/[2(1 + \nu)]$	$= 11.15 \times 10^6$ lb/in ²
Steel specific density (mass per unit volume)	$\rho = 7.324 \times 10^{-4}$ lb/s ² /in ⁴

- c. Velocity of dilatational wave

$$V_1 = [\lambda + 2\mu / \rho]^{1/2} = 2.3084 \times 10^5 \text{ in/s} = 19,237 \text{ ft/s.}$$

Wave travels with the velocity of propagation of dilatation. Displacement is parallel but opposite in direction to wave normal. When reaching a free plane boundary, wave will reflect on itself when wave normal and boundary normal are parallel. Otherwise, a dilatational wave will reflect as two kinds of waves: a dilatational wave with the angle of reflection equal to the angle of incidence, and as a rotational (shear) wave with the angle of reflection smaller than the angle of incidence.

- d. Velocity of rotational (shear) wave

$$V_2 = (\mu / \rho)^{1/2} = 1.2338 \times 10^5 \text{ in/s} = 10,282 \text{ ft/s}$$

Wave travels with the velocity of propagation of rotation. Displacement is perpendicular to wave normal. When reaching a free plane boundary, wave will reflect on itself when wave normal and boundary normal are parallel. Otherwise, a shear wave will reflect as two kinds of waves: a shear wave with the angle of reflection equal to the angle of incidence, and a dilatational wave with the angle of reflection greater than the angle of incidence. Under certain conditions, shear waves are responsible for bending in plates and shells.

- e. The time required for a dilatational wave to travel the distance from the top of the SRB casing to the strain gage location on the HDP's is:

$$\Delta t = 117.0/19,237 = 0.00608 \text{ s}$$

This is one-half of the period of oscillations recorded by the HDP strain gage. The frequency of these oscillations (minima peaks on figure 3-1, left side) is:

$$f = 1/(2 \times 0.00608) = 82.2 \text{ Hz}$$

The coincidence of this frequency with the test data is astonishing, and it prompted this analysis.

- f. Wave propagation and reflection solutions developed in mechanics of continuum, while very rigorous, are also limited in most cases to examples with a single plane boundary. In cases involving multiple boundaries, conditions on these boundaries usually cannot be satisfied and solutions do not exist. A less rigorous solution derived for a prismatical bar states that the wave velocity propagating longitudinally in the bar is:

$$V = (E/\rho)^{1/2} = 1.9899 \times 10^5 \text{ in/s} = 16,582 \text{ ft/s}$$

Formally, this solution can be obtained from the expression for V_1 by assuming Poisson's ratio equal to zero. For steel, the most often cited value of V in the elastic range is 17,000 ft/s. Then, the values of Δt and f corresponding to those derived under e above are:

$$\Delta t = 117.0/16,582 = 0.0071 \text{ s}$$

$$f = 1/(2 \times 0.0071) = 70.4 \text{ Hz}$$

Some of the strain time histories show peak oscillations (after the first peak) occurring at a frequency of about 70 Hz. We are not attempting to provide an explanation why variations in the frequency of oscillations occur. The phenomena of wave reflection are too complex and defy a simplistic explanation. It is worth noting, however, that any exceeding of the elastic range by strains inside the SRB casing should result in a lower velocity of dilatational waves. Frequency domain analysis made with data measured after STS-5 confirms existence of a high peak in PSD's at 70.4 Hz.

Once generated, dilatational wave is reflected from the free boundary of the SRB skirt and from the curved boundary of the dome (forward SRB segment) where it should produce some rotational waves and bending. Because there is very little decay in recorded strain amplitudes (measured about the average strain line) for at least three cycles, one may conclude that a very small amount of

strain energy is transmitted to the gages on HDP's. All wave reflections at the base of SRB occur mainly from the free boundary of the SRB skirt. Therefore, neither stiffness nor mass of HDP supporting structure can have a significant effect on these oscillations.

The appearance of the first and most dominant peak on the strain time history at $T + 0.08$ s requires a different explanation. The time interval between this peak and the first distinct minimum of the incident dilatational wave is about 10 ms. The duration of the peak, the half period, is about:

$$t = 2(10 - 6.08) = 7.84 \text{ ms}$$

which is greater than the half period of dilatational wave. A plausible explanation is that this peak is a result of a pressure shock on the base of the SRB from a rapid ignition. Pressure shock displaces the base of SRB downward by the amount depending (among other factors) on the support stiffness. The peak load on the HDP certainly is proportional to the support stiffness. However, at this instant, the load on the SRB above the skirt joint with the casing should be inversely proportional to the support stiffness because this load is caused by the SRB base displacement. Pressure shock on the SRB base may also generate a dilatational wave traveling up the SRB. The amplitude of this wave is proportional to the downward displacement of the SRB base, and thus, inversely proportional to the stiffness of the support (the MLP). The stiffer the support is, the lower will be the amplitude of upward traveling dilatational wave. The same wave may be responsible for high-frequency oscillations appearing on the HDP strain time history immediately (within 1 to 2 ms) after the first dominant peak. These oscillations and, probably the entire effect of the base-generated dilatational wave, appear to be insignificant.

By far, the major effect on the SRB's, and probably on the entire Shuttle structure, is due to the pressure shock on the SRB dome in forward segment. This shock displaces the dome upward, and this rapid displacement generates a dilatational wave traveling down the SRB. When part of the wave reaches HDP's, the displacement associated with this wave is upward, the load on the post drops, and the first minimum peak appears on the strain time history. The major part of the wave reflects back from the free boundary of the SRB skirt, while a small amount may be reflected from the joint between the skirt and aft segment casing because of boundary direction change at the joint. Also, some shear waves will be generated at both ends of the SRB where reflections take place. Certainly, the amplitude of this dilatational wave does not depend on the stiffness of SRB supports. Because these strain oscillations are caused by a dilatational wave propagating through the steel casing, they are very little (if any) affected by the mass of attached SRB propellant and/or by the attachment of ET. Thus, the standard type of finite element modeling may not be able to explain this phenomenon; or, if forced to do so, it may result in incorrect loads on ET, Orbiter, etc.

KSC-DD-818-TR

In summary, pressure shock at SRB ignition, on the base of SRB, is responsible for the first dominant peak in HDP post strain time history. This peak depends on the stiffness of the SRB supporting structure. The strained part of the SRB is that between its base and supporting structure. The upper part of the SRB, above the joint between the skirt and casing, may be strained, though insignificantly, by the generated dilatational wave at the base.

Peaks in the strain time history, following the first, are caused by a dilatational wave generated at the top of the SRB by the pressure shock on the dome. This wave is bouncing back and forth along the SRB casing, reflecting mainly from the free boundary of the SRB skirt and from the dome; and corresponding base displacements are recorded by the HDP pedestal strain gages. The stiffness and/or mass of the SRB supporting structure has no effect on this wave.

KSR#: GF013R GF015R GF017R GF019R

ALL STRAIN GAGES TYPE 1. SENSORS: KSRGF013R, KSRGF015R, KSRGF017R & KSRGF019R. MLP-1
 SAMPLING RATE 200 Hz. TIME SCALE REFERENCED TO T-ZERO=332:16:00:00 GMT (1983).
 NOTE: EACH STRAIN GAGE IS AN UNCALIBRATED LOAD CELL. TRUE ZERO LOAD (STRAIN) CORRESPONDS TO
 GAGE OUTPUT AFTER T+0.3 SEC. OUTPUT @ T+4.6 SEC CORRESPONDS TO APPROXIMATELY DEAD LOAD
 CONDITION. POSITIVE STRAIN RELATIVE TO NO LOAD CONDITION REPRESENTS COMPRESSION.

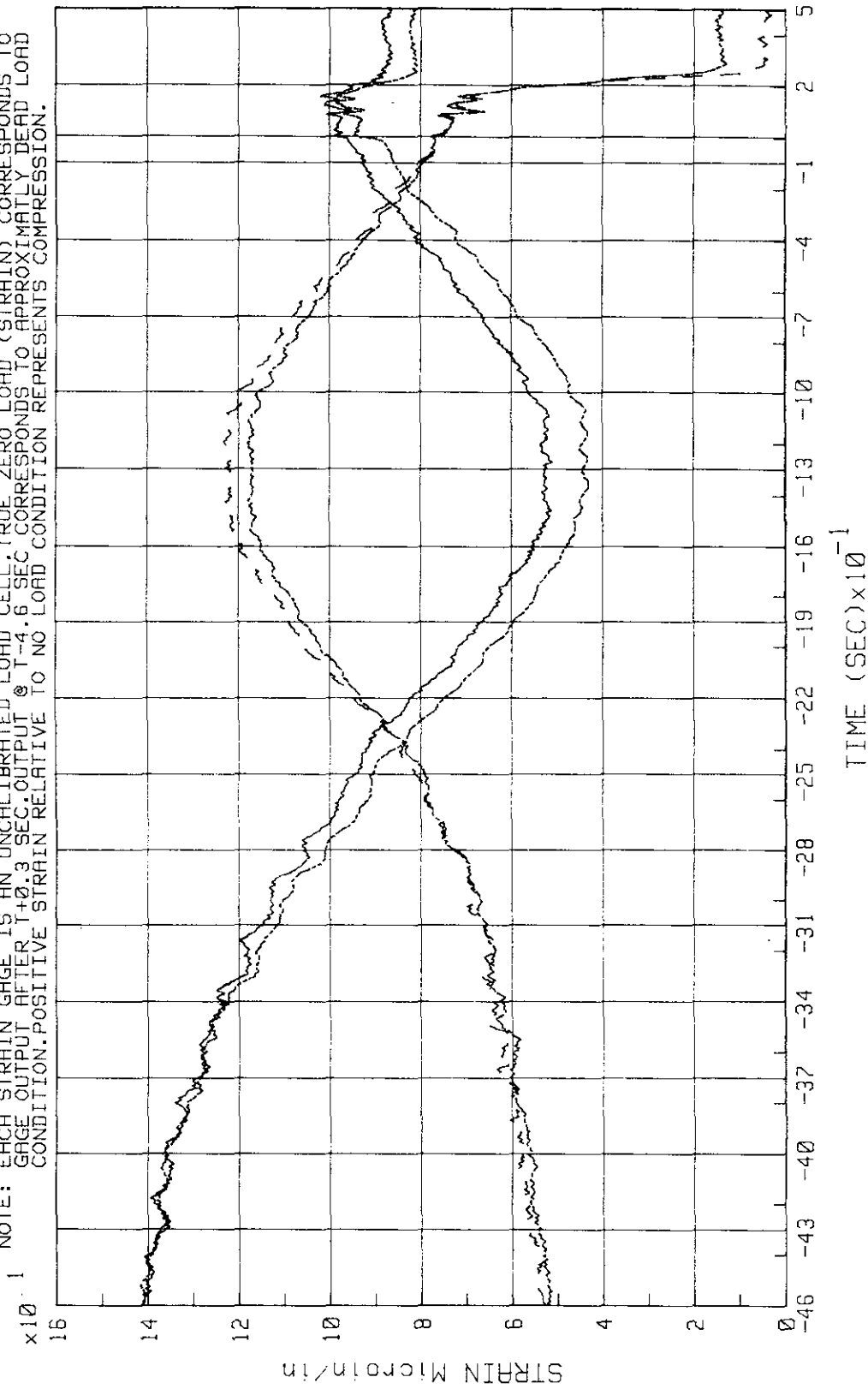


Figure 3-1. STS-9 East SRB HDP Pedestals (1, 2, 3, 4)
 Strains (T - 4.6 to T + 0.5 s (Sheet 1 of 2))

KSC-DD-818-TR

KSR#: GF014R GF016R GF019R GF020R

ALL STRAIN GAGES TYPE 2. SENSORS: KSRGF014R, KSRGF016R, KSRGF018R & KSRGF020R. MLP-1
 SAMPLING RATE 200 Hz. TIME SCALE REFERENCED TO T-ZERO=332:16:00:00 GMT (1983).
 NOTE: EACH STRAIN GAGE IS AN UNCALIBRATED LOAD CELL. TRUE ZERO LOAD (STRAIN) CORRESPONDS TO
 GAGE OUTPUT AFTER T+0.3 SEC. OUTPUT @ T+4.5 SEC CORRESPONDS TO APPROXIMATELY DEAD LOAD
 CONDITION. POSITIVE STRAIN RELATIVE TO NO LOAD CONDITION REPRESENTS COMPRESSION.

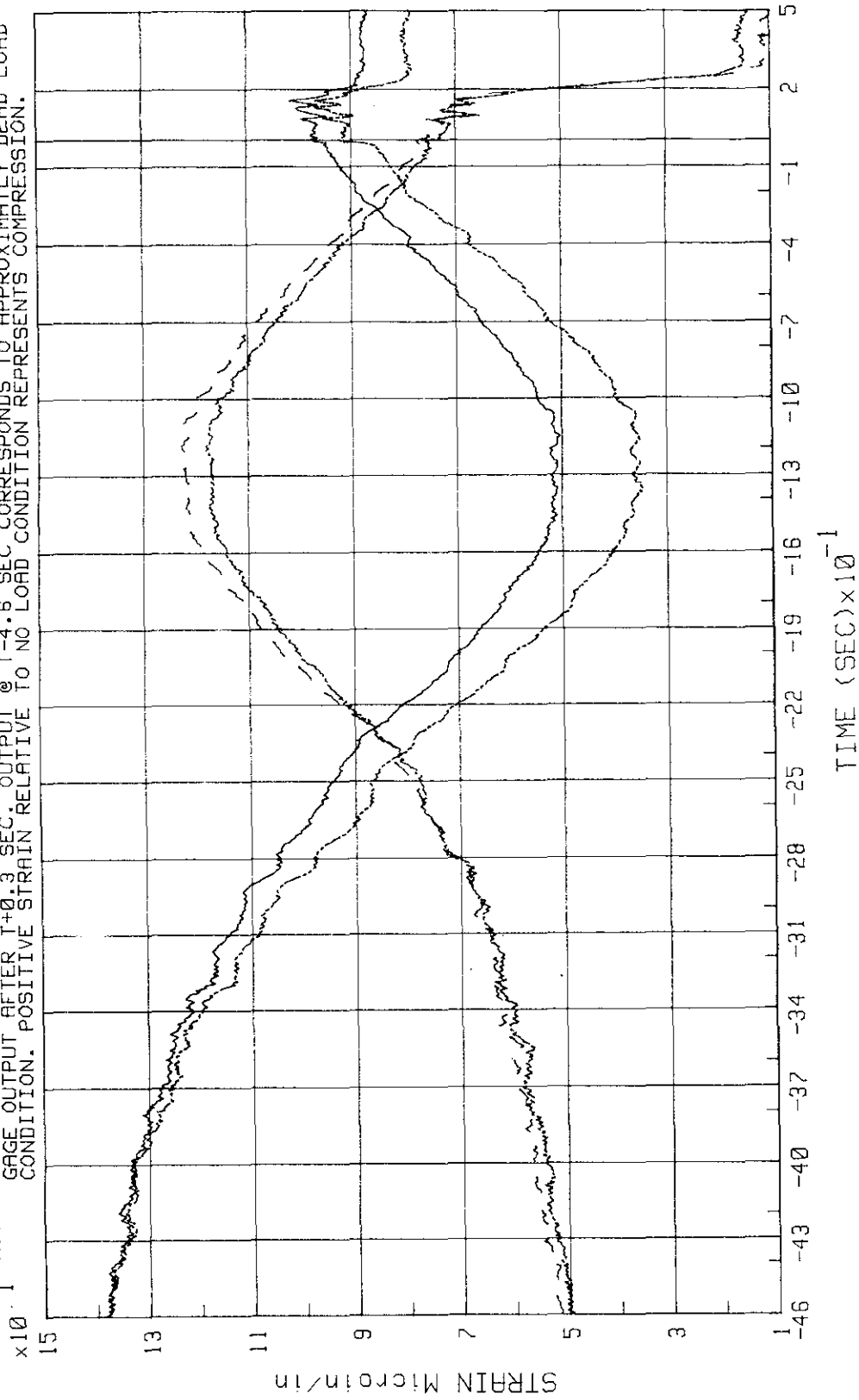


Figure 3-1. STS-9 East SRB HDP Pedestals (1, 2, 3, 4)
 Strains (T - 4.6 to T + 0.5 s (Sheet 2 of 2))

KSR#: GF021R GF023R GF025R GF027R

ALL STRAIN GAGES TYPE 1. SENSORS: KSRGF021A, KSRGF023A, KSRGF025A & KSRGF027A. MLP-1
 SAMPLING RATE 200 Hz. TIME SCALE REFERENCED TO T-ZERO=332:16:00:00.010 GMT (1983).
 NOTE: EACH STRAIN GAGE IS AN UNCALIBRATED LOAD CELL. TRUE ZERO LOAD (STRAIN) CORRESPONDS TO
 GAGE OUTPUT AFTER T+0.3 SEC. OUTPUT @ T-4.6 SEC CORRESPONDS TO APPROXIMATELY DEAD LOAD
 CONDITION. POSITIVE STRAIN RELATIVE TO NO LOAD CONDITION REPRESENTS COMPRESSION.

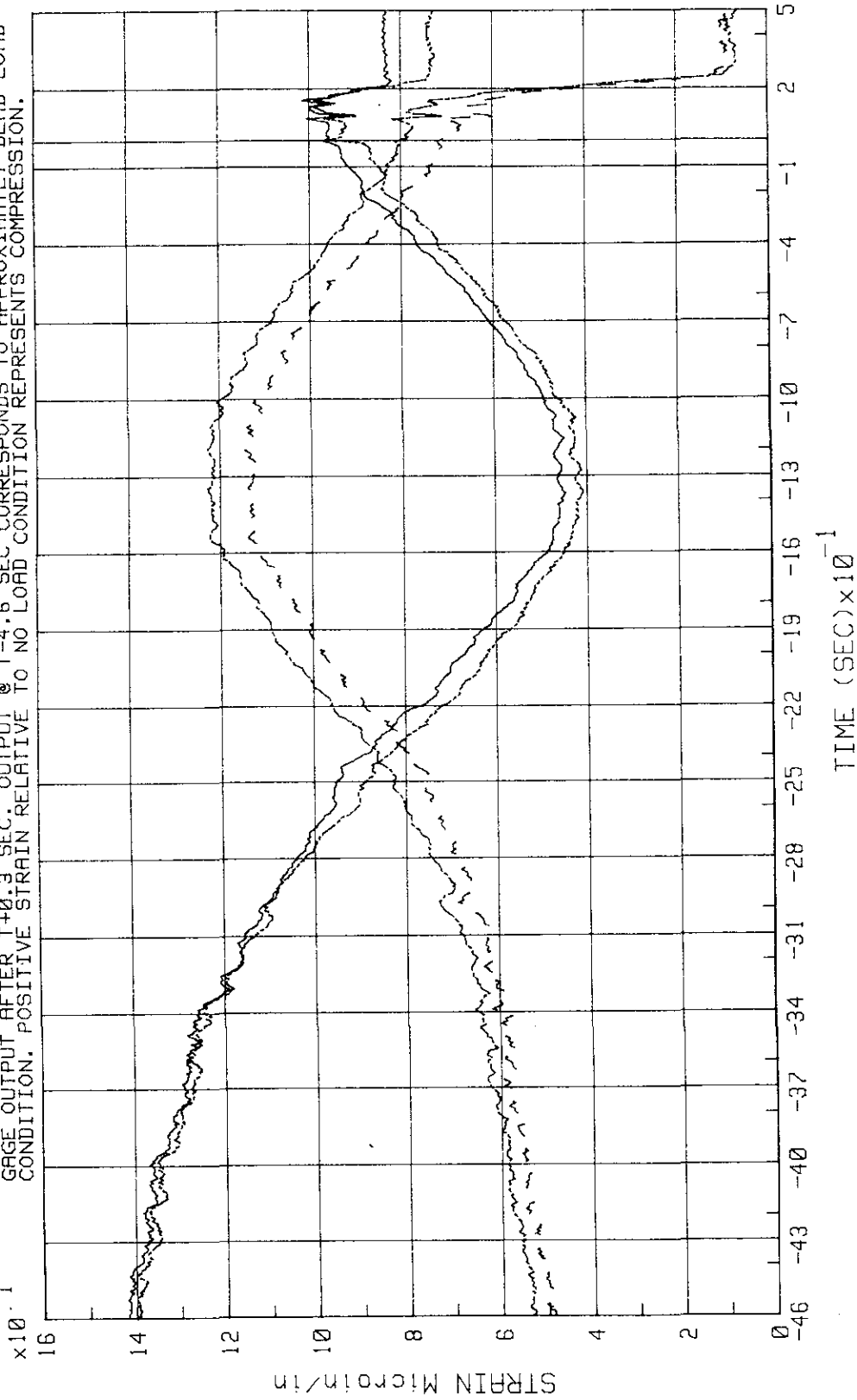


Figure 3-2. STS-9 West SRB HDP Pedestals (5, 6, 7, 8)
 Strains (T - 4.6 to T + 0.5 s (Sheet 1 of 2))

KSC-DD-818-TR

KSR#: GF022R GF024R GF026R GF028R

ALL STRAIN GAGES TYPE 2. SENSORS: KSRGF022R, KSRGF024R, KSRGF026R & KSRGF028R. MLP-1
 SAMPLING RATE 200 Hz. TIME SCALE REFERENCED TO T-ZERO-332:16:00:00.010 GMT (1983).
 NOTE: EACH STRAIN GAGE IS AN UNCALIBRATED LOAD CELL. TRUE ZERO LOAD (STRAIN) CORRESPONDS TO
 GAGE OUTPUT AFTER T+0.3 SEC. OUTPUT @ T+4.6 SEC CORRESPONDS TO APPROXIMATELY DEAD LOAD
 CONDITION. POSITIVE STRAIN RELATIVE TO NO LOAD CONDITION REPRESENTS COMPRESSION.

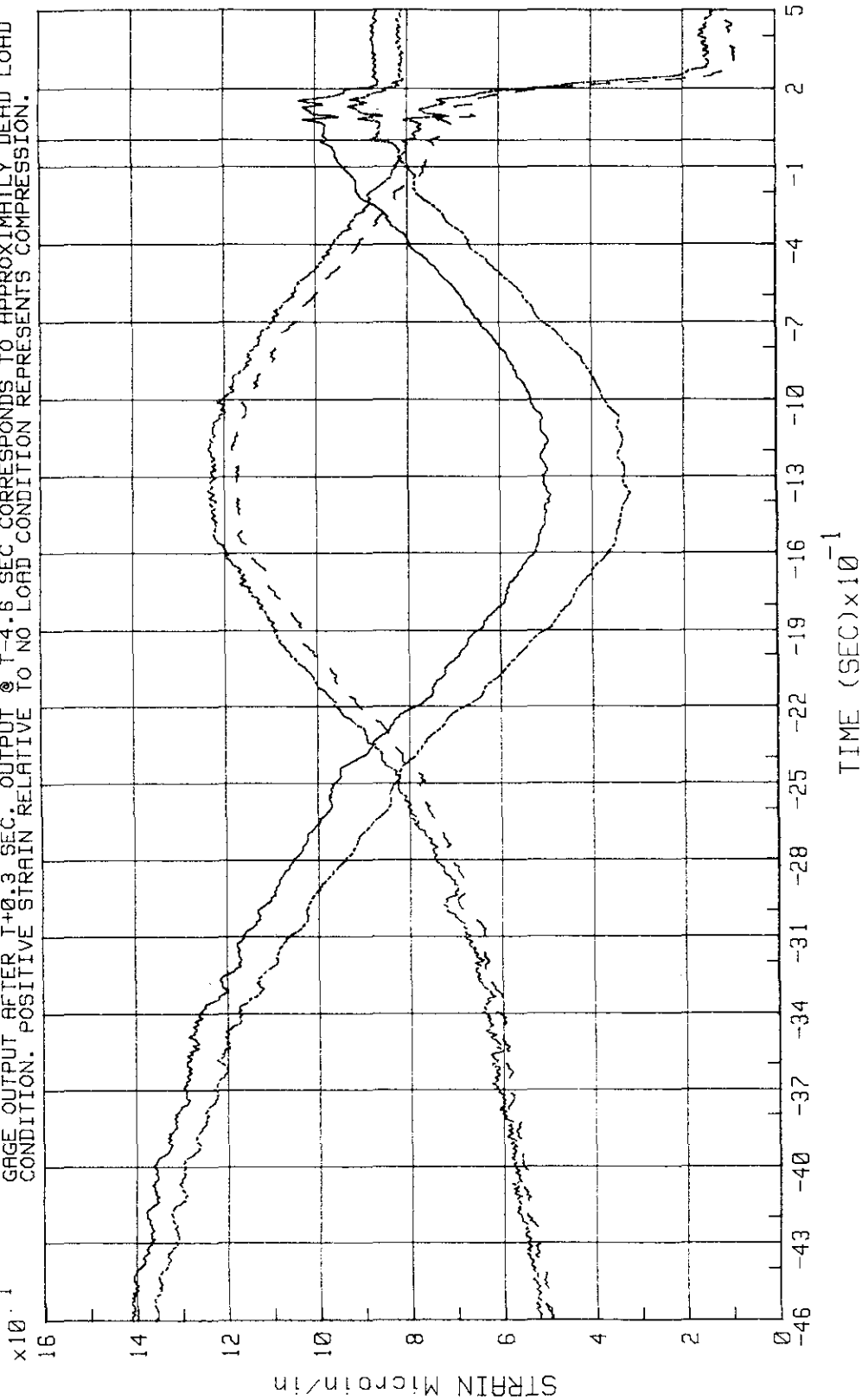


Figure 3-2. STS-9 West SRB HDP Pedestals (5, 6, 7, 8)
 Strains (T - 4.6 to T + 0.5 s (Sheet 2 of 2))

KSR#: GF013T GF015T GF017T GF019T

ALL STRAIN GAGES TYPE 1. SENSORS: KSRGF013A, KSRGF015A, KSRGF017A & KSRGF019A. MLP-1.
SAMPLING RATE 5000 Hz. TIME SCALE REFERENCED TO T-ZERO-332:16:00:00.010 GMT (1983).

x10⁻⁶ THIS PLOT SHOWS SHOCKS (@ T-0.01 SEC) INDUCED BY ACTIVATION OF EXPLOSIVE BOLTS.

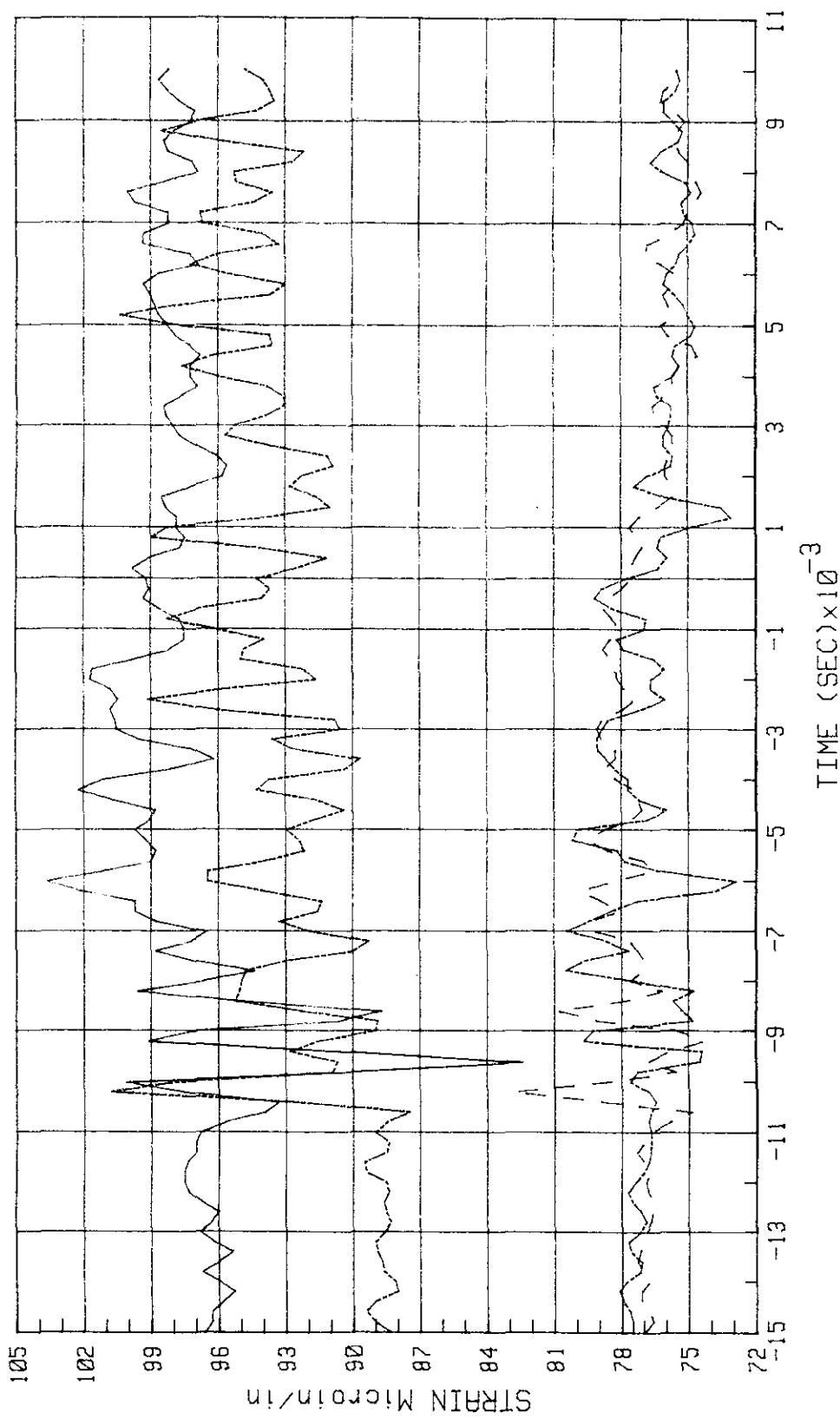


Figure 3-3. STS-9 East SRB HDP Pedestals (1, 2, 3, 4) Strains (T - 0.015 to T + 0.01 s)

KSC-DD-818-TR

KSR#: GF013T GF015T GF017T GF019T

ALL STRAIN GAGES TYPE 1. SENSORS: KSRGF013A, KSRGF015A, KSRGF017A & KSRGF019A. MLP-1
 SAMPLING RATE 5000 Hz. TIME SCALE REFERENCED TO T-ZERO-332:16:00:00.010 GMT (1983).
 THIS PLOT IS FOR ILLUSTRATION ONLY. SEE SINGLE SENSOR DATA PLOT WHICH PROVIDES BETTER SCALE.
 1 NOTE: DYNAMIC COMPONENTS OF THIS AND SIMILAR STRAIN DATA (STS-6 THRU STS-9) WERE USED IN
 COMPUTATIONS OF MEAN AND LIMIT PSD'S PRESENTED ELSEWHERE.

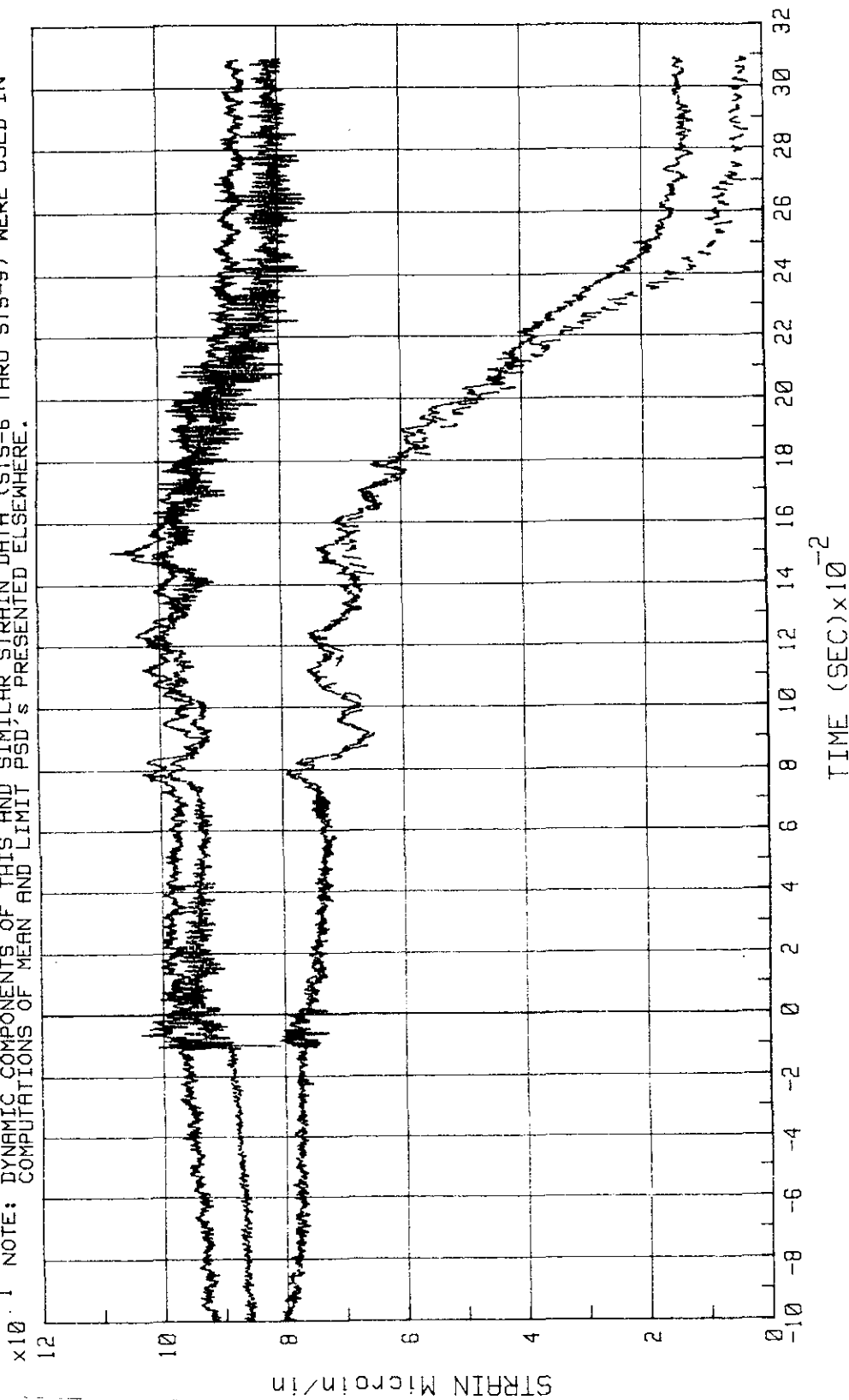


Figure 3-4. STS-9 East SRB HDP Pedestals (1, 2, 3, 4) Strains (T - 0.1 to T + 0.31 s)

KSR#: GF013T GF013L

MLP-1 SENSOR KSRGF013A. SOLID LINE IS RAW DATA. DASH-DOT-DOT LINE IS EXTRACTED TVM.
 SAMPLING RATE 5000 Hz. TIME SCALE REFERENCED TO T-ZERO=332:16:00:00.010 GMT (1983).
 NOTE: THE DIFFERENCE BETWEEN RAW DATA AND TVM (Time Variable Mean) IS DYNAMIC COMPONENT.
 DYNAMIC COMPONENTS OF THIS AND SIMILAR STRAIN DATA (STS-6 THRU STS-9) WERE USED IN
 COMPUTATIONS OF MEAN AND LIMIT PSD'S PRESENTED ELSEWHERE.

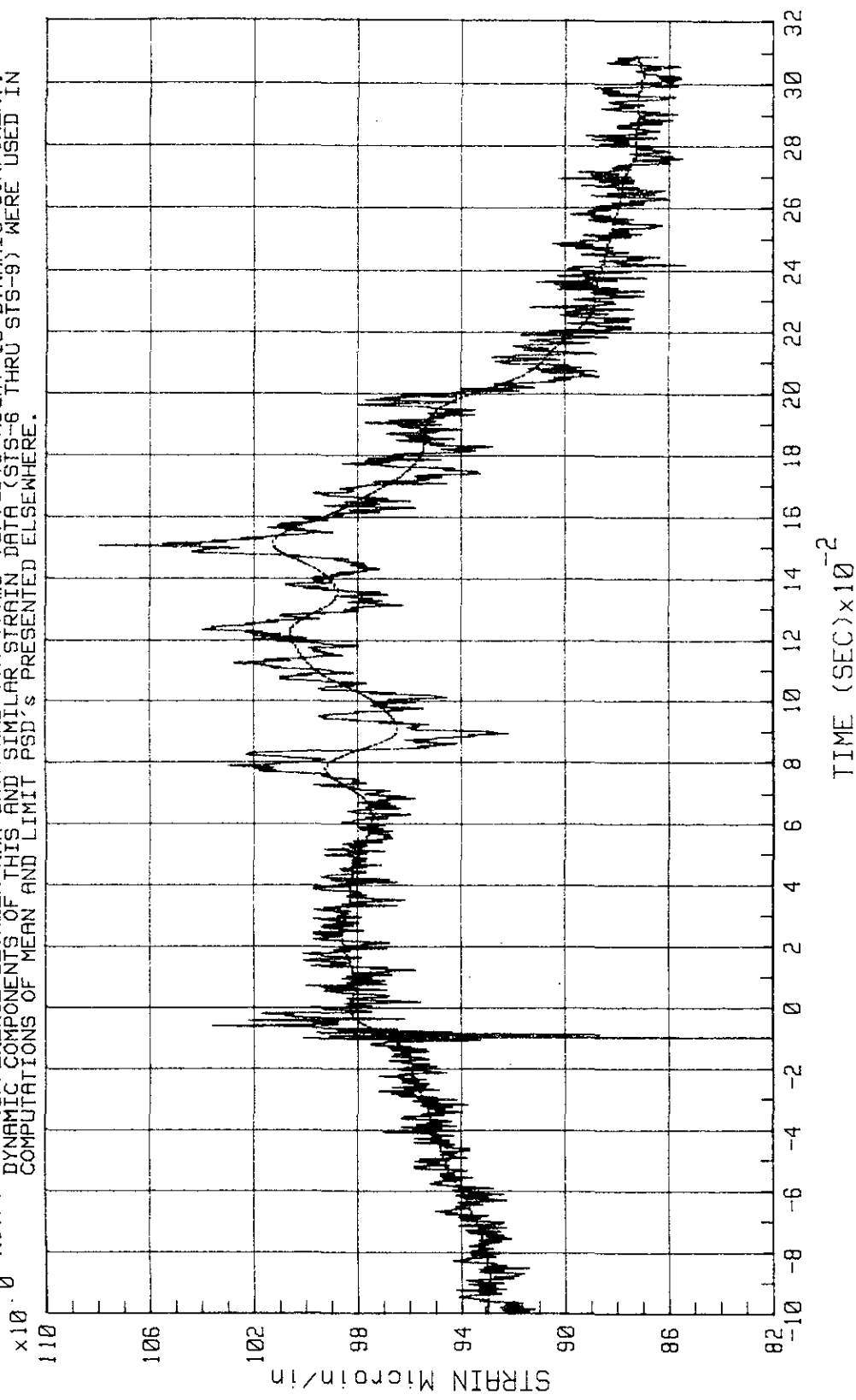


Figure 3-5. STS-9 East SRB HDP Pedestal (1) Strains (T - 0.1 to T + 0.31 s)

KSC-DD-818-TR

KSR#: GF015T GF015L

MLP-1 SENSOR KSRGF015A. SOLID LINE IS RAW DATA. DASH-DOT-DOT LINE IS EXTRACTED TVM.
 SAMPLING RATE 5000 Hz. TIME SCALE REFERENCED TO T-ZERO=332:16:00:00 GMT (1983).
 NOTE: THE DIFFERENCE BETWEEN RAW DATA AND TVM (Time Variable Mean) IS DYNAMIC COMPONENT.
 DYNAMIC COMPONENTS OF THIS AND SIMILAR STRAIN DATA (STS-6 THRU STS-9) WERE USED IN
 COMPUTATIONS OF MEAN AND LIMIT PSD'S PRESENTED ELSEWHERE.

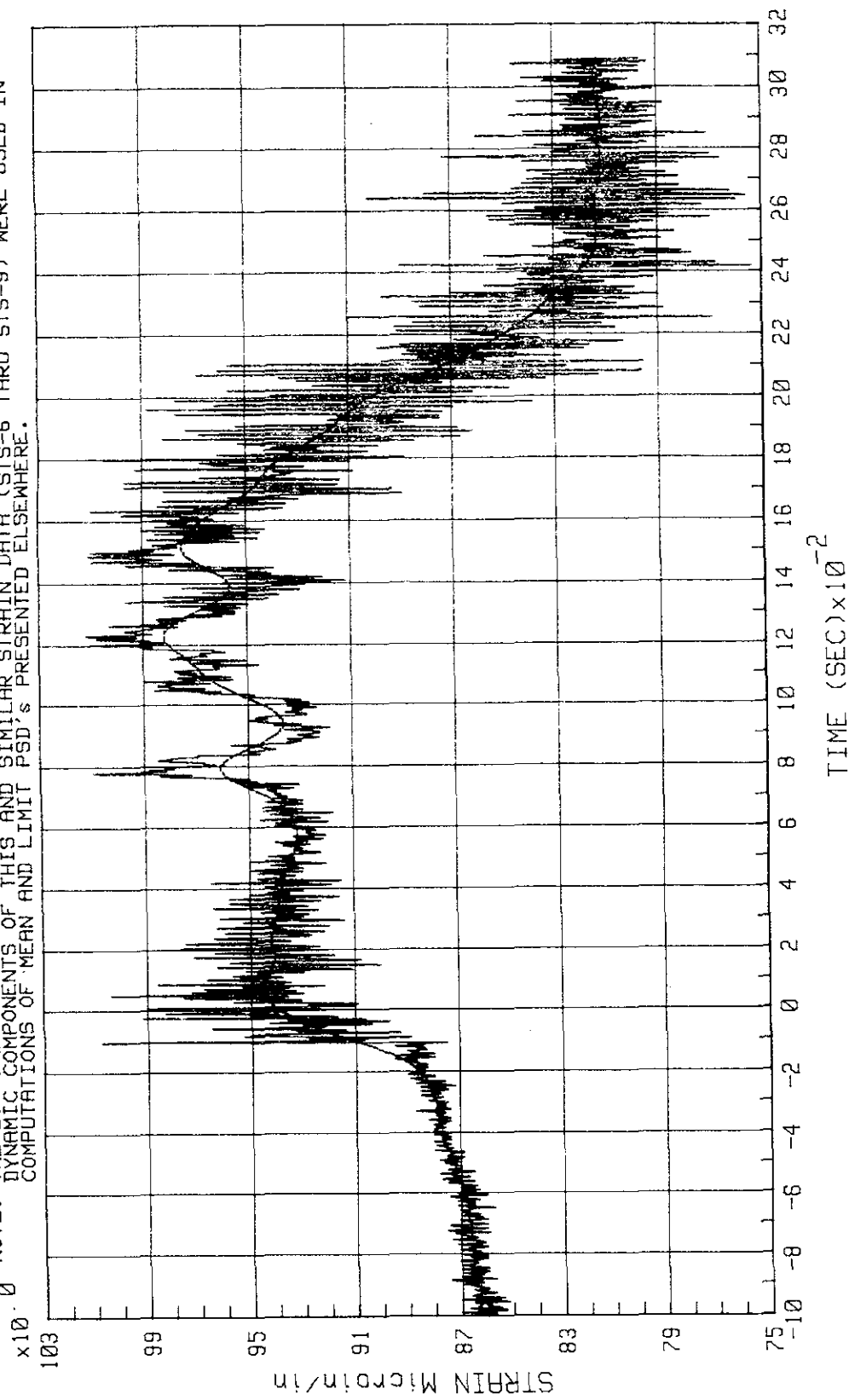


Figure 3-6. STS-9 East SRB HDP Pedestal (2) Strains (T - 0.1 to T + 0.31 s)

KSR#: GF017T GF017L

MLP-1 SENSOR KSRGF017A. SOLID LINE IS RAW DATA. DASH-DOT-DOT LINE IS EXTRACTED TVM.
 SAMPLING RATE 5000 Hz. TIME SCALE REFERENCED TO T-ZERO-332:16:00:00.010 GMT (1983).
 NOTE: THE DIFFERENCE BETWEEN RAW DATA AND TVM (Time Variable Mean) IS DYNAMIC COMPONENT.
 DYNAMIC COMPONENTS OF THIS AND SIMILAR STRAIN DATA (STS-8 THRU STS-9) WERE USED IN
 COMPUTATIONS OF MEAN AND LIMIT PSD'S PRESENTED ELSEWHERE.

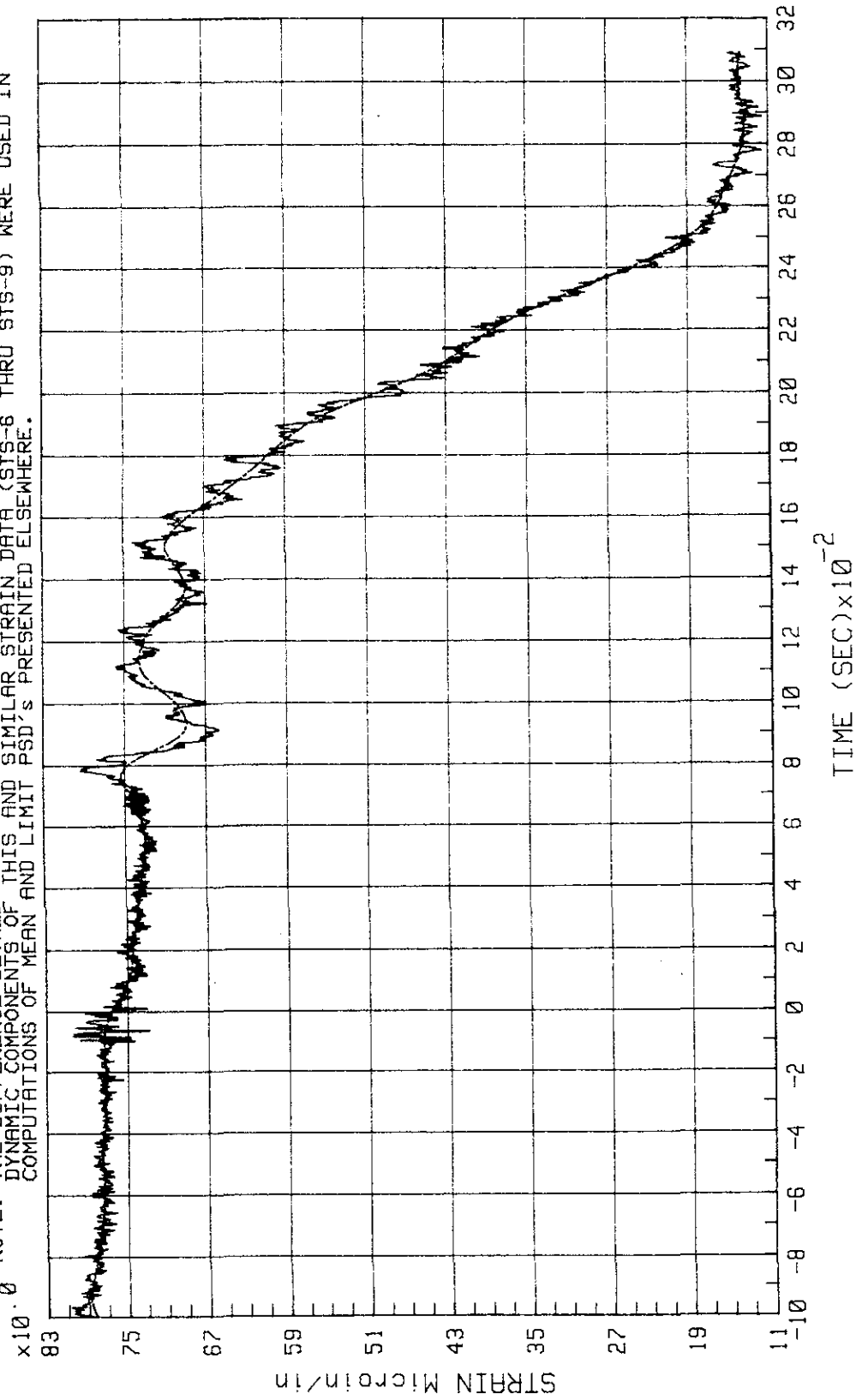


Figure 3-7. STS-9 East SRB HDP Pedestal (3) Strains (T - 0.1 to T + 0.31 s)

KSC-DD-818-TR

KSR#: GF019T GF019L

MLP-1 SENSOR KSRGF019A. SOLID LINE IS RAW DATA. DASH-DOT-DOT LINE IS EXTRACTED TVM.
 SAMPLING RATE 5000 Hz. TIME SCALE REFERENCED TO T-ZERO-332:16:00:00.010 GMT (1983).
 NOTE: THE DIFFERENCE BETWEEN RAW DATA AND TVM (Time Variable Mean) IS DYNAMIC COMPONENT.
 DYNAMIC COMPONENTS OF THIS AND SIMILAR STRAIN DATA (STS-6 THRU STS-9) WERE USED IN
 COMPUTATIONS OF MEAN AND LIMIT PSD'S PRESENTED ELSEWHERE.

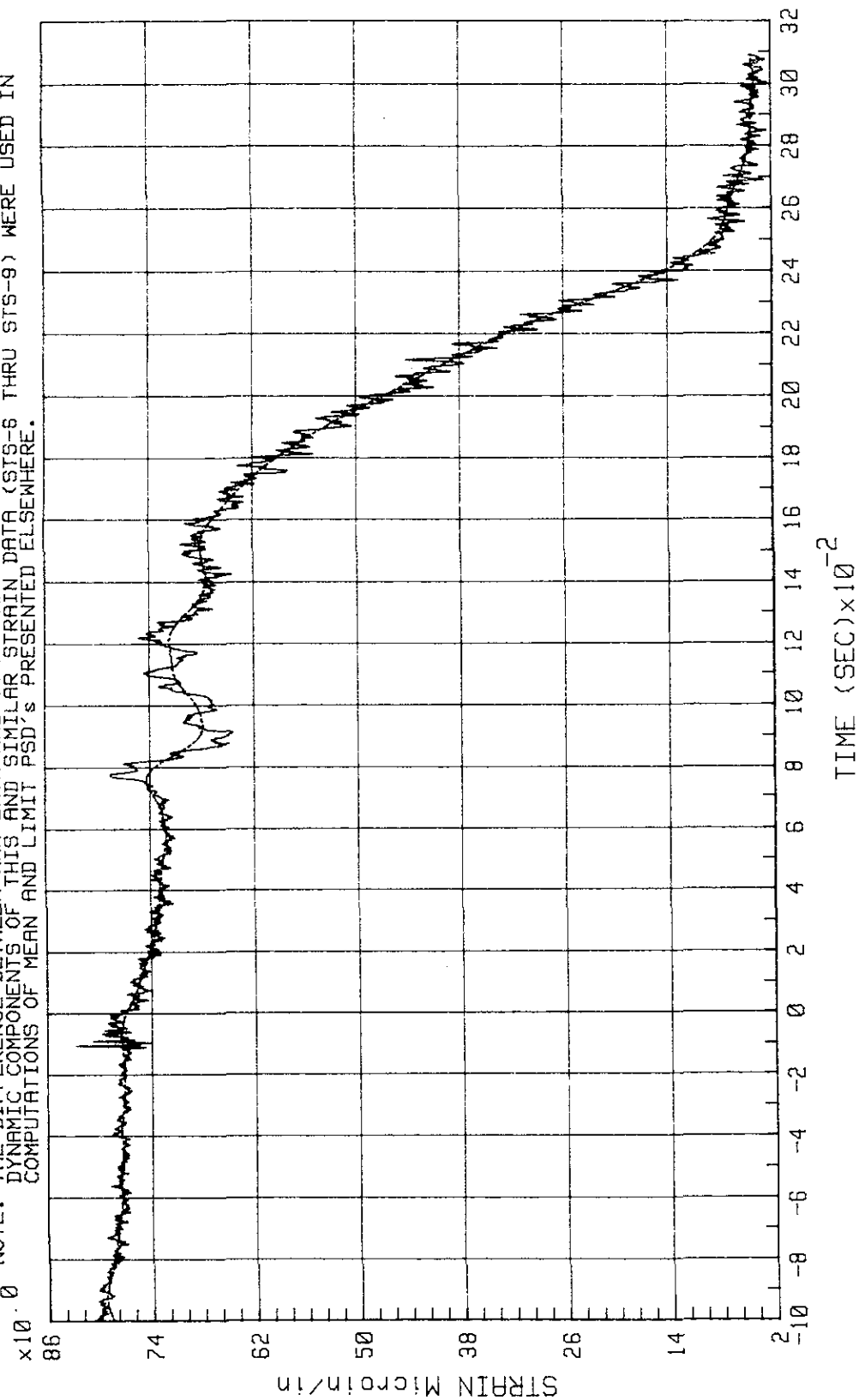


Figure 3-8. STS-9 East SRB HDP Pedestal (4) Strains (T - 0.1 to T + 0.31 s)

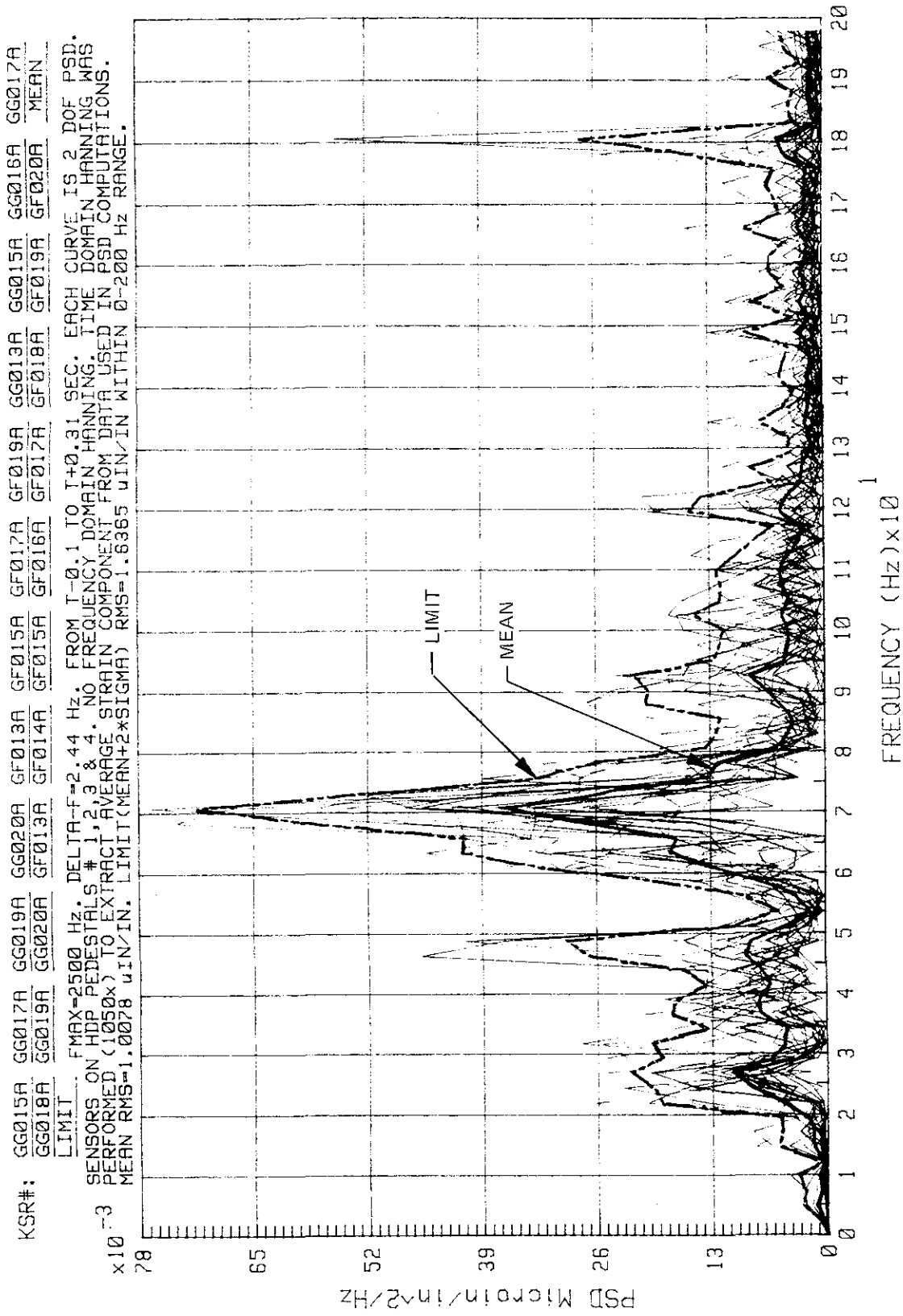


Figure 3-9. STS-6, -7, -8, and -9 East SRB HDP Pedestal Strains at SRB Ignition (Sheet 1 of 2)

KSC-DD-818-TR

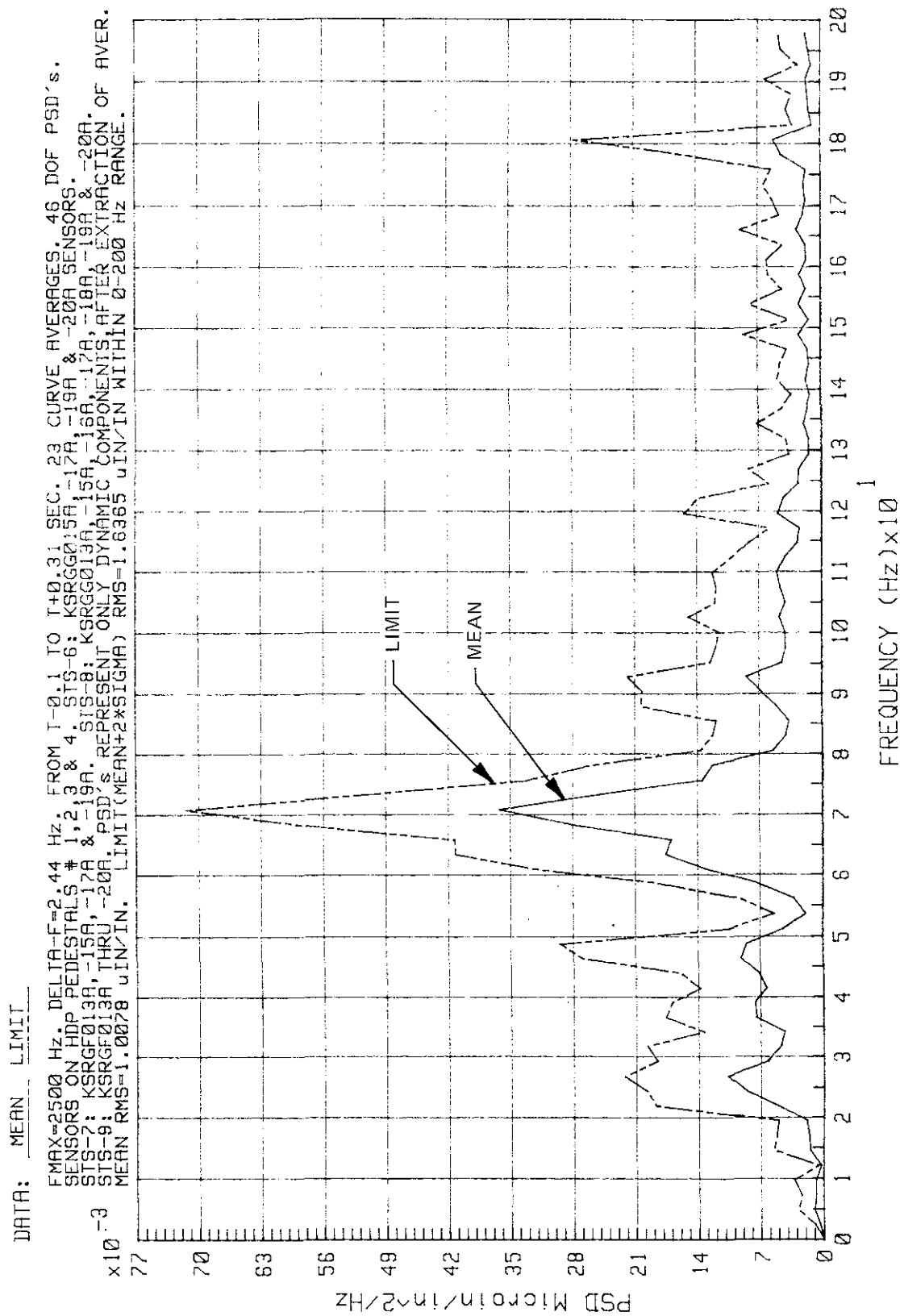


Figure 3-9. STS-6, -7, -8, and -9 East SRB HDP Pedestal Strains at SRB Ignition (Sheet 2 of 2)

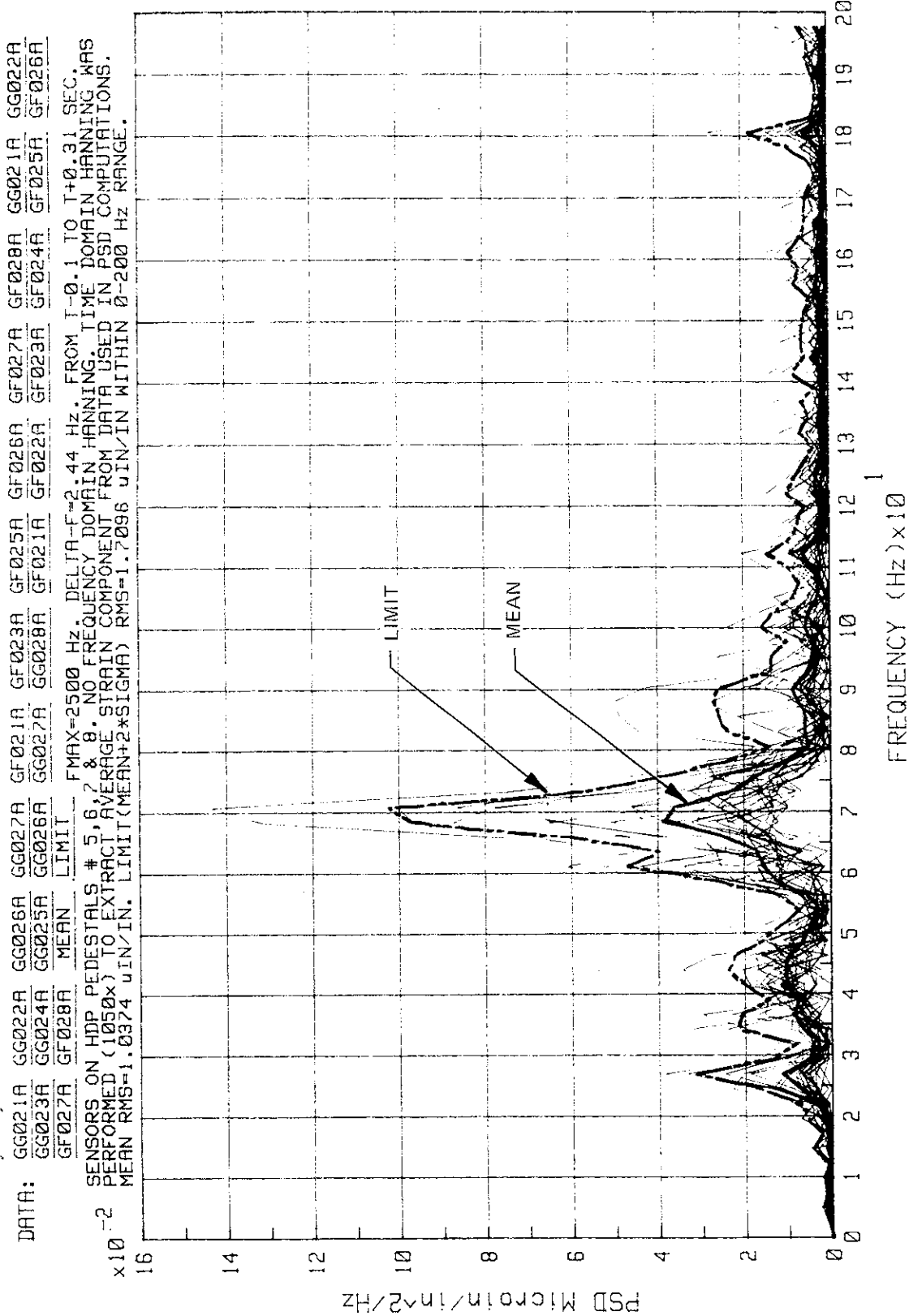


Figure 3-10. STS-6, -7, -8, and -9 West SRB HDP Pedestal Strains at SRB Ignition (Sheet 1 of 2)

KSC-DD-818-TR

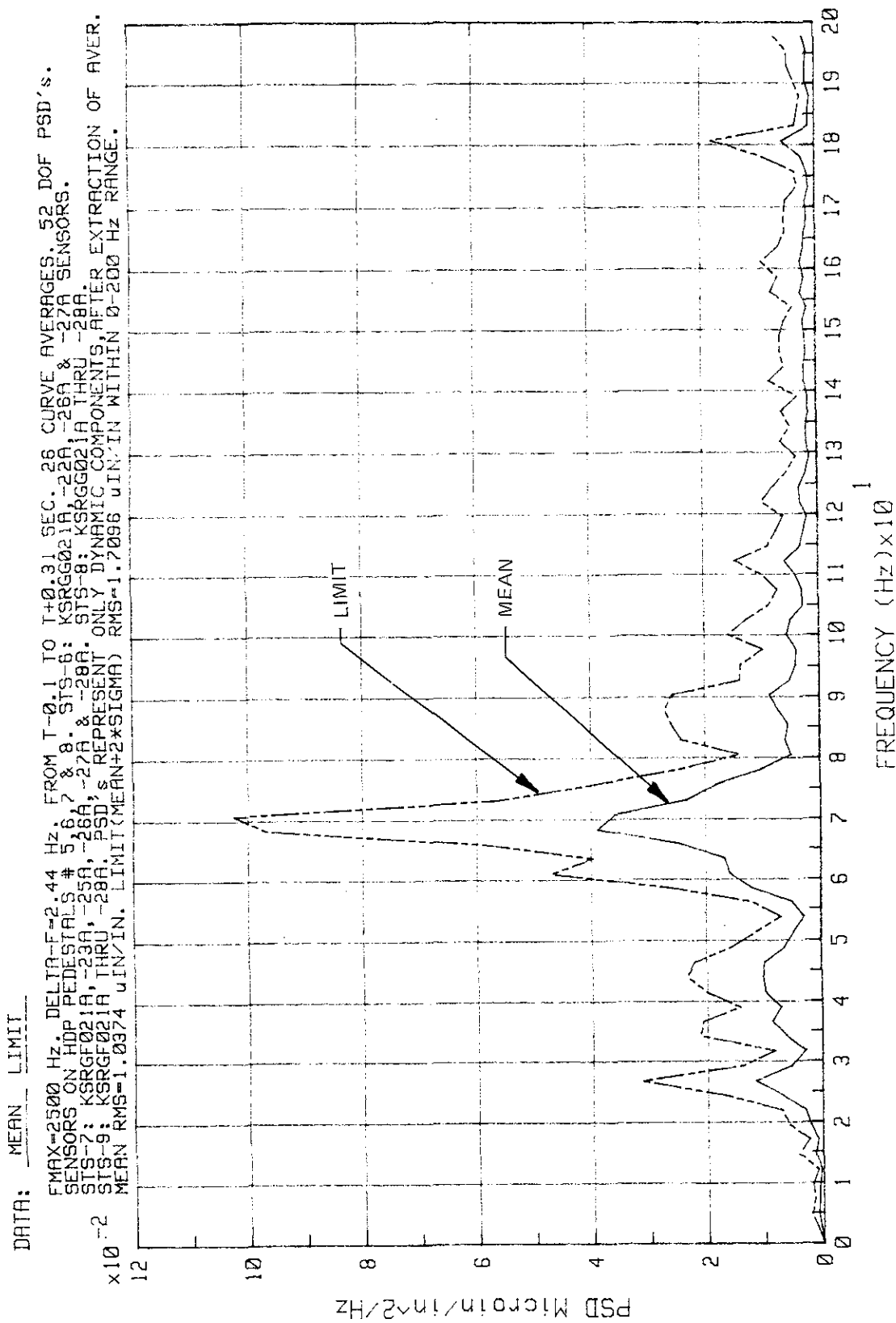


Figure 3-10. STS-6, -7, -8, and -9 West SRB HDP Pedestal Strains at SRB Ignition (Sheet 2 of 2)

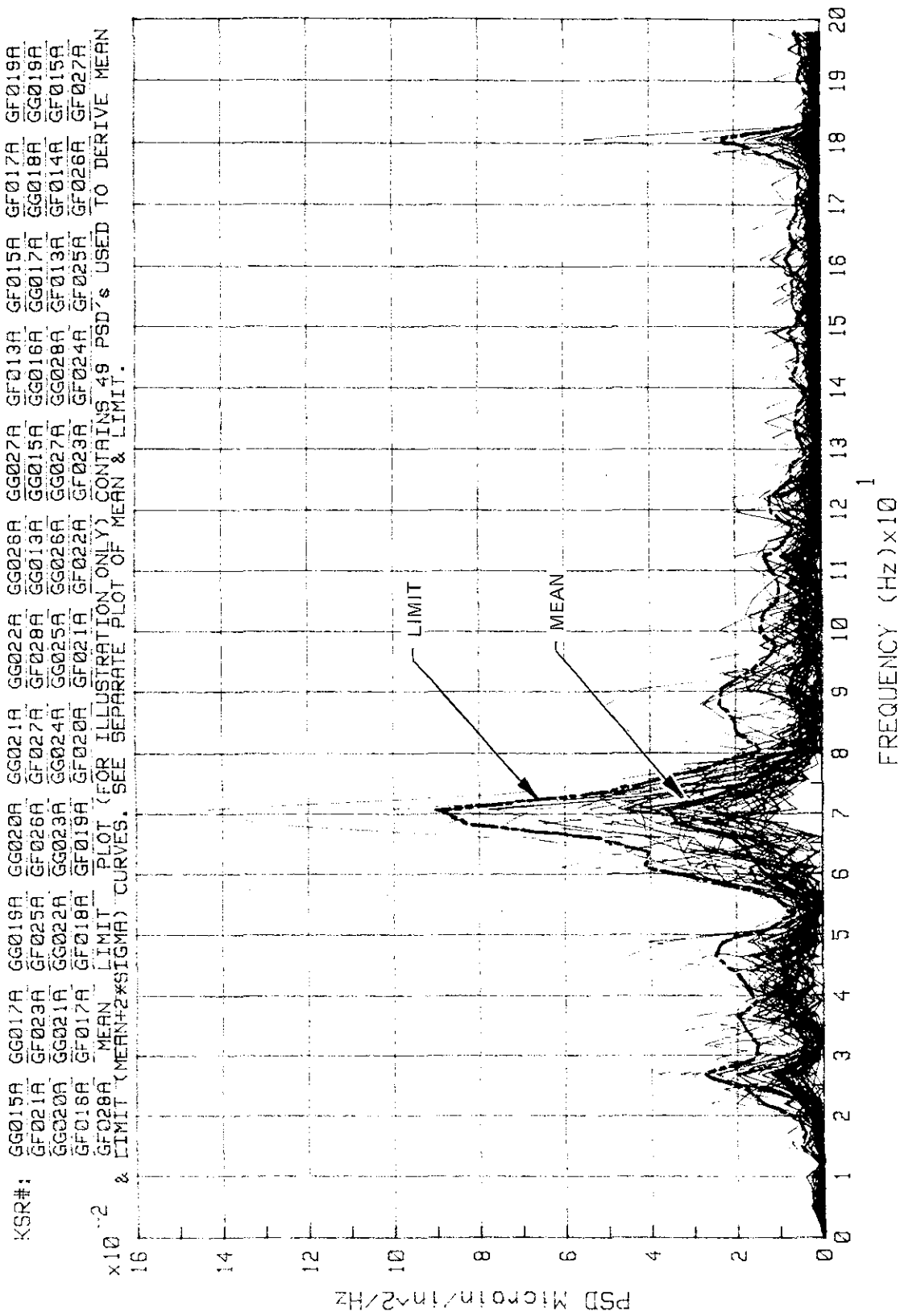


Figure 3-11. STS-6, -7, -8, and -9 Summary of East and West SRB HDP Strains at SRB Ignition
 (Sheet 1 of 3)

KSC-DD-818-TR

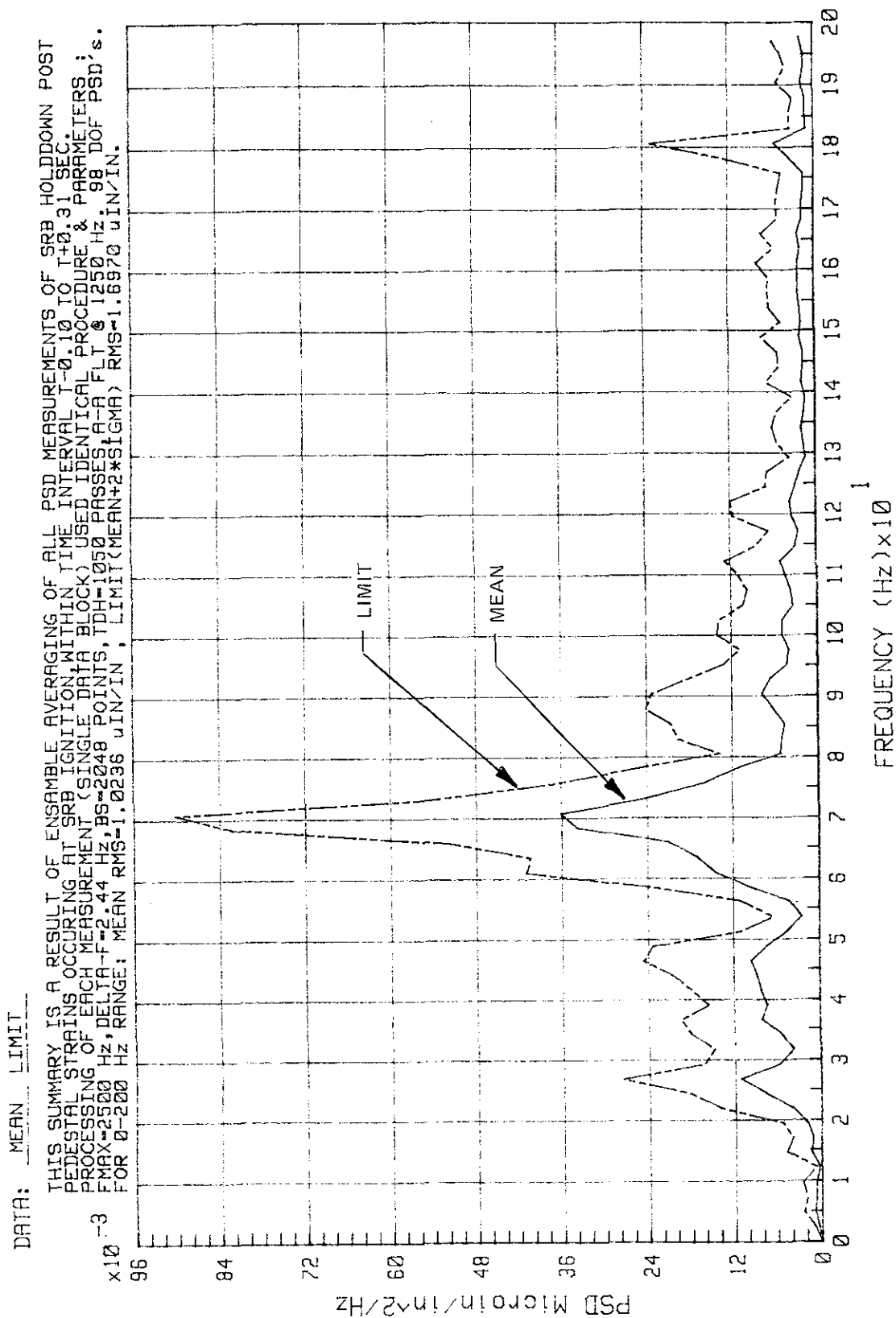


Figure 3-11. STS-6, -7, -8, and -9 Summary of East and West SRB HDP Strains at SRB Ignition
(Sheet 2 of 3)

DATA: MEAN LIMIT

THIS SUMMARY IS A RESULT OF ENSAMBLE AVERAGING OF ALL PSD MEASUREMENTS OF SRB HOLDDOWN POST
PEDESTAL STRAINS OCCURRING AT SRB IGNITION WITHIN TIME INTERVAL $1-0.10$ TO $1+0.31$ SEC.
PROCESSING OF EACH MEASUREMENT (SINGLE DATA BLOCK) USED IDENTICAL PROCEDURE & PARAMETERS:
 $\times 10^{-2}$ FMAX=2500 Hz, DELTA-F=2.44 Hz, BS=2048 POINTS, TDH=1050 PASSES, A-A FLT @ 1250 Hz, 98 DOF PSD'S.
FOR 0-200 Hz RANGE: MEAN RMS=1.0236 $\mu\text{IN}/\text{IN}$, LIMIT(MEAN+3*SIGMA) RMS=1.9483 $\mu\text{IN}/\text{IN}$.

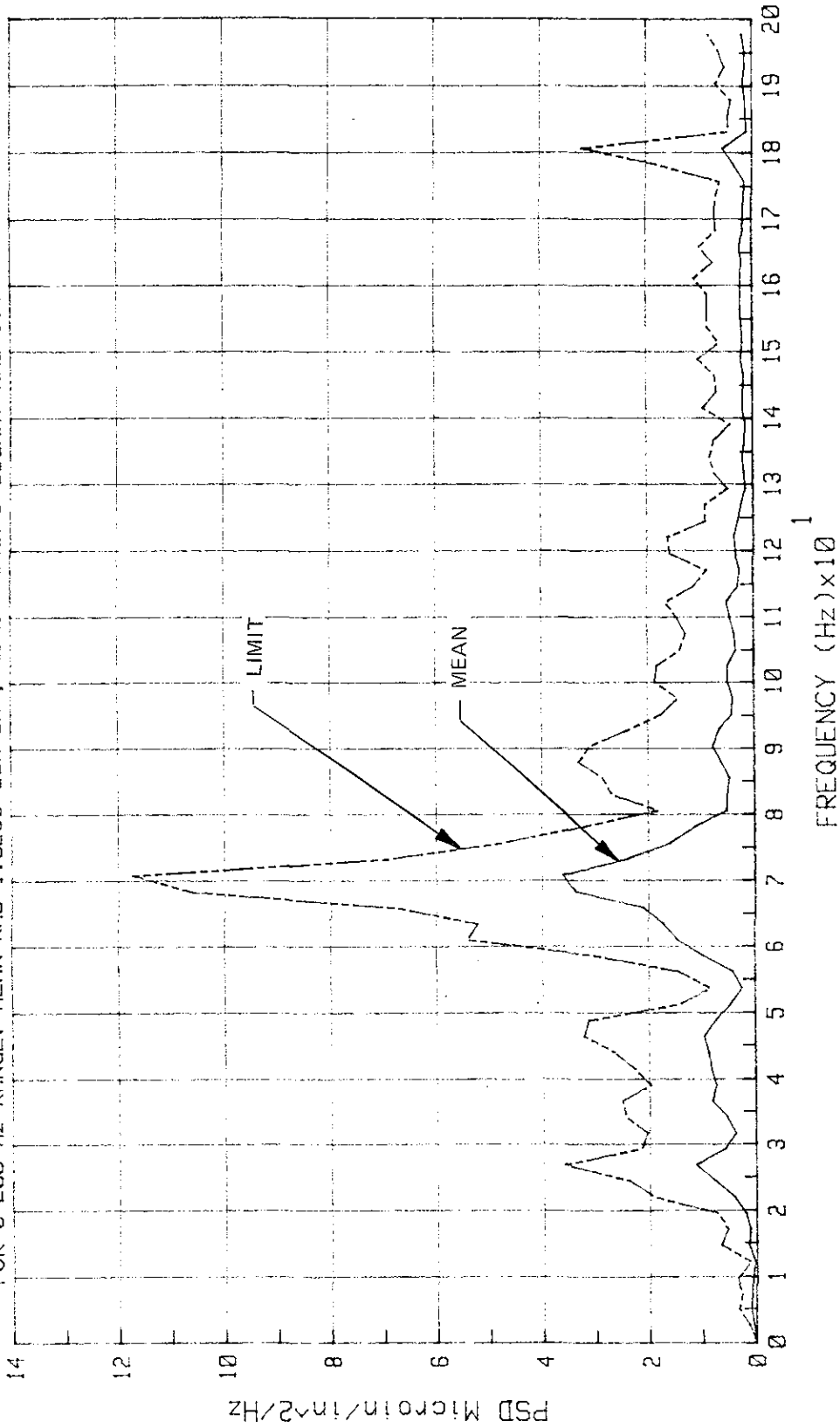


Figure 3-11. STS-6, -7, -8, and -9 Summary of East and West SRB HDP Strains at SRB Ignition
(Sheet 3 of 3)

KSC-DD-818-TR

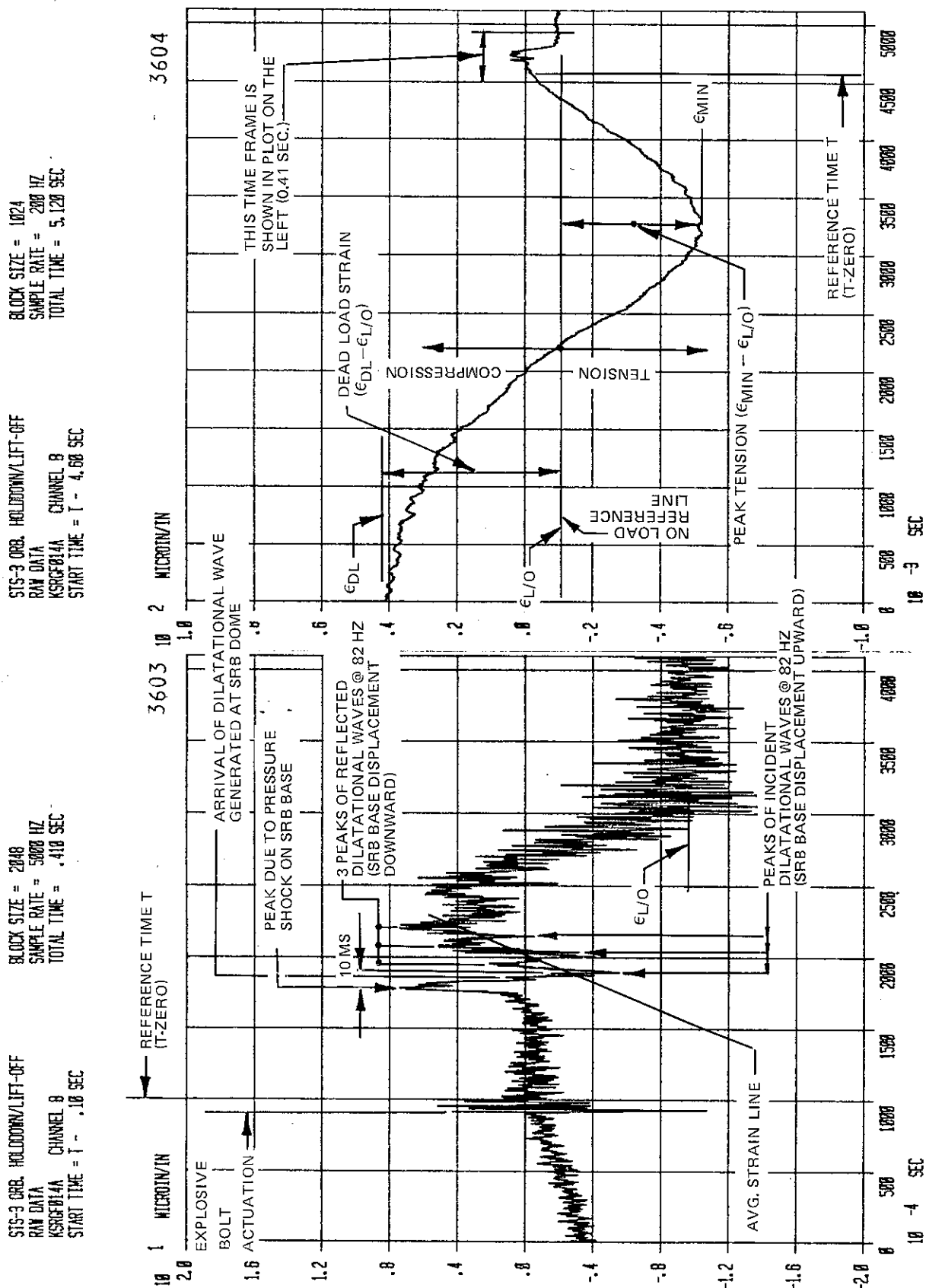


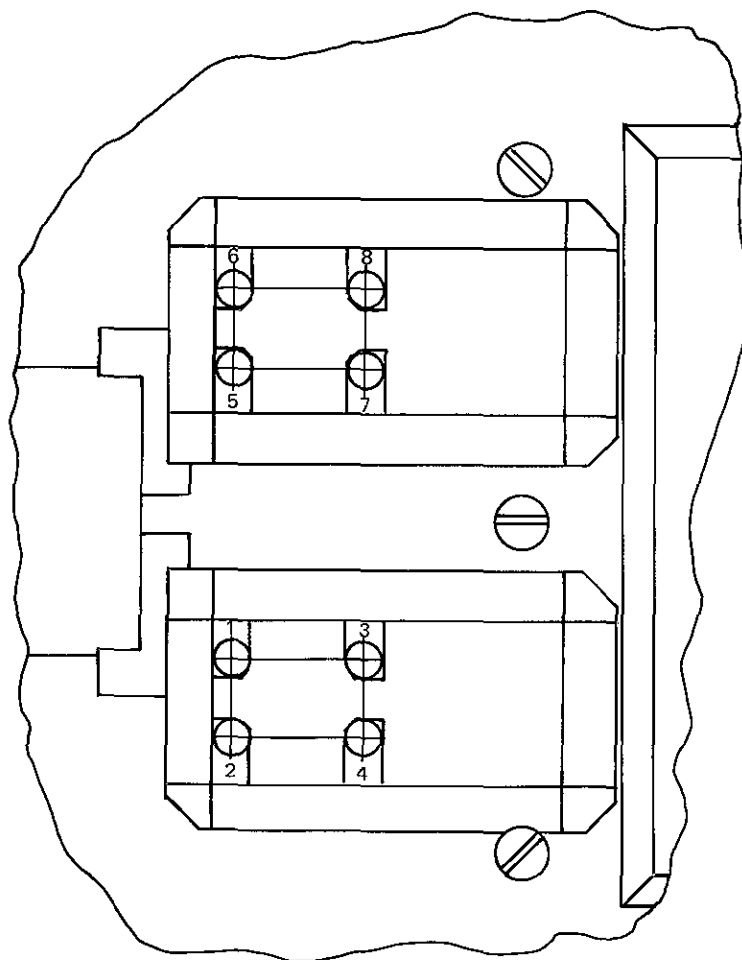
Figure 3-12. Typical Strain Time History and Illustration of Terms in Text

Table 3-1. SRB HDP Loads

HDP No.	KSRGF No.	STS-2				STS-3				STS-5			
		CF (kips/μin/in)	Dead Load $\epsilon_{DL} - \epsilon_{L/O}$ (μin/in)	Peak $\epsilon(t) - \epsilon_{L/O}$ (μin/in)	Peak Load (kips)	CF (kips/μin/in)	Dead Load $\epsilon_{DL} - \epsilon_{L/O}$ (μin/in)	Peak $\epsilon(t) - \epsilon_{L/O}$ (μin/in)	Peak Load (kips)	CF (kips/μin/in)	Dead Load $\epsilon_{DL} - \epsilon_{L/O}$ (μin/in)	Peak $\epsilon(t) - \epsilon_{L/O}$ (μin/in)	Peak Load (kips)
1	13	FAILED				12.70	44	-40	-508.2	11.0	51	-36.5	-401
1	14	9.16	61	-34	-311.6	10.75	52	-45	-483.8	11.0	51	-41.0	-450
2	15	9.81	57	-40	-392.3	8.47	66	-32	-271.0	9.5	59	-48.0	-455
2	16	FAILED				8.60	65	-42	-361.2	8.7	64	-42.0	-367
3	17	15.11	37	104	1,571.2	14.71	38	106	1,559.3	14.3	39	104.0	1,550
3	18	20.70	27	94	1,946.1	18.03	31	107	1,929.5	18.6	30	94.0	1,752
4	19	11.41	49	113	1,289.1	11.89	47	114	1,355.8	12.2	46	110.0	1,337
4	20	15.97	35	110	1,756.9	15.97	35	112	1,789.8	16.9	33	111.0	1,880
5	21	9.02	62	-36	-324.6	9.32	60	-40	-372.7	10.9	52	-42.0	-452
5	22	9.47	59	-31	-293.7	10.75	52	-39	-419.2	11.2	50	-38.0	-425
6	23	8.73	64	-36	-314.4	8.60	65	-34	-292.4	7.8	72	-32.0	-248
6	24	11.18	50	-54	-603.7	10.16	55	-55	-559.0	9.3	60	-50.0	-466
7	25	14.71	38	98	1,441.6	13.63	41	102	1,390.7	14.0	40	108.0	1,510
7	26	16.94	33	103	1,744.8	17.47	32	104	1,816.8	17.5	32	108.0	1,887
8	27	13.98	40	98	1,369.6	14.33	39	92	1,318.7	13.9	40	104.0	1,450
8	28	13.98	40	118	1,649.1	FAILED				12.4	45	113.0	1,400

NOTE: POSITIVE (DOWNWARD) LOADS ARE OVERESTIMATED
AND NEGATIVE (UPWARD) LOADS ARE UNDERESTIMATED.
SEE TEXT FOR EXPLANATION.

KSC-DD-818-TR



LOCATION OF MLP HOLDDOWN POSTS

Figure 3-13. Location of MLP HDP's

SECTION IV

THERMAL DATA SUMMARY

4.1 MLP

MLP-1 was instrumented with eight thermocouples during the launches of STS-1, -3, -4, -5, -7, and -9. For STS-5 launch, two sets of 6- by 6-in steel plates of varying thicknesses, backed with thermal indicator coating, were exposed to direct flame impingement. Figure 4-1 shows the sensor locations and recorded measurements.

During the launches of STS-1 and -3, MLP-1 was instrumented with six calorimeters to detect and record heat rate data. Figure 4-2 shows the calorimeter locations and recorded heat rate.

4.2 FSS

The FSS was instrumented with one calorimeter located at the launch pivot fixture of the ET vent arm. Figure 4-3 shows the measurements of this calorimeter recorded during the launches of STS-3, -6, and -8.

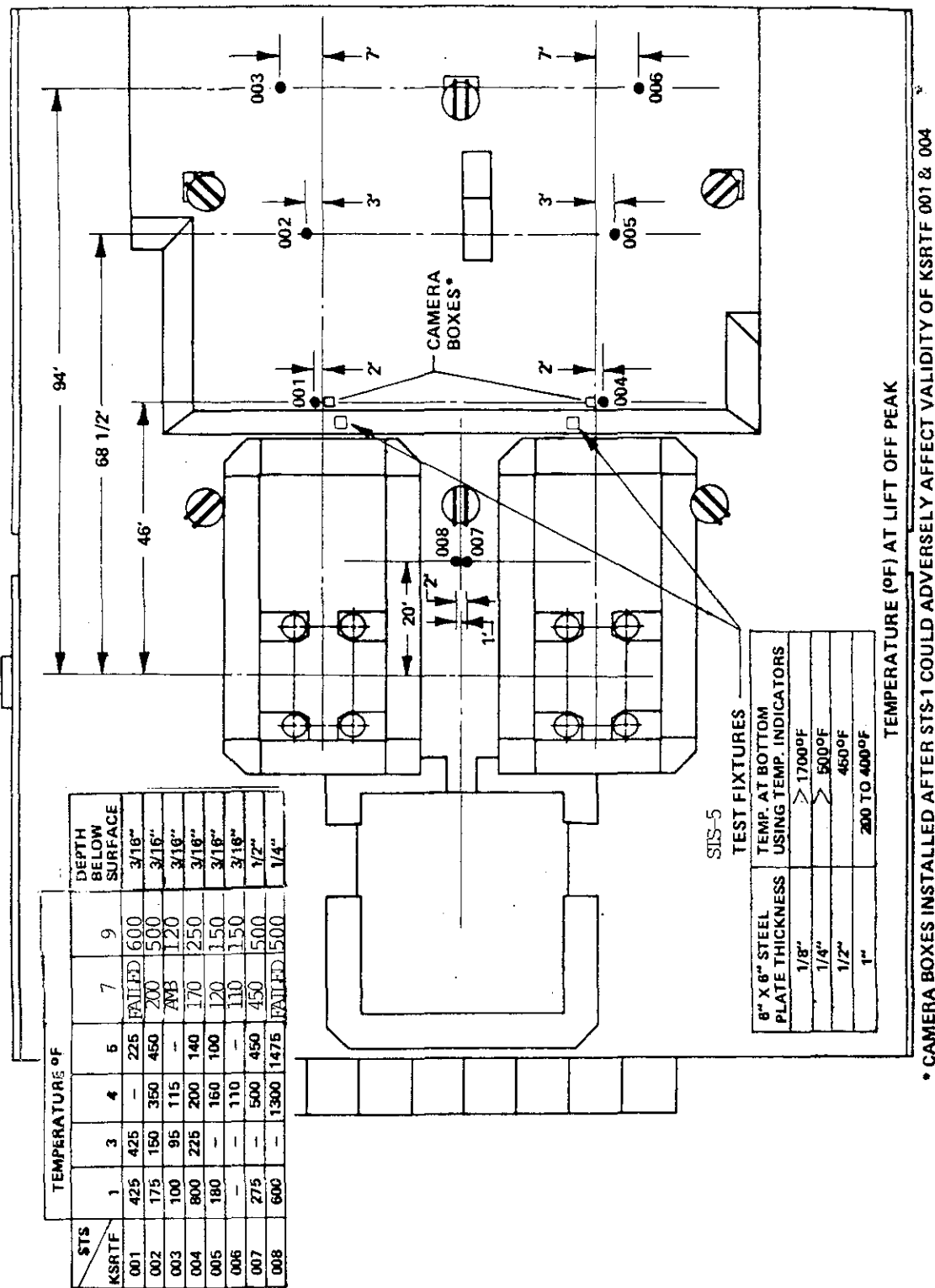


Figure 4-1. MLP-1 Thermal Data Recorded During STS-1, -3, -4, -5, -7, and -9 Launches

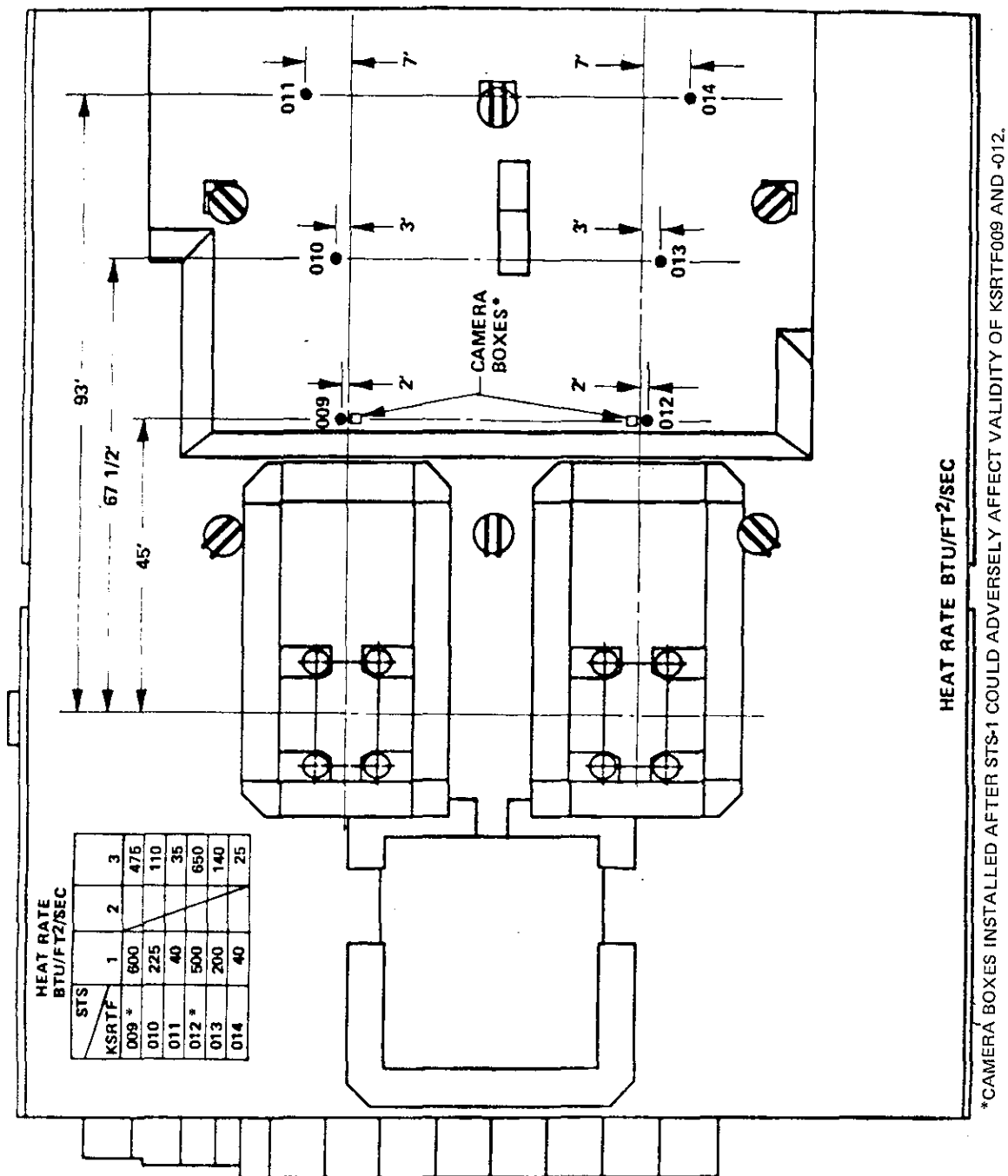
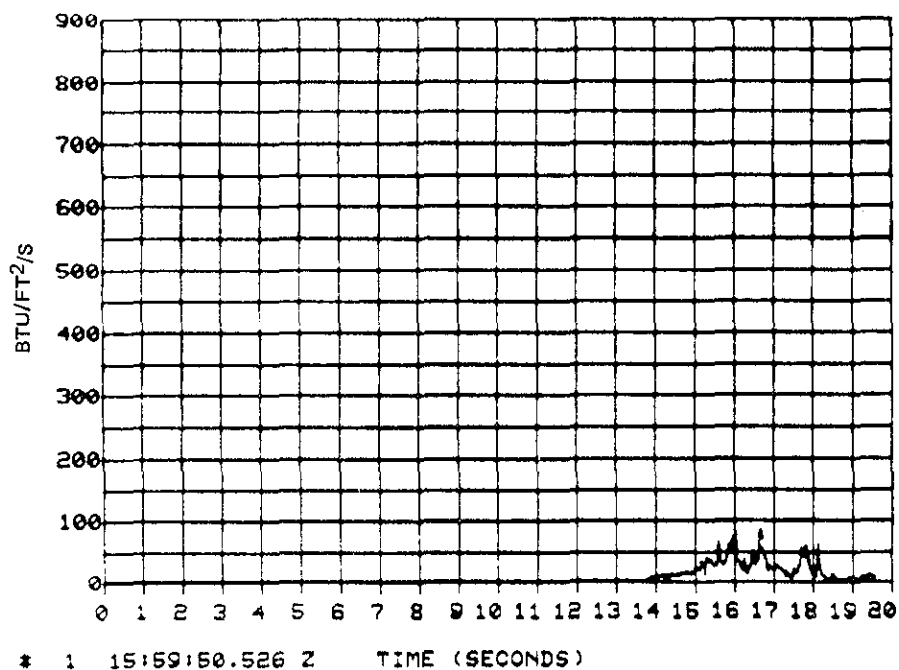


Figure 4-2. MLP-1 Heat Rate Data Recorded During STS-1 and -3 Launches

KSC-DD-818-TR

STS-3 LAUNCH TI-INS 3/22/82

KSATB001A ET HAUNCH PUT FXTR



STS-8 LAUNCH SC-INS 8/30/83

STS-6 LAUNCH TI-INS 4/4/83

KSATB001A ET VENT

KSATB001A ET VENT

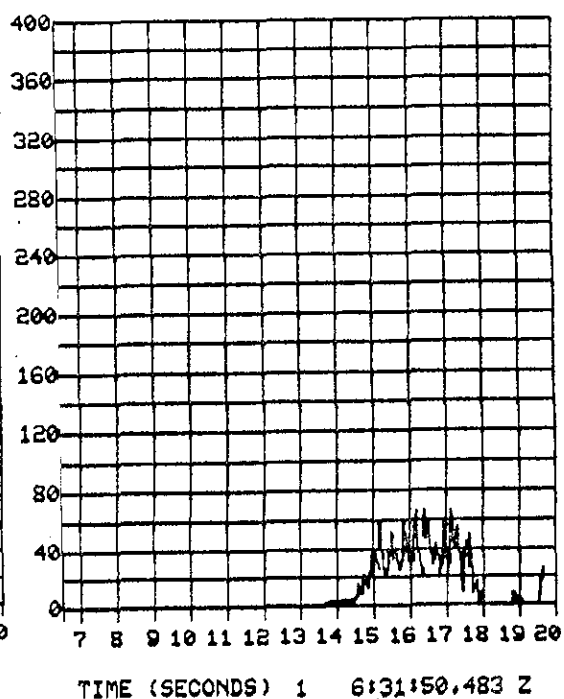
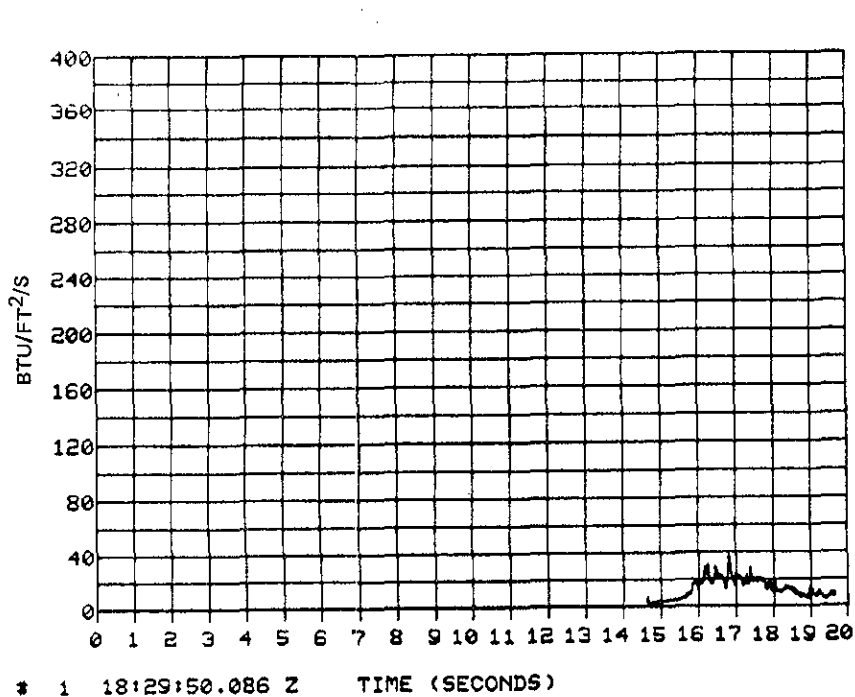


Figure 4-3. FSS Heat Rate Data Recorded During STS-3, -6, and -8 Launches

SECTION V

VIBRATION

5.1 MLP

MLP-1 was instrumented with approximately 182 vibration sensors during the launches of STS-1, -2, and -3. Data that appeared to be valid were processed and published in the documents listed in the bibliography herein. Worst-case samplings of the following elements of the MLP have been selected for this summary and are shown in the applicable figures (figures 5-1 through 5-14). Included are raw data, PD's, PSD's, and rms time histories for the following measurements:

<u>Designation</u>	<u>Location</u>	<u>Room No.</u>	<u>Direction</u>
KSRDF016A	Girder Web Stiffener	43A	Y
KSRDF017A	Girder Web Stiffener	43A	Z
KSRDF021A	6 ft Above Deck B Floor (on wall)	36AB	Z
KSRDF047A	11 ft Above Deck B Floor (on wall)	40AB	X
KSRDF078A	Centerline Bottom Flange Deck 0 Ceiling Beam	7A	Z
KSRDF079A	Centerline Bottom Flange Deck 0 Ceiling Beam	9A	Z
KSRDF119A	Center Floor Beam	41B	X
KSRDF120A	Center Floor Beam	41B	Y
KSRDF037A	Truss T ₂ Vertical	8A	Z
KSRDF038A	Truss T ₁ Vertical	7A	Z
KSRDF080A	Truss T ₂ Top Chord	10A	Z
KSRDF081A	Truss T ₁ Top Chord	10A	Z
KSRDF159A	Floor Framing Stringer (E) (spring-isolated floor)	9B	Z
KSRDF160A	Floor Framing Stringer (W) (spring-isolated floor)	9B	Z

A comparative summary of the vibration inside MLP-2, previously published as appendix E in KSC-DD-712-TR, follows (5.1.1 and 5.1.2). Not included but recommended for additional information is appendix A of KSC-DD-677-TR, which contains data validation criteria, calculated rms displacements, and zoom plots of significant PSD's.

5.1.1 VIBRATION INSIDE MLP-2. This summary of vibration measurements inside MLP-2 during STS-6 launch presents data acquired for the lift-off peak period. Six sensors installed on three structurally different MLP-2 components were used in the analysis. Measurements established that a fundamental vertical MLP-2 vibration mode (after vehicle lift-off) has a natural frequency near 4.4 Hz.

Since STS-6 was the first Shuttle launched from MLP-2, a comparison is made with similar vibration data obtained on MLP-1 during STS-2 and STS-3 launches. This comparison is used to evaluate the new digital Data Acquisition System (DAS) installed in MLP-2.

Six vibration sensors (KSRDG001A through -006A) were installed for STS-6 on MLP-2 deck 0 beams (two), T-2 truss top chord (two), and on deck B floor beams (two). Chosen locations correspond to MLP-1 sensors KSRDF078A and -079A on deck 0 beams, KSRDF080A and -082A on T-2 truss top chord, and KSRDF128A and -129A on deck B floor beams. All MLP-2 sensors were oriented in vertical (Z) direction. It was established that on the MLP-1, sensor KSRDF082A was mistakenly oriented in Y direction; thus, only five sensors were available for data comparison between MLP-1 and MLP-2 vibration environments.

Output of each MLP-2 sensor was processed three times. Each time, a different set of processing parameters was used in order to define the entire frequency range of data and to obtain an optimal resolution from a relatively short record. Governing parameters, such as F_{\max} = Nyquist frequency and ΔF = resolution frequency, are shown on corresponding data plots. In order to distinguish between various computer files containing processed PSD's, the last character in measurement designation (A) has been made variable (A, B, C, etc.), and these new designations appear in figure 5-15 and on all plots that follow in 5.1. Most meaningful comparisons are obtained between similar measurements processed using the same set of parameters. However, in a few cases of STS-2 and STS-3 data processed earlier, different processing parameters were used, mainly in resolution frequencies, which should be considered when making comparisons.

Figure 5-15 presents data processing parameters and calculated rms displacements for all MLP-2 vibration measurements. Figure 5-15 does not include KSRDG001A through -004A processing case for F_{\max} = 5,000 Hz because low data resolution (ΔF = 4.88 Hz) makes this case unsuitable for displacement calculations. The user is referred to the KSC-DD-677-TR (February 1983) containing a description of the technique used to calculate rms displacements from measured acceleration PSD's and for validation criteria. Displacement data from table E-1, KSC-DD-677-TR appendix A, and some STS-2 data (not previously published) are included into comparisons of MLP-1 and MLP-2 vibration environments presented on figures 5-16 through 5-23.

Figures 5-24 through 5-26 present STS-6 vibration environment on MLP-2 deck 0 beams recorded by KSRDG001A and -002A sensors. Both sensors recorded essentially the same and a very severe vibration environment in spite of their different locations. RMS accelerations are 23.5 and 27.7 g (0 to 2 kHz), and rms displacements (0.77 and 0.72 in) indicate that peak displacements (at 99% CL) approach 1.5-in amplitude.

Figures 5-27 through 5-29 present STS-6 vibration environment on two adjacent members of T-2 truss top chord, recorded by KSRDG003A and -004A. These truss members also serve as deck 0 beam supports. Vibration recorded by KSRDG003A located in line with west SRB is slightly more severe than in the midspan of the truss. Also, rms displacement (0.42 in) is greater than that at midspan (0.35 in), indicating that some asymmetric truss modes were excited. The vehicle roll maneuver could be inducing an asymmetric load on the T-2 truss.

Figures 5-30 and 5-31 present STS-6 vibration environment on two deck B floor beams recorded by KSRDG005A and -006A. Both sensors recorded essentially the same vibration environment on floor beams spaced 24 ft apart. These beams have a distinct resonance at 15.6 Hz and about 0.2 in rms displacements associated with local bending of the beams. The total rms displacements are between 0.49 and 0.62 in.

Figure 5-32, left frame, presents PSD's obtained from all MLP-2 vibration sensors when data were processed at the same resolution of 0.781 Hz. All data have a peak at 4.69 Hz, indicating that a fundamental MLP-2 resonance is near this frequency. The right frame on figure 5-24, where data from two measurements have a resolution of 0.39 Hz, shows that a more accurate figure for the MLP-2 resonance is 4.4 Hz.

5.1.2 MLP-1 AND MLP-2 VIBRATION DATA COMPARISON. In an effort to evaluate the new permanent measurement system (PMS), vibration measurements on MLP-2 (STS-6) recorded with the new system were compared to corresponding data recorded on MLP-1 (STS-2 and -3). These comparisons and pertinent comments are presented on figures 5-16 through 5-23.

Comparison of deck 0 beam and T-2 truss top chord vibration measurements, figures 5-16 and 5-18, shows that the effect of baseline drift (STS-3, KSRDF079A and KSRDF080A) extends up to 25 to 30 Hz. New PMS measurements do not show any effect of baseline drift. Perhaps this could be attributed to different sensors (piezo-resistive versus piezo-electric type) and to different cables used with these sensors.

Figure 5-17 shows that above 30 Hz, STS-6 data on deck 0 are higher than that of STS-3, while rms displacements, governed by the very low frequency components, remain about the same.

The best data correlation is obtained for measurements on deck B floor beams shown on figures 5-19 through 5-22 and figure 5-23, left frame. Here, good correlation exists within the entire examined range, 0 to 250 Hz, figures 5-20

KSC-DD-818-TR

through 5-22. The fundamental beam resonance frequency of MLP-2 is slightly higher (15.6 Hz) than that of MLP-2 (14.8 Hz), possibly because of different local dead loads on these beams.

Figure 5-23, right frame, presents data on deck B floor beams pertinent to comparison on MLP-1 and MLP-2 fundamental resonances. Both MLP's have a fundamental resonance near 4.4 to 4.6 Hz. However, on deck B, MLP-1 has also a peak around 7.3 Hz, which on MLP-2 is observed only in deck 0 to T-2 truss data. This indicates another MLP mode, possibly local, which is different on each MLP (see figure 5-16 for comparison).

In summary, valid vibration data recorded by fm DAS on MLP-1 and pcm DAS on MLP-2 correlate well in most examined cases. Data recorded by fm DAS often exhibited a baseline drift, which results in too high and invalid PSD amplitudes within 0 to 25 Hz range. MLP-2 data recorded by pcm DAS has a better quality than MLP-1 data, and it is not subject to a malfunction resulting in baseline drift. STS-6 MLP-2 vibration levels are slightly higher than those of MLP-1 (STS-2 and STS-3), but rms displacements governed by PSD components below 5 Hz are lower than on MLP-1.

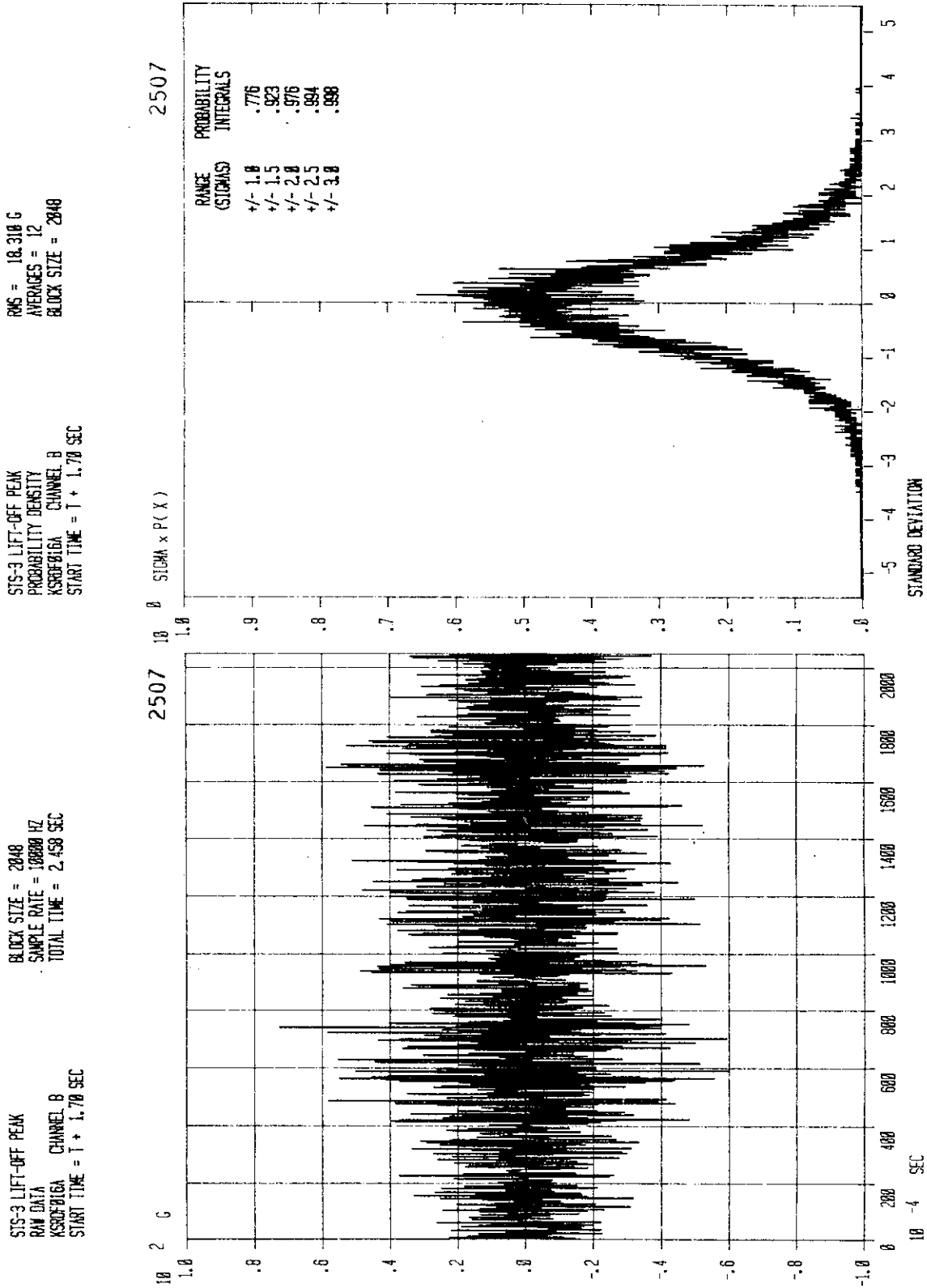


Figure 5-1. Room 43A - Girder Web Stiffener, Y Direction (Sheet 1 of 2)

KSC-DD-818-TR

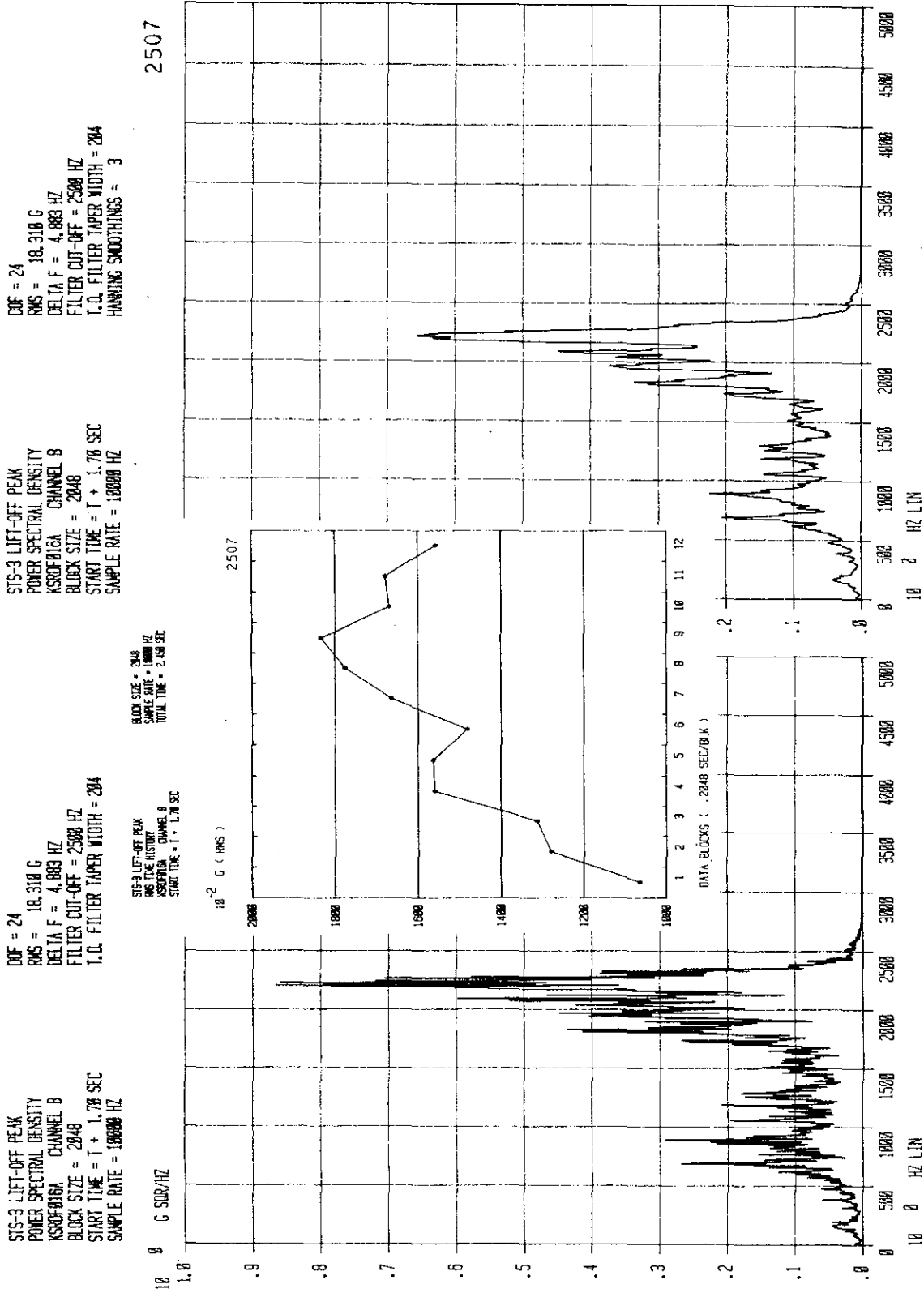


Figure 5-1. Room 43A - Girder Web Stiffener, Y Direction (Sheet 2 of 2)

STS-3 LIFT-OFF PEAK
RAW DATA
KSC00017A CHANNEL C
START TIME = 1 + 1.70 SEC

BLOCK SIZE = 2048
SAMPLE RATE = 10000 HZ
TOTAL TIME = 2.450 SEC

STS-3 LIFT-OFF PEAK
PROBABILITY DENSITY
KSC00017A CHANNEL C
START TIME = 1 + 1.70 SEC
RMS = 14.884 G
AVERAGES = 12
BLOCK SIZE = 2048

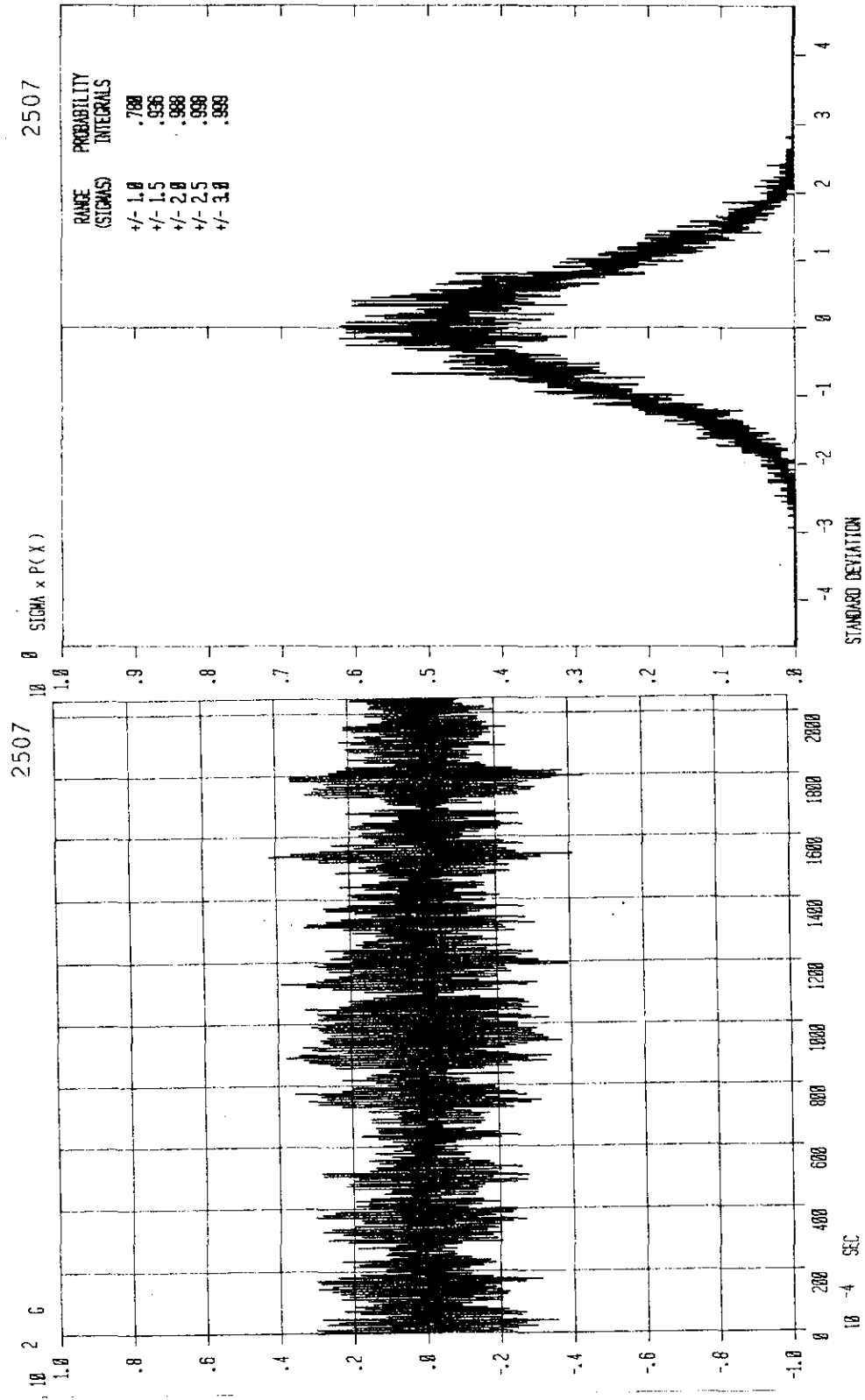


Figure 5-2. Room 43A - Girder Web Stiffener, Z Direction (Sheet 1 of 2)

KSC-DD-818-TR

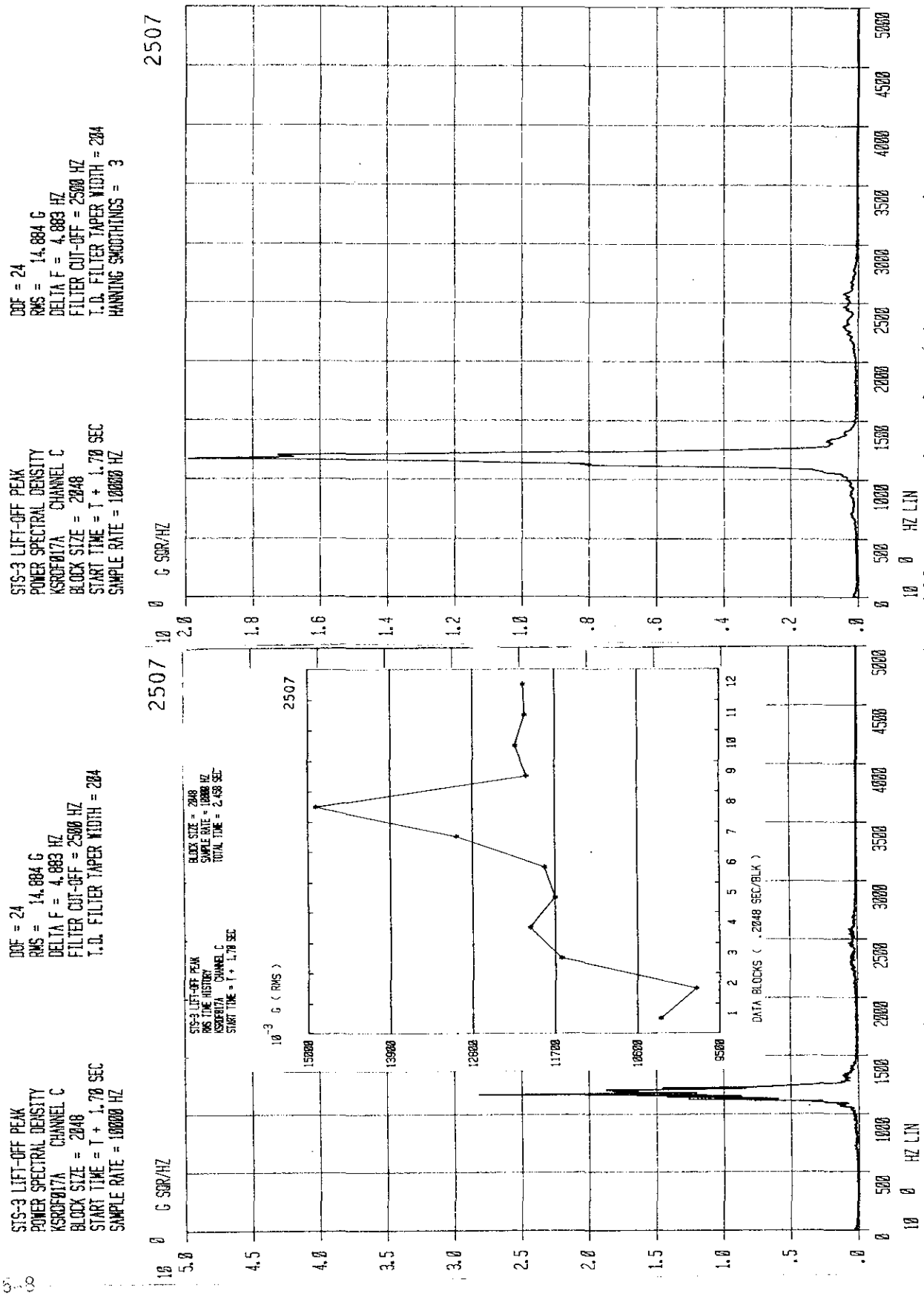


Figure 5-2. ROOM 45A - Girder Web Stiffener, Z Direction (Sheet 2 of 2)

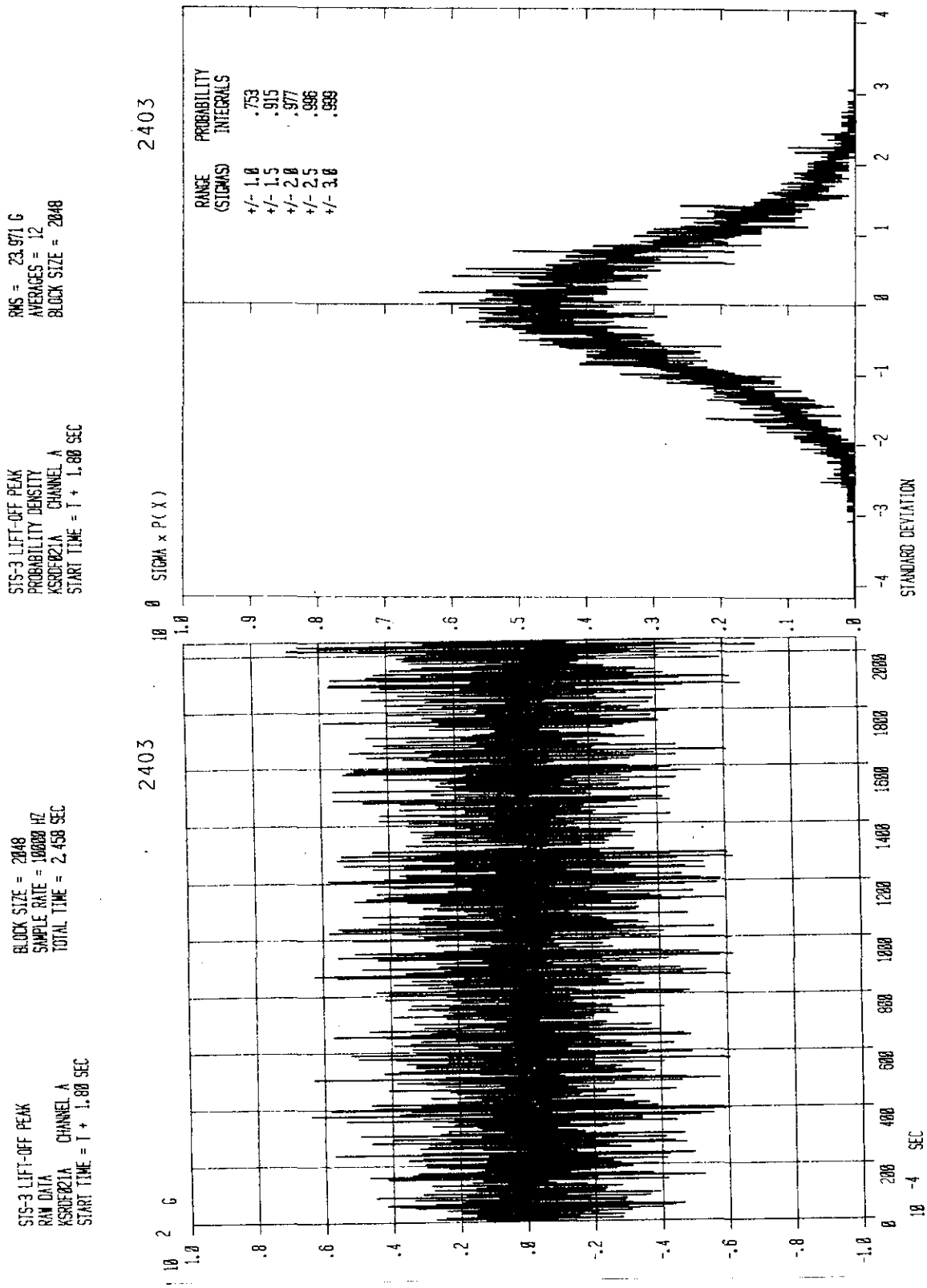


Figure 5-3. Room 36AB - Above Deck B Floor (6 ft), Z Direction (Sheet 1 of 2)

KSC-DD-818-TR

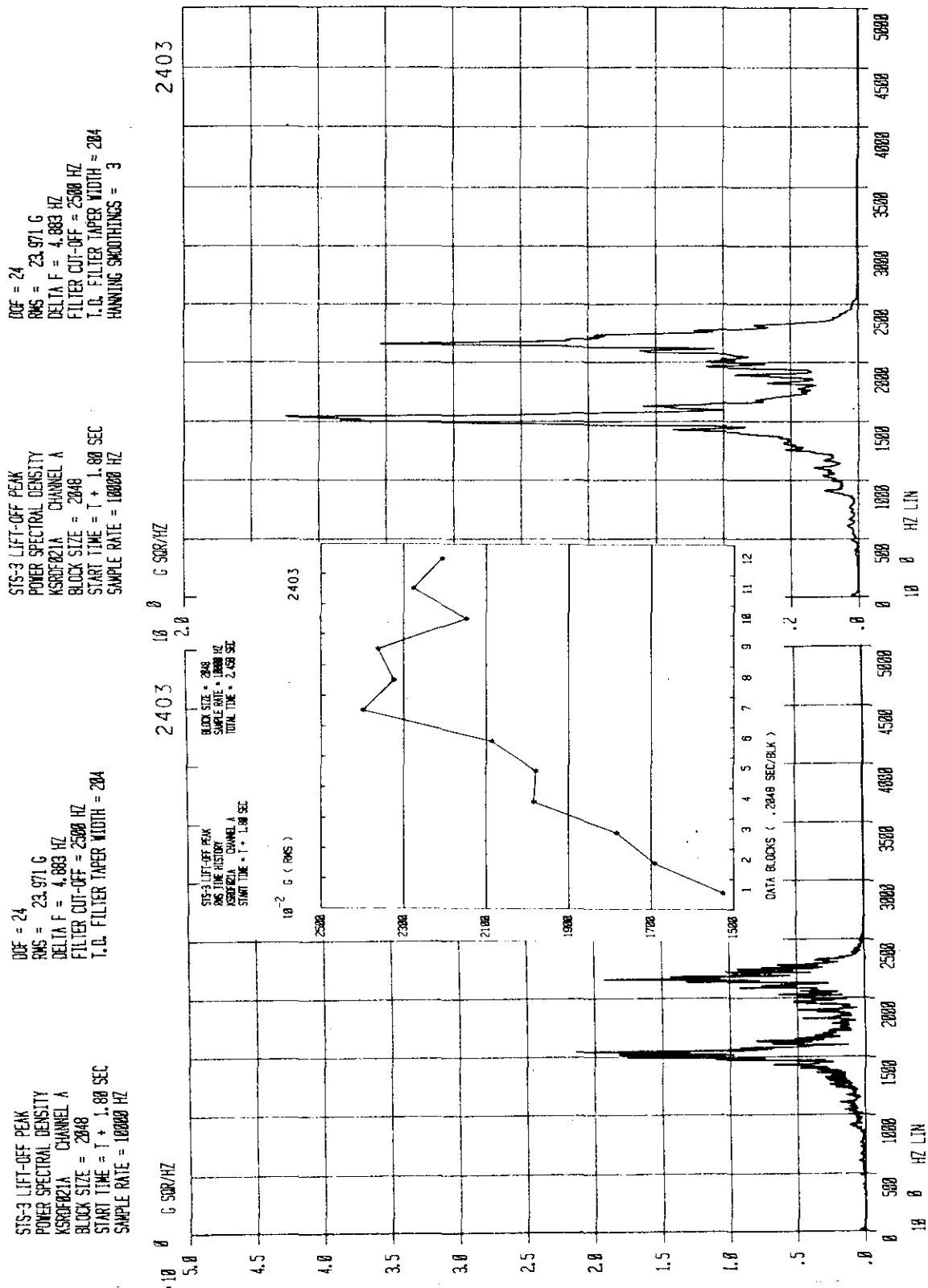


Figure 5-3. Room 36AB - Above Deck 3 Floor (6 ft), Z Direction (Sheet 2 of 2)

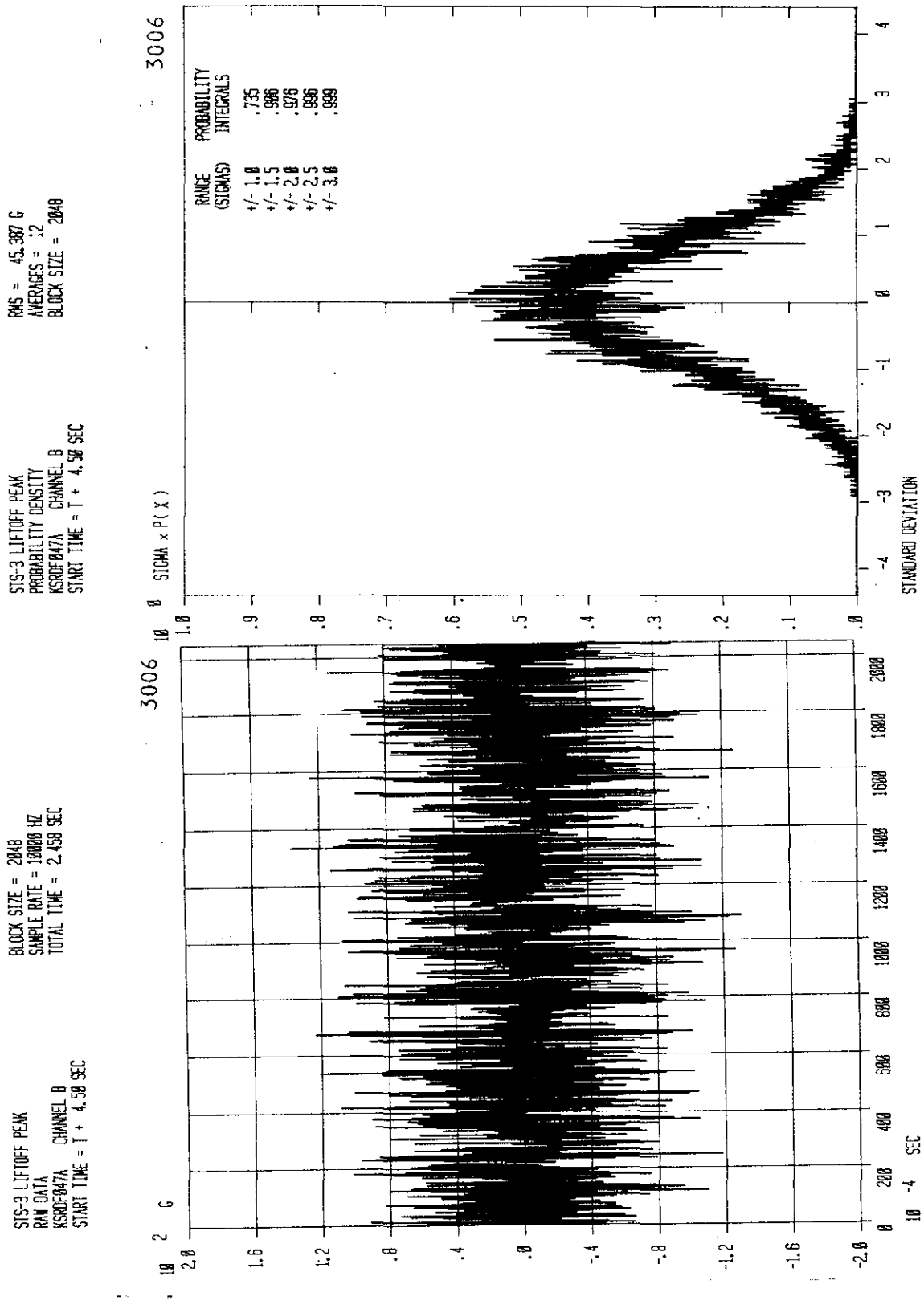


Figure 5-4. Room 40AB - Above Deck B Floor (11 ft), X Direction (Sheet 1 of 2)

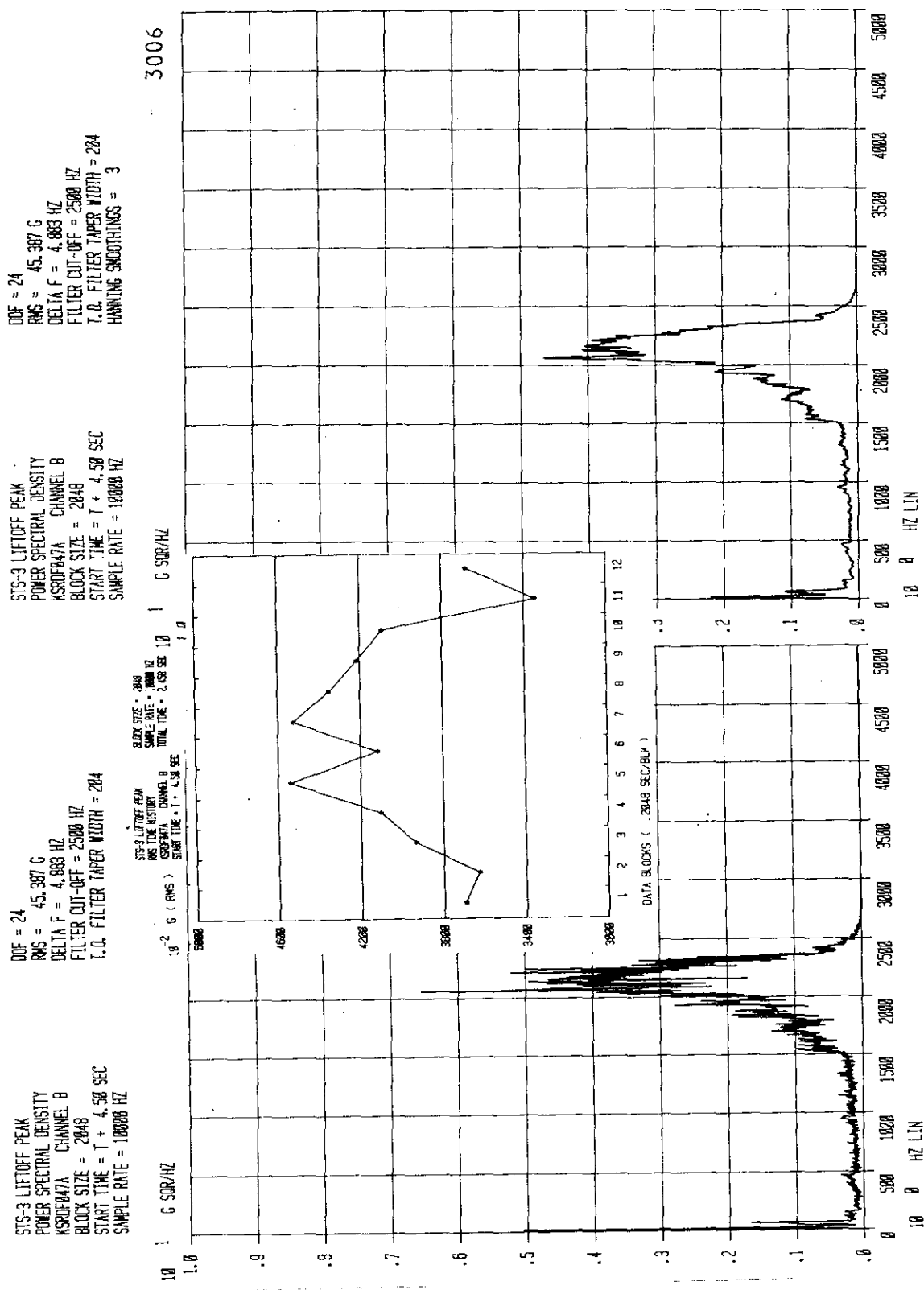


Figure 5-4. Room 40AB - Above Deck B Floor (.11 ft), X Direction (Sheet 2 of 2)

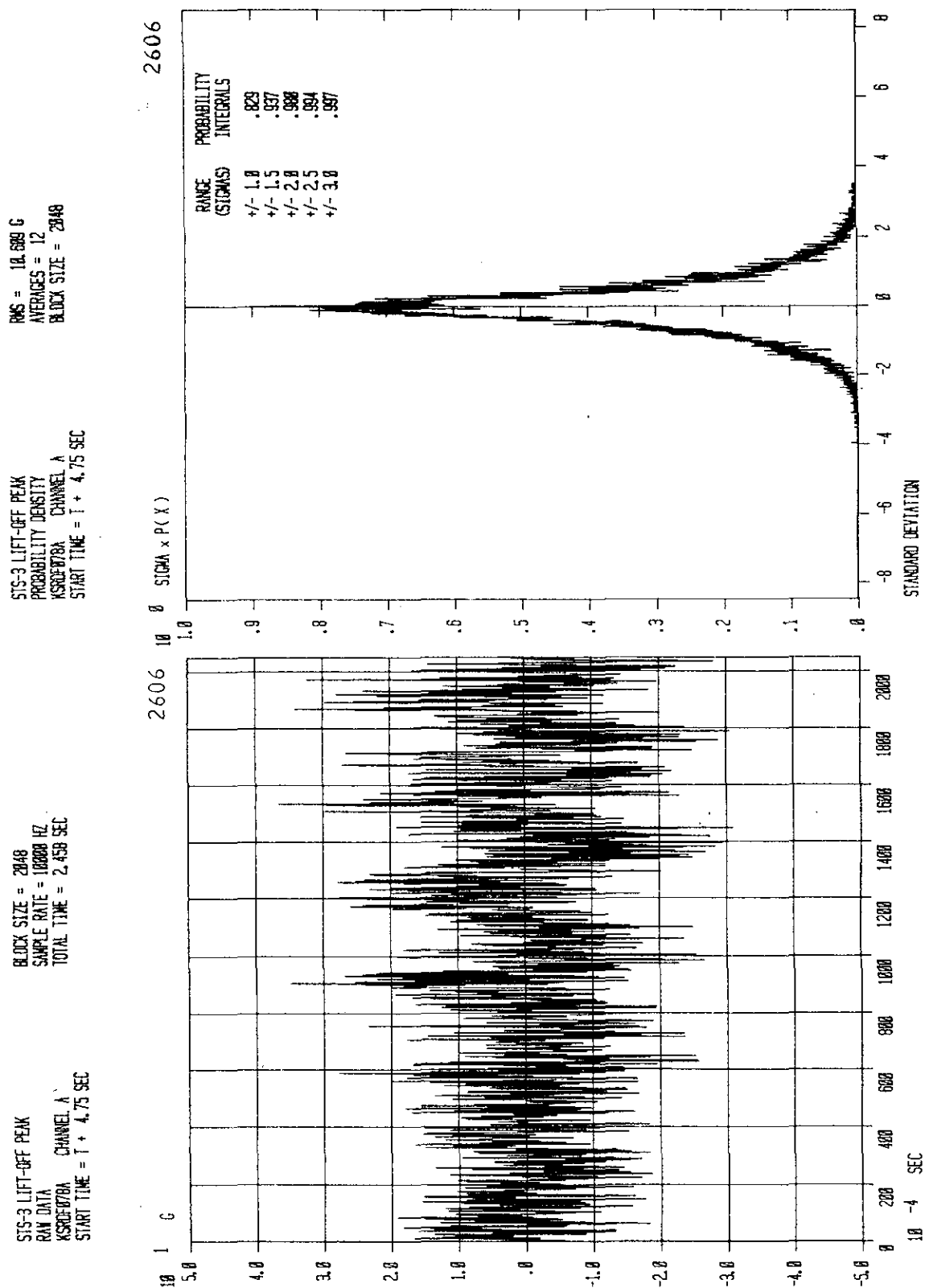


Figure 5-5. Room 7A - CL Bottom Flange Deck 0 Beam, Z Direction (Sheet 1 of 2)

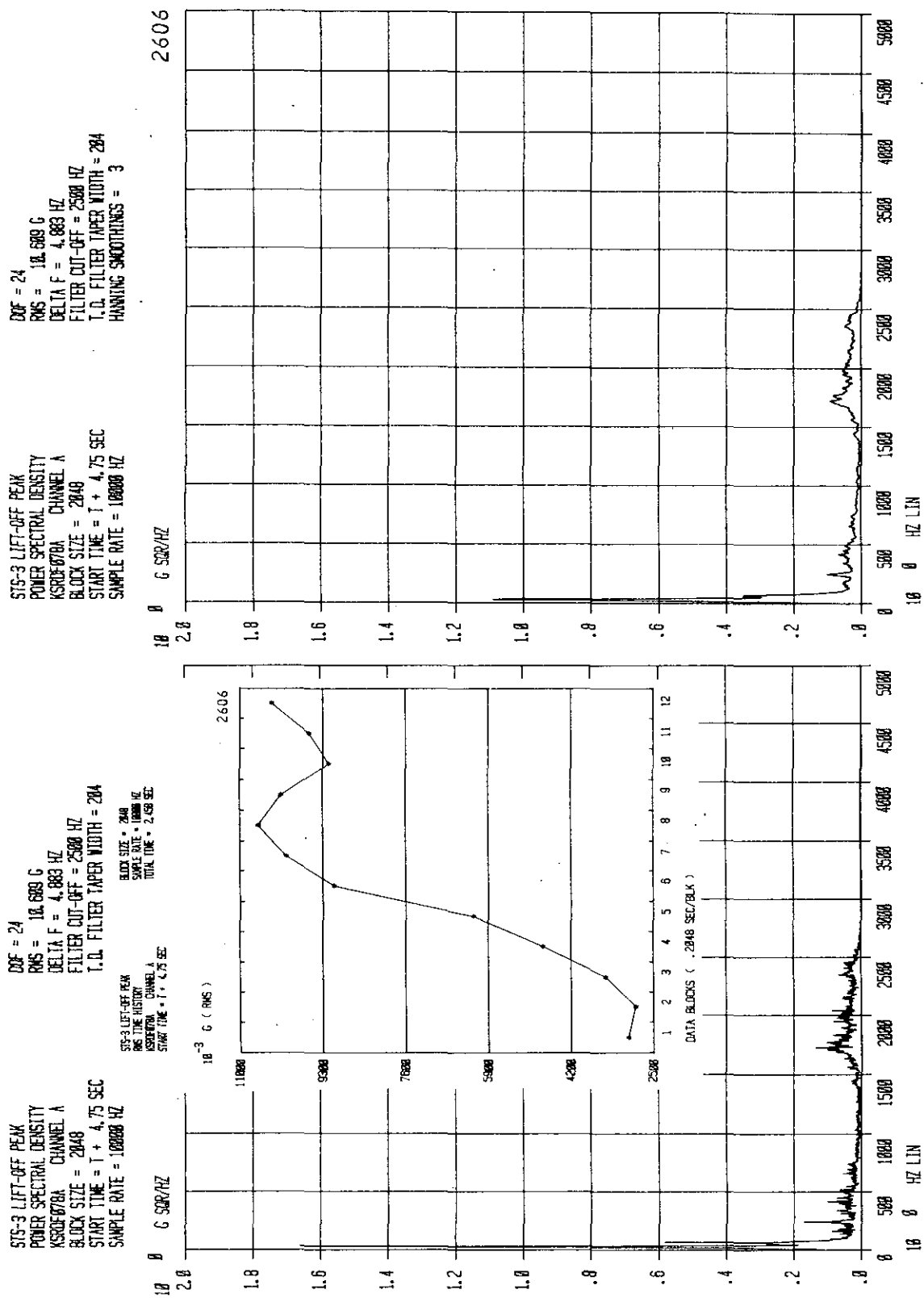


Figure 5-5. Room 7A - C_L Bottom Flange Deck 0 Beam, Z Direction (Sheet 2 of 2)

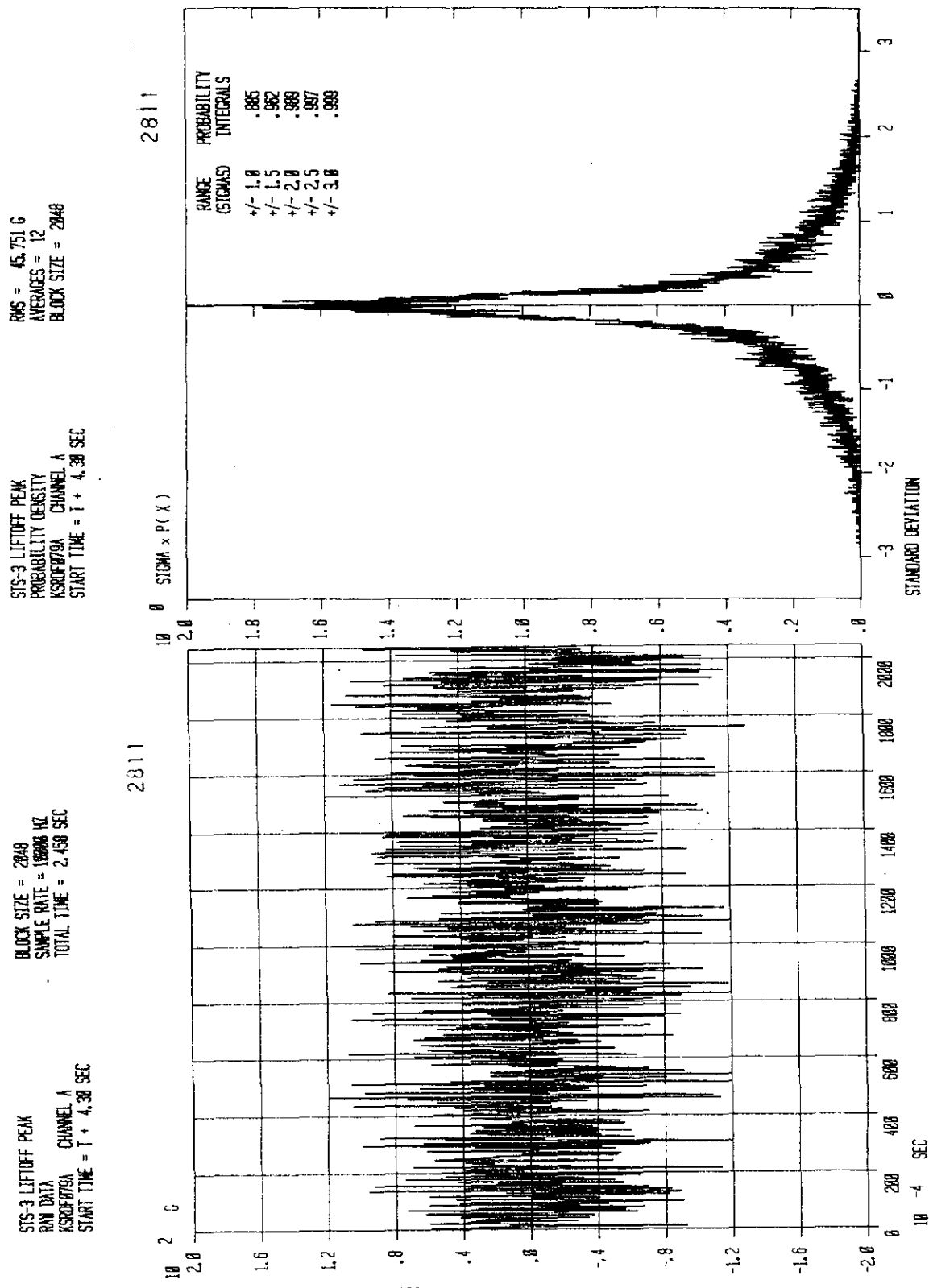


Figure 5-6. Room 9A - CL Bottom Flange Deck 0 Beam, Z Direction (Sheet 1 of 2)

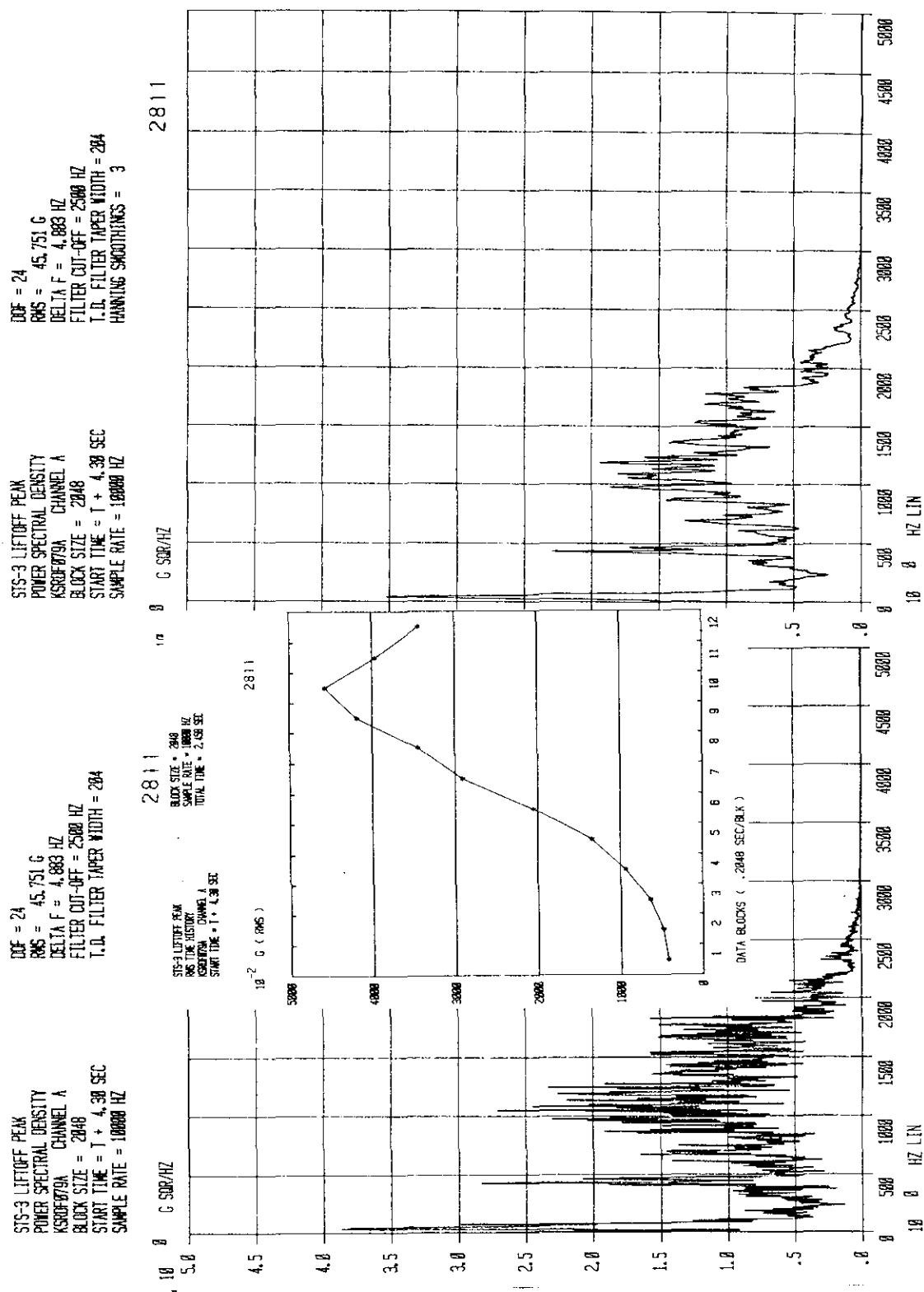


Figure 5-6. Room 9A - CL Bottom Flange Deck 0 Beam (Sheet 2 of 2)

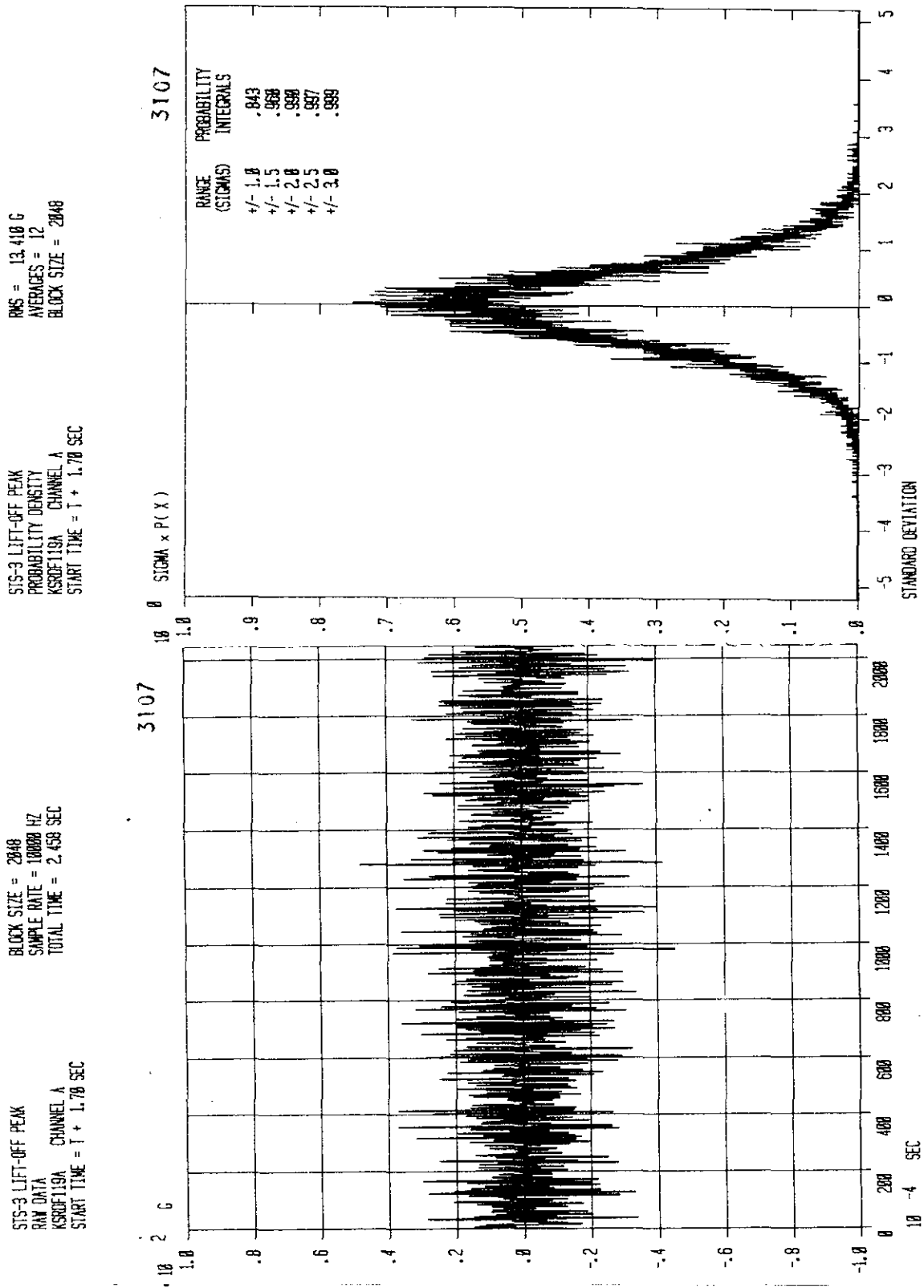


Figure 5-7. Room 41B - Center Floor Beam, X Direction (Sheet 1 of 2)

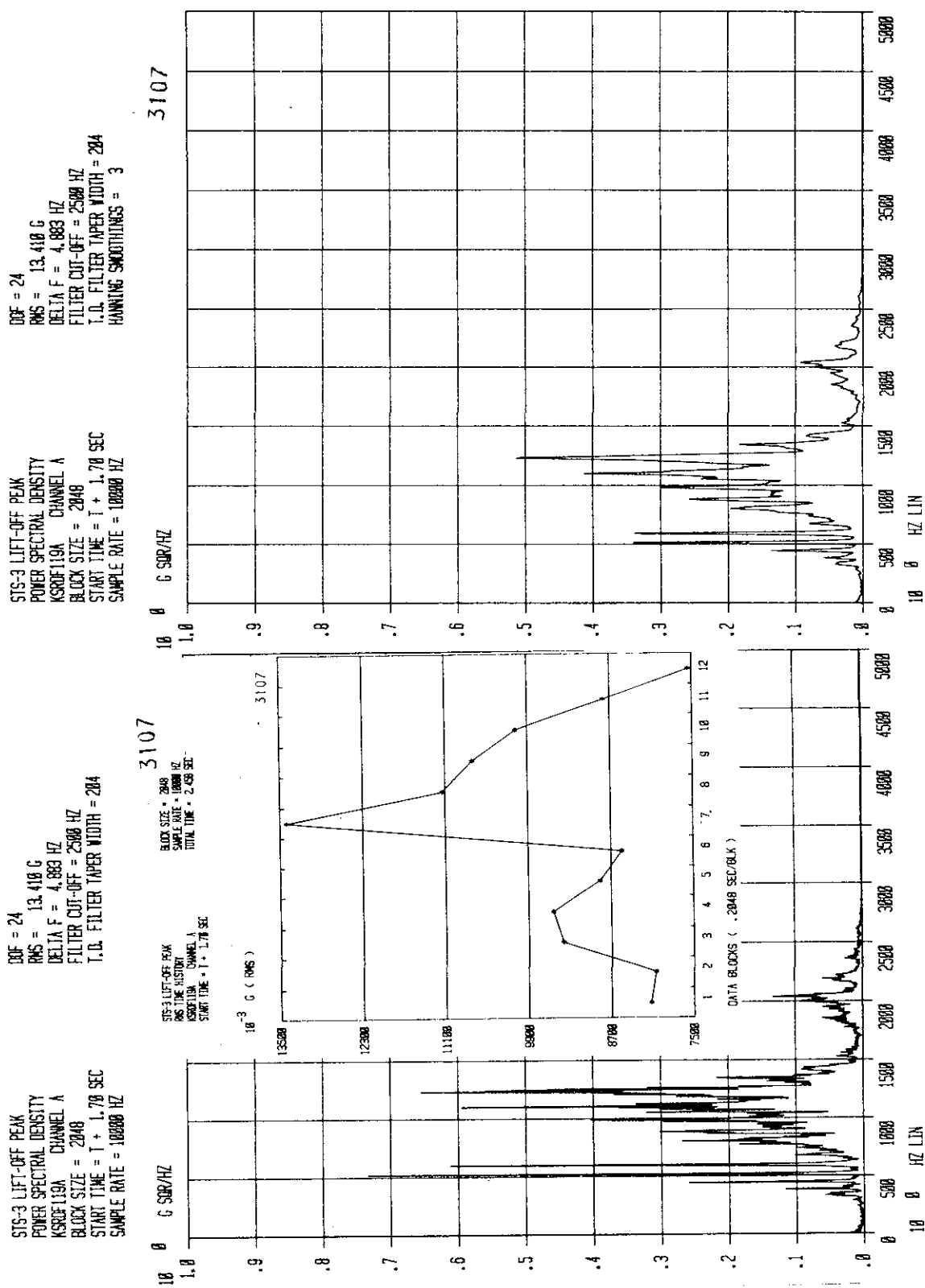


Figure 5-7. Room 41B - Center Floor Beam, X Direction (Sheet 2 of 2)

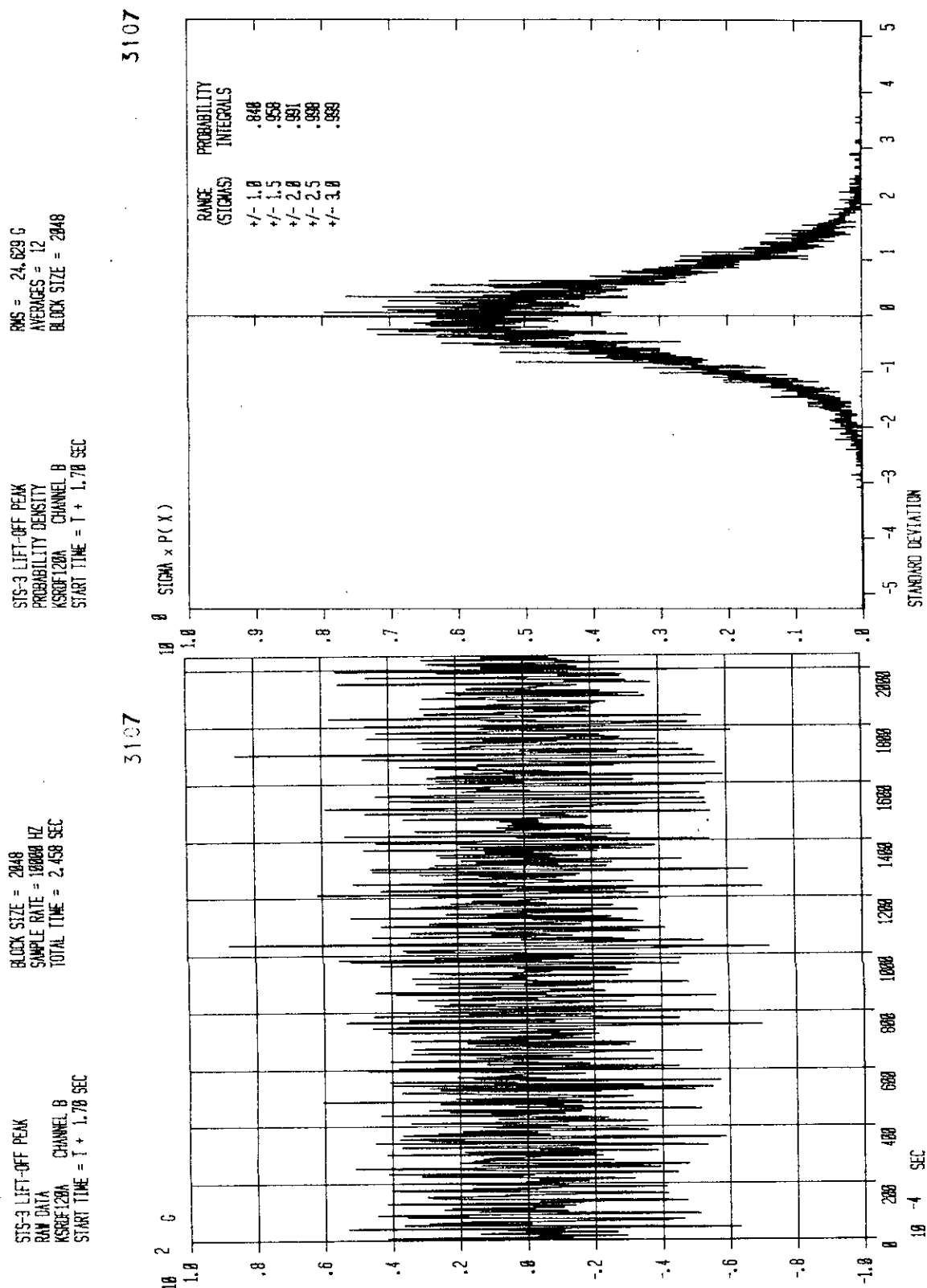


Figure 5-8. Room 41B - Center Floor beam, Y Direction (Sheet 1 of 2)

KSC-DD-818-TR

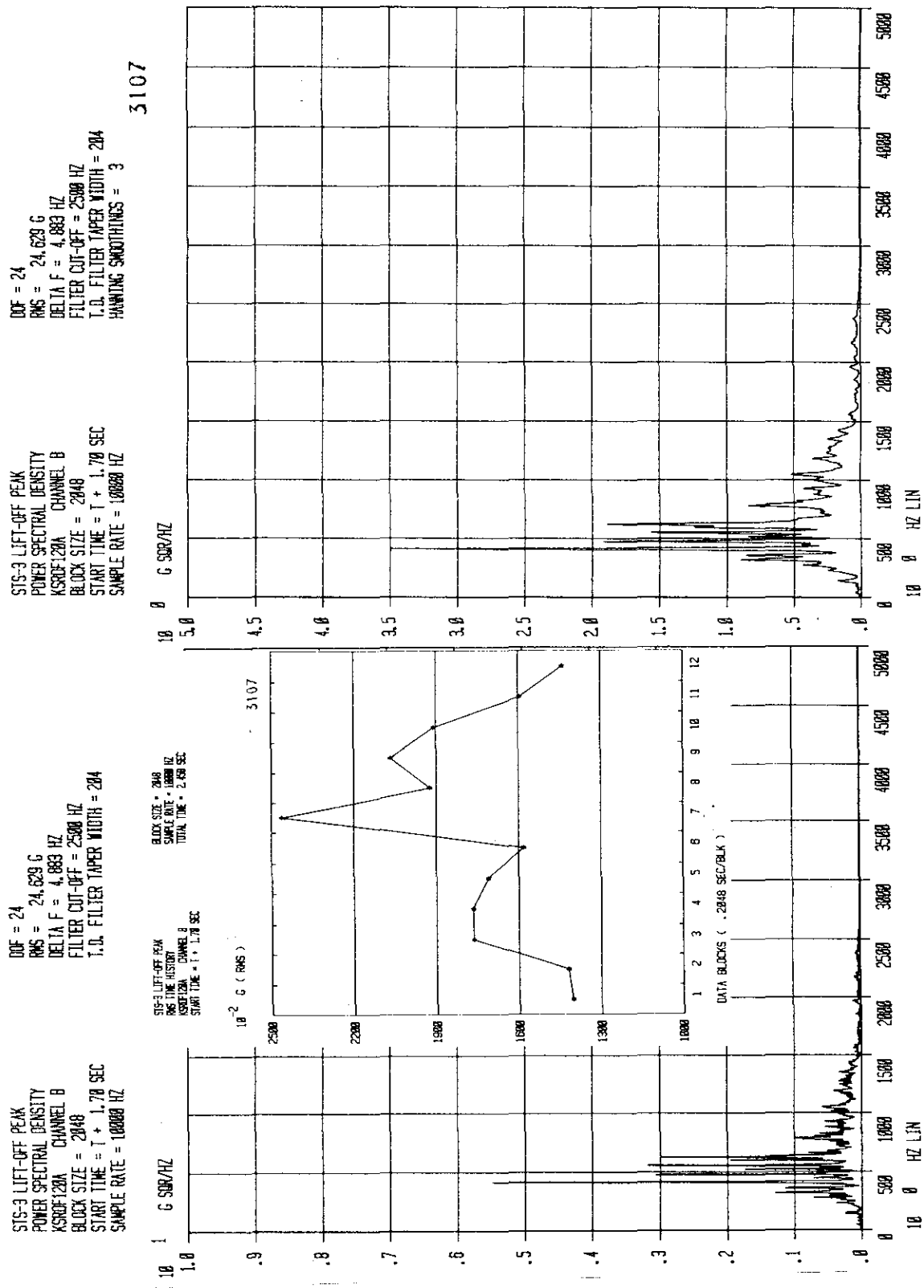


Figure 5-8. Room 41B - Center Floor beam, Y Direction (Sheet 2 of 2)

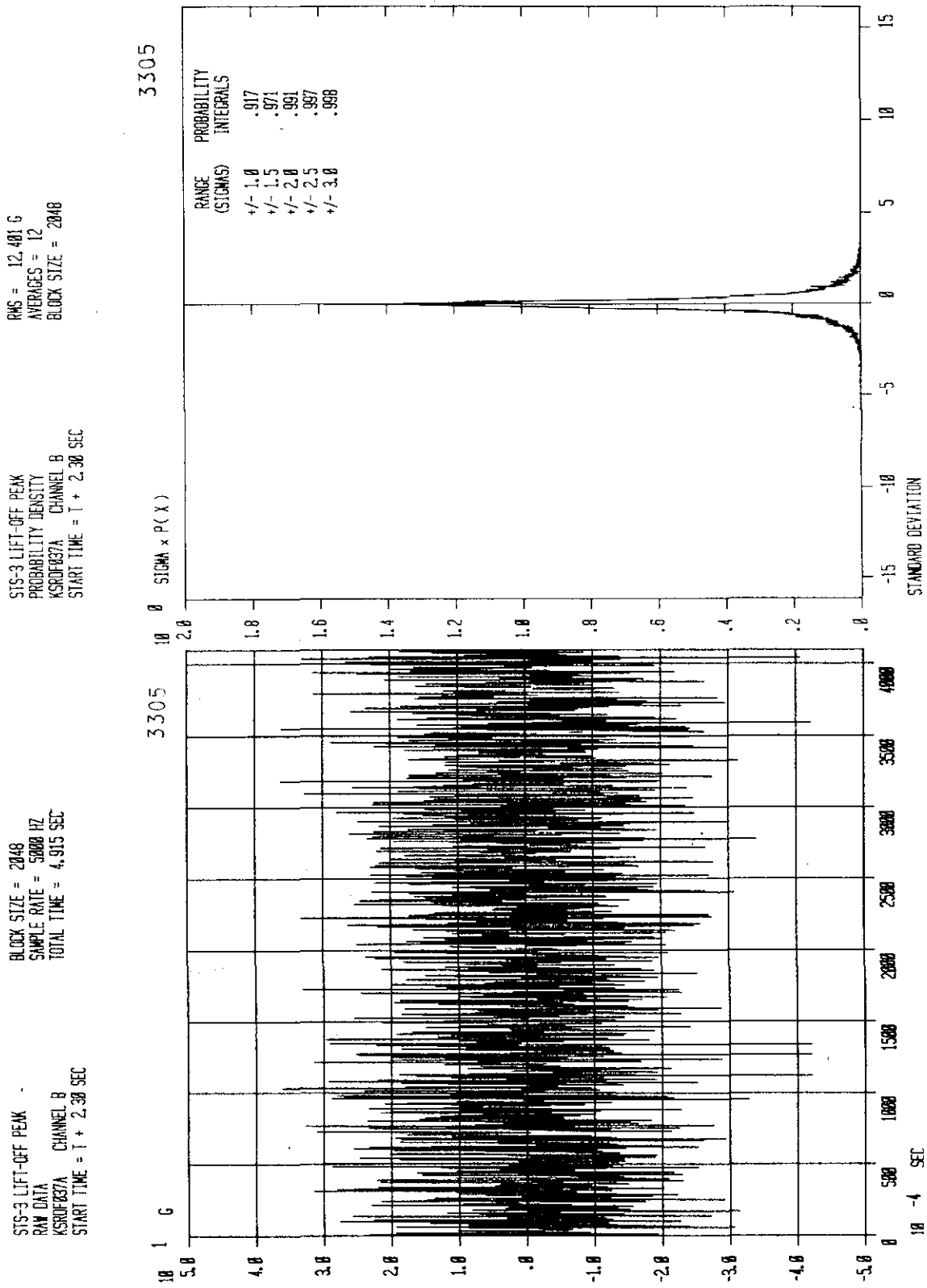


Figure 5-9. Room 8A - Truss T2 Vertical, Z Direction (Sheet 1 of 2)

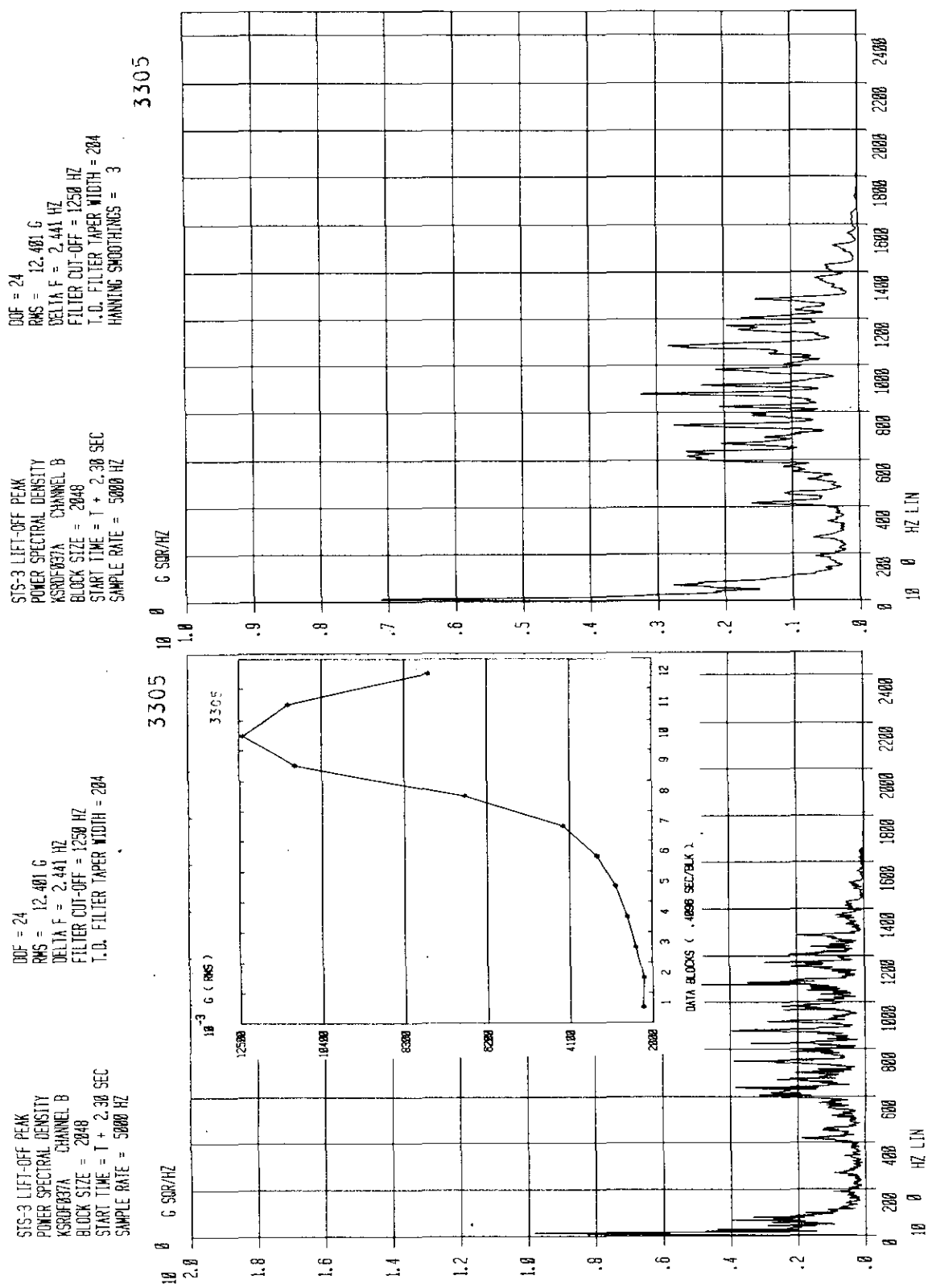


Figure 5-9. Room 8A - Truss T2 Vertical, Z Direction (Sheet 2 of 2)

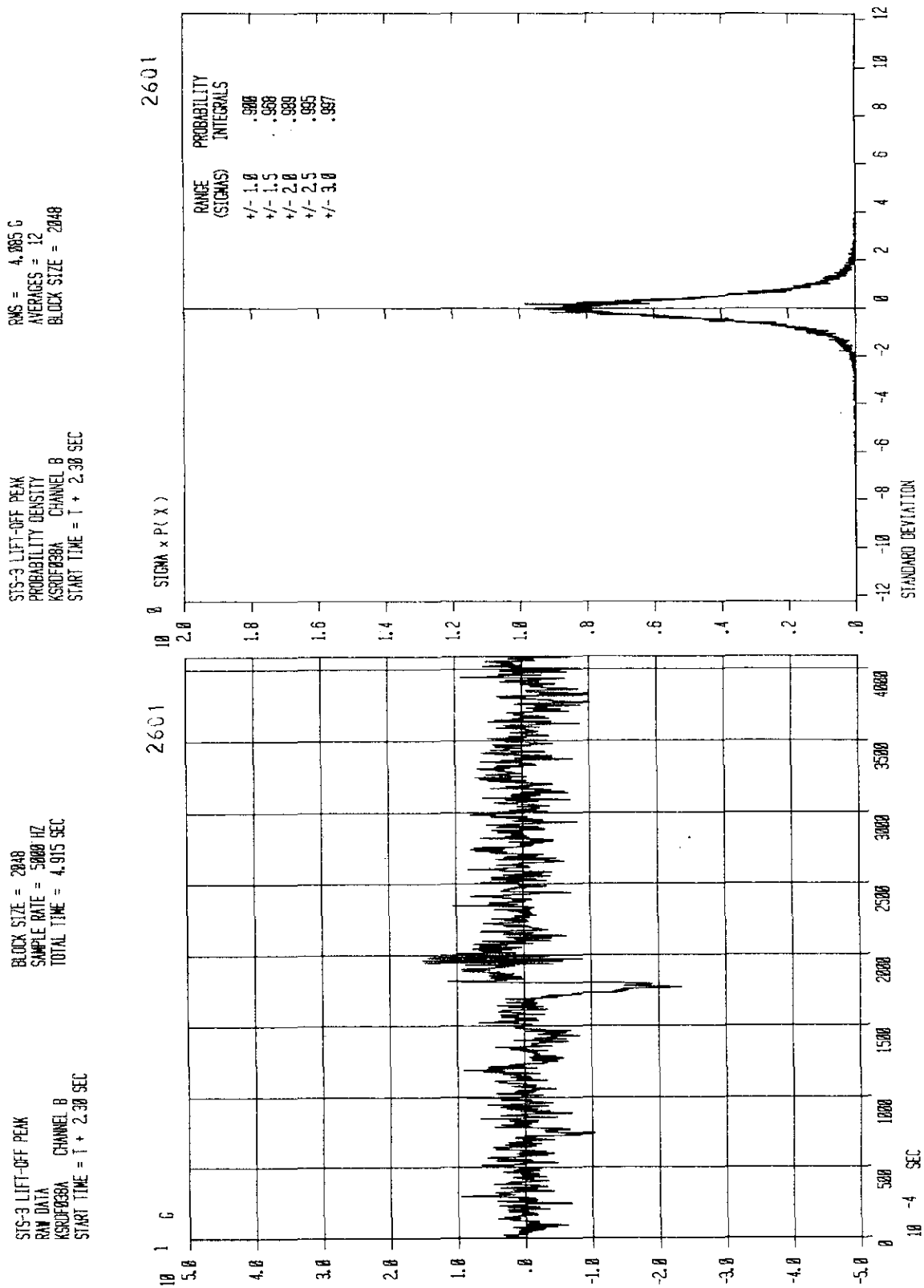


Figure 5-10. Room 7A - Truss T1 Vertical, Z Direction (Sheet 1 of 2)

KSC-DD-818-TR

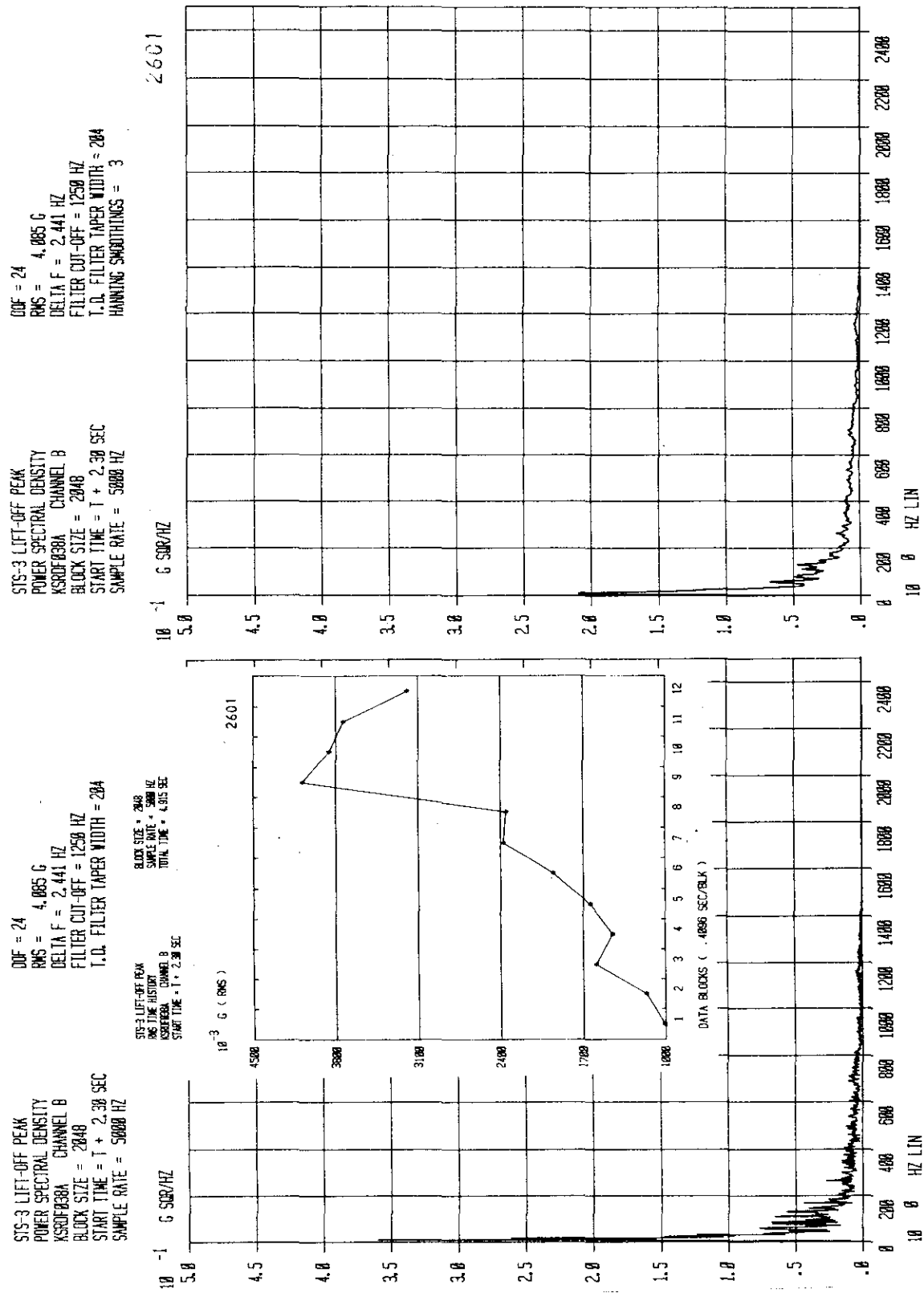


Figure 5-10. Room 7A - Truss T1 Vertical, Z Direction (Sheet 2 of 2)

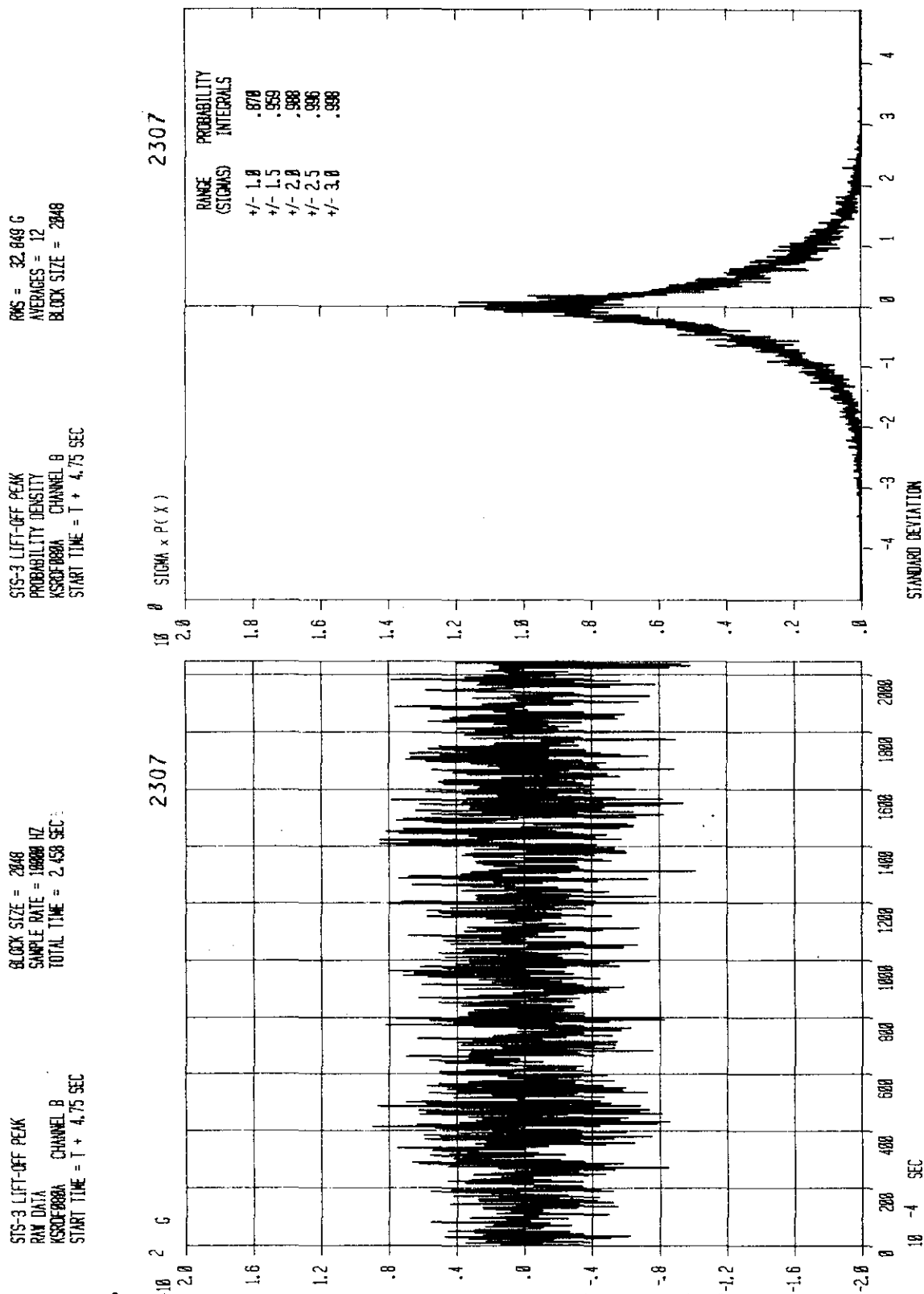


Figure 5-11. Room 10A - Truss T₂ Top Chord, Z Direction (Sheet 1 of 2)

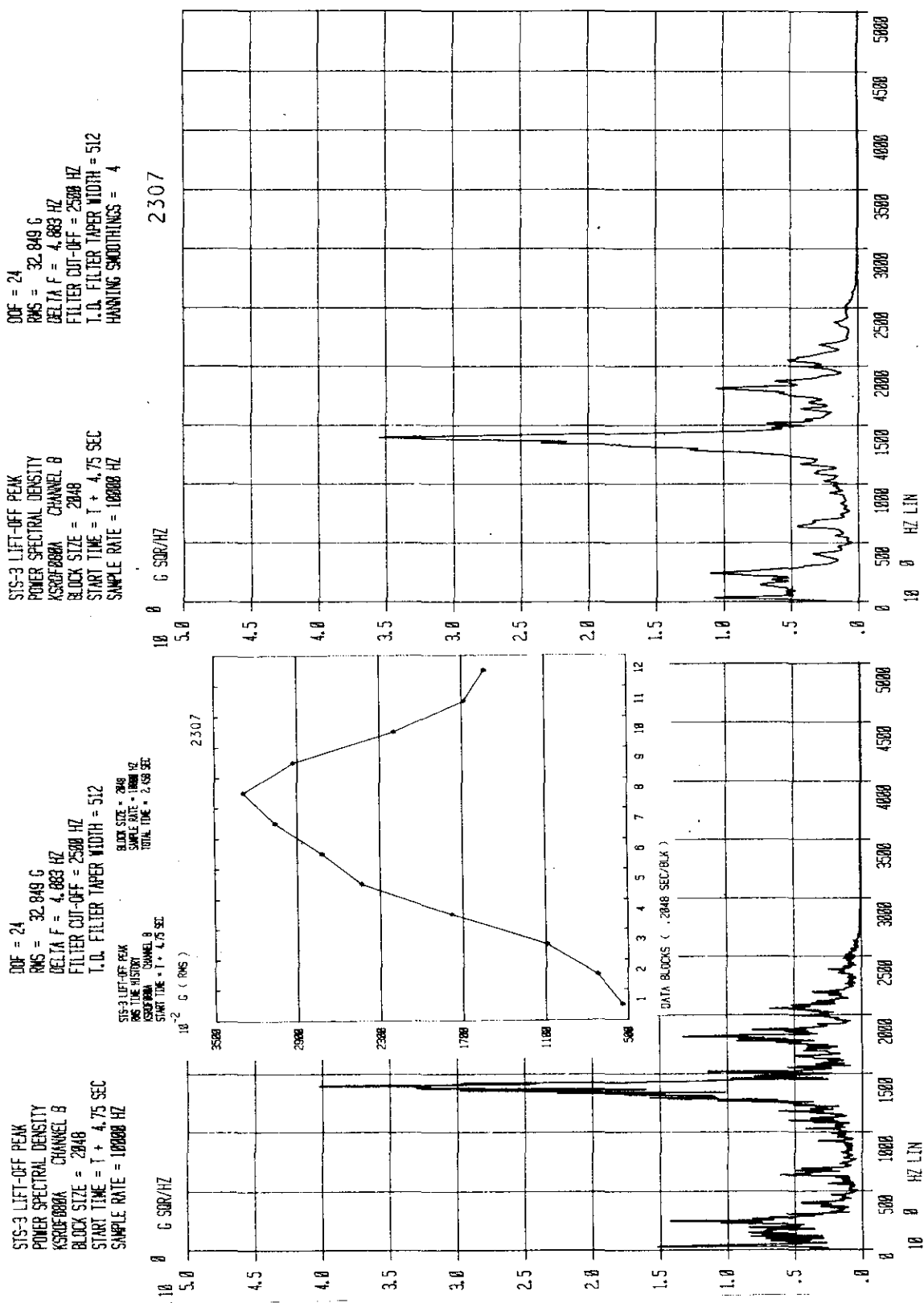
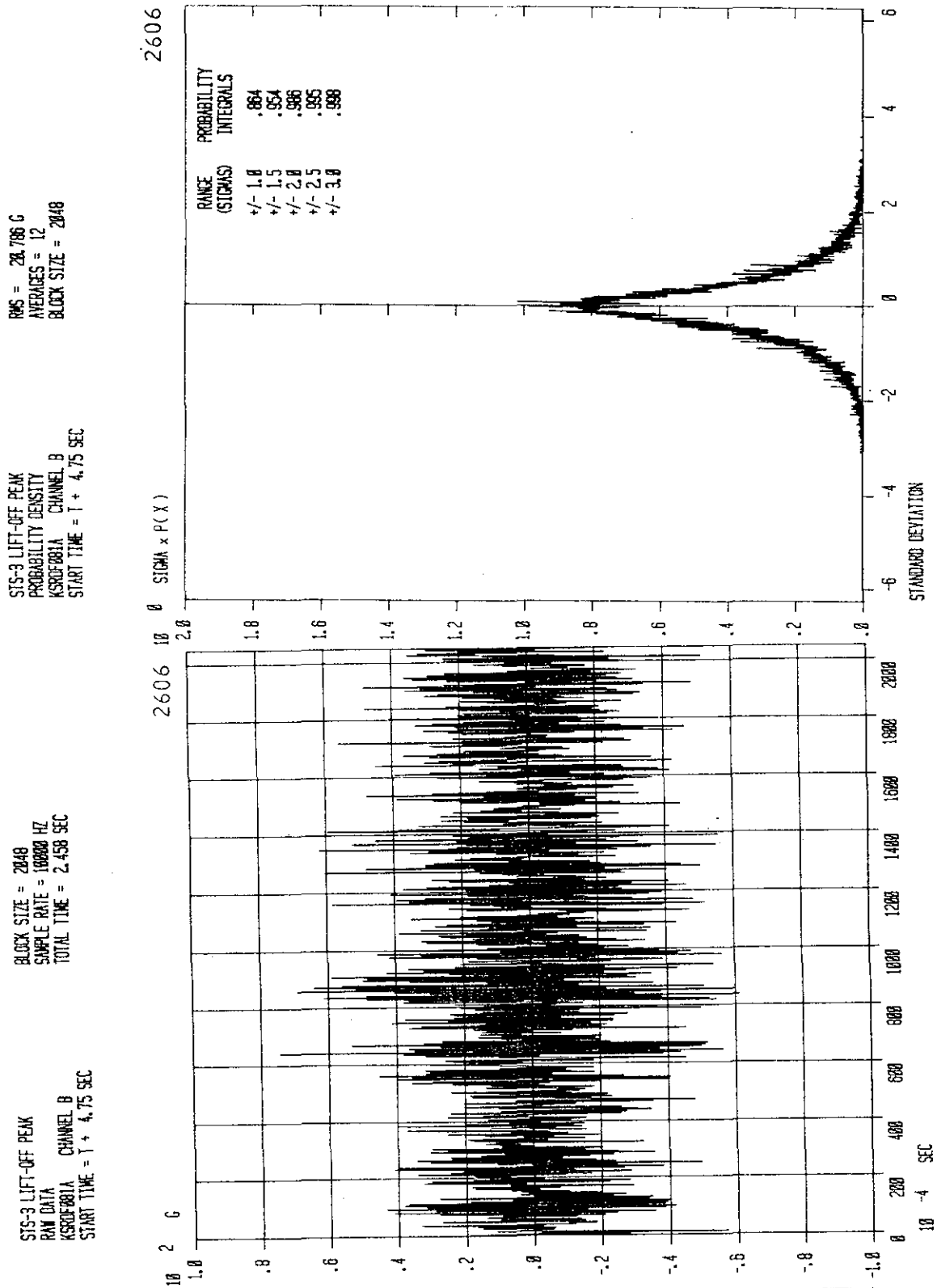


Figure 5-11. Room 10A - Truss T₂ Top Chord, Z Direction (Sheet 2 of 2)

Figure 5-12. Room 10A - Truss T₁ Top Chord, Z Direction (Sheet 1 of 2)

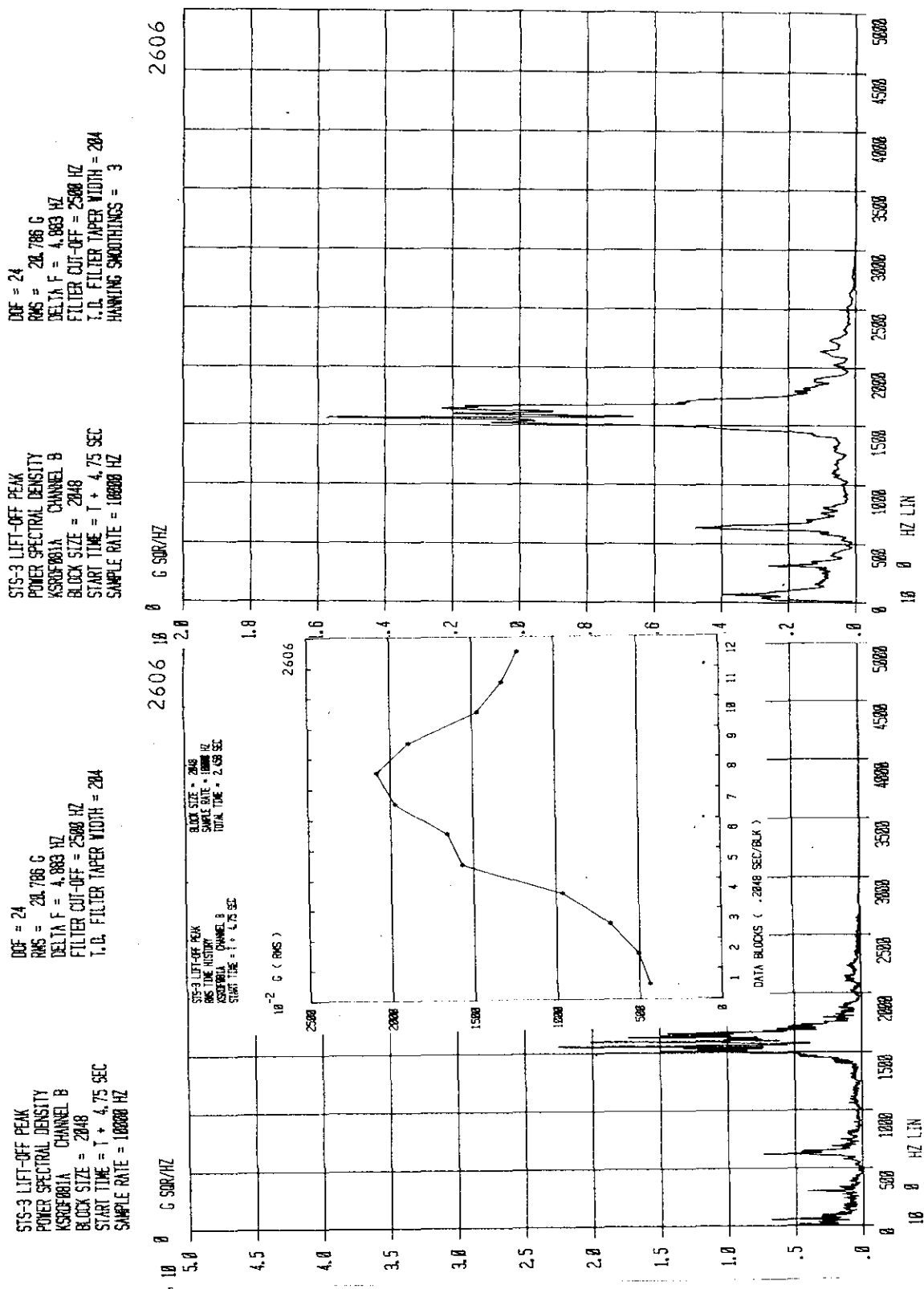


Figure 5-12. Room 10A - Truss T₁ Top Chord, Z Direction (Sheet 2 of 2)

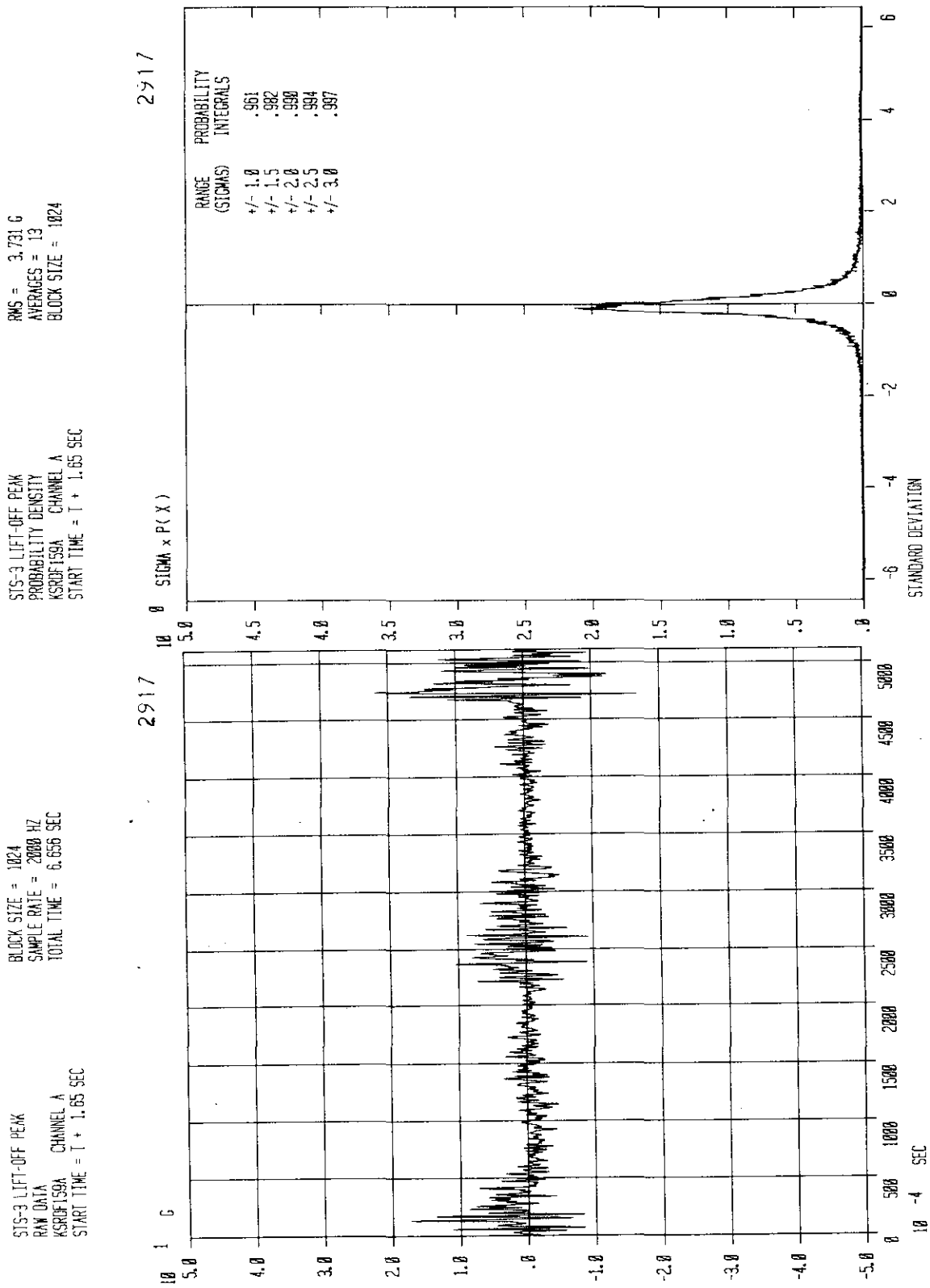


Figure 5-13. Room 9B - Floor Framing Stringer (E), Z Direction (Sheet 1 of 2)

KSC-DD-818-TR

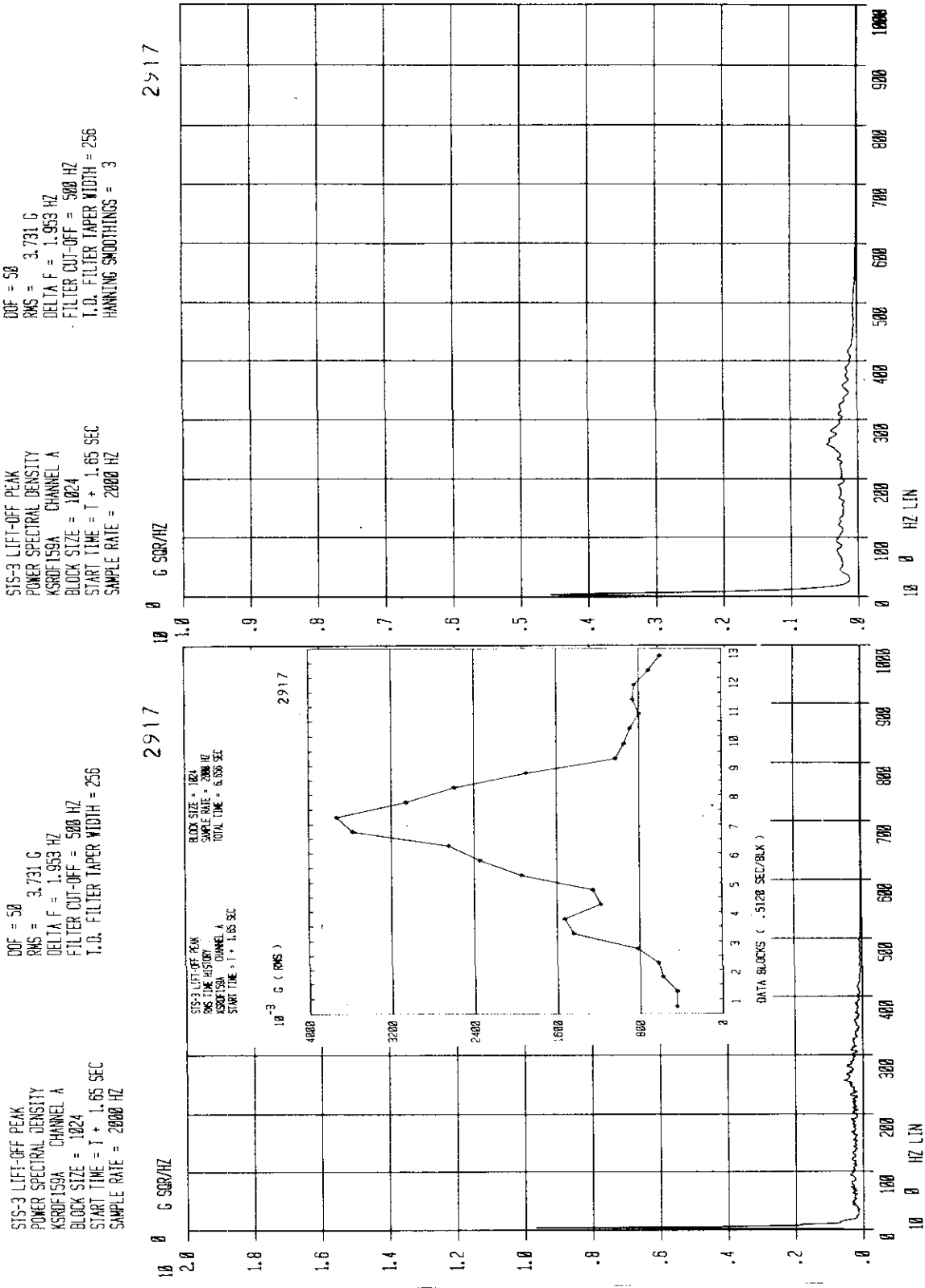


Figure 5-13. Room 9B - Floor Framing Stringer (E), Z Direction (Sheet 2 of 2)

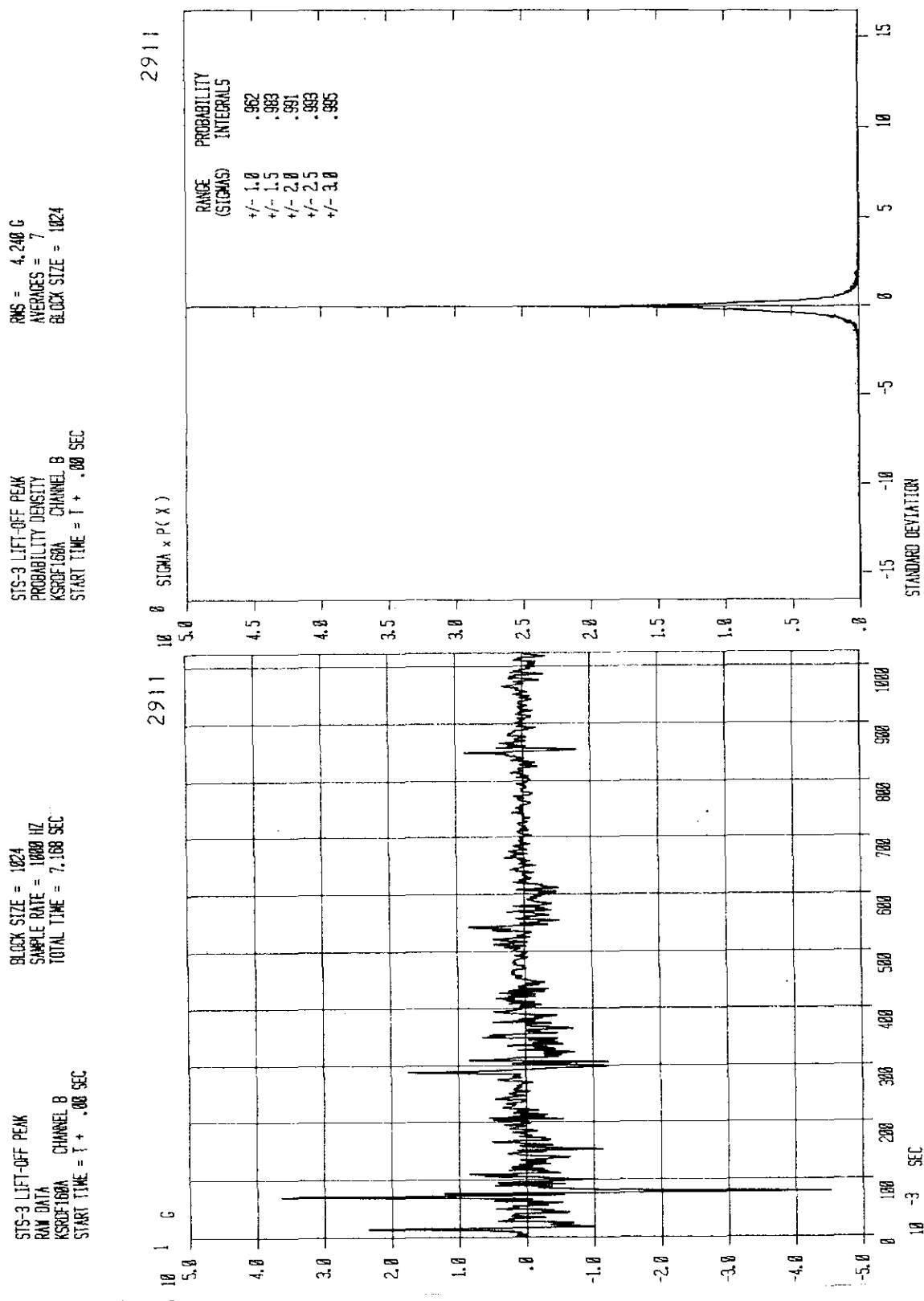


Figure 5-14. Room 9B - Floor Framing Stringer (W), Z Direction (Sheet 1 of 2)

KSC-DD-818-TR

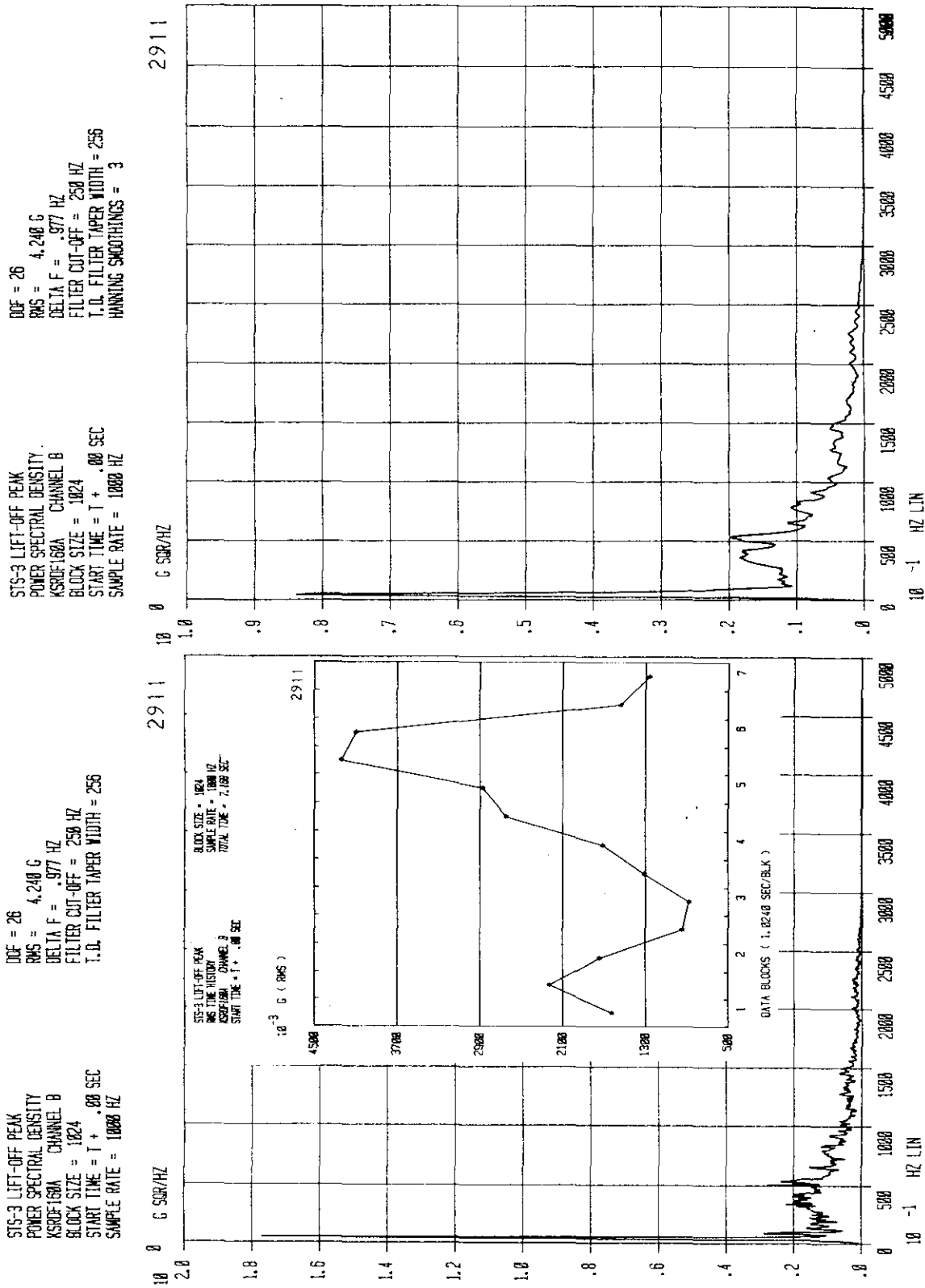


Figure 5-14. Room 9B - Floor Framing Stringer (W), Z Direction (Sheet 2 of 2)

MEAS.KSRDG #			001C	002C	003C	004C	005A
PROC.PARAM.	Fmax(Hz)		100	100	100	100	500
	BLOCK SIZE		256	256	256	256	1024
	DELTA F		.781	.781	.781	.781	.976
	TOTAL TIME		7.69	7.69	7.69	7.69	8.20
	START TIME		To+1.80	To+1.80	To+1.80	To+1.80	To
PERIOD LOCATION DIR/FREQ.RANGE			L/O PEAK LEV 0 Z/O-2K	L/O PEAK LEV 0 Z/O-2K	L/O PEAK T-2 Z/O-2K	L/O PEAK T-2 Z/O-2K	L/O PEAK FL BEAM Z/O-2K
FILTER@ (Hz)	0 *	DISPL. (IN.)	2.980	5.940	.8970	.7500	1.618
	2		.7706	.7162	.4204	.3504	.707
	3		.7182	.6538	.3960	.3314	.590
	4		.5650	.5393	.3295	.2802	.514
	5		.3768	.3680	.2571	.2304	.398

MEAS.KSRDG #			006A	005B	006B	005C	006C
PROC.PARAM.	Fmax(Hz)		500	100	100	100	100
	BLOCK SIZE		1024	256	256	512	512
	DELTA F		.9770	.7813	.7813	.390	.390
	TOTAL TIME		8.20	8.97	8.97	7.69	7.69
	START TIME		To	To	To	To+1.20	To+1.20
PERIOD LOCATION DIR/FREQ.RANGE			L/O PEAK FL BEAM Z/O-2K	L/O PEAK FL BEAM Z/O-2K	L/O PEAK FL BEAM Z/O-2K	L/O PEAK FL BEAM Z/O-2K	L/O PEAK FL BEAM Z/O-2K
FILTER@ (Hz)	0 *	DISPL. (IN.)	1.639	1.539	2.158	4.155	4.184
	2		.7340	.4865	.6250	.3471	.4000
	3		.6390	.4307	.5590	.2904	.3514
	4		.5490	.3865	.5005	.2750	.3290
	5		.4233	.3040	.3872	.2325	.2716

*Note: RMS displacements calculated without a filter (filter at 0 Hz) are not valid. Refer to KSC-DD-677-TR, page 6, for validation criteria.

Figure 5-15. STS-6 MLP-2 Vibration Data Processing Parameters and Calculated RMS Displacements (Sheet 1 of 2)

KSC-DD-818-TR

MEAS. KSRDG #			001B	002B	003B	004B	
PROC. PARAM.	Fmax(Hz)		1000	1000	1000	1000	
	BLOCK SIZE		1024	1024	1024	1024	
	DELTA F		1.95	1.95	1.95	1.95	
	TOTAL TIME		6.67	6.67	6.67	6.67	
	START TIME		To+2.00	To+2.00	To+2.00	To+2.00	
PERIOD LOCATION DIR/FREQ. RANGE			L/O PEAK LEV 0 Z/O-2K	L/O PEAK LEV 0 Z/O-2K	L/O PEAK T-2 Z/O-2K	L/O PEAK T-2 Z/O-2K	
FILTER@ (Hz)	0 *	DISPL. (IN.)	.9316	1.102	.8973	.7203	
	2		.8163	.9657	.8000	.6488	
	3		.4750	.5617	.5278	.4546	
	4		.4208	.4965	.4780	.4173	
	5		.2744	.3192	.3582	.3250	

*Note: RMS displacements calculated without a filter (filter at 0 Hz) are not valid. Refer to KSC-DD-677-TR, page 6, for validation criteria.

Figure 5-15. STS-6 MLP-2 Vibration Data Processing Parameters and Calculated RMS Displacements (Sheet 2 of 2)

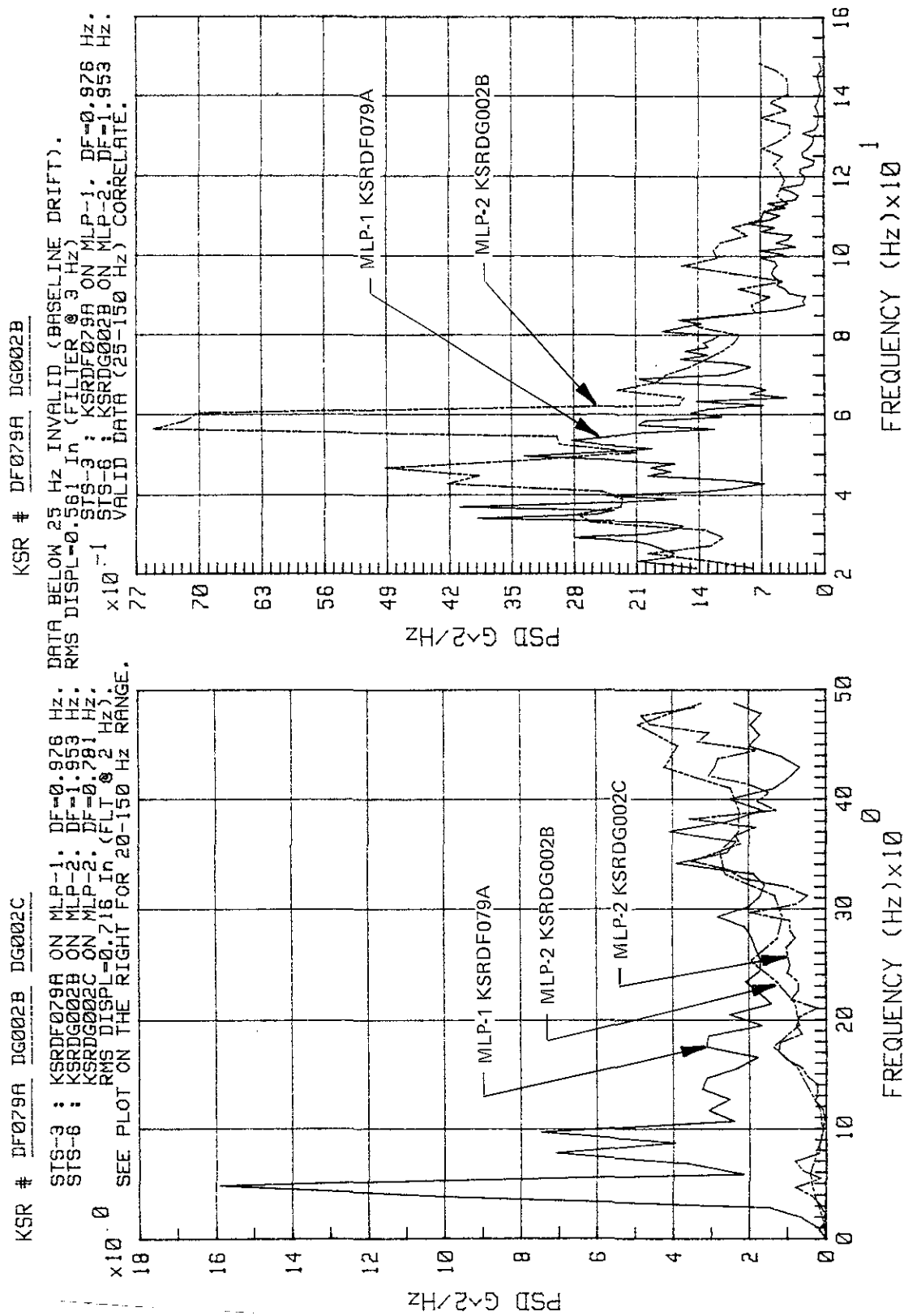


Figure 5-16. MLP-1 and MLP-2 Vibration, Deck 0 Beam, Room 9A at Centerline of East SRB, Z Direction

KSC-DD-818-TR

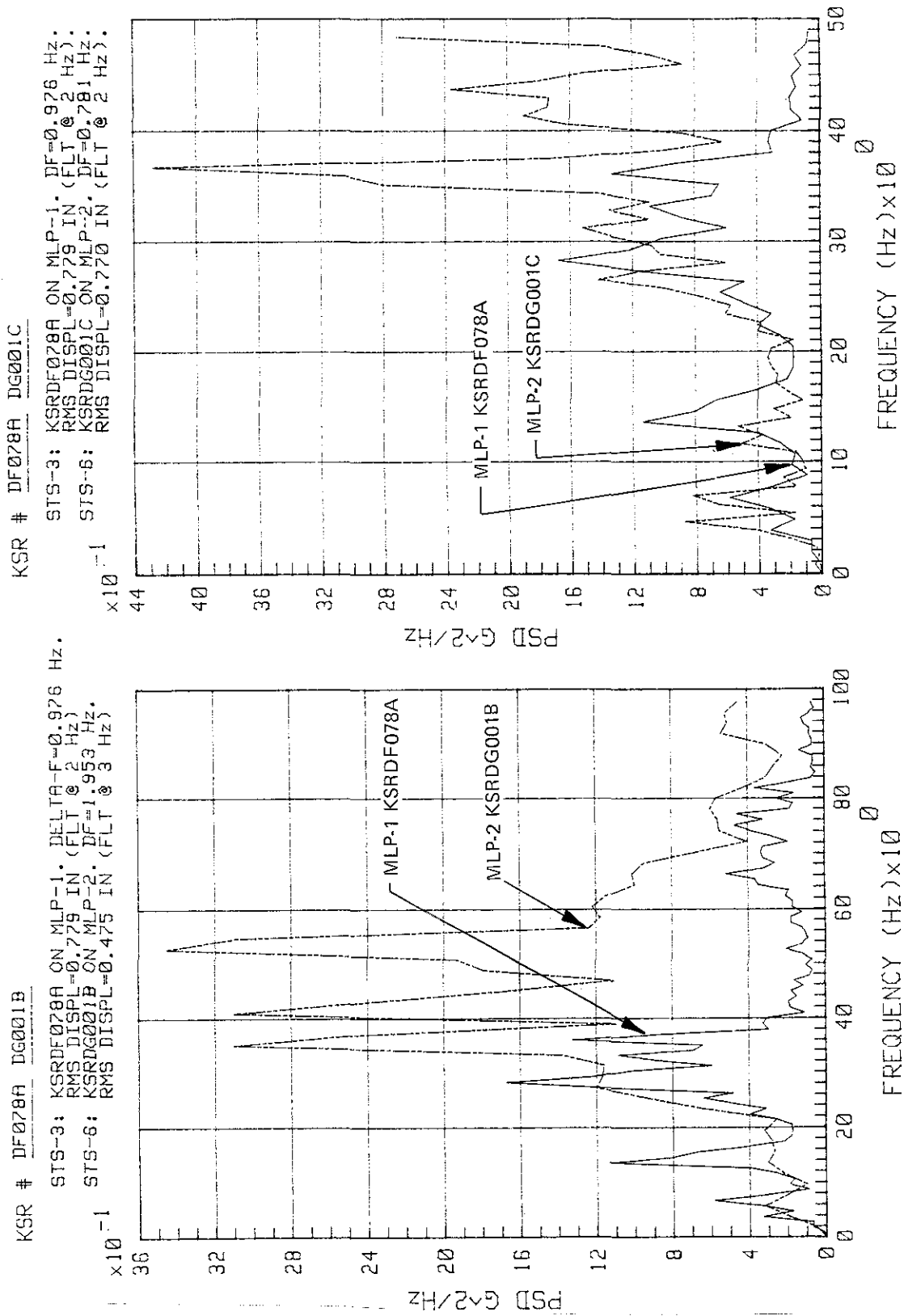


Figure 5-17. MLP-1 and MLP-2 Vibration, Deck 0 Beams, Room 7A, Z Direction

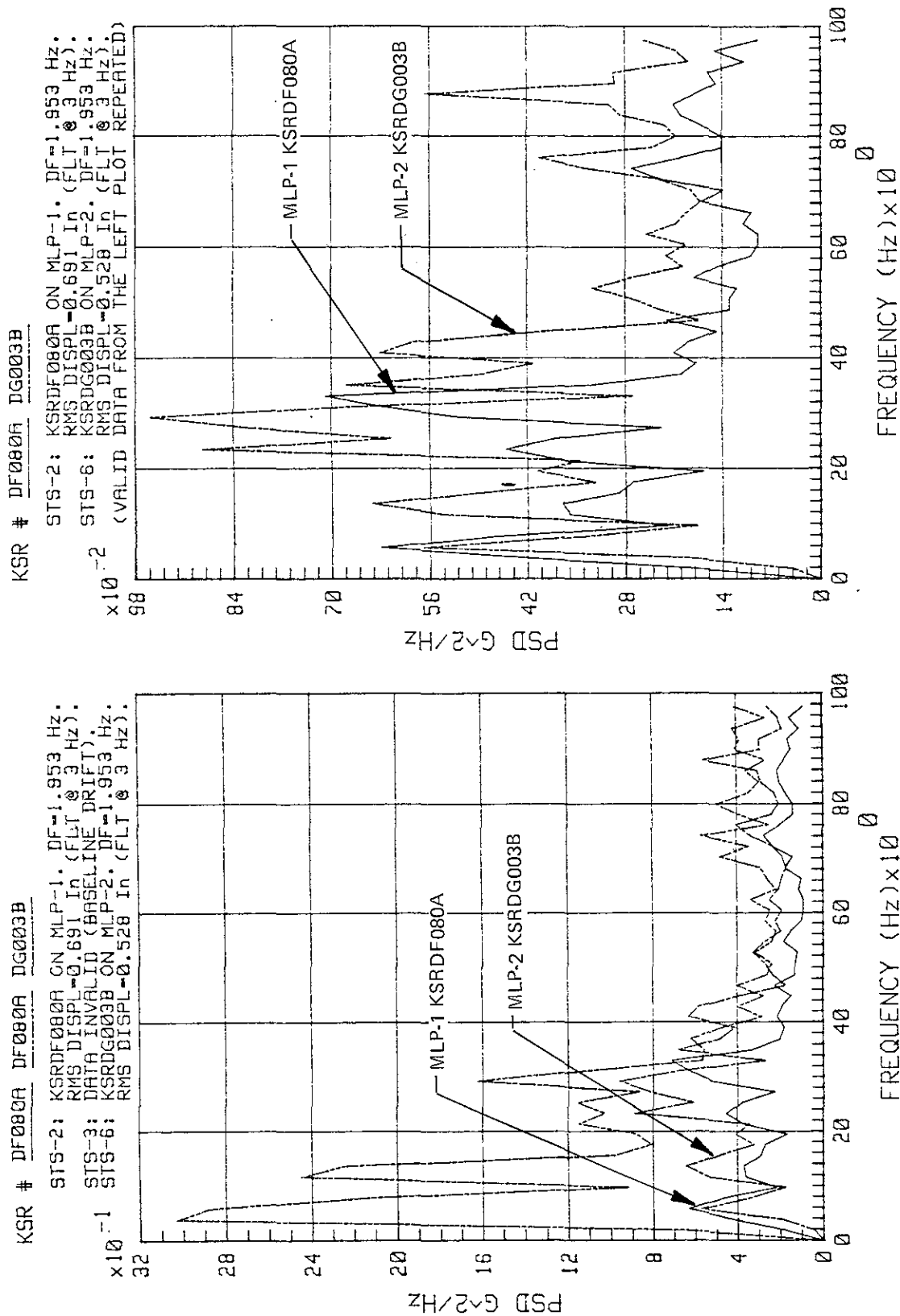


Figure 5-18. MLP-1 and MLP-2 Vibration, T-2 Truss Top Chord, Room 10A, Z Direction

KSC-DD-818-TR

KSR # DF129B DF129A DG006A

SIS-2 : KSRDF129B ON MLP-1. DELTA-F=0.926 Hz. RMS DISPL=0.773 in (FILTER @ 2 Hz).
 SIS-3 : KSRDF129A ON MLP-1. DELTA-F=1.553 Hz. RMS DISPL=0.647 in (FILTER @ 3 Hz).
 SIS-6 : KSRDG006A ON MLP-2. DELTA-F=0.926 Hz. RMS DISPL=0.625 in (FILTER @ 2 Hz).
 0 NOTE : IN ORDER TO OBTAIN BETTER PLOT RESOLUTION, THE SAME DATA ARE REPEATED ON THE FOLLOWING PLOTS.

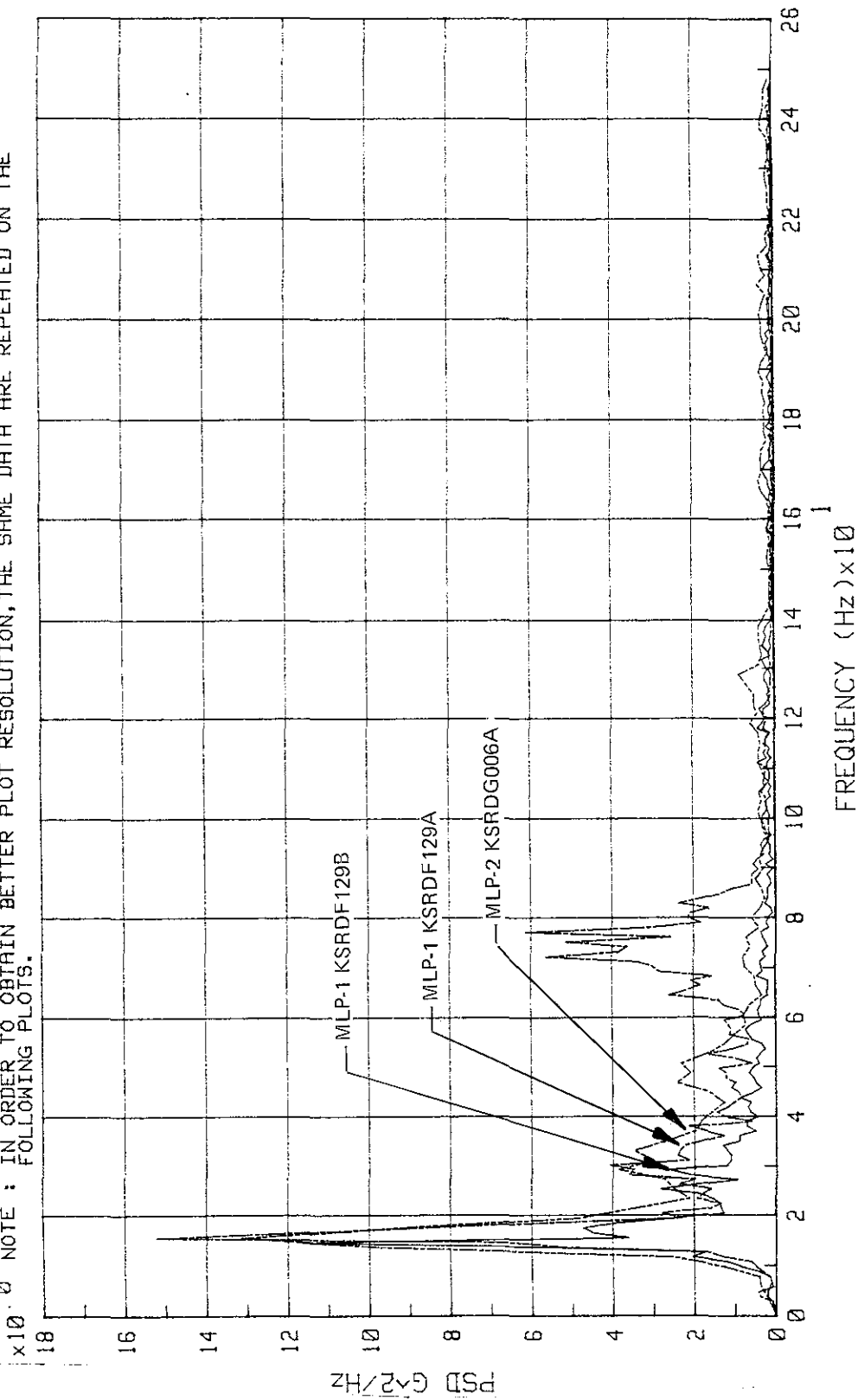


Figure 5-19. MLP-1 and MLP-2 Vibration, Deck B Floor Beam, Room 9B, Z Direction

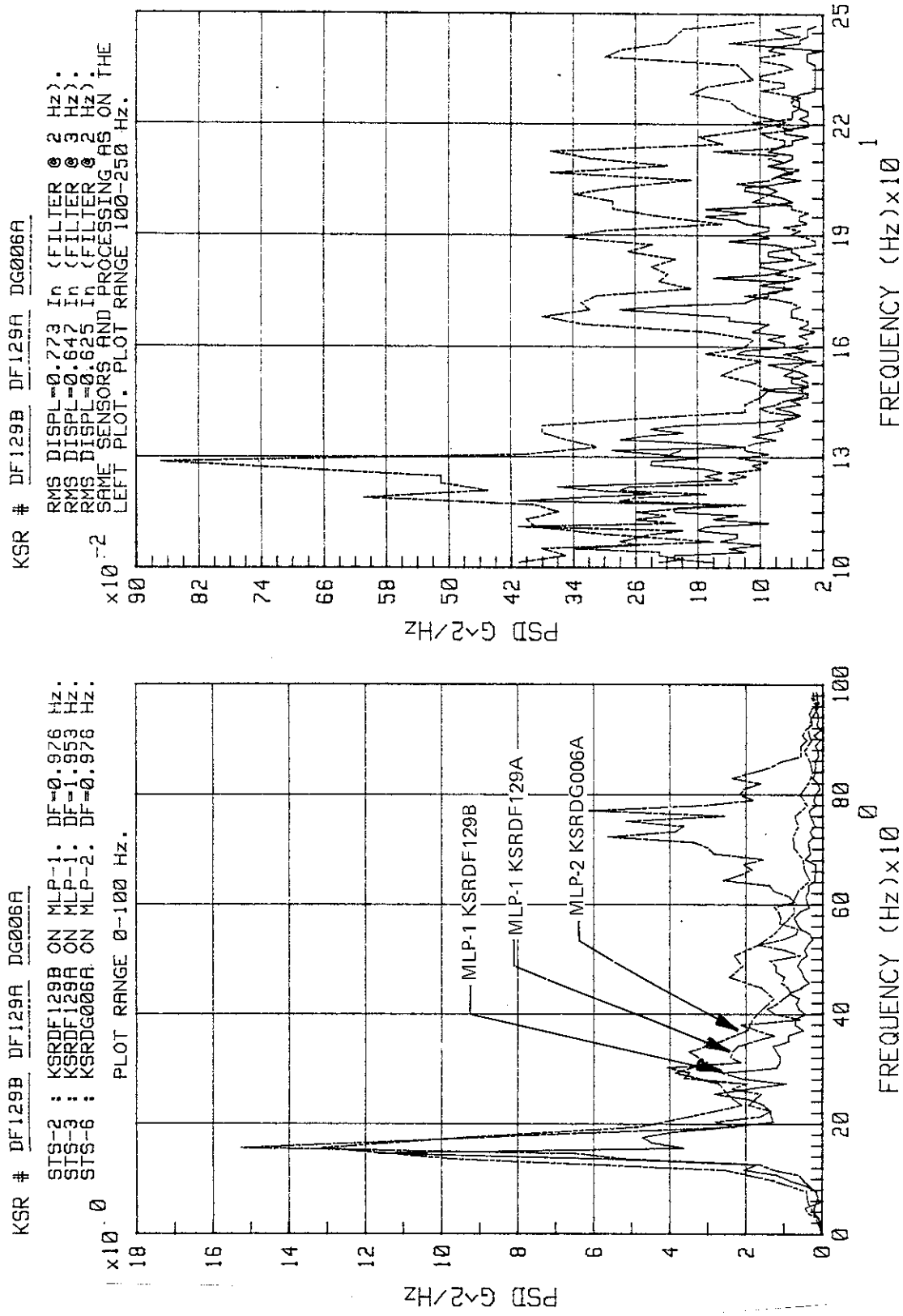


Figure 5-20. MLP-1 and MLP-2 Vibration, Deck 8 Floor Beam, Room 9B, Z Direction, KSRDF129B, -DF129A, -DG006A

KSC-DD-818-TR

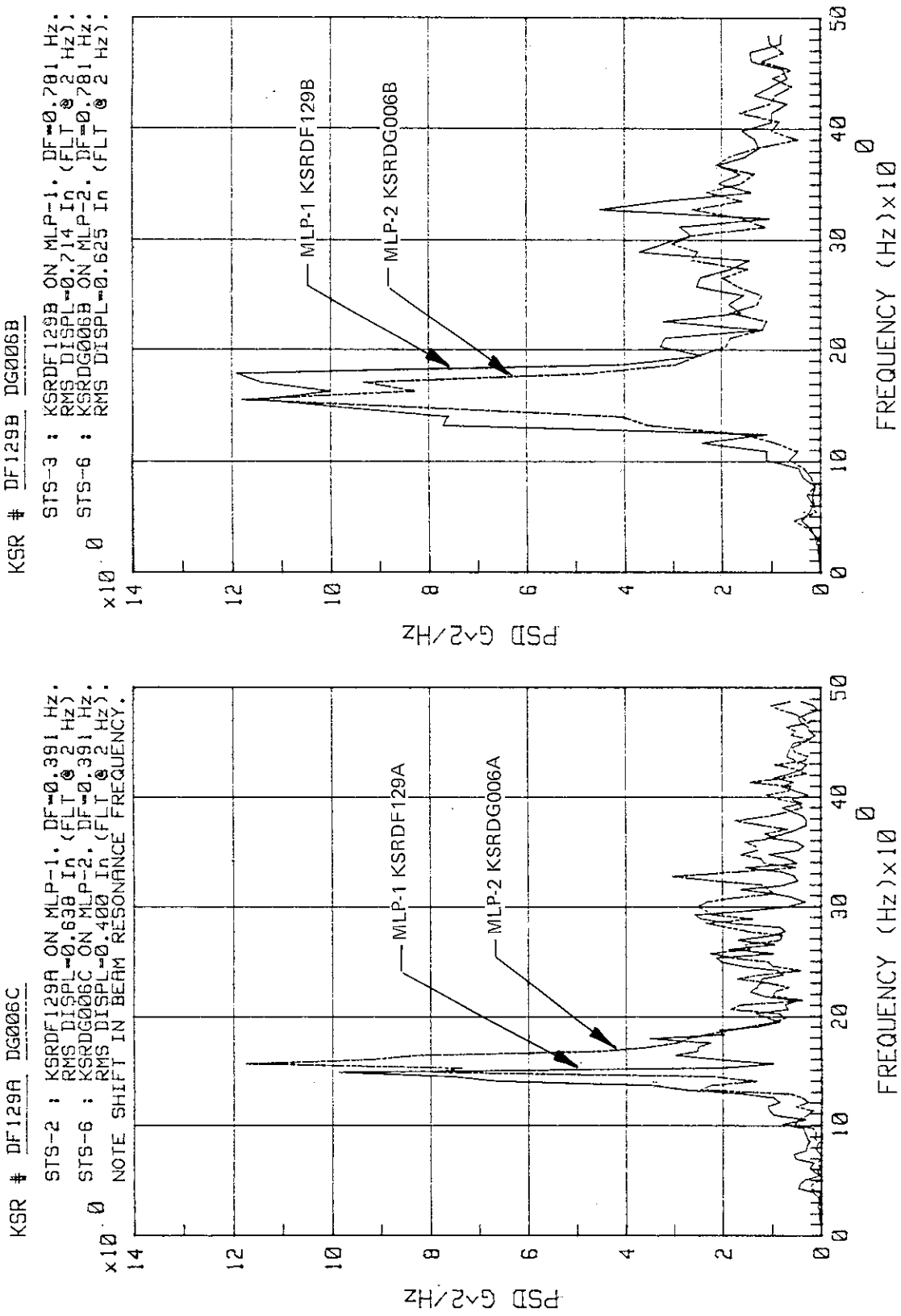


Figure 5-21. MLP-1 and MLP-2 Vibration, Deck B Floor Beam, Room 9B, Z Direction, KSRDF129A, -DG006C, -DF129B, -DG006B

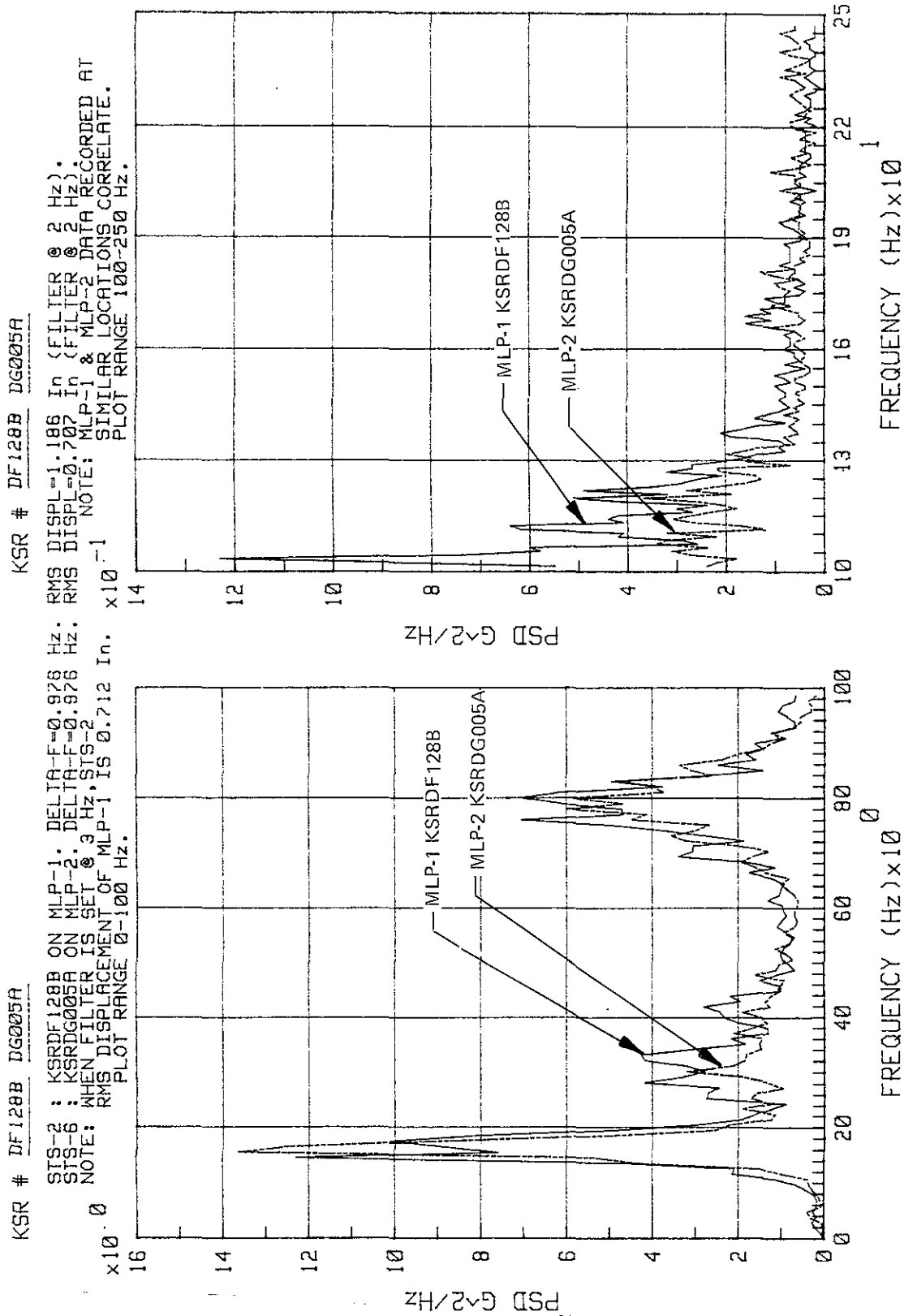


Figure 5-22. MLP-1 and MLP-2 Vibration, Deck 8 Floor Beam, Room 9B, at West SRB, Z Direction, KSRDF128B, -DG005A

KSC-DD-818-TR

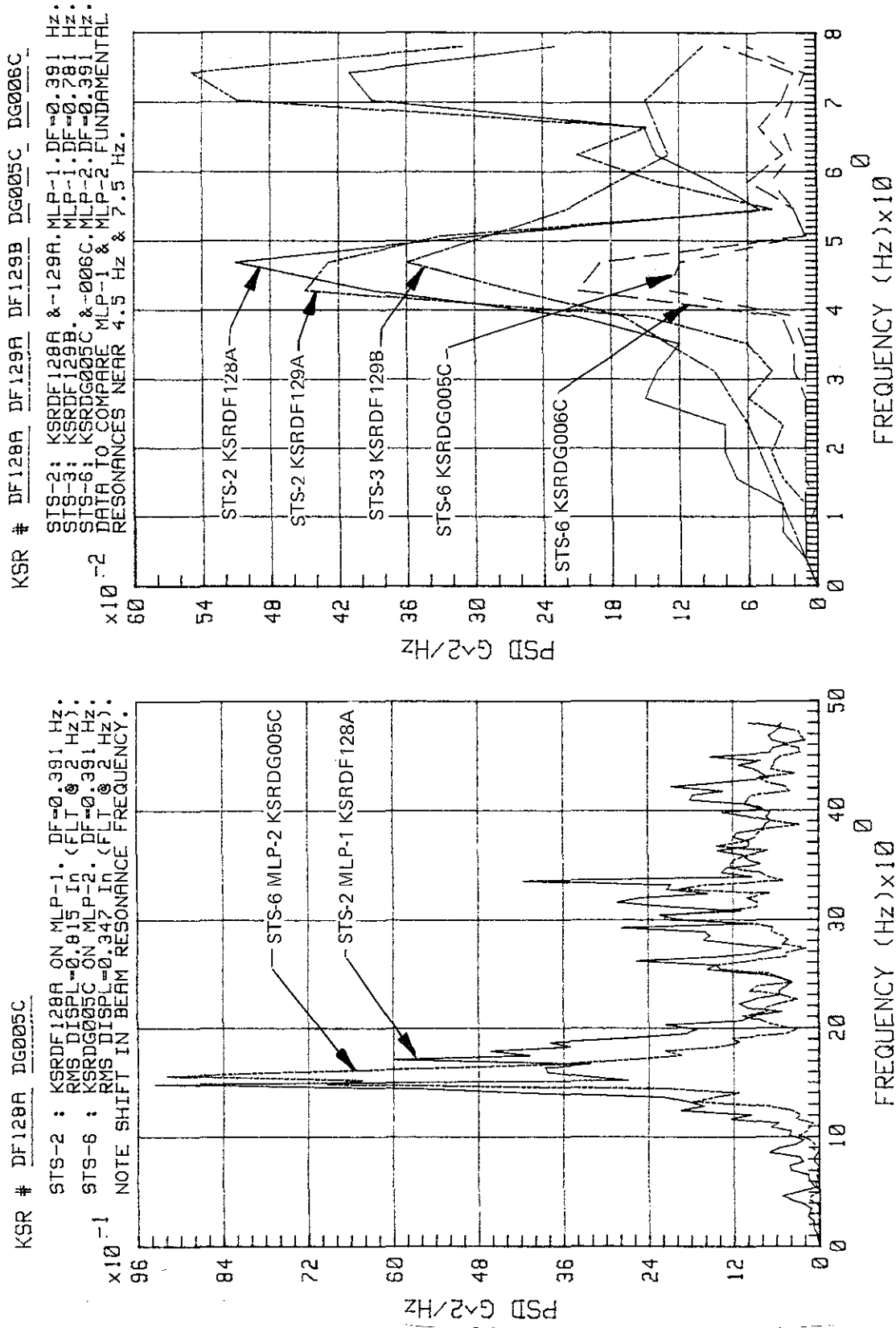


Figure 5-23. MLP-1 and MLP-2 Vibration, Deck B Floor Beam, Room 9B, at West SRB, Z Direction,
KSRDF128A, -DG005C, and KSRDF128A, -DF129A, -DG005C, -DG006C

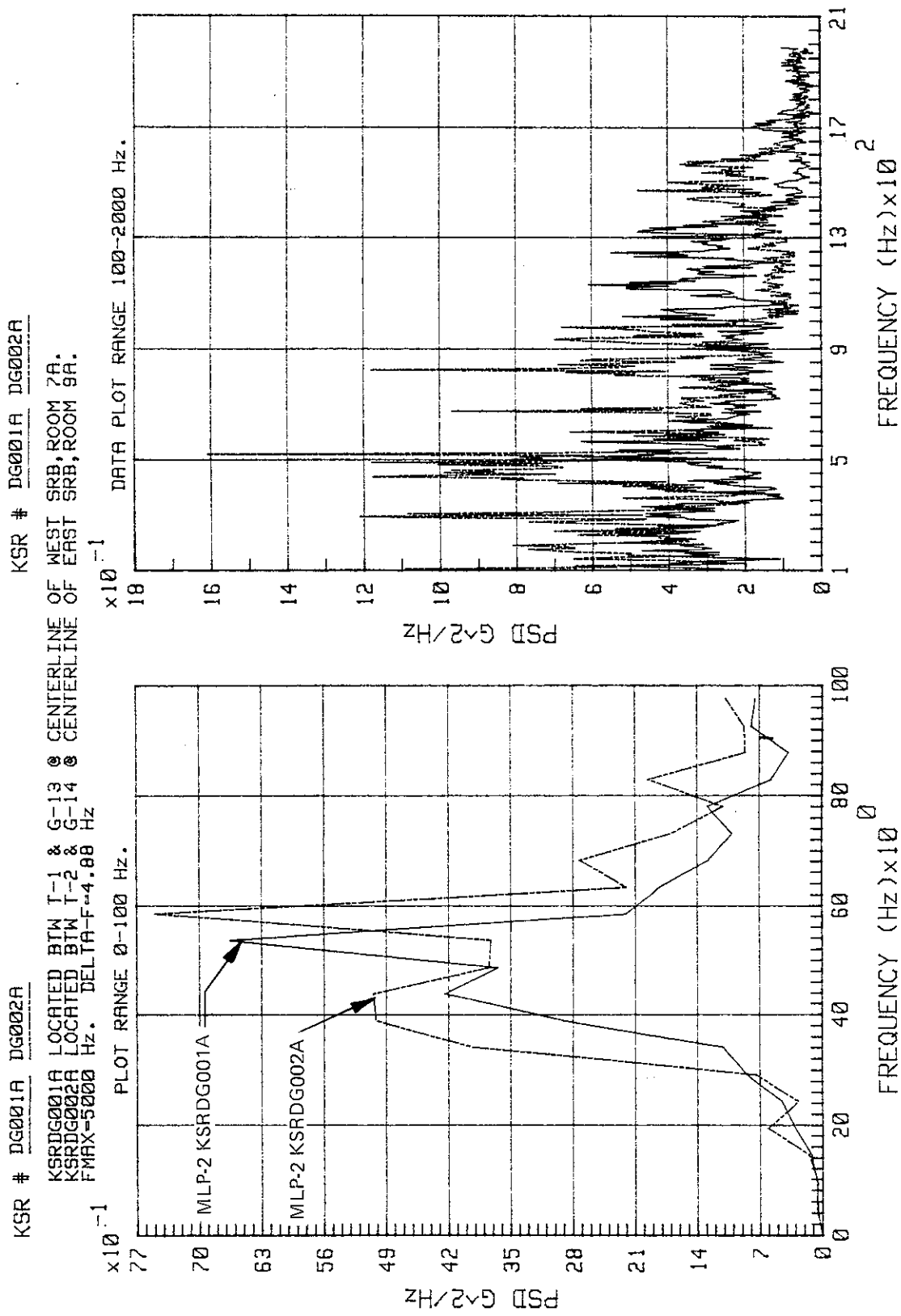


Figure 5-24. STS-6 MLP-2 Vibration of Deck 0 Beams, Z Direction, 0 to 100 Hz and 100 to 2,100 Hz

KSC-DD-818-TR

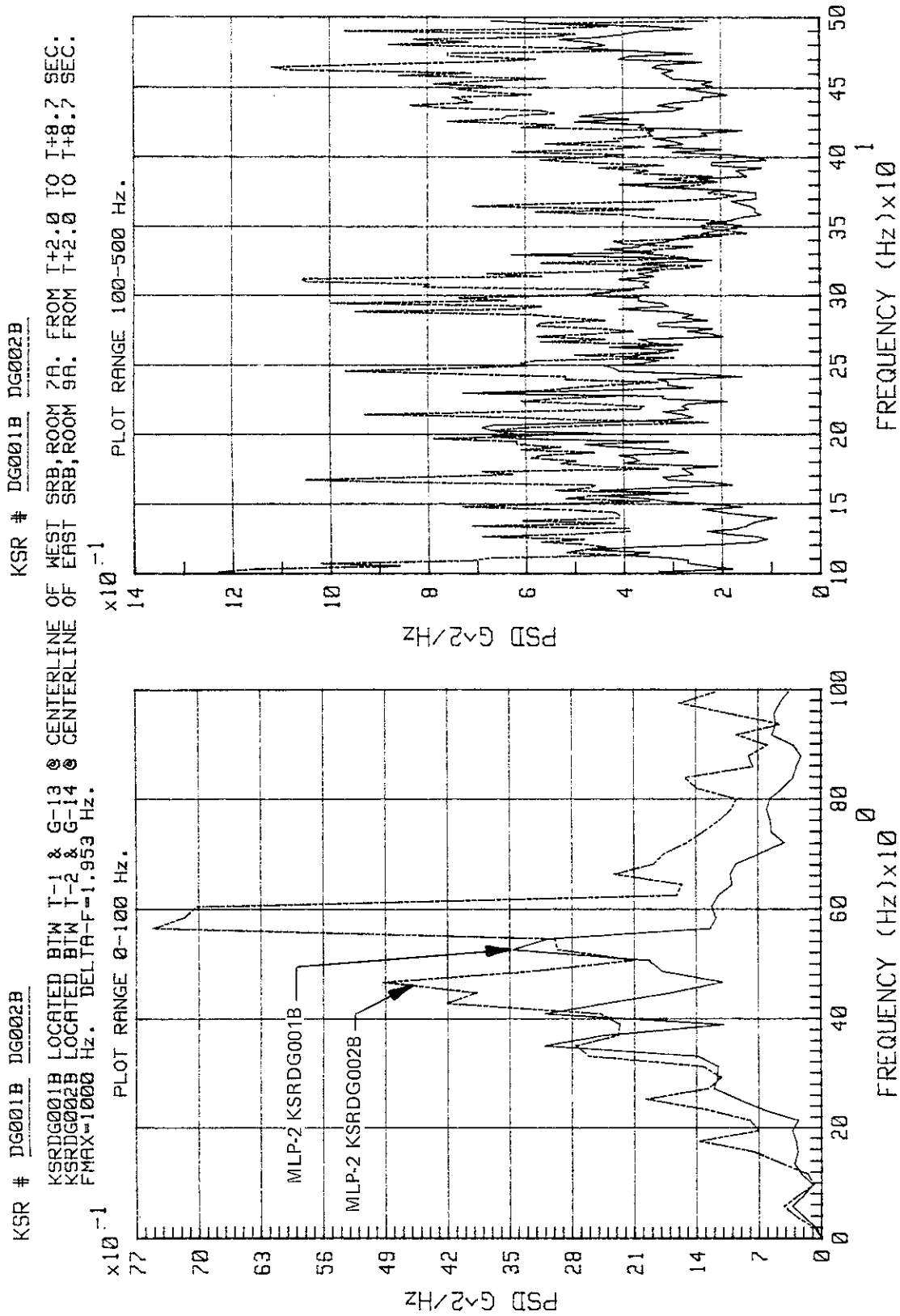


Figure 5-25. STS-6 MLP-2 Vibration of Deck 0 Beams, Z Direction, 0 to 100 Hz and 100 to 500 Hz

KSR # DG001C DG002C

KSRDG001C LOCATED BTW I-1 & G-13 @ CENTERLINE OF WEST SRB, ROOM 7A. FROM I+1.8 TO I+9.5 SEC.
 KSRDG002C LOCATED BTW I-2 & G-14 @ CENTERLINE OF EAST SRB, ROOM 9A. FROM I+1.8 TO I+9.5 SEC.
 FMAX=100 Hz. DELTA-F=0.781 Hz. ANTI-ALIASING FILTER @ 50 Hz. AVERAGING BLOCK TIME 1.28 SEC.

NOTE: PLOT RANGE 0-100 Hz CONTAINS DATA AFFECTED BY ANTI-ALIASING FILTER.

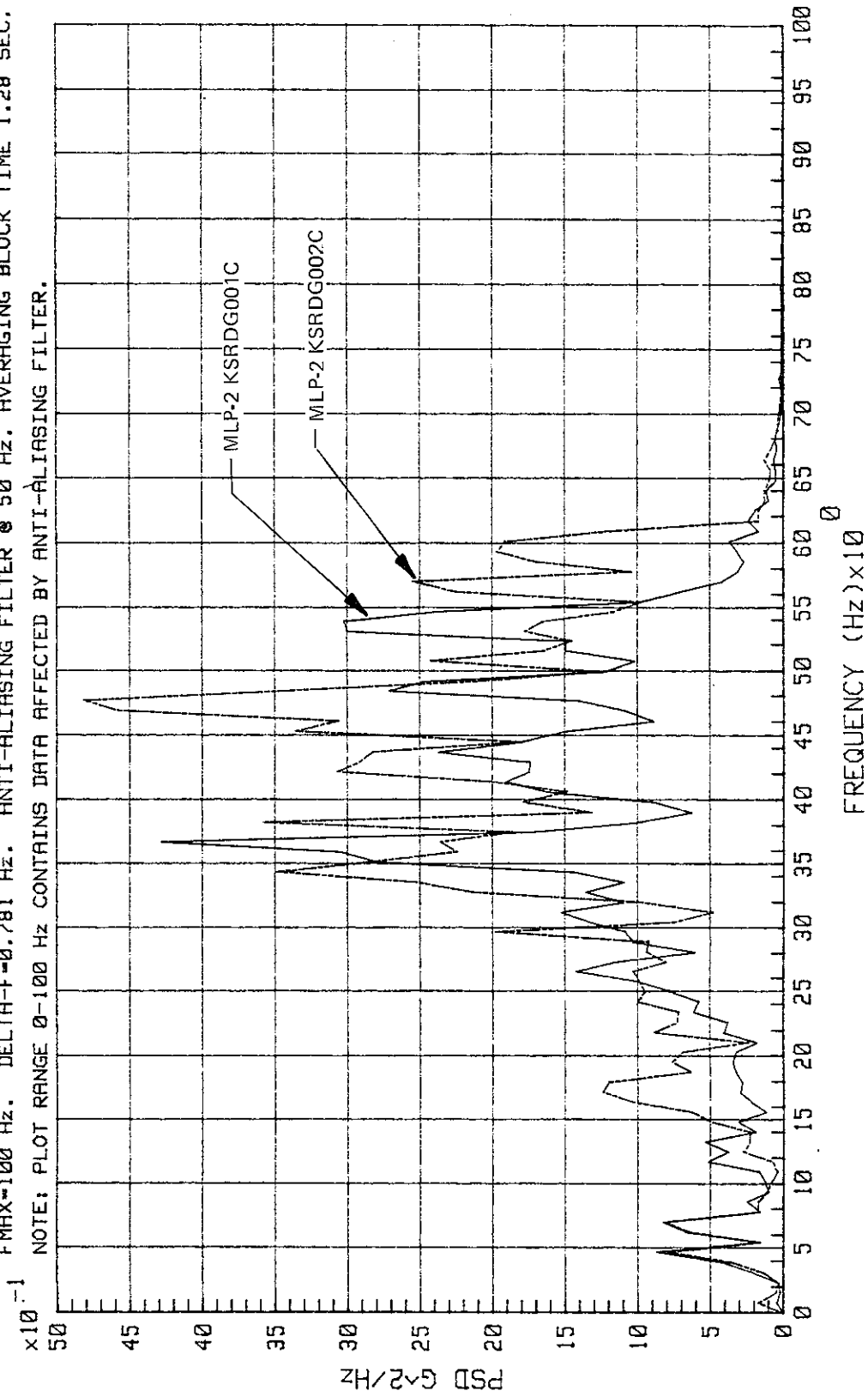
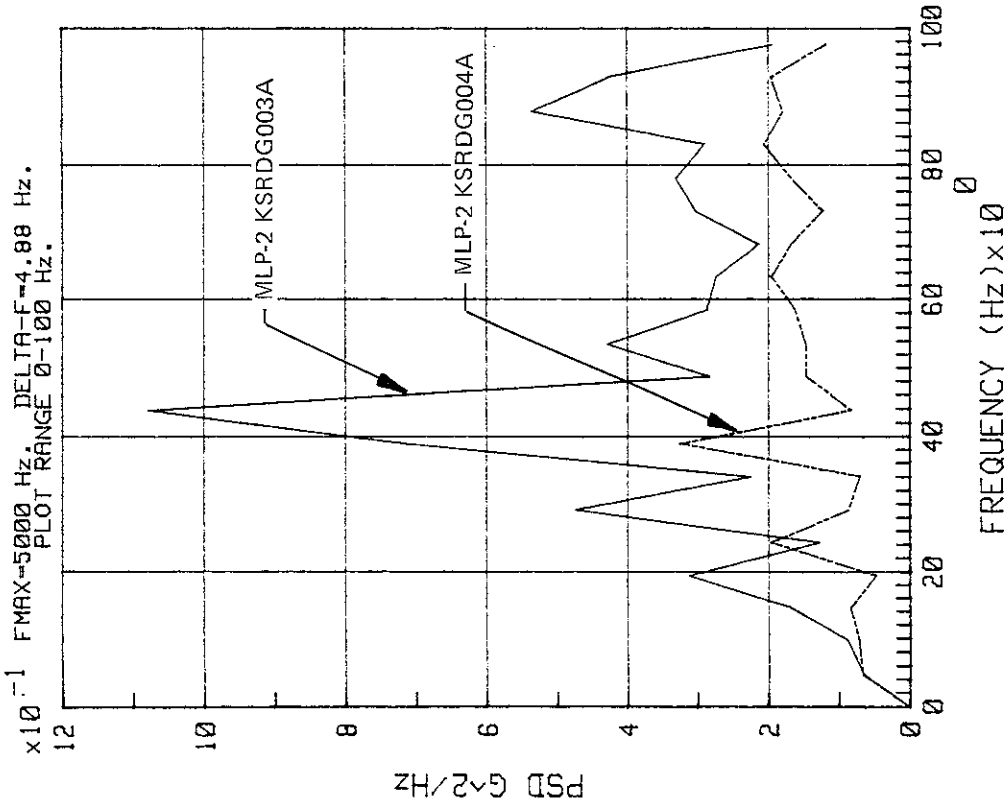


Figure 5-26. STS-6 MLP-2 Vibration of Deck 0 Beams, Z Direction, 0 to 100 Hz

KSC-DD-818-TR

KSR # DG003A DG004A

KSRDG004A LOCATED @ MIDSPAN OF T-2, @ MIDSPAN OF CENTER PANEL.
KSRDG003A LOCATED @ SECOND PANEL, ADJACENT TO TRUSS MIDSPAN.
x10⁻¹ FMAX=5000 Hz. DELTA-F=4.88 Hz.
PLOT RANGE 0-100 Hz.



KSR # DG003A DG004A

KSRDG004A LOCATED @ MIDSPAN OF CENTER PANEL. FROM T+5.2 TO T+7.7 SEC.
KSRDG003A LOCATED @ SECOND PANEL, ADJACENT TO TRUSS MIDSPAN. FROM T+5.2 TO T+7.7 SEC.

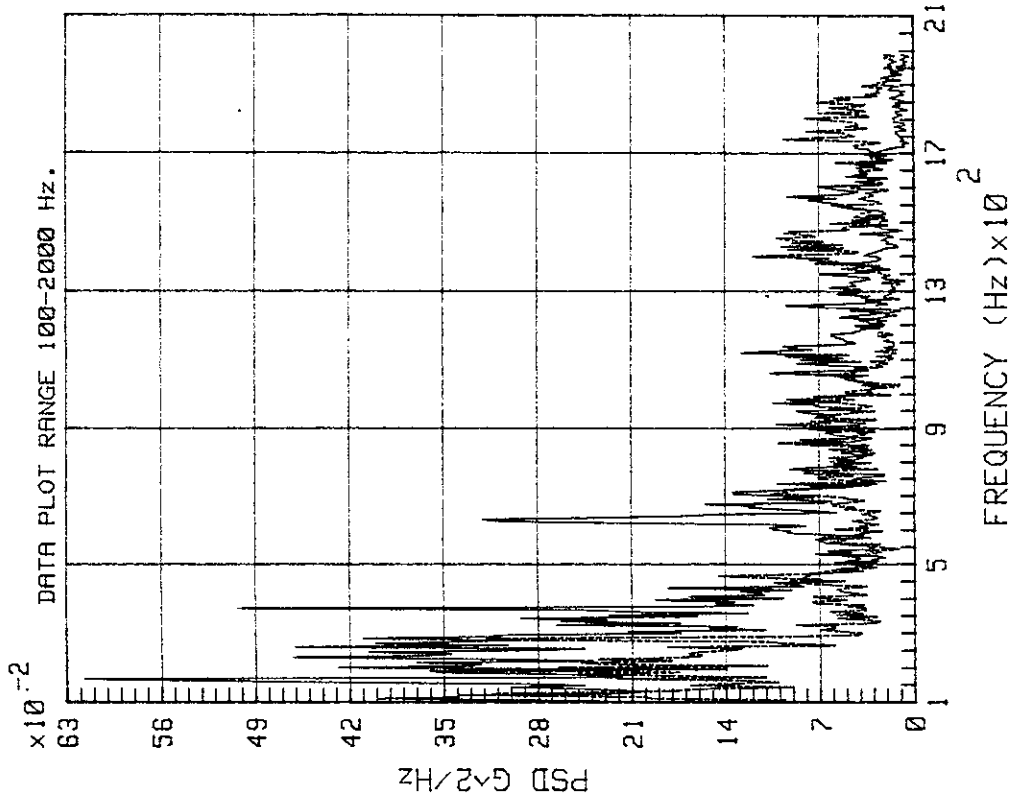


Figure 5-27. STS-6 MLP-2 Vibration of T-2 Truss Top Chord, Z Direction, 0 to 100 Hz and 100 to 2,100 Hz

KSR # DG003B DG004B

KSR # DG003B DG004B

KSRDG004B LOCATED @ MIDSPAN OF T-2, @ MIDSPAN OF CENTER PANEL. FROM T+2.0 TO T+8.7 SEC.
 KSRDG003B LOCATED @ SECOND PANEL, ADJACENT TO TRUSS MIDSPAN. FROM T+2.0 TO T+8.7 SEC.
 FMAX=1000 Hz. DELTA-F=1.953 Hz.

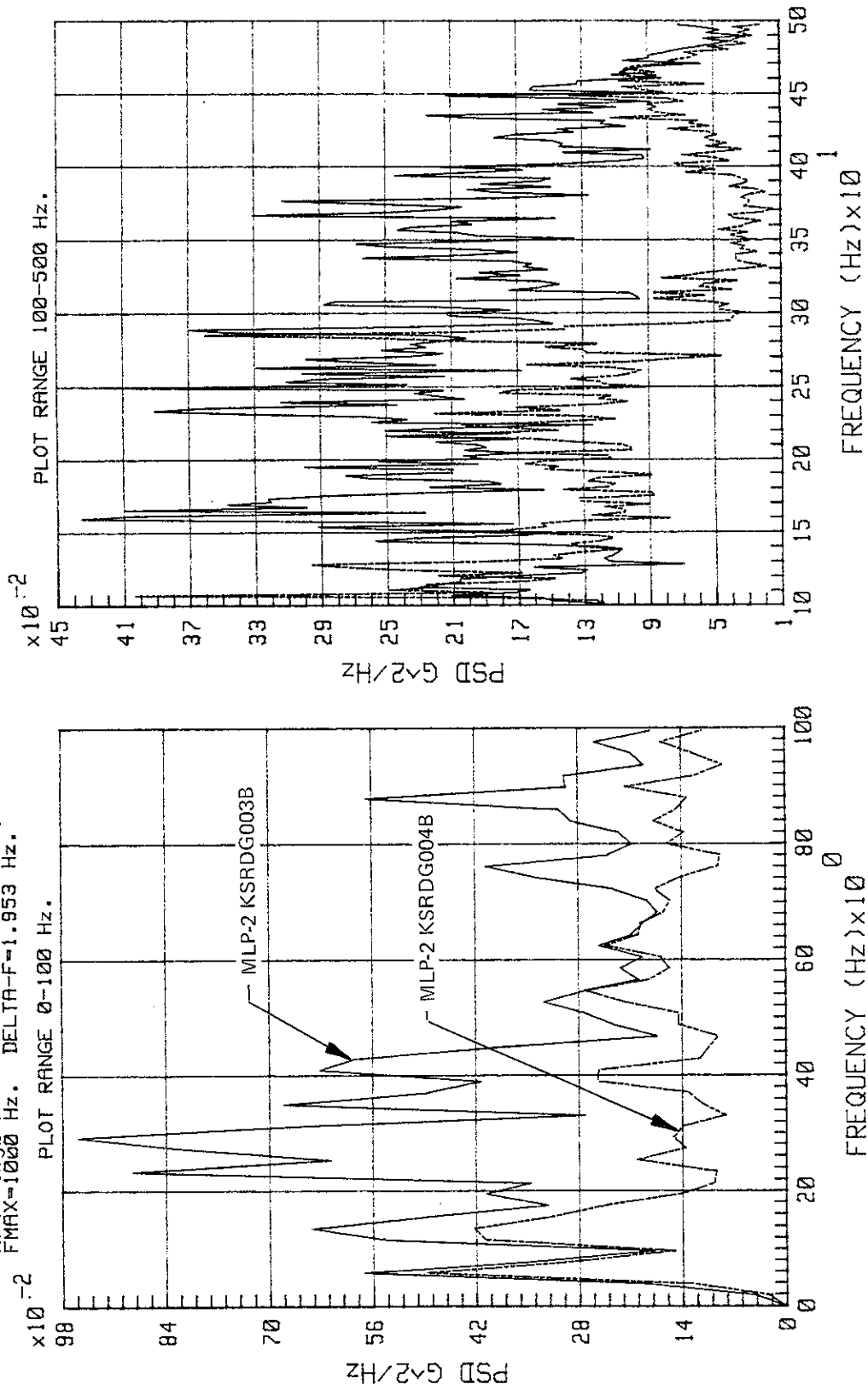


Figure 5-28. STS-6 MLP-2 Vibration of T-2 Truss Top Chord, Z Direction, 0 to 100 Hz and 100 to 500 Hz

KSC-DD-818-TR

KSR # DG003C DG004C

KSRDG004C LOCATED @ MIDSPAN OF T-2, @ MIDSPAN OF CENTER PANEL. FROM T+1.8 TO T+9.5 SEC.
 KSRDG003C LOCATED @ SECOND PANEL, ADJACENT TO TRUSS MIDSPAN. FROM T+1.8 TO T+9.5 SEC.
 FMAX=100 Hz. DELTA-F=0.781 Hz. ANTI-ALIASING FILTER @ 50 Hz. AVERAGING BLOCK TIME 1.28 SEC.
 NOTE: PLOT RANGE 0-100 Hz CONTAINS DATA AFFECTED BY ANTI-ALIASING FILTER.
 NOTE: KSRDG003C IN LINE WITH WEST SRB, RECORDED HIGHER VIBRATION THAN AT MIDSPAN OF T-2.

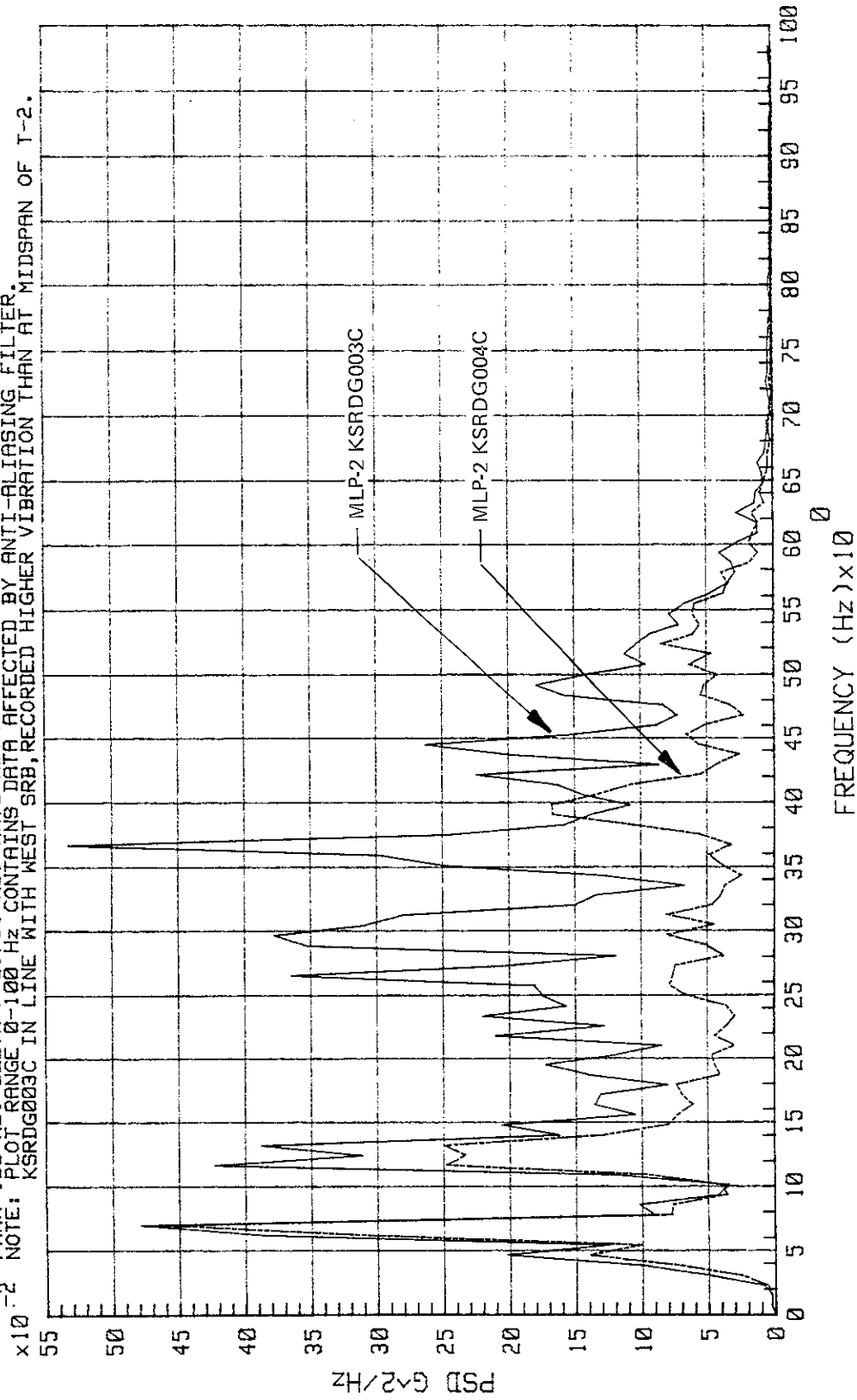


Figure 5-29. STS-6 MLP-2 Vibration of T-2 Truss Top Chord, Z Direction, 0 to 100 Hz

KSR # DG005A DG006A

KSRDG005A LOCATED BTW I-2 & G-14 @ CENTERLINE OF WEST SRB ROOM 9B. FROM I+0.0 TO I+8.2 SEC.
 KSRDG006A LOCATED BTW I-2 & G-14 @ CENTERLINE OF MLP-2 ROOM 9B. FROM I+0.0 TO I+8.2 SEC.
 FMAX=500 Hz. DELTA-F=0.976 Hz.

KSR # DG005A DG006A

BOTH SENSORS SHOW THE SAME VIBRATION
 -2 ENVIRONMENT AT EITHER LOCATION.
 PLOT RANGE 100-250 Hz.

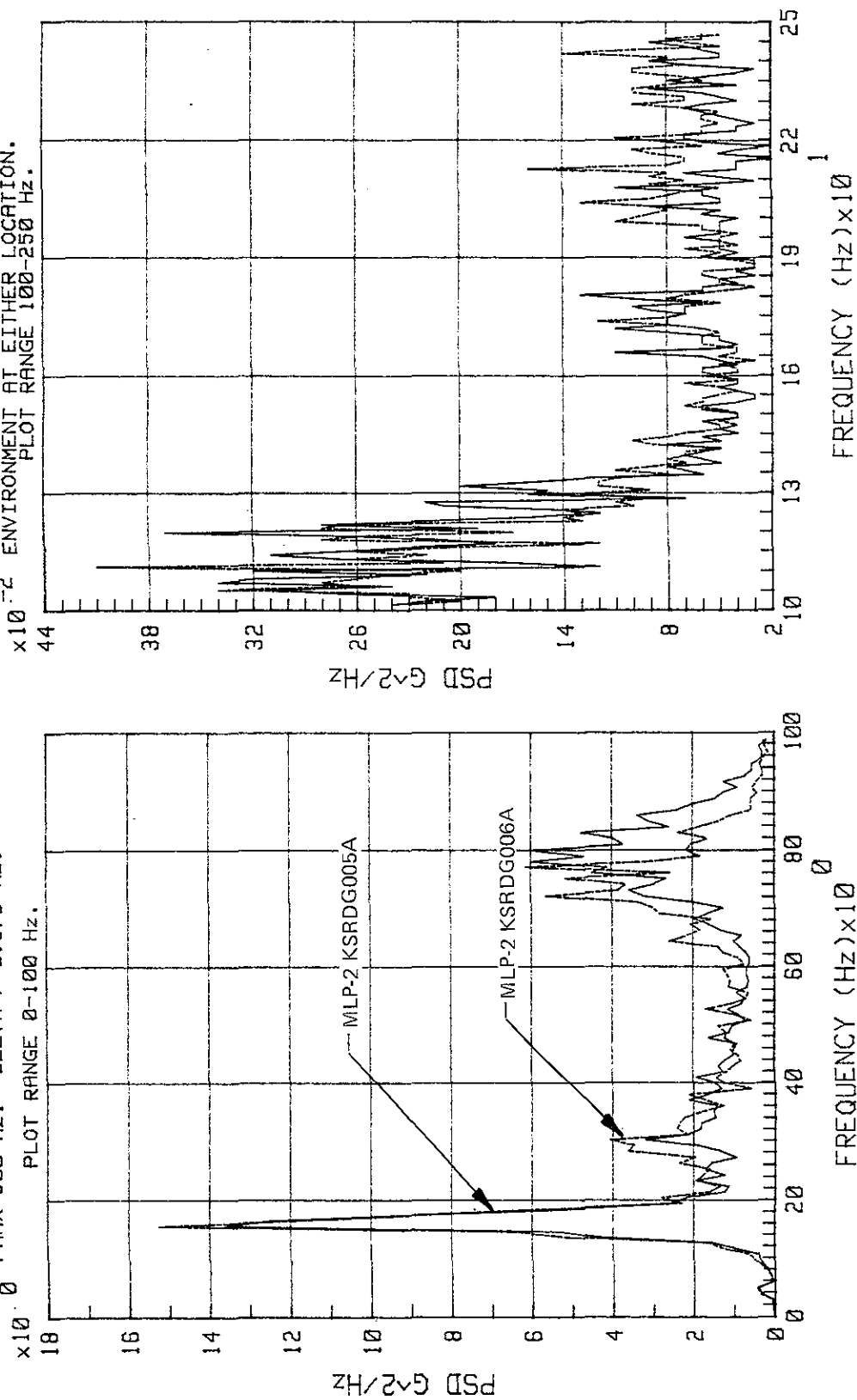
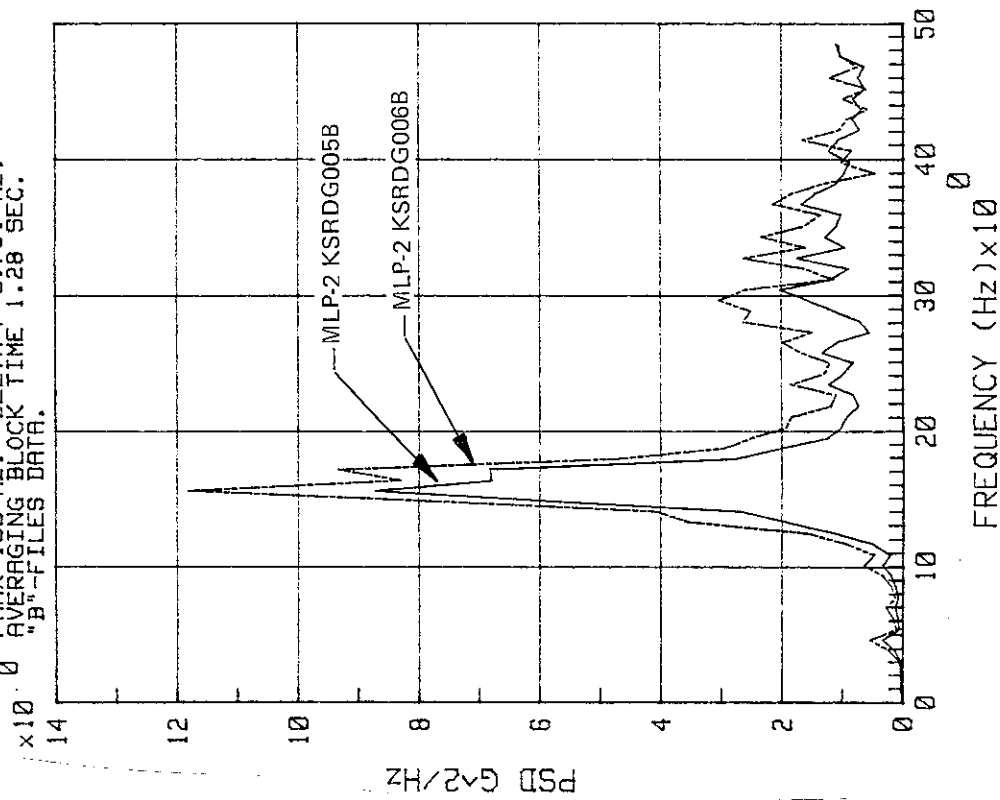


Figure 5-30. STS-6 MLP-2 Vibration of Deck B Floor Beams, Z Direction, 0 to 100 Hz and 100 to 250 Hz

KSC-DD-818-TR

KSR # DG005B DG006B

KSRDG005B LOCATED BTW I-2 & G-14 @ CENTERLINE OF WEST SRB, ROOM 9B. FROM I+0.0 TO I+9.0 SEC.
 KSRDG006B LOCATED BTW I-2 & G-14 @ CENTERLINE OF MLP-2 ROOM 9B. FROM I+0.0 TO I+9.0 SEC.
 FMAX=100 Hz. DELTA-F=0.781 Hz.
 AVERAGING BLOCK TIME 1.28 SEC.
 "B"-FILES DATA.



KSR # DG005C DG006C

KSRDG005C LOCATED BTW I-2 & G-14 @ CENTERLINE OF WEST SRB, ROOM 9B. FROM I+0.0 TO I+9.0 SEC.
 KSRDG006C LOCATED BTW I-2 & G-14 @ CENTERLINE OF MLP-2 ROOM 9B. FROM I+0.0 TO I+9.0 SEC.
 FMAX=100 Hz. DELTA-F=0.391 Hz.
 AVERAGING BLOCK TIME 2.56 SEC.
 "C"-FILES DATA.

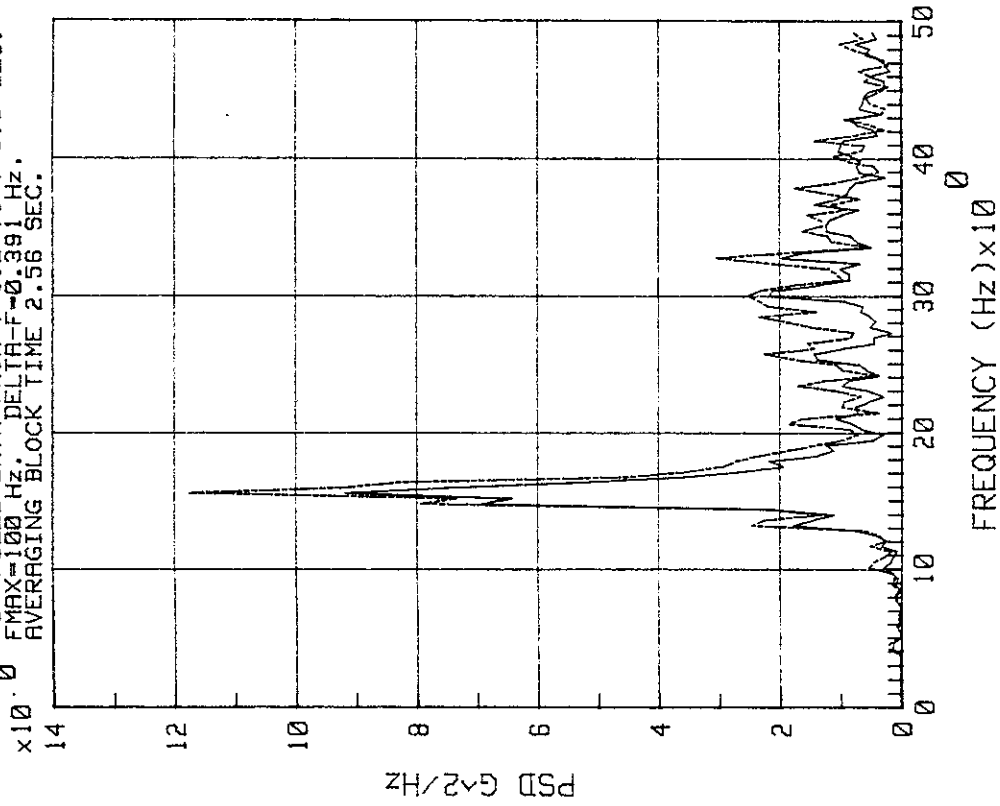


Figure 5-31. STS-6 MLP-2 Vibration of Deck B Floor Beams, Z Direction, 0 to 50 Hz

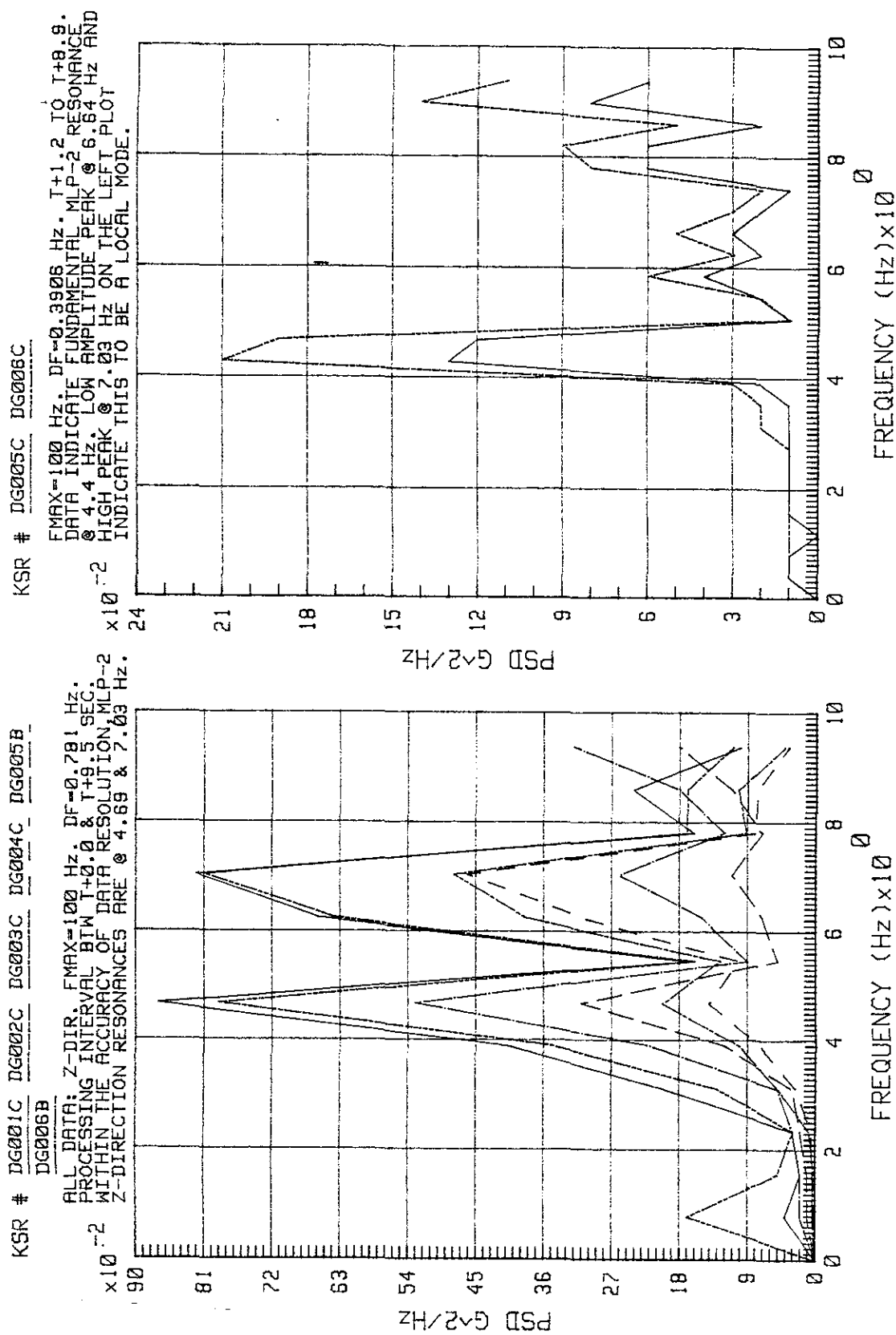


Figure 5-32. STS-6 Data Pertinent to MLP-2 Fundamental Resonances After SRB Ignition

5.2 FSS

The FSS was instrumented with approximately 50 vibration sensors during the launches of STS-1, -2, and -3. All sensors were located on floor beams and at 75-, 115-, 145-, 215-, and 255-ft levels except for a triaxial sensor that was mounted on the ET arm vertical member at the 215-ft level. During STS-4 and -5 launches, the LH₂ and LO₂ Dewar gage panels were instrumented with 18 vibration sensors located on the 155-ft level. The resulting data were processed and published in the documents listed in the bibliography herein. Worst-case samplings of the following elements of the FSS have been selected for this summary and are shown in the applicable figures (figures 5-33 through 5-42). Included are raw data, PD's, PSD's, and rms time histories for the following measurements:

<u>Designation</u>	<u>Location</u>	<u>Level (ft)</u>	<u>Direction</u>
KSADB002A	Floor Beam - Side 2 (between supports)	75	Z
KSADB013A	Floor Beam - Side 4 (between supports)	115	Z
KSADB014A	Floor Beam Center - Side 1 (near main structural support)	115	Z
KSADB033A	Floor Beam - Side 1 (between supports)	195	Z
KSADB035A	Floor Beam Center - Side 1 (near main structural support)	195	Z
KSADB046A	Floor Beam - Side 1 (between supports)	255	Z
KSADB047A	Floor Beam Center - Side 1 (near main structural support)	255	Z
KSADB050A	ET Arm (vertical member)	215	Z
KFHDB007A	LH ₂ Dewar (gage panel center)	155	X
KFODB007A	LO ₂ Dewar (gage panel center)	155	X

STS-3 FSS multiple plot summary PSD's for various levels and directions, previously published as appendix C in KSC-DD-651-TR, are included in this summary (figures 5-43 through 5-61). Not included, but recommended for additional information is appendix C of KSC-DD-677-TR, which contains data validation criteria, calculated rms displacements, and zoom plots of significant PSD's.

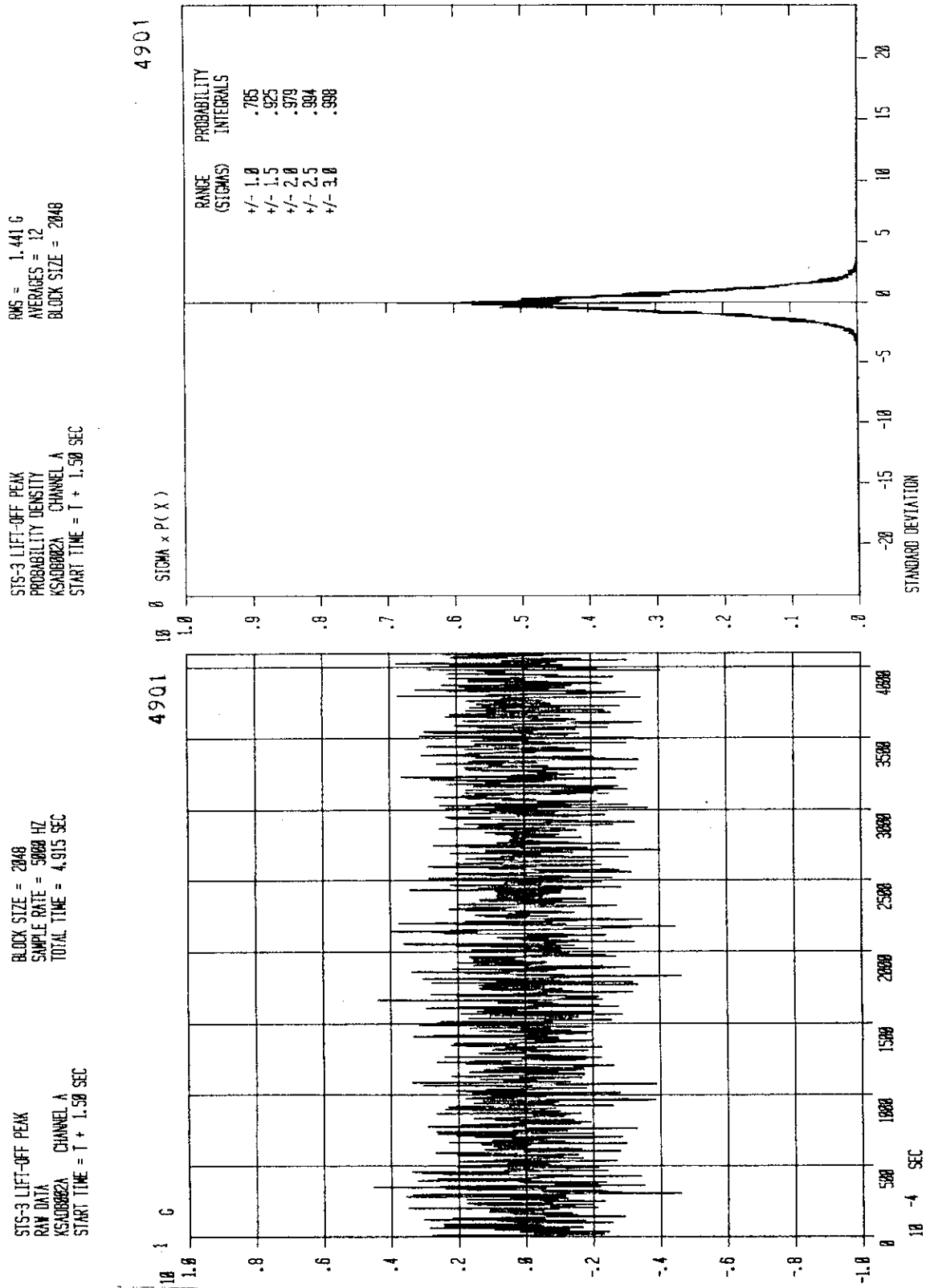


Figure 5-33. Floor Beam Side 2, 75-ft Level, Z Direction (Sheet 1 of 2)

KSC-DD-818-TR

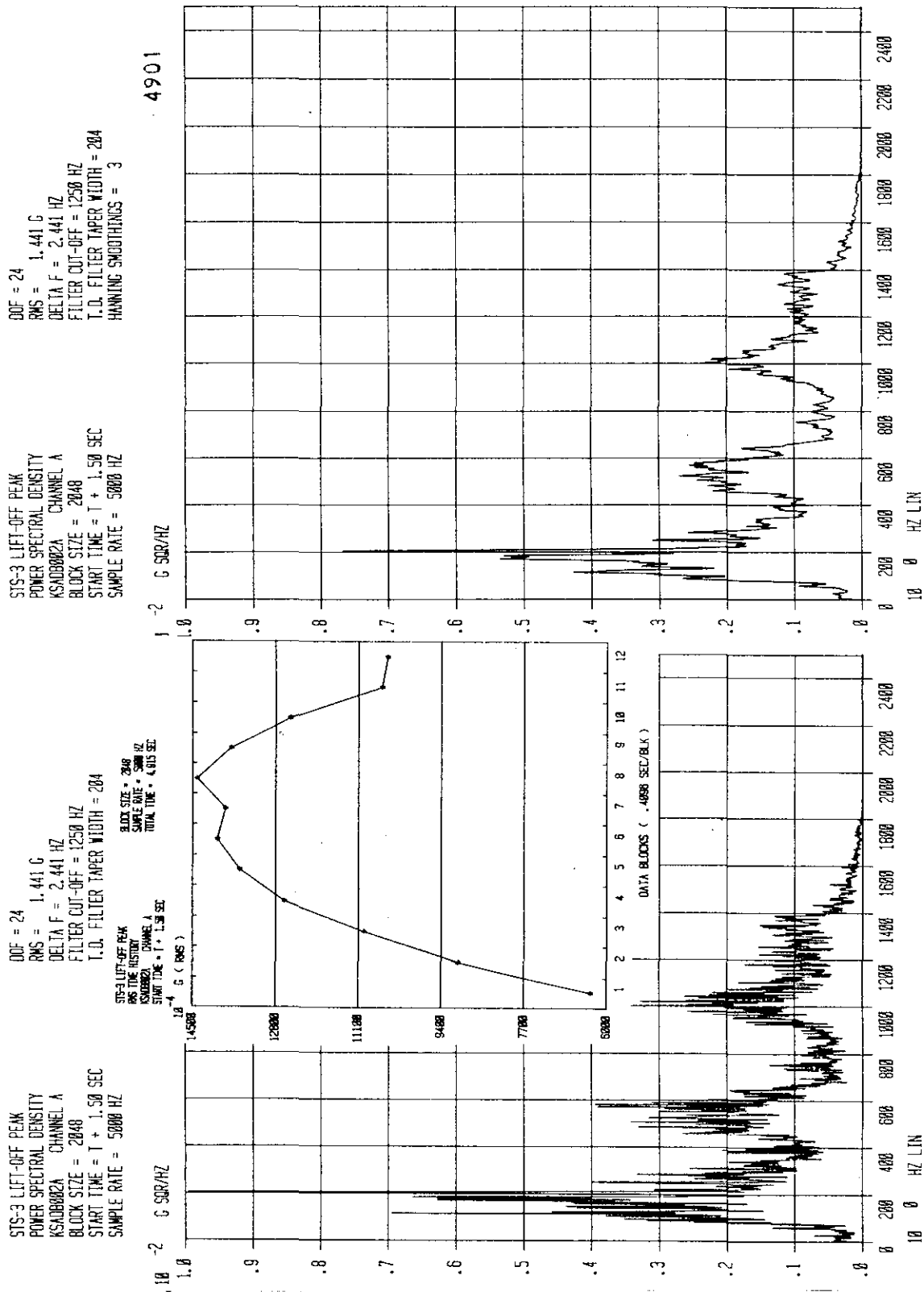


Figure 5-33. Floor Beam Side 2, 75-ft Level, Z Direction (Sheet 2 of 2)

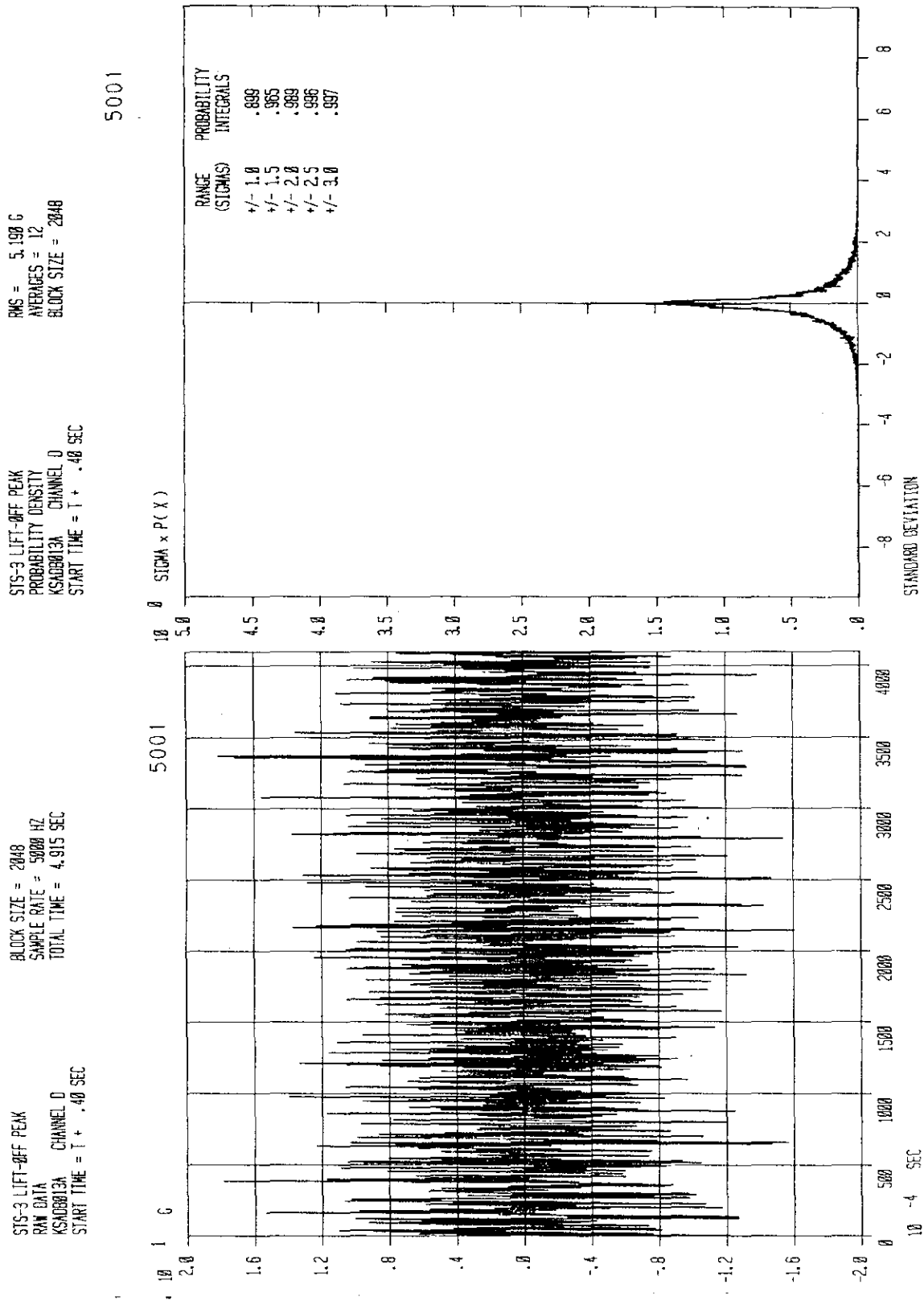


Figure 5-34. Floor Beam Center Side 4, 115-ft Level, Z Direction (Sheet 1 of 2)

KSC-DD-818-TR

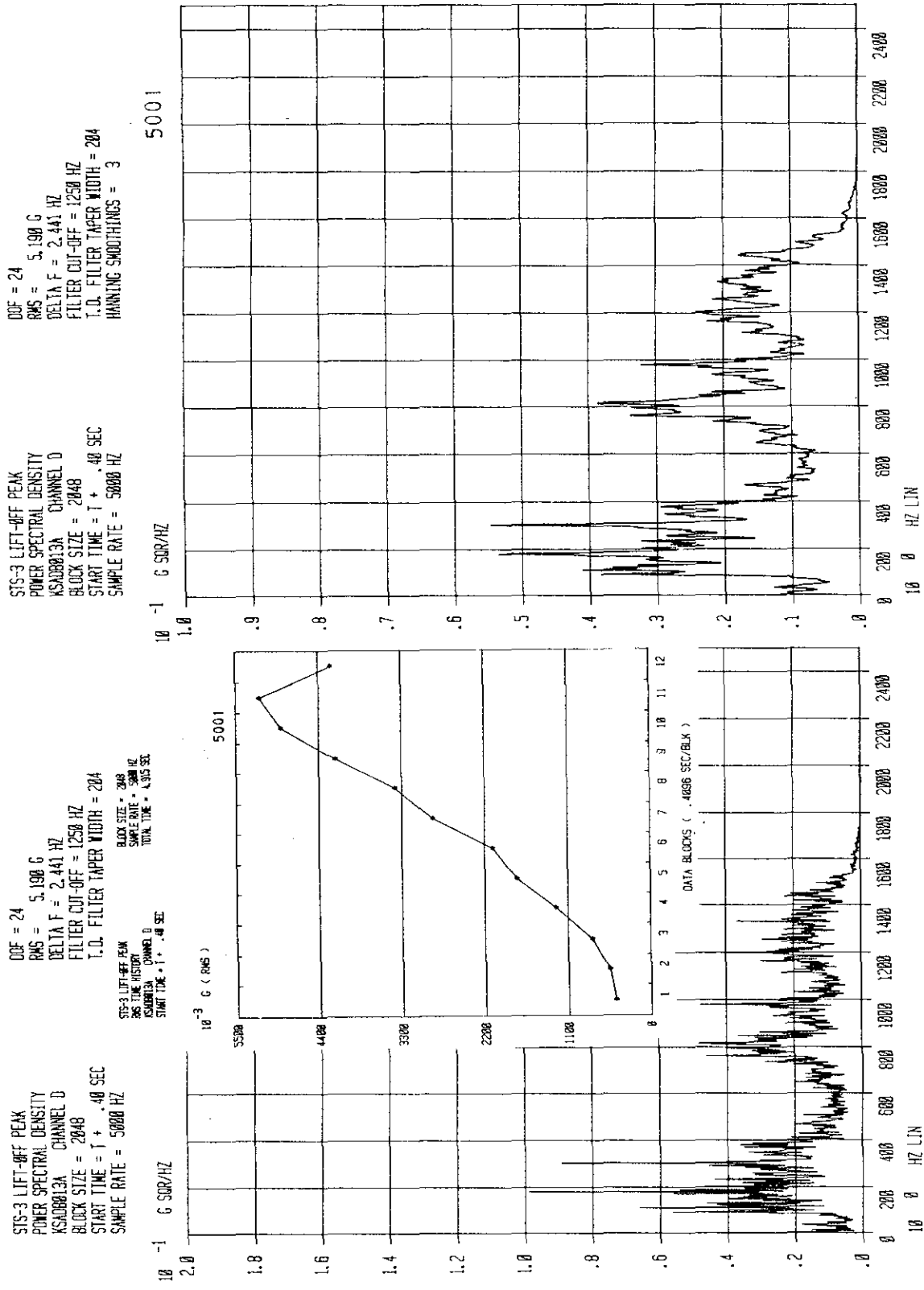


Figure 5-34. Floor Beam Center Side 4, 115-ft Level, Z Direction (Sheet 2 of 2)

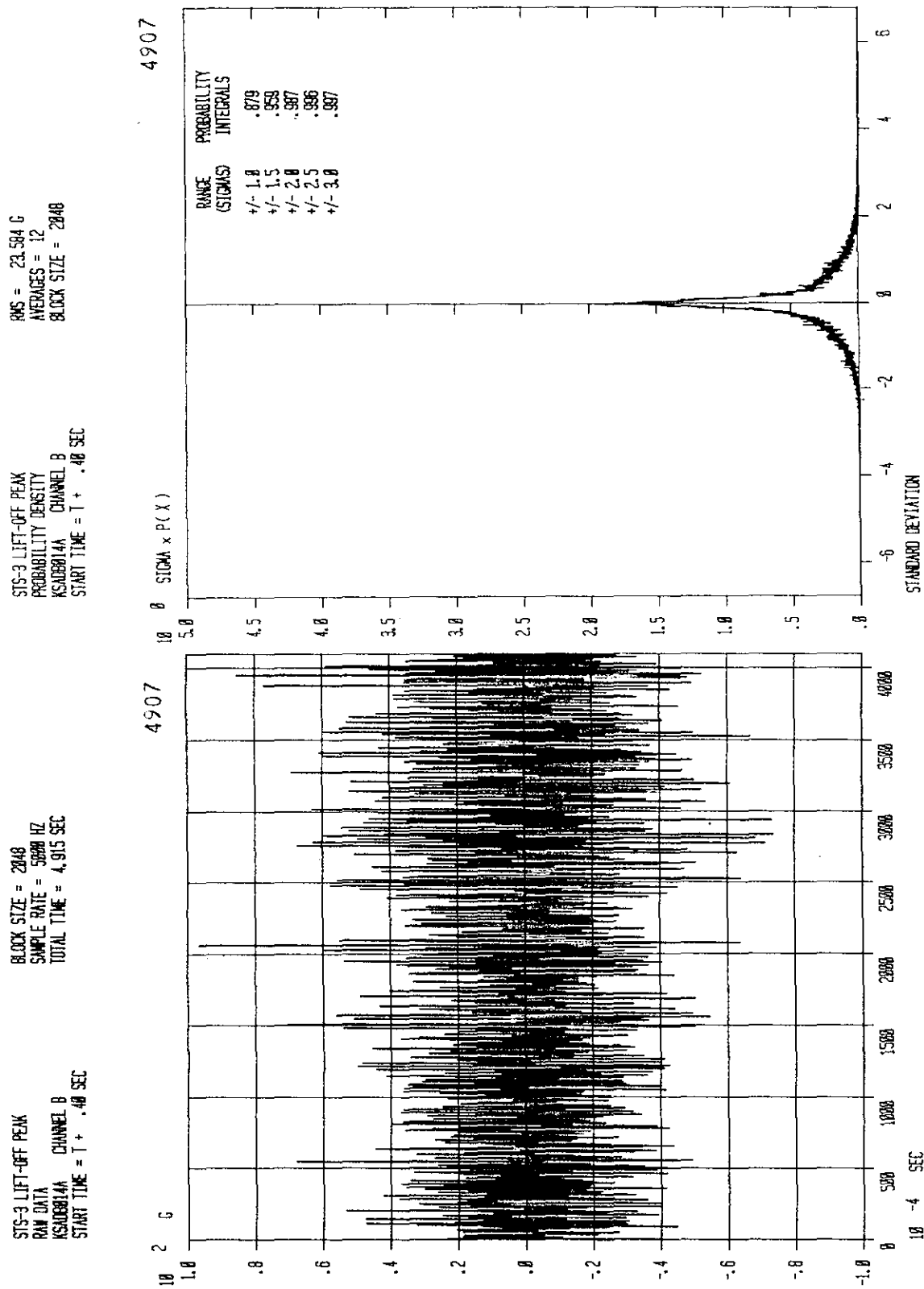


Figure 5-35. Floor Beam Center Side 1, 115-ft Level, Z Direction (Sheet 1 of 2)

KSC-DD-818-TR

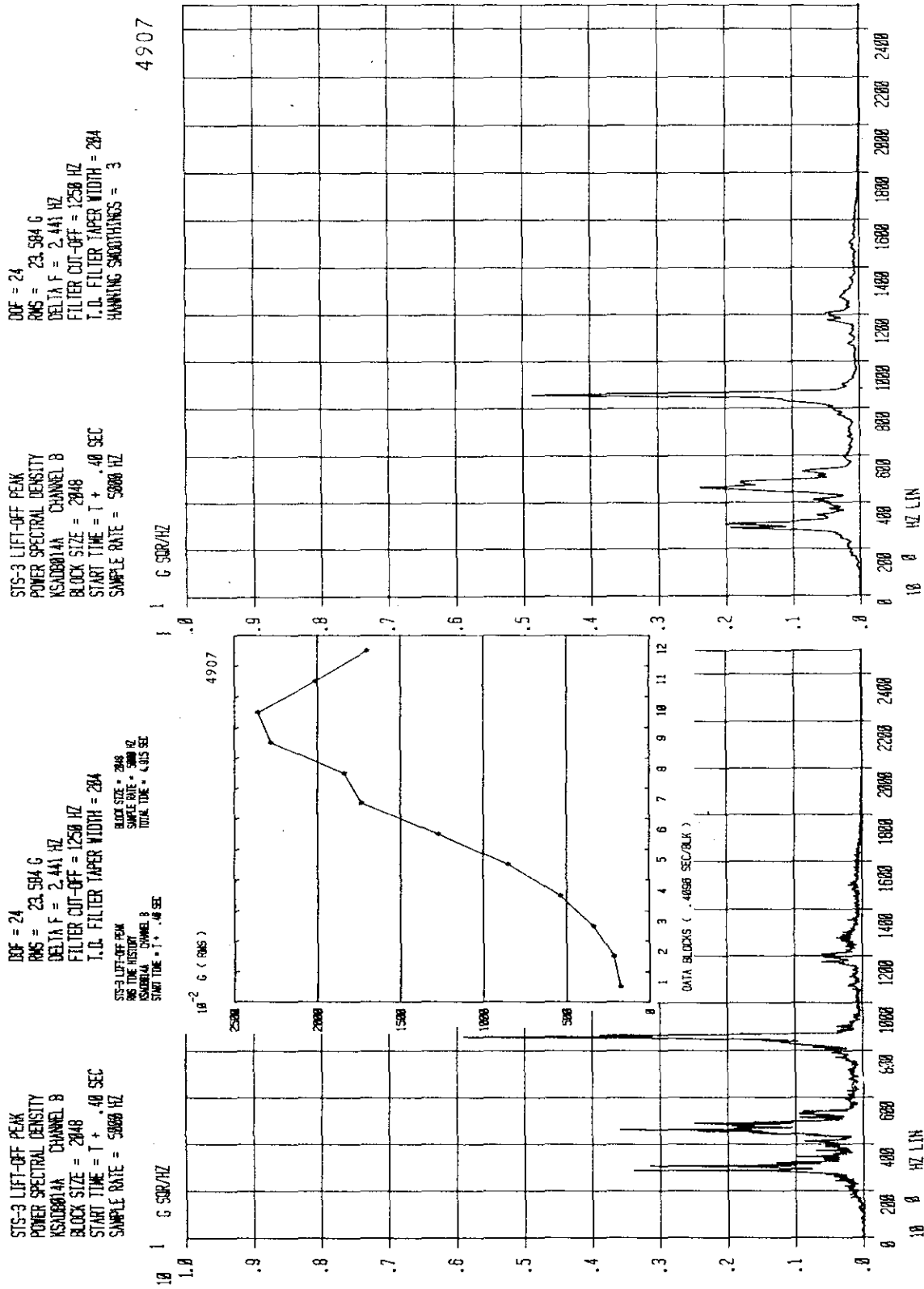


Figure 5-35. Floor Beam Center Side 1, 115-ft Level, Z Direction (Sheet 2 of 2)

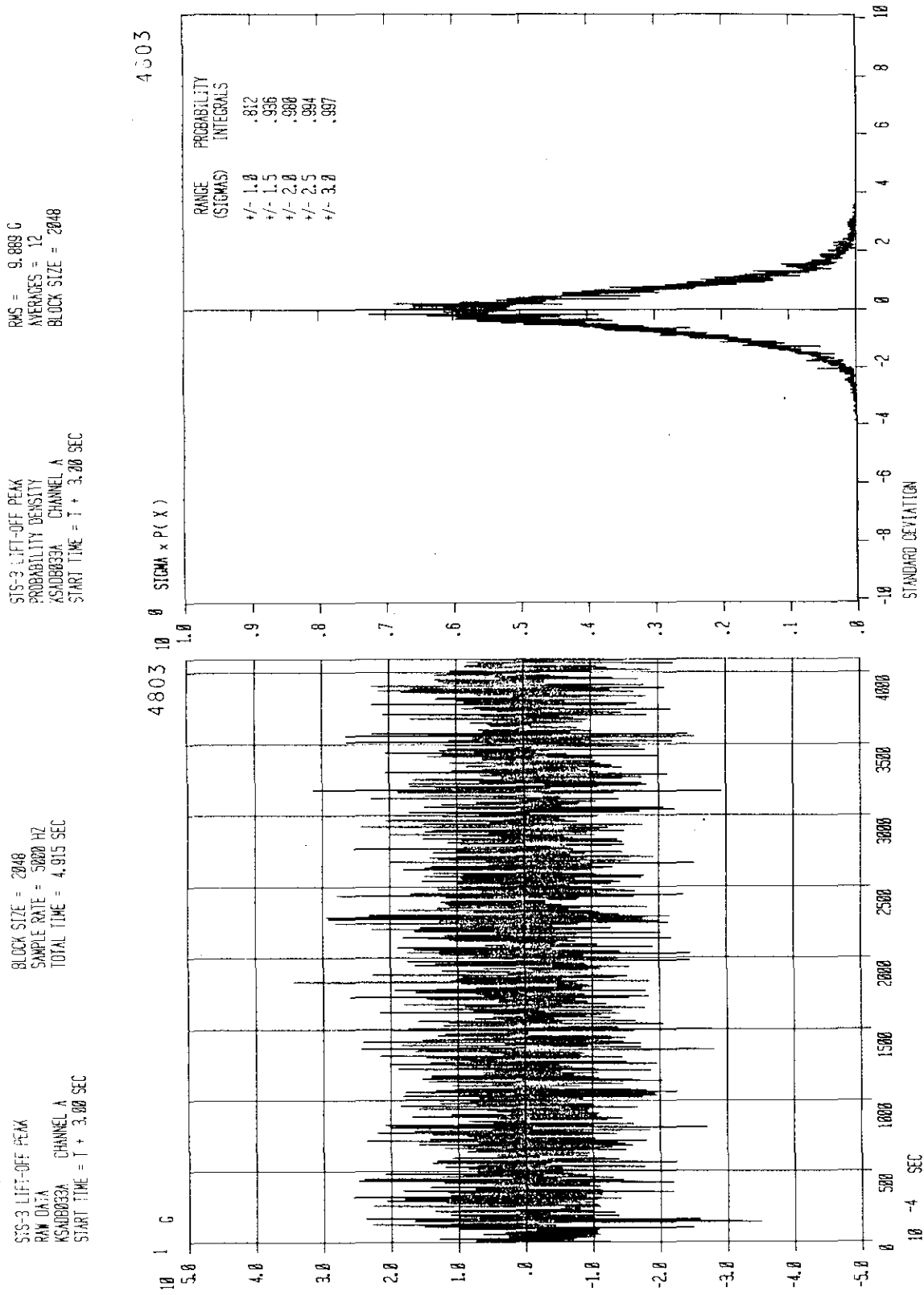


Figure 5-36. Floor Beam Side 1, 195-ft Level, Z Direction (Sheet 1 of 2)

KSC-DD-818-TR

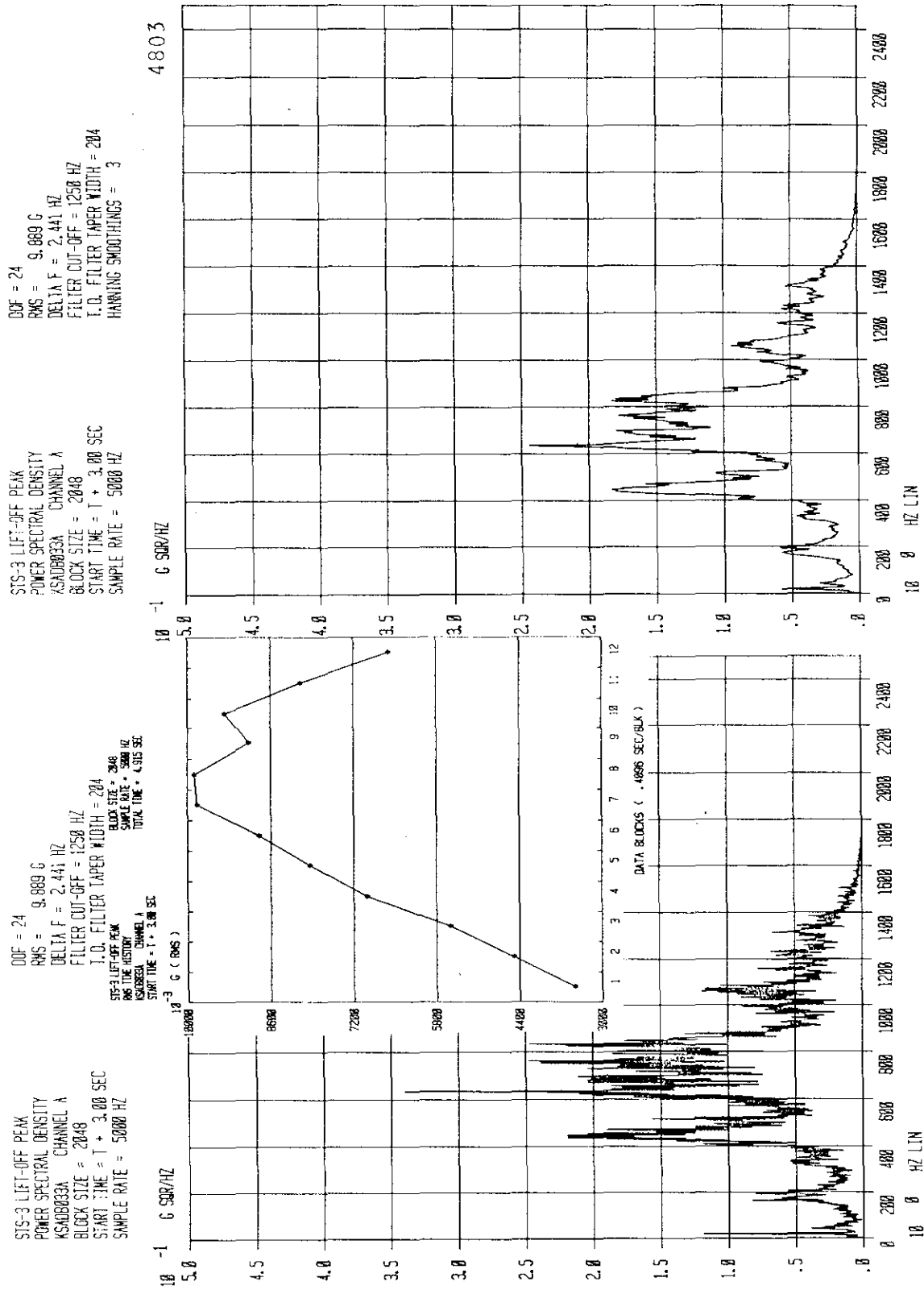


Figure 5-36. Floor Beam Side 1, 195-ft Level, Z Direction (Sheet 2 of 2)

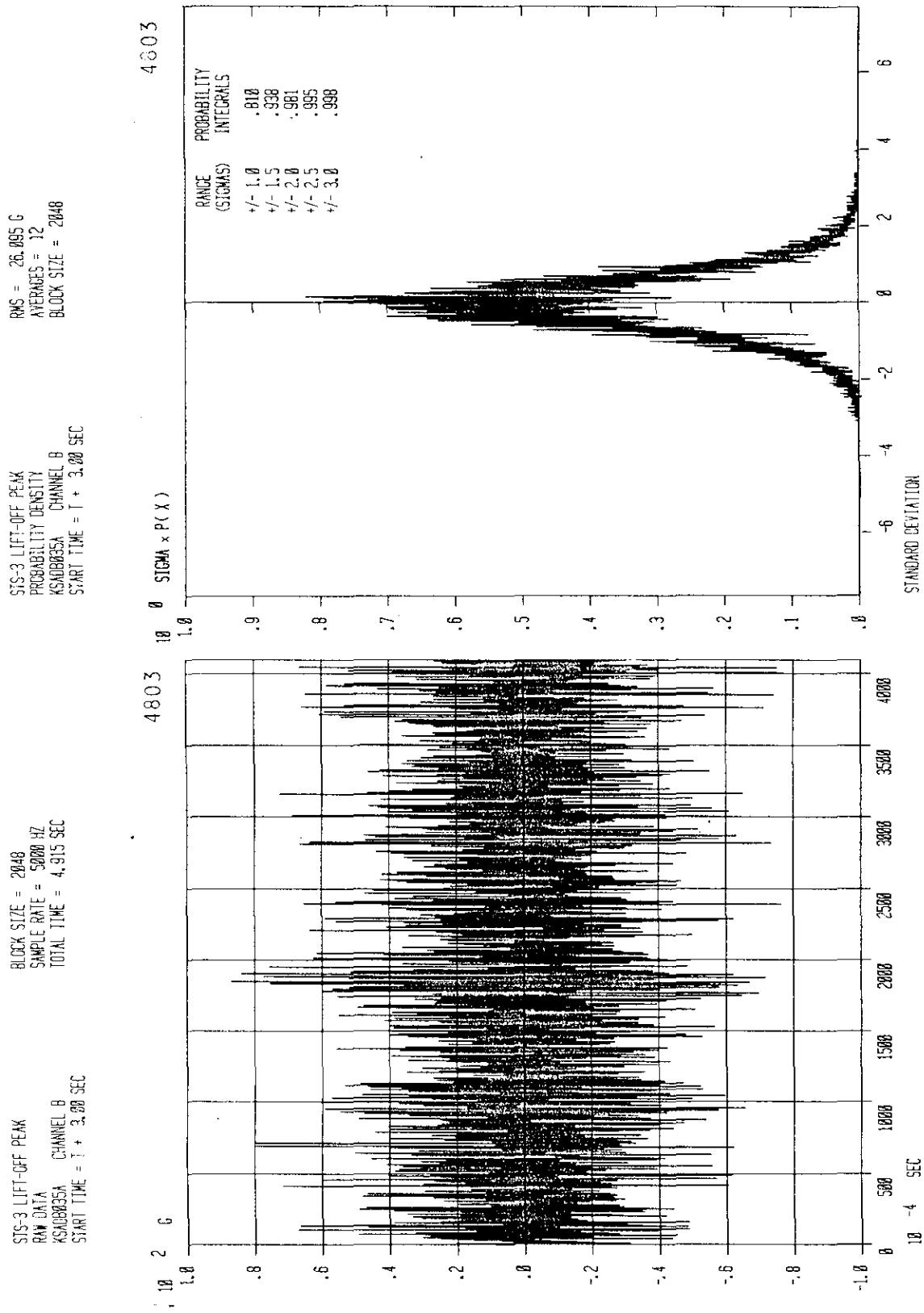


Figure 5-37. Floor Beam Center Side 1, 195-ft Level, Z Direction (Sheet 1 of 2)

KSC-DD-818-TR

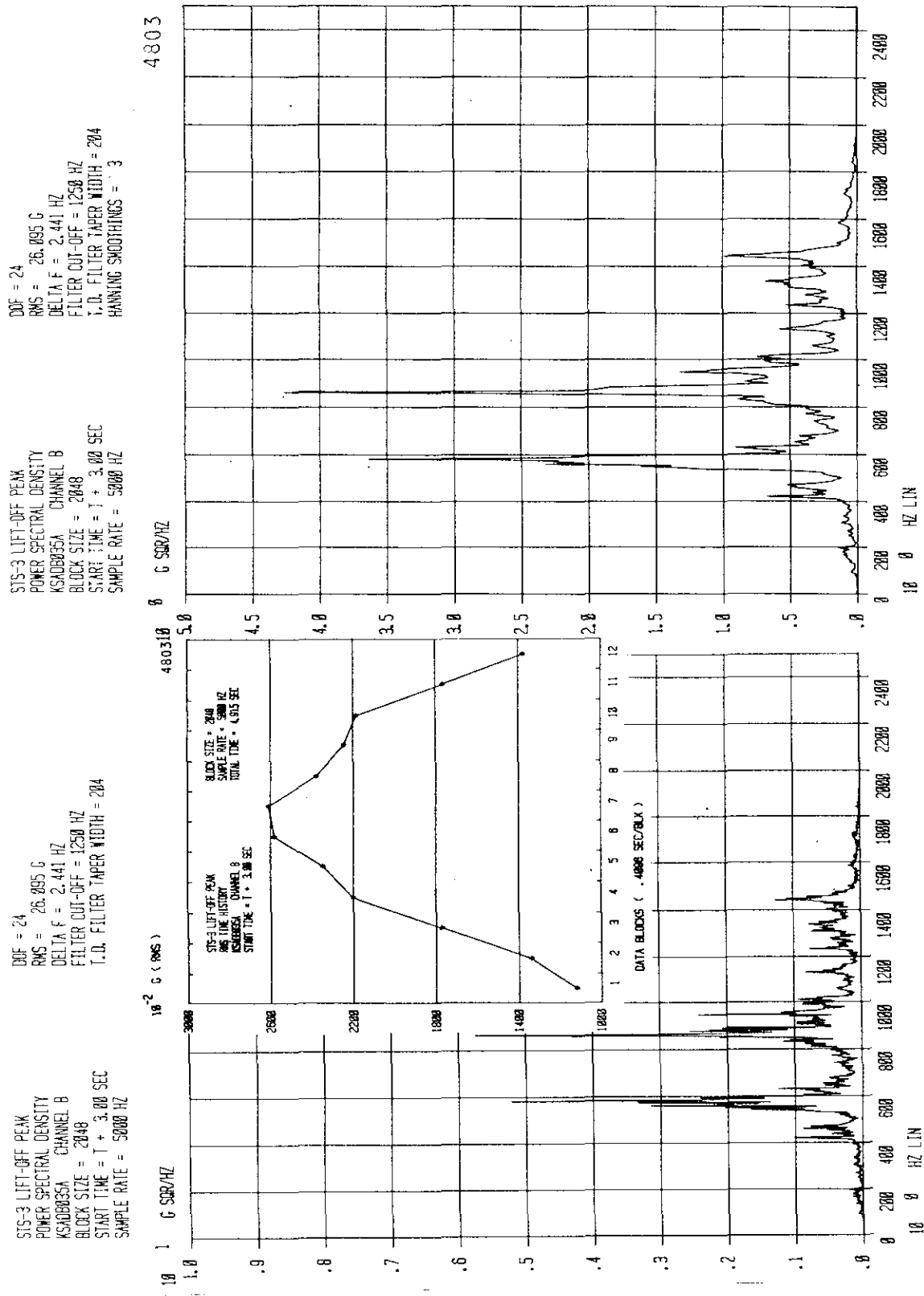


Figure 5-37. Floor Beam Center Side 1, 195-ft Level, Z Direction (Sheet 2 of 2)

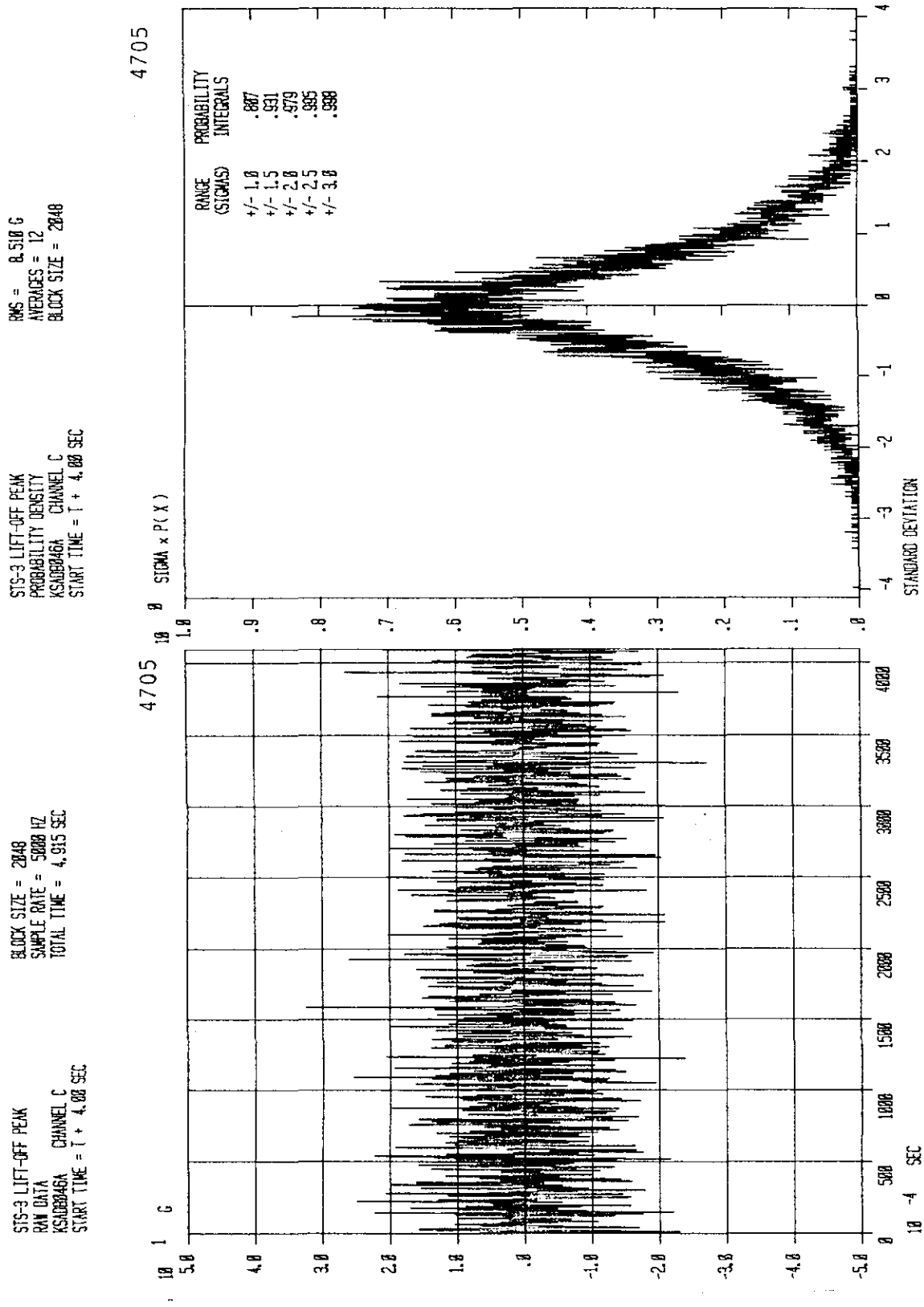


Figure 5-38. Floor Beam Side 1, 255-ft Level, Z Direction (Sheet 1 of 2)

KSC-DD-818-TR

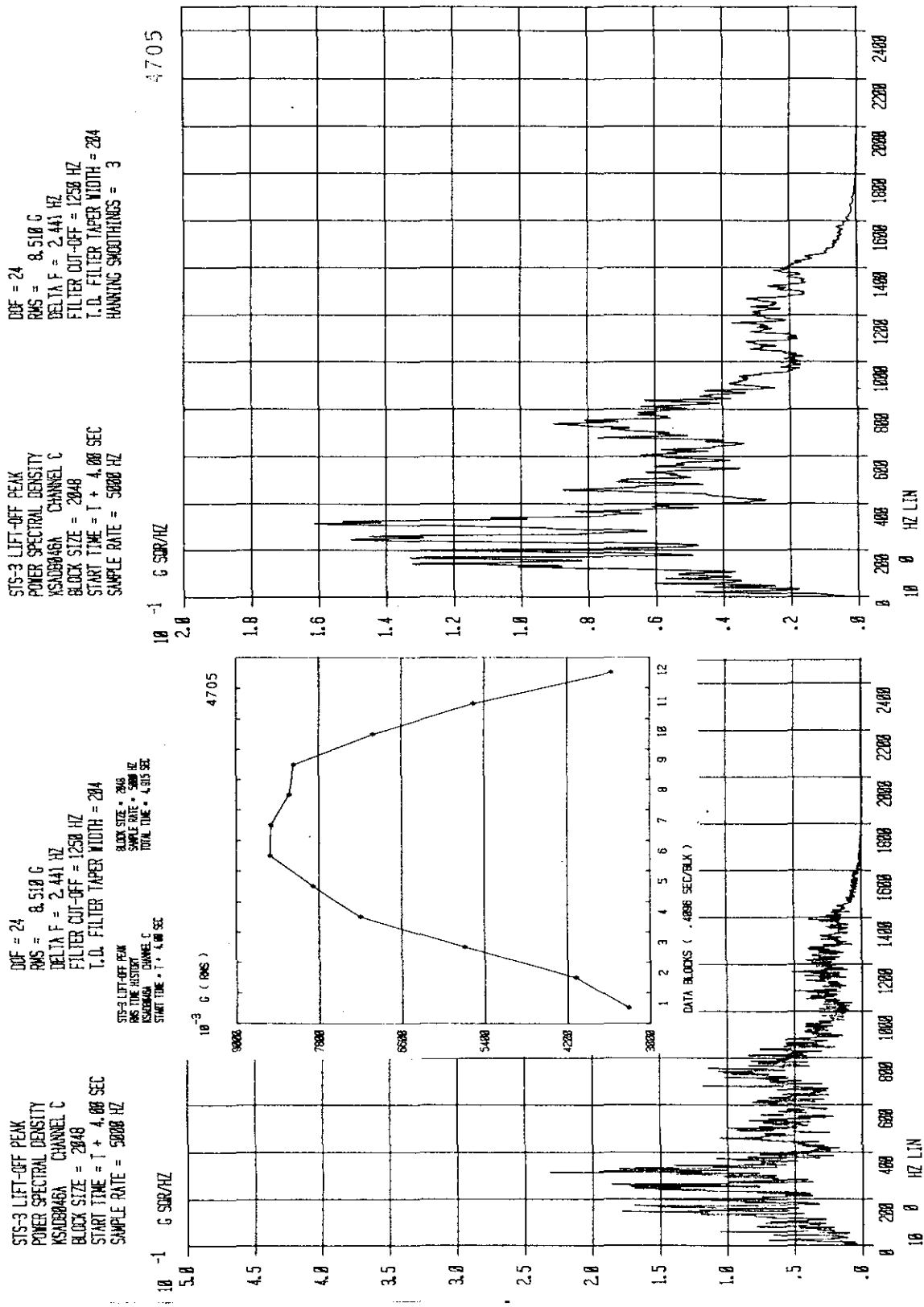


Figure 5-38. Floor Beam Side 1, 255-ft Level, Z Direction (Sheet 2 of 2)

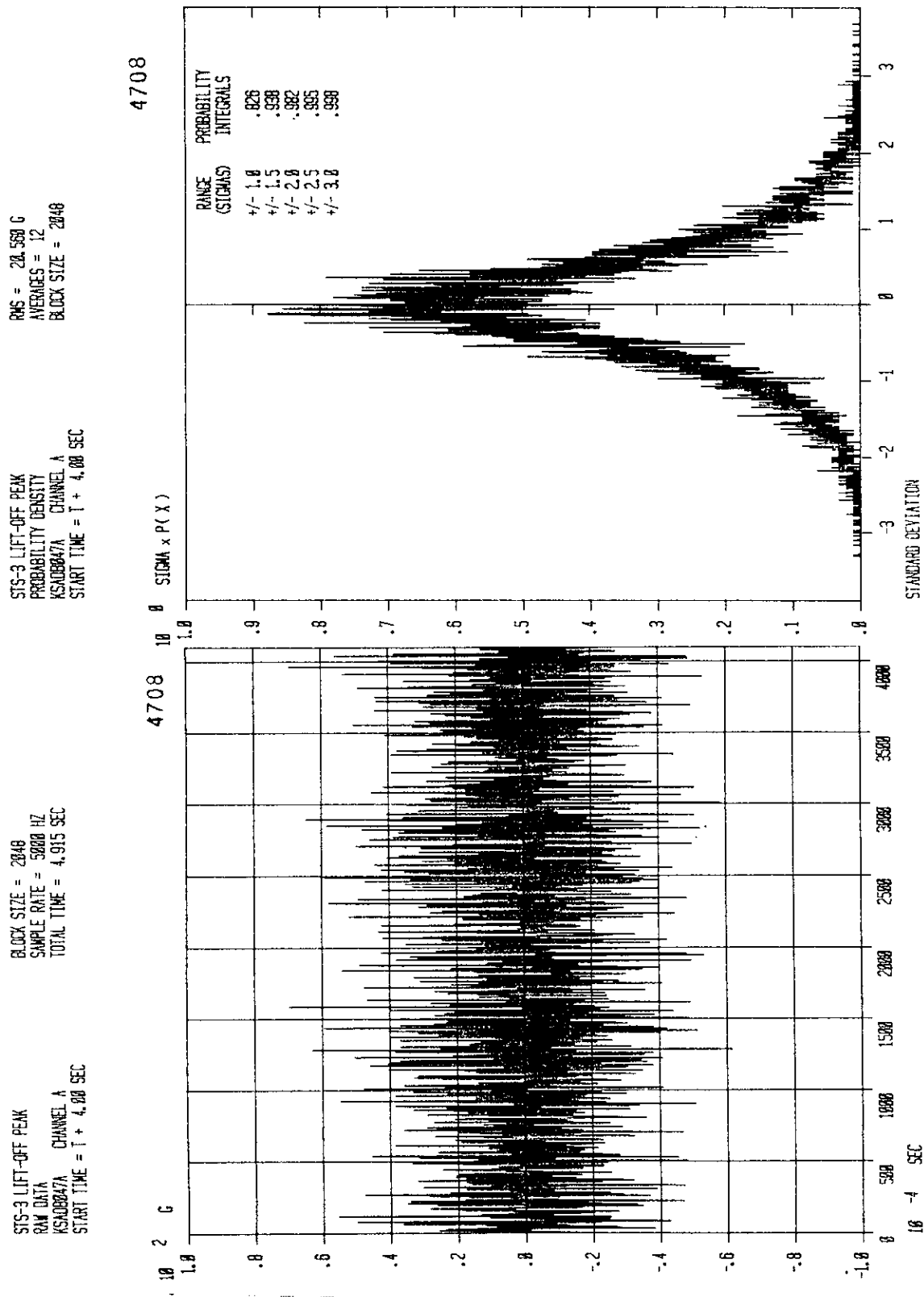


Figure 5-39. Floor Beam Center Side 1, 255-ft Level, Z Direction (Sheet 1 of 2)

KSC-DD-818-TR

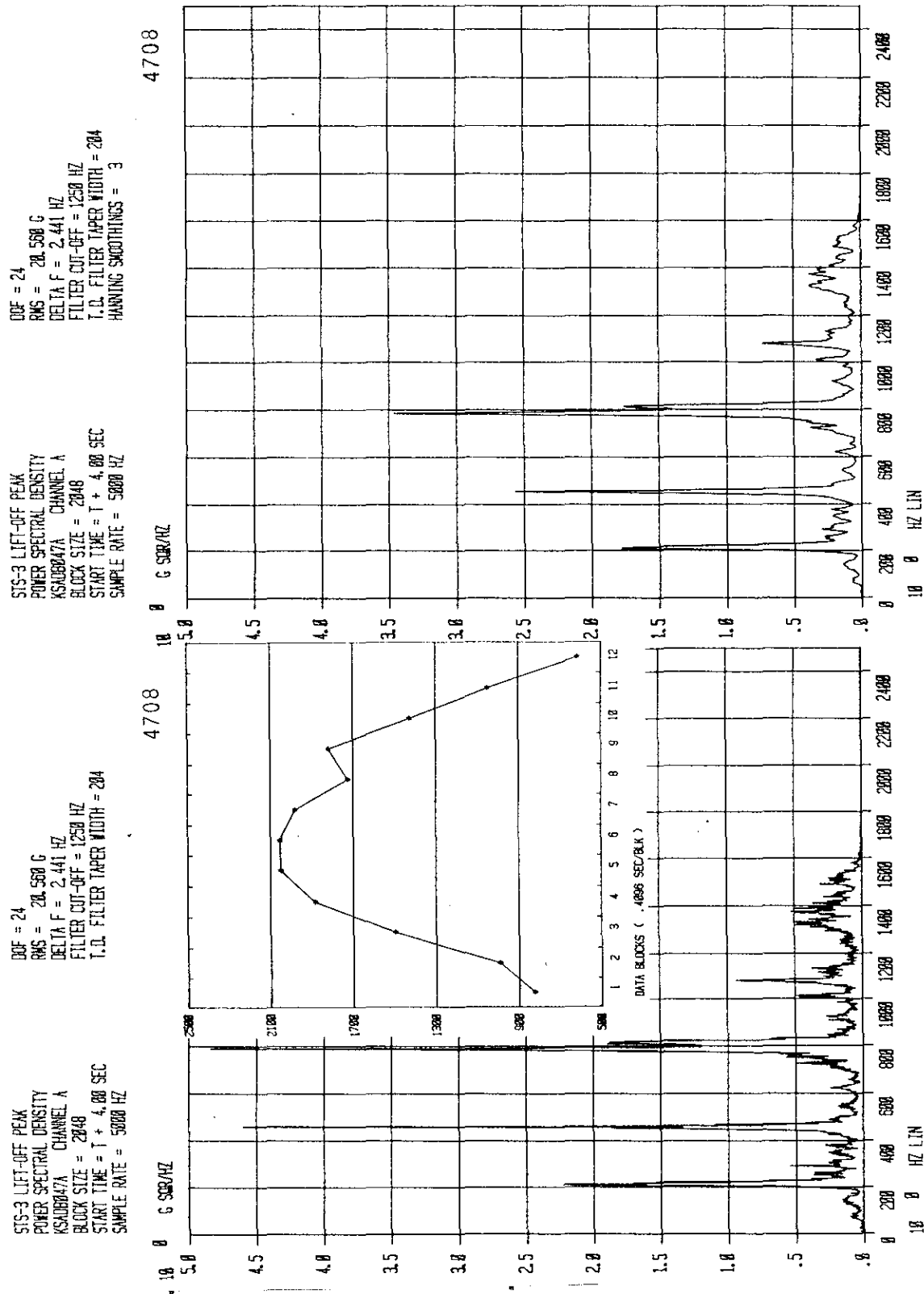


Figure 5-39. Floor Beam Center Side 1, 255-ft Level, Z Direction (Sheet 2 of 2)

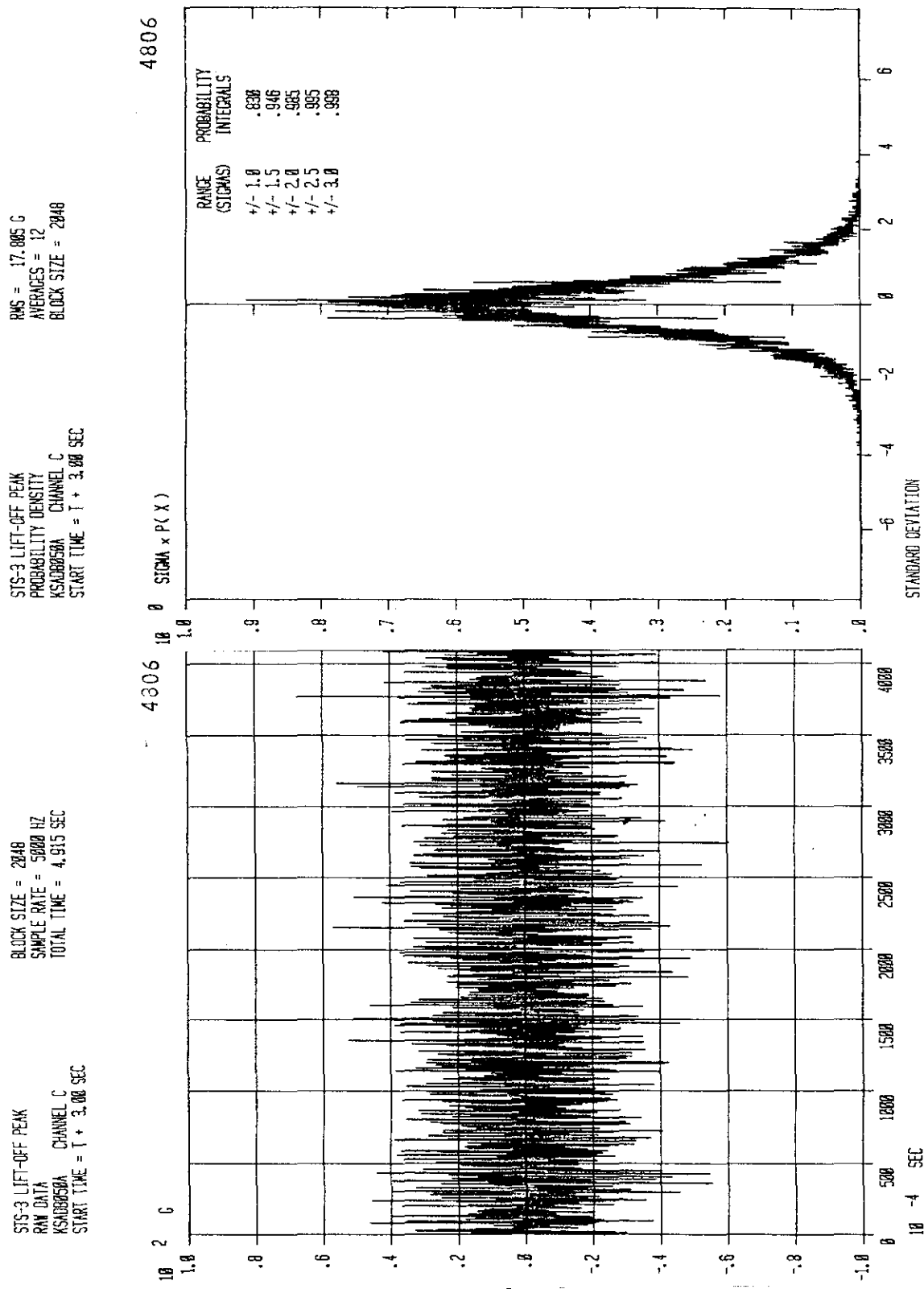


Figure 5-40. ET Arm Vertical Member, 215-ft Level, Z Direction (Sheet 1 of 2)

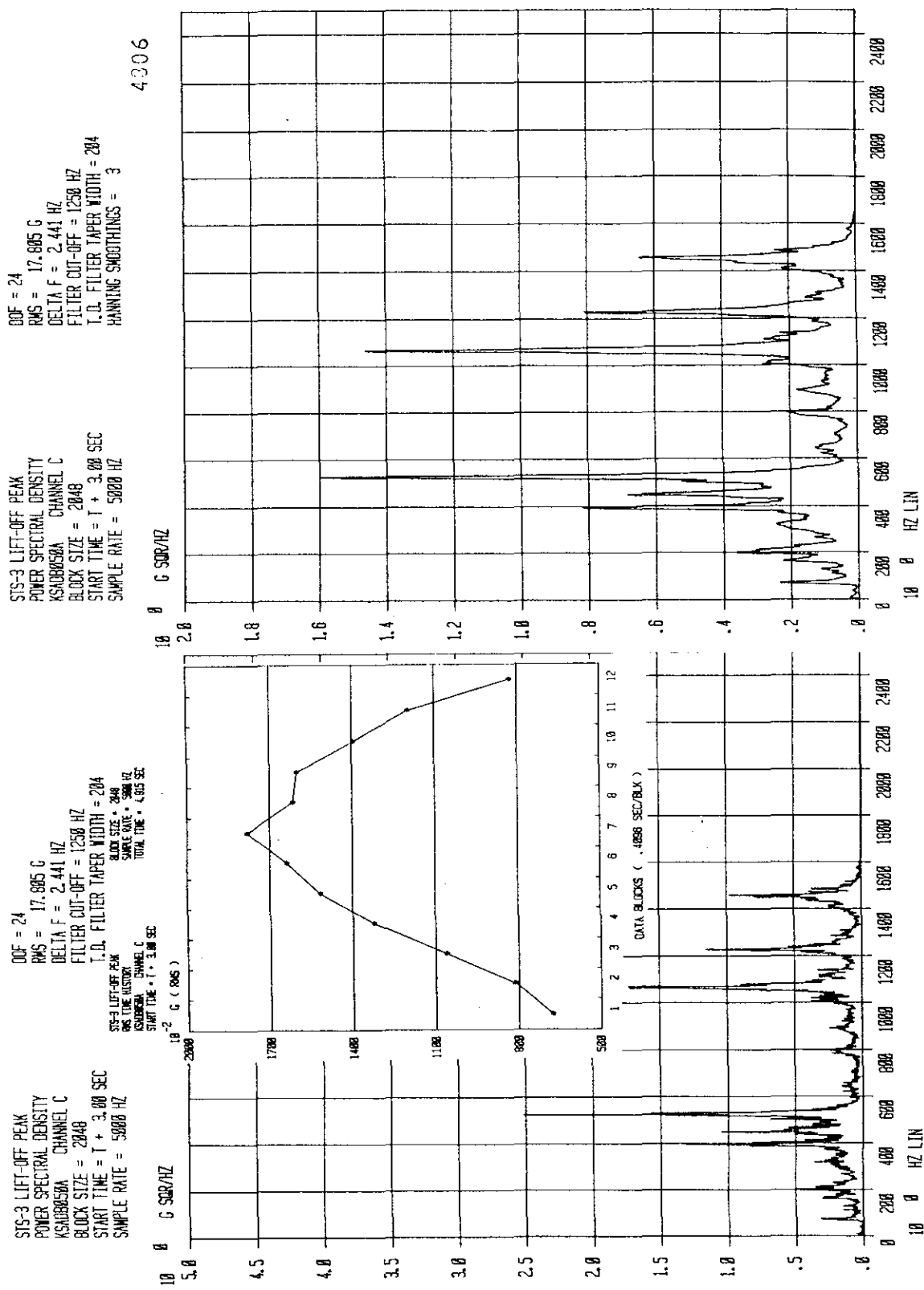


Figure 5-40. ET Arm Vertical Member, 21.5-ft Level, Z Direction (Sheet 2 of 2)

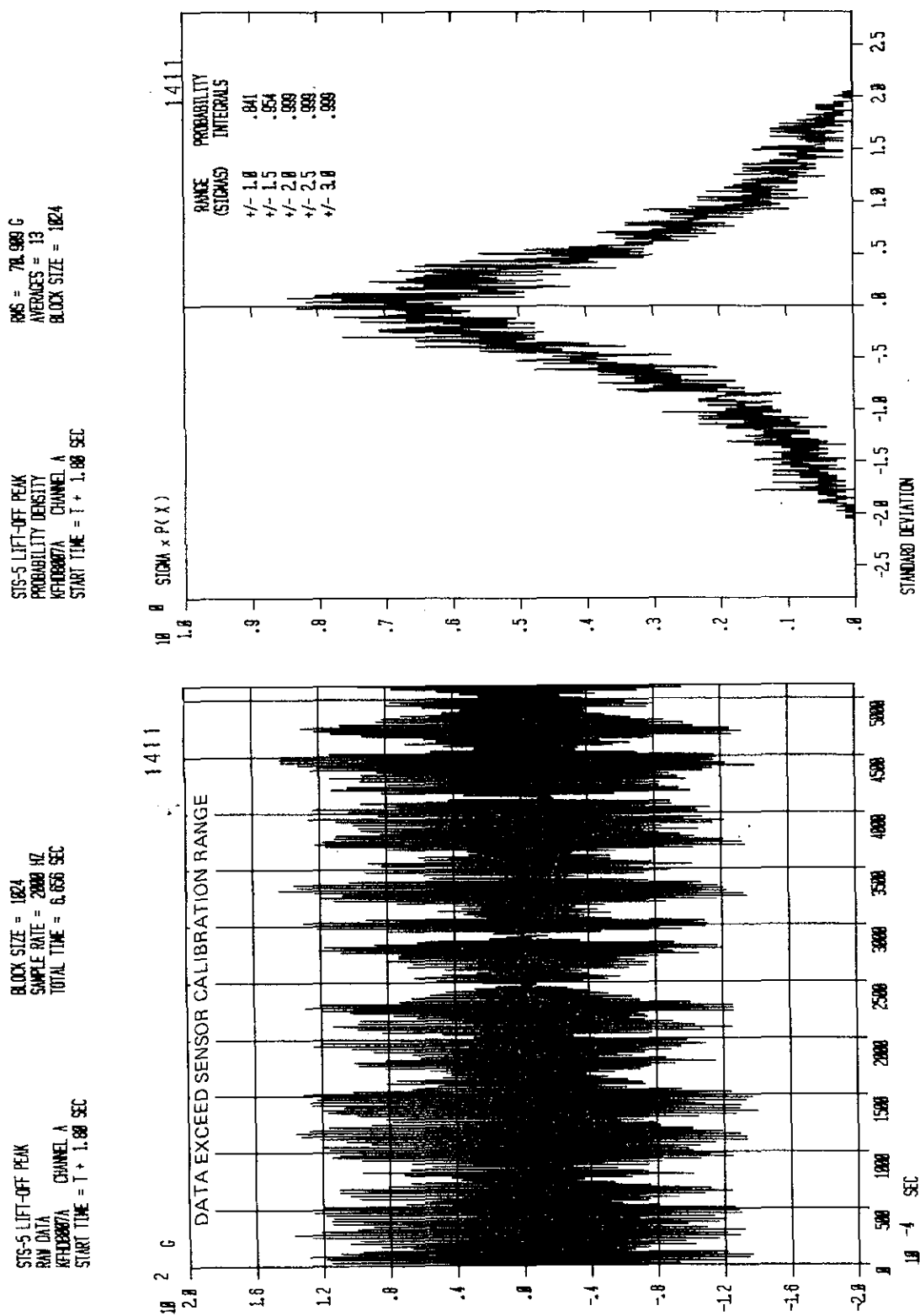


Figure 5-41. LH2 Dewar Gage Panel Center, 155-ft Level, X Direction (Sheet 1 of 2)

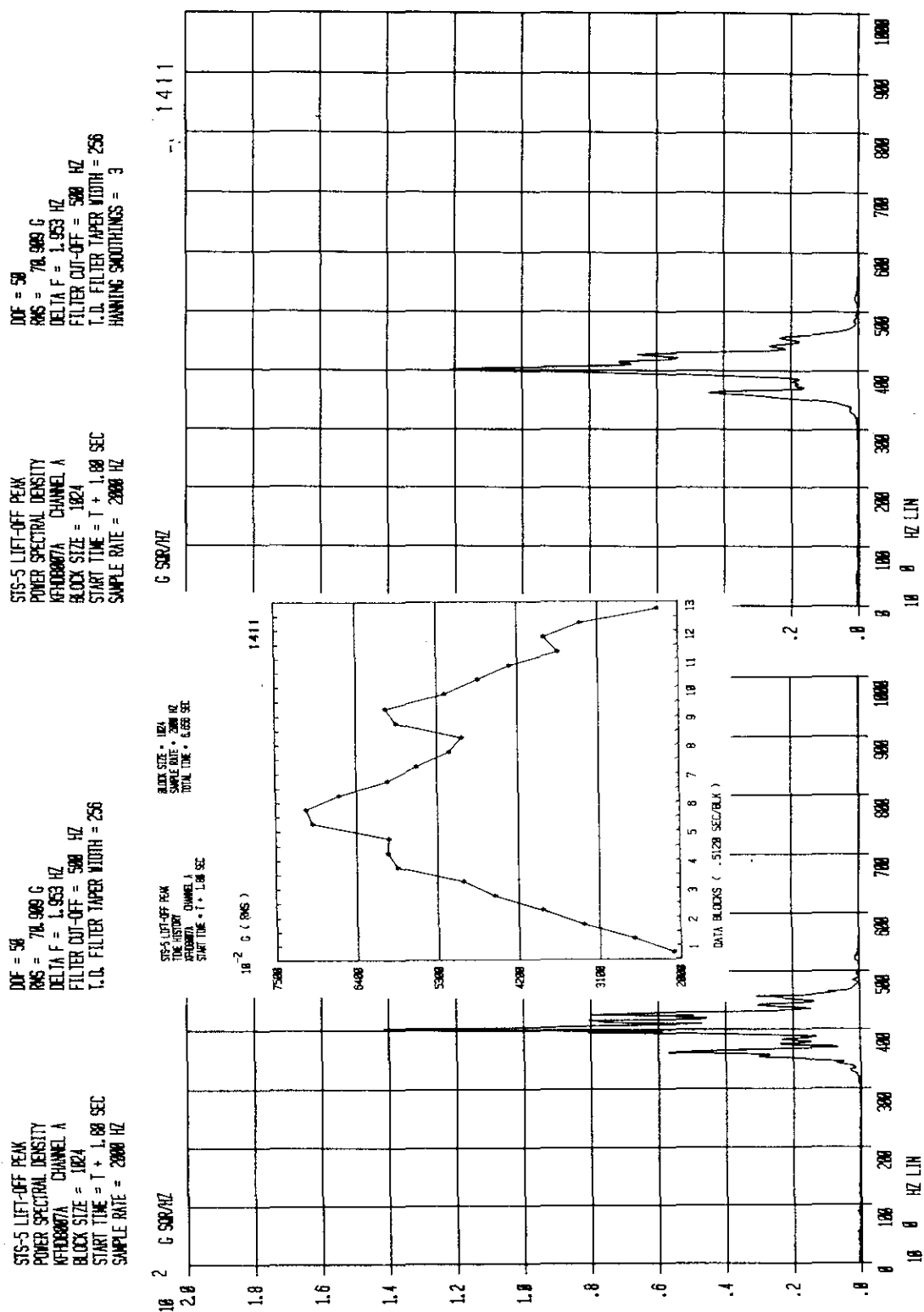


Figure 5-41. LH₂ Dewar Gage Panel Center, 155-ft Level, X Direction (Sheet 2 of 2)

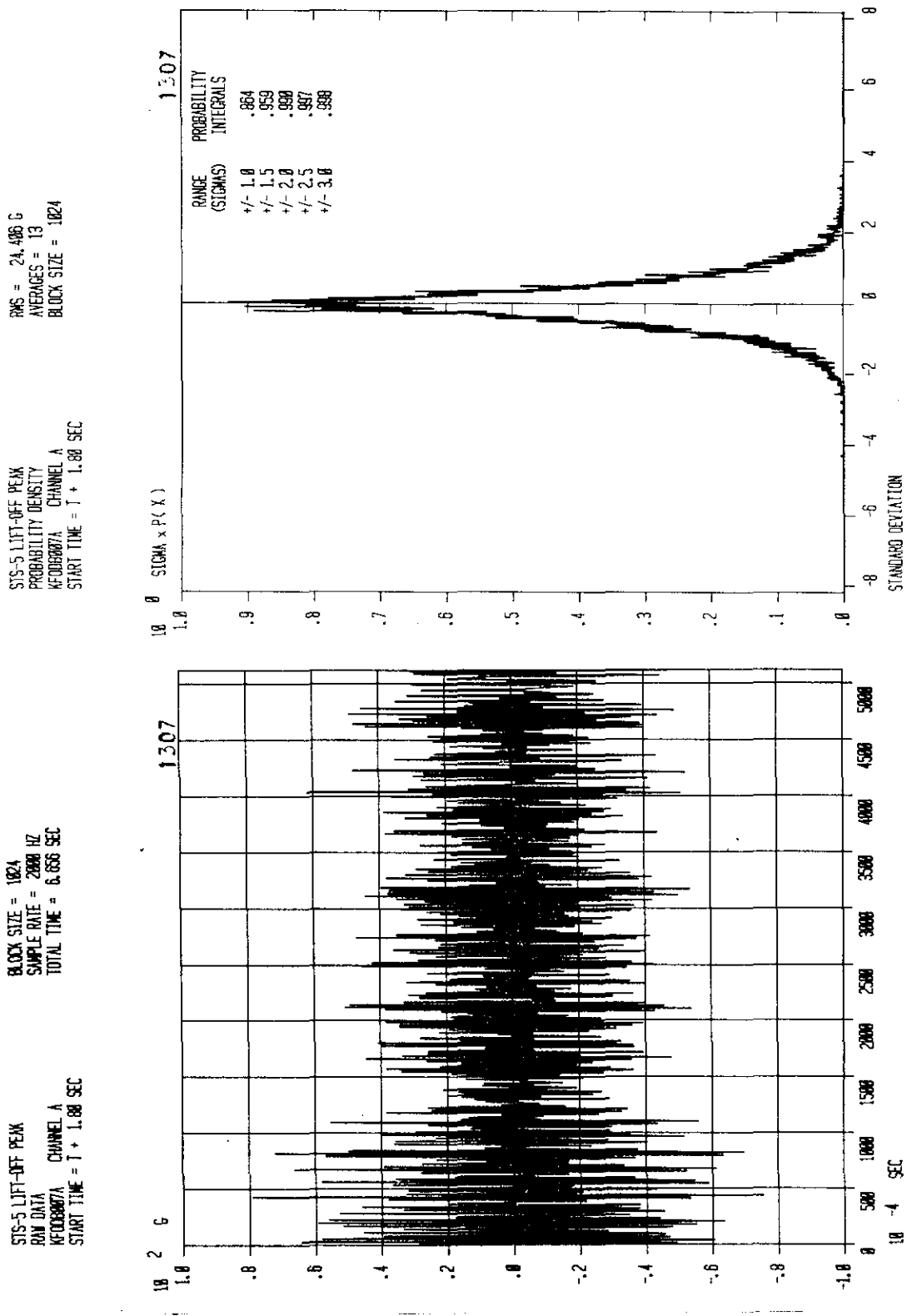
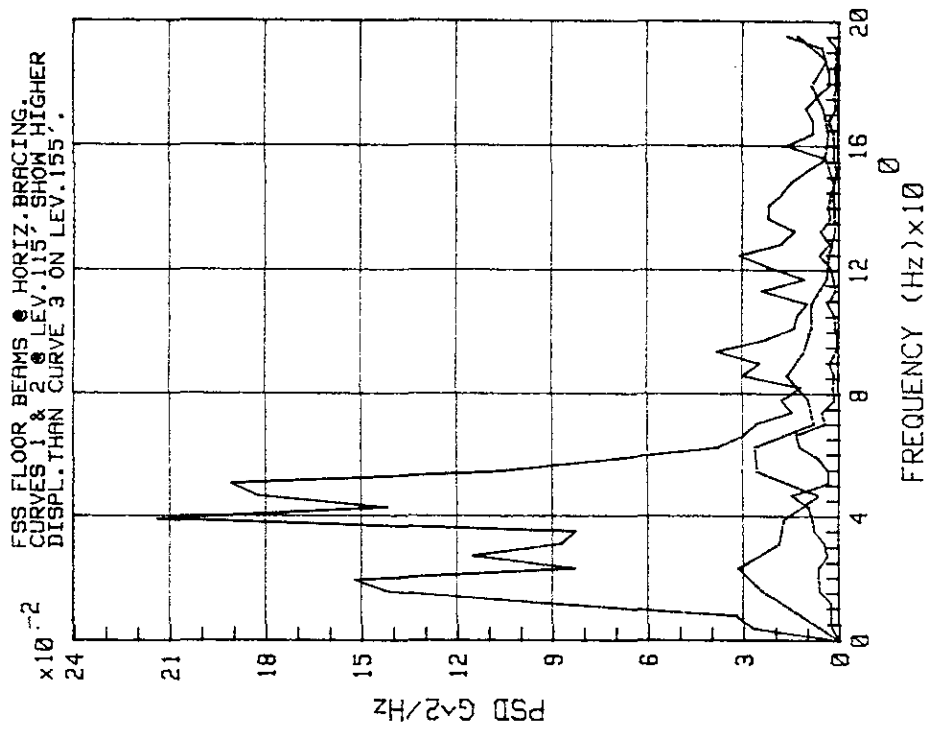


Figure 5-42. L02 Dewar Gage Panel Center, 155-ft Level, X Direction (Sheet 1 of 2)

Figure 5-42. L02 Dewar Gage Panel Center, 155-ft Level, X Direction (Sheet 2 of 2)

STS-3, FSS VIBR. @ LEV. 115' & 155', Y-DIR.

KSA # DB005A DB011B DB020B



STS-3, FSS VIBR. @ LEV. 115' & 155', X-DIR

KSA # DB010B DB019A

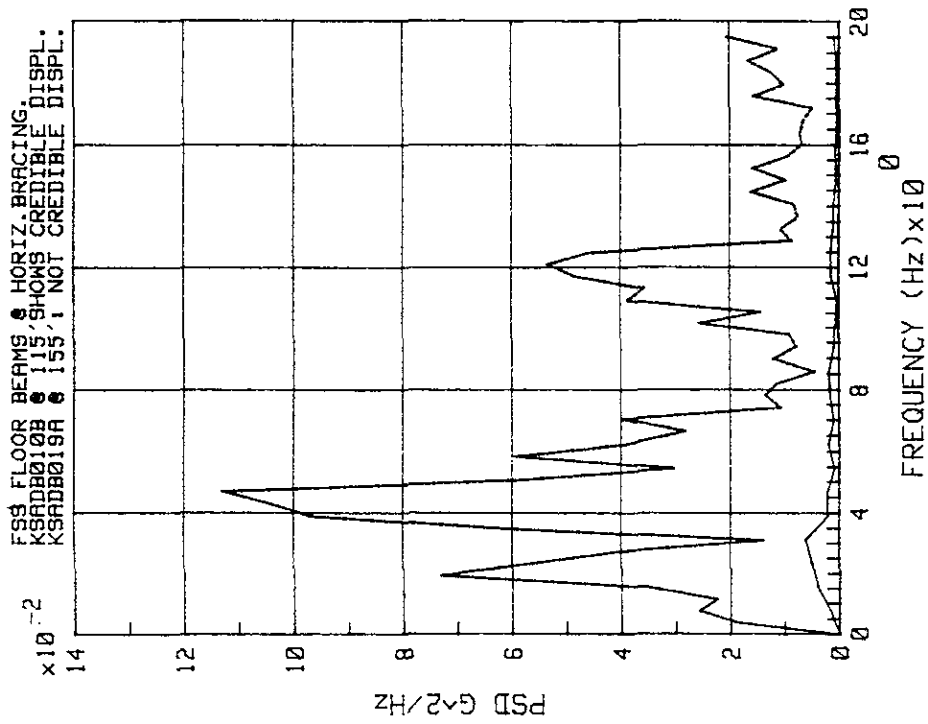


Figure 5-43. STS-3 FSS Vibration at 115- and 155-ft Levels, X and Y Directions

KSC-DD-818-TR

KSA # DB003A DB006B DB007A DB012B DB013B DB014A

FSS FLOOR BEAMS. KSADB003A -006B AND -014A PROCESSED FROM 1+0.0 TO 1+10.2 SEC. DELTA-F=0.39 Hz.
 REMAINING MEASUREMENTS PROCESSED FOR AVAILABLE TIME PRIOR TO LOSS OF DATA. DELTA-F VARIES.
 DATA DISPERSION AT THE LOW FREQUENCIES IS HIGH. DATA CREDIBILITY IS QUESTIONABLE.

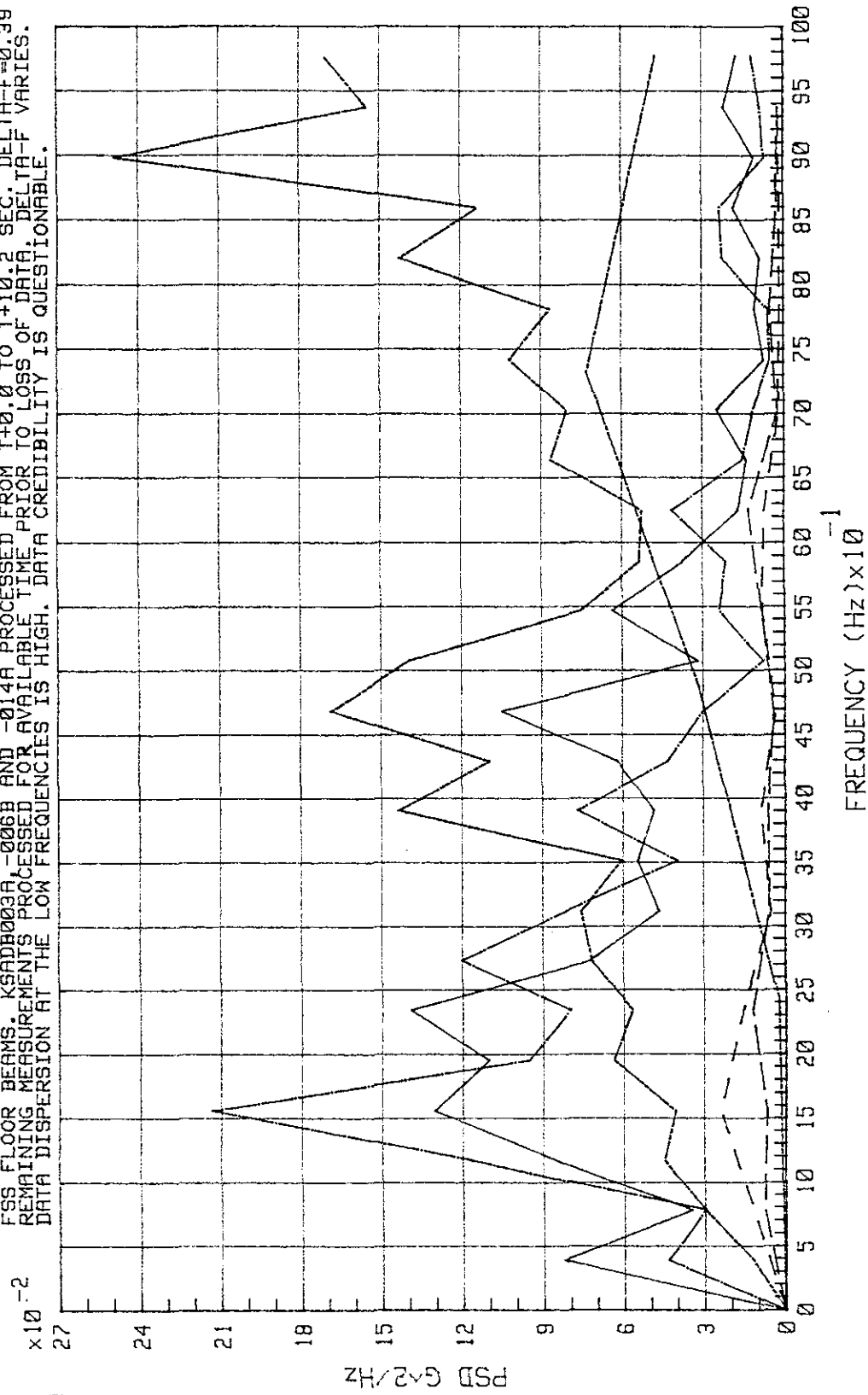


Figure 5-44. STS-3 Lift-Off Peak - FSS Vibration at 115-ft Level, Z Direction

KSA # DB003B DB006A DB007A DB012A DB013A DB014B

FSS FLOOR BEAMS. ALL DATA PROCESSED BETWEEN T+0.0 AND T+6.4 SEC AT PEAK. DELTA-F=2.44 Hz.
IN THE PLOT SCALE ONLY KSADB014B CAN BE SEEN.
SEE NEXT PLOT FOR REMAINING MEASUREMENTS.

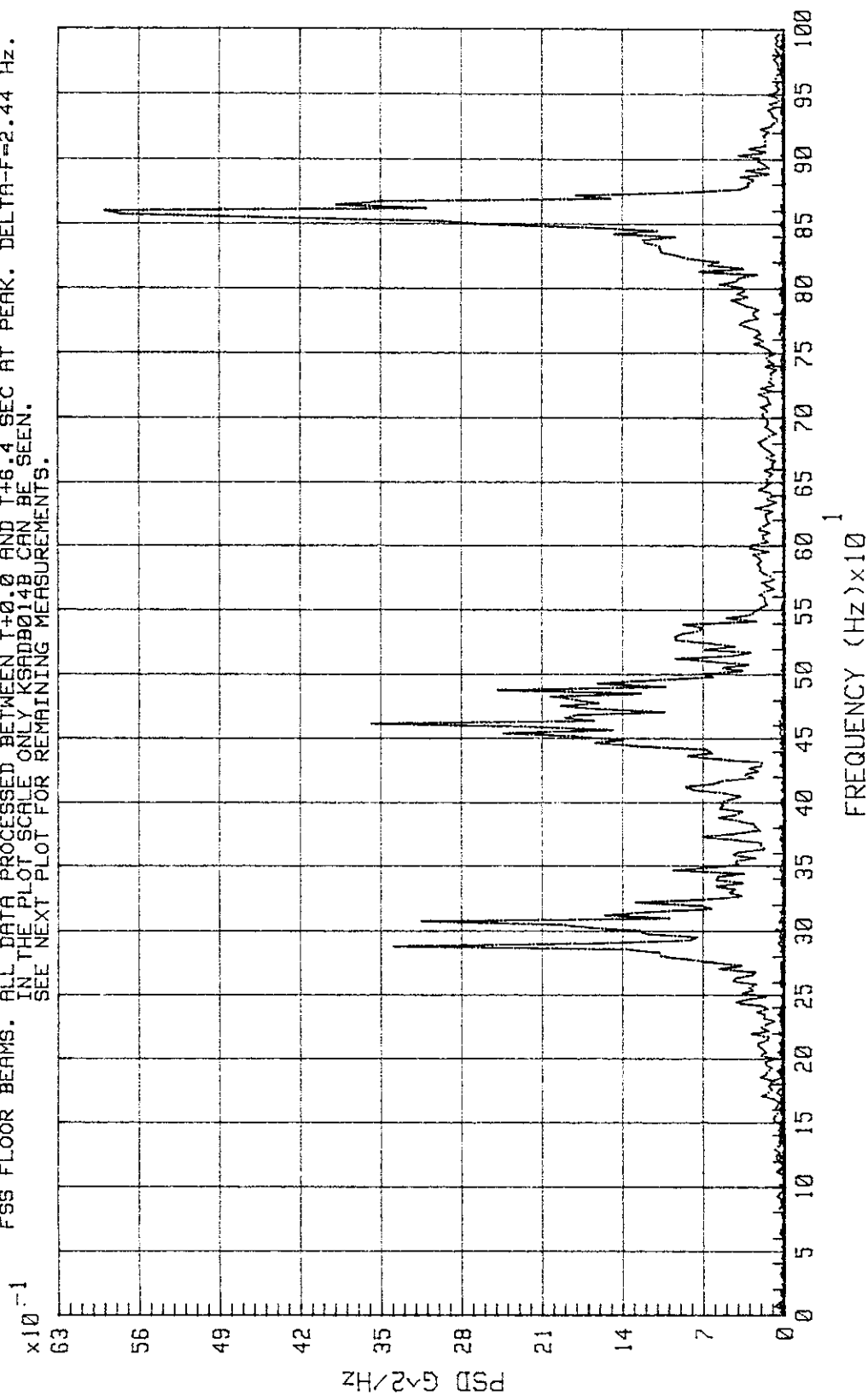


Figure 5-45. STS-3 Lift-Off Peak -- FSS Vibration at 115-ft Level,
Z Direction (Only KSADB014B Is Visible)

KSC-DD-818-TR

KSA # DB003B DB006A DB007A DB012A DB013A

FSS FLOOR BEAMS. ALL DATA PROCESSED BETWEEN T+0.0 AND T+6.4 SEC AT PEAK. DELTA-F=2.44 Hz.

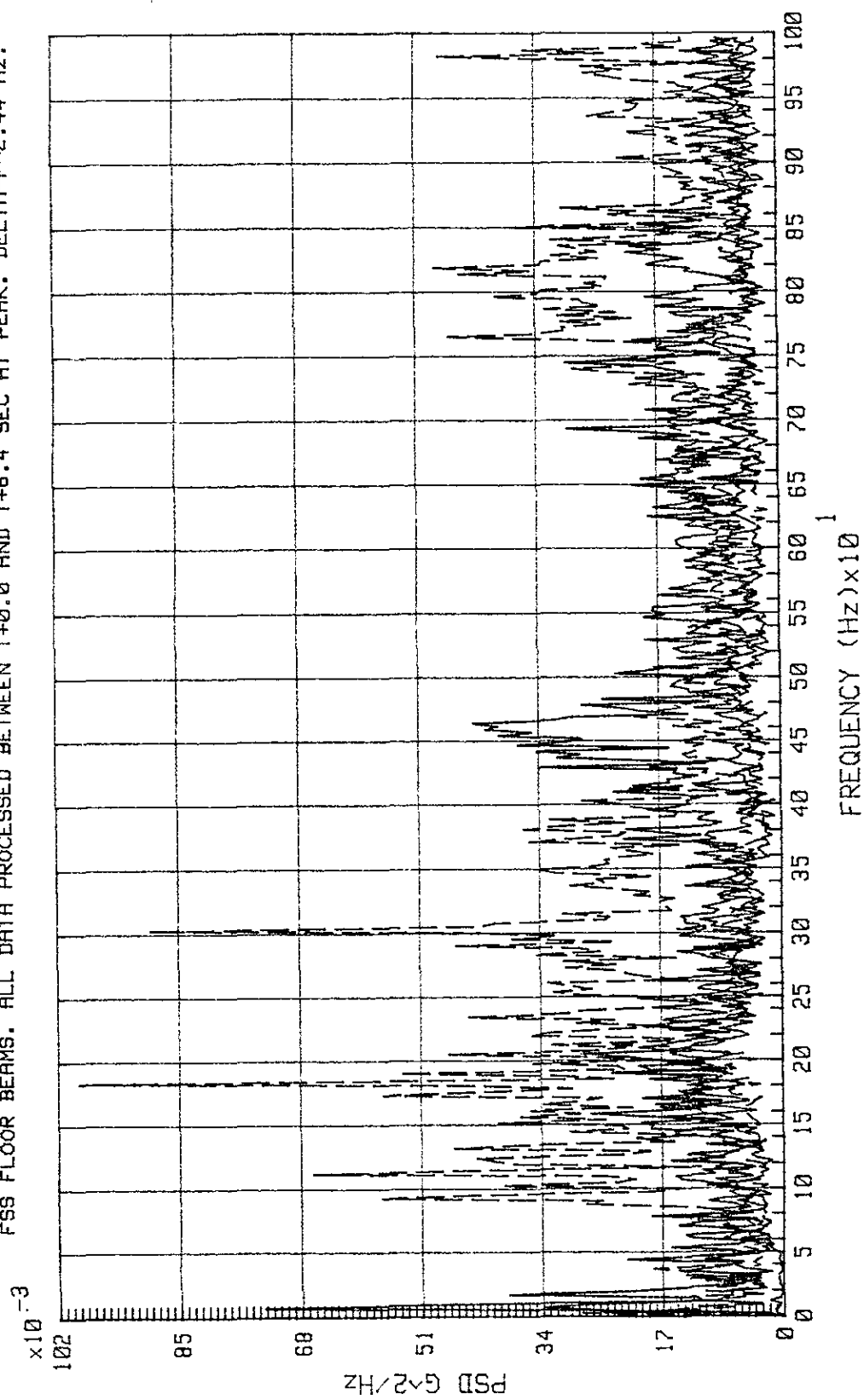


Figure 5-46. STS-3 Lift-Off Peak - FSS Vibration at 115-ft Level, Z Direction

KSA # DB003B DB006A DB007A DB012A DB013A

FSS FLOOR BEAMS. ALL DATA PROCESSED BETWEEN T+0.0 AND T+6.4 SEC AT PEAK. DELTA-F=2.44 Hz.
ALL PSD'S HANNED 3x.

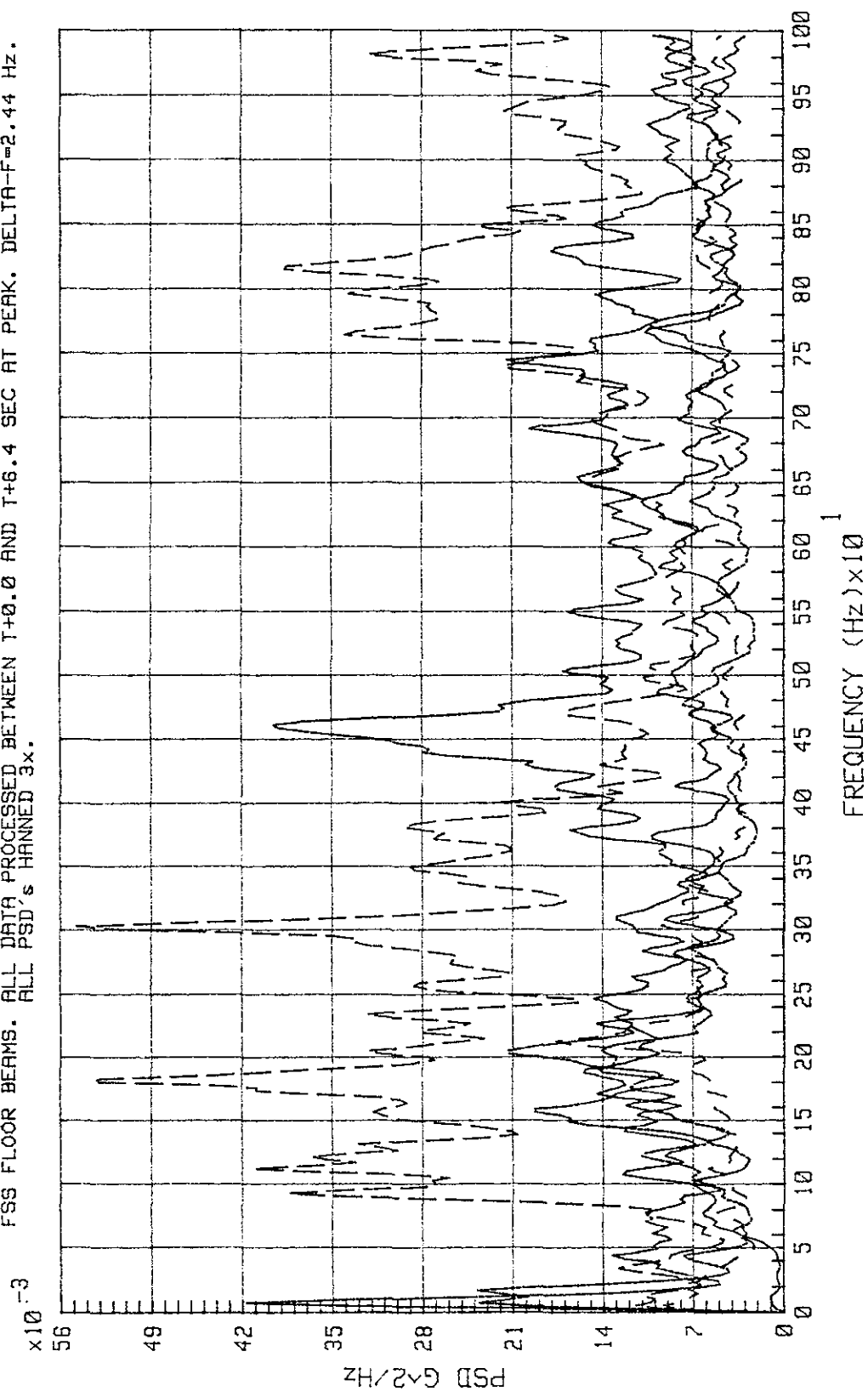


Figure 5-47. STS-3 Lift-Off Peak - FSS Vibration at 115-ft Level, Z Direction (All PSD'S Hanned)

KSC-DD-818-TR

KSA # DB015A DB016A DB017A DB021B DB022B

FSS FLOOR BEAMS. ALL DATA PROCESSED FROM T+0.0 TO T+10.2 SEC AT PEAK, DELTA-F=0.3906 Hz.
 DATA FROM KSADB015A AND KSADB017A ARE NOT CREDIBLE (TOO HIGH DISPL s)
 FOR KSADB016A, KSADB021A AND KSADB022B SEE NEXT PLOT.

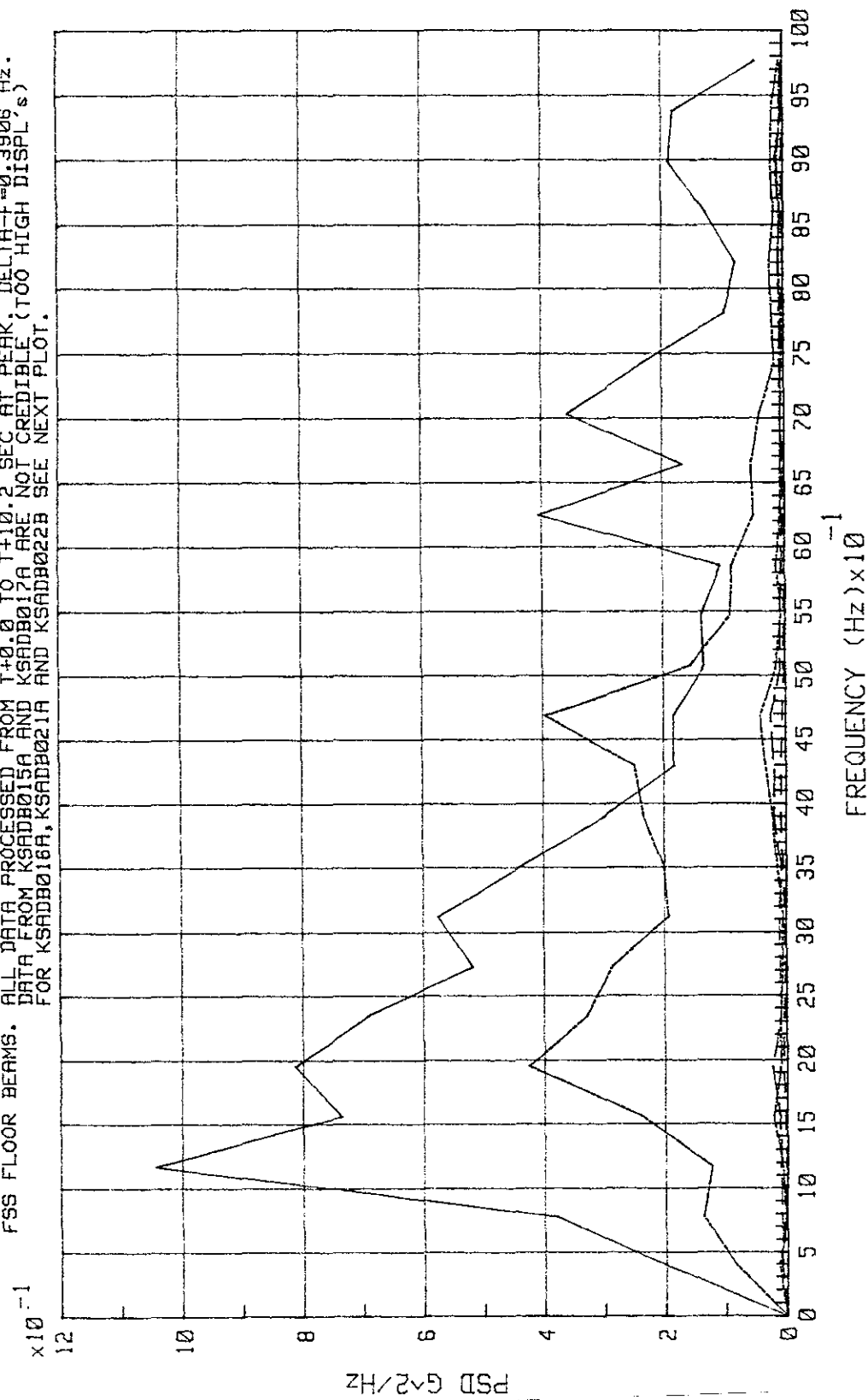


Figure 5-48. STS-3 Lift-Off Peak - FSS Vibration at 155-ft Level, Z Direction
 (KSADB015A, -16A, -17A, -21B, and -22B)

KSA # DB016A DB021B DB022B

FSS FLOOR BERMS. ALL DATA PROCESSED FROM T+0.0 TO T+10.2 SEC AT PEAK. DELTA-F=0.3906 Hz.
 KSADB016A AND KSADB022B AMPLITUDES BELOW 3 Hz ARE INVALID (HIGH DISPL²s).

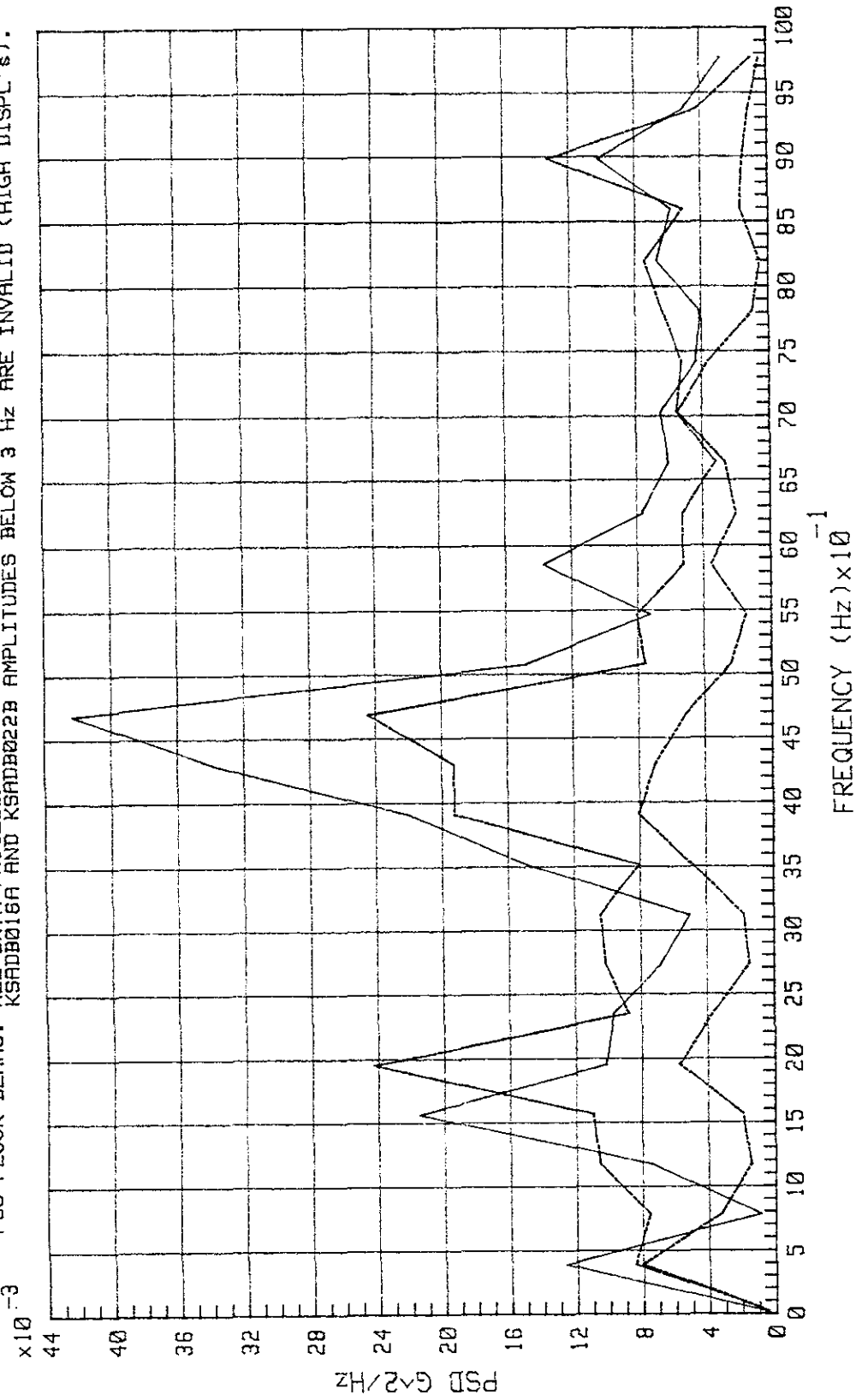


Figure 5-49. STS-3 Lift-Off Peak -
 FSS Vibration at 155-ft Level, Z Direction (KSADB016A, -21B, and -22B)

KSC-DD-818-TR

KSA # DB015B DB016B DB017B DB021A DB022A

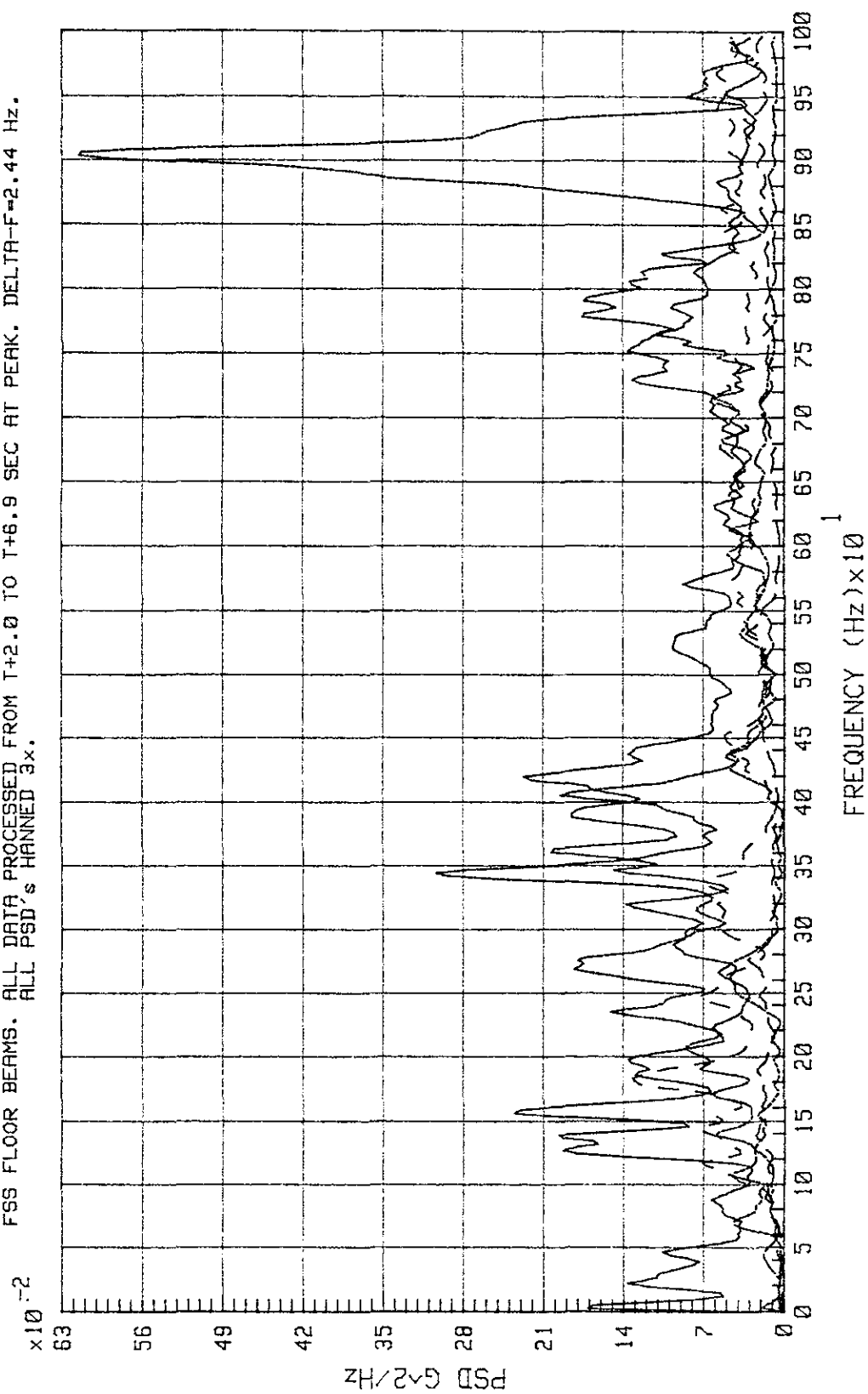
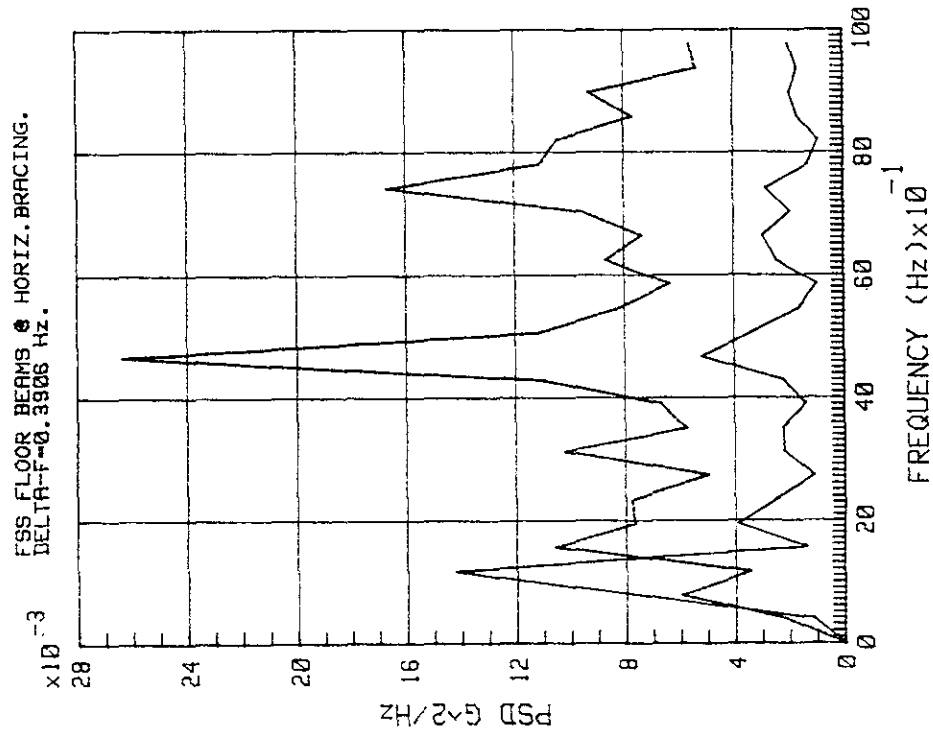
FSS FLOOR BEAMS. ALL DATA PROCESSED FROM T+2.0 TO T+6.9 SEC AT PEAK. DELTA-F=2.44 Hz.
ALL PSD's HANNED 3x.

Figure 5-50. STS-3 Lift-Off Peak - FSS Vibration at 155-ft Level, Z Direction (All PSD's Hanned)

STS-3, FSS VIBR. @ LEVEL 195, X-DIR.

KSA # DB025B DB030B



STS-3, FSS VIBR. @ LEVEL 195, Y-DIR.

KSA # DB026B DB031B

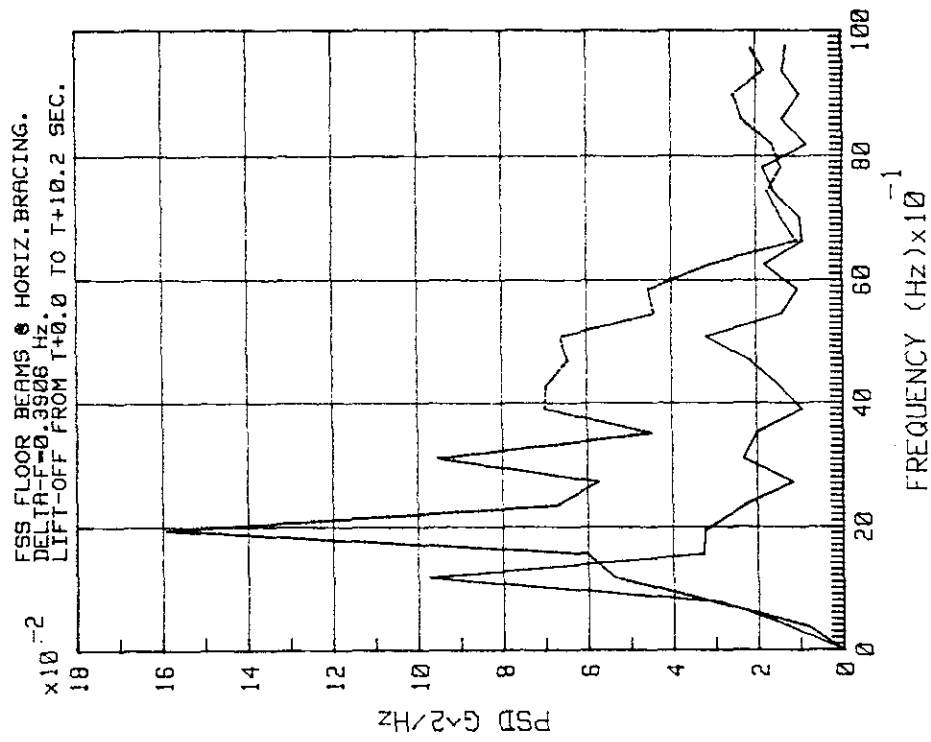


Figure 5-51. STS-3 FSS Vibration at 195-ft Level, X and Y Directions

KSC-DD-818-TR

KSA # DB023A DB029A DB035B DB024B

FSS FLOOR BEAMS. ALL DATA PROCESSED FROM T+0.0 TO T+10.2 SEC.
DELTA F = 0.3906 Hz.

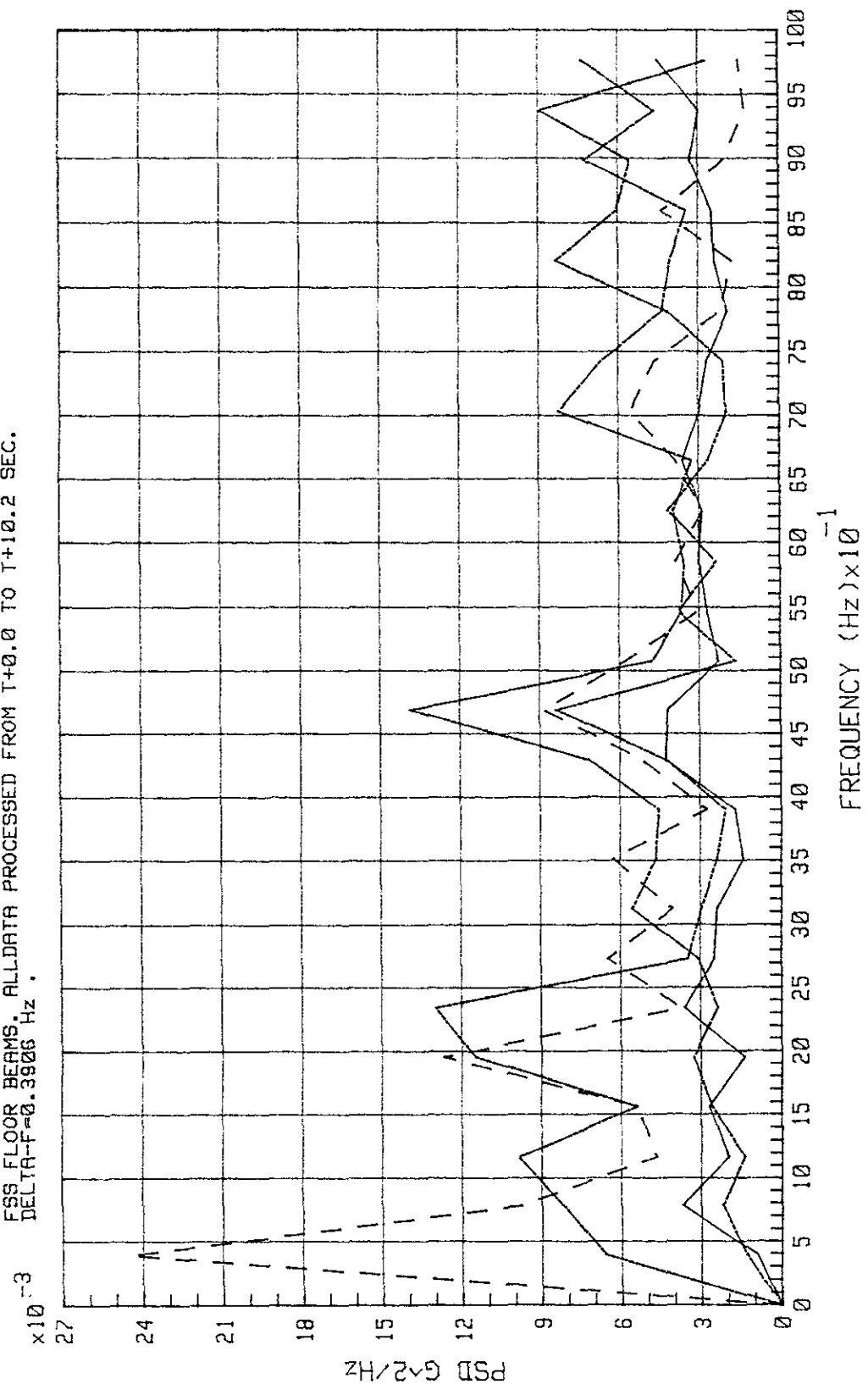


Figure 5-52. STS-3 Lift-Off Peak - FSS Vibration at 195-ft Level, Z Direction
(KSADB023A, -29A, -24B, and -35B; Delta F = 0.3906 Hz)

KSR # DB023A DB024B DB027A DB028A DB029A DB032B DB033B DB034B DB035B

FSS FLOOR BEAMS. ALL DATA PROCESSED FROM T+0.0 TO T+10.2 SEC.
DELTA-F=0.3906 Hz ALL EXCEPT KSADB034B (DELTA-F=0.488 Hz)

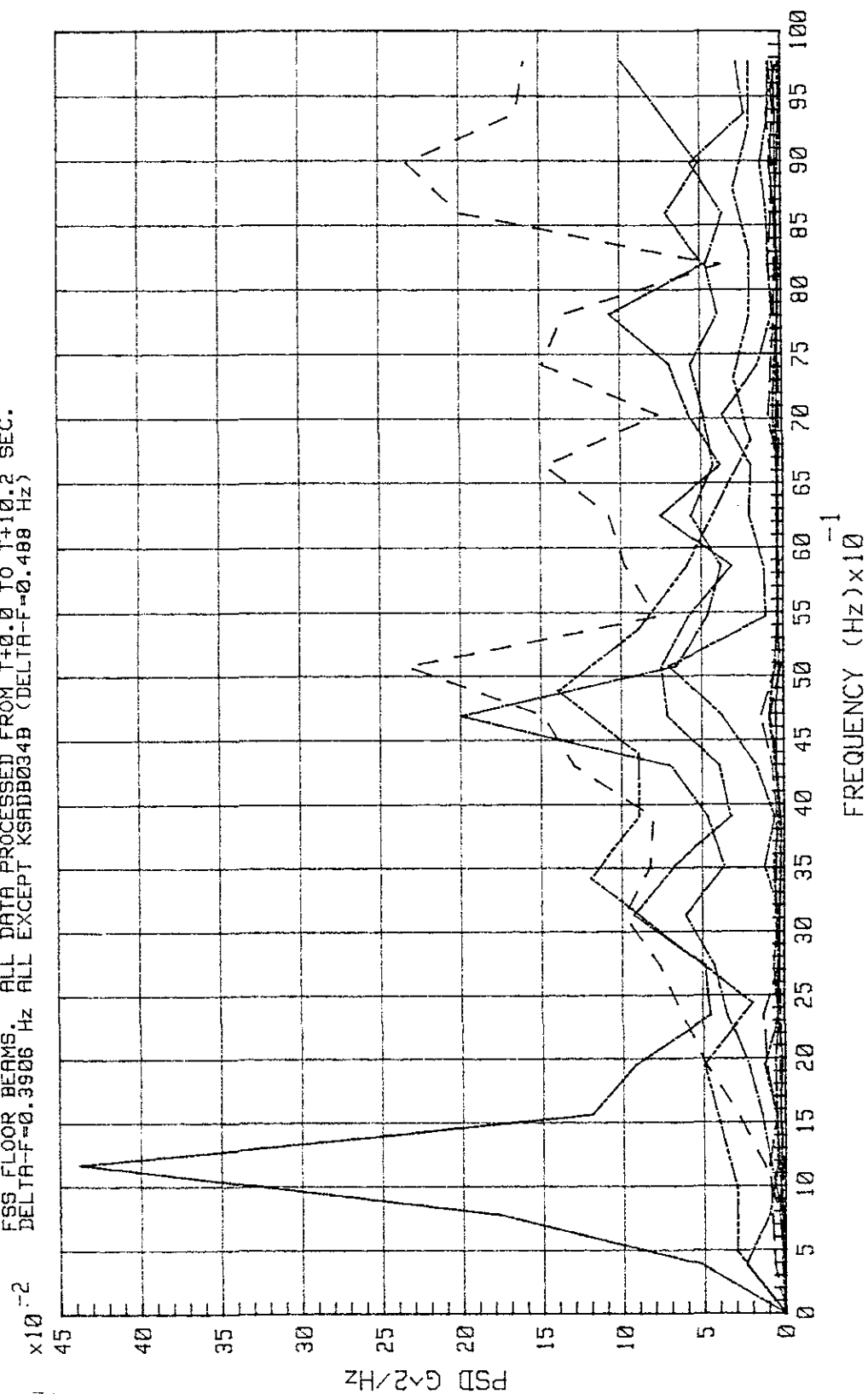


Figure 5-53. STS-3 Lift-Off Peak - FSS Vibration at 195-ft Level, Z Direction

KSC-DD-818-TR

KSR # DB023B DB024A DB027B DB028B DB029B DB032A DB033A DB034A

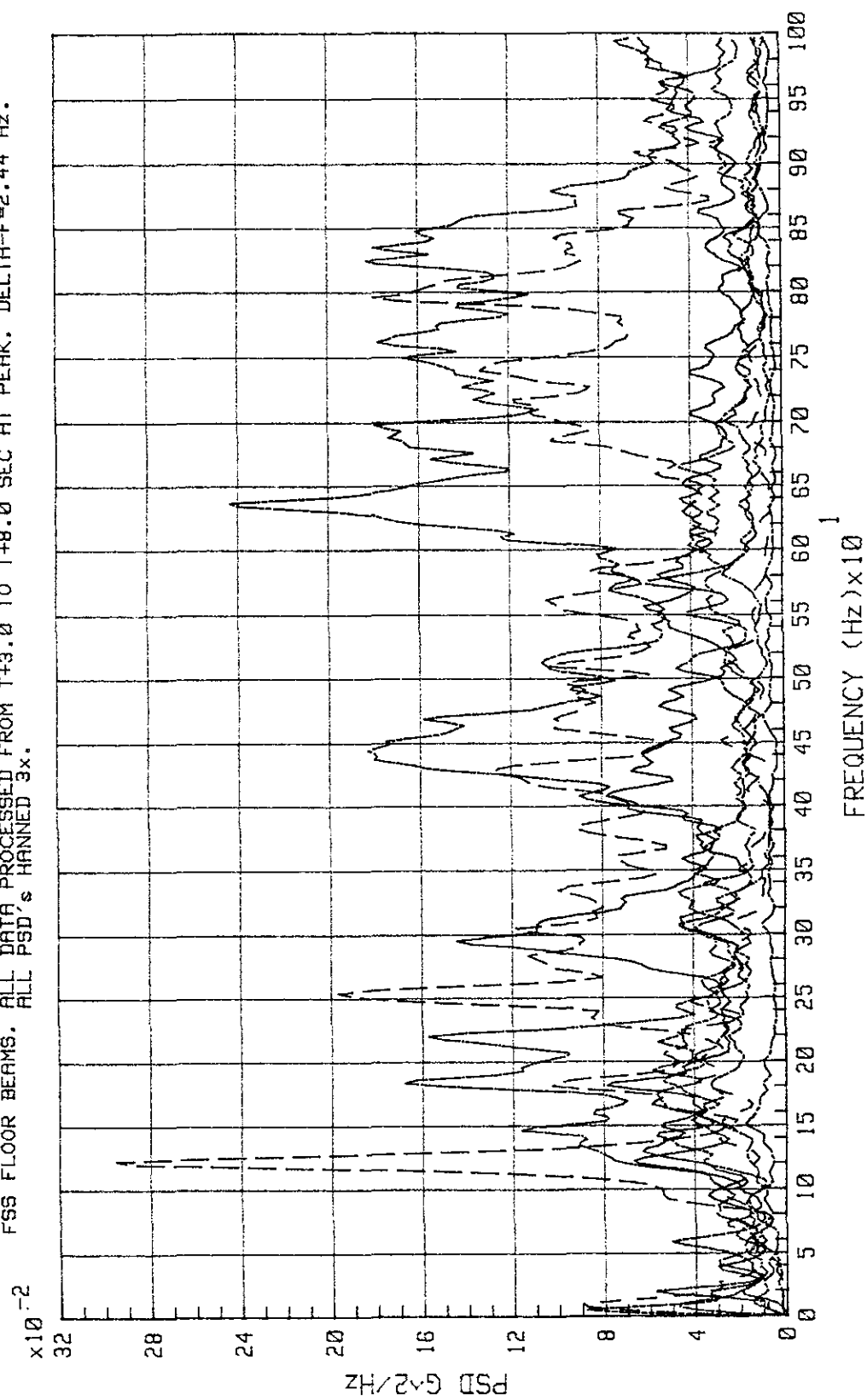
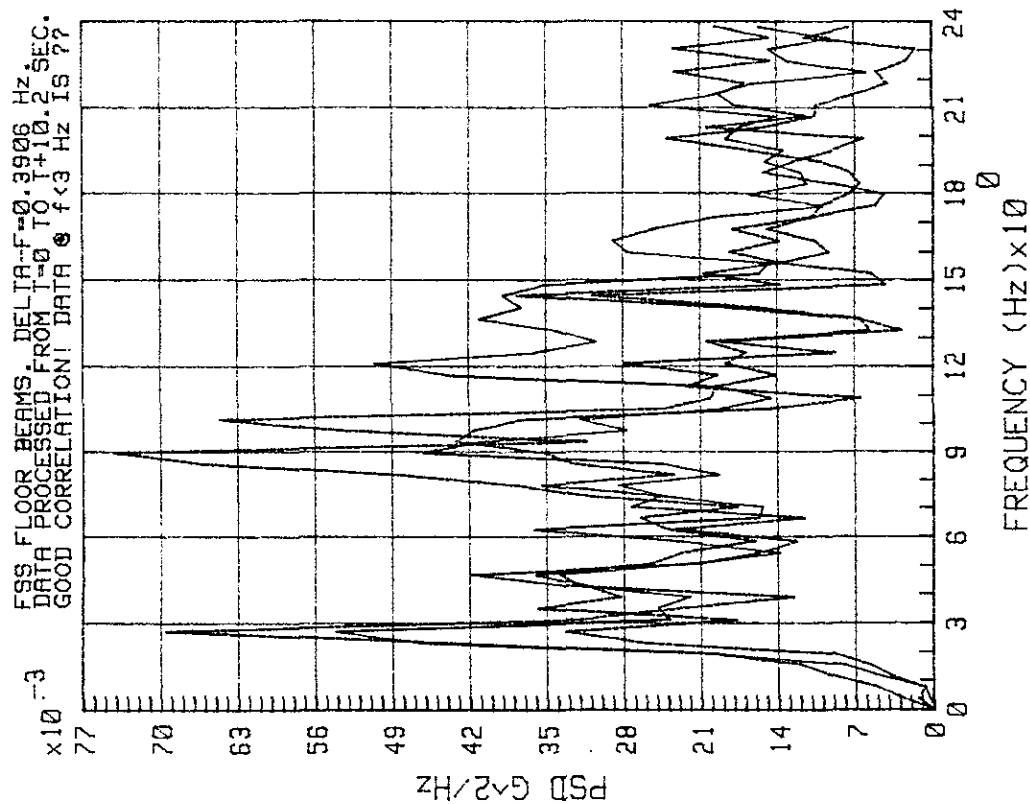
FSS FLOOR BEAMS. ALL DATA PROCESSED FROM T+3.0 TO T+8.0 SEC AT PEAK. DELTA-F=2.44 Hz.
ALL PSD's HANNED 3x.

Figure 5-54. STS-3 Lift-Off Peak - FSS Vibration at 195-ft Level, Z Direction (All PSD's Hanned)

KSA # DB037A DB038A DB039A



KSA # DB036A DB037A DB038A DB039A

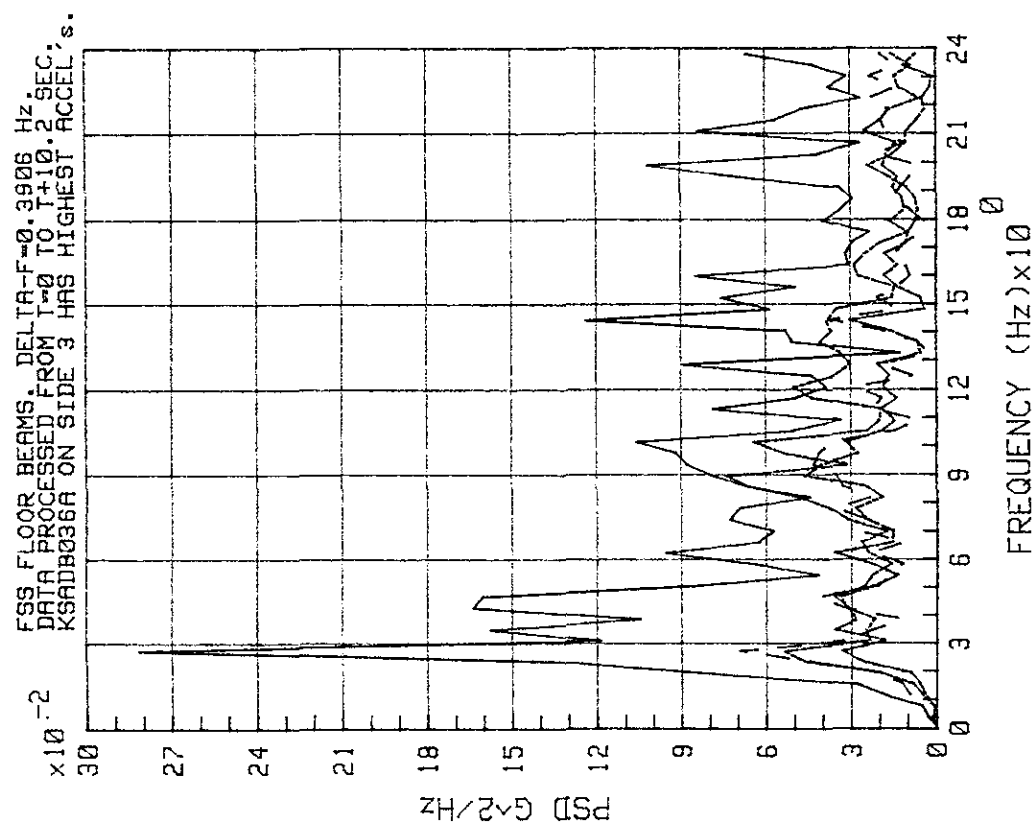
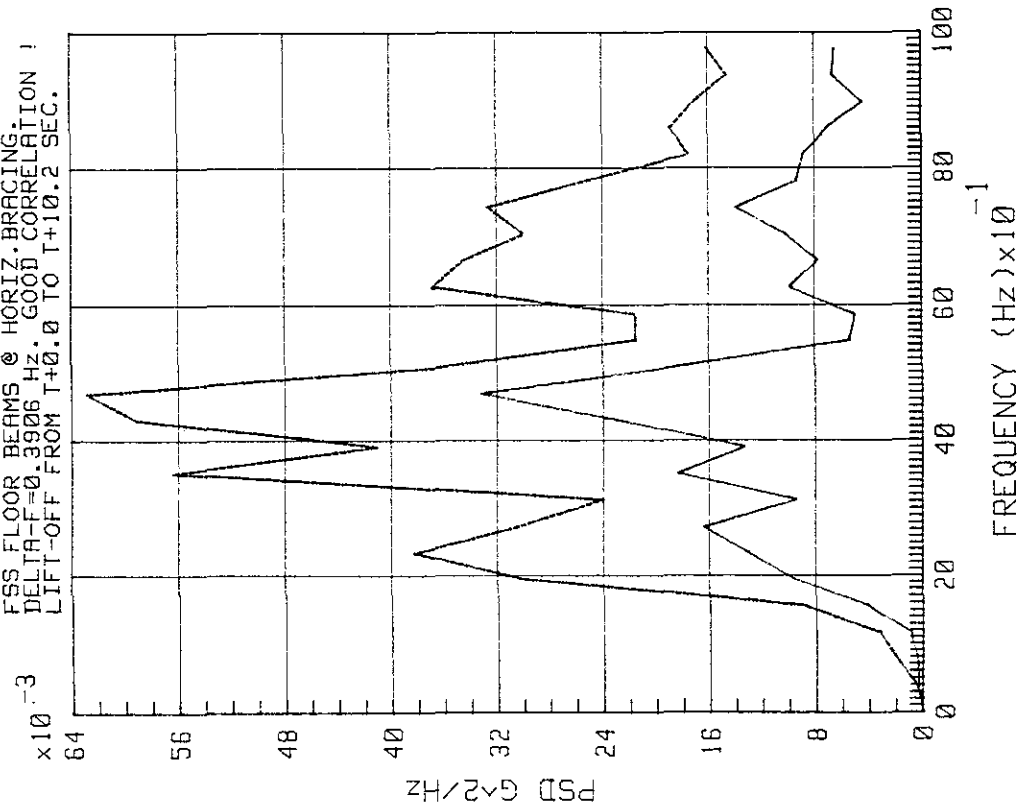


Figure 5-55. STS-3 FSS Vibration at 215-ft Level, Z Direction

KSC-DD-818-TR

KSA # DB040B DB043A

FSS FLOOR BEAMS @ HORIZ. BRACING.
 DELTA-F=0.3906 Hz. GOOD CORRELATION !
 LIFT-OFF FROM T+0.0 TO T+10.2 SEC.



KSA # DB040B DB043A

SAME DATA AS PLOT ON THE LEFT.
 ALL PEAKS UP TO 20 Hz CORRELATE !!!
 GOOD CORRELATION EXISTS THROUGHOUT.

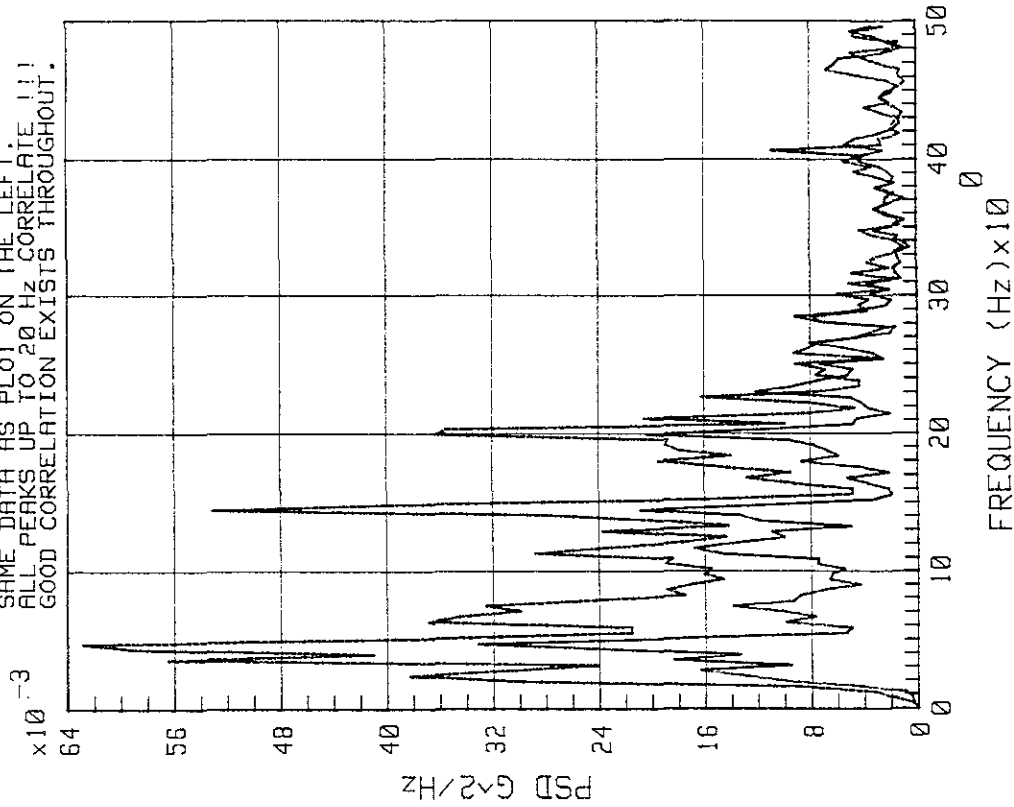
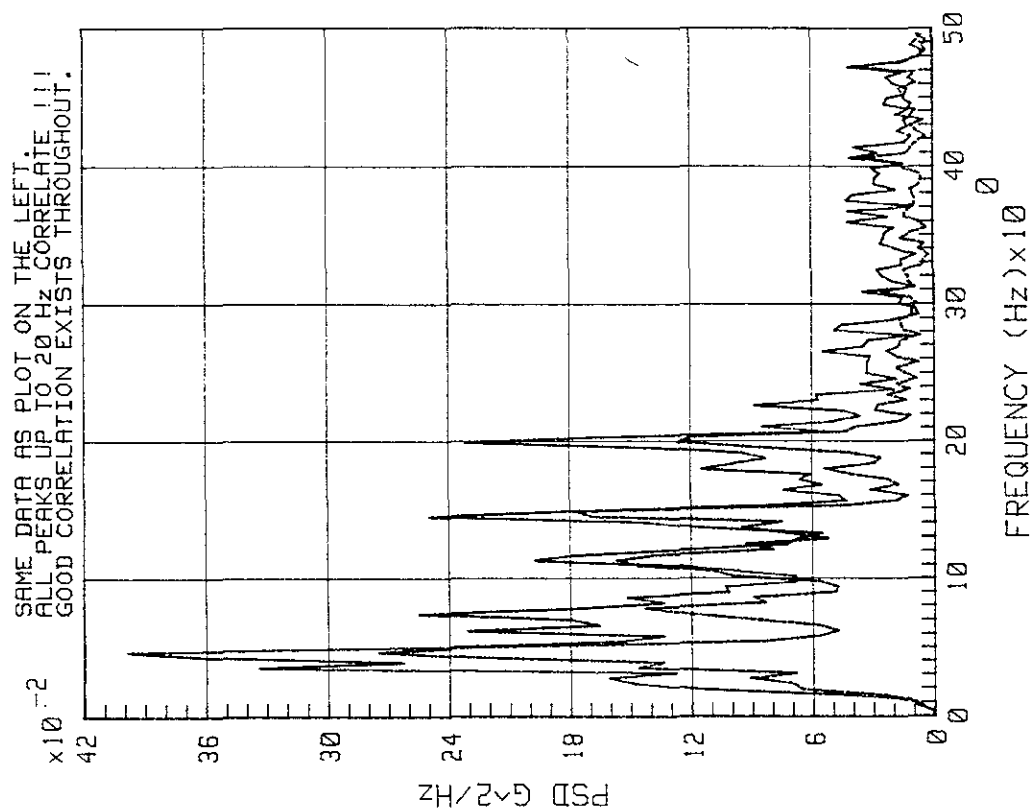


Figure 5-56. STS-3 FSS Vibration at 255-ft Level, X Direction

KSA # DB041B DB044B



KSA # DB041B DB044B

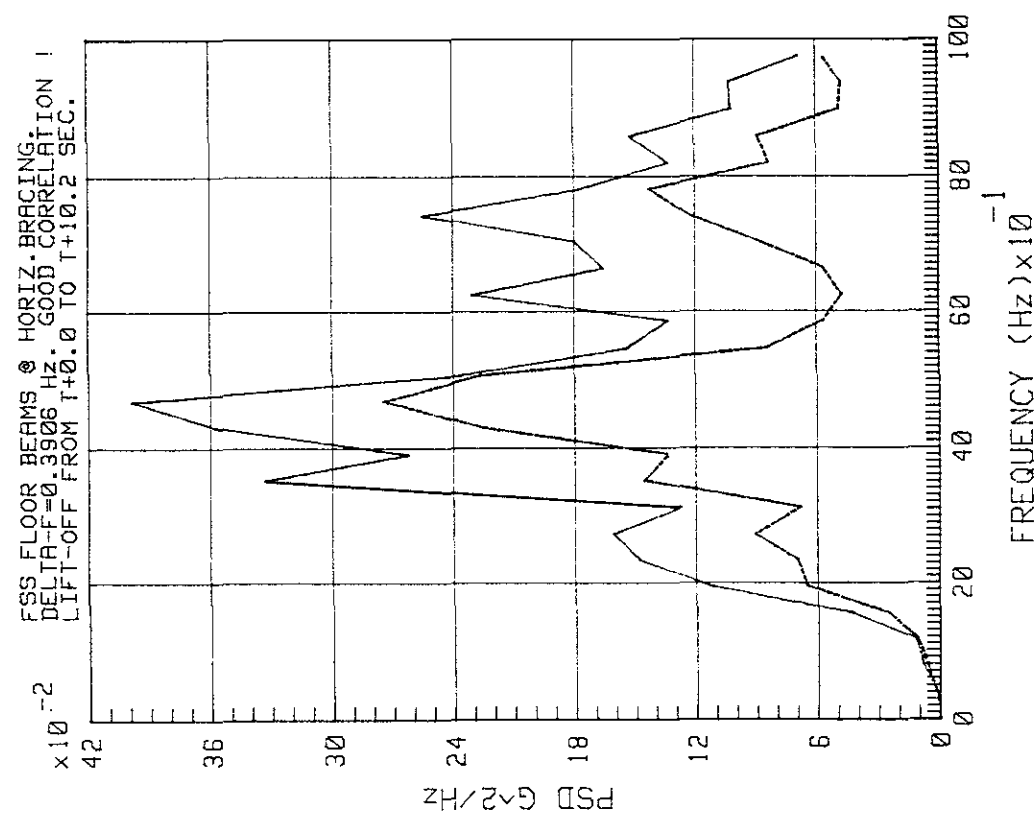
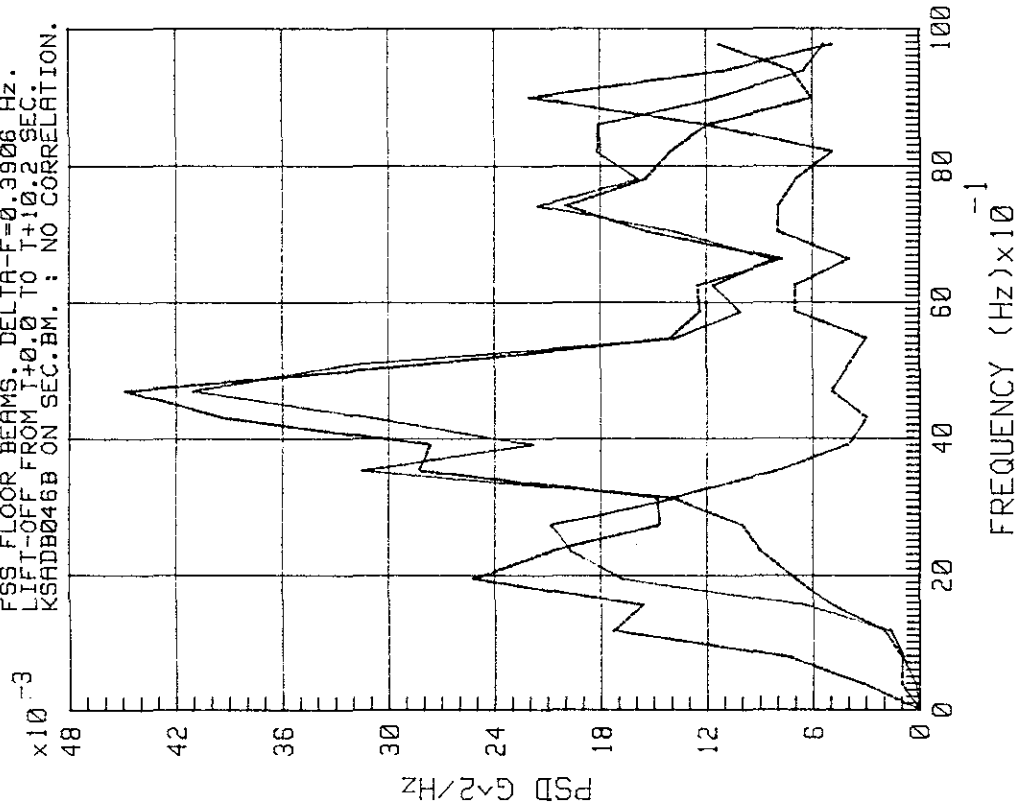


Figure 5-57. STS-3 FSS Vibration at 255-ft Level, Y Direction

KSC-DD-818-TR

KSA # DB042A DB045B DB046B

FSS FLOOR BEAMS. DELTA-T=0.3906 Hz.
LIFT-OFF FROM T+0.0 TO T+10.2 SEC.
KSADB046B ON SEC.BM. ; NO CORRELATION.



KSA # DB042A DB045B DB046B

SAME DATA AS PLOT ON THE LEFT.
KSADB042A AND -045B HAVE GOOD CORREL.
KSADB046B PLOT TO 15 Hz. POOR CORREL.

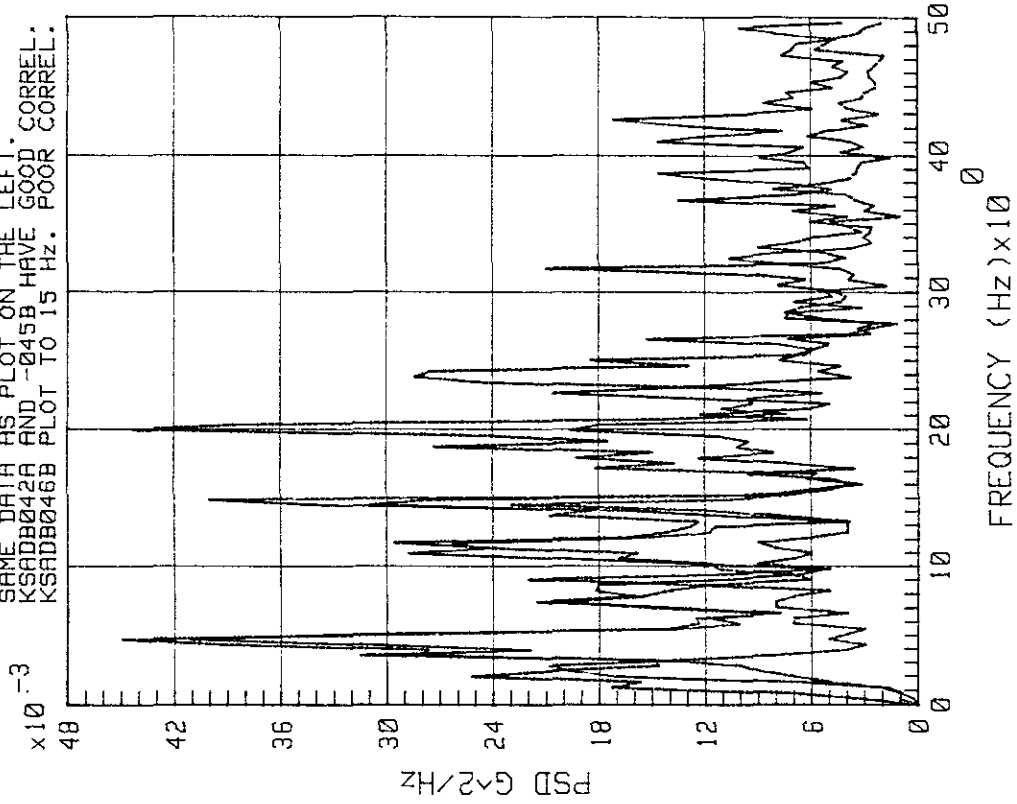


Figure 5-58. STS-3 FSS Vibration at 255-ft Level, Z Direction

KSA # DB042B DB045A DB046A

$\times 10^{-2}$
 FSS FLOOR BEAMS. ALL DATA PROCESSED FROM T+4.0 TO T+8.9 SEC AT PEAK. DELTA-F=2.44 Hz.
 ALL PSD's HANNED 3x. PLOT RANGE: 50-1500 Hz. KSADB042B AND KSADB045A ON
 MAIN FLOOR BEAMS CORRELATE THROUGHOUT. KSADB046A ON SEC.FL.BM. IS NOT EXPECTED TO CORRELATE.

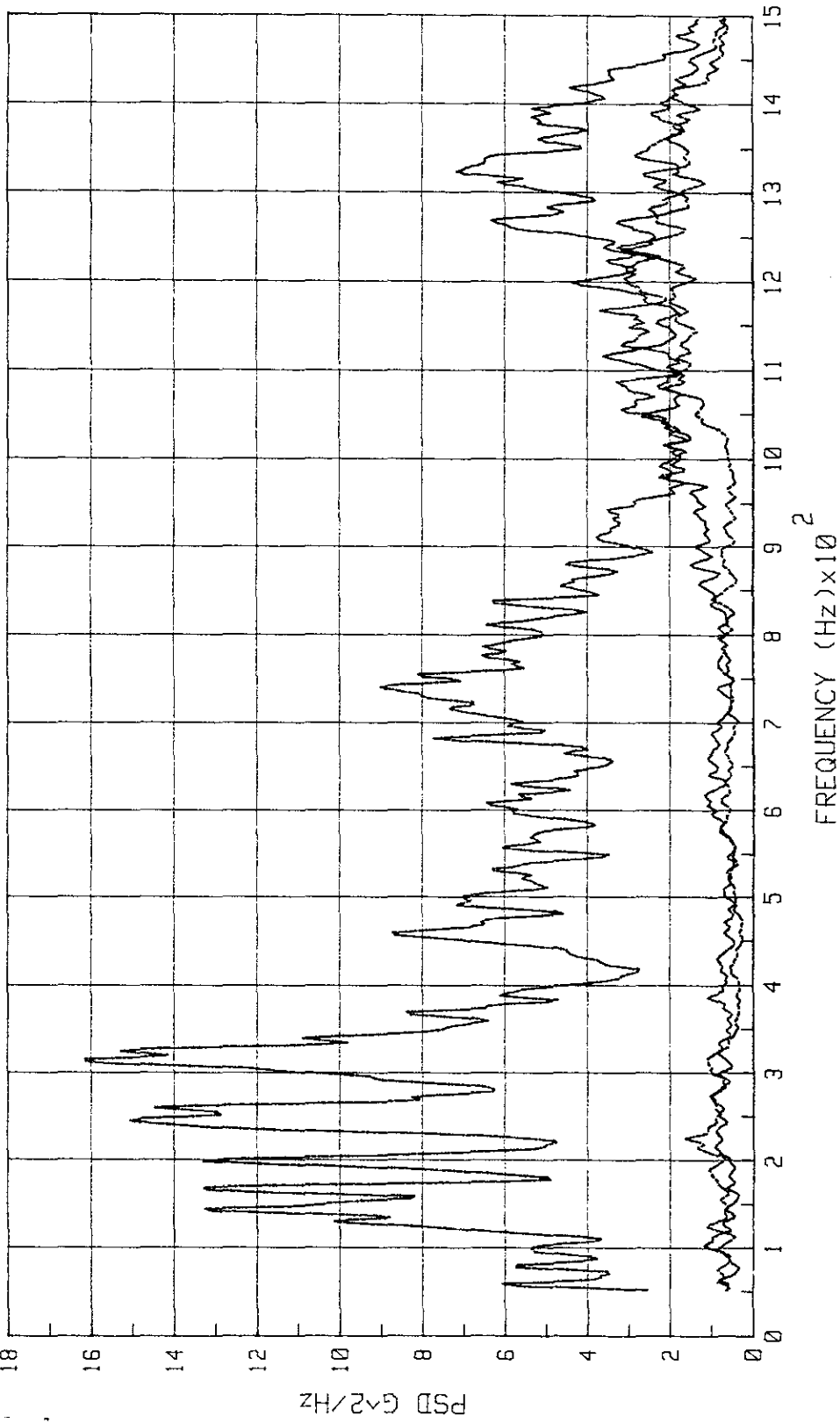


Figure 5-59. STS-3 Lift-Off Peak - FSS Vibration at 255-ft Level, Z Direction (All PSD's Hanned)

KSC-DD-818-TR

KSR # DB014B DB035A DB047B

FSS SIDE 1 MAIN BEAMS @ MIDSPAN, @ JOINT WITH DIAGONAL MEMBERS. DELTA-F=2.44 Hz.
ALL PSD'S HANNED 3x. DATA PROCESSED BETWEEN T+3.0 AND T+8.9 SEC AT PEAK.
FOR KSHDB047B SEE NEXT PLOT. IT'S DATA DIFFERS FROM STS-2.

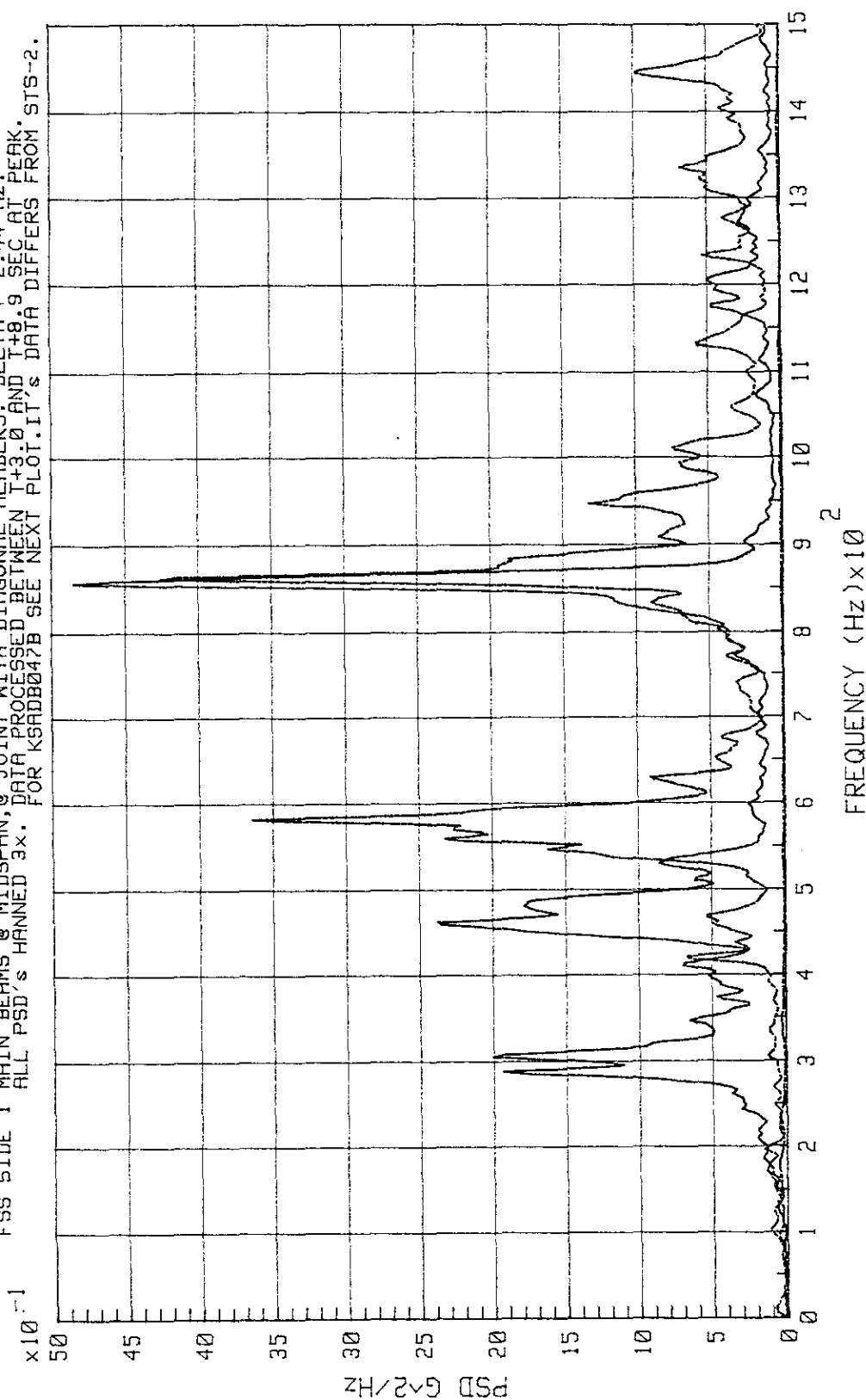


Figure 5-60. STS-3 Lift-Off Peak -
FSS Vibration on Side 1 at 115-, 195-, and 255-ft Levels, Z Direction

KSA # DB047B

FSS SIDE 1 MAIN BEAM @ MIDSPAN, @ JOINT WITH DIAGONAL MEMBER. DELTA-T=2.44 HZ.
 PSD HANNED 3x. DATA PROCESSED FROM T+4.0 TO T+8.9 SEC AT PEAK. STS-3 DATA FREQ.

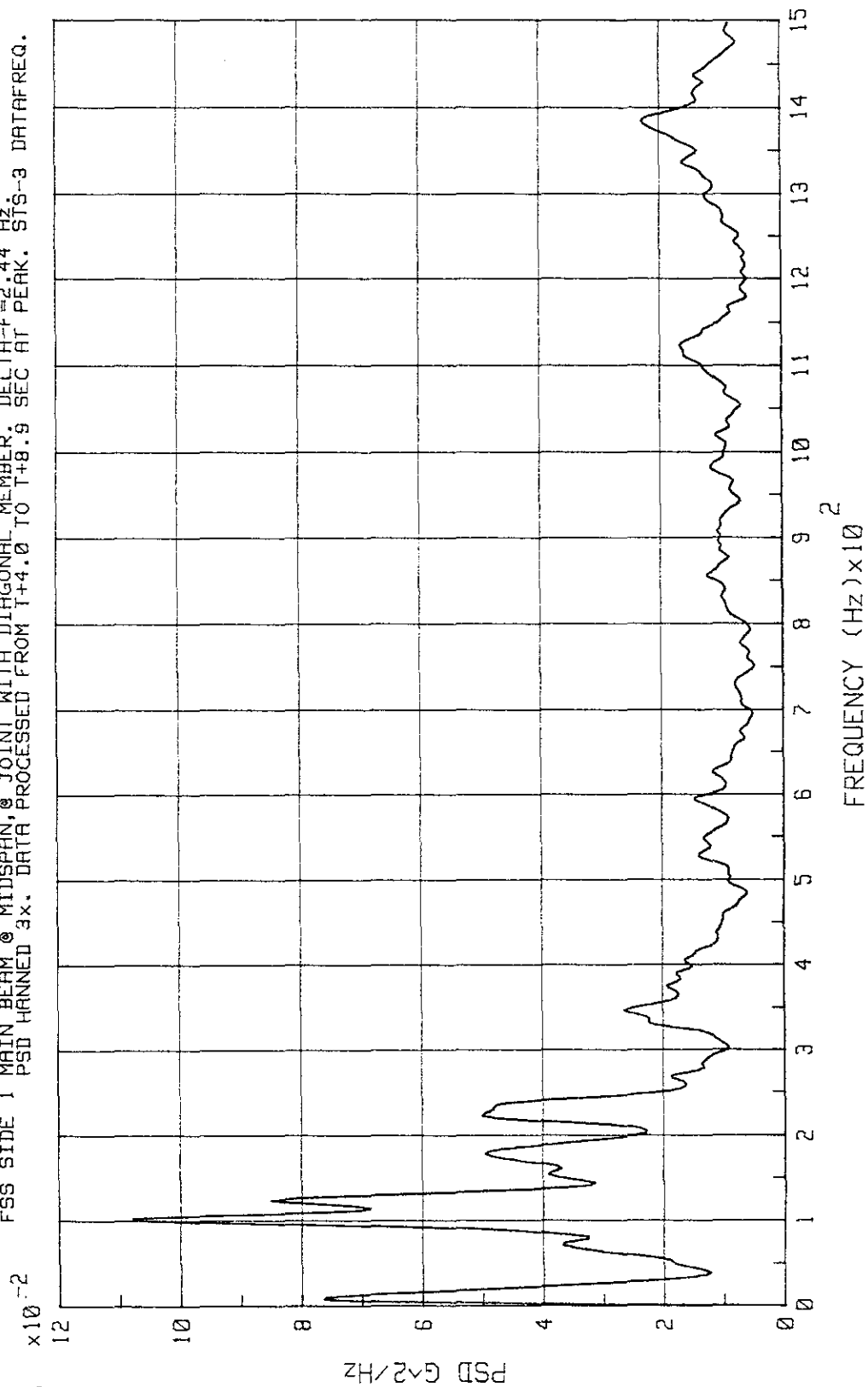


Figure 5-61. STS-3 Lift-Off Peak - FSS Vibration on Side 1 at 255-ft Level, Z Direction

KSC-DD-818-TR

5.3 RSS

The RSS was instrumented with approximately 50 vibration sensors during the launches of STS-1, -2, and -3. Sensors were installed at various levels on floor beams, bottom flanges, and outside flanges. The resulting data were processed and published in documents listed in the bibliography herein. This summary contains sampling data from various levels, recorded during the lift-off peak of STS-3 (figures 5-62 through 5-68). Included are raw data, PD's, PSD's, and rms time histories for the following measurements:

<u>Designation</u>	<u>Location</u>	<u>Level</u>	<u>Direction</u>
KSRDC011A	Main Floor Beam	107-ft	Z
KSRDC015A	Floor Beam, Side 4	158-ft, 5-in	Z
KSRDC016A	Platform 2-In Floor Beam, Side 3	131-ft	Z
KSRDC019A	Outside Flange, Side 4	135-ft	Y
KSRDC025A	Platform Floor Beam	107-ft	X
KSRDC032A	Platform Floor Beam	107-ft	X
KSRDC041A	Platform Floor beam, Middle	120-ft	X

Multiple plot summary PSD's for various levels and directions, published as appendix B in KSC-DD-651-TR, are included (figures 5-69 through 5-93). Not included but recommended for additional information is appendix B of KSC-DD-677-TR, containing data validation criteria, zoom plots of significant PSD's, and calculated rms displacements.

STS-3 LIFT-OFF PEAK
 RMS = 2.677 G
 AVERAGES = 12
 BLOCK SIZE = 2048
 KSR02011A CHANNEL C
 START TIME = T + 2.00 SEC

STS-3 LIFT-OFF PEAK
 BLOCK SIZE = 2048
 SAMPLE RATE = 5000 HZ
 TOTAL TIME = 4.915 SEC
 KSR02011A CHANNEL C
 START TIME = T + 2.00 SEC

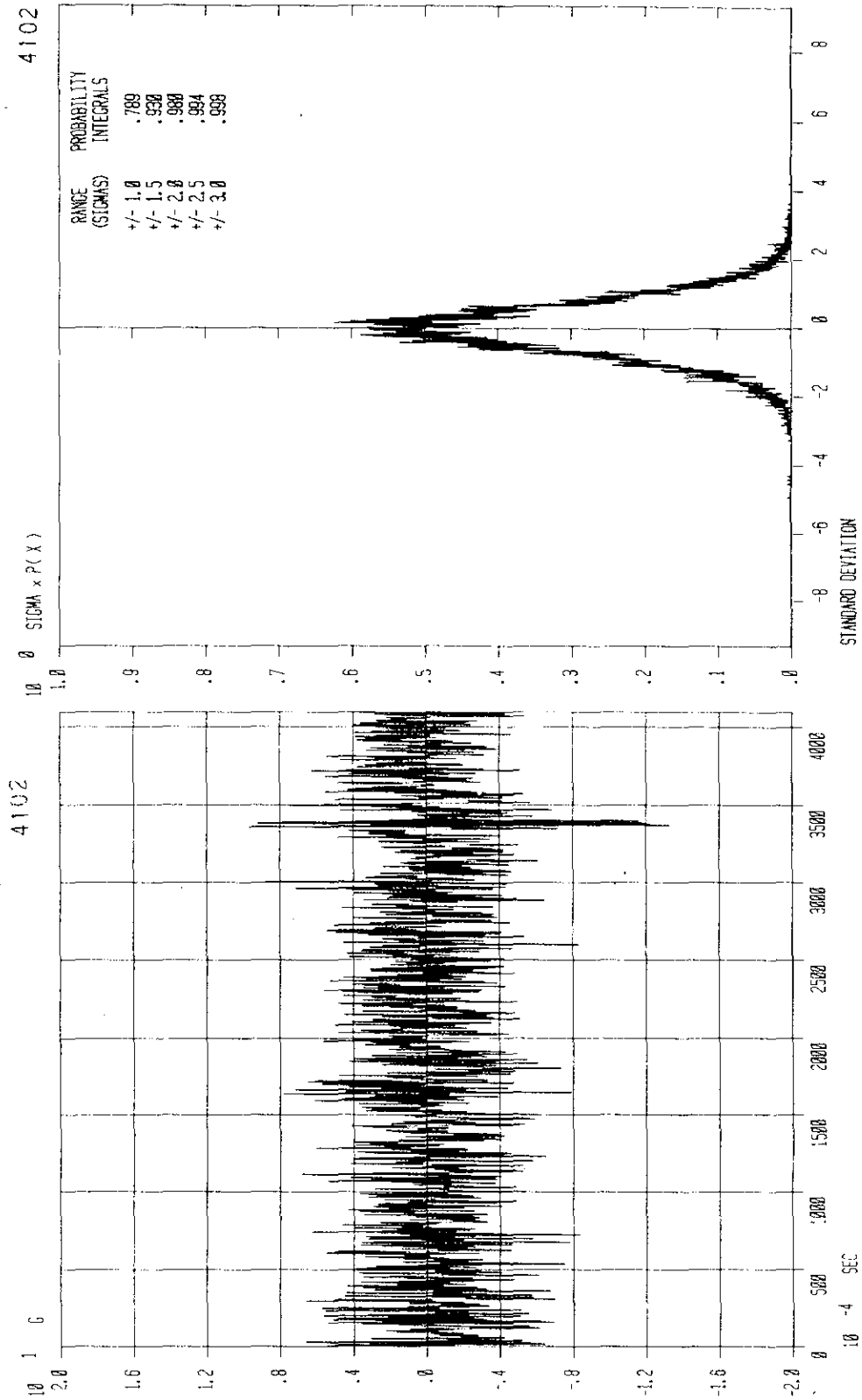


Figure 5-62. Main Floor Beam, 107-ft Level, Z-Direction (Sheet 1 of 2)

KSC-DD-818-TR

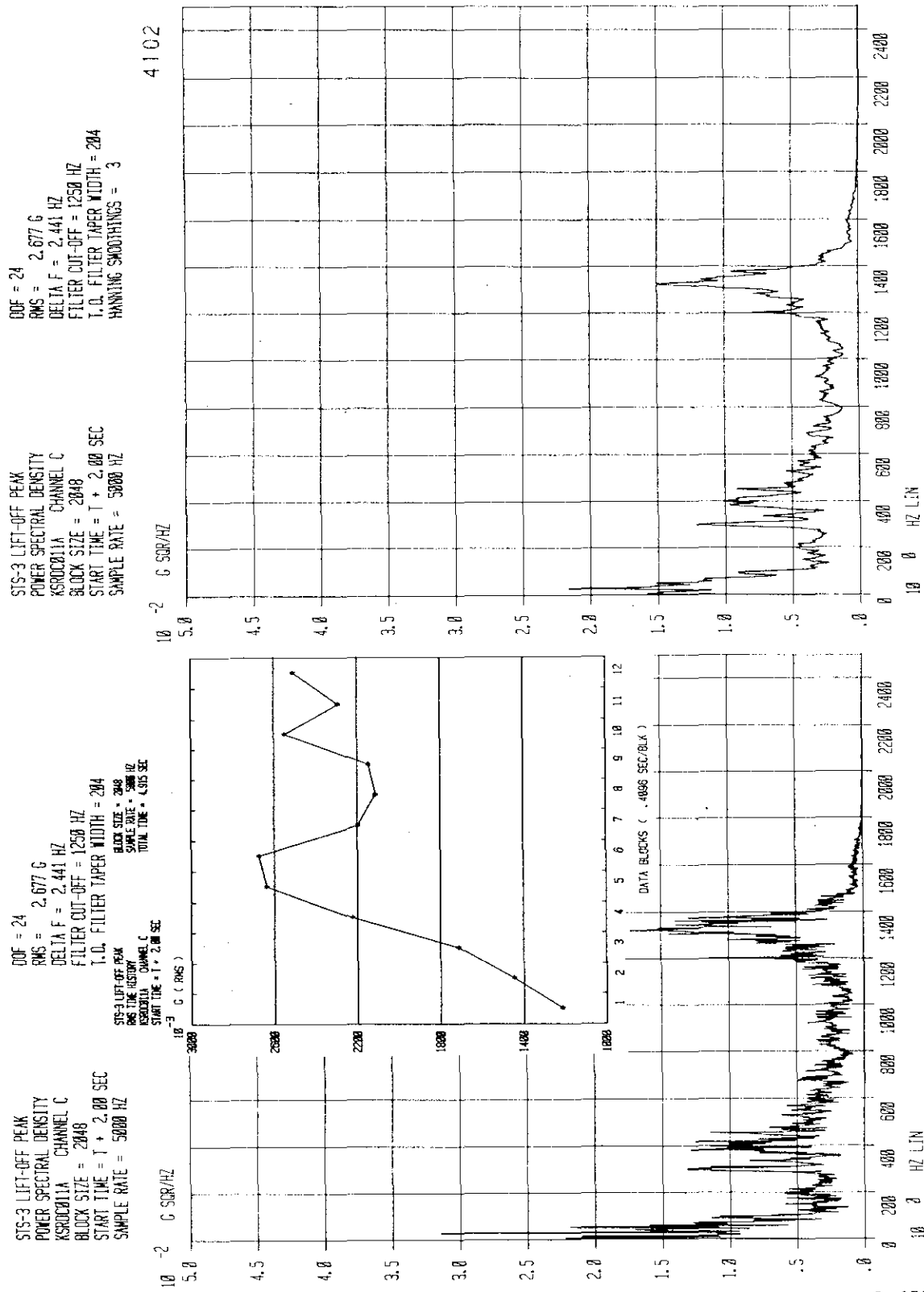


Figure 5-62. Main Floor Beam, 107-ft Level, Z-Direction (Sheet 2 of 2)

STS-3 LIFT-OFF
 RAW DATA
 KSC00015A CHANNEL B
 START TIME = T + 1.20 SEC
 BLOCK SIZE = 2048
 SAMPLE RATE = 5000 HZ
 TOTAL TIME = 4.915 SEC

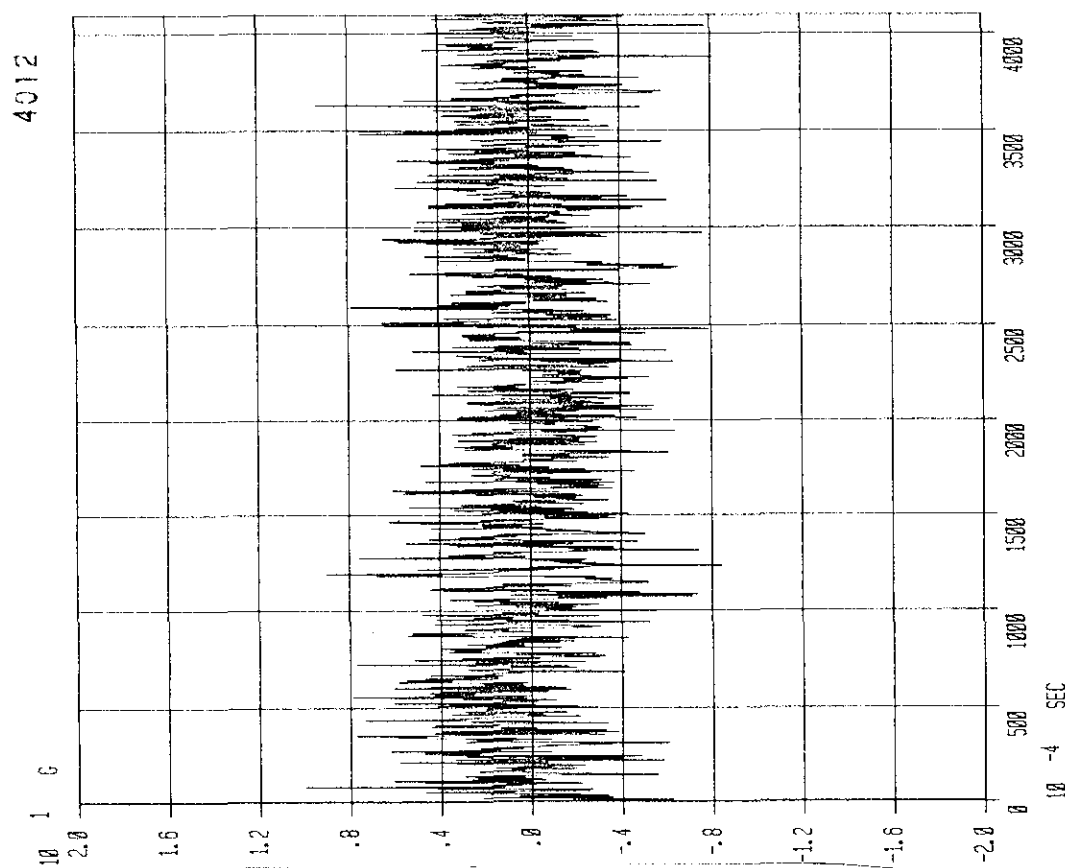


Figure 5-63. Floor Beam, Side 4, 158-ft 5-in- Level, Z-Direction (Sheet 1 of 2)

KSC-DD-818-TR

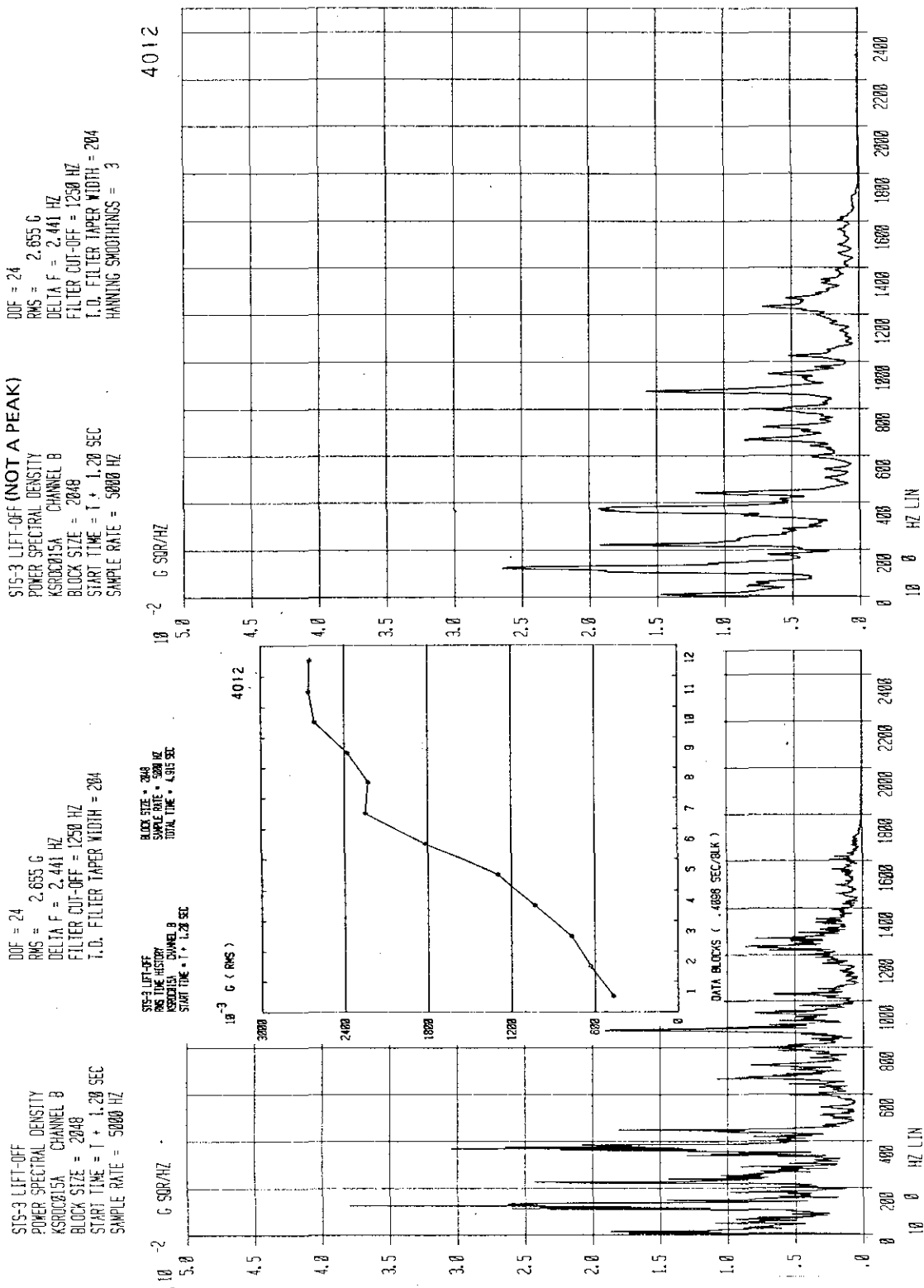


Figure 5-63. Floor Beam, Side 4, 158-ft 5-in- Level, Z-Direction (Sheet 2 of 2)

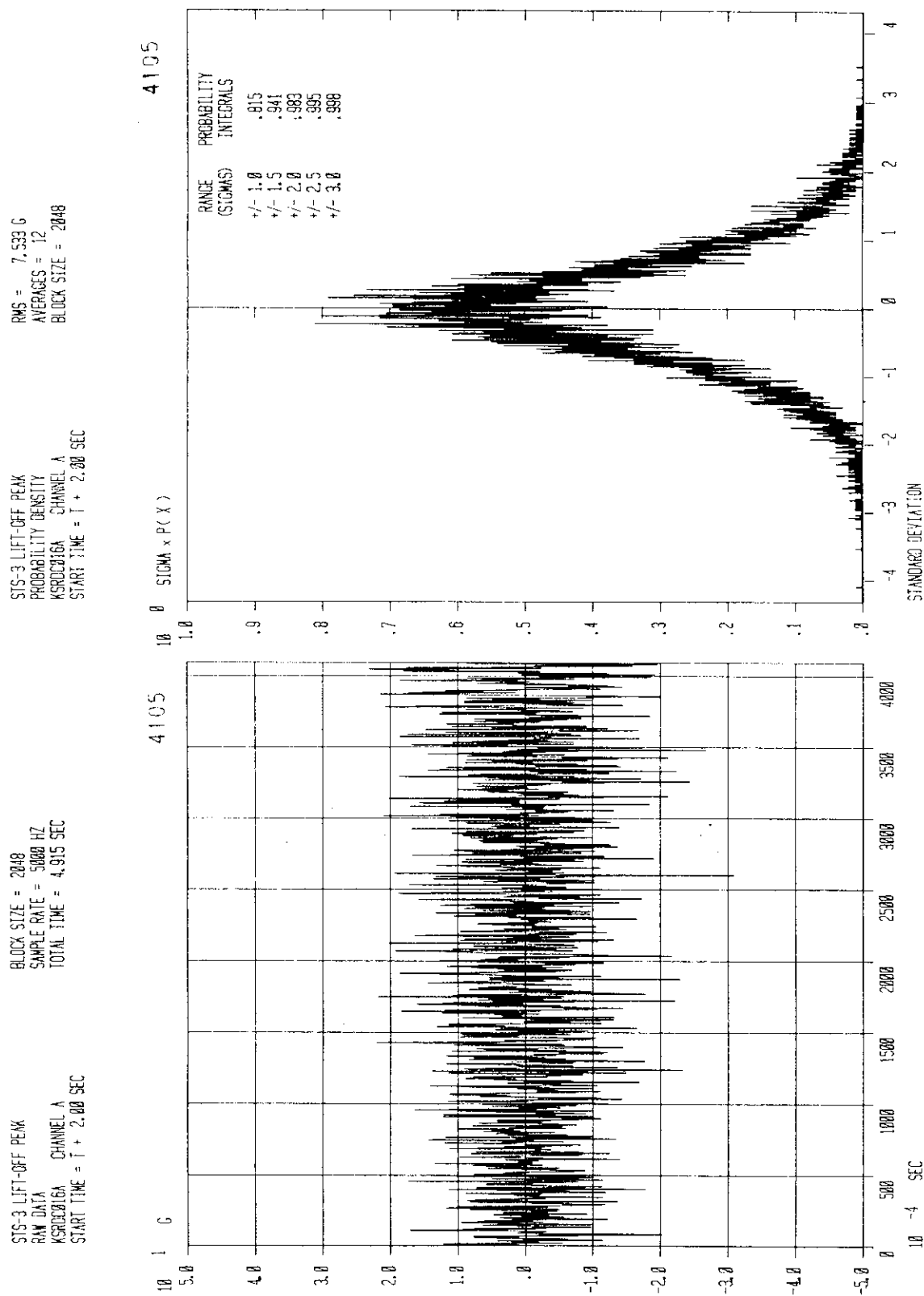


Figure 5-64. Platform 2-in-Floor Beam, Side 3, 131-ft Level (Sheet 1 of 2)

KSC-DD-818-TR

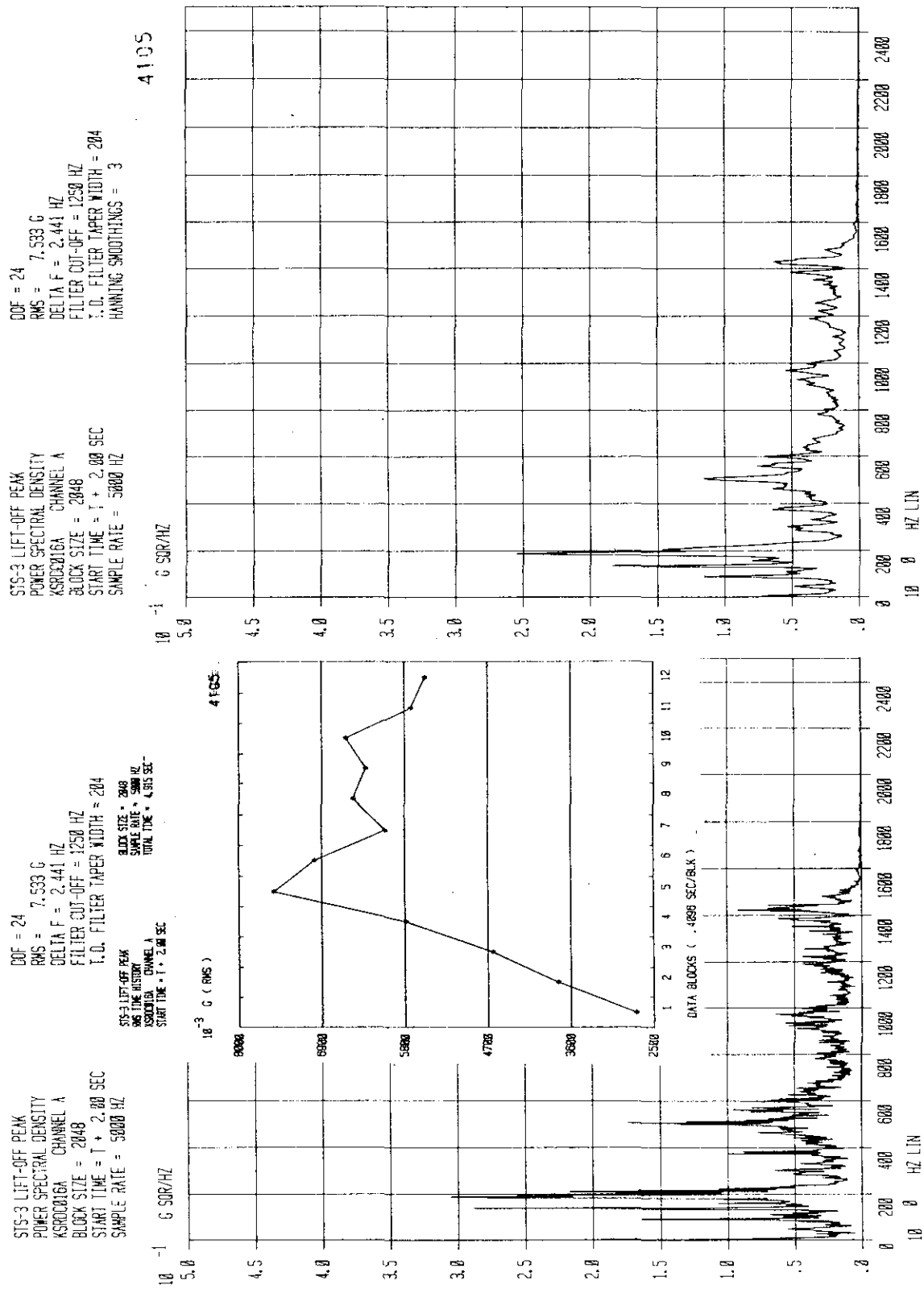


Figure 5-64. Platform 2-in-Floor Beam, Side 3, 131-ft Level (Sheet 2 of 2)

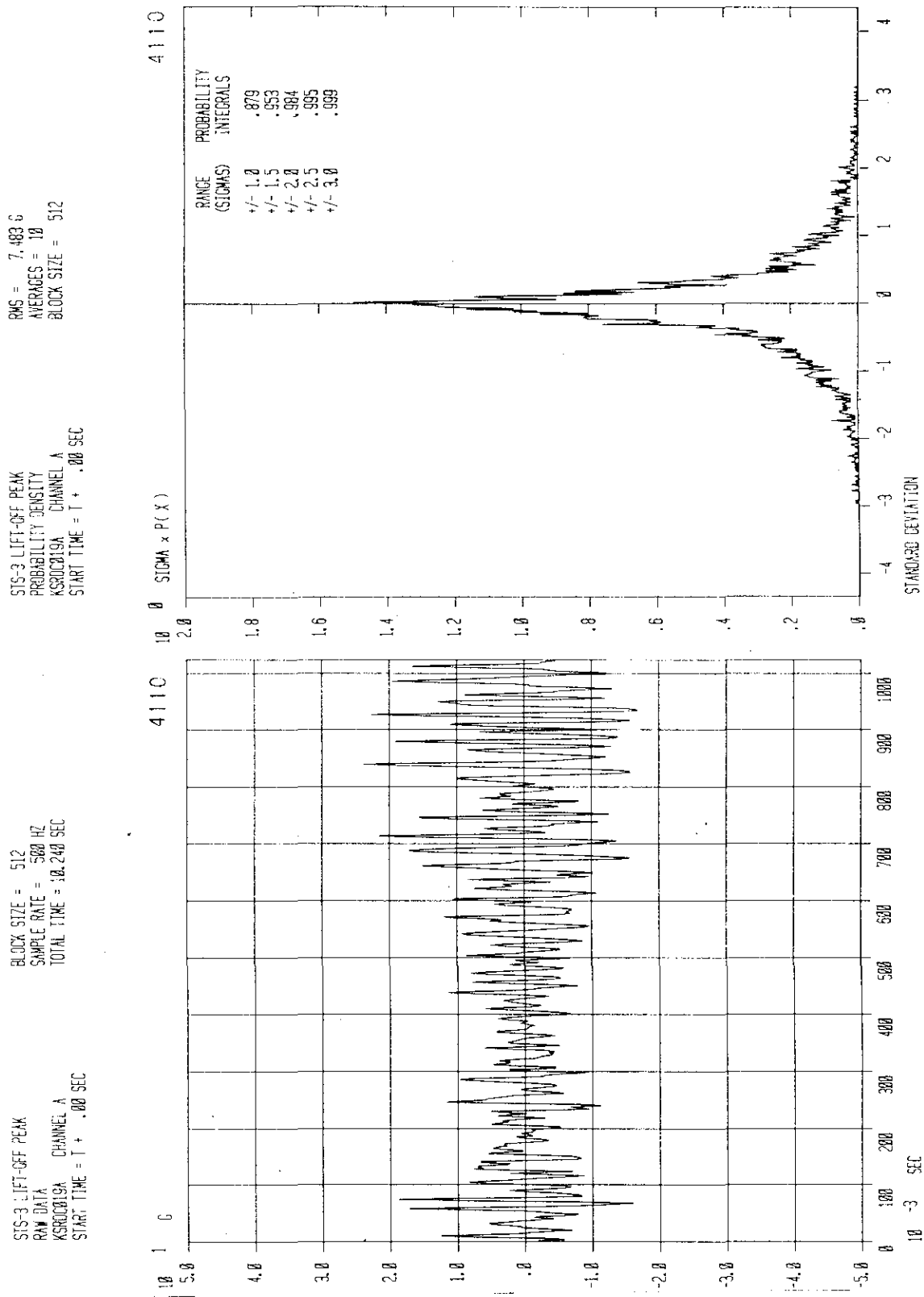


Figure 5-65. Outside Flange, Side 4, 135-ft Level (Sheet 1 of 2)

KSC-DD-818-TR

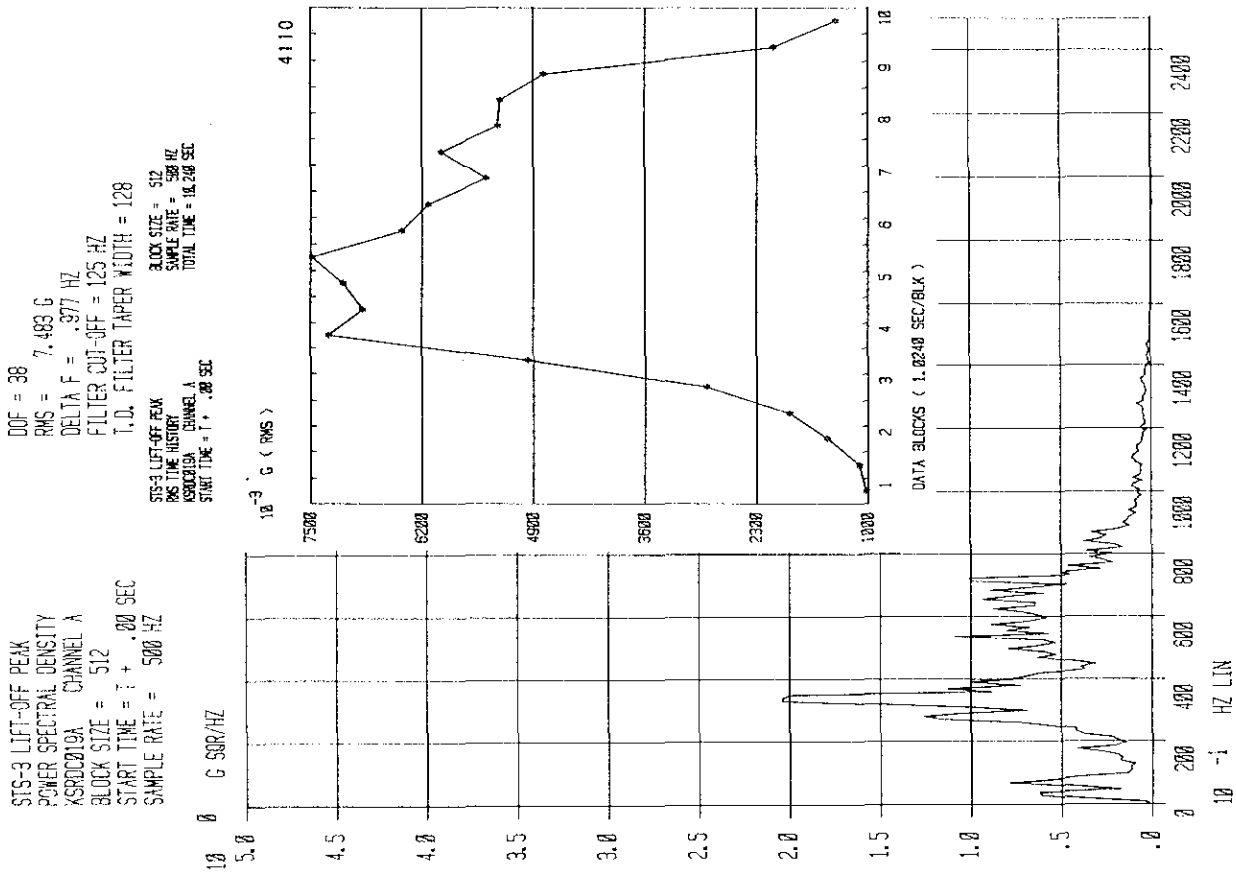


Figure 5-65. Outside Flange, Side 4, 135-ft Level (Sheet 2 of 2)

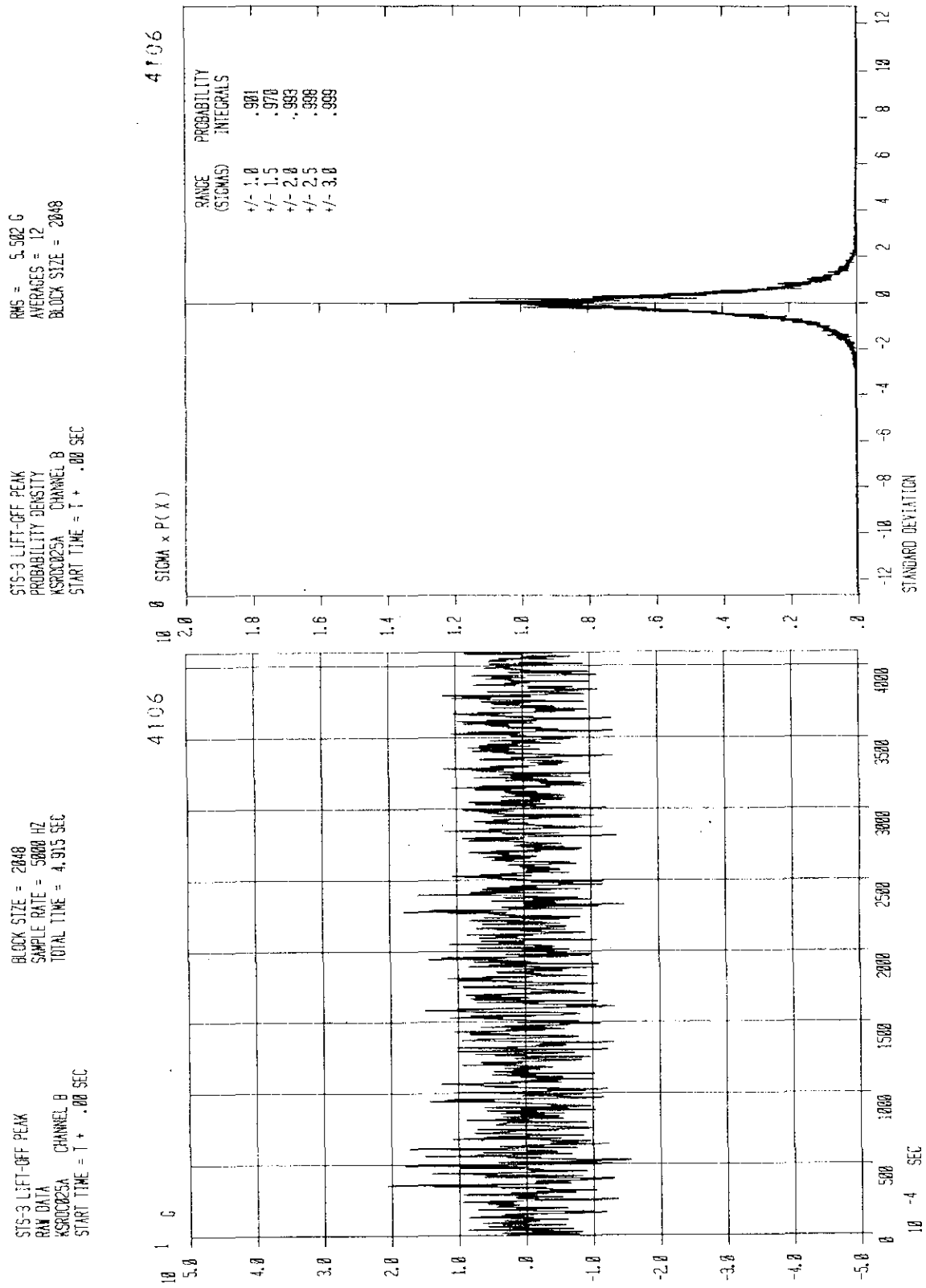


Figure 5-66. Platform Floor Beam (Point 1), 107-ft Level (Sheet 1 of 2)

KSC-DD-818-TR

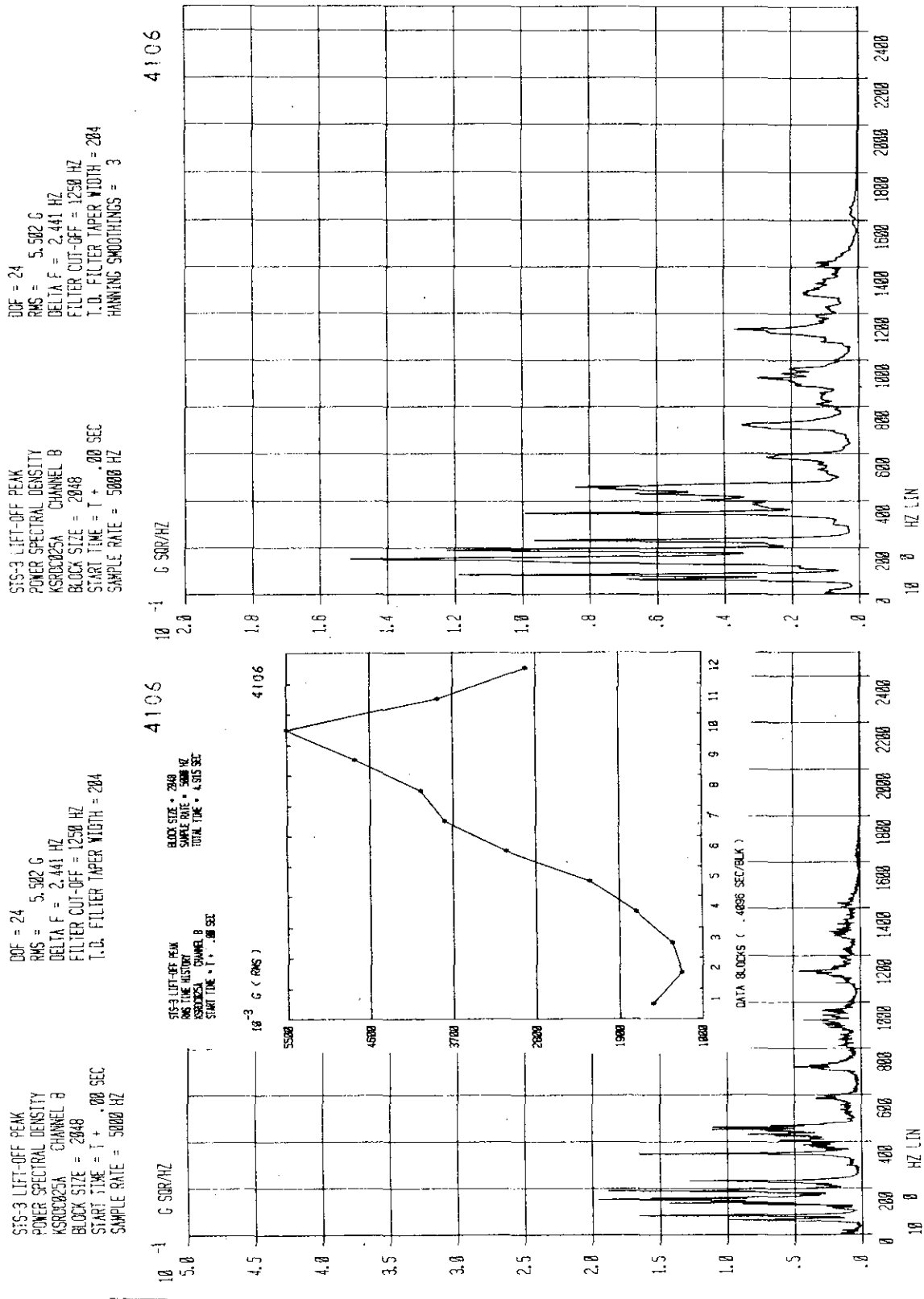


Figure 5-66. Platform Floor Beam (Point 1), 107-ft Level (Sheet 2 of 2)

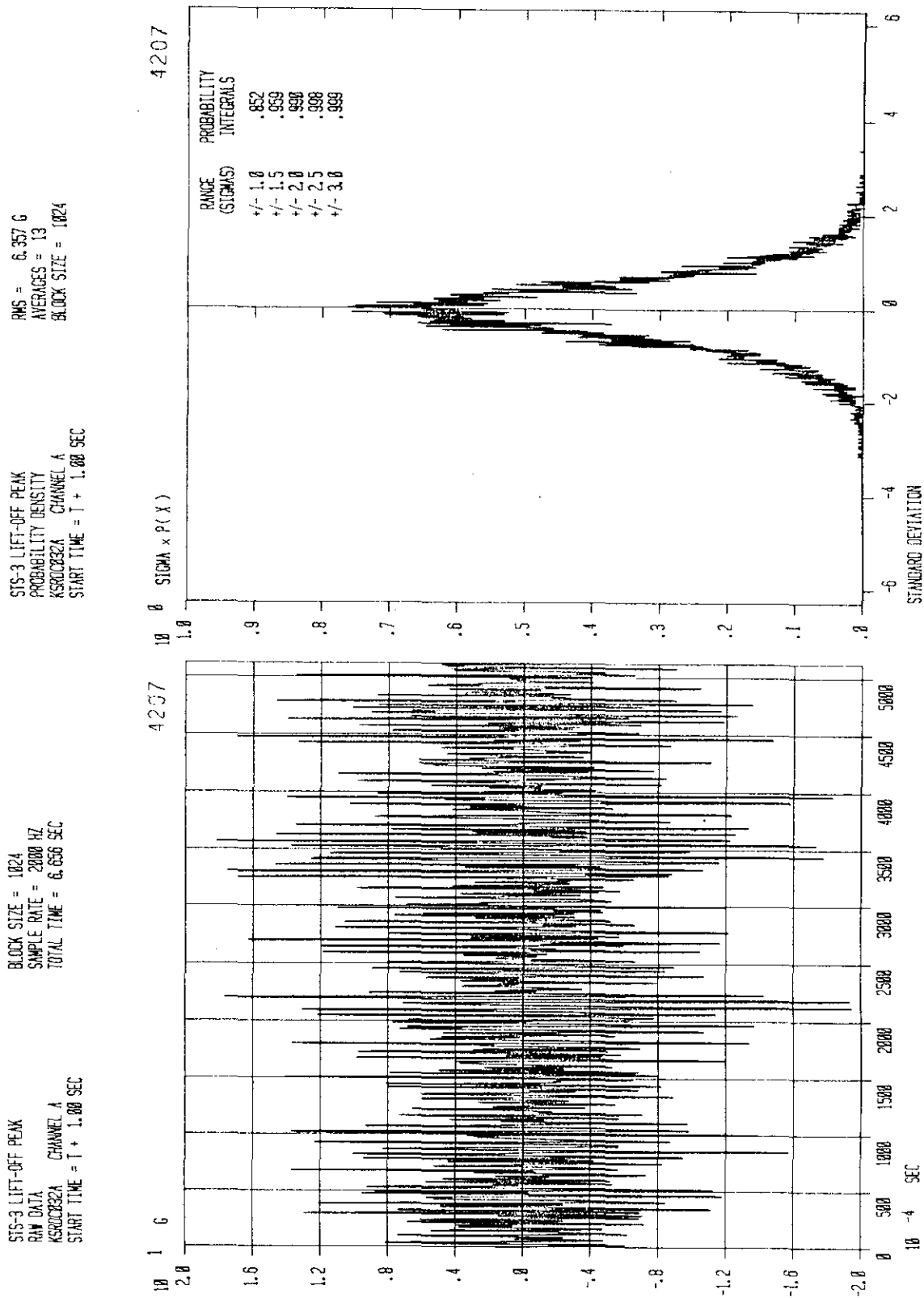


Figure 5-67. Platform Floor Beam (Point 2), 107-ft Level (Sheet 1 of 2)

KSC-DD-818-TR

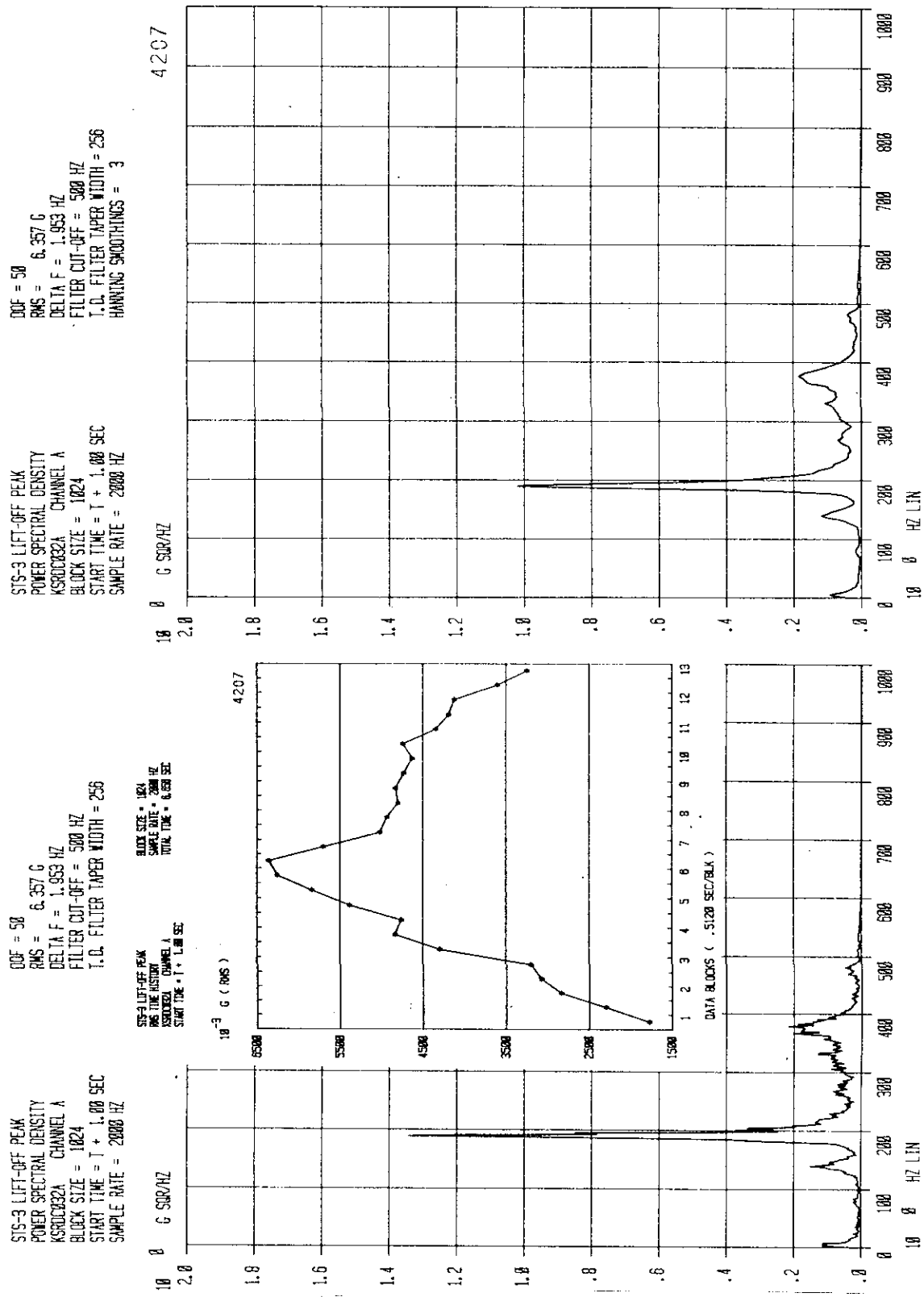


Figure 5-67. Platform Floor Beam (Point 2), 107-ft Level (Sheet 2 of 2)

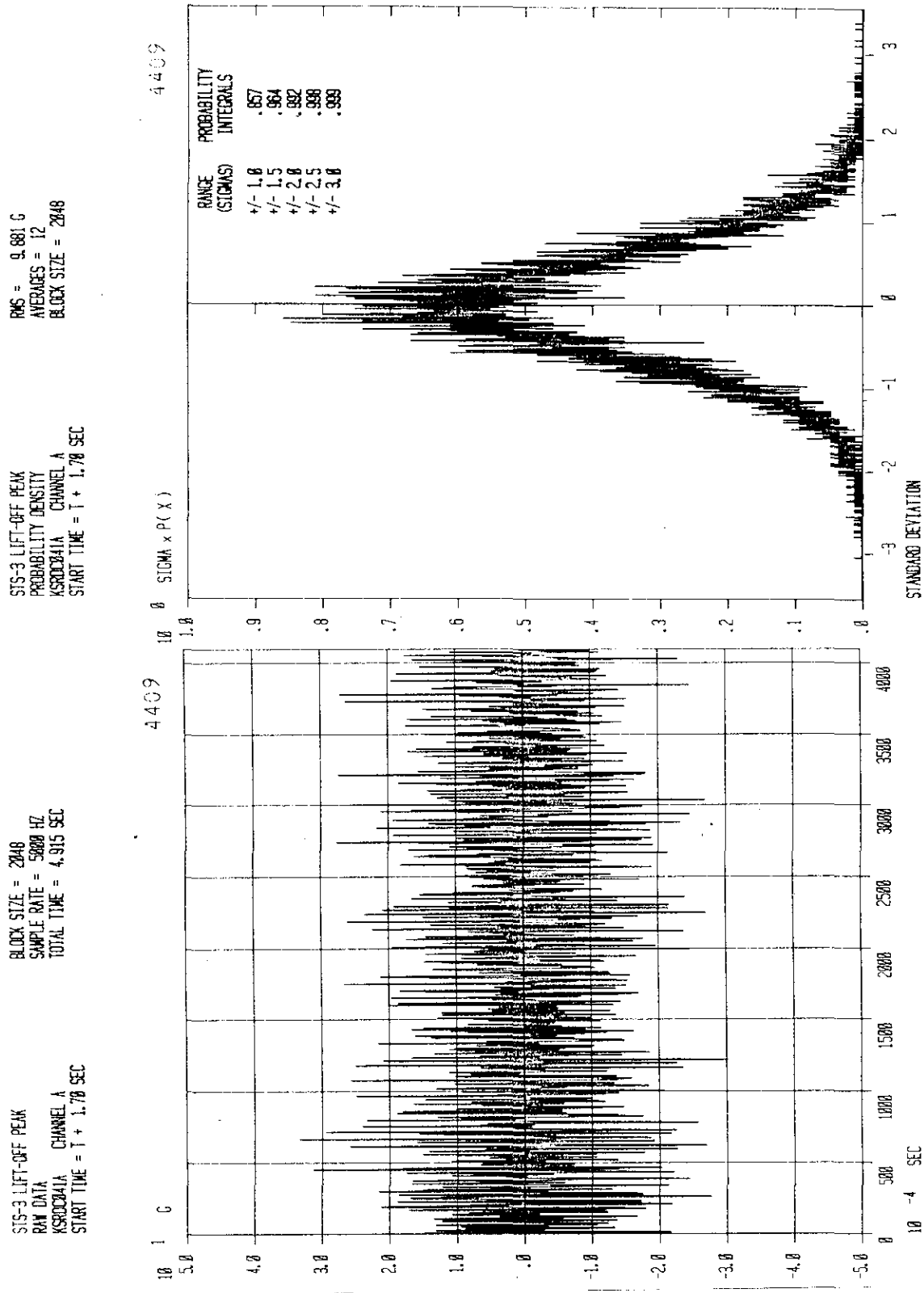


Figure 5-68. Platform Floor Beam (Middle), 107-ft Level (Sheet 1 of 2)

KSC-DD-818-TR

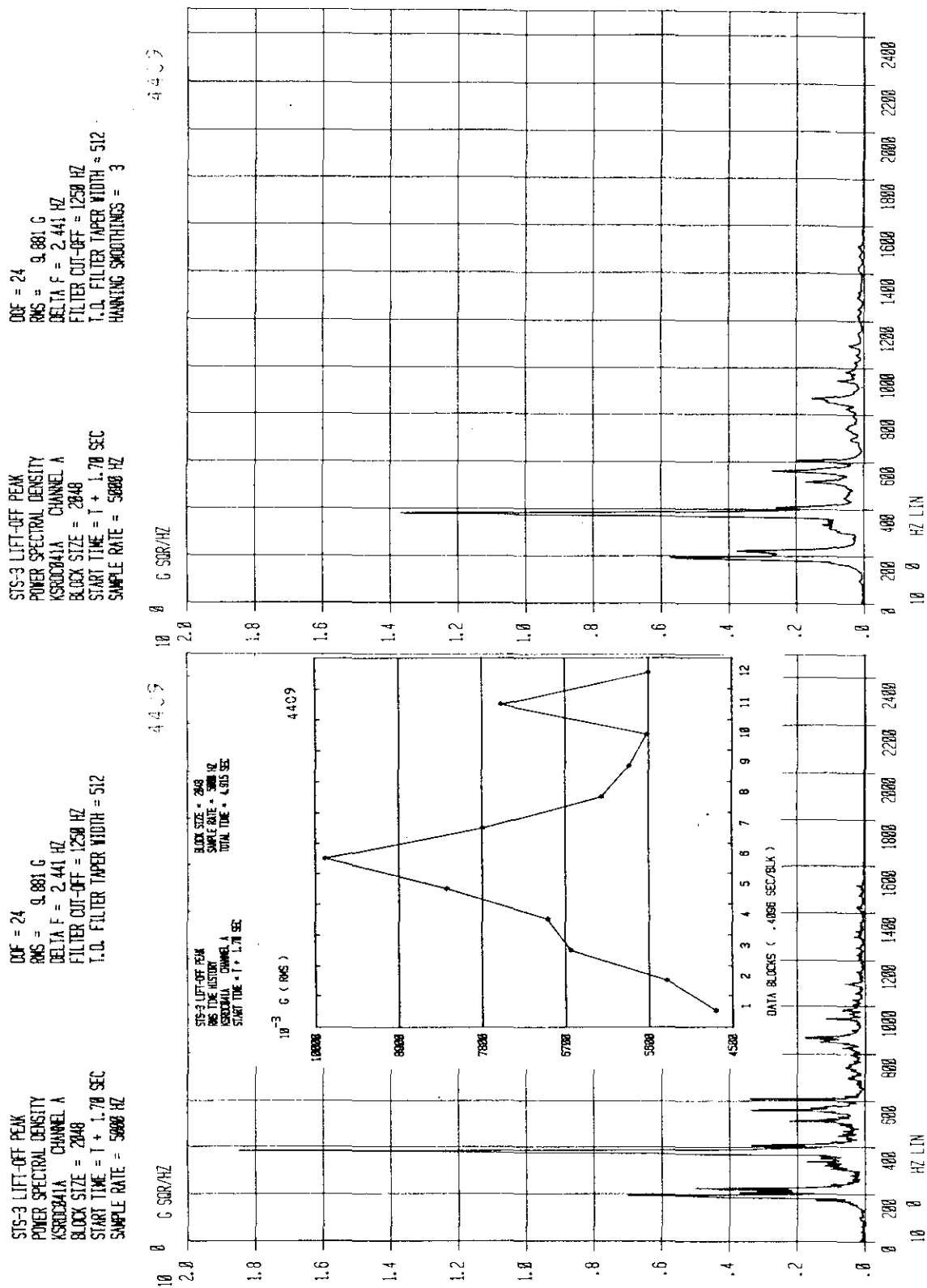
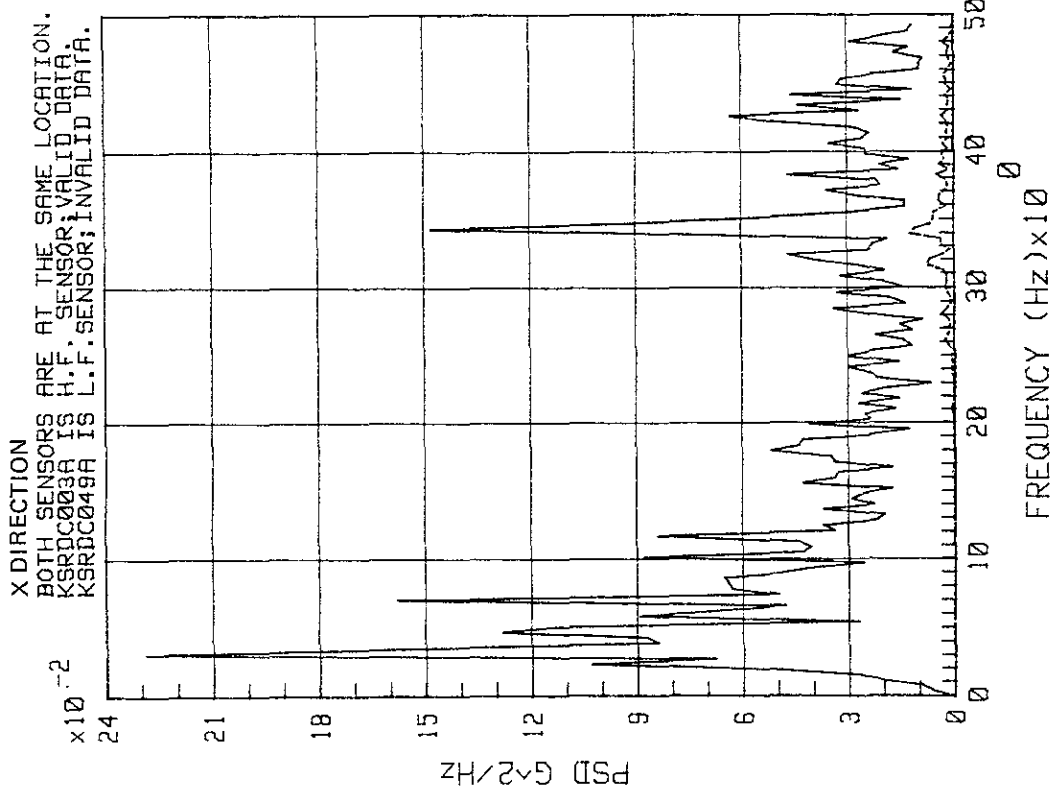


Figure 5-68. Platform Floor Beam (Middle), 107-ft Level (Sheet 2 of 2)

KSR # DC003A DC049C



KSR # DC004B DC050C

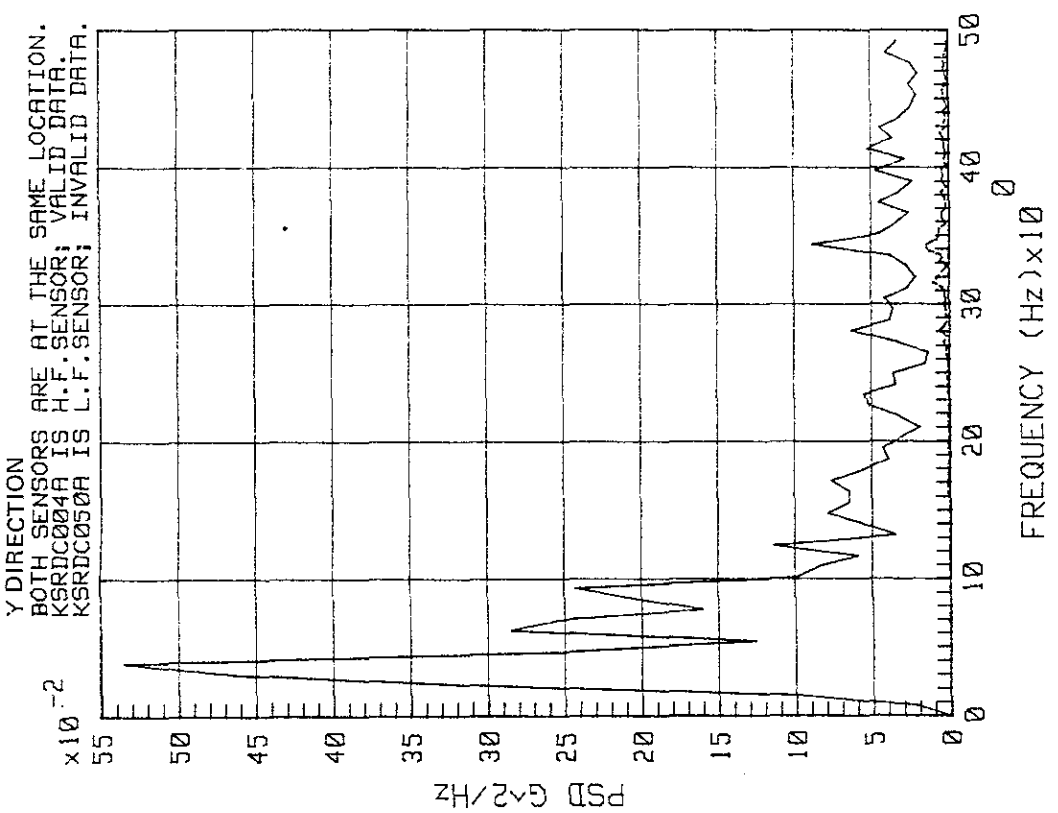


Figure 5-69. STS-3 RSS Vibration Data Comparison, Bottom Flange, 130-ft 7-in Level

STS-3, RSS VIBR. ON HYPERGOL PLATF. X-DIR.
KSR # DC032A DC035C

STS-3, RSS VIBR. ON HYPERGOL PLATF. Y-DIR.
KSR # DC033A DC036C

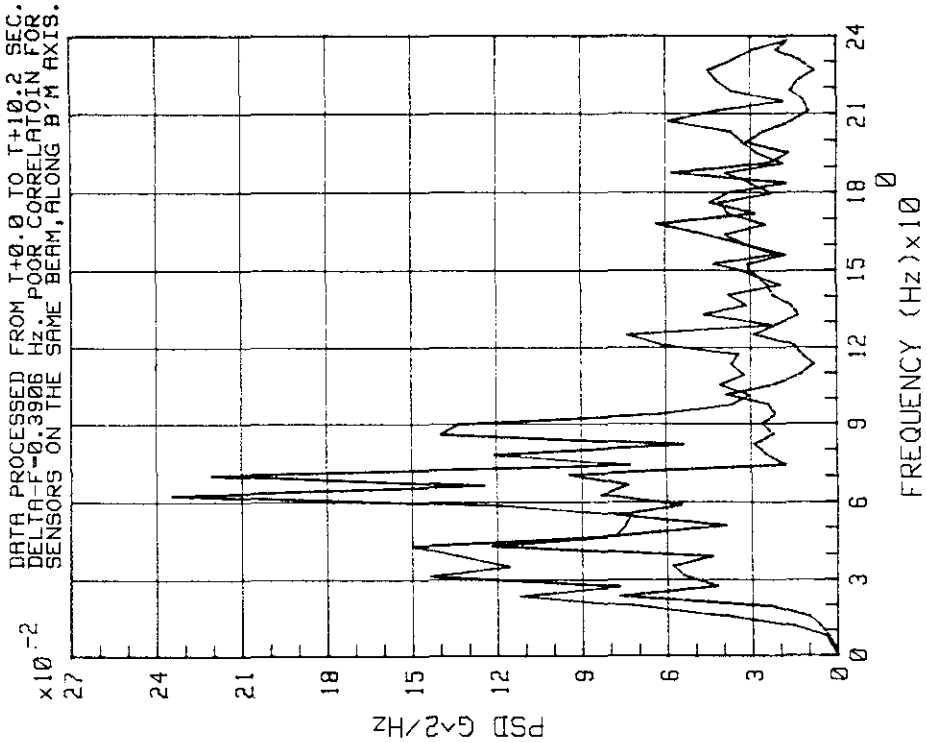
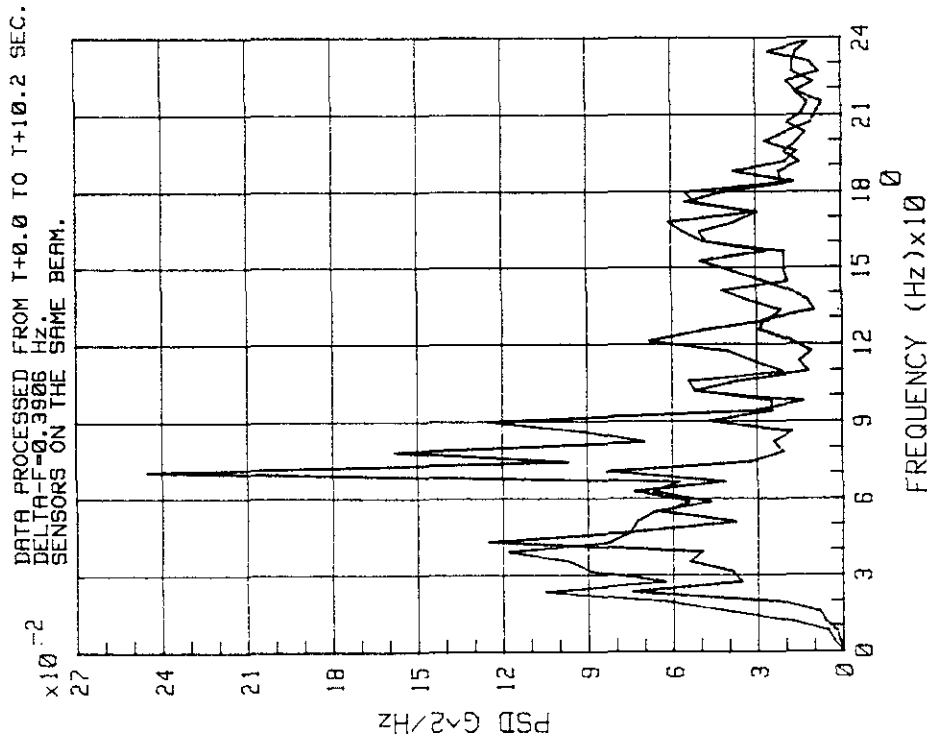


Figure 5-70. STS-3 RSS Vibration on Hypergol Platform, X and Y Directions

KSR # DC037C DC038A DC039A DC040C DC034D

DATA PROCESSED FROM T+0.0 TO T+10.2 SEC. DELTA-F=0.3906 Hz.
DATA FROM KSRDC034D CANNOT BE SEEN IN THIS SCALE. SEE NEXT PLOT WHERE DATA WAS HANNED.

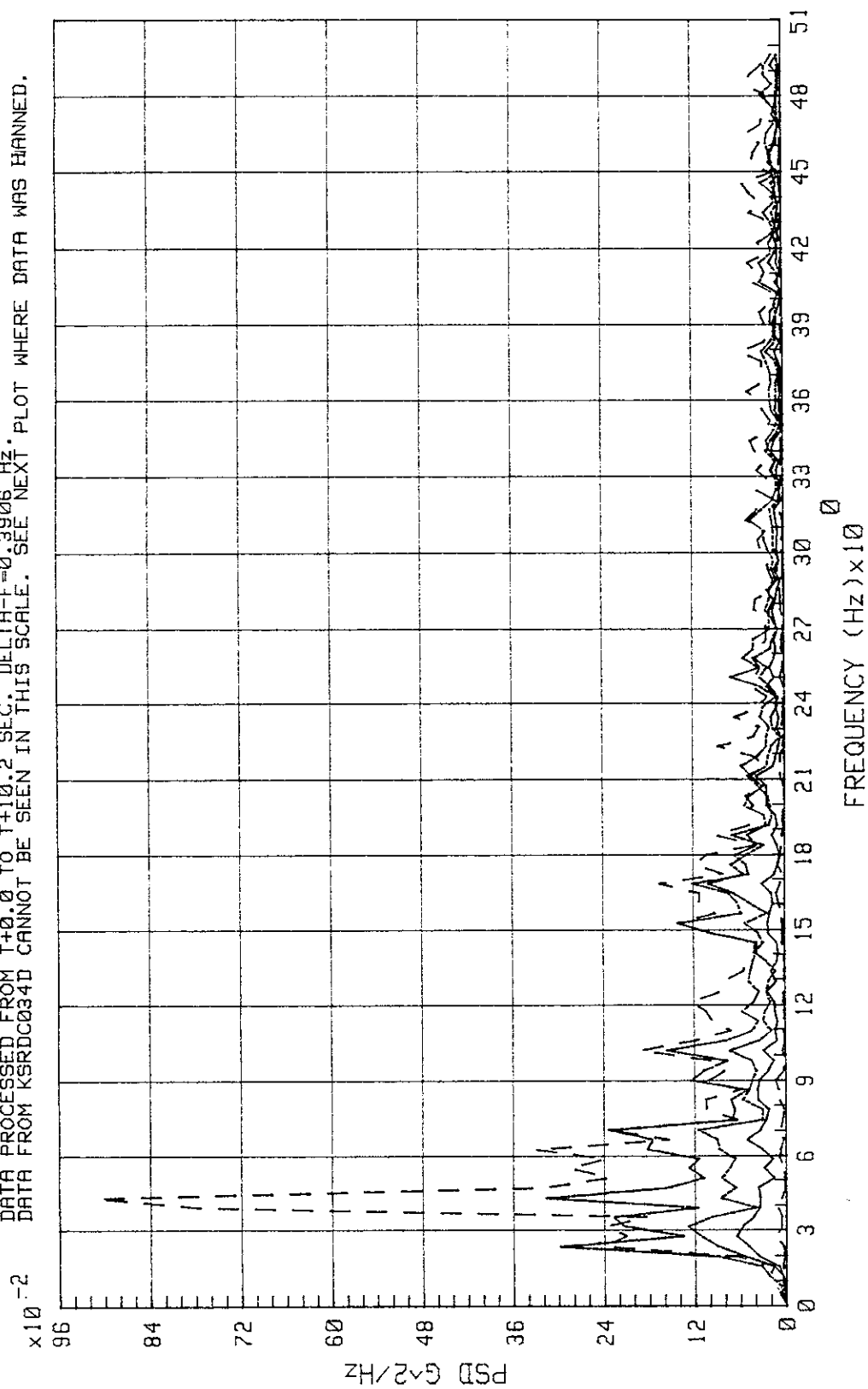


Figure 5-71. STS-3 RSS Vibration on Hypergol Platform, Z Direction (Sheet 1 of 2)

KSC-DD-818-TR

KSR # DC037C DC038A DC039A DC040C DC034D

DATA PROCESSED FROM T+0.0 TO T+10.2 SEC. DELTA-F=0.3906 Hz. ALL PSD's HANNED 3x.
DATA FROM KSRDC034D CANNOT BE SEEN IN THIS SCALE.

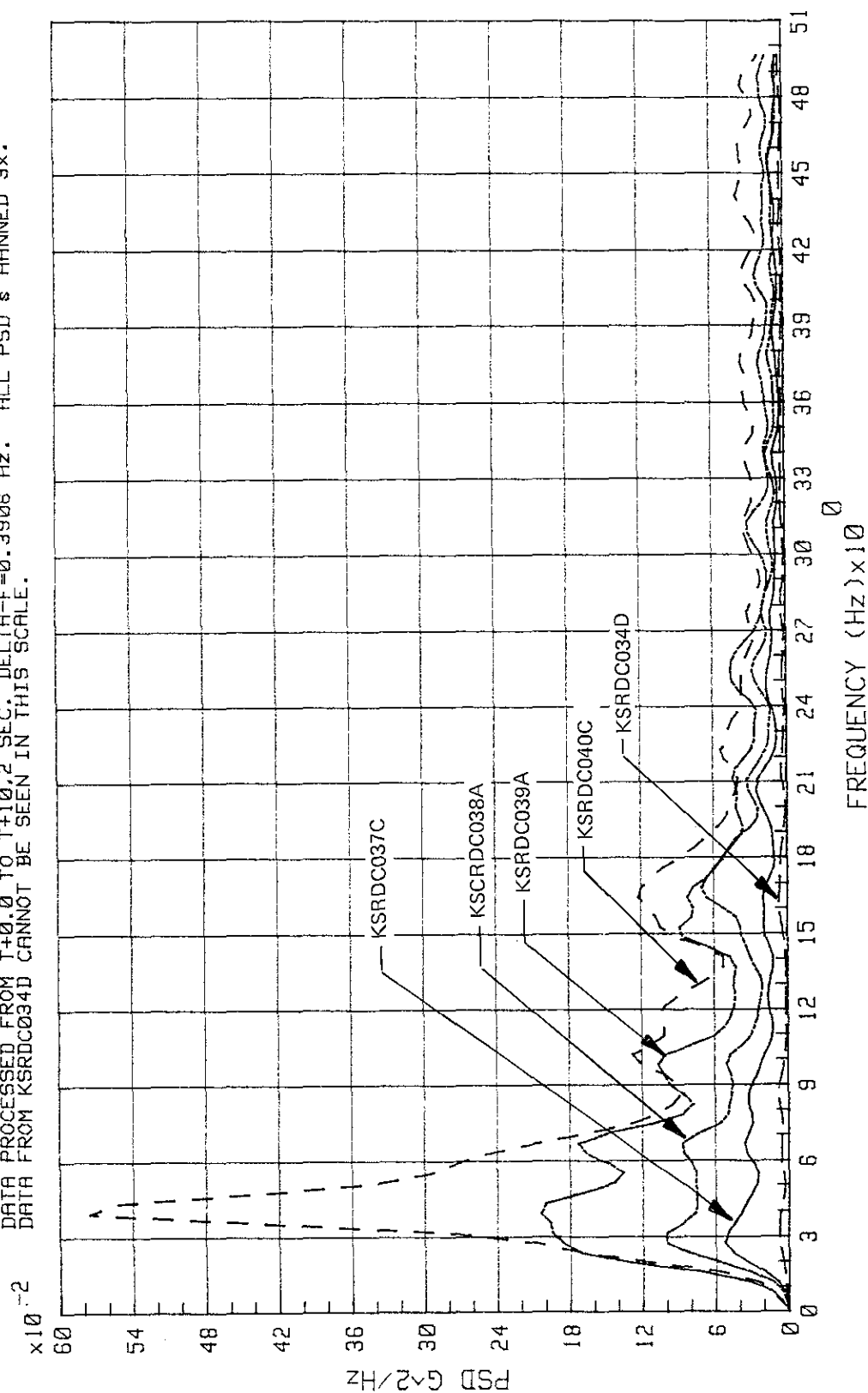


Figure 5-71. STS-3 RSS Vibration on Hypergol Platform, Z Direction (Sheet 2 of 2)

KSR # DC001B DC002C DC002A DC041B

$\times 10^{-1}$ ALL DATA PROCESSED AT LIFT-OFF PEAK. ALL PSD'S HANNED 3x.
HIGH PEAKS OF KSRDC041B SUPPRESSED REMAINING DATA.

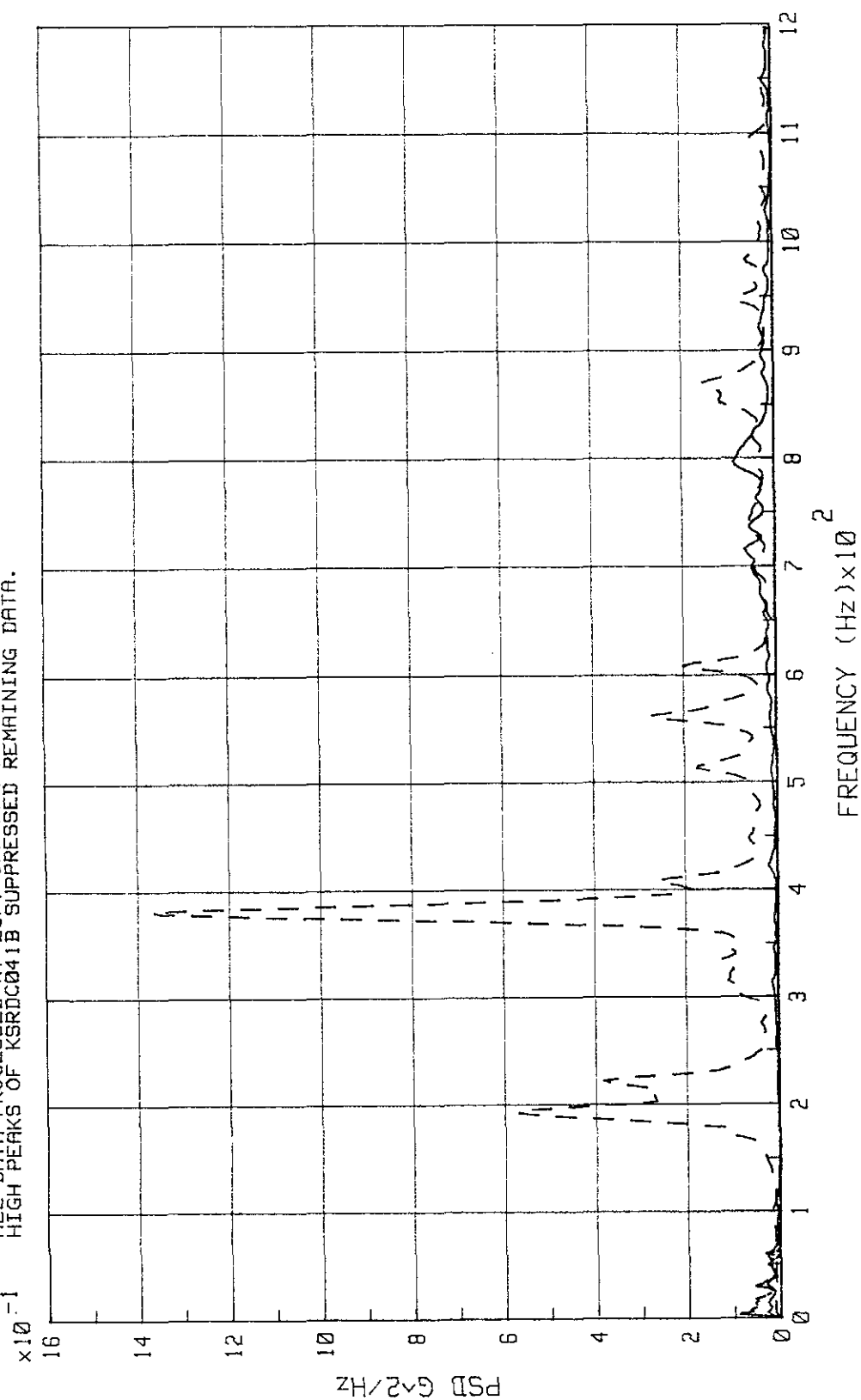


Figure 5-72. STS-3 RSS Vibration on APU Platform, Z Direction (Sheet 1 of 2)

KSC-DD-818-TR

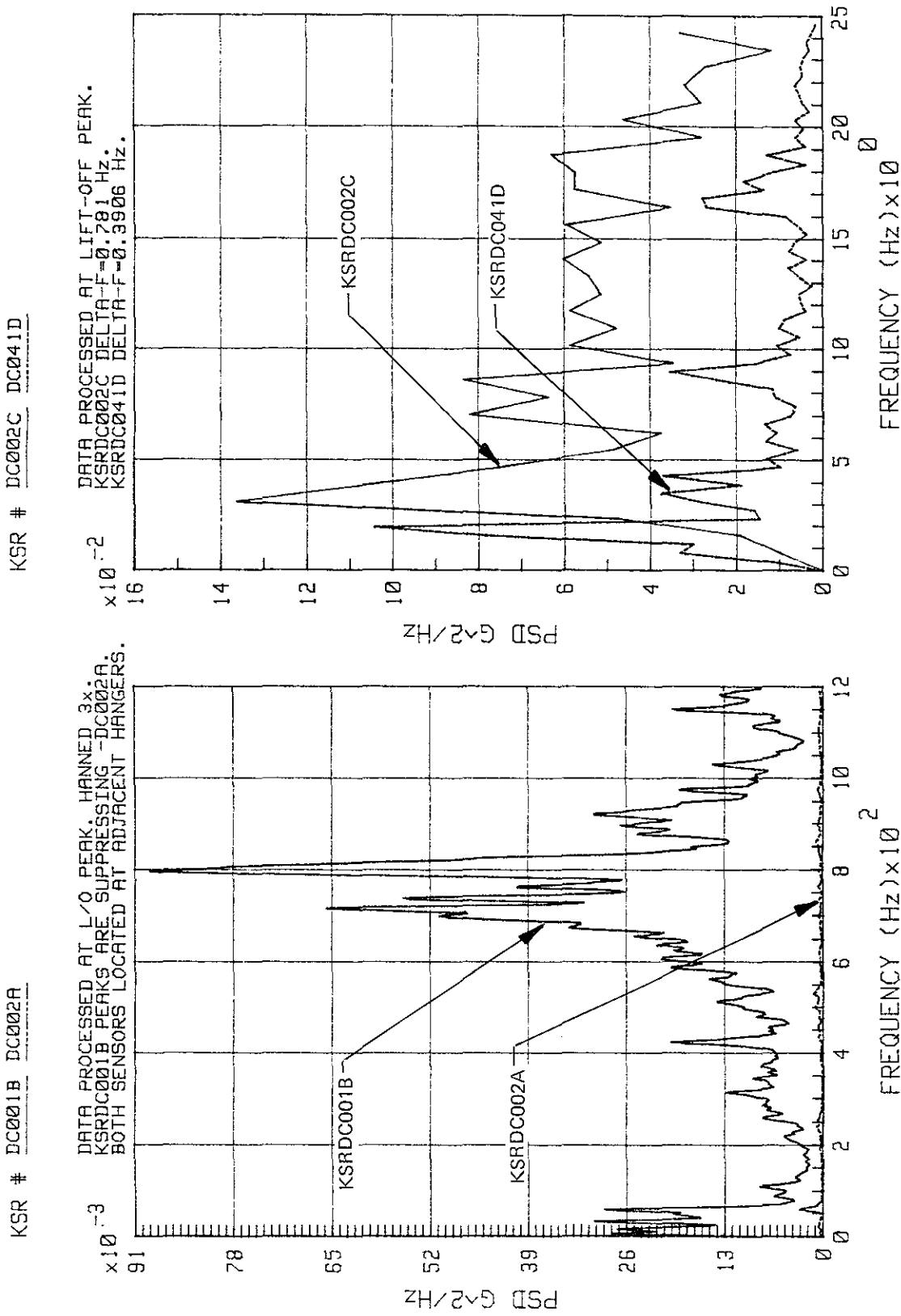


Figure 5-72. STS-3 RSS Vibration on APU Platform, Z Direction (Sheet 2 of 2)

KSR # DC005A DC009A DC010A DC011A

ALL DATA PROCESSED FROM T+0.0 TO T+10.2 SEC. DELTA-F=0.3908 Hz. SENSOR RANGE 5-2000 Hz.
 GOOD CORRELATION CONSIDERING WIDE SPREAD BETWEEN SENSORS.

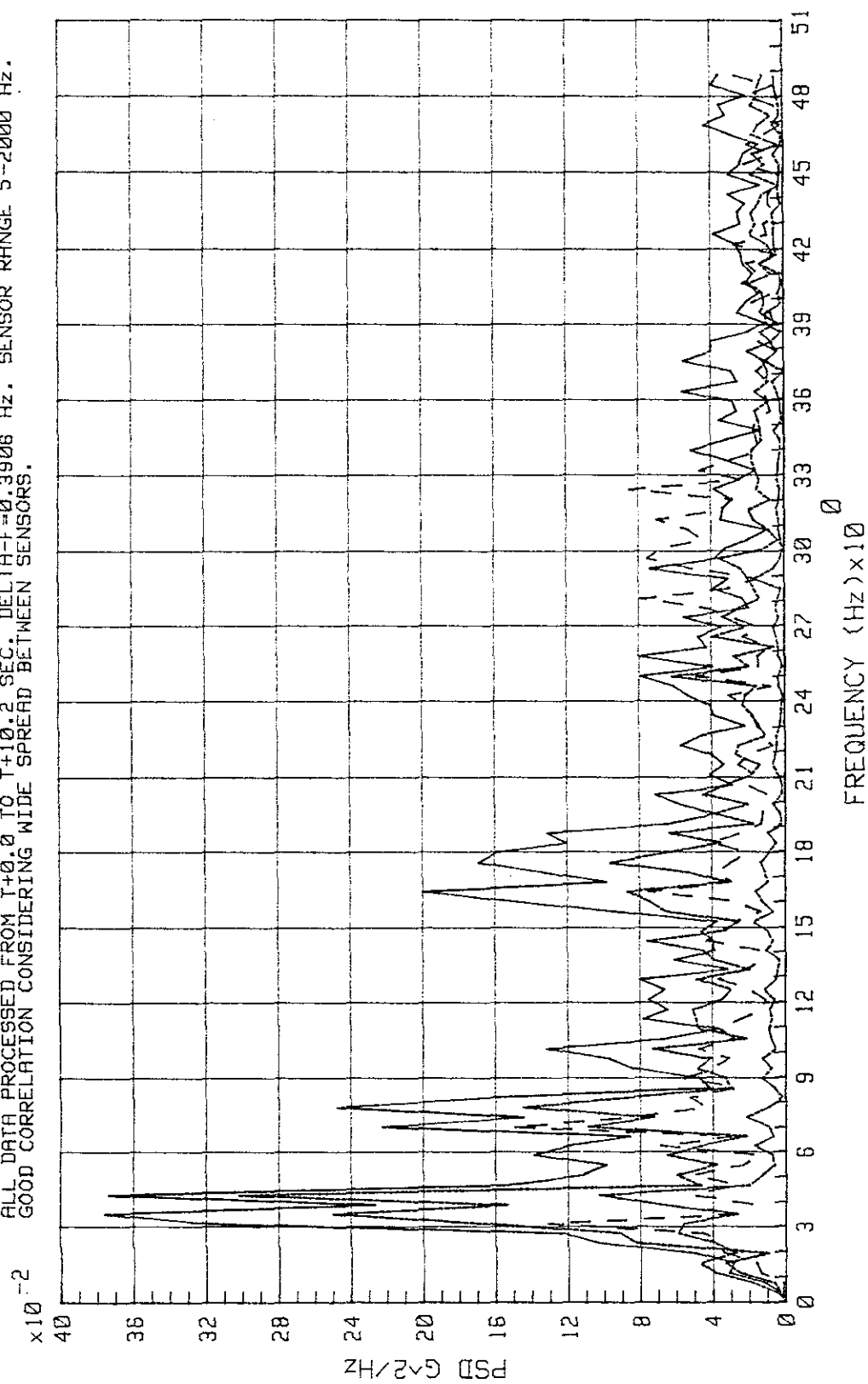


Figure 5-73. STS-3 RSS Vibration on PCR Floor, Z Direction

KSC-DD-818-TR

KSR # DC003A DC024A DC032A DC035C

ALL DATA PROCESSED FROM T+0.0 TO T+10.2 SEC EXCEPT KSRDC024A (T+0.0 TO T+7.69 SEC).
DELTA-F=0.3906 Hz ALL EXCEPT KSRDC024A DELTA-F=0.781 Hz.
SENSOR RANGE 5-2000 Hz.

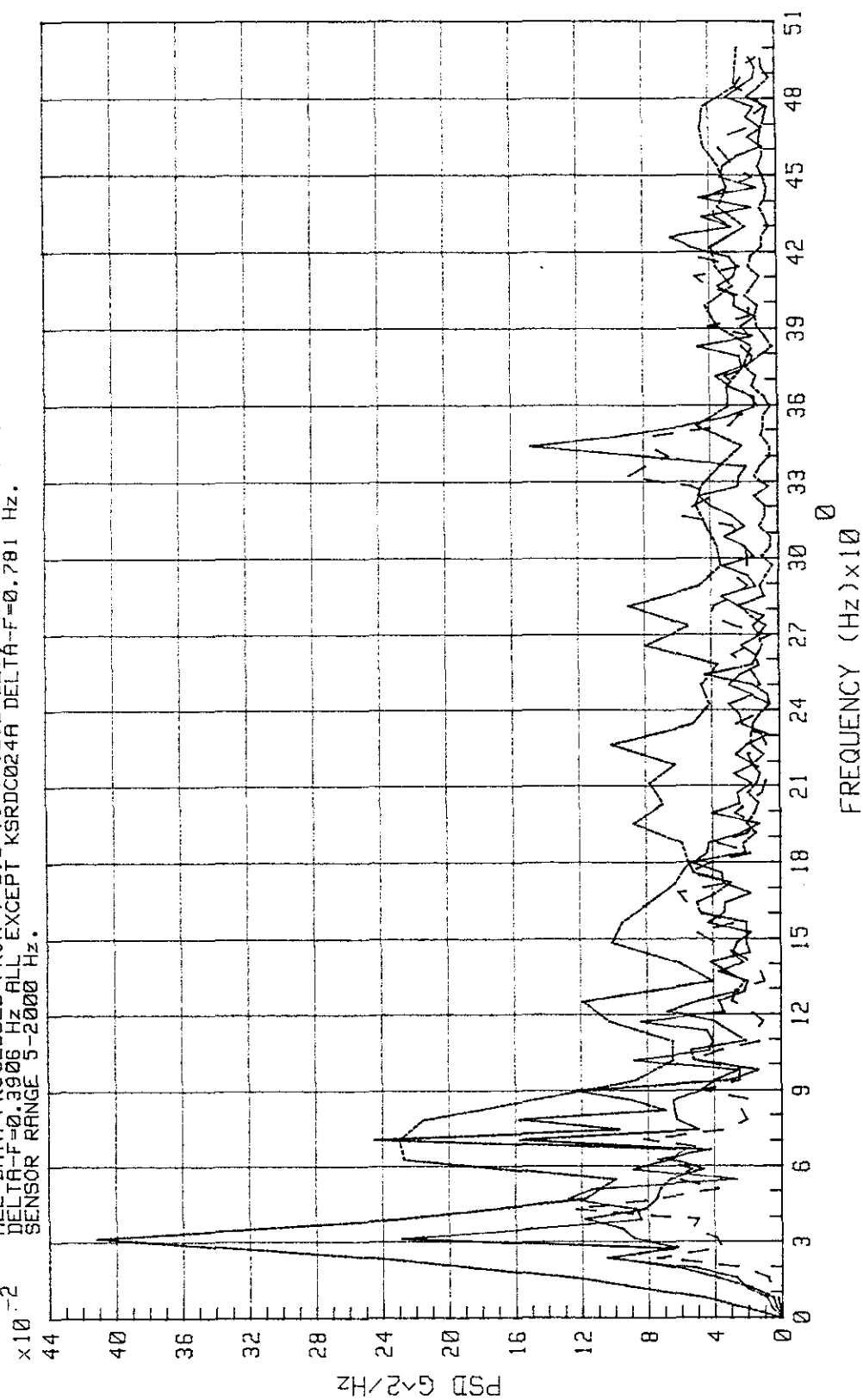


Figure 5-74. STS-3 RSS Vibration, High-Frequency Sensors on Floors, X Direction

KSR # DC004B DC025A DC033A DC036C

ALL DATA PROCESSED FROM T+0.0 TO T+10.2 SEC EXCEPT KSRDC004B (T+0.4 TO T+6.81 SEC).
 DELTA F=0.3906 Hz ALL EXCEPT KSRDC004B DELTA F=0.781 Hz. SENSOR RANGE 5-2000 Hz.
 KSRDC025A HAS QUESTIONABLE AMPLITUDES BELOW 3 Hz.

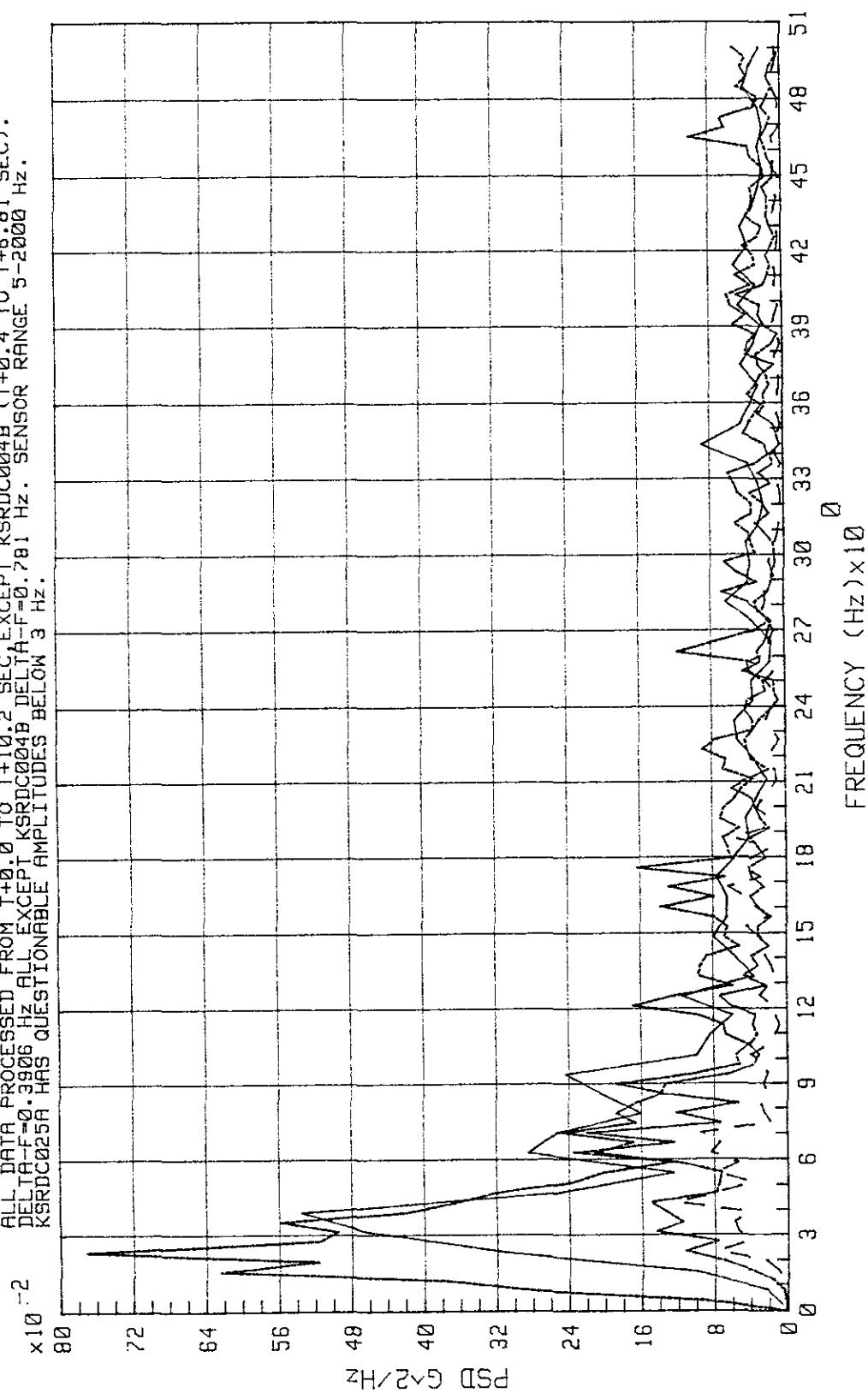


Figure 5-75. STS-3 RSS Vibration, High-Frequency Sensors on Floors, Y Direction (Sheet 1 of 2)

KSC-DD-818-TR

KSR # DC004B DC025A DC033A DC036C

5-116

ALL DATA PROCESSED FROM T+0.0 TO T+10.2 SEC, EXCEPT KSRDC004B (T+0.4 TO T+6.81 SEC).
 DELTA-F=0.3906 Hz ALL EXCEPT KSRDC004B DELTA-F=0.781 Hz. SENSOR RANGE 5-2000 Hz.
 KSRDC004B AND KSRDC025A DATA BELOW 5 Hz ARE EXCLUDED FROM PLOT. GOOD CORRELATION WITHIN PLOT.

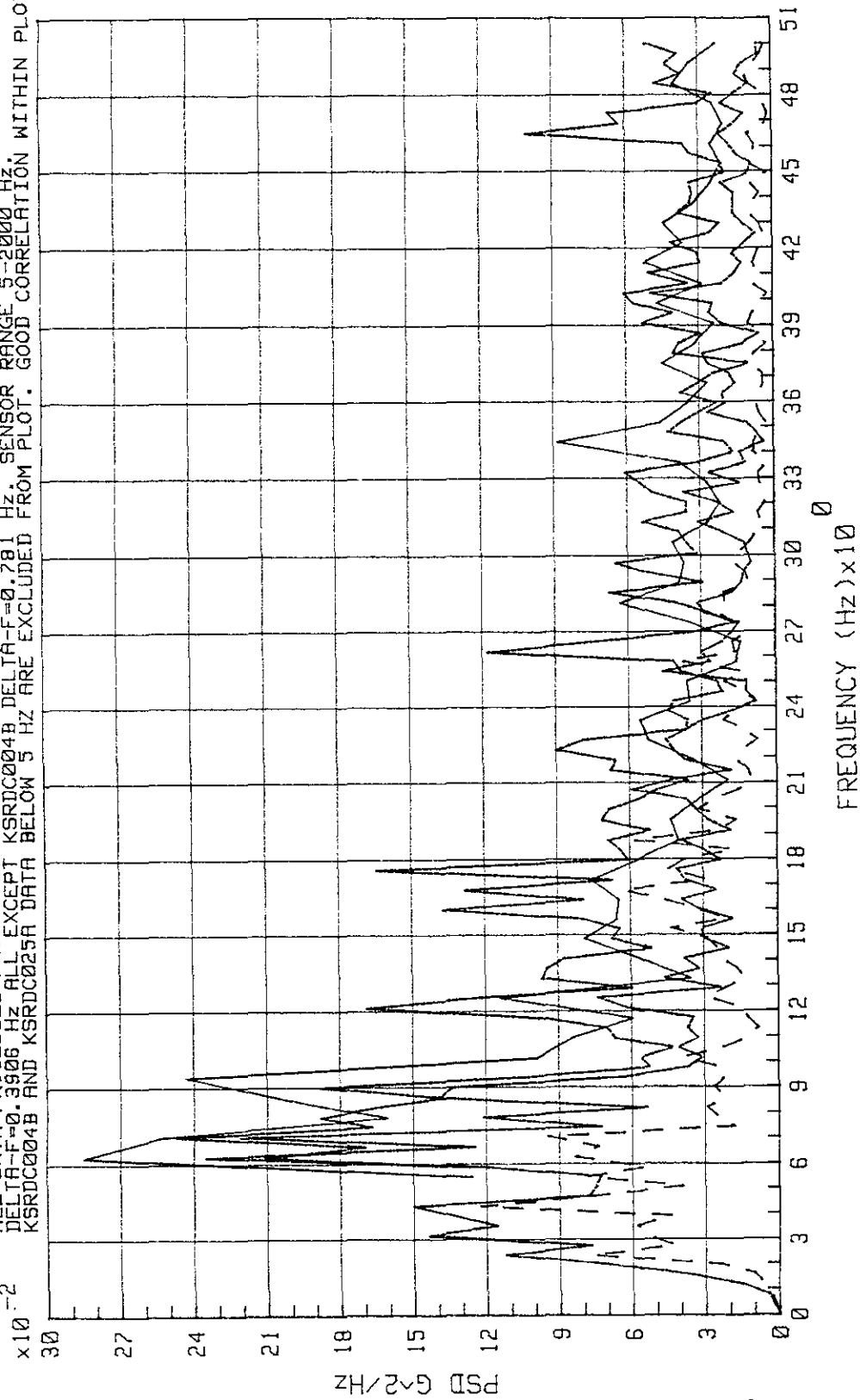


Figure 5-75. STS-3 RSS Vibration, High-Frequency Sensors on Floors, Y Direction (Sheet 2 of 2)

KSR # DC017A DC018A DC023A

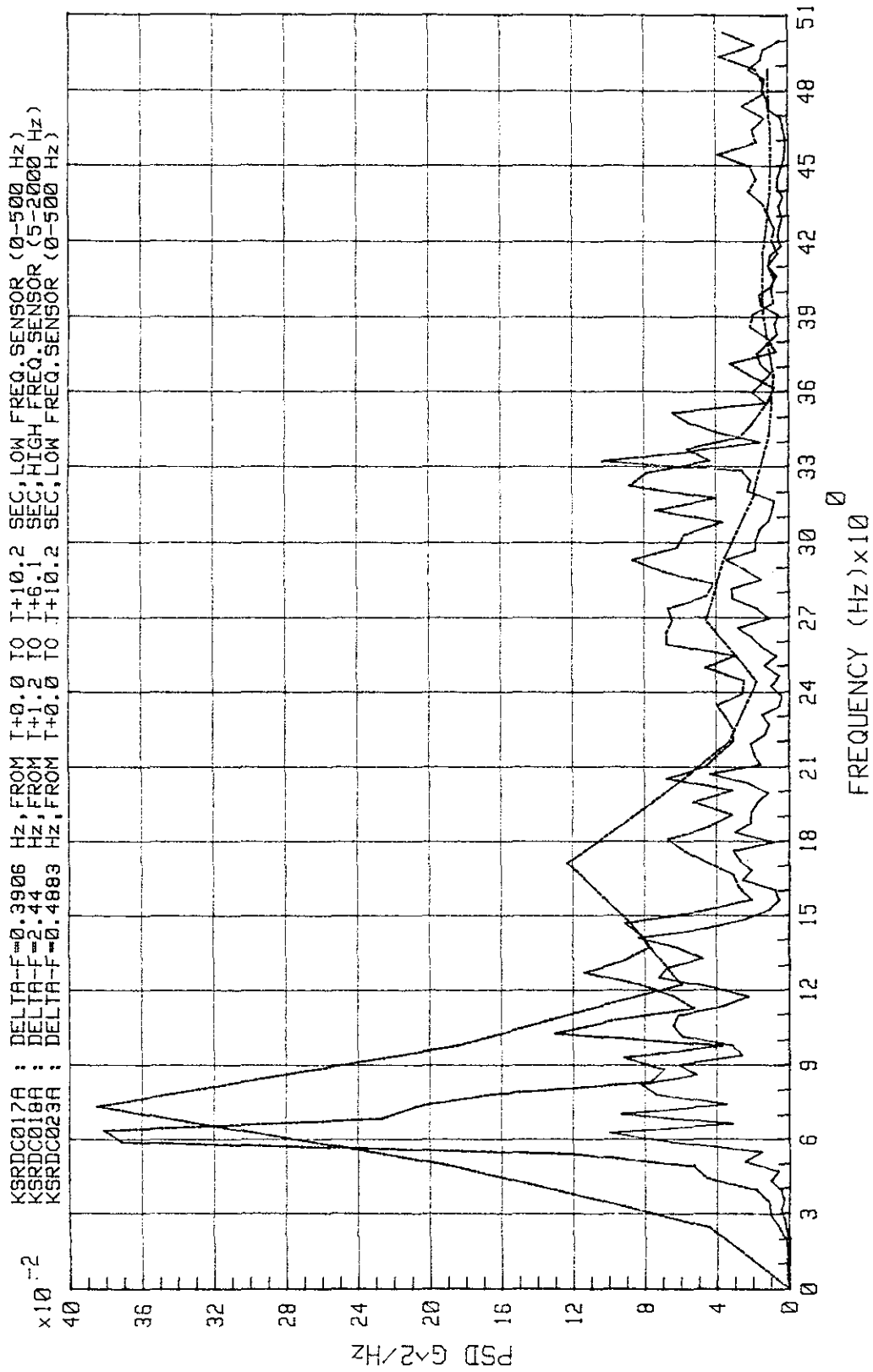


Figure 5-76. STS-3 RSS Vibration, Side 4 Girts, X Direction

KSC-DD-818-TR

KSR # DC020 DC021A DC022B

$\times 10^{-1}$
 KSRDC020 PROCESSED FROM T+0.0 TO T+10.2 SEC. DELTA F=0.3906 HZ. DATA VALID.
 KSRDC021A AND KSRDC022B PROCESSED FROM T+0.0 TO T+12.8 SEC. DATA ARE QUESTIONABLE-CONTAIN
 BASELINE DRIFT. LOW FREQUENCY ENDS OF PSD'S ARE EXCLUDED FROM PLOT BECAUSE OF TOO HIGH SCALE.

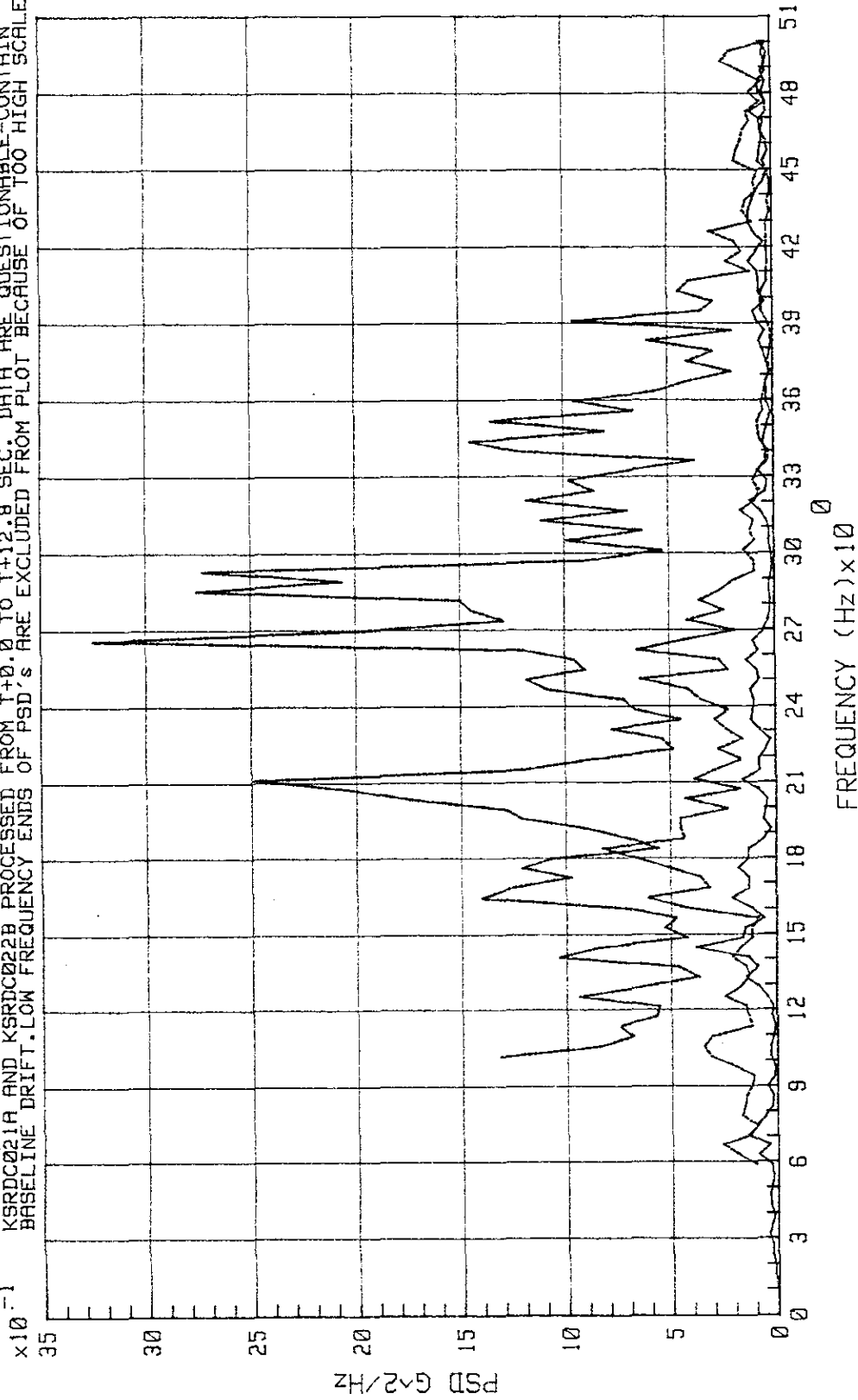


Figure 5-77. STS-3 RSS Vibration, Side 3 Girts, Y Direction

KSR # DC042C DC043C DC044C

ALL SENSORS : DELTA-F=0.781 Hz. PROCESSING FROM T+1.1 TO T+6.2 SEC. SENSOR RANGE 5-2000 Hz.
KSRDC042A (X), KSRDC043A (Y) AND KSRDC044A (Z) ARE INSTALLED ON THE SAME MOUNT.
DATA ARE VALID. COMPARE THESE PSD's WITH PSD's PROCESSED FOR INTERVAL T+6.2 TO T+16.45 SEC
WHEN A MALFUNCTION OCCURED.

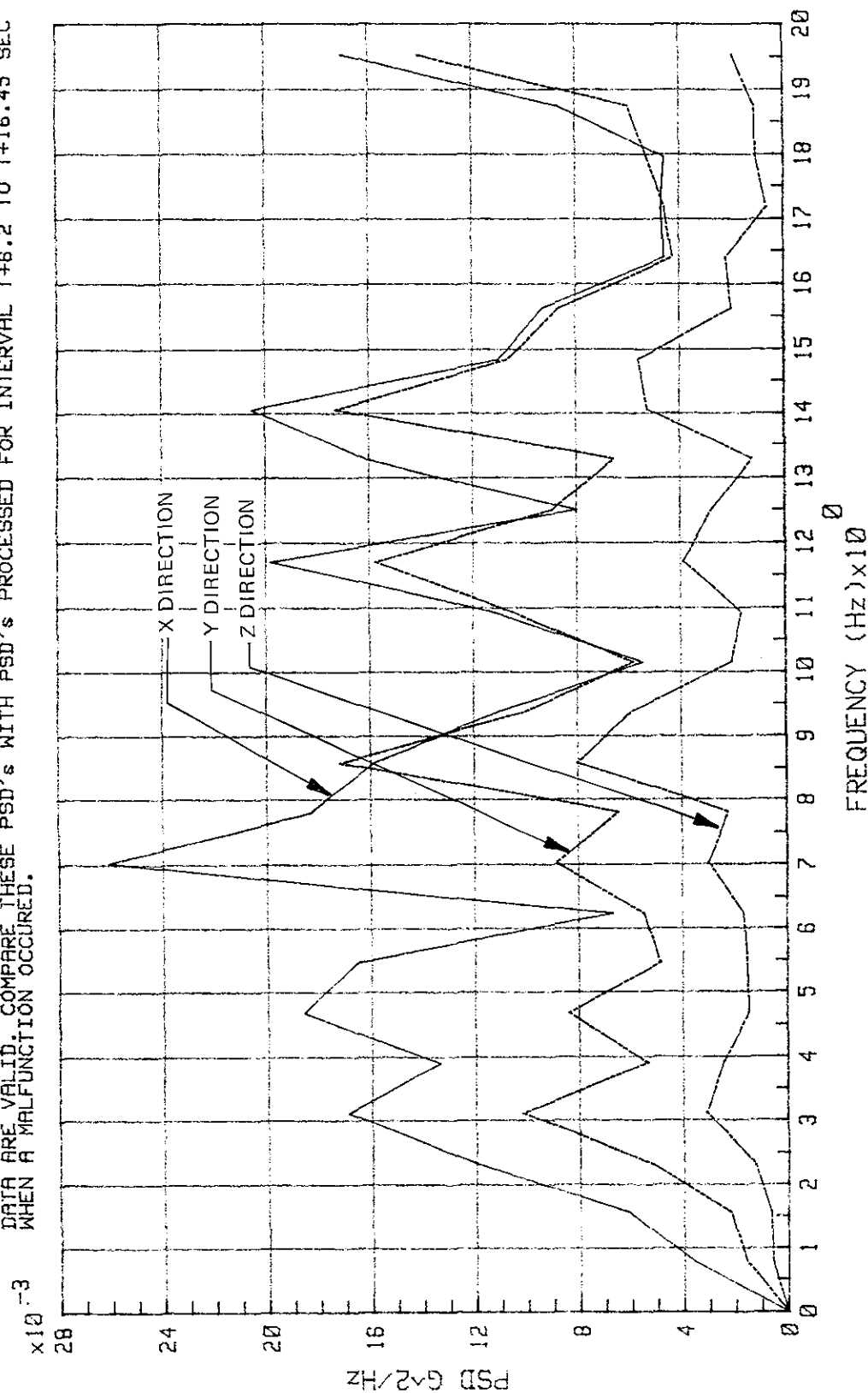


Figure 5-78. STS-3 Lift-Off - Vibration Inside HIM Rack 6396A1, Sensors in X, Y, and Z Directions

KSC-DD-818-TR

KSR # DC042D DC043D DC044D

ALL SENSORS : DELTA-F-0.391 Hz. PROCESSING FROM T+6.2 TO T+18.45 SEC. SENSOR RANGE 5-2000 Hz.
 SENSORS ARE LOCATED INSIDE HIM RACK #6388A1 ON THE SAME MOUNT. MALFUNCTION BEGINS AT T+6.3 SEC.
 SENSORS ARE IDENTICAL. RECORDED TIME HISTORIES DID NOT ORIGINATE FROM SENSOR OUTPUTS, RATHER
 PSD'S ARE IDENTICAL. WITHIN THE DATA ACQUISITION SYSTEM, IDENTICAL PSD'S CAN OCCUR ONLY FROM
 THE SAME AND COMMON SIGNAL. SENSOR OUTPUT IS SUPPRESSED BY MUCH HIGHER EXTRANEIOUS SIGNAL.

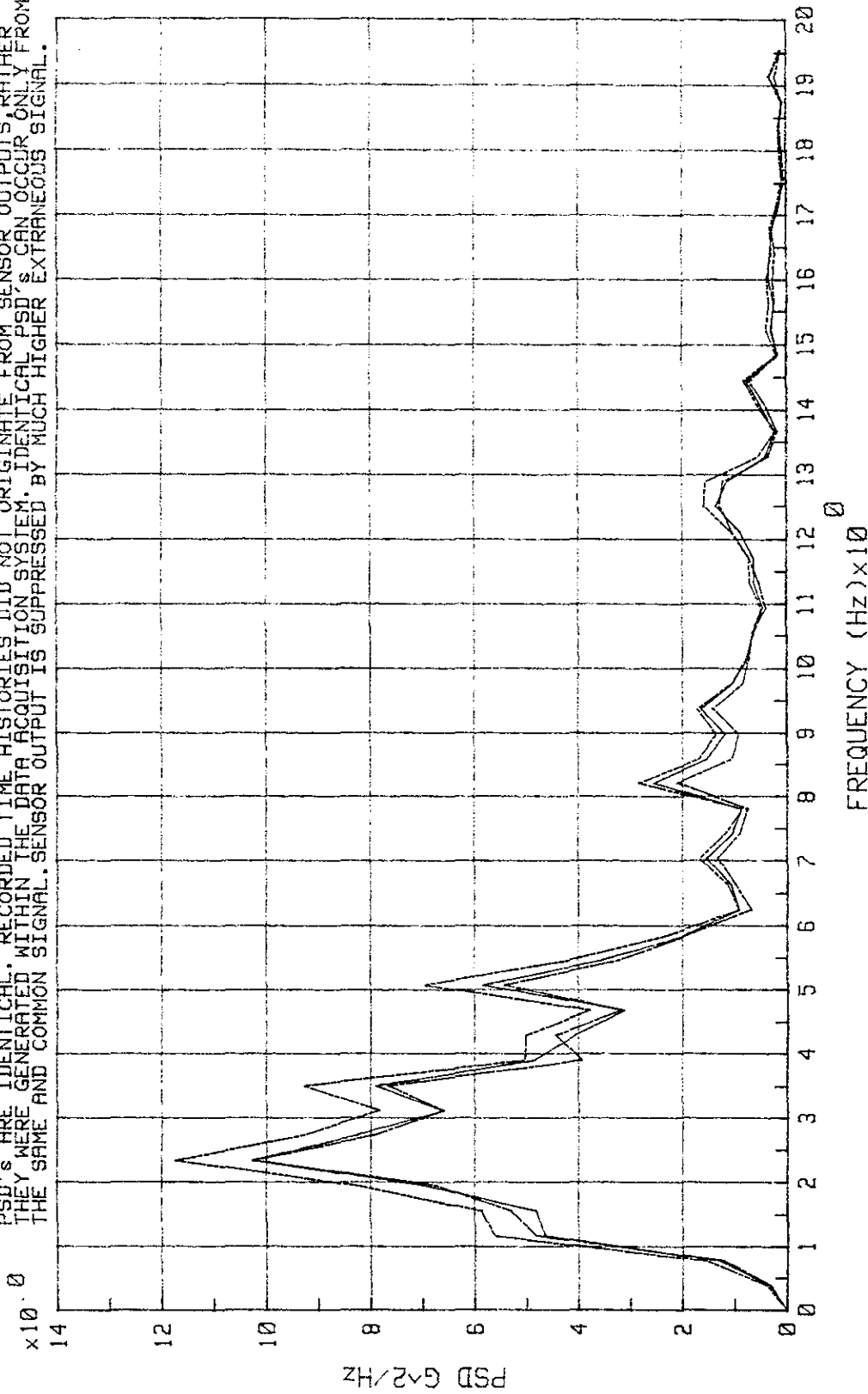


Figure 5-79. STS-3 Malfunction of High-Frequency Sensors KSRDC042A (X), -43A (Y), and -44A (Z)

KSR # DC042C DC043C DC044C DC042D DC043D DC044D

CURVES 1 THRU 3 (ALL "C" FILES) : DELTA-F=0.781 Hz. T+1.0 TO T+6.2 SEC. VALID DATA.
 CURVES 4 THRU 6 (ALL "D" FILES) : DELTA-F=0.391 Hz. T+6.2 TO T+16.4 SEC. INVALID DATA.
 MALFUNCTION OCCURRED AT 6.3 SEC AFTER T=ZERO AND PERSISTED THROUGHOUT THE END OF DATA RECORD.
 MALFUNCTION IS AFFECTING PSD'S FROM 0 Hz TO AT LEAST 50 Hz, THE SAME EXTRANEOUS SIGNAL
 APPEARS IN ALL "D" FILES REGARDLESS OF SENSOR ORIENTATION (X, Y, Z-DIRECTIONS).

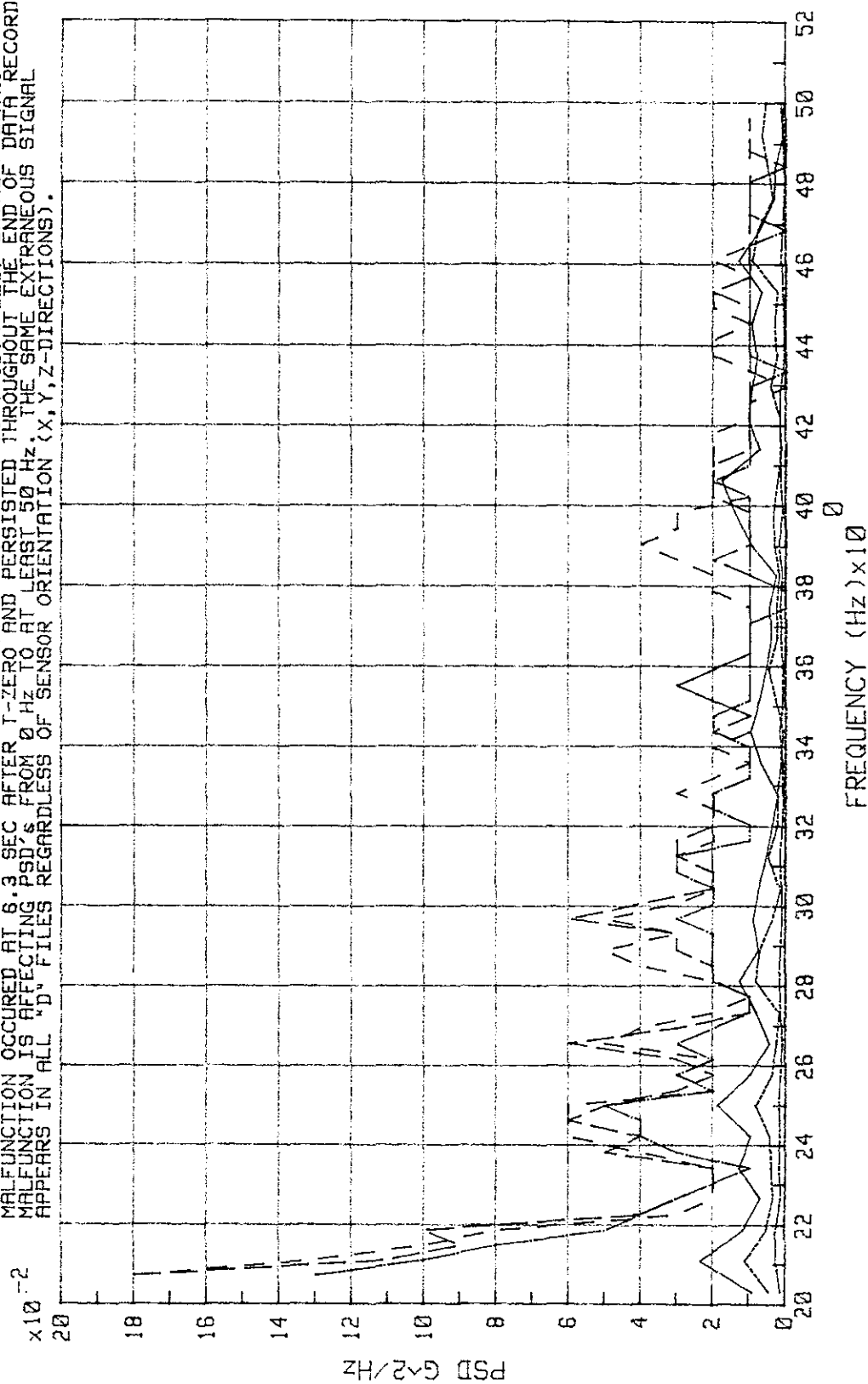


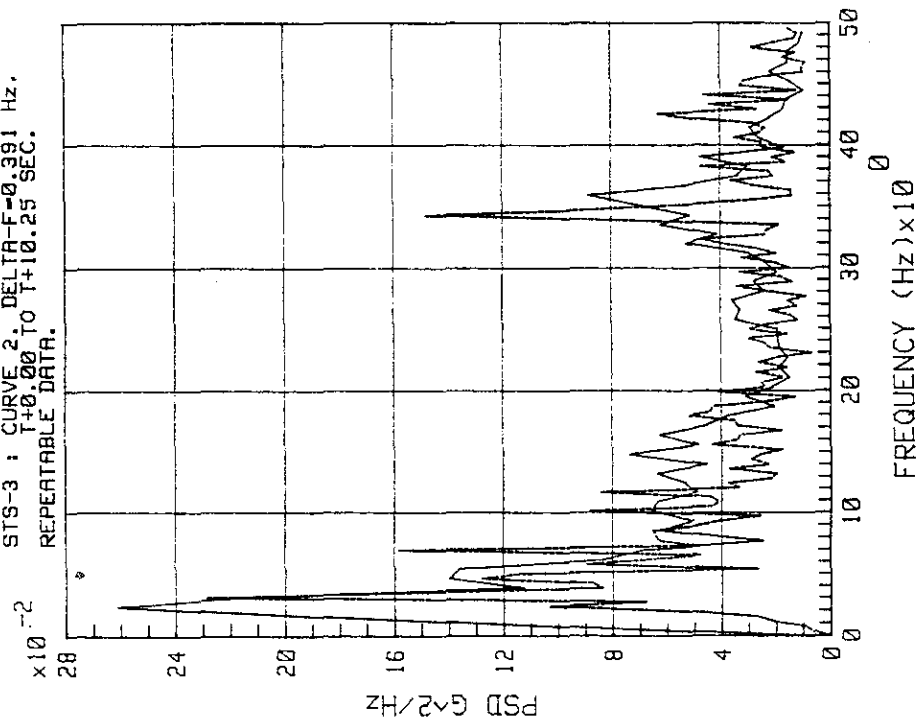
Figure 5-80. STS-3 KSRDC042A (X), -43A (Y), and -44A (Z) Before and After Malfunction

KSC-DD-818-TR

STS-2 & STS-3, PCR FL.BM. X-DIR.

KSR # DC003B DC003A

STS-2 : CURVE 1. DELTA-F=0.781 Hz.
T+0.00 TO T+10.25 SEC.
STS-3 : CURVE 2. DELTA-F=0.391 Hz.
T+0.00 TO T+10.25 SEC.
REPEATABLE DATA.



STS-2 & STS-3, PCR FL.BM. Y-DIR.

KSR # DC004B DC004B

STS-2 : CURVE 1. DELTA-F=0.781 Hz.
T+0.00 TO T+10.25 SEC.
STS-3 : CURVE 2. DELTA-F=0.781 Hz.
T+0.40 TO T+6.41 SEC.
STS-3 DATA LOST @ T+6.9 SEC. NOT A PEAK.

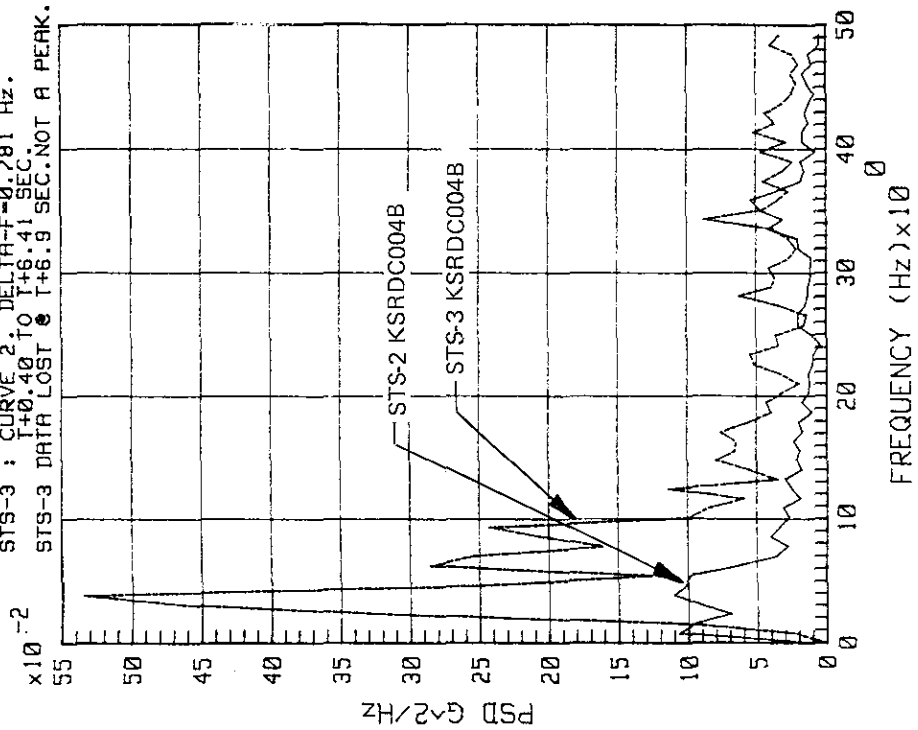


Figure 5-81. STS-2 and -3 PCR Floor Beam, X and Y Directions

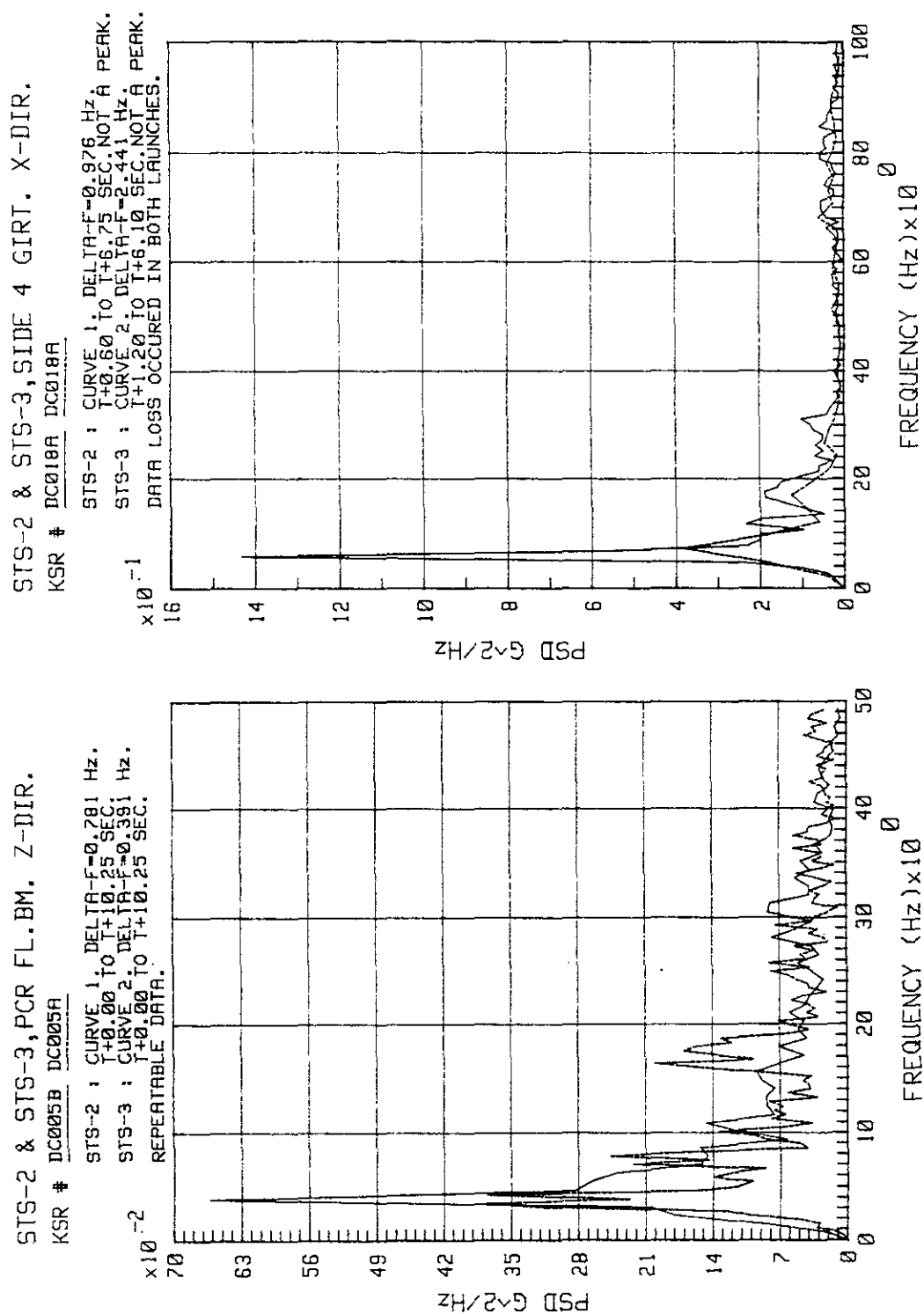


Figure 5-82. STS-2 and -3 PCR Floor Beam, Z Direction, and Side Girt, X Direction

KSC-DD-818-TR

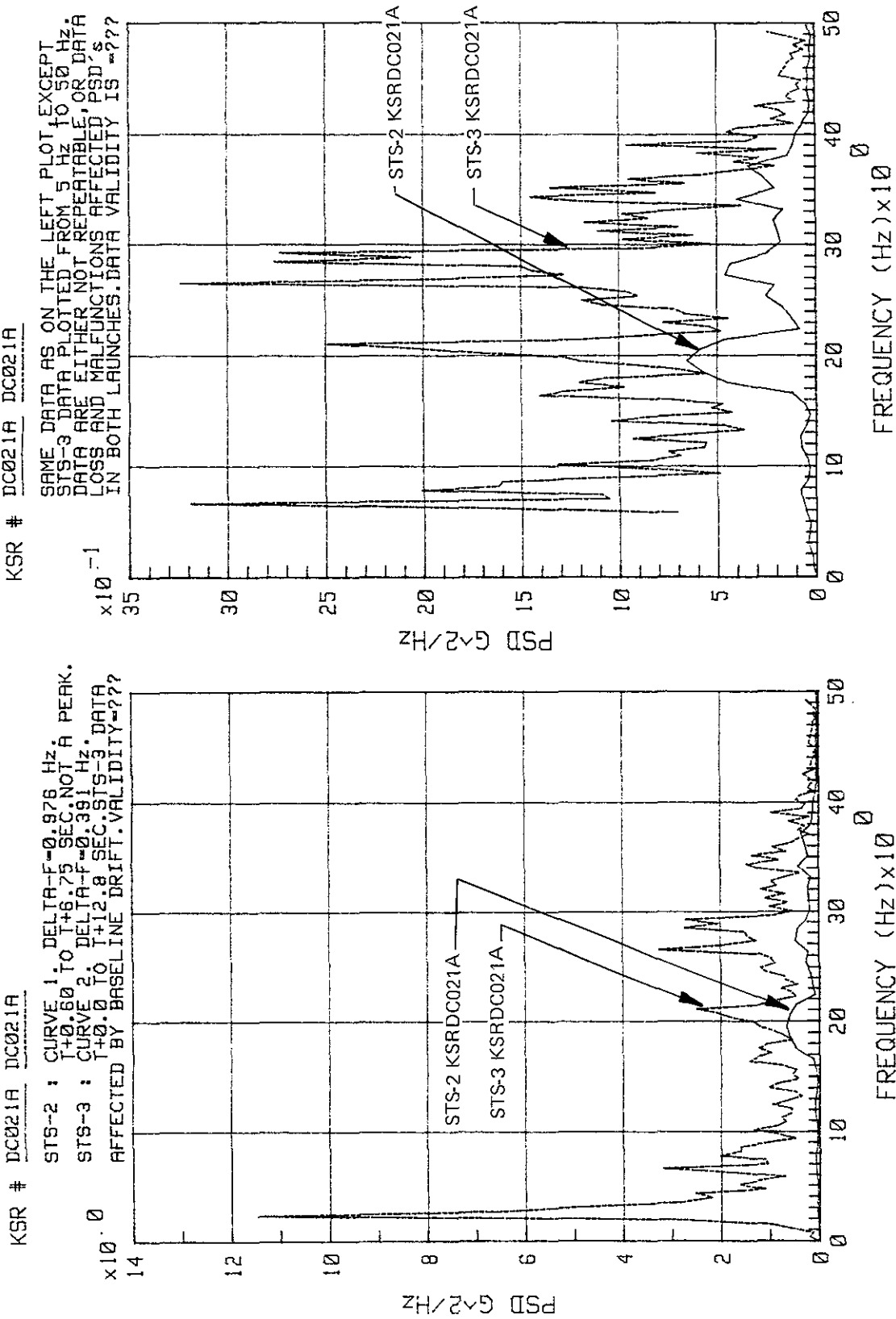
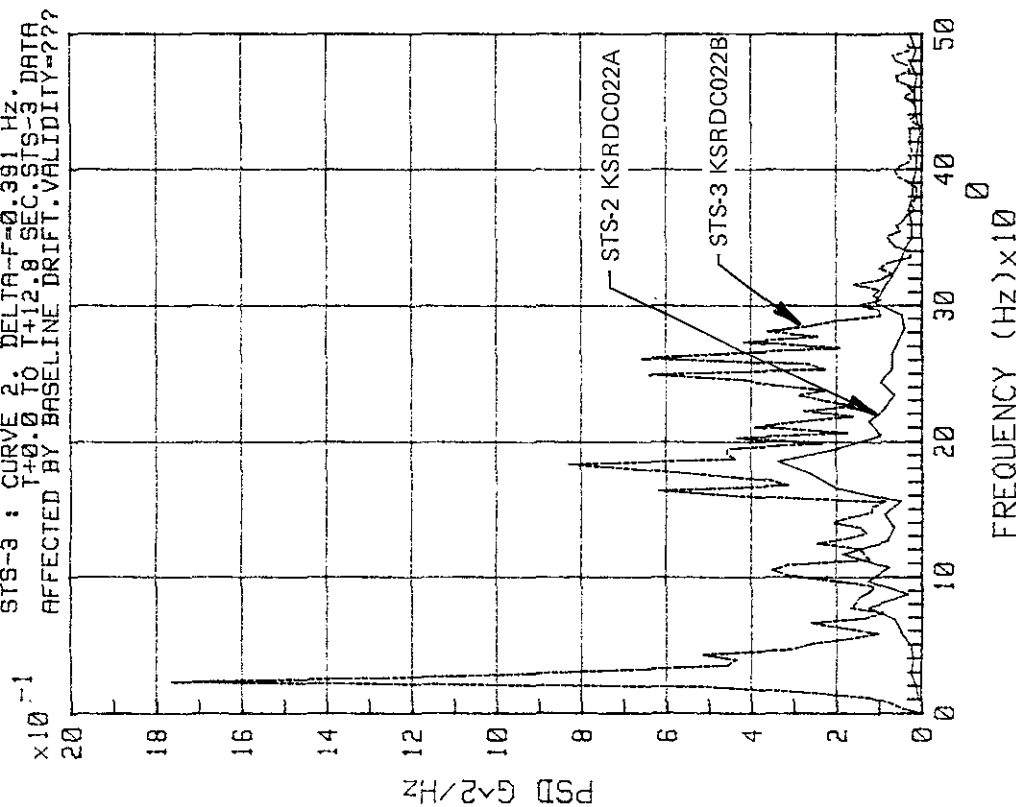


Figure 5-83. STS-2 and -3 Side 3 Girt, Y Direction (Sheet 1 of 2)

KSR # DC022A DC022B

STS-2 : CURVE 1. DELTA-F=0.976 Hz.
 T+0.0 TO T+6.15 SEC. NOT A PEAK.
 STS-3 : CURVE 2. DELTA-F=0.391 Hz. DATA
 T+0.0 TO T+12.8 SEC. STS-3 DATA
 AFFECTED BY BASELINE DRIFT. VALIDITY=???



KSR # DC022A DC022B

SAME DATA AS ON THE LEFT PLOT EXCEPT
 STS-3 DATA PLOTTED FROM 5 Hz TO 50 Hz.
 WITHIN THE PLOTTED RANGE DATA ARE FAIRLY
 REPEATABLE. EXCLUDED STS-3 DATA BELOW 5
 Hz YIELD UNREALISTIC 2.1 IN RMS DISPL.

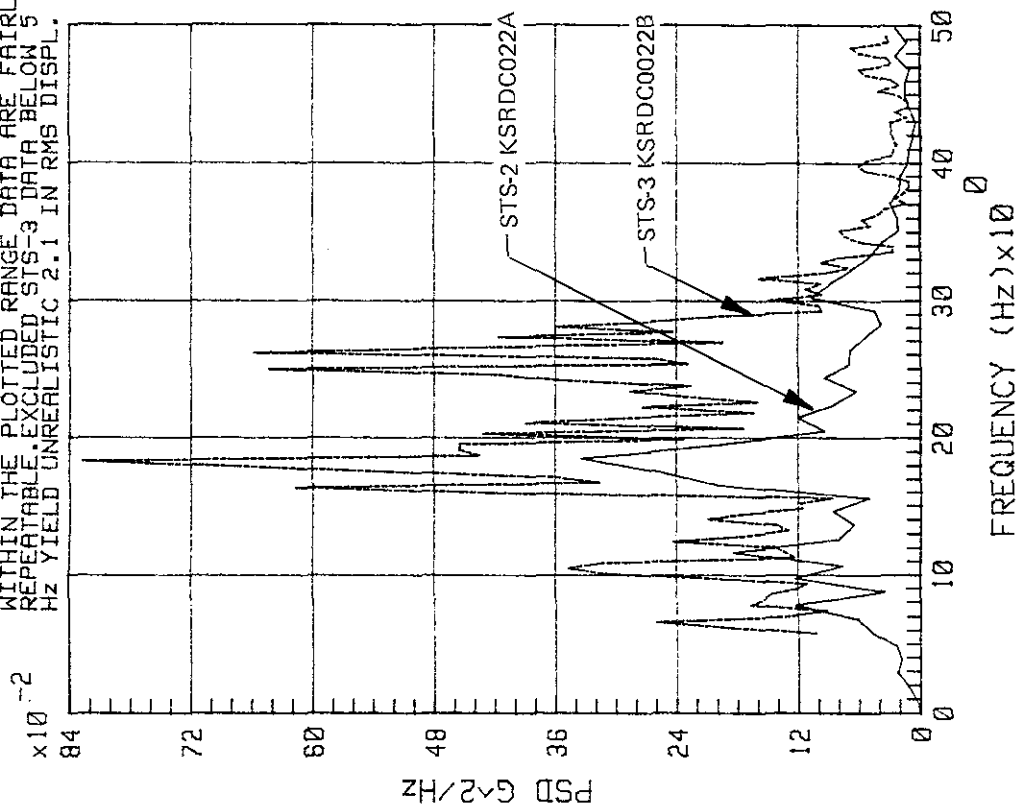


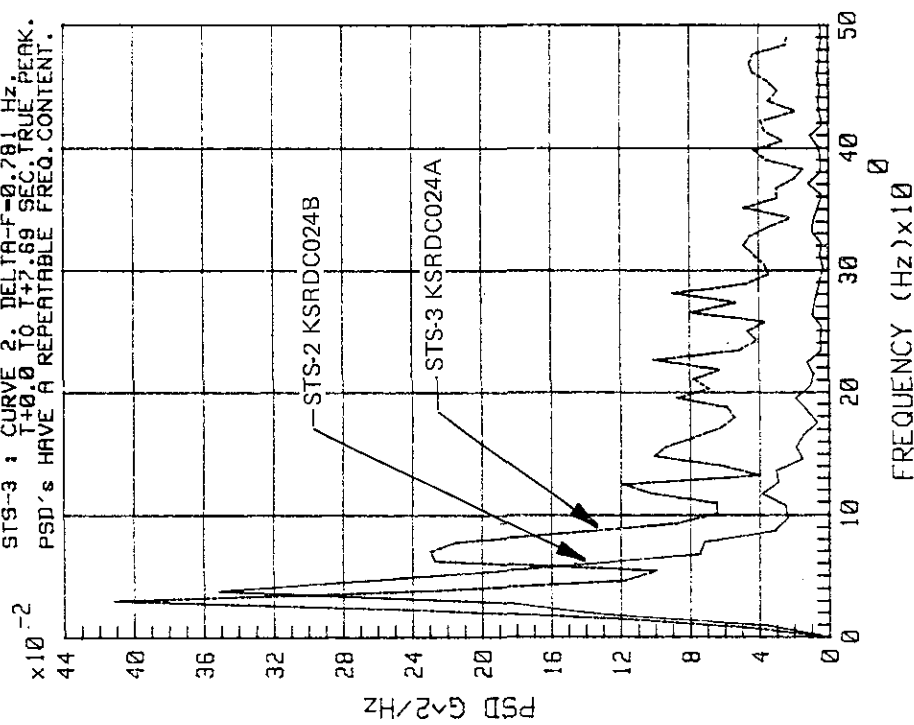
Figure 5-83. STS-2 and -3 Side 3 Girt, Y Direction (Sheet 2 of 2)

KSC-DD-818-TR

STS-2 & STS-3, APS FL. BM. X-DIR.

KSR # DC024B DC024A

STS-2 : CURVE 1: DELTA-F-0.976 Hz.
T+0.0 TO T+5.13 SEC. NOT A PEAK.
STS-3 : CURVE 2: DELTA-F-0.781 Hz. PEAK.
T+0.0 TO T+7.69 SEC. TRUE PEAK.
PSD's HAVE A REPEATABLE FREQ. CONTENT.



STS-2 & STS-3, APS FL. BM. Y-DIR.

KSR # DC025B DC025A

STS-2 : CURVE 1: DELTA-F-0.976 Hz.
T+0.0 TO T+8.20 SEC.
STS-3 : CURVE 2: DELTA-F-0.391 Hz.
T+0.0 TO T+10.25 SEC.
REPEATABLE DATA.

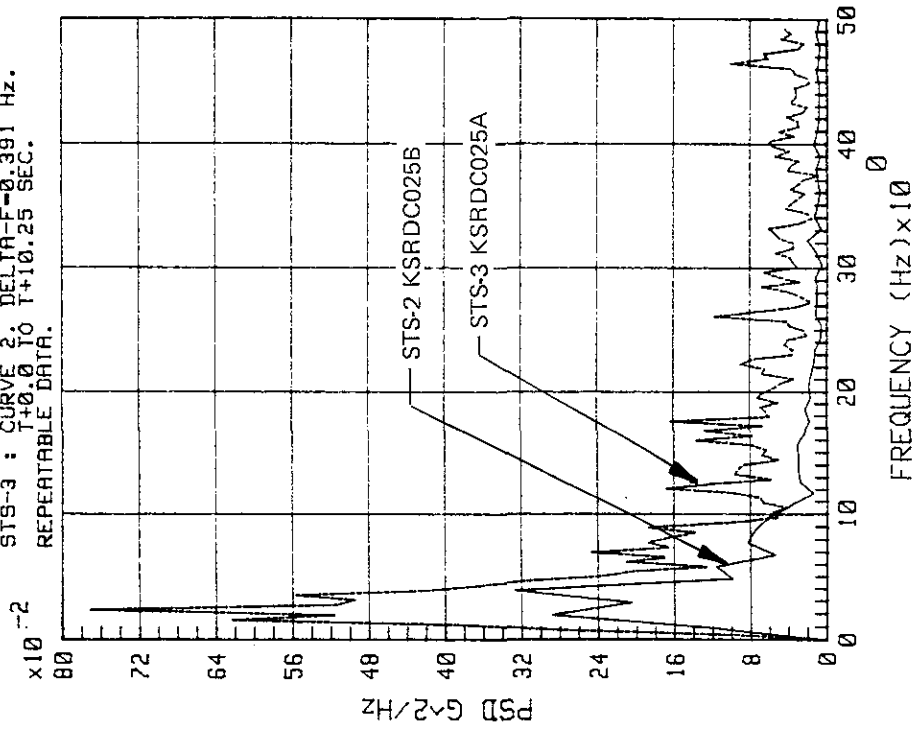


Figure 5-84. STS-2 and -3 APS Floor Beam, X and Y Directions

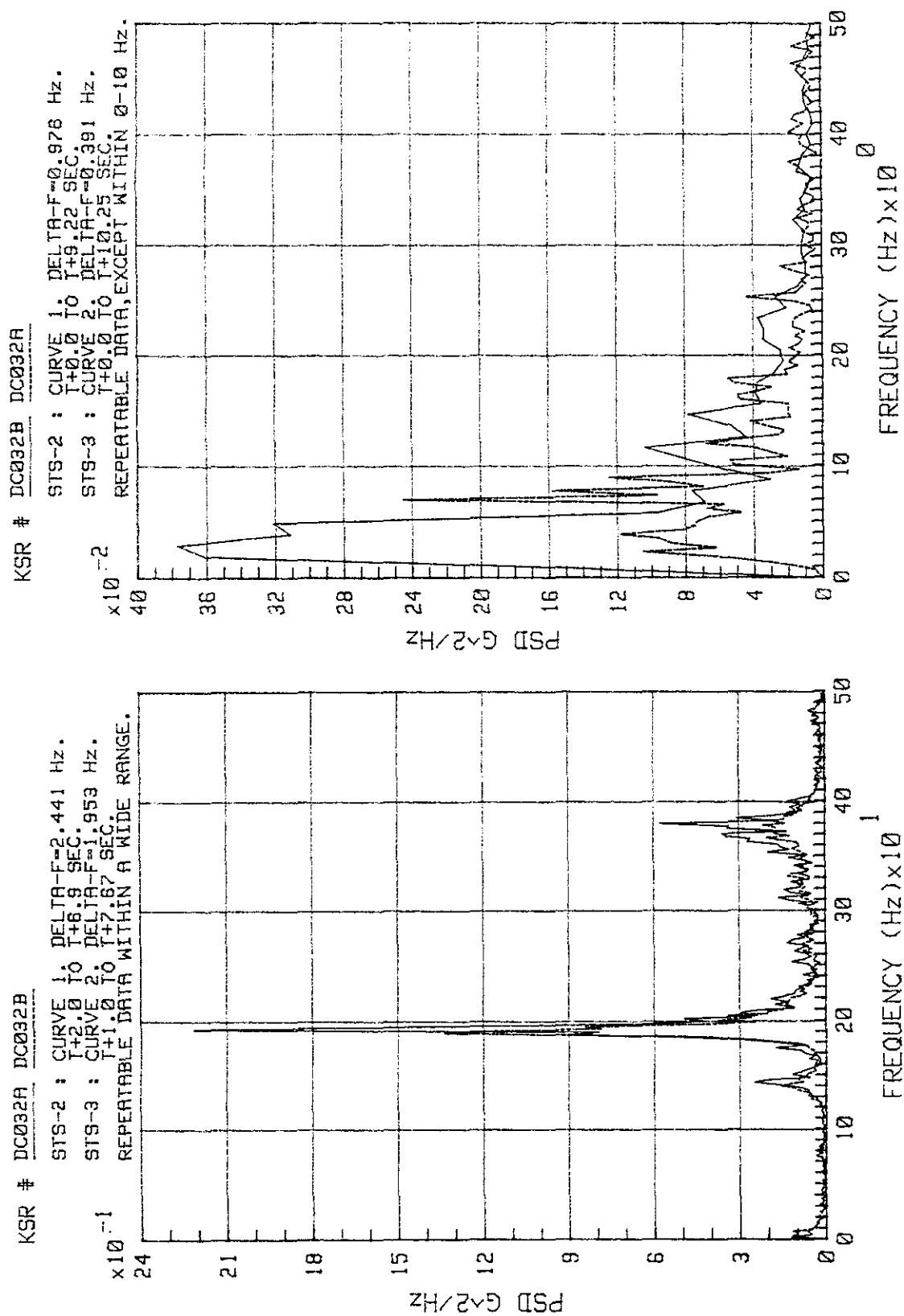


Figure 5-85. STS-2 and -3 Hypergol Electronic Equipment Platform Floor Beam at 117-ft Elevation, X Direction

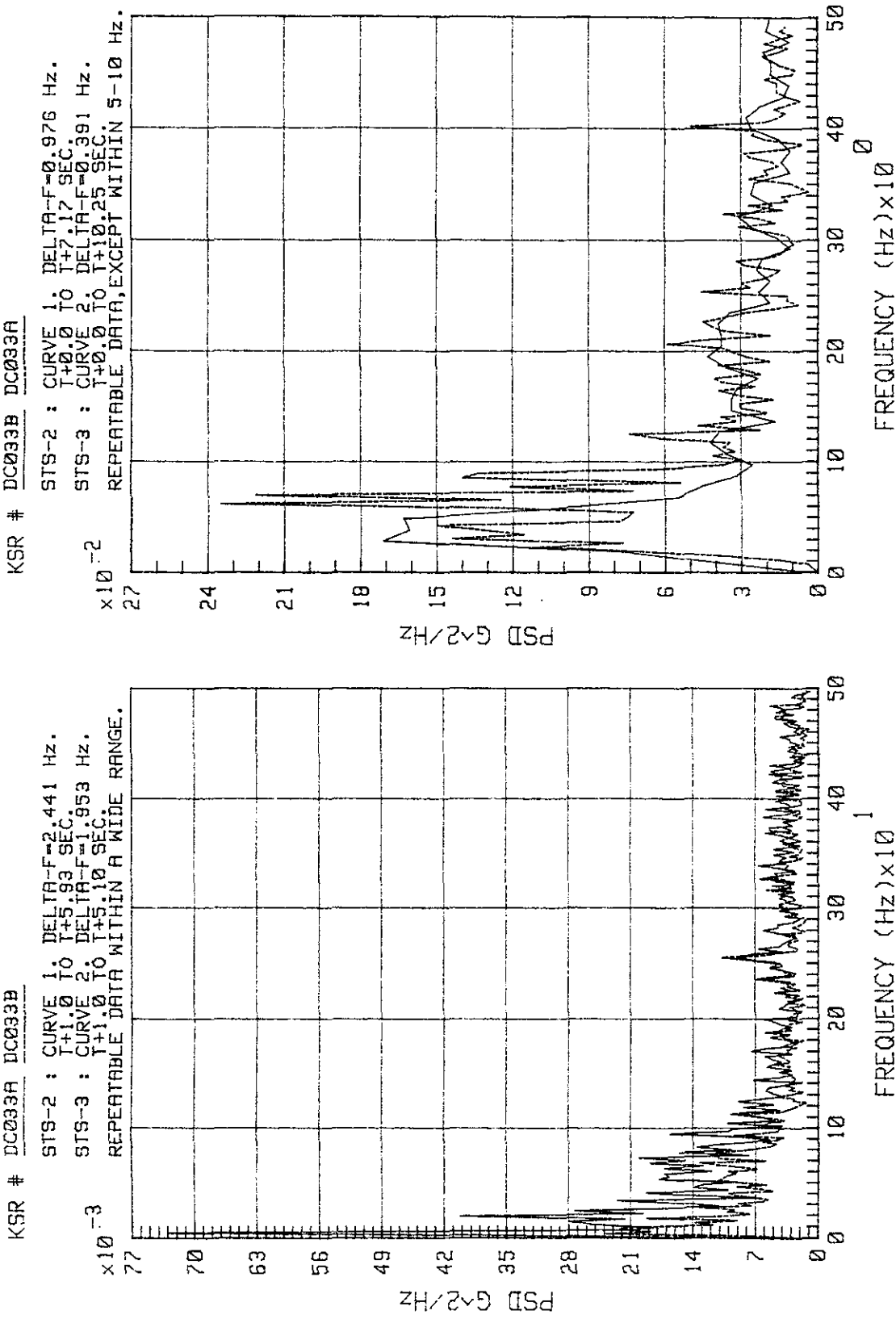


Figure 5-86. STS-2 and -3 Hypergol Electronic Equipment Platform Floor Beam at 117-ft Elevation, Y Direction

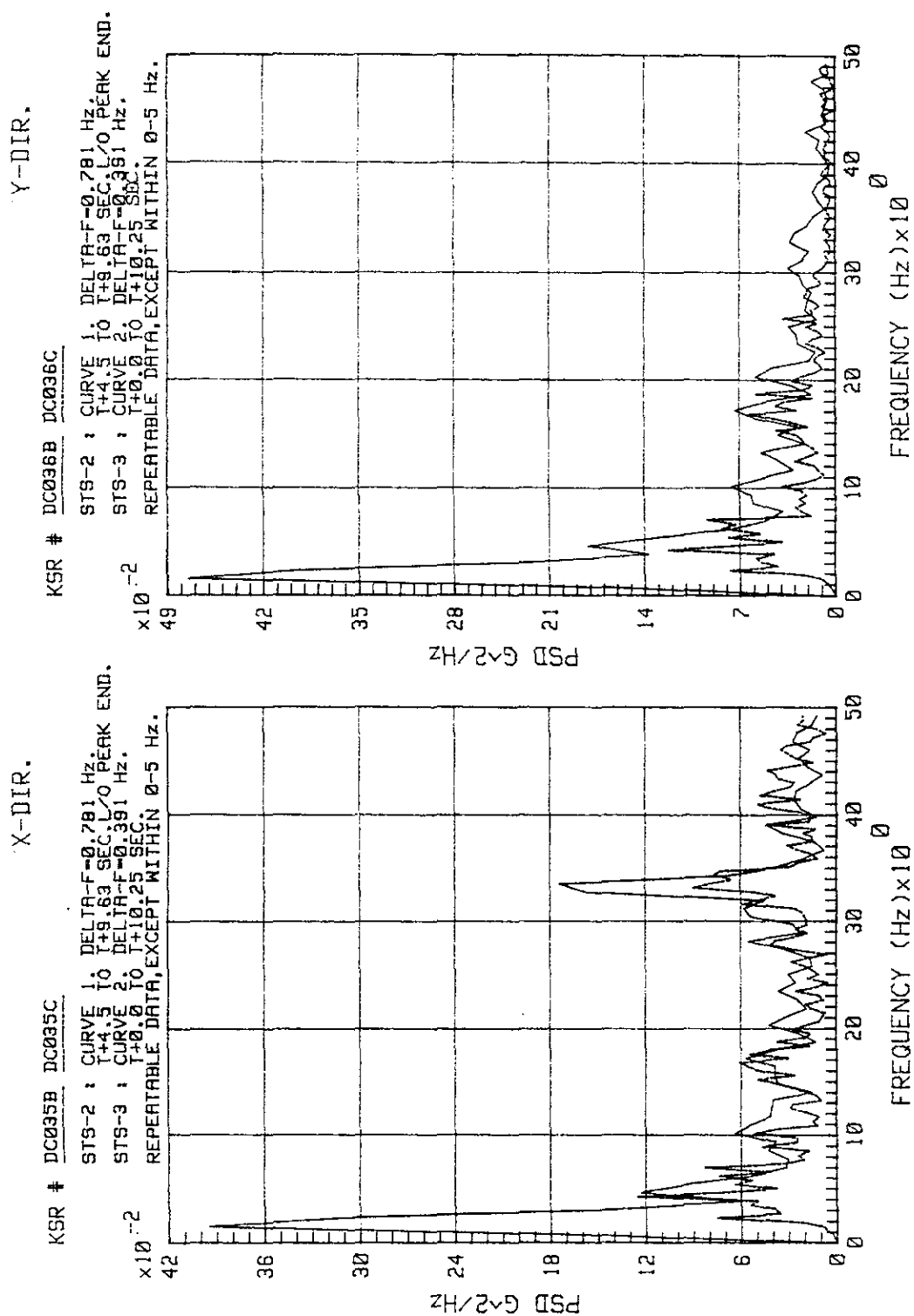


Figure 5-87. STS-2 and -3 Hypergol Electronic Equipment Platform Floor Beam, X and Y Directions

KSC-DD-818-TR

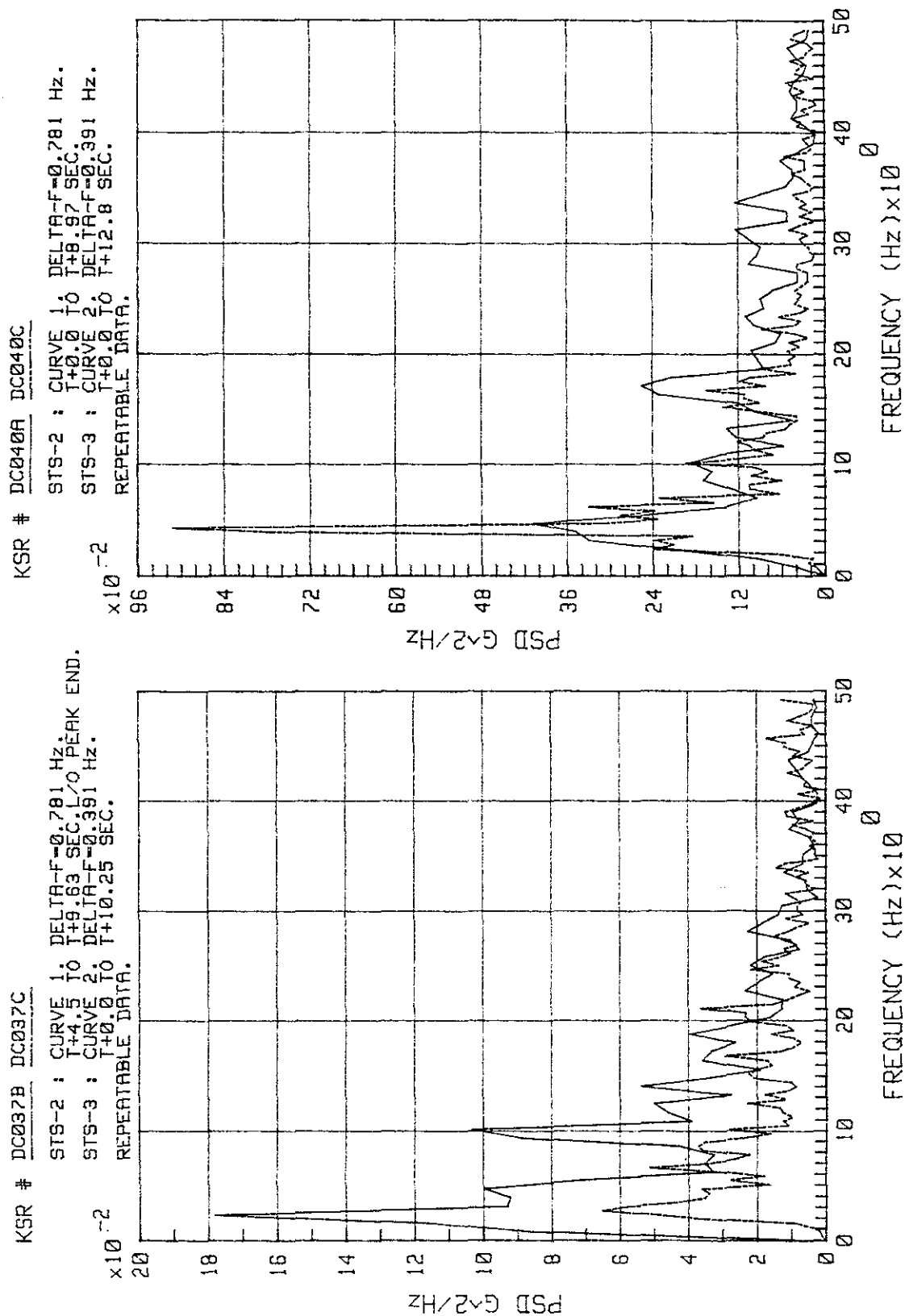


Figure 5-88. STS-2 and -3 Hypergol Electronic Equipment Platform Floor Beam, Z Direction

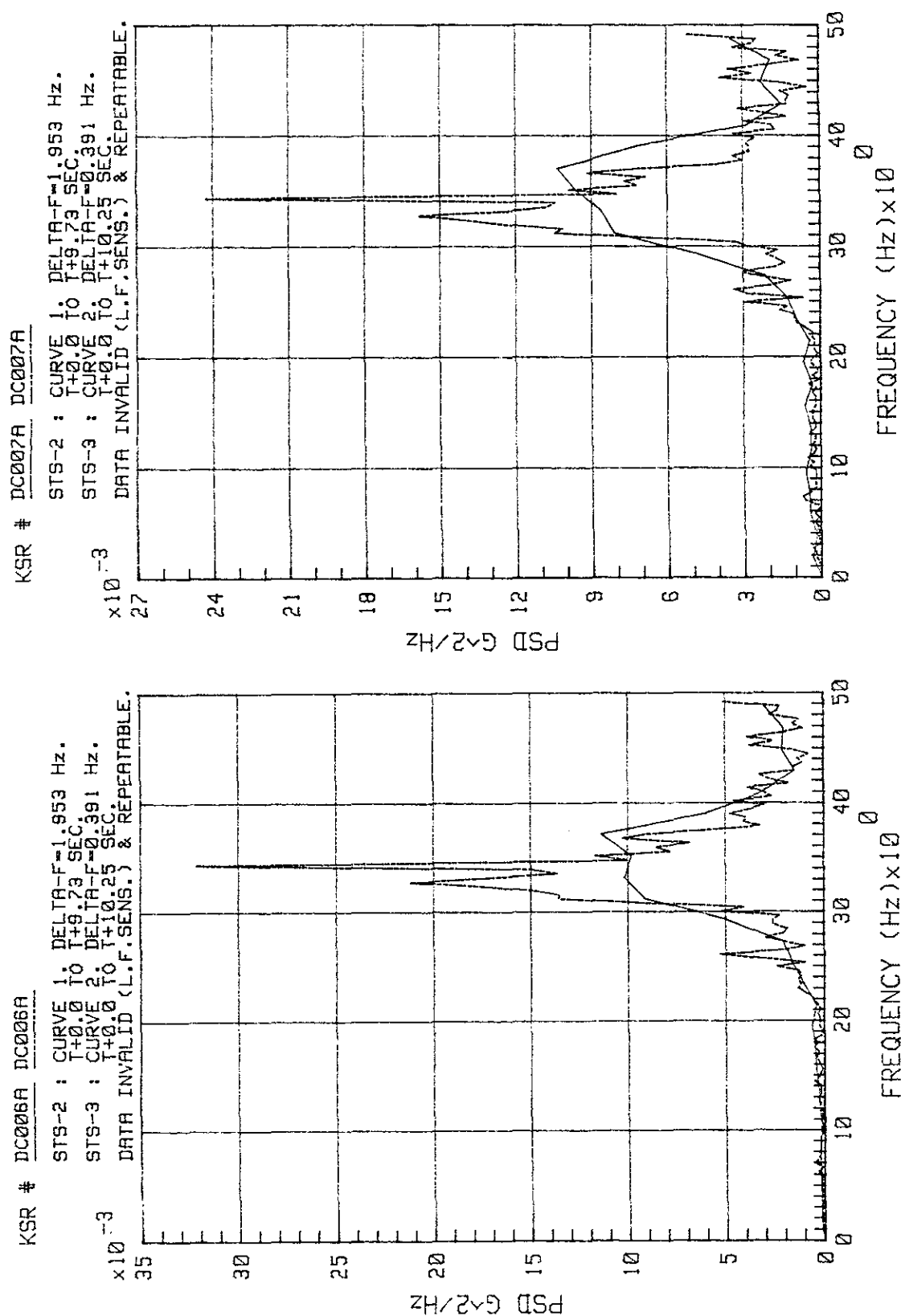


Figure 5-89. STS-2 and -3 PCR Floor Beam, X and Y Directions

KSC-DD-818-TR

KSR # DC006A DC007A

BOTH SENSORS : DELTA-F=1.953 Hz. DATA PROCESSED FROM 1+0.0 TO 1+9.73 SEC.
 BOTH SENSORS ARE LOCATED ON THE SAME BASE MOUNT ON PCR FLOOR BEAM @ ELEVATION 130'-7".
 PSD's ARE ALMOST IDENTICAL WITHIN A RANGE FROM 0 Hz TO 230 Hz. SUCH SIMILARITY IS NOT CREDIBLE.
 DATA WERE INVALIDATED ON THE BASIS OF DISPLACEMENT CHECK (RMS DISPL.=0.041 & 0.056 INCHES).
 PSD's SIMILARITY INDICATES A COMMON SOURCE OF MALFUNCTION.

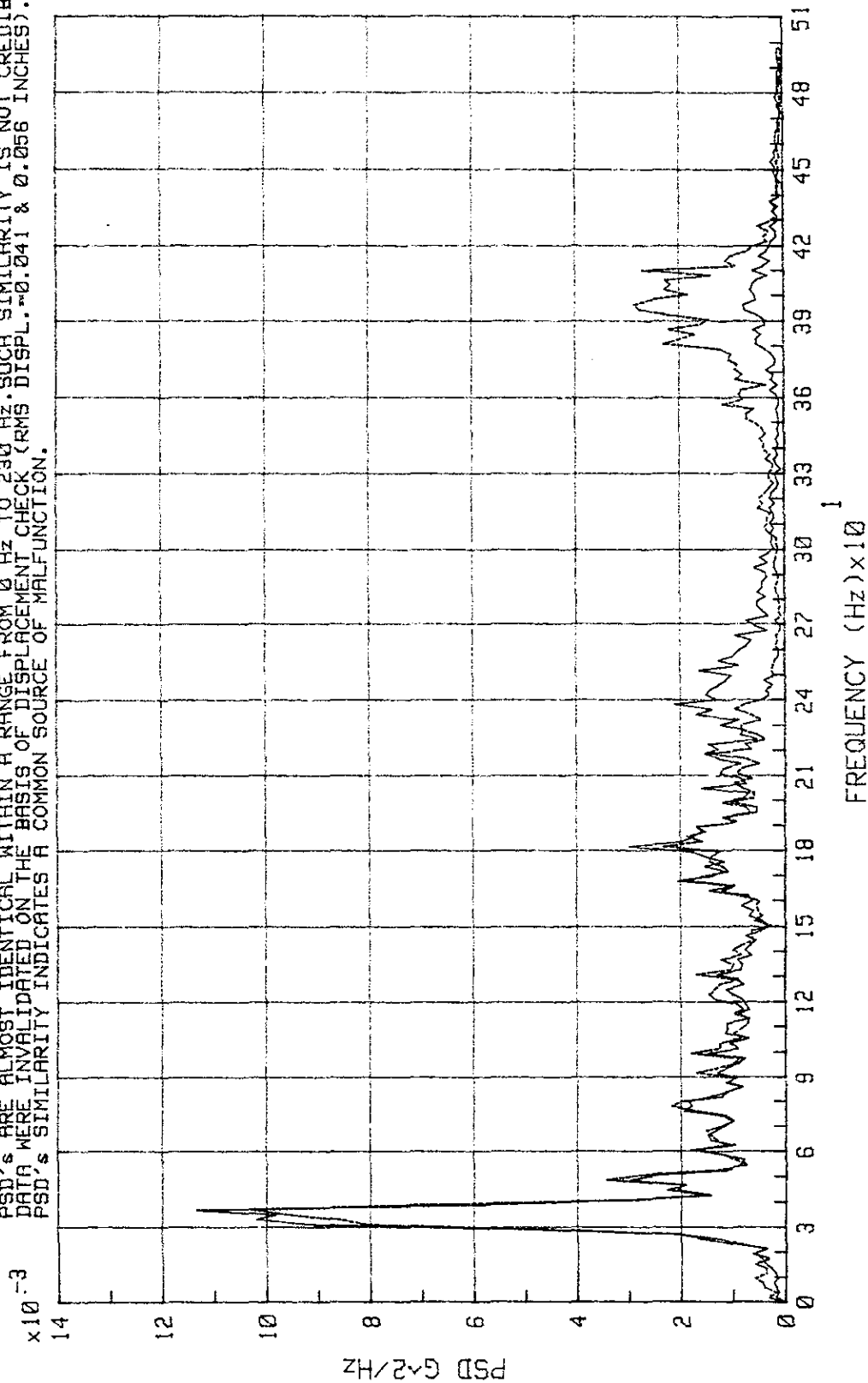


Figure 5-90. STS-2 Lift-Off Peak - Comparison Between KSRDC006A (X) and -007A (Y) (Sheet 1 of 2)

KSR # DC006A DC007A

BOTH SENSORS : DELTA-F=0.391 Hz. DATA PROCESSED FROM T+0.0 TO T+10.25 SEC.
 BOTH SENSORS ARE LOCATED ON THE SAME BASE MOUNT, ON PCR FLOOR BEAM @ ELEVATION 130'-7".
 PSD'S ARE ALMOST IDENTICAL, ALL PEAKS MATCH. SUCH SIMILARITY IS NOT CREDIBLE (X & Y DIR'S).
 DATA WERE INVALIDATED ON THE BASIS OF DISPLACEMENT CHECK (RMS DISPL.=0.023 & 0.031 INCHES).
 PSD'S SIMILARITY INDICATES A COMMON SOURCE OF MALFUNCTION.

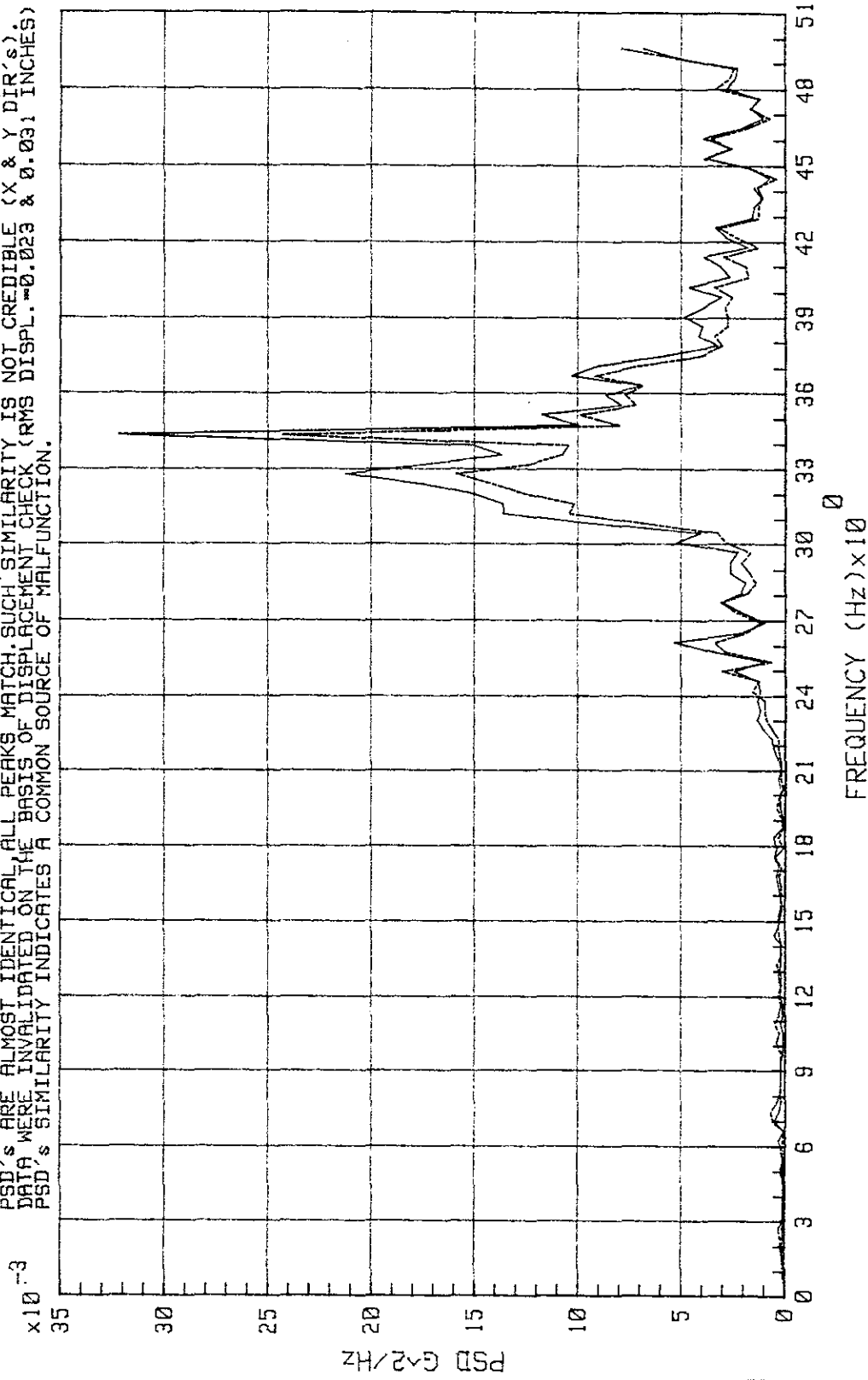


Figure 5-90. STS-2 Lift-Off Peak - Comparison Between KSRDC006A (X) and -007A (Y) (Sheet 2 of 2)

KSC-DD-818-TR

KSR # DC049B DC050B

BOTH SENSORS 1 DELTA-F=2.44 Hz. PROCESSING FROM T+2.5 TO T+2.4 SEC. SENSOR RANGE 0-500 Hz. BOTH SENSORS ARE LOCATED ON THE SAME BASE MOUNT, ON PCR FLOOR BEAM @ ELEVATION 130'-7". PSD's ARE ALMOST IDENTICAL, ALL PEAKS MATCH. SUCH SIMILARITY IS NOT CREDIBLE (X & Y DIR's). DATA WERE INVALIDATED ON THE BASIS OF DISPLACEMENT CHECK. PSD's SIMILARITY AND COINCIDENCE OF MAJOR PEAKS SUGGEST THAT RECORDED SIGNALS DID NOT ORIGINATE FROM SENSOR OUTPUTS.

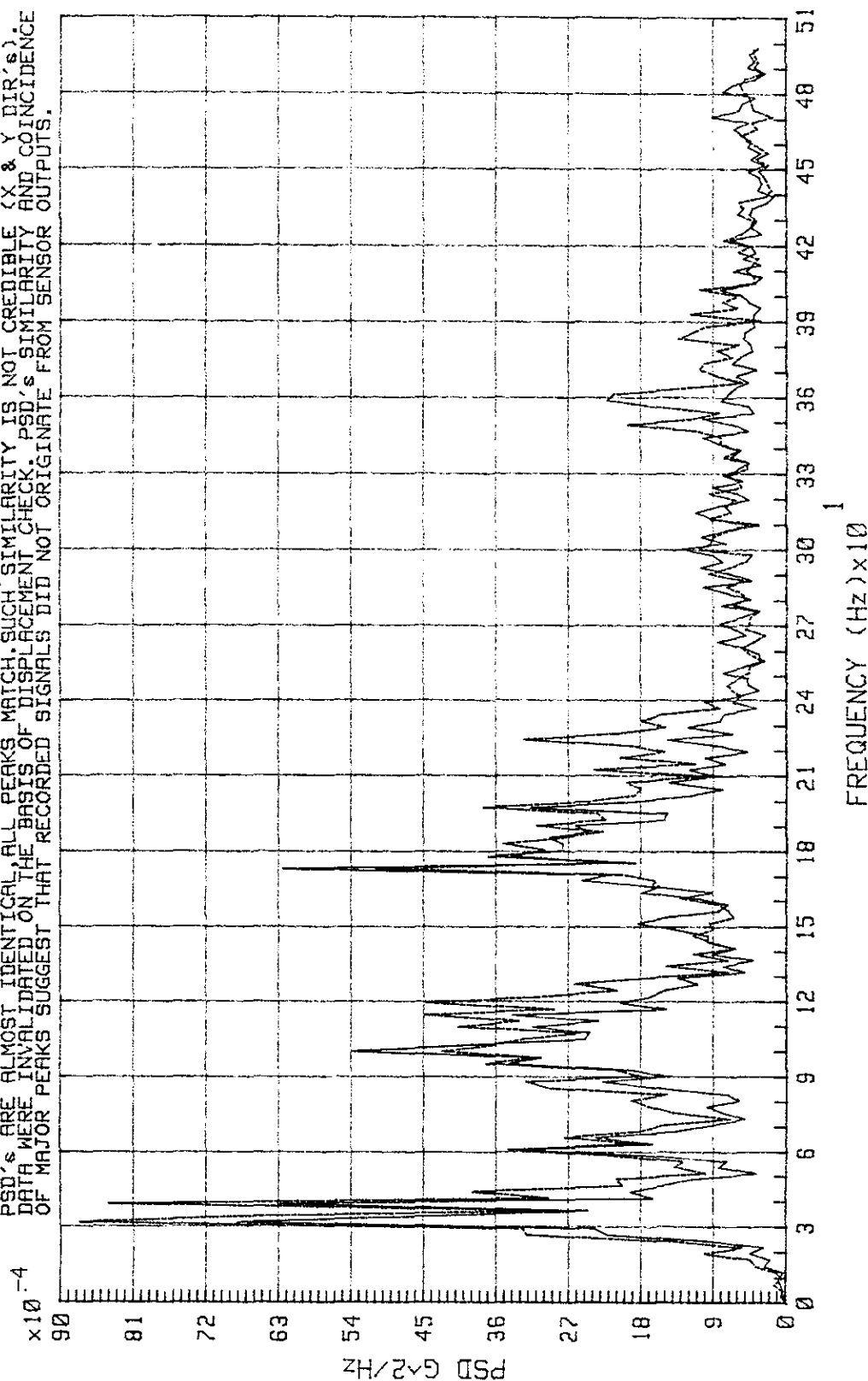


Figure 5-91. STS-3 Lift-Off Peak - Comparison Between KSRDC049A (X) and -050A (Y) (Sheet 1 of 3)

KSR # DC049B DC050B

BOTH SENSORS : DELTA-F=2.44 Hz. PROCESSING FROM T+2.5 TO T+7.4 SEC. SENSOR RANGE 0-500 Hz. BOTH SENSORS ARE LOCATED ON THE SAME BASE MOUNT, ON PCR FLOOR BEAM @ EL.130'. 7" PROCESSED. DATA ARE BEYOND THE NOMINAL SENSOR FREQUENCY RANGE. PSD's ARE ALMOST IDENTICAL; MAJOR PEAKS AND TREND MATCH. BOTH DATA RECORDS ORIGINATE FROM THE SAME SOURCE AND NOT FROM THE SENSOR OUTPUTS (ACCELERATIONS IN X & Y DIRECTIONS CANNOT COINCIDE IN THE HIGH FREQUENCY RANGE).

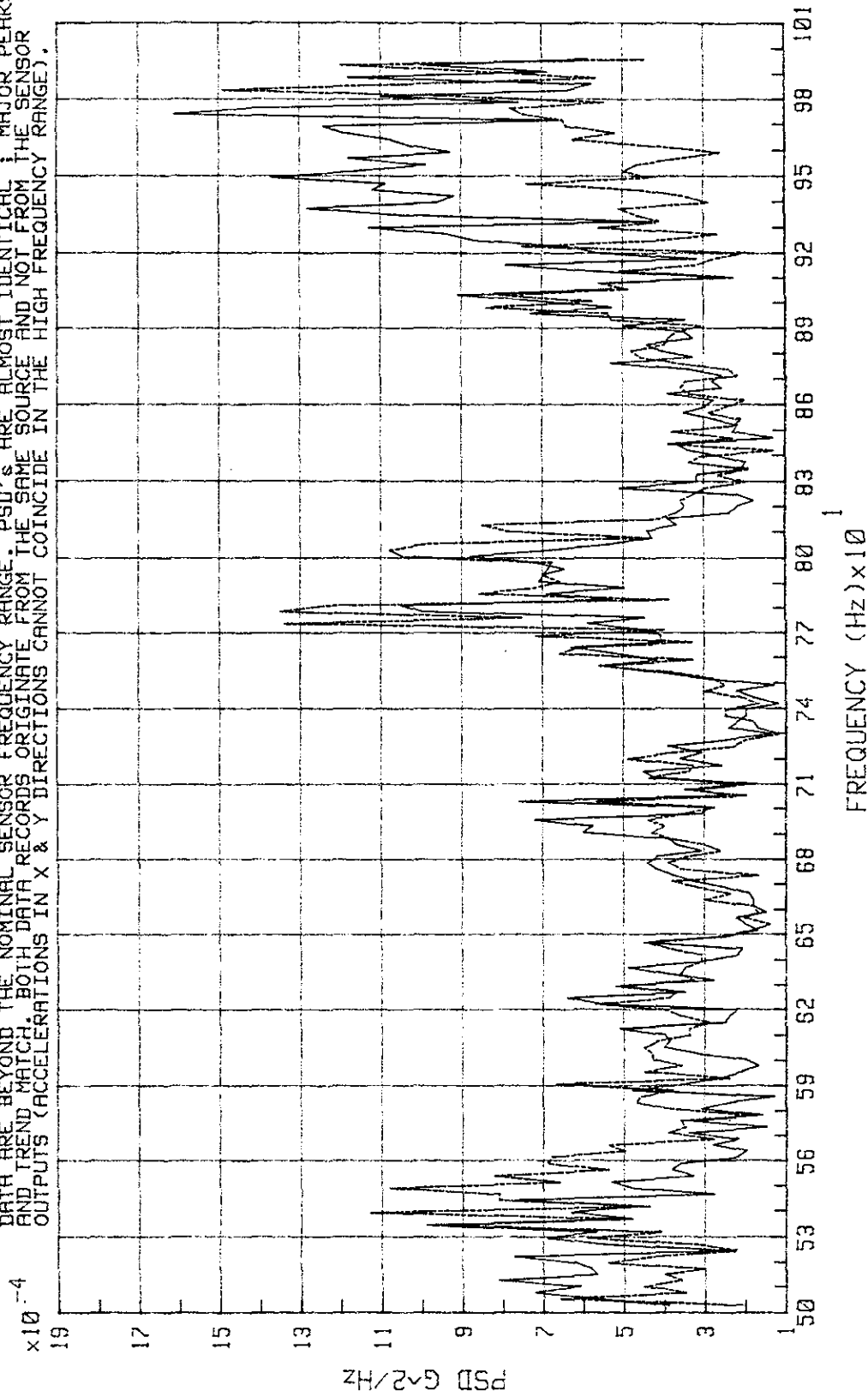


Figure 5-91. STS-3 Lift-Off Peak - Comparison Between KSRDC049A (X) and -050A (Y) (Sheet 2 of 3)

KSC-DD-818-TR

KSR # DC049C DC050C

BOTH SENSORS : DELTA-F-0.391 Hz. DATA PROCESSED FROM T+0.0 TO T+10.25 SEC.
 BOTH SENSORS ARE LOCATED ON THE SAME BASE MOUNT, ON PCR FLOOR BEAM @ ELEVATION 130'-2".
 PSD's ARE ALMOST IDENTICAL, ALL PEAKS MATCH, SUCH SIMILARITY IS NOT CREDIBLE (X & Y DIR's).
 DATA WERE INVALIDATED ON THE BASIS OF DISPLACEMENT CHECK (RMS DISPL.=0.020 & 0.028 INCHES).
 PSD's SIMILARITY INDICATES A COMMON SOURCE OF MALFUNCTION.

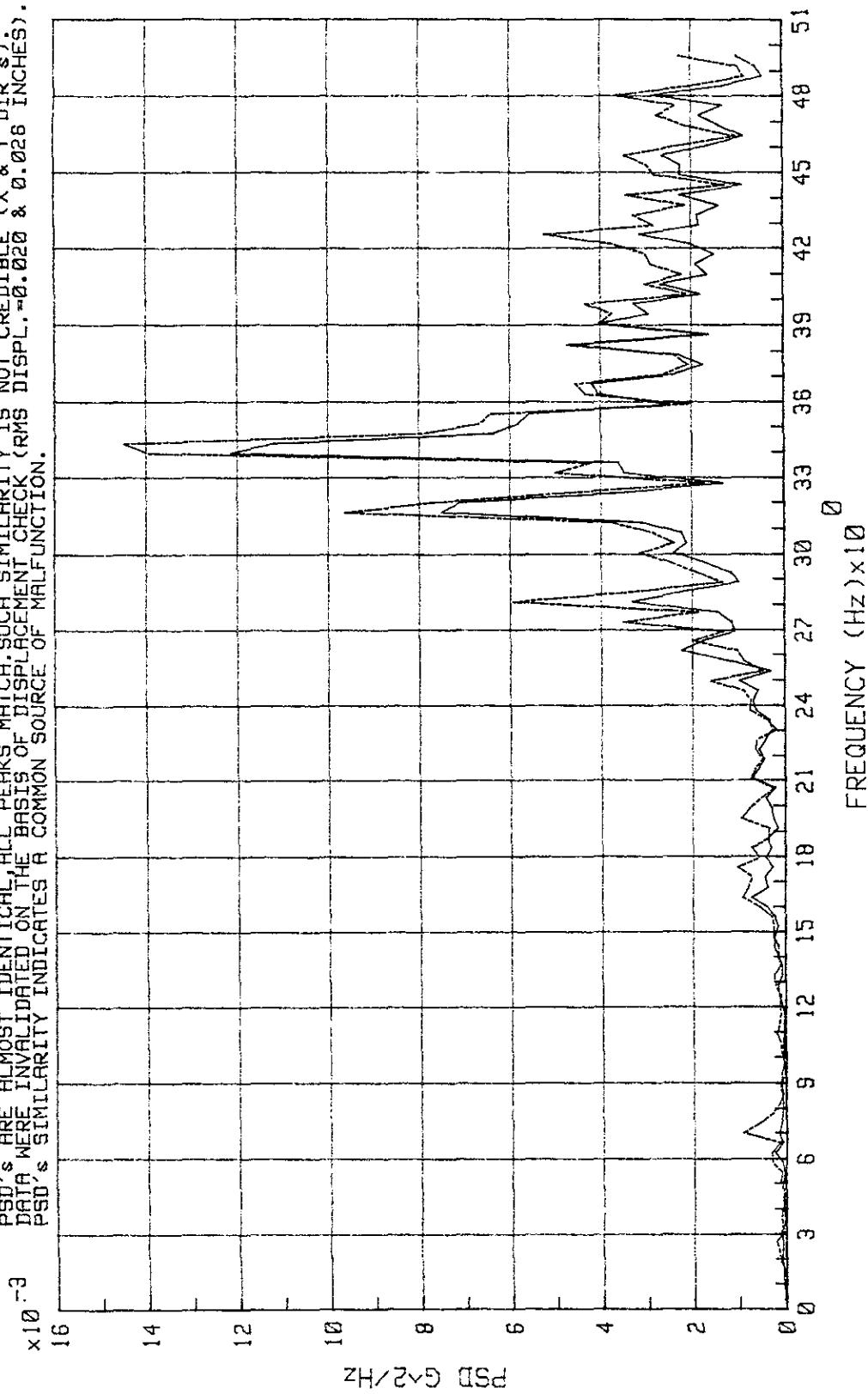


Figure 5-91. STS-3 Lift-Off Peak - Comparison Between KSRDC049A (X) and -050A (Y) (Sheet 3 of 3)

KSR # DC006A DC007A DC049C DC050C

ALL SENSORS : DELTA-F-0.391 Hz. PROCESSING FROM 1+0 TO 1+10.25 SEC. SENSOR RANGE 0-500 Hz.
 SENSORS ARE LOCATED AT TWO DIFFERENT LOCATIONS ON PCR FLOOR BEAMS @ EL. 130'-7". OCCUR BECAUSE
 ALL PSD'S ARE IN THE NOISE DOMAIN. FLAT PORTIONS OF PSD'S (KSRDC006A & -007A) OCCUR BECAUSE
 OF COMPUTATIONAL ROUNDING (DATA ARE BELOW COMPUTATIONAL RANGE GOVERNED BY THE HIGHEST PSD PEAK).
 ALL PSD'S ARE INVALID. LOW FREQUENCY COMPONENTS, 0-20 Hz, ARE ABSENT. A "DAS" PROBLEM/MISMATCH.

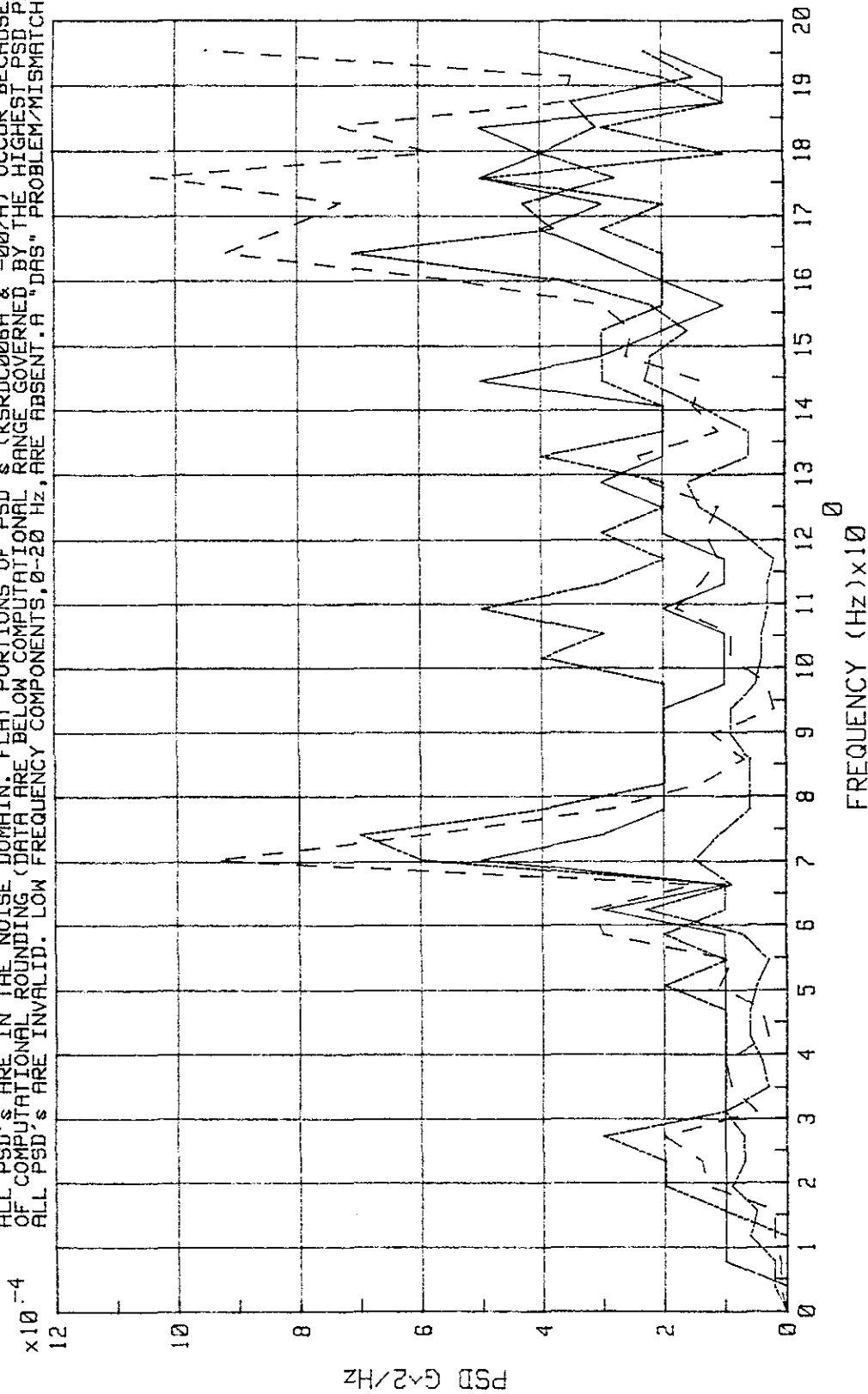


Figure 5-92. STS-3 Lift-Off Peak - Low-Frequency Sensors KSRDC006A (X), -007A (Y), -049A (X),
 and -050A (Y) (Sheet 1 of 2)

KSC-DD-818-TR

KSR # DC006A DC007A DC049C DC050C

ALL SENSORS : DELTA F=0.391 Hz. PROCESSING FROM T+0 TO T+10.25 SEC. SENSOR RANGE 0-500 Hz.
 SENSORS ARE LOCATED AT TWO DIFFERENT LOCATIONS ON PCR FLOOR BEAMS @ EL. 130' ± 2".
 ALL PSD'S ARE INVALID. PSD'S SIMILARITY AND COINCIDENCE OF MAJOR PEAKS SUGGEST THAT RECORDED
 SIGNALS DID NOT ORIGINATE FROM SENSOR OUTPUTS. SENSOR OUTPUTS WERE SUPPRESSED BY SOME MISMATCH
 IN THE DATA ACQUISITION SYSTEM. A DATA LOSS/FAILURE WAS NEVER OBSERVED IN T.H. RECORDS OF L.F. SENS.

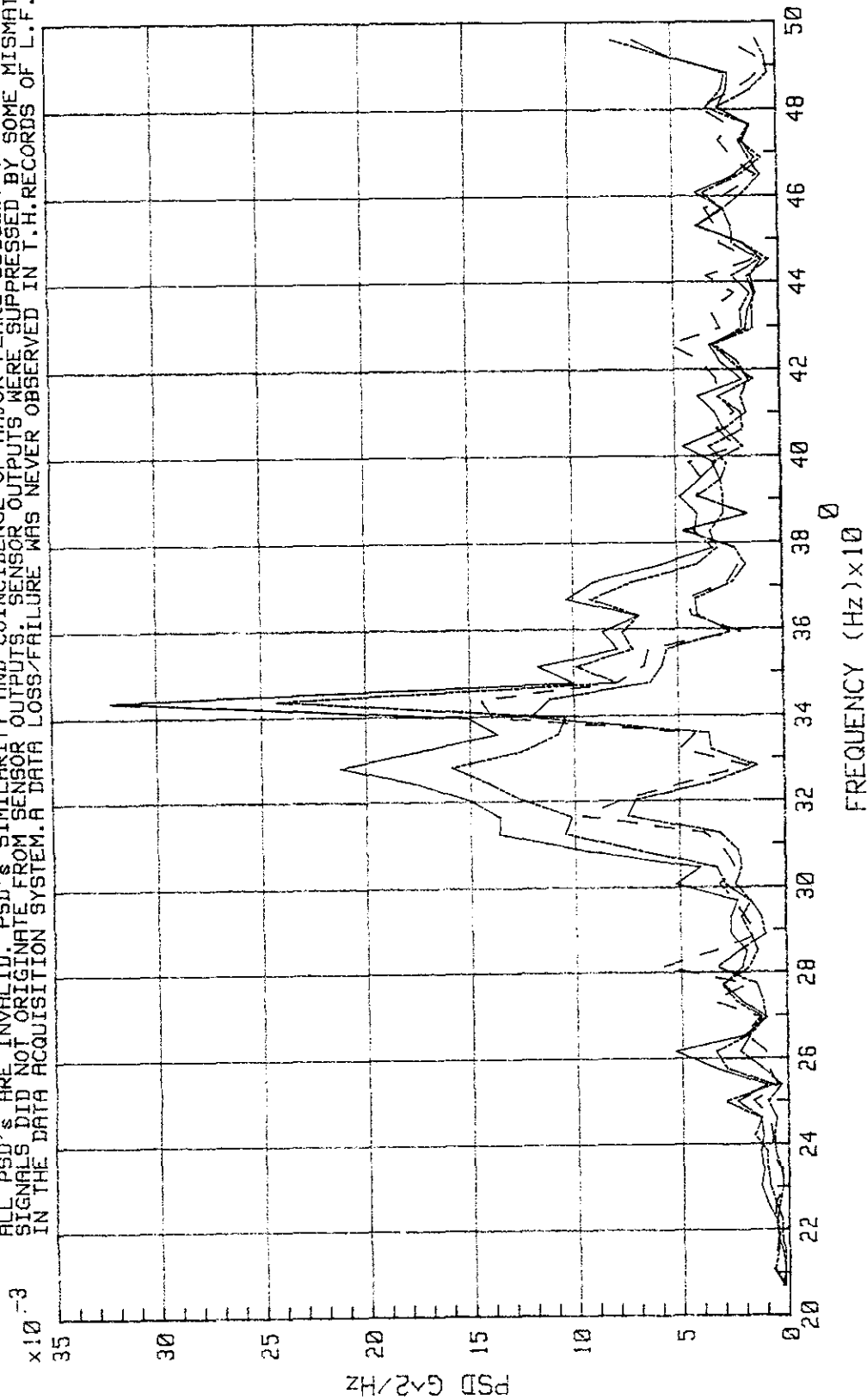


Figure 5-92. STS-3 Lift-Off Peak - Low-Frequency Sensors KSRDC006A (X), - 007A (Y), -049A (X),
 and -050A (Y) (Sheet 2 of 2)

KSR # DC045A DC046A DC047A DC048A

ALL SENSORS : DELTA-F=0.391 Hz. PROCESSING FROM T+5.7 TO T+13.4 SEC. SENSOR RANGE 5-2000 Hz.
 KSRDC045A (X), -DC046A (Y) -DC047A (Z) ARE LOCATED ON DRAWER SUPPORTING RAIL (SAME MOUNT).
 KSRDC048A (Z) IS LOCATED AT MIDSPAN OF FAN SUPPORT PANEL. HIGH AMPLITUDE LOW FREQUENCY
 COMPONENTS BEGUN TO APPEAR AT T+6.0 SEC. CALCULATED RMS DISPLACEMENTS ARE UNREALISTIC (4.05,
 3.65, 2.82 AND 1.44 IN RESPECTIVELY). PSD'S ARE INVALID AND RESULT FROM A MALFUNCTION IN DAS.

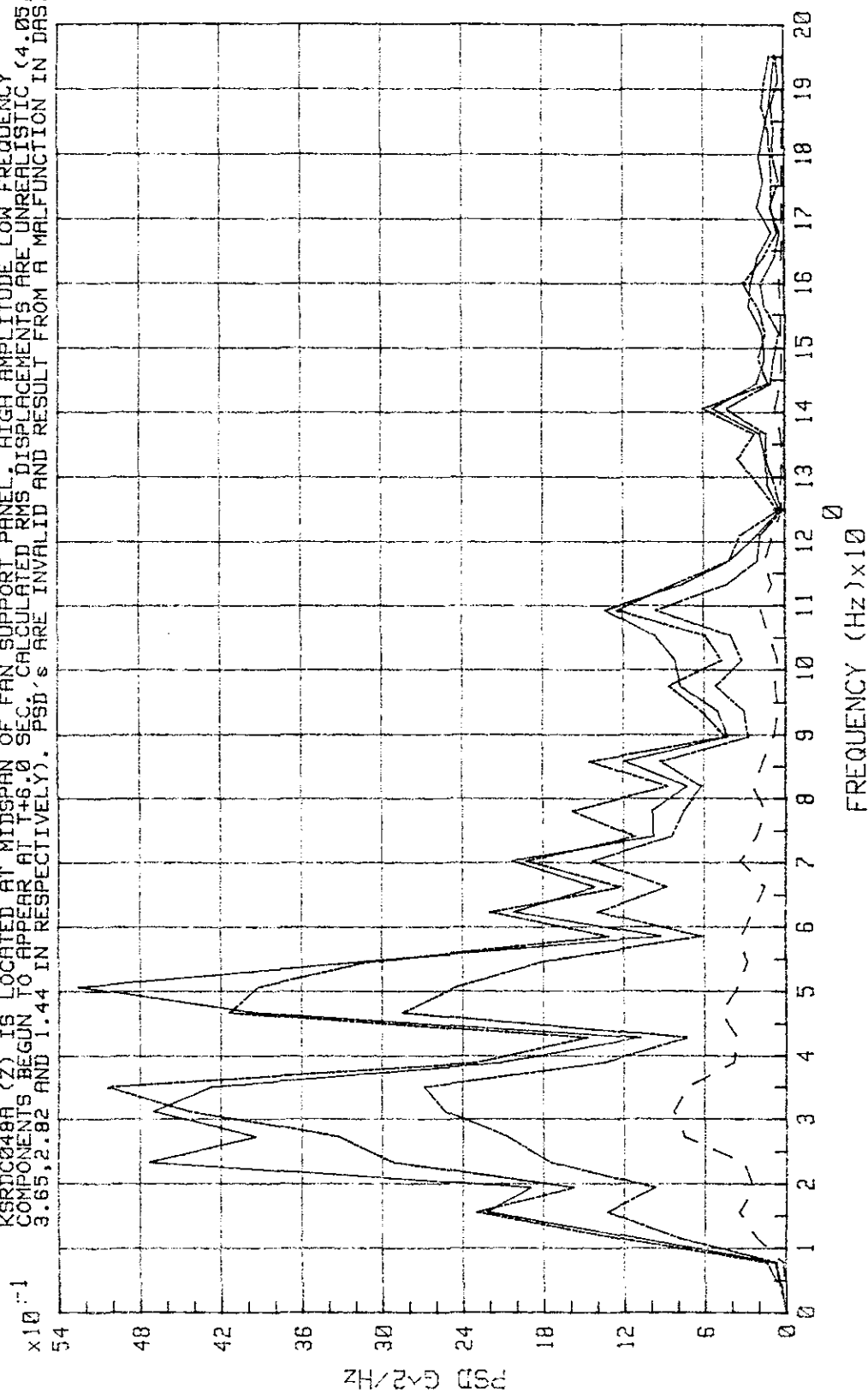


Figure 5-93. STS-2 Lift-Off Peak End - High-Frequency Sensors Inside HIM Rack 6396A1